SECTION 5.8: METEOROLOGY

File name: 598690_ESK_DSSR 5.8 Meteorology Rev

Author's declaration: I declare that appropriate diligence and quality assurance was applied in the compilation of this report. As such I am confident in the results here described and the conclusions drawn.

AIRSHED

Name: Dr L W Burger

Date: 10/01/2024

Peer Reviewer: I declare that this report has undergone independent peer review by myself, that comments were addressed to my satisfaction, and that as such, it is considered fit for publication.

Universiteit van Pretoria
University of Pretoria
Yunibesithi ya Pretoria

Name: Prof C de W Rautenbach

Date: 10/01/2024

Project Manager Authorisation:

SRK Consulting - Certified Electronic Signature
srk consulting
598690/45363/Report
9630-[illegible]-14/03/2024
This signature has been printed digitally. The Author has given permission for its use for this document. The details are stored in the SRK Signature Database

Holmes

Name: D Holmes

Date: 14/03/2024

Project Partner Authorisation:

SRK Consulting - Certified Electronic Signature
srk consulting
598690/45363/Report
5038-9071-5622-ENGE-14/03/2024
This signature has been printed digitally. The Author has given permission for its use for this document. The details are stored in the SRK Signature Database

Name: B Engelsman

Date: 14/03/2024

Eskom NSS Technical Lead Acceptance:

Kilian

Name: A Kilian

Date: 2024-03-14

Eskom NSS Employer's Agent Acceptance:

Name: F van Mosseveld

2024-03-15
Date:

AMENDMENT RECORD			
Rev	**Draft**	**Date**	**Amendment**
0		04 May 2016	New section, replacing old KSSR Rev 0. Original submission to the NNR
1		31 March 2022	Revised by SRK, accepted by Eskom
1a		14 March 2024	Revised by Airshed to include additional monitoring data and to address NNR comments

Executive Summary

This chapter of this Site Safety Report (SSR) presents an evaluation of the prevailing meteorological, corrosion and climatological characteristics for the Duynefontyn site, with specific attention also to the extreme values of meteorological variables such as rainfall, air temperature and wind speed, and rare meteorological phenomena that occur infrequently. Future projections of these parameters due to climate change are also accommodated.

These characteristics have been investigated in support of the identification of external events and potential hazards to the nuclear installation(s) on the site.

The following meteorological parameters were identified for onsite monitoring and inclusion in this SSR:

- wind speed and direction;
- ambient air temperature and temperature difference between vertical levels;
- precipitation;
- relative humidity;
- ambient pressure;
- solar radiation;
- atmospheric stability;
- evapotranspiration rate;
- corrosivity.

The analysis of historical records also details of the following meteorological parameters, some of which are rare and extreme:

- hail;
- frost;
- fog;
- lightning;
- tornadoes;
- snow, avalanches, ice, ice cover and blizzards;
- thunder;
- extreme weather (wind speed, rainfall and temperature).

- tornado/tropical cyclones.

Meteorological parameters are monitored at the Koeberg Weather Station (wind speed and dry-bulb temperature at four different heights on a 120-m tower, and atmospheric pressure and rainfall at surface) as well as a separate automatic weather station (Duynefontyn Weather Station (WS)) measuring dry-bulb temperature at two heights, wind speed, solar radiation, relative humidity, atmospheric pressure, rainfall, visibility and lightning events. Measurements on the 120-m tower are made at 10 m, 50 m, 85 m and 120 m, above ground level. Additional meteorological history was also obtained from the South African Weather Services (SAWS) reports, and monitoring data from SAWS.

Measurements on the 120-m tower included the period 1980 to 2022 (plus 9 months data in 2023). The Duynefontyn WS was commissioned 29 September 2017. Data gathering interruption occurred following an Eskom Stop Work Order of 6 February 2019, which took effect from 1 April 2019. The Resume Work Order was received on 9 July 2019, and with effect from 10 July 2019, regular data checks and collections were again performed.

Eskom Standard 238-52 – Meteorological Requirements for Nuclear Installations (Eskom, 2017) and the analytical procedures provided in the IAEA Specific Safety Guide No. SSG-18 (International Atomic Energy Agency, 2011) were used as a basis for conducting the meteorological analyses.

Corrosivity was determined according to using measurement of sulfate and chloride deposition rates at the site following the methods specified in the International Organisation for Standardisation (ISO) 9225 on corrosion of metals and alloys-corrosivity of atmospheres (International Organisation for Standardisation, 2012c). This included four measurement campaigns, namely, from May 2008 to January 2009, October 2012 to September 2013, October 2017 to April 2019 and September 2019 to September 2020.

Summaries of meteorological parameters are provided in ***Table 5.8.A*** and ***Table 5.8.B***. Please note that the use of “mean” in the table and throughout the report refers to the “arithmetic mean” which is the same as “average”.

Table 5.8.A includes the analyses of climate change projections published by the SAWS and the 5th Assessment Report of the Intergovernmental Panel on Climate Change (IPCC) (ARP5) (Intergovernmental Panel on Climate Change, 2013), as well as detailed analyses of downscaled global climate model simulations for the site, which were performed by the Council for Scientific and Industrial Research (CSIR).

Table 5.8.A
Site Specific Parameters Part 1

Meteorological Parameter		Baseline	Climate Change Projections (Including 95% Confidence Intervals)			
			2044	2064	2110	2130
Annual Average		4.1	4.2 ± 0.2	4.3 ± 0.2	4.4 ± 0.2	4.5 -0.3+0.2
Hourly Maximum Wind Speed [m/s] (10 m above site ground level)	Extreme Observed & Projected	17.2	17.4 ±0.3	17.5 ±0.3	17.7 ±0.3	17.9 ±0.3
	10 Year Return	16.9 ± 1.0	17.3 ± 1.0	17.6 ± 1.0	18.3 ± 1.0	18.7 ± 1.0
	100 Year Return	21.6 ± 1.5	22.1 ± 1.5	22.5 ± 1.5	23.4 ± 1.5	23.9 ± 1.5
	1 000 Year Return	26.3 ± 2.2	26.9 ± 2.2	27.3 ± 2.2	28.4 ± 2.2	29.0 ± 2.2
	10 000 Year Return	30.9 ± 2.8	31.6 ± 2.8	32.1 ± 2.8	33.4 ± 2.8	34.1 ± 2.8
	100 000 Year Return	35.5 ± 3.5	36.4 ± 3.5	36.9 ± 3.5	38.4 ± 3.5	39.2 ± 3.5
	1 000 000 Year Return	40.2 ± 4.2	41.1 ± 4.2	41.7 ± 4.2	43.4 ± 4.2	44.3 ± 4.2
	10 000 000 Year Return	44.8 ± 4.8	45.8 ± 4.8	46.5 ± 4.8	48.4 ± 4.8	49.4 ± 4.8
	100 000 000 Year Return	49.4 ± 5.5	50.5 ± 5.5	51.3 ± 5.5	53.4 ± 5.5	54.5 ± 5.5
Wind peaks (**gusts**) [m/s] (10 m above site ground level)	Extreme Observed & Projected	38.8	39.2 -0.6+0.5	39.4± 0.6	40.0 ± 0.7	40.3 ± 0.7
	10 Year Return	33.8 ± 2.7	34.1 ± 2.7	34.2 ± 2.7	34.8 ± 2.7	35.1 ± 2.7
	100 Year Return	43.3 ± 4.8	43.7 ± 4.8	43.9 ± 4.8	44.6 ± 4.8	45.0 ± 4.8
	1 000 Year Return	52.7 ± 6.8	53.2 ± 6.8	53.4 ± 6.8	54.3 ± 6.8	54.8 ± 6.8
	10 000 Year Return	62.0 ± 8.9	62.6 ± 8.9	62.9 ± 8.9	64.0 ± 8.9	64.5 ± 8.9
	100 000 Year Return	71.4 ± 11.0	72.1 ± 11.0	72.4 ± 11.0	73.6 ± 11.0	74.2 ± 11.0
	1 000 000 Year Return	80.8 ± 13.1	81.5 ± 13.1	81.9 ± 13.1	83.3 ± 13.1	84.0 ± 13.1

Meteorological Parameter		Baseline	Climate Change Projections (Including 95% Confidence Intervals)			
			2044	2064	2110	2130
	10 000 000 Year Return	90.1 ± 15.2	90.9 ± 15.2	91.4 ± 15.2	92.9 ± 15.2	93.7 ± 15.2
	100 000 000 Year Return	99.5 ± 17.3	100.4 ± 17.3	100.9 ± 17.3	102.6 ± 17.3	103.4 ± 17.3
Ambient temperature [°C]	Mean daily maximum dry bulb temperature	20.1	21.1 -0.4+0.5	21.8 -0.4+0.5	23.7 -0.4+0.5	24.7 -0.4+0.5
	- coincident wet bulb temperature (a)	16.0	18.0 -0.3+0.1	18.3 -0.4+0.2	19.1 -0.5+0.2	19.4 -0.7+0.2
	Mean daily maximum wet bulb temperature (a)	16.2	18.2 -0.2+0.2	18.5 -0.2+0.4	19.3 -0.2+0.6	19.7 -0.3+0.6
	Extreme Observed & Projected dry-bulb maximum	38.8	39.8 -0.5+0.4	40.5 -0.5+0.4	42.4 -0.5+0.4	43.5 -0.5+0.4
	10 Year Return	37.5 ± 0.9	40.3 ± 1.8	41.1 ± 1.8	43.4 ± 2.0	44.5 ± 2.0
	100 Year Return	40.4 ± 2.0	42.6 ± 2.7	43.4 ± 2.8	45.6 ± 2.9	46.8 ± 3.0
	1 000 Year Return	43.3 ± 3.2	44.9 ± 3.7	45.7 ± 3.8	47.9 ± 3.9	49.1 ± 4.0
	10 000 Year Return	46.2 ± 4.3	47.1 ± 4.7	48.0 ± 4.8	50.2 ± 4.9	51.3 ± 4.9
	100 000 Year Return	49.1 ± 5.5	49.4 ± 5.7	50.2 ± 5.8	52.4 ± 5.9	53.6 ± 5.9
	1 000 000 Year Return	52.0 ± 6.7	51.7 ± 6.7	52.5 ± 6.8	54.7 ± 6.9	55.9 ± 6.9
	10 000 000 Year Return	54.9 ± 7.9	53.9 ± 7.7	54.7 ± 7.7	57.0 ± 7.9	58.1 ± 7.9
	100 000 000 Year Return	57.8 ± 9.0	56.2 ± 8.7	57.0 ± 8.7	59.2 ± 8.9	60.4 ± 8.9
	Maximum temperature of 3-hour duration (b)	37.0 Corresponding Wet Bulb Temperature 19.0	37.9 -0.5+0.3	38.6 -0.5+0.4	40.5 -0.6+0.5	41.4 -0.8+0.5
	Maximum temperature of 6-hour duration (b)	36.1	37.0 -0.5+0.3	37.7 -0.5+0.4	39.6 -0.6+0.5	40.5 -0.8+0.5

Meteorological Parameter		Baseline	Climate Change Projections (Including 95% Confidence Intervals)			
			2044	2064	2110	2130
		Corresponding Wet Bulb Temperature 18.9				
	Maximum temperature of 7-day duration (b)	18.5 Corresponding Wet Bulb Temperature 15.5	19.4 -0.5+0.3	20.1 -0.5+0.4	22.0 -0.6+0.5	22.9 -0.8+0.5
	Mean daily minimum dry bulb temperatures	13.1	13.8 -0.3+0.3	14.2 -0.3+0.3	15.4 -0.3+0.3	16.1 -0.2+0.3
	- coincident wet bulb temperature (a)	11.5	12.9 -0.2+0.1	13.1 -0.2+0.1	13.7 -0.4+0.2	14.0 -0.5+0.2
	Mean daily minimum wet bulb temperature (a)	11.0	12.4 -0.1+0.2	12.6 -0.1+0.2	13.1 -0.2+0.4	13.4 -0.2+0.5
	Extreme Observed & Projected dry-bulb minimum	3.0	3.9 -0.5+0.4	4.6 -0.5+0.4	6.5 -0.7+0.6	7.5 -0.8+0.7
	10 Year Return	3.5 ± 0.5	3.4 ± 0.8	4.1 ± 0.8	5.8 ± 0.9	6.7 ± 0.9
	100 Year Return	1.6 ± 1.0	2.0 ± 1.2	2.7 ± 1.2	4.4 ± 1.3	5.3 ± 1.3
	1 000 Year Return	-0.2 ± 1.5	0.7 ± 1.6	1.3 ± 1.7	3.0 ± 1.7	3.9 ± 1.7
	10 000 Year Return	-2.1 ± 2.0	-0.7 ± 2.1	-0.1 ± 2.1	1.6 ± 2.1	2.5 ± 2.2
	100 000 Year Return	-3.9 ± 2.5	-2.1 ± 2.5	-1.5 ± 2.5	0.2 ± 2.6	1.1 ± 2.6
	1 000 000 Year Return	-5.8 ± 3.0	-3.5 ± 2.9	-2.9 ± 3.0	-1.2 ± 3.0	-0.2 ± 3.0
	10 000 000 Year Return	-7.6 ± 3.5	-4.9 ± 3.4	-4.3 ± 3.4	-2.6 ± 3.5	-1.6 ± 3.5
	100 000 000 Year Return	-9.5 ± 4.0	-6.3 ± 3.8	-5.7 ± 3.8	-4.0 ± 3.9	-3.0 ± 3.9
	Minimum temperature of 3-hour duration (b)	4.5	5.4 -0.5+0.3	6.1 -0.5+0.4	8.0 -0.6+0.5	8.9 -0.8+0.5

Meteorological Parameter		Baseline	Climate Change Projections (Including 95% Confidence Intervals)			
			2044	2064	2110	2130
		Corresponding Wet Bulb Temperature 3.6				
	Minimum temperature of 6-hour duration (b)	4.8 Corresponding Wet Bulb Temperature 4.0	5.7 -0.5+0.3	6.4 -0.5+0.4	8.3 -0.6+0.5	9.2 -0.8+0.5
	Minimum temperature of 7-day duration (b)	14.0 Corresponding Wet Bulb Temperature 12.1	14.9 -0.5+0.3	15.6 -0.5+0.4	17.5 -0.6+0.5	18.4 -0.8+0.5
Rainfall [mm]	Average Annual Total	372.4	318.3 -8.8+8.4	300.3 -1.7+12.5	254.7 -1.9+5.5	229.6 -1.1+0.6
	Extreme Annual Total	640.4	Projections indicate reduction. Worst-case assumption assumes same as baseline			
	Annual Re-occurrences:					
	10 Year Return	471.1 ± 45.3	Projections indicate reduction. Worst-case assumption assumes same as baseline			
	100 Year Return	611.9 ± 85.7				
	1 000 Year Return	750.1 ± 127.0				
	10 000 Year Return	888.1 ± 168.7				
	100 000 Year Return	1026.1 ± 210.5				
	1 000 000 Year Return	1164.1 ± 252.4				
	10 000 000 Year Return	1302.1 ± 294.4				
	100 000 000 Year Return	1440.1 ± 336.4				
	Extreme 24-hour Storm	70	Projections indicate reduction. Worst-case assumption assumes same as baseline			
	24-Hour Re-occurrences:					

Meteorological Parameter		**Baseline**	**Climate Change Projections (Including 95% Confidence Intervals)**			
			2044	**2064**	**2110**	**2130**
	10 Year Return	49.0 ± 7.3	Projections indicate reduction. Worst-case assumption assumes same as baseline			
	100 Year Return	69.0 ± 12.8				
	1 000 Year Return	88.6 ± 18.3				
	10 000 Year Return	108.1 ± 23.7				
	100 000 Year Return	127.7 ± 29.2				
	1 000 000 Year Return	147.2 ± 34.7				
	10 000 000 Year Return	166.7 ± 40.2				
	100 000 000 Year Return	186.3 ± 45.7				
	Extreme 1-hour Storm	23.6	Insufficient data to make projection. Assume same as baseline			
Mean Sea Level Atmospheric pressure [hPa]	Daily Minimum	910.6 (September)	Not available	Not available	Not available	Not available
	Daily Maximum	1040.0 (July)	Not available	Not available	Not available	Not available
	Extreme Lower (Hourly)	932.5	932.3 -0.3+0.2	932.1 -0.4+0.3	931.7 -0.3+0.4	930.7 -0.4+0.3
	Mean Annual	1016.2	1015.9 -0.3+0.3	1015.7 -0.3+0.4	1015.3 -0.4+0.3	1015.0 -0.4+0.4
	Extreme Upper (Hourly)	1046.9	1046.9 -0.0+0.1	1046.9 -0.0+0.0	1046.9 -0.0+0.0	1046.9 -0.0+0.0

Notes:

(a) Wet-bulb temperature projections are not part of the primary meteorological variables provided by the climate change mode used in the analyses. The projections provided in the table are based on using the daily minimum, mean and maximum temperature projected increases and assuming ±25% variation in the corresponding moisture content.

(b) Temperatures of 3-hour, 6- hour and 7-day durations assumed projected temperature increases as per the climate change model.

Table 5.8.B
Site Specific Parameters Part 2

Meteorological Parameter			Value			
Tornadoes	Tornado Probability (EF - Enhanced Fujita Scale)	Based on 116-year database 1905 -2020	All(2)	1.0 x 10^{-5} per year per km²		
			EF0	7.0 x 10^{-6} per year per km²		
			EF1	2.4 x 10^{-6} per year per km²		
			EF2	5.6 x 10^{-7} per year per km²		
			EF3	1.0 x 10^{-8} per year per km²		
			EF4	<1.0 x 10^{-8} per year per km²		
		Based on 34-year database 1987 - 2020 (1)	All(2)	2.2 x 10^{-5} per year per km²		
			EF0	1.7 x 10^{-5} per year per km²		
			EF1	5.2 x 10^{-6} per year per km²		
			EF2	1.2 x 10^{-6} per year per km²		
			EF3	2.2 x 10^{-8} per year per km²		
			EF4	<2.2 x 10^{-8} per year per km²		
	10^{-7} per year wind speed: - maximum wind speed - maximum translational - maximum rotational		 75.0 m/s 15.0 m/s 60.0 m/s			
			Lower Quartile	Upper Quartile	Median	Average
	Path Width [m]:					
	EF0 tornado (70% to 74% probability)		22.9	68.6	45.7	54.9
	EF1 tornado (23% to 24% probability)		68.6	182.9	91.4	163.8
	EF2 tornado (5% to 6% probability)		137.2	402.3	228.6	344.1
	EF3 tornado (<0.01% probability)		339.5	1005.8	548.6	736.3
	Path Length [km]					
	EF0 tornado (70% to 74% probability)		0.29	2.7	0.8	2.27
	EF1 tornado (23% to 24% probability)		1.77	9.33	4.4	7.1
	EF2 tornado (5% to 6% probability)		4.53	19.25	10	14.3
	EF3 tornado (<0.01% probability)		12.38	36.34	23	29.1
	Pressure drop for 10^{-7} per year wind speed		40 hPa			
	Maximum rate of pressure drop for 10^{-7} per year wind speed		13 hPa/s			
Atmospheric Turbulence (Delta-T Method)	Convective (A)		1.55%			
	Unstable (B)		2.02%			

Meteorological Parameter		Value	
(120-m Tower)	Moderately Unstable (C)	3.28%	
	Neutral (D)	33.86%	
	Moderately Stable (E)	37.44%	
	Stable (F)	16.54%	
	Very Stable (G)	5.30%	
Prolonged Inversions	Likelihood	Annual	22%
		Summer	14%
		Winter	30%
Snowfall (3)	Average	0.0 mm/h	
	Maximum load	0.0 N/m^3	
Lightning	Flashes/year/km^2	0.3 flashes/year/km^2 (range 0.2 to 1.6)	
	Average strokes per flash	13.75	
	Maximum strokes per flash	25	
	Average peak current	25 kA	
	Highest peak current	166 kA	
Thunder	No. days with thunder	7.0 days/year	
Hail	No. days with hail	1.0 days/year	
Frost	No. days with frost	0 days/year	
Fog	No. days with fog	60 days/year	
Relative humidity	Summer (relative humidity at 37 ºC, dry bulb)	14.6%	
	Winter (relative humidity at -25 ºC, dry bulb)	91.1% at lowest temperatures Assume 100% at -25ºC	
Solar Radiation	Lowest daily total	8.3 MJ/m^2.day (June)	
	Highest daily total	30.9 MJ/m^2.day (December)	
Penman Evapotranspiration	Monthly Total Minimum	76.3 mm (June)	
	Monthly Total Maximum	237.0 mm (December)	
Corrosivity	Rate in 1st year	Carbon steel	85.8 μm/year
		Zinc	3.4 μm/year
		Copper	1.9 μm/year
		Aluminium	1.2 μm/year
	Average rate over 20 years	Carbon steel	20.0 μm/year
		Zinc	1.9 μm/year
		Copper	0.7 μm/year

Meteorological Parameter		Value	
		Aluminium	0.5 µm/year

Notes:

(1) Tornado activity has increased since 1987 within an 80 km radius from the site. Whilst climate change may have contributed to increases in tornado frequencies, it may also simply be that the reporting of tornadoes has increased due to population spread as well as the associated damage to property.

(1) The “All” tornado entry combines all frequencies from EF0 to EF4 in the table.

(2) This reflects current observation; however extreme minimum temperatures (excluding climate change projections indicate temperatures well below freeze point for water and may result in the occurrence of snow at the site

CONTENTS

TABLES

FIGURES

APPENDICES

5.8 METEOROLOGY

The meteorological and climatological characteristics for the site have been investigated in support of the identification of external events[1] and potential hazards to the nuclear installation(s) on the site. This chapter of this Site Safety Report (SSR) presents the approach to evaluation of these site characteristics, with specific attention to the extreme values of meteorological variables such as air temperature and wind speed and rare meteorological phenomena that occur infrequently (International Atomic Energy Agency, 2019).

5.8.1 Introduction

The approach to be followed during the evaluation of the Duynefontyn site (the site) for locating nuclear installation(s) has been provided in ***Chapter 4*** (Site Investigation Approach) for the various scenarios of KNPS and possible new nuclear installation(s) as described in ***Chapter 3*** (Overview of Planned Activities at the Site) and in the meteorology section of the SSR Technical Specification (Eskom, 2021). The most important requirement for completing the meteorology section is the provision of sufficient data to perform the analyses required for this section, which include historical data and reports, and on-site meteorological parameter measurements. The information must serve to confirm that the site is suitable for its intended use and to provide the site characteristics in a manner that is fit for use in the Safety Analysis Report (SAR) that will demonstrate the adequacy of the design of the nuclear installation(s) to protect public health, safety, plant security and provide environmental protection.

The key meteorological aspects have been identified as follows:

- wind field parameters, including average and extreme wind speeds, average and extreme wind gusts, wind directions and turbulence (derived from the standard deviation of wind direction) - These parameters are necessary to calculate the atmospheric dispersion of air emissions from the nuclear installation(s), under normal operating conditions and upset or accidental releases. Wind speed data are also required to estimate extreme oceanographic events, such as extreme storm surges. The extremes of wind speeds, including tornadoes and cyclones, are also required to establish the adequacy of the nuclear installation design.
- air temperature, including dry- and wet-bulb temperatures - The nuclear installation design should accommodate the effects of

---

[1] Events originating outside the nuclear installation(s) with the potential to cause adverse conditions or even damage to safety important structures, systems or components (Eskom, 2022).

temperature extremes, including both very high and low temperatures.

- rainfall, including the amount, type and durations are important to design surface water holding and drainage systems;
- snow - This is an important parameter in regions where snow may represent a significant load factor in the design of plant structures.
- lightning - Lightning transients exhibit extremely high voltages, currents and current rise rates and knowledge on lightning expected at the site is required for the design of insulators to minimise damage.
- blizzards, dust and sandstorms, drought, icing and hail – These rare meteorological phenomena are included owing to their possible impact on plant safety.
- solar radiation - The measurement of the solar radiation is required to determine the development of the day-time atmospheric structure and evapotranspiration rates.
- barometric pressure - Required to estimate extreme oceanographic events.
- corrosivity potential - Required to enable the selection of appropriate construction and fabrication material. It is also required to assist with the selection of protective coating systems, if implemented.

Eskom has been collecting meteorological data at the Koeberg Weather Station since 1980, with the erection of two towers of 50 m and 120 m in height. The focus of the measurement on the towers (wind speed and air temperatures) has been to fulfil the requirements of the emergency preparedness of the existing nuclear power station. However, since it was identified that solar radiation, relative humidity and dry-bulb temperature at 2 m above ground level were also required for the SSR, these instruments were later (1 January 2009) added to the Koeberg Weather Station. These instruments were operating on a temporary basis and were decommissioned on 30 September 2013 (first monitoring campaign). In addition to the weather station at Koeberg, Eskom has been collecting meteorological data at six other locations in the vicinity of the site since 1985. All of these data have been made available for analyses for the completion of the SSR.

A second monitoring campaign recommenced on 29 September 2017 with the establishment of a new weather station (Duynefontyn WS) on the site (approximately 490 m west of the Koeberg Weather Station) and continued until 31 March 2019. Data gathering interruption occurred following the Stop Work Order of 6 February 2019 (Eskom, 2019a), which took effect from 1 April 2019, and during which only occasional data checks were done on the information collected in the logger. The Resume Work Order was received on 9 July 2019, and with effect from 10 July 2019, regular data checks and collections were again performed until 30 April 2022.

Whilst the 120-m tower meteorological data provide for a relatively long-term database, data accumulated over longer periods improve the accuracy of estimating extreme weather conditions. Additional information was therefore also obtained from the SAWS reports, and monitoring data from SAWS.

5.8.2 Purpose and Scope

The purpose of the meteorological investigation of the site is to:

- provide baseline information for site evaluation and this SSR that will be updated over the life cycle of the nuclear installation(s);
- confirm the suitability of the site through the identification of external events and potential hazards for the nuclear installation(s);
- develop the atmospheric structure (including wind and turbulent fields) to enable atmospheric dispersion predictions necessary for the assessment of potential radiological impact to the public and the environment in ***Chapter 7*** (Potential Radiological Impact on the Public and the Environment, PRIPE) and the evaluation of the feasibility of the emergency planning in ***Chapter 8*** (Emergency Planning);
- define the local air quality with specific reference to corrosion potential.

The results of the meteorological analysis also provide input into the:

- selection of appropriate dispersion models for the site and the assessment of the atmospheric dispersion of radionuclides to the environment;
- demonstration of compliance with the National Nuclear Regulator's (NNR's) licensing requirements for operating a nuclear installation in terms of radiological protection to ensure public health and safety;
- establishment of limits for nuclear installation design performance.

These additional functions, however, require additional data and detail that depends on the nuclear installation design.

5.8.3 Regulatory Framework

The overall legal and regulatory basis for this SSR is outlined in ***Chapter 2*** (Legal and Regulatory Basis) of this SSR. The main national regulations specifically relevant to a meteorological investigation for site evaluation are the Regulations on Siting of New Nuclear Installations (Department of Energy, 2011). These require the SSR to present the characteristics of the proposed site, which include *inter alia*:

- [Regulation 4(5)] Natural phenomena and potential man-made hazards must be appropriately accounted for in the design of the new nuclear installation(s), and that adequate emergency plans and nuclear security measures can be developed.
- [Regulation 5(3)] The characteristics of the site relevant to the design assessment, risk and dose calculations, including inter alia:
  - [Regulation 5(3)(a)] external events (and in this case of natural origin); and
  - [Regulation 5(3)(b)] meteorological data.

5.8.4 Requirement Documents and Guides

The Regulation is complemented by the following NNR documents:

- Interim Guidance for the Siting of Nuclear Facilities, Regulatory Guide RG-0011, Rev 0 – Sections 7.2.2 and 8.3 (National Nuclear Regulator, 2016a)
- Consideration of External Events for New Nuclear Installations, Position Paper PP-0014, Rev 0 – Sections 11.3, 11.4, 11.5 and 11.9 (National Nuclear Regulator, 2012a);
- Emergency Planning Technical Basis For New Nuclear Installations, Position Paper PP-0015, Rev 0 – Sections 7.3.2.3 and 7.3.4 (National Nuclear Regulator, 2012b);
- Guidance on the Verification and Validation of Evaluation and Calculation Models used in Safety and Design Analyses, Regulatory Guide RG-0016, Rev 0 (National Nuclear Regulator, 2016b);
- Quality and Safety Management Requirements for Nuclear Installations. Requirement Document No. RD-0034 (National Nuclear Regulator, 2008).
- Emergency Prepared and Response Requirements. Requirement Document No. RD-014 (National Nuclear Regulator, 2005)

- Demonstration of compliance with the NNR requirements has also been performed following the available NNR guidelines and internationally accepted safety standards and supporting documents, US regulatory guidance and Eskom standards as follows:
    - International Atomic Energy Agency (IAEA) Safety Requirement No. SSR-1 on Site Evaluation for Nuclear Installations (International Atomic Energy Agency, 2019);
    - IAEA Specific Safety Guide No. SSG-18 on Meteorological and Hydrological Hazards in Site Evaluation for Nuclear Installations (International Atomic Energy Agency, 2011);
    - IAEA Safety Guide No.NS-G-3.2 on Dispersion of Radioactive Material in Air and Water and Consideration of Population Distribution in Site Evaluation for Nuclear Power Plants (International Atomic Energy Agency, 2002);
    - IAEA Specific Safety Guide No. SSG-68 on Design of Nuclear Installations Against External Events Excluding Earthquakes (International Atomic Energy Agency, 2021);
    - IAEA Safety Report Series No. 19. on Generic Models for Use in Assessing the Impact of Discharge of Radioactive Substances to the Environment (International Atomic Energy Agency, 2001);
    - United States Nuclear Regulatory Commission (US NRC) NUREG 0800 (Parts 2.3.1 to 2.3.4.) (United States Nuclear Regulatory Commission, 2007a);
    - US NRC Regulatory Guide 1.145 on Atmospheric Dispersion Models for Potential Accident Consequence Assessments at Nuclear Power Plants (United States Nuclear Regulatory Commission, 1983);
    - US NRC Regulatory Guide No. 1.76 on Design Basis Tornado and Tornado Missiles for Nuclear Power Plants (United States Nuclear Regulatory Commission , 2007b);
    - US NRC Regulatory Guide No. 1.23 on Meteorological Monitoring Programs for Nuclear Power Plants (United States Nuclear Regulatory Commission, 2007c);
    - American Nuclear Society – Determining Meteorological Information at Nuclear Facilities, American Nuclear Society, ANSI/ANS-3.11-2015 (American National Standard, 2015);
    - EPA-454/R-99-005 on Meteorological Monitoring Guidance for Regulatory Modelling Applications (United States Environmental Protection Agency, 2000);

- ISO 9223 on Corrosion of Metals and Alloys-Corrosivity of Atmospheres – Classification (International Organisation for Standardisation, 2012a);
- Eskom Standard 238-52 – Meteorological Requirements for Nuclear Installations (Eskom, 2017)[2].

Regulatory Guide 1.23 Rev 1 (United States Nuclear Regulatory Commission, 2007c) was used as reference for the specification of meteorological instruments and operation of the weather station since the start of the monitoring programme at the site. This guide reflects the regulatory requirements and best practices, using guidance provided in ANSI/ANS-3.11-2005 *"Determining Meteorological Information at Nuclear Facilities*. Although the latter standard has subsequently been revised to ANSI/ANS-311-2015 (ANS 2015), the meteorological monitoring specification in the current campaign still conforms to the listed criteria.

5.8.5 Evaluation Approach

This Subsection provides the background to the meteorological information on which the analyses are based. This includes information on both on- and off-site meteorological data.

5.8.5.1 Meteorological Data Analysis

The following steps have been identified (Eskom, 2022) to evaluate the meteorological characteristics of the site:

- identification of key meteorological parameters required to characterise events that are likely to occur within the site (both rare and extreme);
- desk study evaluation of existing meteorological information including key historical data, analyses, reports and related information;
- analysis of monitored onsite meteorological data;
- identification, quantification and management of uncertainties;
- identification of any further work required prior to or during construction and operation of the nuclear installation(s).

The analytical procedures provided in the IAEA Specific Safety Guide No. SSG-18 (International Atomic Energy Agency, 2011) were used as a basis

---

[2] This section of this SSR identifies the criteria for establishing and implementing an onsite meteorological measurements programme that aims to demonstrate compliance with the National Nuclear Regulator (NNR) requirements for collection of basic meteorological data. At the time of writing, no specific NNR requirements for the collection of basic meteorological data have been provided. In the interim, the Eskom Standard 238-52 – Radiation Protection: Meteorological Requirements (***Eskom, 2017***) will be followed.

for conducting the meteorological analyses. The main tasks in the meteorological analysis included the following:

- to assess the meteorological and climatological characteristics for the region around the site;
- to describe the basic meteorological parameters, regional orography and phenomena including wind speed and direction, air temperature, precipitation, humidity, solar radiation, atmospheric stability parameters, prolonged inversions and dispersion potential;
- to determine extreme values of meteorological variables (e.g. wind speed, precipitation, snow and temperature);
- to determine the potential frequency and severity of lightning;
- to determine the potential occurrence of tornadoes in the region;
- to determine the potential for tropical cyclones, hurricanes and hurricane force winds;
- to establish a monitoring programme for meteorological measurements (including a review of existing meteorological measurements at the existing Koeberg Weather Station, which has been operating since 1980, to inform the emergency response system with the meteorological parameters required for emergency planning and execution);
- to determine uncertainties in the measurements and to take them into account in the evaluation.

The monitoring requirements (and any potentially additional requirements) will continue throughout the nuclear installation operation and up until decommissioning (International Atomic Energy Agency, 2002) and (Eskom, 2017)).

5.8.5.2 Meteorological Measurement

The site was investigated with regard to the meteorological characteristics that could be significant to safety in respect of external naturally induced events. The following are addressed in the subsections:

- the available data prior to site investigations;
- the meteorological measurements performed (and on-going) for the purpose of this SSR;
- the meteorological stations;
- data resources;

- the evaluation techniques used;
- the methods for analysis of data.

5.8.5.2.1 Availability of Data

The meteorological monitoring site (Koeberg Weather Station), established in 1979, is located about 1 km from the coast on a 24-m sand ridge aligned south-southeast to north-northwest. In 1984, with the advent of Koeberg Nuclear Power Station operation, the monitoring system was upgraded to include instruments to measure wind speed and temperature at different elevations on meteorological towers of 50 m and 120 m at the Koeberg weather station. The 120-m tower was later (1988) replaced after it blew over, with the current 120-m tower.

The 50 m tower is a back-up of the main 120-m tower (Eskom, 1997; Eskom, 2023a). The 120-m tower is located at 33° 40’ 58.16”S; 18° 26’ 27.20”E. The base of the Koeberg Weather Station is at 24 m amsl. Wind speed and dry-bulb temperature measurements are made at 10 m, 50 m, 85 m and 120 m, above ground level. Instrumentation to measure the wind vector at 50 m and 120 m consists of anemometers placed in each of the north-south (i.e. ‘v’ wind vector), east-west (i.e. ‘u’ wind vector) and vertical (i.e. ‘w’ wind vector) planes. At the 10 m and 85 m levels, no vertical (i.e. ‘w’ wind vector) wind speed measurements are recorded. The standard deviation of horizontal and vertical direction, i.e. ‘sigma theta’ and ‘sigma phi’, are also determined from these measurements. Dry-bulb temperatures are recorded at each of the four 120-m tower levels. Atmospheric pressure and rainfall have been measured near ground level.

Instruments for the measurement of solar radiation, relative humidity and dry-bulb temperature at 2 m above ground level were added to the Koeberg Weather Station in January 2009 and continued until 30 September 2013, when these instruments were decommissioned following stoppage of the new build programme. A new meteorological station (Duynefontyn WS) was subsequently established approximately 490 m west of the 120-m tower. Parameters measured at this weather station include wind speed and direction, dry-bulb temperature at 2 m and 8 m above ground level, solar radiation, relative humidity, atmospheric pressure, rainfall, visibility and lightning events.

Five additional weather stations (remote Eskom Weather Stations) were installed by Eskom in 1985 at Bok Point, Atlantis, Rondekuil, Milnerton and Robben Island (Eskom, 2023b), as shown in ***Figure 5.8.1*** and summarised in ***Table 5.8.1***. The measured meteorological parameters at these stations include wind speed at 10 m and dry bulb temperature.

5.8.5.3 Onsite Meteorological Instrumentation

Whilst wind speed and direction, and dry bulb temperatures are measured at different levels on the 120-m tower, relative humidity, solar radiation, atmospheric pressure and rainfall values are measured near ground level. For the period from 1 January 2009 to 30 September 2013, these measurements were made at the same location as the 120-m tower. On 29 September 2017 the Duynefontyn WS was commissioned at a different location (33° 40’ 57.01”S; 18° 26’ 8.08”E) and at an altitude of 10 m amsl. Data gathering interruption occurred following an Eskom Stop Work Order of 6 February 2019 (Eskom, 2019a), which took effect from 1 April 2019, and during which only occasional data checks were done on the information collected in the logger. The Resume Work Order was received on 9 July 2019, and with effect from 10 July 2019, regular data checks and collections were again performed up until 30 April 2022.

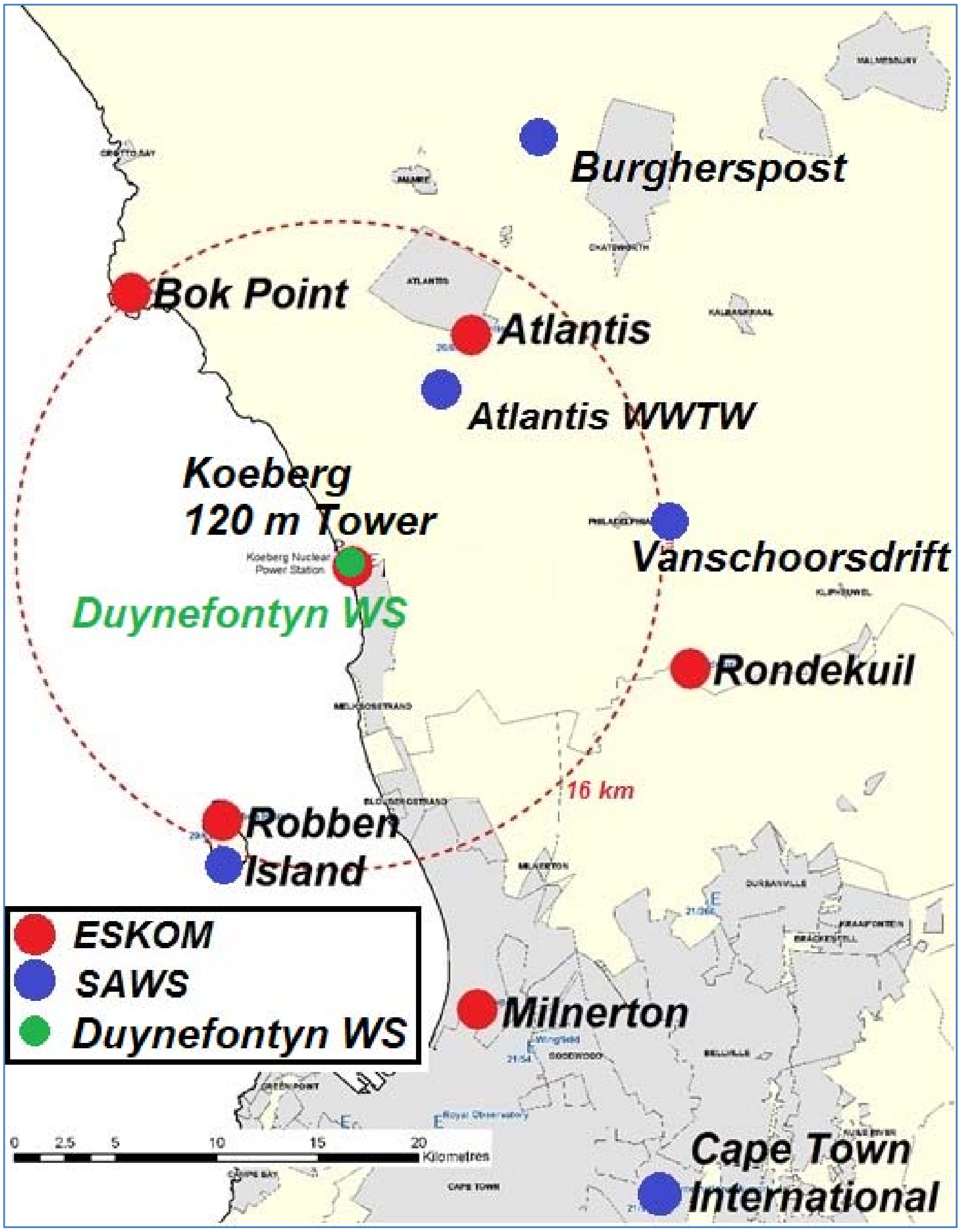

Figure 5.8.1
Location of Weather Monitoring Stations

Table 5.8.1
Meteorological Stations and Measurements

Station	Distance from Site	Meteorological Parameters Measured	Availability
Duynefontyn	1.8 km	Precipitation, Air temperature, Ambient pressure, Wind Speed/Direction, Relative Humidity, Solar radiation, visibility, lightning events	29 September 2017 to 30 April 2022
Koeberg(1) [Eskom]	2 km South-southeast	Precipitation, Air temperature, Ambient pressure, Wind Speed/Direction(2), Air Temperature at 2 m(4), Relative Humidity, Solar radiation	1979 to 2023(3)(4)
Bok Point [Eskom]	16.5 km	Air temperature, Wind Speed/Direction	1985 to 2019(5)
Atlantis [Eskom]	11.5 km northeast	Air temperature, Wind Speed/Direction	1985 to 2023(4)
Rondekuil [Eskom]	16.5 km	Air temperature, Wind Speed/Direction	1985 to 2023(4)
Milnerton [Eskom]	22.5 km south	Air temperature, Wind Speed/Direction	1985 to 2022(6)
Robben Island [Eskom]	14.5 km southwest	Air temperature, Wind Speed/Direction	1985 to 2023(4)
Cape Town International Airport (0021178A3 & 0021178B8) [SAWS]	35.0 km south	Precipitation, Air temperature, Ambient pressure, Wind Speed/Direction, Relative Humidity	1960 to 2022
Robben Island (0020649 03) [SAWS]	17.7 km southwest	Precipitation	1850 to 2019
Atlantis Wastewater Treatment Works (0020846 4) [SAWS]	9.0 km northeast	Precipitation	1979 to 2019
Vanschoorsdrift (0021130) [SAWS]	16.2 km east	Precipitation	1860 to 2011(7)
Burgherspost (0041060) [SAWS]	21.0 km north-northeast	Precipitation	1858 to 2011(8)

Notes:

(1) Wind speed and dry-bulb temperature are monitored at four levels (10m, 50m, 85m and 120m) above ground on the 120-m tower. For the period 1 January 2009 to 30 September 2013, relative humidity, solar radiation, dry-bulb temperature, and precipitation were also monitored at 2 m above ground level. The temperature measurement at 10 m on the 120-m tower also accounts for the temperature measurement at 8 m on the Duynefontyn WS.

(2) The wind speed and direction are monitored with ‘u, v, w’ anemometers at 50 m and 120 m levels. The ‘u, v, w’ anemometers measure the wind speed in three directions, namely east-west wind component with the ‘u’ anemometer, north-south wind component with the ‘v’ anemometer and vertical wind component with the ‘w’ anemometer. Measurements at 10 m and 85 m levels are with ‘u, v’ anemometers, i.e., only horizontal wind vector is monitored.

(3) Electronic data only available from 1 October 1997. Prior to this date, all data were provided as hardcopy tables.

(4) Monitoring data for 2023 included months from January to September.
(5) Monitoring data for 2019 included months from January to June, thereafter no data available for this weather station.
(6) Monitoring data for 2019 included January to June, and only October during 2020. Observations again from 26 January 2021 to 26 June 2022. Thereafter no data available for this weather station.
(7) Temperature at 2 m above ground level, solar radiation and relative humidity recorded only for the period from 1 January 2009 to 30 September 2013
(8) Monitoring stations decommissioned.

Regarding the establishment of historical trends, it is considered acceptable to collect meteorological information from nearby weather stations (International Atomic Energy Agency, 2019)). The closest SAWS monitoring station with long-term observations of a comprehensive set of meteorological parameters is located at Cape Town International Airport (CTIA) (***Figure 5.8.1***). Since this station falls within the same prevailing atmospheric air mass flow as the site (Preston-Whyte & Tyson, 1988), the meteorological observations are included for comparative purposes. The parameters measured at this station include the wind vector (speed and direction), ambient temperature, relative humidity, atmospheric pressure and rainfall. Wind speed and direction measurements are made at approximately 10 m above ground level.

Two different data capturing systems are used on the site, namely:

- computer-based direct link from the 120-m tower instrumentation;
- an automatic data logger to record the meteorological parameters measured at the Duynefontyn WS which are not part of the emergency preparedness programme.

The 3-second, 120-m tower data are stored on a database, whilst 10-minute averages from the Duynefontyn WS are stored on the automatic data logger in electronic format (Eskom, 2022; International Atomic Energy Agency, 2002; International Atomic Energy Agency, 2011). The following information is recorded:

- 120-m tower:
  - location, date and time;
  - horizontal wind direction (degrees) and wind speed (m/s) (including wind gusts) at 10 m, 50 m, 85 m and 120 m;
  - standard deviation of wind direction (degrees) in horizontal and vertical planes, known as “sigma theta” (σ_θ) and “sigma phi” ($\sigma\varphi$), respectively at 50 m and 120 m;
  - vertical wind speed (m/s) (including wind gusts) at 50 m, and 120 m;
  - standard deviation of vertical wind speed (m/s), known as “sigma w” (σ_w) at 50 m, and 120 m;

- ambient air temperature[3] (°C) at 10 m, 50 m, 85 m and 120 m;
- ambient temperature gradients (lapse rates) between levels 10 m-50 m and 10 m–120 m (°C);
- barometric pressure (hPa);
- precipitation (mm);

- Additional instruments at Koeberg Weather Station (1 January 2009 – 30 September 2013):
  - location, date and time;
  - atmospheric moisture (per cent);
- solar radiation (kW/m²);
- Duynefontyn WS (29 September 2017 – 31 April 2022):
  - location, date and time;
  - horizontal wind direction (degrees) and wind speed (m/s) (including wind gusts) at 10m;
  - standard deviation of wind direction (degrees) in horizontal plane (“sigma theta”) at 10m;
  - ambient air temperature (°C) at 2 m and 8 m;
  - ambient temperature gradients (lapse rates) between levels 2 m and 8 m (°C);
  - atmospheric moisture (per cent);
  - precipitation (mm);
  - solar radiation (kW/m²);
  - barometric pressure (hPa);
  - visibility (km);
  - lightning events (counts).

Corrosivity of the local atmosphere was measured on site using the coupon-based method (CLIMAT) and the ISO Standard 9223 methodology (International Organisation for Standardisation, 2012a; International Organisation for Standardisation, 2012b; Burger, 2022). The CLIMAT method involves the exposure of metallic coupons to the environment and subsequently classifying the resultant corrosion. The ISO Standard 9223 methodology utilises the measured temperature and relative humidity from the local weather station together with the deposition rate of sulfur dioxide and airborne salinity to determine the corrosivity rate.

---

[3] A measure of the hotness or coldness of the ambient air, as measured by a suitable instrument (American National Standard, 2015).

5.8.5.4 Instrument Accuracy

As part of the management of uncertainties (see ***Subsection 5.8.9***) all instrumentation is within the accuracy specifications contained in the SSR Technical Specification (Eskom, 2022). The required instrument accuracies, ranges and measurement resolutions of the instrumentation included on the Duynefontyn WS are summarised in ***Table 5.8.2*** (Eskom, 2022; American National Standard, 2015). These accuracies equal or better the requirements of the US NRC (United States Nuclear Regulatory Commission, 2007c). The technical specifications of the meteorological instrumentation for the Duynefontyn WS are given in ***Appendix 5.8.D***.

The meteorological instrumentation is checked on a monthly basis as part of the maintenance programme described in ***Subsection 5.8.8***. More specific maintenance such as sensor calibration, sensor performance testing and sensor component replacement are done on a bi-annual basis (United States Nuclear Regulatory Commission, 2007c).

Validation of the data includes the following steps:

- identify period during which instrument calibration activity occurred and remove data during this period since it would include data generated by the calibration process (when applicable);
- check that all data are within valid ranges. Two range checks are:
  - instrument ranges;
  - ranges based on actual extreme observations;
- check that the readings from the instruments are not fixed on a value for extended periods and that no sudden jumps occurred.

If any of these conditions are not met, the data are automatically flagged. Flagged data are subsequently checked by the data analyst and replaced by a missing parameter identifier (“-9999”) if they are suspected to be invalid. These data validation checks would identify instrument malfunction. The necessary actions to rectify any issues are initiated and executed as soon as possible, to minimise data loss.

Table 5.8.2
Instrument Accuracies and Resolutions

Measurement Parameter	**Duynefontyn WS Instrument Specification**		**ANSI/ANS-3.11-2015 (*American National Standard, 2015*)**	
	System Accuracy and Range	**Measurement Resolution**	**Required Accuracy and Range**	**Required Measurement Resolution**
Wind speed	± 0.2 m/s with starting threshold of less than 0.4 m/s Range 0 to 50 m/s	0.1 m/s	±0.2 m/s or 5% of observed wind speed starting threshold < 0.45 m/s (1)	0.1 m/s
Wind direction	± 3° of azimuth, with starting threshold of less than 0.5 m/s Range 0 to 360 m/s	1°	± 5° of azimuth, with starting threshold of less than 0.5 m/s	1°
Sigma theta	Degrees azimuth	0.1	Not applicable	0.1
True North	± 3°	1°	None stated	None stated
Ambient Air Temperature	± 0.5 °C Range -50 to +50 °C	0.1 °C	±0.5 °C	0.1 °C
Solar Radiation	±5%, linearity 1% max up to 3 000 W/m², stability <±2% per year, operating temperature of -20 to +65°C and minimum response time of 10 µS Range 400-1 100 nanometre	0.1 W/m²	5% of observed	±1 W/m²
Relative Humidity	±2 % at 20 °C:, stability: better than ±1 % per year and response time of 10 seconds (without filter) Range 0 to 100%	0.1%	±4%	0.1%
Precipitation	2% up to 25 mm/hr 3% up to 50 mm/hr	0.1 mm	±10% for a volume equivalent to 2.54 mm of precipitation at a rate < 50 mm/hr	0.25 mm
Atmospheric Pressure	±0.5 hPa (mbar) at -50 to +60°C Range 600 to 1 100 hPa (mbar)	0.1 hPa	±3 hPa	0.1 hPa
Time	±5 min	1 min	±5 min	1 min
Note				

Measurement Parameter	**Duynefontyn WS Instrument Specification**		**ANSI/ANS-3.11-2015** (***American National Standard, 2015***)	
	System Accuracy and Range	**Measurement Resolution**	**Required Accuracy and Range**	**Required Measurement Resolution**
(1) The starting threshold defines calm wind conditions. Any wind speed below the starting threshold of the wind speed or direction sensor; or any wind speed below that which is appropriate for input into plume models, whichever is greater. In the United States of America, calm is typically defined as any speed less than 1 mph, i.e. 0.45 m/s.				

The availability of the measured meteorological parameters on the 120-m tower at the site for the period 1 October 1997 to 30 September 2023 (Eskom, 2023a) is given below:

- horizontal wind speed, direction and standard deviation of wind direction:
  - 10 m : 99.92 per cent
  - 50 m : 99.92 per cent
  - 85 m : 98.19 per cent
  - 120 m : 98.09 per cent
- vertical wind speed, direction and standard deviation of wind direction:
  - 50 m : 99.86 per cent
  - 120 m : 96.838 per cent
- ambient air temperature:
  - 10 m : 99.94 per cent
  - 50 m : 99.92 per cent
  - 85 m : 98.54 per cent
  - 120 m : 98.73 per cent
- vertical temperature difference:
  - 10 m – 50 m : 99.65 per cent
  - 10 m – 120 m : 99.02 per cent
- precipitation : 99.99 per cent
- barometric pressure : 99.66 per cent

The availability of the measured meteorological parameters on the surface station at the 120-m tower site for the period 1 January 2009 to 30 September 2013 (Eskom, 2023a) is given below:

- ambient air temperature : 94.55 per cent
- relative humidity : 94.55 per cent
- solar radiation : 92.38 per cent

The availability of the measured meteorological parameters on the Duynefontyn WS for the period 29 September 2017 to 22 February 2022 (excluding Stop Work Order period from1 April 2019 to 9 July 2019) (Eskom, 2023a) is given below:

- horizontal wind speed, direction and standard deviation of wind direction at 10m : 97.17 per cent
- ambient air temperature:
  - 2 m : 97.10 per cent
  - 8 m : 94.68 per cent
- vertical temperature difference: 94.07 per cent
- barometric pressure : 93.16 per cent
- relative humidity : 94.90 per cent
- solar radiation : 100 per cent
- rainfall : 97.37 per cent
- visibility : 86.11 per cent
- lightning events : 96.14 per cent

Instrument calibrations were performed by an ISO 17025 (International Organisation of Standardisation, 2017) accredited laboratory on a biannual basis.

5.8.5.5 Macro and Micro Siting of Instrumentation

Local topographical characteristics and surface features can sufficiently influence atmospheric transport and dispersion to warrant consideration when planning or evaluating a monitoring programme. The topography in the immediate vicinity (5 km) is fairly flat with elevations reaching up to 50 m amsl. As shown in ***Figure 5.8.2***, the major topographical features are to be found more inland, beyond 10 km. Proceeding towards the northeast, the topography first rises gradually to about 200 m and then to above 500 m amsl (Dassenberg Mountain). Dassenberg Mountain is about 22 km from the site. Other mountains in this area include Bobbejaanberg (370 m amsl) at about 20 km from the site and Contreberg (460 m amsl) at 25 km from the site.

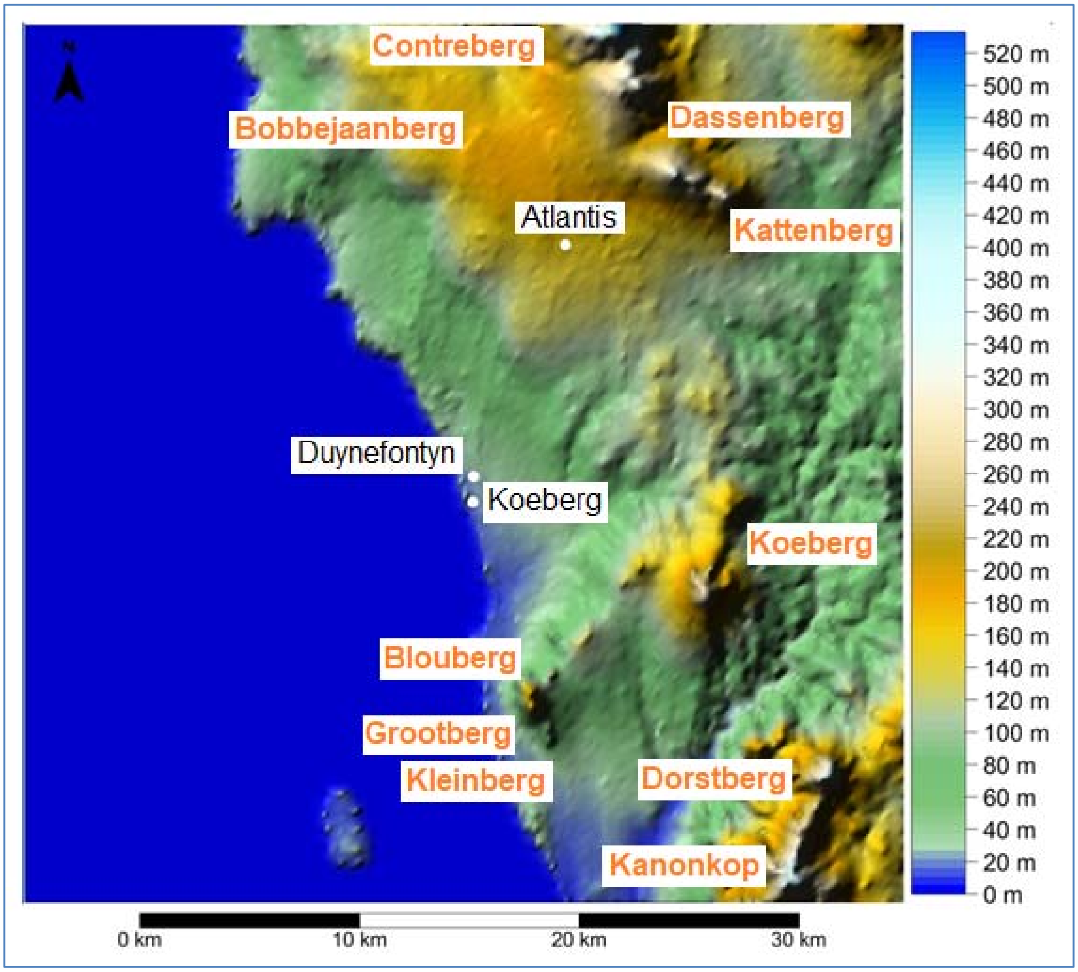

Figure 5.8.2
Topography of the 40 km by 40 km Study Area

The terrain to the east-northeast of the site is relatively flat, rising gradually to about 120-m amsl. Koeberg Mountain (363 m amsl) lies at about 11 km east-southeast. The closest mountain is Blouberg Mountain (220 m amsl) at about 8.6 km, and Grootberg (220 m amsl) about 9.5 km south-southeast from the site. The topography exceeds 400 m amsl at about 21 km when reaching Dorstberg (425 m amsl) and Kanonkop (432 m amsl), towards the east-southeast of the site.

The description above indicates that the terrain around the site is relatively flat up to approximately 10 km radius. The meteorological observations at the Koeberg Weather Station and at the Duynefontyn WS, which are approximately 2 km south-southeast of the Duynefontyn footprint, are therefore expected to provide very similar readings to the atmospheric conditions at the nuclear installation footprint.

The atmospheric structure located near the ocean can be influenced by sea and land breezes, and long-range transport of stable plumes over water. A feature of shoreline sites is the thermal internal boundary layer (TIBL) at the coastline, which deepens with increasing distance away from the water body. The ANSI/ANS -3.11-2015 standard (American National Standard, 2015) recommends that at least one measurement level shall be located within the TIBL. The Duynefontyn WS as well as the lower levels on the 120-m tower are located within the TIBL. The base of the 120-m tower is at a height of 24 m amsl and the Duynefontyn WS at 10 m amsl.

Despite the relatively low relief, it is expected that the prevailing wind speed or direction vary slightly across the region, especially towards the elevated region in the east of the study area. A comparison of the wind measurements made at the 120-m tower, the Duynefontyn WS and the more remote Eskom Weather Stations at Bok Point, Atlantis, Rondekuil, Milnerton and Robben Island, is discussed later in ***Subsection 5.8.6.1.1***.

It is important and necessary to gain a good understanding of atmospheric conditions near the nuclear installation(s) and therefore the location of the onsite weather station was selected in such a manner to be free from any nearby structures, which include natural (e.g. dunes) and man-made structures. The selection of a suitable location for the mast and all instrumentation took several factors into account to ensure the quality of the measurements.

Guided by the ANSI/ANS-3.11 (American National Standard, 2015) considerations in the siting of meteorological observation instrumentation, the following micro-siting measures were applied in the installation of the instruments to prevent local effects from unduly altering the values of the meteorological parameters to be measured:

- wind speed and direction measurements are at and above 10 m above ground level;
- the nearby buildings and other structures at the site do not influence the wind readings;
- the measurement locations are clear from any dunes, trees or other vegetation that could influence the wind readings;
- the meteorological mast is located on an elevation which would represent as closely as possible the same meteorological characteristics as the surface layer into which any airborne material will be released.

5.8.5.6 Length of Monitoring

The length of monitoring (monitoring timeframes) includes the prevailing (near-current) meteorology as well as long-term historical records. The latter information is specifically needed to improve the accuracy of predicting extreme values for wind speeds, dry bulb temperature and rainfall rates.

All meteorological data are collected on site. The 120-m tower data are collected and stored directly into a Microsoft database as raw 3-second readings. There are no raw data from the towers prior to 2006 when the new system was implemented. Electronic hourly/daily data are available from October 1997 to 2006, but only hard copies of the observations were available prior to October 1997. The data analysed prior to 1997 included annual maximum wind speeds, gusts, rainfall and maximum 24-hour rainfall events, which were included in the extreme value calculations.

Data from the temporary instruments at the Koeberg Weather Station (1 January 2009 to 30 September 2013), were logged on a Campbell CR10X logger, from where the data were then downloaded to a portable computer. The CR10X data logger was programmed to sample all meteorological parameters once every 10 seconds, and to provide the average of these over a 10-minute period, which was stored in the data logger memory. The 60-minute period coincided with the start of every hour of the day. Daily averages and maximums and radiation totals are also stored in the logger.

Similarly, data from the instruments at the Duynefontyn WS (operating from 29 September 2017) are logged on a Campbell CR1000 logger, from where the data are downloaded remotely via a modem and mobile phone connection. As a backup option, the data may also be downloaded locally via cable onto a portable computer. The data logger was programmed to sample all meteorological parameters once per second, and to provide the average of these over a 10-minute period, which was stored in the data logger memory. All parameters are provided as 10-minute averages or totals (i.e. solar radiation and rainfall) using 360 readings per sampling period. The recorded logger date and time coincided with the start of every 10-minute monitoring period.

The following statistical analyses are followed on the validated meteorological data (note “mean”, as used in this context and throughout the report is understood to be “arithmetic mean”, which is the same as “average”):

- short-term wind gusts, hourly mean values for all meteorological parameters, and averages of daily maximums and minimums for rainfall, relative humidity and ambient dry-bulb temperature These values are reported per month to illustrate the seasonal behaviour. Extreme values (minimums and maximums) are also determined per month for rainfall (highest 1- and 24-hour totals), dry bulb temperatures (hourly means) and wind speed (hourly means and gusts).

- a joint frequency distribution of hourly mean wind speed and wind direction data - The prevailing wind field is best described through a joint frequency which is normally displayed in tabular form and wind roses[4].
- atmospheric stability classification - The atmospheric stability is typically classified into one of seven categories ranging from very stable to convective conditions. The classification is determined through the rate of temperature increase (stable) or decrease (unstable) with height above ground level (International Atomic Energy Agency, 2002). Temperature difference measurements are made at 3 second intervals between 10 m and 50 m, and 10 m and 120 m, respectively. These are provided as hourly means. The fluctuations in wind direction are also used to provide a measure of atmospheric turbulence (International Atomic Energy Agency, 2002). The standard deviation of wind speed (‘sigma-theta’) is calculated using the 3 second wind direction readings at 50 m and 120 m and are provided as hourly means.
- hourly-totalled solar radiation levels - Solar radiation levels, in combination with the hourly mean wind speed, ambient air temperature and atmospheric stability allow a full description of the atmospheric structure (International Atomic Energy Agency, 2002) suitable for use in the atmospheric dispersion model. The effects of both routine air discharges and accidental air releases from the nuclear installation(s) are calculated using the dispersion on an hourly average basis, using the hourly means of wind speed, wind direction, dry bulb temperature, relative humidity and the hourly totals for solar radiation and rainfall. These dispersion calculations are then used to estimate exposures for longer periods, for example, 2-hourly, 8-hourly, 24-hourly, 3-daily, monthly and annually.

---

[4] A wind rose comprises 16 spokes which represent the directions from which winds blew during the period. The colours/shades of grey or box width reflect the different categories of wind speeds, the box closest to the inner circle, for example, represent winds of 1 m/s to 2 m/s. The dotted circles provide information regarding the frequency of occurrence of wind speed and direction categories. For the wind roses provided in this analysis, each dotted circle represents 5 per cent frequency of occurrence. The figure given in the centre of the circle describes the frequency with which calms occurred, i.e. periods during which the wind speed was below 1 m/s, i.e. calm-wind conditions.

- extreme value analyses of long-term meteorological parameter values are based on the methodologies given in (International Atomic Energy Agency, 2011).

The accuracy of estimated statistical parameters improves with longer term monitoring. The World Meteorology Organisation (WMO) states that the optimal length of record for predictive use of normals[5] varies with element, geography and secular trend (World Meteorological Organisation, 2011). The WMO further states that in general, the most recent 5- to 10-year period of record has as much predictive value as a 30-year record (World Meteorological Organisation, 2011). For elements that show a substantial underlying trend (such as mean temperature), predictive accuracy is improved by updating the averages and period averages frequently (World Meteorological Organisation, 2011). The surface meteorological data covered a period of 9 years (4 years covering the period 2009 to 2013 with the instruments for relative humidity, solar radiation and temperature at 2 m located at the Koeberg Weather Station near the 120 m tower, and 5 years covering the period 2017 to 2020 with the Duynefontyn WS). The analyses of these data are therefore considered adequate to draw statistical conclusions. Extrapolating extreme meteorological parameters from observations typically requires more than 30 years of data. Instead, therefore, the extreme temperature analyses were conducted using the observations made at the 10 m level on the 120 m tower that included a 43-year data period from 1980 to 2022 (plus 9 months data in 2023).

Corrosion monitoring was first initiated by Eskom in 1991. This monitoring campaign continued from June 1991 to January 1993 and was done at two sites. The first site was approximately 50 m from the high tide mark, just south of the Koeberg Nuclear Power Station, and the second site situated at the weather mast, approximately 700 m from the high tide mark. A second campaign was done on the site and continued from 11 April 2008 to 10 April 2009, a third campaign from 10 October 2012 to 12 September 2013 and a fourth campaign from 10 October 2017 to 18 September 2020 (Burger, 2022). As per ISO 9225 Sulfation Plate Method (International Organisation for Standardisation, 2012c), mean gas concentrations can be calculated using diffusive sampling devices. As per the ISO 9225 Standard, standardized corrosivity estimation is based on information on levels of the dominating environmental parameters: the temperature-humidity complex, and pollution with SO_2 and airborne chlorides (International Organisation for Standardisation, 2012c). According to the ISO 9225 Standard, the period of measurement is preferably one year

---

[5] Under the WMO Technical Regulations, climatological standard normals are averages of climatological data computed for the following consecutive periods of 30 years: 1 January 1901 to 31 December 1930, 1 January 1931 to 31 December 1960, and so forth (World Meteorological Organisation, 2011). The latest normal covers the period 1 January 1991 to 31 December 2010.

in order to cover seasonal variations of relative humidity, temperature and pollution concentrations, and because the classification system is based on yearly average values (International Organisation for Standardisation, 2012c). Since the completed monitoring periods include four years and six months continuous monitoring (October 2017 to April 2022), as well as a full year from April 2008 to April 2009, and an eleven-month period from October 2012 to September 2013, the monitoring campaigns are considered adequate to conclude corrosion rates with current conditions. As per the International Standard, annual corrosion rates based on these measurements may be used to project up to 20 years (International Organisation for Standardisation, 2012b). The International Standard also indicate that for some engineering applications, more general guiding corrosion values defined in intervals of average corrosion rates for corrosivity categories may be used. Average corrosion rates of up to 10 years are considered to correspond to the initial period of exposure. Average corrosion rates for periods longer than 10 years are considered steady-state corrosion rates, but that the uncertainty level for guiding corrosion values defined as averages for initial and steady-state periods is high. Changes in the affecting parameters, namely relative humidity, temperature and pollution concentrations, may affect the corrosion rate. This could be as a result of natural variations in the climate, projected climate change and/or the increase or decrease in air pollution levels. Although these parameters are not expected to vary significantly over the near future, continued corrosion monitoring should identify changes in the rates.

5.8.6 Meteorological Parameters

The following meteorological parameters were identified for onsite monitoring and inclusion in this SSR:

- wind speed and direction;
- ambient air temperature and temperature difference;
- precipitation;
- relative humidity;
- ambient pressure;
- solar radiation;
- atmospheric stability (derived temperature gradient and from the standard deviation of horizontal wind direction, or ‘sigma theta’, wind speed and solar radiation);

- evapotranspiration rate (derived from the ambient air temperature, wind speed, solar radiation and relative humidity);
- corrosivity.

Also, details of the following regional meteorological parameters have been obtained from the SAWS:

- hail;
- frost;
- fog;
- lightning;
- tornadoes;
- extreme weather (wind speed, rainfall and temperature);
- snow, avalanches, ice, ice cover and blizzards;
- thunder.

In addition, and in line with the international recommendations (International Atomic Energy Agency, 2011) the severe and rare phenomena at the proposed site were identified using historical records compiled by the SAWS, and include:

- lightning;
- extreme winds;
- tornado/tropical cyclones;
- extreme meteorological variability.

5.8.6.1 Site Meteorological Parameters

This section addresses the measurement and evaluation of the site meteorological characteristics, augmented where necessary due to limited data recordings by observations made at SAWS stations, which involve slightly longer monitoring periods.

5.8.6.1.1 Wind Speed and Direction

The atmospheric dispersion of air emissions from the site is largely a function of the wind speed and direction. The wind speed influences both the distance of downward transport and the rate of dilution. The generation of mechanical turbulence is similarly a function of the wind speed and the wind direction determines the advection path.

(a) Prevailing Wind Patterns

From the nearly 25 years of historical electronic data set produced by Eskom (Eskom, 2023a), it is clear that the most dominant wind direction in this region is from the south-southeast and south (***Figure 5.8.3***). The wind roses in this figure represent the wind speed and directional patterns as observed at the Koeberg 120 m tower (October 1997 – September 2023), and the five offsite Eskom automatic weather stations (AWS) located at Robben Island (January 1998 – September 2023), Bok Point (January 1998 – June 2019), Atlantis (January 1998 – September 2023), Rondekuil (January 1998 – September 2023), and Milnerton (January 1998 – June 2019, October 2020, 26 January 2021 – 26 June 2022).

The observation at the 10 m level on the 120-m tower indicate annual mean wind speeds varying between 3.7 m/s (2003) and 4.8 m/s (2008) with an average of 4.1 m/s, with most of these occurring from the south-southeast, followed by southeast winds. The highest hourly mean wind speed at this level on the 120-m tower was 16.5 m/s.

The observation at the Duynefontyn WS indicate annual mean wind speeds varying between 4.0 m/s (2020) and 4.3 m/s (2019) with an average of 4.1 m/s, with most of these occurring from the south-southeast, followed by southeast winds. The highest hourly mean wind speed at this weather station was 15.4 m/s.

Bok Point experienced annual mean wind speeds varying between 4.6 m/s (2019) and 5.7 m/s (2010) with an average of 5.2 m/s, with most of these occurring from the south-southeast, followed by southerly and then northerly winds. The highest hourly mean wind speed at Bok Point was 18.9 m/s. However, Robben Island experienced a higher maximum hourly mean wind speed of 20.3 m/s and annual mean wind speeds varying between 4.3 m/s (2022) and 5.6 m/s (2000) with an average of the annual means of 5.0 m/s. Rondekuil WS also experienced a higher maximum hourly mean wind speed of 19.7 m/s, and annual mean wind speeds varying between 3.7 m/s (2022) and 4.7 m/s (2005) with an average of the annual means of 4.2 m/s. Excluding the years 2020 to 2022, since they were not full annual periods, the Milnerton WS experienced a maximum hourly mean wind speed of 13.6 m/s and annual mean wind speeds varying between 3.6 m/s (2019) and 4.8 m/s (1998) with an average of the annual means of 3.6 m/s. Atlantis WS experienced the lowest maximum hourly mean wind speed of 11.8 m/s and annual mean wind speeds varying between 2.7 m/s (1998) and 3.4 m/s (2013) with an average of the annual means of 3.0 m/s.

Apart from the southerly wind sector, the wind observations at Robben Island reflect a similar wind directional distribution as at Bok Point. Atlantis also observed similar wind directions, albeit shifted to the south from south-east, but significantly lower wind conditions (hourly mean and maximum of 3.7 m/s and 11.8 m/s, respectively). The most dominant wind direction at the Atlantis WS is southerly (11.1 per cent), followed by south-southeasterly winds (9.5 per cent).

The effect of the general sheltering effect of the elevated inland terrain to the east, as well as the greater valley flow conditions running southwest between the Dorstberg and Kanonkop (towards the south), and Koeberg (towards the north) of the Rondekuil weather station is reflected in the significantly reduced winds from the south-southeast with increased frequency of winds from the southwest.

The wind observations at the Atlantis weather station similarly reflect reduced southeasterly winds. Although this may be due to the effect of the mountain range north and northeast this may also be due to a different mechanism, such as the extensive built-up area to the east and southeast.

Calm wind conditions, i.e. wind speeds below 0.5 m/s, at the Rondekuil and Atlantis experienced 2.7 per cent and 2.2 per cent calm wind conditions, respectively. Calm wind conditions were lower at the other sites, namely 1.5 per cent (120-m tower), 0.5 per cent (Duynefontyn WS), 0.2 per cent (Bok Point WS), 1.3 per cent (Milnerton WS) and 0.8 per cent (Robben Island). The following seasonal frequencies of calm wind conditions were experienced (autumn, winter, spring, summer):

- 120-m tower (10 m level) – 4.6 per cent, 3.3 per cent, 3.0 per cent and 3.7 per cent
- Duynefontyn WS – 1.0 per cent, 0.2 per cent, 0.3 per cent and 0.4 per cent
- Atlantis – 3.3 per cent, 1.9 per cent, 1.8 per cent and 1.7 per cent
- Rondekuil – 5.2 per cent, 2.2 per cent, 1.2 per cent and 2.1 per cent
- Robben Island – 1.4 per cent, 0.9 per cent, 0.5 per cent and 0.2 per cent
- Milnerton – 2.1 per cent, 1.9 per cent, 0.7 per cent and 0.4 per cent
- Bok Point –0.3 per cent, 0.4 per cent, 0.1 per cent and 0.10 per cent

The wind pattern at the Koeberg 120-m tower (at 10 m) reflects the dominance of the south-southeasterly wind component observed at Bok Point to the north, as well as the conditions at Robben Island and Milnerton to the south. The strongest winds were mostly observed from the south-southeasterly sector, i.e. 120-m tower (10m level) (12.2 per cent), Duynefontyn WS (11.2 per cent), Atlantis (11.1 per cent), Milnerton (33.4

per cent), Robben Island (19.5 per cent), Bok Point (14.2 per cent), or the southern sector, i.e. Rondekuil (12.3 per cent). Although strong winds were also observed from the northwesterly sector, the frequencies were less, i.e. 120-m tower (10m level) (6.7 per cent), Duynefontyn WS (5.8 per cent), Atlantis (4.9 per cent), Milnerton (8.3 per cent), Robben Island (10.2 per cent), Rondekuil (2.7 per cent) and Bok Point (5.6 per cent).

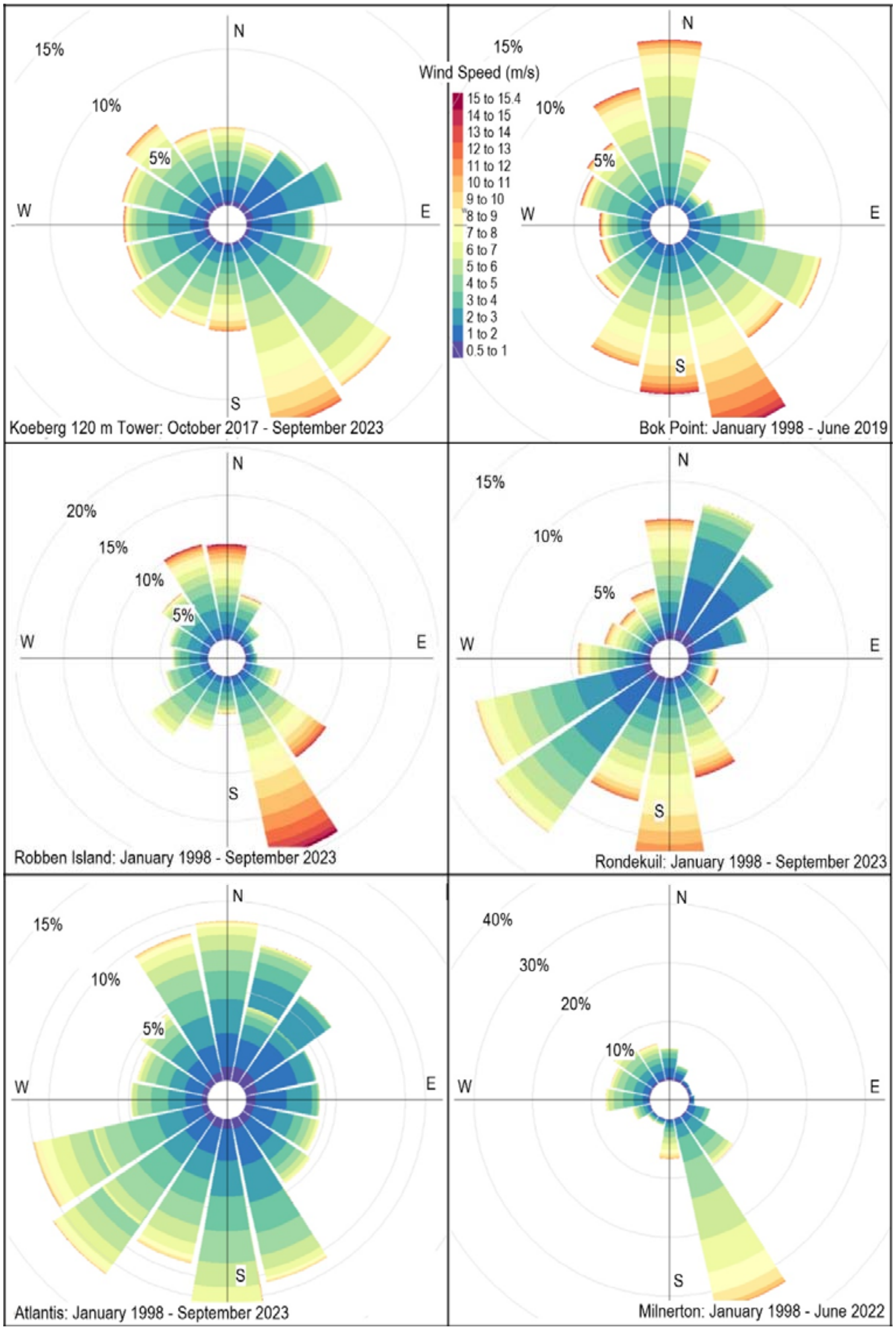

Figure 5.8.3

Comparison of Long-Term Wind Roses (120-m Tower: 1997 to 2023, Eskom AWS:1998 to 2023)

Rondekuil observed 12.5 per cent from the southwest and 9.1 per cent from the north-northeast. Less frequent observations were made at the 10 m level on the 120-m tower, i.e. 6.2 per cent and 4.3 per cent, respectively; as well as at the Duynefontyn WS (5.1 per cent and 4.5 per cent). The other offsite Eskom AWS locations also observed lower frequencies of winds from these sectors, i.e. Atlantis WS (7.5 per cent and 4.5 per cent), Milnerton WS (1.3 per cent and 2.8 per cent), Robben Island WS (7.8 per cent and 4.8 per cent), and Bok Point WS (4.4 per cent and 3.7 per cent).

The northerly winds observed at the Koeberg 120-m tower (5.1 per cent) were similar to Milnerton (5.6 per cent) but not as significant as at Bok Point (10.7 per cent), Atlantis (9.1 per cent), Rondekuil (7.9 per cent) and Robben Island (10.0 per cent). Both the 120-m tower and the Duynefontyn WS observed low frequency of winds directly from the north. This may suggest that the land-sea interface (i.e. land and sea breeze circulation) have a significant effect by distributing the winds from the north over a larger sector. When considering the combined sector from northwest to northeast the frequencies are more comparable, i.e. Koeberg 120-m tower (21.2 per cent), Milnerton (23.3 per cent), Bok Point (28.0 per cent), Atlantis (26.9 per cent), Rondekuil (23.1 per cent) and Robben Island (31.3 per cent). Apart from the south-southeasterly and southeasterly sectors, all other wind directions at Koeberg occurred with very similar frequency of between 4 and 7 per cent. South-southeasterly winds occurred for about 19.5 per cent of the period at Robben Island and about 33.4 per cent at Milnerton WS. This is followed by southeasterly winds, i.e. 9.9 per cent at Milnerton WS and 10.7 per cent at Robben Island WS. Whilst it is expected that the observation made at both Robben Island and Milnerton are influenced by the presence of Table Mountain towards the south, more channelling of the south-southeasterly winds was observed at the Milnerton WS, i.e. 33.4 per cent compared with 19.5 per cent at Robben Island, whereas the southeasterly winds were similar, i.e. 9.9 per cent compared with 10.7 per cent at Robben Island, respectively.

A comparison of the wind patterns between the observations at the 10 m level on the 120-m tower and the Duynefontyn WS is shown in ***Figure 5.8.4***. The period (2017-2022) wind roses are very similar, with the main differences being slightly higher frequencies of southerly and northeasterly winds observed at the Duynefontyn WS. The mean wind speed was 4.14 m/s and 4.14 m/s at the 120-m tower and Duynefontyn WS, respectively. A similar comparison of the diurnal wind patterns between the observations at the 10 m level on the 120-m tower and the Duynefontyn WS is shown in ***Figure 5.8.5***. The day-time wind roses are similar, but the night-time conditions at the Duynefontyn WS observed more north and northeasterly winds than at the 120-m tower. This is more pronounced at wind speeds less than 3 m/s.

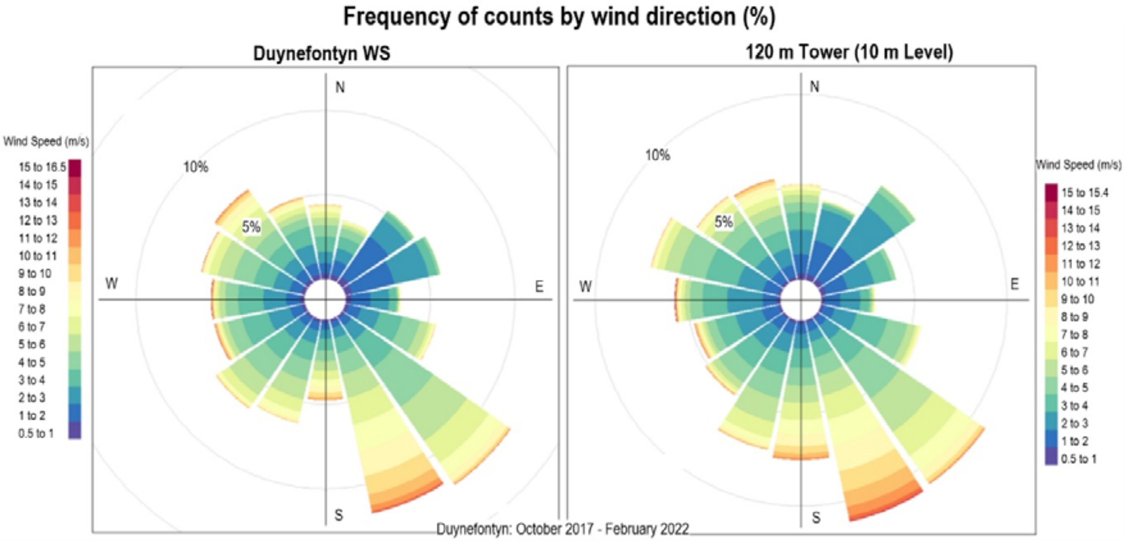

Duynefontyn: October 2017 - February 2022

Figure 5.8.4
Comparison of 120-m Tower and Duynefontyn WS Wind Roses (2017 to 2022)

There is very little difference between the 120-m tower and Duynefontyn WS wind speeds. The mean wind speed during day-time hours for the period (2017-2022) was 4.31 m/s and 4.45 m/s at the 120-m tower and Duynefontyn WS, respectively. The mean wind speed during night-time hours was 3.97 m/s and 3.88 m/s at the 120-m tower and Duynefontyn WS, respectively. The calculated bias is however 0. The wind direction has a bias of +7.8°, i.e. winds at the Duynefontyn WS have a directional bias of 7.8° clockwise.

Figure 5.8.6 is a comparison of the observations of day-time winds at the six weather stations (120-m tower (10 m level), Robben Island, Bok Point, Atlantis, Rondekuil, and Milnerton). Whilst the predominance of the main wind directions (south-southwesterly, southerly and south-southeasterly) are still maintained, increased frequency of westerly winds was observed at the 120-m tower, north- and southwesterly winds at Bok Point and southwesterly winds at Atlantis. Little difference between the period (day- and night-time combined) wind roses and day-time wind roses for Robben Island and Rondekuil was evident. The dominance of the south-southwest to north-northeast valley wind flow condition (i.e. between Dorstberg and Kanonkop, towards the south and Koeberg, towards the north) result in very similar day- and night-time wind roses for Rondekuil.

An increase in the northwesterly winds was observed at Milnerton. The westerly winds are due to the replacement of the rising hot air which develops over land during the day. Understandably, this was not observed at Robben Island due to the relative smaller size of the exposed land.

Since Rondekuil is located more inland, the diurnal wind patterns are more dominated by local influences such as the Dorstberg mountain (425 m amsl) south-southeast of the Rondekuil weather, as opposed to land-sea breeze circulation observed during the day-night cycle and therefore not manifested as clearly as at the other stations closer to the sea.

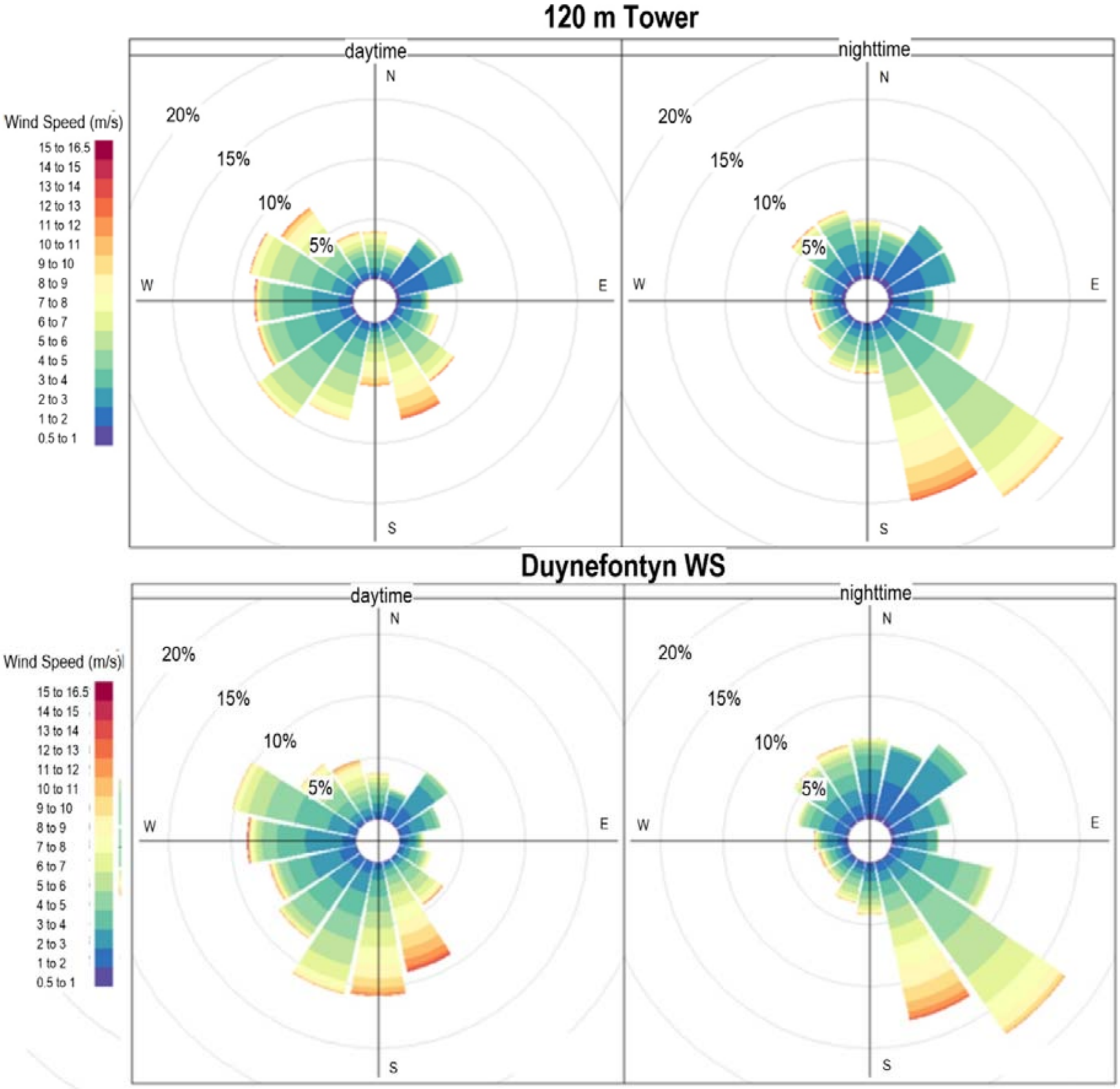

Figure 5.8.5
Comparison of 120-m Tower and Duynefontyn WS Day- and Night-time Wind Roses (2017 to 2022)

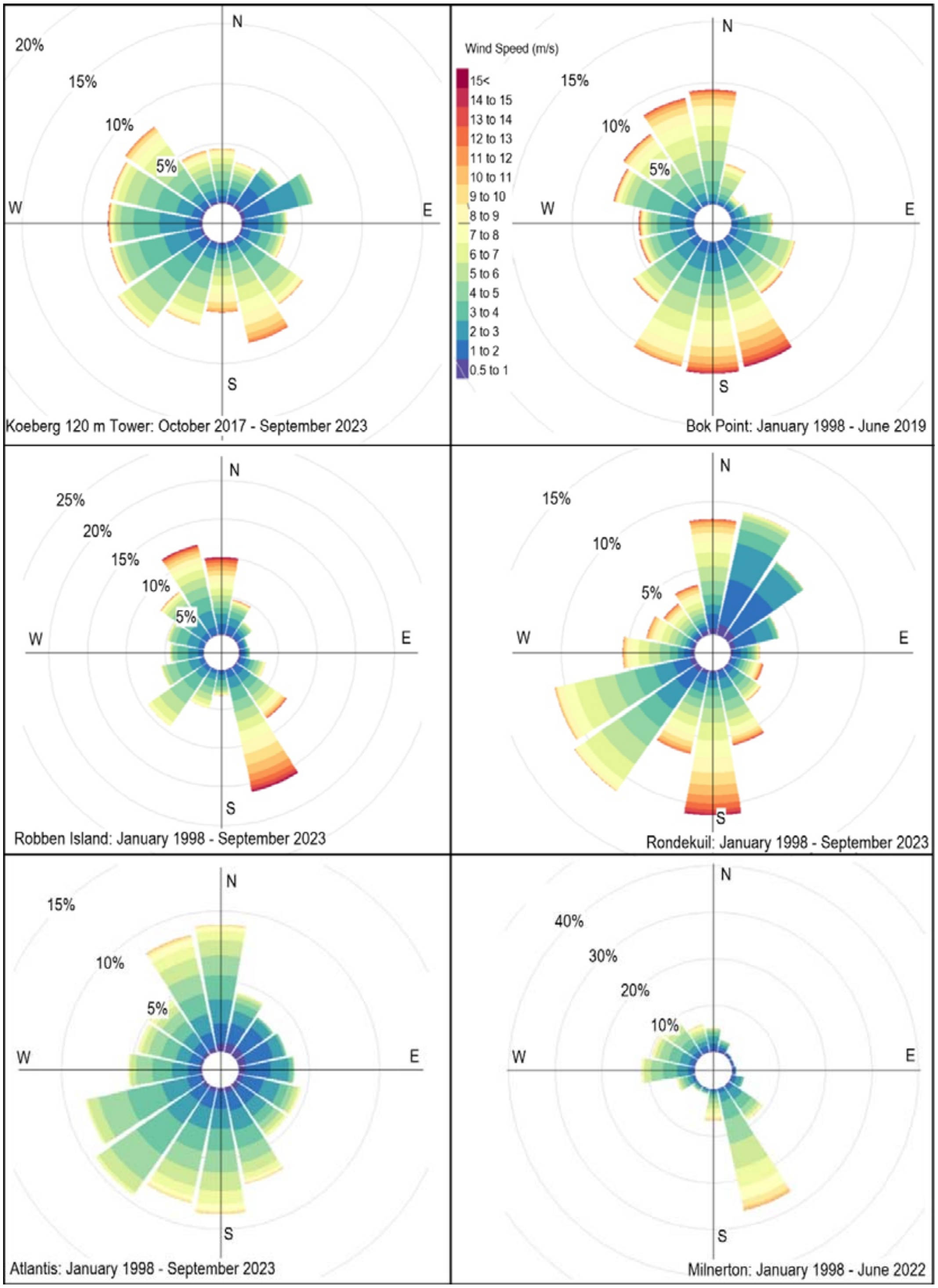

Figure 5.8.6
Comparison of Day-time Wind Roses (120-m Tower 1997 to 2023, Eskom AWS 1998 to 2023)

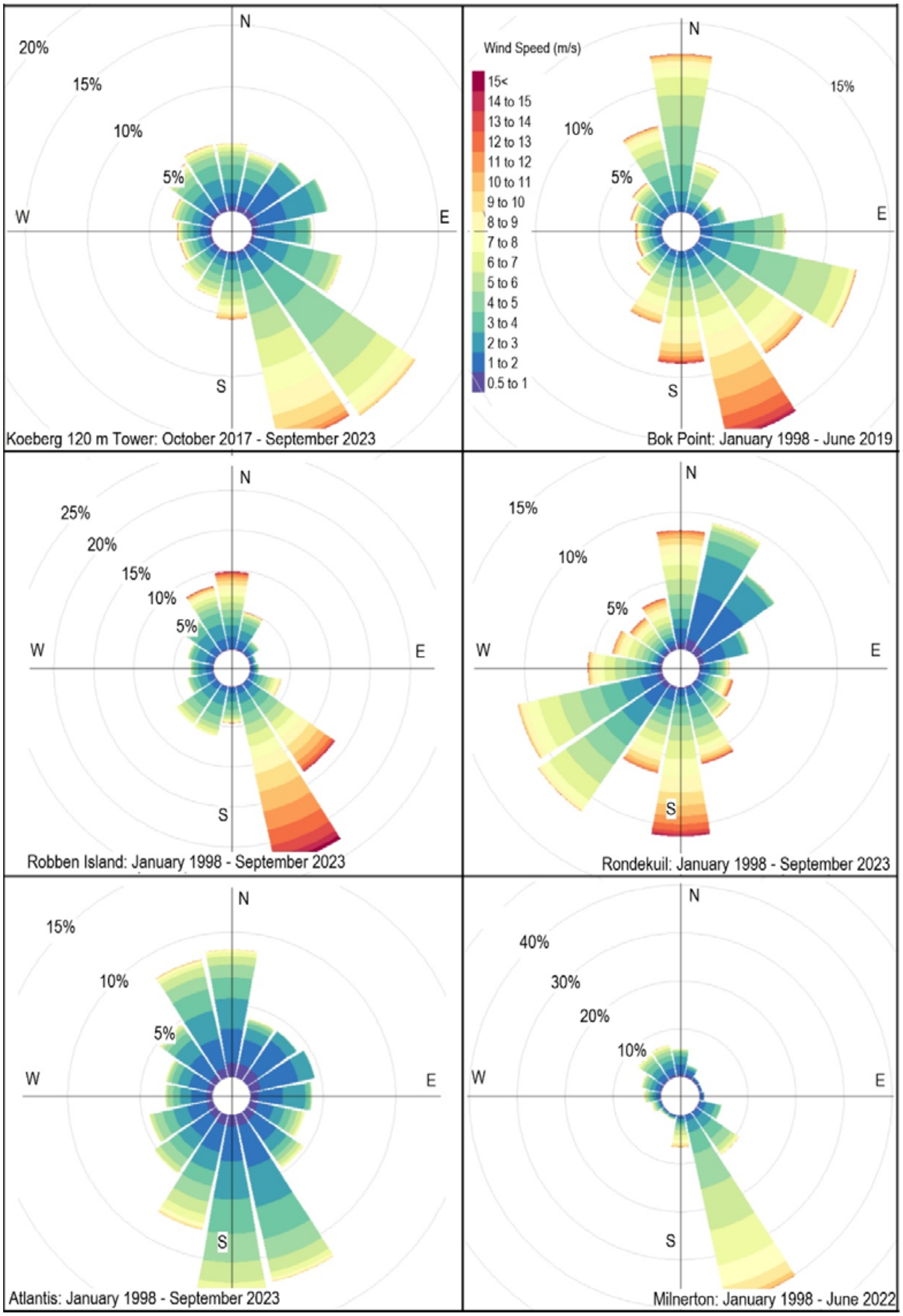

Figure 5.8.7
Comparison of Night-time Wind Roses (120-m Tower 1997 to 2023, Eskom AWS 1998 to 2023)

Since Rondekuil is located more inland, the diurnal wind patterns are more dominated by local influences such as the Dorstberg mountain (425 m amsl) south-southeast of the Rondekuil weather, as opposed to land-sea breeze circulation observed during the day-night cycle and therefore not manifested as clearly as at the other stations closer to the sea.

The wind speed at the 120-m Tower tended to increase towards mid-afternoon as the instability is highest at around 14h00 to 17h00 (***Table 5.8.3***).

Table 5.8.3
Wind Speed as Function of Time of Day at the 120-m Tower (10 m Level) (October 1997 to September 2023)

Hour of Day	Wind Speed [m/s] at 10 m level	
	Average	95th Percentile
01h00	3.5	7.4
02h00	3.4	7.3
03h00	3.4	7.2
04h00	3.3	7.1
05h00	3.3	7.1
06h00	3.2	6.9
07h00	3.2	6.9
08h00	3.2	7.3
09h00	3.5	7.7
10h00	3.8	8.0
11h00	4.2	8.3
12h00	4.6	8.7
13h00	5.0	9.1
14h00	5.2	9.6
15h00	5.3	9.9
16h00	5.4	10.1
17h00	5.3	10.2
18h00	5.1	10.2
19h00	4.7	9.9
20h00	4.4	9.3
21h00	4.2	8.8
22h00	4.0	8.4
23h00	3.8	7.9
24h00	3.6	7.6

As the air over land cools down during the night, it is expected that the sea breeze would disappear and may even result in the development of a land breeze. This is well illustrated by the infrequent occurrence of winds from the ocean (westerly sector) shown in the night-time wind roses summarised in ***Figure 5.8.5***. The offshore flows are characterised by slow (less than 3 m/s) wind speeds.

Conditions at Bok Point indicate an increased southeasterly wind component during the night. An increased frequency of southeasterly winds was also observed at Koeberg. Apart from the decrease in winds from the westerly sector at Atlantis and Milnerton, little difference was observed in the other wind directions.

According to the long-term observations which were carried out during the period October 1997 to September 2023 (Eskom, 2023a) at 10 m above ground level on the 120-m tower, south-southeasterly winds dominate with 12.123 per cent occurrences (see ***Table 5.8.4***). This wind direction also experienced a relatively high frequency of strong winds (0.95 per cent above 10 m/s), i.e. winds in excess of 10 m/s.

The second highest frequency (0.29 per cent) of strong winds comes from the south, followed by northwesterly (0.14 per cent), north-northwesterly (0.08 per cent) westerly and southeasterly (both 0.07 per cent), winds.

As a comparison, albeit for a shorter period (October 2017 to February 2022) (Eskom, 2023a) the Duynefontyn WS also observed the highest wind direction prevalence from the south-southeast with 11.21 per cent occurrences (see ***Table 5.8.5***). This wind direction also experienced a high frequency of strong winds (1.50 per cent above 10 m/s). The second highest frequency (0.35 per cent) of strong winds comes from the south, followed by north-northwesterly (0.13 per cent), then west-southeasterly and westerly (both 0.09 per cent) winds.

As shown in ***Table 5.8.6*** the two highest hourly average winds, averaged per sector, at the 120-m tower (10 m height) during the October 1997 to September 2023 period occurred from the south-southeast with wind speed of 6.3 m/s, followed by winds from the south with an average wind speed of 5.4 m/s. Northeasterly winds have the lowest average wind speed of 2.0 m/s. The highest wind speeds measured in each cardinal wind direction is also presented in ***Table 5.8.6***. The top two hourly maximum wind speeds per sector, occurred from the west with maximum wind speed of 16.5 m/s[6] and the west-south-west with an hourly maximum wind speed of 16.1 m/s.

---

[6] According to historical records of annual maximum wind speed and gusts (Eskom, 1997) a record high maximum hourly average wind speed of 17.2 m/s was recorded at the 10 m level on the120-m tower during 1984.

Similarly, as shown in ***Table 5.8.7***, the two highest hourly winds, averaged per sector, at the Duynefontyn WS during the October 2017 to February 2022 period also occurred from the south-southeast with a wind speed of 7.2 m/s, followed by the southern sector with a wind speed of 5.7 m/s. North-northeasterly winds have the lowest average wind speed of 2.2 m/s. The highest hourly wind speeds measured in each cardinal wind (***Table 5.8.7***) occurred from the west with maximum wind speed of 15.4 m/s followed by south-southeast with maximum wind speed of 14.4 m/s.

The persistence (continuous duration) of hourly average winds above 10 m/s, 12 m/s, 14 m/s and 16 m/s at the 120-m tower was observed to be maximum 31 hours (August), 19 hours (June), 13 hours (August) and 1 hour (June, July and August), respectively (***Table 5.8.8***).

Table 5.8.4
Wind Speed and Direction Categorisation at the 120-m Tower (10 m Level) (October 1997 to September 2023)

Wind Direction	Wind Speed [m/s] at 10 m level												Total (%)
	<0.5	**0.5-1.0**	**1.0-2.0**	**2.0-3.0**	**3.0-4.0**	**4.0-5.0**	**5.0-6.0**	**6.0-8.0**	**8.0-10.0**	**10.0-13.0**	**13.0-18.0**	**>18.0**	
N	0.11%	0.28%	0.71%	0.82%	0.98%	0.73%	0.53%	0.70%	0.23%	0.03%	0.00%	0.00%	5.13%
NNE	0.11%	0.33%	0.90%	0.78%	0.75%	0.54%	0.33%	0.41%	0.11%	0.02%	0.00%	0.00%	4.28%
NE	0.12%	0.42%	2.14%	1.41%	0.41%	0.16%	0.06%	0.03%	0.01%	0.00%	0.00%	0.00%	4.75%
ENE	0.11%	0.41%	2.16%	2.44%	0.89%	0.23%	0.06%	0.02%	0.00%	0.00%	0.00%	0.00%	6.32%
E	0.11%	0.30%	1.25%	1.49%	0.85%	0.22%	0.08%	0.08%	0.03%	0.00%	0.00%	0.00%	4.40%
ESE	0.09%	0.22%	0.85%	1.27%	1.45%	0.96%	0.42%	0.26%	0.08%	0.02%	0.00%	0.00%	5.62%
SE	0.07%	0.18%	0.59%	1.20%	2.17%	2.62%	2.09%	1.99%	0.48%	0.07%	0.00%	0.00%	11.46%
SSE	0.07%	0.15%	0.45%	0.72%	1.07%	1.47%	1.62%	3.38%	2.32%	0.95%	0.03%	0.00%	12.23%
S	0.08%	0.16%	0.40%	0.59%	0.77%	0.72%	0.63%	1.20%	0.87%	0.29%	0.00%	0.00%	5.71%
SSW	0.07%	0.16%	0.45%	0.70%	0.97%	1.04%	0.90%	0.98%	0.23%	0.03%	0.00%	0.00%	5.52%
SW	0.07%	0.18%	0.61%	1.00%	1.22%	1.21%	0.99%	0.81%	0.09%	0.02%	0.00%	0.00%	6.21%
WSW	0.08%	0.21%	0.75%	1.28%	1.34%	0.82%	0.40%	0.31%	0.13%	0.07%	0.01%	0.00%	5.38%
W	0.11%	0.25%	0.89%	1.36%	1.35%	0.71%	0.31%	0.26%	0.14%	0.07%	0.02%	0.00%	5.47%
WNW	0.09%	0.22%	0.71%	1.01%	1.19%	1.00%	0.72%	0.54%	0.13%	0.06%	0.01%	0.00%	5.69%
NW	0.09%	0.23%	0.70%	0.88%	1.02%	0.99%	0.88%	1.26%	0.51%	0.14%	0.01%	0.00%	6.69%
NNW	0.11%	0.25%	0.67%	0.98%	0.96%	0.66%	0.47%	0.66%	0.29%	0.08%	0.00%	0.00%	5.13%
TOTAL	1.51%	3.96%	14.31%	18.04%	17.42%	14.06%	10.44%	12.79%	5.59%	1.80%	0.09%	0.00%	100.00%

Table 5.8.5
Wind Speed and Direction Categorisation at the Duynefontyn WS (October 2017 to February 2022)

Wind Direction	Wind Speed [m/s] at 10 m level												Total (%)
	<0.5	0.5-1.0	1.0-2.0	2.0-3.0	3.0-4.0	4.0-5.0	5.0-6.0	6.0-8.0	8.0-10.0	10.0-13.0	13.0-18.0	>18.0	
N	0.03%	0.27%	1.09%	1.34%	0.97%	0.54%	0.43%	0.44%	0.14%	0.01%	0.00%	0.00%	5.25%
NNE	0.04%	0.31%	1.91%	1.77%	0.26%	0.10%	0.05%	0.08%	0.01%	0.00%	0.00%	0.00%	4.53%
NE	0.04%	0.29%	2.20%	2.73%	0.99%	0.36%	0.05%	0.03%	0.01%	0.00%	0.00%	0.00%	6.69%
ENE	0.02%	0.29%	1.21%	1.52%	0.99%	0.25%	0.02%	0.00%	0.00%	0.00%	0.00%	0.00%	4.31%
E	0.04%	0.18%	0.86%	1.11%	0.50%	0.11%	0.08%	0.12%	0.02%	0.00%	0.00%	0.00%	3.02%
ESE	0.03%	0.14%	0.62%	1.21%	1.69%	1.12%	0.41%	0.25%	0.06%	0.00%	0.00%	0.00%	5.54%
SE	0.01%	0.13%	0.48%	0.92%	1.59%	2.27%	2.16%	2.61%	0.70%	0.13%	0.00%	0.00%	11.01%
SSE	0.05%	0.13%	0.51%	0.59%	0.89%	1.02%	1.11%	2.82%	2.51%	1.50%	0.09%	0.00%	11.21%
S	0.02%	0.15%	0.57%	0.81%	1.06%	0.93%	0.89%	1.67%	0.99%	0.35%	0.00%	0.00%	7.44%
SSW	0.03%	0.15%	0.65%	1.02%	1.19%	1.25%	1.28%	1.17%	0.27%	0.05%	0.00%	0.00%	7.06%
SW	0.03%	0.12%	0.72%	1.23%	1.24%	0.93%	0.40%	0.27%	0.11%	0.07%	0.00%	0.00%	5.12%
WSW	0.03%	0.13%	0.90%	1.38%	1.06%	0.45%	0.17%	0.25%	0.17%	0.09%	0.01%	0.00%	4.65%
W	0.04%	0.17%	0.78%	1.88%	1.24%	0.65%	0.28%	0.32%	0.11%	0.09%	0.03%	0.00%	5.59%
WNW	0.04%	0.14%	0.86%	1.38%	1.71%	1.41%	0.83%	0.59%	0.13%	0.03%	0.00%	0.00%	7.12%
NW	0.01%	0.14%	0.67%	1.05%	1.27%	0.97%	0.68%	0.73%	0.22%	0.02%	0.00%	0.00%	5.76%
NNW	0.05%	0.17%	0.67%	0.93%	0.99%	0.83%	0.57%	0.90%	0.47%	0.13%	0.00%	0.00%	5.71%
TOTAL	0.50%	2.94%	14.70%	20.86%	17.66%	13.18%	9.40%	12.24%	5.92%	2.48%	0.13%	0.00%	100.00%

Table 5.8.6
Mean and Maximum Hourly Wind Speed per Direction at the 120-m Tower (10 m Level) (October 1997 to September 2023)

Sector-Averaged Hourly Wind Speed		Sector Maximum Hourly Wind Speed	
Wind Direction	**Wind Speed (m/s)**	**Wind Direction**	**Wind Speed (m/s)**
SSE	6.3	**W**	16.5
S	5.4	**WSW**	16.1
SE	4.7	**SSE**	15.9
NW	4.6	**WNW**	15.6
SSW	4.4	**NW**	14.6
SW	4.1	**S**	14.1
NNW	4.0	**SE**	14.1
WNW	3.9	**N**	13.9
N	3.9	**ESE**	13.9
WSW	3.6	**SW**	13.8
W	3.4	**NNW**	13.5
ESE	3.4	**NNE**	13.0
NNE	3.3	**SSW**	12.9
E	2.5	**E**	11.9
ENE	2.2	**ENE**	11.4
NE	2.0	**NE**	10.1

Table 5.8.7

Mean and Maximum Hourly Wind Speed per Direction at the Duynefontyn WS (October 2017 to February 2022)

Sector-Averaged Hourly Wind Speed		Sector Maximum Hourly Wind Speed	
Wind Direction	**Wind Speed (m/s)**	**Wind Direction**	**Wind Speed (m/s)**
SSE	7.2	**W**	15.4
S	5.7	**SSE**	14.4
SE	5.4	**WSW**	13.9
SSW	4.7	**SE**	13.1
NNW	4.6	**SW**	13.0
NW	4.2	**NNW**	12.7
WNW	4.0	**SSW**	12.7
SW	3.8	**NW**	12.5
ESE	3.7	**S**	12.4
W	3.7	**WNW**	11.9
WSW	3.6	**N**	11.1
N	3.4	**NNE**	9.2
E	2.6	**ESE**	8.8
ENE	2.5	**E**	8.5
NE	2.4	**NE**	8.4
NNE	2.2	**ENE**	6.2

Table 5.8.8
Sustained Wind Speeds at the 120-m Tower (10 m Level) (October 1997 to September 2023)

Month	Hourly Persistence (Continuous Duration)			
	10 m/s	12 m/s	14 m/s	16 m/s
January	14	7	2	0
February	11	7	4	0
March	16	10	3	0
April	8	2	0	0
May	12	2	0	0
June	25	19	11	1
July	23	11	6	1
August	31	17	13	1
September	19	9	5	0
October	12	5	1	0
November	14	7	1	0
December	14	10	1	0

Seasonal wind roses based on the wind data measured at the 120-m tower (10 m level) and the Duynefontyn WS for the observational period of October 2017 to February 2022 are compared in ***Figure 5.8.8***. The wind roses for the two sites are very similar. Spring observed more frequent northeasterly winds at the Duynefontyn WS than at the 120-m tower (***Table 5.8.9*** and ***5.8.10***). Increased occurrence of east-southeasterlies and west-northwesterlies were observed at the Duynefontyn WS during summer. More frequent southerly, northeasterly and west-northwesterly winds were observed at the Duynefontyn WS during autumn and during winter, more frequent south-south--westerly winds were observed at the Duynefontyn WS.

The longer data period of 1997 to 2023 for the 120-m tower (10m level) were also compared with the observations at the five AWS for the 1998 to 2023 monitoring period (Eskom, 2023b) and provided in ***Figures 5.8.9*** to ***5.8.12***.

Table 5.8.9
Seasonal Wind Direction Occurrence at the Duynefontyn WS (October 2017 to February 2022)

Wind Direction	Frequency of Occurrence			
	Spring	Summer	Autumn	Winter
N	4.44%	2.48%	4.74%	9.53%
NNE	3.07%	1.66%	6.03%	7.85%
NE	4.60%	1.51%	7.75%	13.48%
ENE	3.35%	1.05%	4.27%	8.68%
E	3.23%	1.69%	3.15%	3.82%
ESE	7.00%	5.69%	5.47%	3.80%
SE	11.96%	15.62%	10.98%	4.76%
SSE	12.00%	17.76%	10.53%	3.21%
S	8.17%	10.51%	7.61%	3.37%
SSW	8.46%	8.90%	5.21%	5.45%
SW	6.19%	5.30%	4.41%	4.46%
WSW	4.64%	5.47%	4.65%	4.28%
W	5.53%	6.27%	5.51%	5.43%
WNW	6.78%	8.41%	7.64%	5.86%
NW	5.34%	5.06%	6.60%	6.26%
NNW	5.25%	2.61%	5.44%	9.76%
TOTAL	100.00%	100.00%	100.00%	100.00%

Table 5.8.10
Seasonal Wind Direction Occurrence at the 120-m Tower (10 m Level) (October 1997 to September 2023)

Wind Direction	Frequency of Occurrence			
	Spring	Summer	Autumn	Winter
N	4.16%	2.20%	5.22%	8.82%
NNE	3.16%	1.60%	4.74%	7.51%
NE	3.19%	1.29%	5.56%	8.83%
ENE	4.00%	1.32%	7.11%	12.69%
E	3.45%	2.50%	4.61%	6.98%
ESE	6.08%	4.55%	6.29%	5.53%
SE	12.71%	14.59%	11.65%	7.01%
SSE	13.63%	19.03%	11.31%	5.18%
S	6.06%	9.26%	5.39%	2.25%

Wind Direction	Frequency of Occurrence			
	Spring	Summer	Autumn	Winter
SSW	6.37%	7.71%	4.87%	3.22%
SW	7.58%	8.12%	5.01%	4.21%
WSW	6.36%	6.29%	4.57%	4.34%
W	5.94%	6.21%	5.21%	4.55%
WNW	5.84%	6.39%	5.72%	4.82%
NW	6.85%	5.89%	7.07%	6.94%
NNW	4.60%	3.04%	5.68%	7.13%
TOTAL	100.00%	100.00%	100.00%	100.00%

Overall, the most common summer winds were from the general southeastern sector, i.e. including the combined east-southeast, southeast and south-southeast. For the Duynefontyn WS and 120-m tower these occurrences were 39.07 per cent (***Table 5.8.9***) and 38.17 per cent (***Table 5.8.10***), respectively. Similar conditions were also observed at Milnerton (57.2 per cent, ***Table 5.8.12***), Bok Point (34.5 per cent, ***Table 5.8.11***) and Robben Island (38.8 per cent, ***Table 5.8.14***). However, the summer wind directions at Rondekuil (***Table 5.8.13***) and Atlantis (***Table 5.8.15***) were more prevalent from the south, i.e. 20.2 per cent and 18.8 per cent, respectively. Winter conditions observed winds mainly from the north-northwest and north. Atlantis WS observed 13.7 per cent frequency from north-northwest, which is similar than the observations at the Robben Island WS of 10.7 per cent from the north-northwest. Milnerton observed 10.7 per cent from the north-northwest and 10.8 per cent from the north, whereas the wind conditions at the Rondekuil WS was spread from the north (13.6 per cent), north-northeast (15.6 per cent) and northeast (13.2 per cent). Winter winds are dominated by northerly winds (40.1%) at the Bok Point WS. Although the most common winds at the 120-m tower during winter were from the east-northeast (approximately 12.7 per cent), strong winds were more from the northern and western sectors.

The wind direction during strong wind conditions at the Robben Island WS (***Appendix 5.8.A*** ***Table 5.8.A.4***) and Milnerton WS (***Appendix 5.8.A*** ***Table 5.8.A.2***) were mostly south-southeast, i.e. 19.5 per cent and 33.4 per cent respectively. Rondekuil WS (***Appendix 5.8.A*** ***Table 5.8.A.3***), Atlantis WS (***Appendix 5.8.A*** ***Table 5.8.A.5***) and Bok Point (***Appendix 5.8.A*** ***Table 5.8.A.6***) observed strong wind mostly from the south, i.e. 12.3 per cent, 11.1 per cent and 14.2 per cent, respectively.

Table 5.8.11
Seasonal Wind Direction Occurrence at the Bok Point (January 1998 to June 2019)

Wind Direction	Frequency of Occurrence			
	Spring	Summer	Autumn	Winter
N	8.21%	5.40%	11.70%	17.51%
NNE	2.50%	1.19%	3.74%	7.48%
NE	0.74%	0.54%	1.44%	2.65%
ENE	1.12%	0.68%	2.10%	3.14%
E	3.75%	2.30%	6.05%	6.91%
ESE	7.99%	6.23%	10.53%	9.52%
SE	7.90%	8.01%	9.28%	6.09%
SSE	15.24%	20.26%	13.18%	7.84%
S	11.09%	14.86%	7.98%	4.94%
SSW	10.29%	11.02%	5.40%	4.40%
SW	5.37%	5.41%	3.37%	3.28%
WSW	3.94%	3.60%	2.56%	3.03%
W	3.93%	3.61%	3.11%	3.58%
WNW	5.12%	5.22%	4.65%	4.48%
NW	5.59%	5.31%	5.92%	5.57%
NNW	7.22%	6.36%	9.00%	9.56%
TOTAL	100%	100%	100%	100%

Table 5.8.12
Seasonal Wind Direction Occurrence at the Milnerton (January 1998 to June 2022)

Wind Direction	Frequency of Occurrence			
	Spring	Summer	Autumn	Winter
N	4.38%	1.33%	5.40%	10.82%
NNE	1.93%	0.44%	2.12%	6.56%
NE	0.66%	0.20%	0.81%	1.93%
ENE	0.49%	0.12%	0.66%	1.53%
E	0.74%	0.24%	1.04%	1.97%
ESE	2.83%	1.17%	4.63%	6.72%
SE	10.04%	5.89%	12.27%	11.75%
SSE	36.91%	50.28%	30.75%	16.38%
S	7.37%	11.46%	5.52%	2.49%

Wind Direction	Frequency of Occurrence			
	Spring	Summer	Autumn	Winter
SSW	1.07%	1.29%	1.50%	0.97%
SW	1.19%	1.17%	1.20%	1.61%
WSW	3.61%	2.74%	2.93%	3.66%
W	8.44%	8.15%	7.68%	6.28%
WNW	7.01%	6.50%	7.37%	7.16%
NW	8.11%	6.38%	9.03%	9.50%
NNW	5.24%	2.62%	7.10%	10.66%
TOTAL	100.00%	100.00%	100.00%	100.00%

Table 5.8.13

Seasonal Wind Direction Occurrence at the Rondekuil (January 1998 to September 2023)

Wind Direction	Frequency of Occurrence			
	Spring	Summer	Autumn	Winter
N	6.53%	2.80%	8.54%	13.59%
NNE	6.87%	3.50%	10.60%	15.61%
NE	5.73%	2.19%	7.50%	13.23%
ENE	3.25%	1.25%	3.65%	7.74%
E	1.81%	1.00%	1.76%	2.73%
ESE	2.24%	1.78%	2.34%	1.68%
SE	3.48%	2.93%	3.52%	2.51%
SSE	7.47%	7.20%	6.82%	4.66%
S	13.58%	20.24%	10.33%	5.16%
SSW	8.82%	13.03%	6.96%	3.92%
SW	12.29%	17.41%	13.10%	7.04%
WSW	12.37%	15.87%	11.74%	6.11%
W	5.40%	4.93%	4.17%	4.18%
WNW	3.69%	2.43%	2.67%	3.50%
NW	3.08%	1.68%	2.65%	3.40%
NNW	3.38%	1.75%	3.65%	4.92%
TOTAL	100.00%	100.00%	100.00%	100.00%

Table 5.8.14
Seasonal Wind Direction Occurrence at the Robben Island (January 1998 to September 2023)

Wind Direction	Frequency of Occurrence			
	Spring	Summer	Autumn	Winter
N	7.71%	5.49%	10.93%	15.26%
NNE	3.36%	2.30%	5.73%	7.67%
NE	1.42%	0.94%	2.24%	4.30%
ENE	0.76%	0.57%	1.12%	1.86%
E	1.00%	0.63%	1.24%	2.32%
ESE	3.02%	1.70%	3.86%	6.64%
SE	10.66%	8.97%	11.88%	11.22%
SSE	20.71%	28.15%	19.49%	10.52%
S	4.36%	4.99%	3.94%	2.45%
SSW	7.31%	7.63%	4.79%	3.56%
SW	9.76%	10.08%	6.56%	5.19%
WSW	5.31%	5.01%	4.11%	3.99%
W	4.27%	3.61%	3.07%	3.75%
WNW	4.51%	4.05%	3.73%	4.45%
NW	6.18%	6.56%	6.31%	6.13%
NNW	9.69%	9.31%	11.00%	10.67%
TOTAL	100.00%	100.00%	100.00%	100.00%

Table 5.8.15
Seasonal Wind Direction Occurrence at the Atlantis (January 1998 to September 2023)

Wind Direction	Frequency of Occurrence			
	Spring	Summer	Autumn	Winter
N	7.01%	3.05%	9.54%	16.56%
NNE	3.24%	1.52%	4.93%	7.99%
NE	2.70%	1.20%	4.75%	6.92%
ENE	3.50%	1.58%	5.03%	6.60%
E	4.12%	2.35%	4.72%	5.75%
ESE	4.73%	3.86%	4.90%	3.94%
SE	5.41%	5.10%	4.87%	3.66%
SSE	9.98%	13.94%	9.15%	5.01%
S	11.61%	18.75%	9.92%	4.39%

Wind Direction	Frequency of Occurrence			
	Spring	Summer	Autumn	Winter
SSW	9.68%	13.22%	7.06%	3.72%
SW	8.56%	10.89%	6.83%	3.92%
WSW	7.33%	9.02%	6.39%	3.91%
W	4.91%	4.78%	4.16%	3.55%
WNW	4.70%	3.44%	3.94%	4.38%
NW	5.04%	3.39%	4.93%	5.99%
NNW	7.49%	3.90%	8.89%	13.72%
TOTAL	100.00%	100.00%	100.00%	100.00%

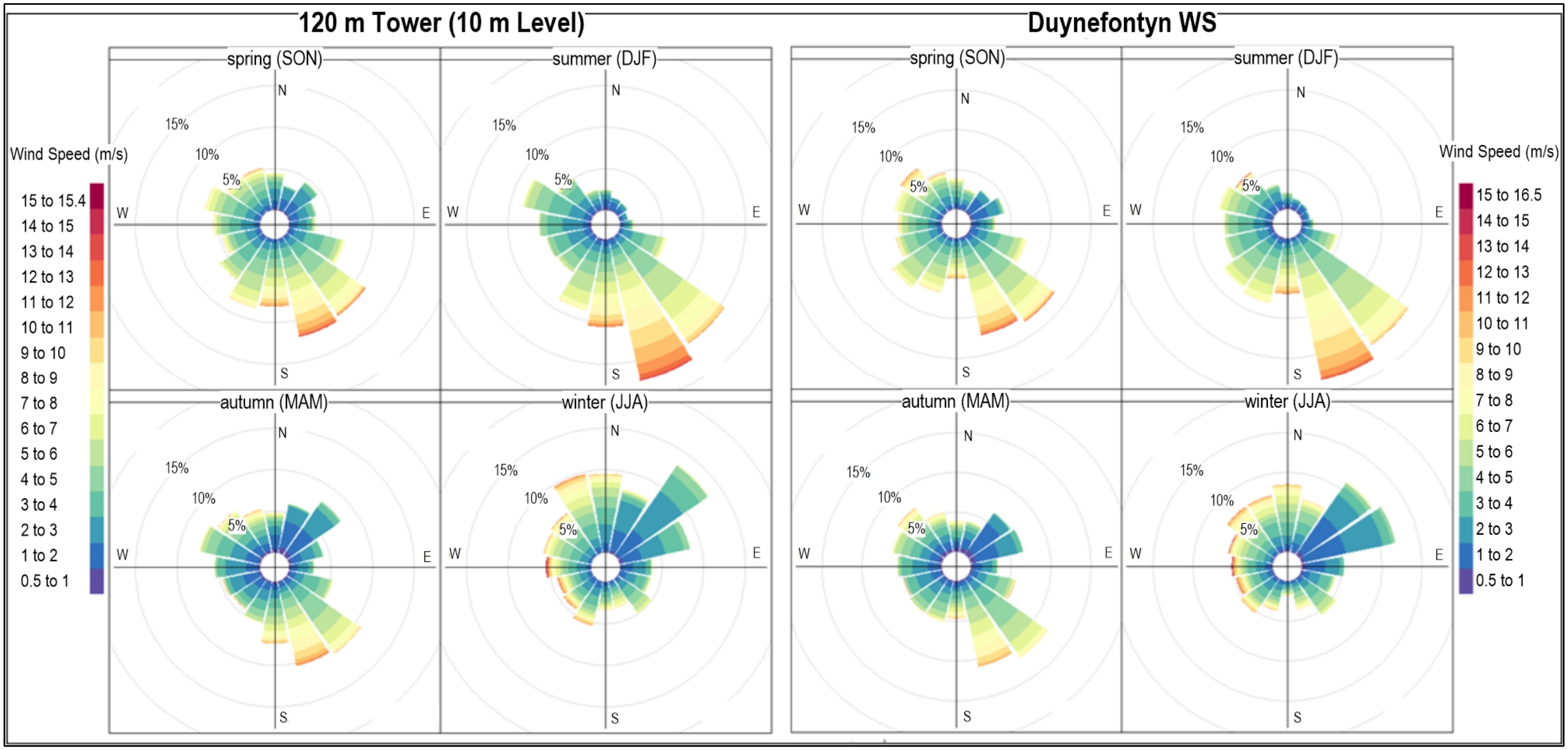

Figure 5.8.8
Comparison of Seasonal Wind Roses (120-m Tower 2017 to 2022, Duynefontyn 2017 to 2022)

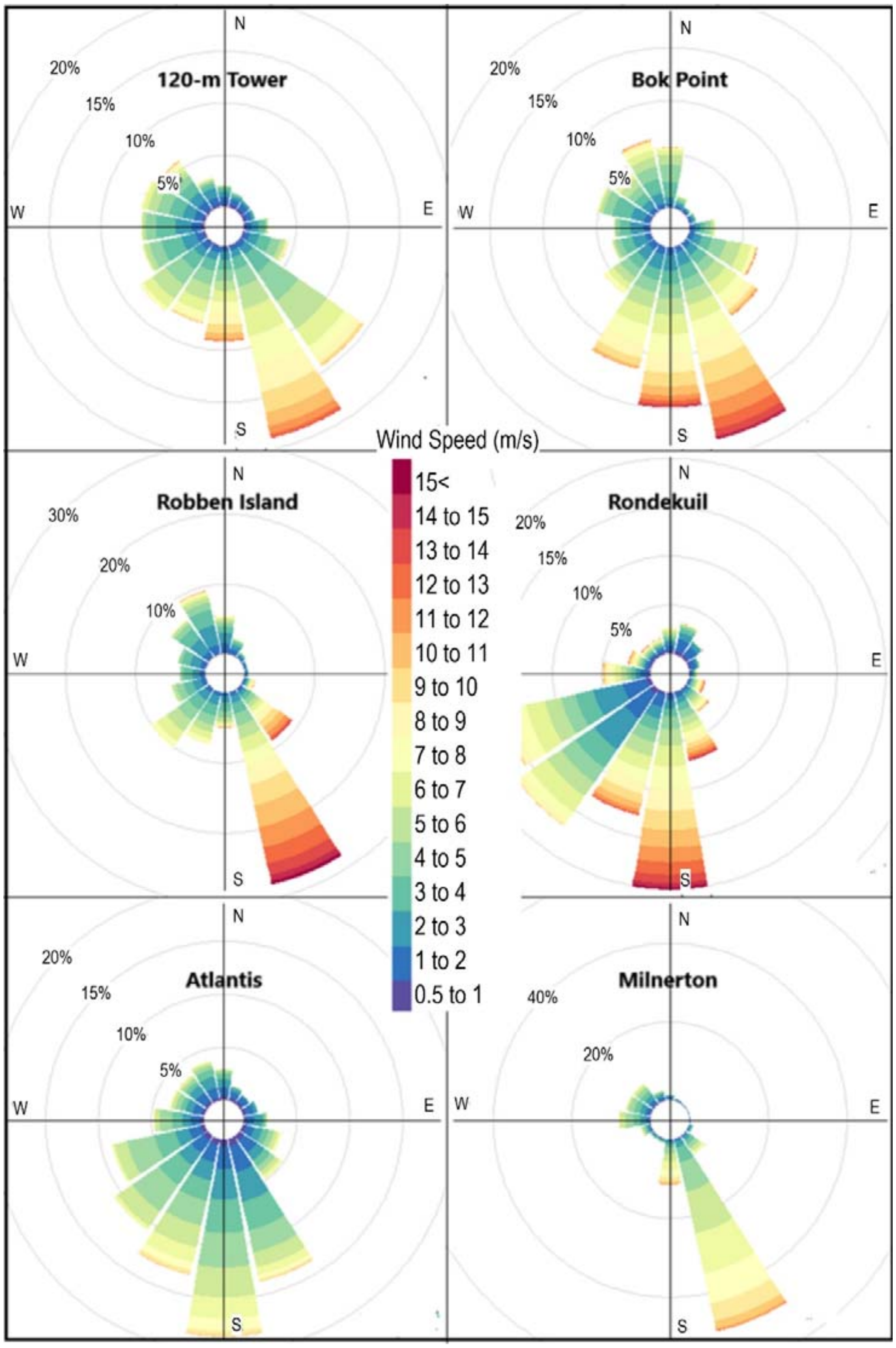

Figure 5.8.9
Comparison of Summer Wind Roses (Koeberg 1997 to 2023, All Other Stations 1998 to 2023)

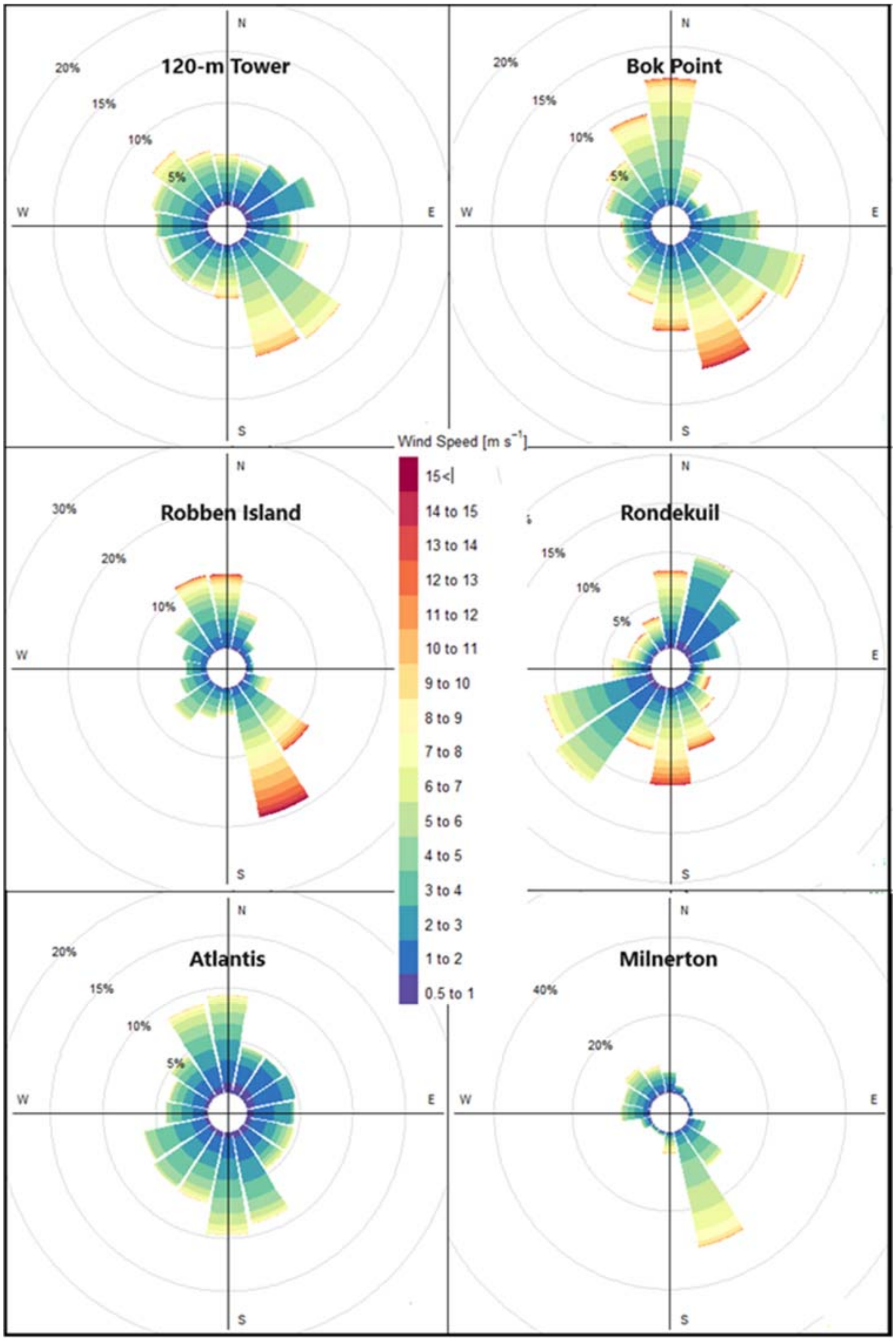

Figure 5.8.10
Comparison of Autumn Wind Roses (Koeberg 1997 to 2023, All Other Stations 1998 to 2023)

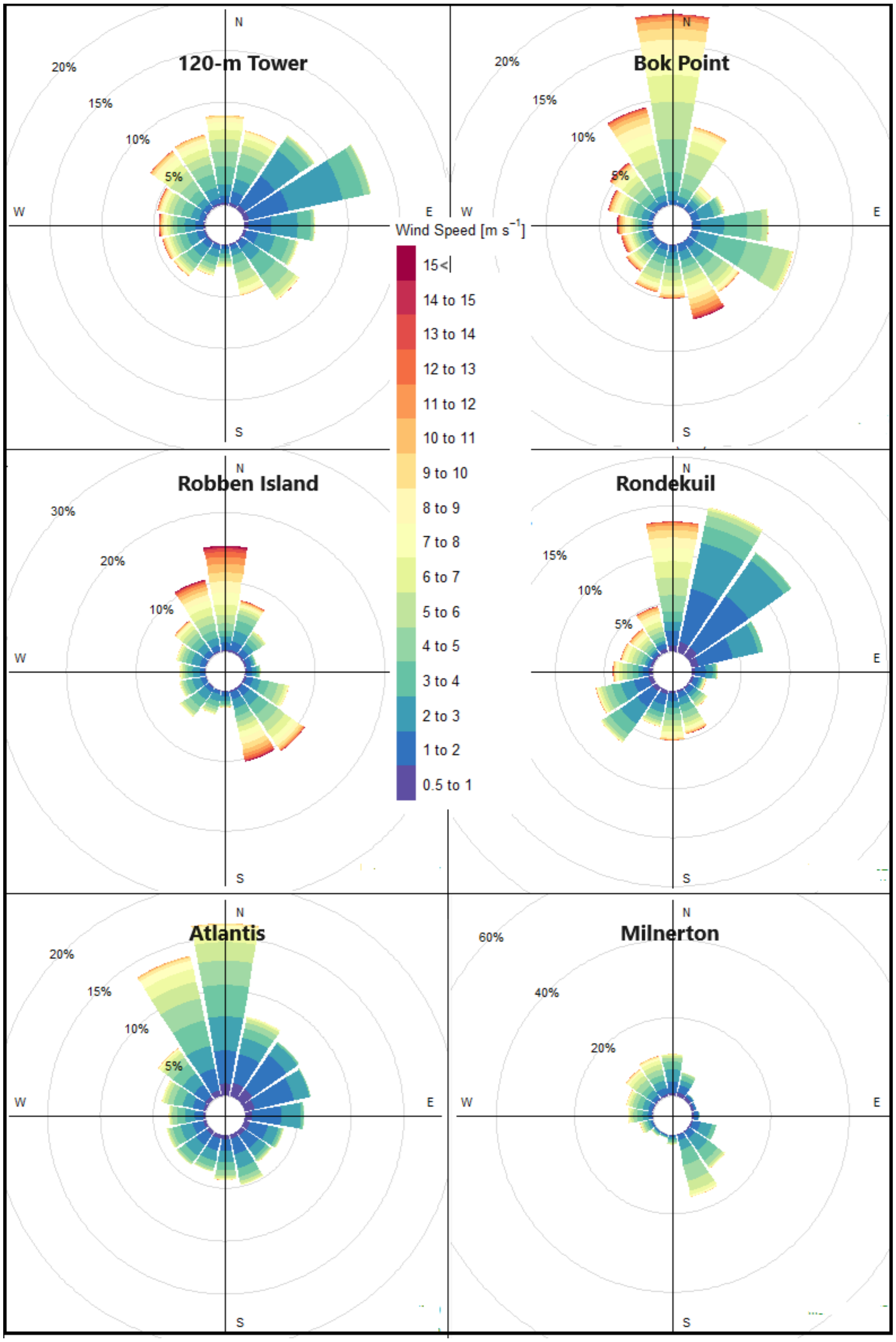

Figure 5.8.11
Comparison of Winter Wind Roses (Koeberg 1997 to 2023, All Other Stations 1998 to 2023)

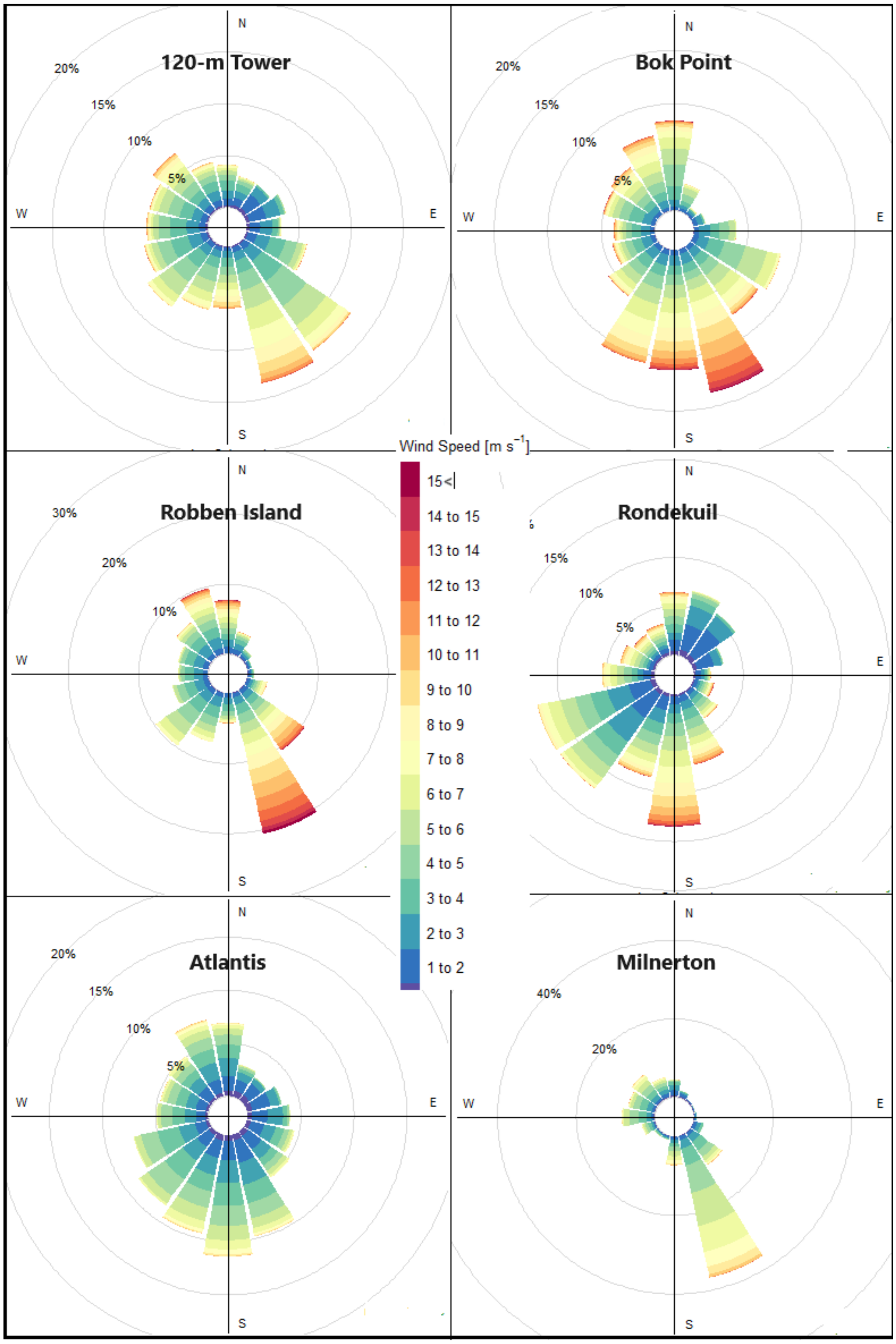

Figure 5.8.12
Comparison of Spring Wind Roses (Koeberg 1997 to 2020, All Other Stations 1998 to 2023)

The conditions during winter are therefore marginally calmer than during summer. Autumn and spring exhibit general wind direction changes from southeasterly and southerly (summer) to northwesterly and northerly (winter), and vice versa. Although wind direction changes occurred between the seasons, similar calm wind conditions were experienced as during summer and winter; spring had similar calm wind conditions during summer and autumn had similar calm wind conditions as during winter.

Monthly average and maximum wind speeds observed at the 120-m tower (10 m level) and at the Duynefontyn WS are provided in ***Table 5.8.16*** to ***Table 5.8.19***.

A summary of the highest hourly average and wind gusts recorded at the 120-m tower during the January 1980 to September 2023 period and the Duynefontyn WS for October 2017 to February 2022 is provided in ***Table 5.8.20*** (Eskom, 2023a). The site experienced exceptionally strong winds in May 1987 (highest gust of 38.8 m/s). Most of the gusts above 20 m/s during the period January 1980 to September 2023 occurred during south-southeasterly winds (36.60 per cent), followed by west-northwesterly (11.78 per cent) and westerly winds (10.17 per cent), as summarised in ***Table 5.8.21***.

Albeit a much shorter period (October 2017 to February 2022), the observations at the Duynefontyn WS also indicate most of the gusts above 20 m/s to be south-southeasterly winds, i.e. 28.26 per cent. This latter period also recorded the highest occurrence of gusts from the south-southeasterly winds (40.74 per cent) at the 120-m tower, followed by westerly and west-southwesterly (14.81 per cent) and west-northwesterly winds (7.41 per cent.

Table 5.8.16
Average Wind Speed per Month at the 120-m Tower (10 m Level) (October 1997 to September 2023)

Wind Direction	Wind Speed [m/s] at 10 m level per Month												Annual
	Jan	Feb	Mar	Apr	May	Jun	Jul	Aug	Sep	Oct	Nov	Dec	
N	2.3	2.2	2.4	3.2	4.1	4.6	4.7	4.6	4.1	3.4	3.3	2.5	3.9
NNE	2.1	1.9	2.1	2.7	3.3	4.0	4.2	3.9	3.4	2.8	2.5	2.1	3.4
NE	1.6	1.5	1.5	1.8	2.0	2.2	2.4	2.3	2.0	1.7	1.7	1.6	2.1
ENE	1.6	1.7	1.8	2.1	2.2	2.4	2.4	2.4	2.2	2.1	1.8	1.7	2.3
E	2.6	2.7	2.5	2.6	2.4	2.3	2.4	2.4	2.3	2.5	2.9	2.8	2.5
ESE	3.5	3.5	3.5	3.7	3.3	2.9	2.8	3.0	3.0	3.7	3.9	3.9	3.4
SE	5.3	5.1	4.9	4.4	4.0	3.5	3.9	3.8	4.1	4.7	5.2	5.1	4.8
SSE	7.3	6.9	6.4	5.6	4.3	4.2	4.6	5.0	5.5	6.2	6.7	7.0	6.4
S	6.3	5.9	5.5	4.7	3.2	3.0	3.2	4.2	4.6	5.5	5.8	6.1	5.5
SSW	4.8	4.6	4.4	3.8	2.9	3.0	3.5	4.2	4.5	4.7	5.0	5.1	4.5
SW	4.3	4.2	3.6	3.1	2.8	3.1	3.8	4.1	4.2	4.4	4.7	4.5	4.2
WSW	3.3	3.1	2.7	2.6	2.7	4.1	3.9	4.5	4.1	3.8	3.8	3.7	3.6
W	3.0	2.9	2.6	2.5	2.7	4.1	4.4	4.3	4.4	3.6	3.5	3.3	3.5
WNW	3.7	3.6	3.1	3.1	3.3	4.4	4.6	4.5	4.6	4.0	4.0	3.9	4.0
NW	4.0	3.5	3.6	4.1	4.7	5.1	5.1	5.5	5.5	4.8	4.9	4.4	4.7
NNW	3.0	2.5	2.9	3.4	4.2	4.6	4.9	4.8	4.5	3.5	3.5	2.9	4.0
TOTAL	4.9	4.5	4.1	3.6	3.3	3.5	3.7	3.9	4.1	4.3	4.7	4.7	4.1

Table 5.8.17
Maximum Wind Speed per Month at the 120-m Tower (10 m Level) (October 1997 to September 2023)

Wind Direction	**Wind Speed [m/s] at 10 m level per Month**												**Annual**
	Jan	**Feb**	**Mar**	**Apr**	**May**	**Jun**	**Jul**	**Aug**	**Sep**	**Oct**	**Nov**	**Dec**	
N	7.3	7.4	7.5	10.6	11.9	13.9	12.6	11.8	10.6	9.9	12.4	8.7	13.9
NNE	7.5	7.3	7.1	9.4	11.4	13.0	12.4	11.6	10.5	10.3	8.5	6.5	13.0
NE	4.3	7.1	7.2	6.4	10.1	8.4	9.9	9.2	4.9	8.9	6.2	5.2	10.1
ENE	7.5	6.1	6.5	6.1	10.0	9.3	8.6	6.2	6.5	6.9	6.8	11.4	11.4
E	9.3	9.7	8.6	9.2	10.0	10.8	7.5	7.7	9.7	9.9	10.1	11.9	11.9
ESE	9.6	8.9	9.9	13.9	11.2	10.3	9.2	9.4	10.5	11.2	12.7	13.3	13.9
SE	12.2	11.2	11.8	10.8	11.7	10.5	14.1	13.0	11.5	13.7	12.8	11.5	14.1
SSE	15.9	15.7	14.4	12.3	10.4	11.4	12.5	12.7	12.2	14.4	14.6	14.1	15.9
S	13.2	14.1	13.2	11.7	8.7	8.5	9.3	9.4	12.2	12.6	12.3	12.9	14.1
SSW	11.2	10.7	10.1	12.9	10.4	10.9	12.2	11.5	10.5	11.2	11.2	11.8	12.9
SW	10.7	9.5	9.0	10.9	13.1	11.8	11.6	13.8	11.3	10.6	11.5	8.9	13.8
WSW	7.2	7.3	7.5	8.4	13.1	15.7	13.9	16.1	14.1	11.0	11.7	9.8	16.1
W	7.5	7.6	8.1	9.8	13.0	16.0	16.5	16.2	13.2	11.0	9.9	10.0	16.5
WNW	10.1	8.6	9.3	10.8	12.6	15.6	15.4	14.3	15.4	10.8	9.9	9.2	15.6
NW	13.6	10.5	10.6	11.5	12.9	14.3	13.6	14.5	14.6	12.9	11.8	13.3	14.6
NNW	10.5	9.7	10.2	12.1	12.4	11.6	13.5	12.7	12.7	12.0	12.8	10.1	13.5
Maximum	15.9	15.7	14.4	13.9	13.1	16.0	16.5	16.2	15.4	14.4	14.6	14.1	16.5

Table 5.8.18

Average Wind Speed per Month at the Duynefontyn WS (October 2017 to February 2022)

Wind Direction	Wind Speed [m/s] at 10 m level per Month												Annual
	Jan	Feb	Mar	Apr	May	Jun	Jul	Aug	Sep	Oct	Nov	Dec	
N	2.3	2.1	1.9	2.8	3.3	4.2	4.3	3.6	3.6	3.0	2.5	2.4	3.4
NNE	1.7	1.9	1.6	1.9	1.9	2.6	2.5	2.2	2.4	1.9	1.9	2.0	2.2
NE	1.9	2.1	1.9	2.0	2.1	2.6	2.7	2.4	2.6	2.1	2.0	2.1	2.4
ENE	1.9	2.0	2.0	2.3	2.3	2.5	2.7	2.4	2.6	2.3	2.1	2.0	2.5
E	2.8	2.5	2.5	2.3	2.4	2.1	2.4	2.6	2.5	3.0	3.1	3.6	2.6
ESE	4.0	3.9	3.5	3.4	2.8	2.7	2.4	3.2	3.2	4.1	3.6	3.7	3.7
SE	5.5	5.4	5.0	4.7	4.3	3.7	3.7	4.0	4.4	5.2	5.7	5.8	5.4
SSE	7.7	7.3	6.6	5.9	4.6	4.1	4.2	5.1	6.0	6.1	7.3	7.9	7.2
S	6.0	5.7	5.4	4.5	3.0	3.1	3.7	4.8	5.1	5.4	6.2	6.2	5.7
SSW	4.9	4.6	3.6	3.4	2.4	3.5	4.2	4.9	4.7	4.6	5.0	4.7	4.7
SW	3.6	3.3	2.7	2.5	3.1	3.8	4.7	4.3	3.8	3.8	3.8	3.4	3.8
WSW	2.8	2.6	2.2	2.2	2.5	4.8	5.1	4.8	3.5	3.9	3.2	3.3	3.6
W	2.8	2.7	2.4	2.5	2.2	5.1	5.4	4.6	4.4	3.2	3.4	3.4	3.7
WNW	3.5	3.5	2.9	3.0	3.4	4.2	4.8	4.4	5.0	3.8	3.8	3.8	4.0
NW	3.1	2.9	3.0	3.6	4.4	4.7	4.8	4.7	4.7	4.5	4.1	3.6	4.2
NNW	2.3	2.7	3.0	3.5	4.7	5.3	5.5	5.0	4.7	4.6	3.3	3.3	4.6

Table 5.8.19
Maximum Wind Speed per Month at the Duynefontyn WS (October 2017 to February 2022)

Wind Direction	Wind Speed [m/s] at 10 m level per Month												Annual
	Jan	Feb	Mar	Apr	May	Jun	Jul	Aug	Sep	Oct	Nov	Dec	
N	5.9	6.5	5.0	9.2	8.7	11.1	10.3	8.3	8.8	8.9	8.3	9.2	11.1
NNE	3.9	4.9	3.0	7.2	4.2	9.2	7.5	5.4	5.2	4.4	3.8	5.3	9.2
NE	4.4	6.5	6.4	4.7	5.0	8.4	6.1	4.8	6.3	4.5	6.9	5.8	8.4
ENE	3.7	3.7	3.5	4.6	4.8	5.1	5.2	4.5	6.0	6.2	3.7	4.3	6.2
E	7.4	6.3	7.9	6.4	4.8	6.8	4.4	8.4	6.8	8.3	8.5	8.5	8.5
ESE	8.6	8.8	8.7	7.6	6.4	6.7	5.4	7.2	8.3	8.8	6.7	7.7	8.8
SE	12.6	10.6	11.1	10.2	9.4	6.9	7.9	7.6	9.0	13.1	12.2	11.6	13.1
SSE	14.4	13.1	12.6	11.4	9.5	9.0	9.4	9.1	11.8	11.8	14.0	14.1	14.4
S	12.4	11.3	11.2	10.4	6.4	7.5	8.7	10.7	10.8	11.4	12.3	12.2	12.4
SSW	9.1	7.7	8.0	7.0	8.8	10.4	12.7	11.9	11.2	9.5	9.1	8.6	12.7
SW	6.7	6.4	6.1	4.7	11.5	13.0	11.4	11.7	8.5	10.9	12.5	7.0	13.0
WSW	5.2	5.4	4.8	7.7	11.6	13.4	13.9	12.4	9.2	10.1	10.8	9.8	13.9
W	4.8	6.5	5.3	5.9	9.8	15.2	15.4	12.4	9.4	10.2	6.7	8.5	15.4
WNW	7.5	8.4	8.2	8.4	7.2	11.9	11.8	9.4	8.9	11.0	8.4	8.3	11.9
NW	6.7	8.0	9.6	8.3	8.6	12.3	12.5	10.5	9.6	9.3	9.1	7.5	12.5
NNW	5.8	7.0	9.5	9.8	11.1	12.7	12.6	11.6	11.9	11.8	6.4	7.5	12.7

Table 5.8.20
Monthly Maximum Hourly Average and Wind Gusts (m/s) at the 120-m Tower and Duynefontyn WS

Month	120-m Tower (10m level)				Duynefontyn WS	
	January 1980 – September 2023		October 2017 – February 2022		October 2017 – February 2022	
	Max of Hour Average	Highest Gust	Max of Hour Average	Highest Gust	Max of Hour Average	Highest Gust
January	15.9	30.2	13.9	22.5	14.4	22.7
February	15.7	28.8	12.3	21.3	13.1	20.4
March	16.3	32.0	11.7	20.3	12.6	20.0
April	13.9	37.1	12.1	18.4	11.4	20.5
May	17.2	38.8	13.1	23.8	11.6	23.0
June	16.0	37.8	15.8	25.3	15.2	25.6
July	16.5	38.8	16.5	31.0	15.4	28.7
August	16.2	31.5	12.9	23.0	12.4	22.8
September	15.4	37.6	12.2	19.8	11.9	20.3
October	14.4	27.2	13.7	21.9	13.1	21.2
November	14.6	27.8	14.0	22.5	14.0	23.2
December	14.1	36.9	14.0	23.8	14.1	23.5
Annual	17.2	38.8	16.5	31.0	15.4	28.7

Table 5.8.21
Gusts Above 20 m/s Directional Occurrence and Maximum Gusts at 120-m Tower (10 m Level) and Duynefontyn WS

Wind Direction	120-m Tower (10m level)				Duynefontyn WS	
	January 1980 – September 2023		October 2017 – February 2022		October 2017 – February 2022	
	Frequency Distribution of Gust Above 20 m/s	Highest Gust (m/s)	Frequency Distribution of Gust Above 20 m/s	Highest Gust (m/s)	Frequency Distribution of Gust Above 20 m/s	Highest Gust (m/s)
N	2.95%	28.0	0.00%	0.0	0.00%	18.7
NNE	0.57%	24.5	0.00%	18.4	0.00%	14.9
NE	0.45%	20.8	0.00%	0.0	0.00%	16.0
ENE	0.74%	22.6	0.00%	0.0	0.00%	12.7
E	1.72%	35.9	0.00%	0.0	0.00%	14.6
ESE	1.44%	36.9	0.00%	18.4	1.09%	21.2
SE	3.24%	23.9	7.41%	23.8	6.52%	21.2
SSE	36.60%	27.8	40.74%	22.5	28.26%	23.5
S	7.21%	37.1	0.00%	0.0	0.00%	18.9
SSW	0.66%	26.4	0.00%	0.0	2.17%	20.3

Wind Direction	120-m Tower (10m level)				Duynefontyn WS	
	January 1980 – September 2023		October 2017 – February 2022		October 2017 – February 2022	
	Frequency Distribution of Gust Above 20 m/s	Highest Gust (m/s)	Frequency Distribution of Gust Above 20 m/s	Highest Gust (m/s)	Frequency Distribution of Gust Above 20 m/s	Highest Gust (m/s)
SW	1.23%	20.9	7.41%	20.8	5.43%	22.6
WSW	7.76%	38.8	14.81%	23.8	19.57%	26.4
W	10.17%	31.5	14.81%	31.0	14.13%	28.7
WNW	11.78%	34.4	7.41%	27.3	8.70%	22.8
NW	4.44%	26.3	3.70%	23.5	2.17%	25.6
NNW	9.03%	32.0	3.70%	21.4	11.96%	22.5
Total/Max	100.00%	38.8	100.00%	31.0	100.00%	28.7

(b) Valley Flow and Land/Sea Breeze Interactions

The differential heating of slopes can potentially give rise to anabatic (up-valley) flow during the day and katabatic (down-valley) flow during the night. However, apart from very small micro-climates, the study area contains no significant valley flow scenarios. On the other hand, diurnal land/sea breeze conditions are evident. The large heat capacity of oceans reduces water-surface temperature change to near-zero values during a diurnal cycle. The land surface, however, warms and cools more dramatically because of the small molecular conductivity and heat capacity in soil prevents the diurnal temperature signal from propagating rapidly away from the surface. As a result, the land is warmer than the water during the day and cooler at night. During the morning, when the nocturnal surface boundary layer has been eliminated, air begins to rise over the warm land near the shoreline, and cooler air from the water flows in to replace it. This is known as the sea-breeze. A return circulation (the anti-sea-breeze) brings the warmer air back out to sea where it descends toward the sea surface to close the circulation. At night, land surfaces usually cool faster than the neighbouring water bodies, reversing the temperature gradient that was present during the day. The result is a land breeze: cool air from land flows out to sea at low levels, warms, rises, and returns aloft toward land (anti-land-breeze) where it eventually descends to close the circulation (Stull, 1997).

Low to moderate wind regimes at the site largely reflect the land/sea breezes with increased frequency of westerlies (sea breeze) observed during the day-time and increased frequency of easterlies (land breeze) occurring during the night-time.

5.8.6.1.2 Ambient Air Temperature

Temperature is a primary climatological parameter that is used as an index of the energy status of the environment. The monitoring levels for air temperature at the 120-m tower are at heights applicable to the Koeberg emergency programme requirements, i.e. 10 m, 50 m, 85 m and 120 m above ground level. Similarly, monitoring levels for temperature differences are representative of and characterise the magnitude of atmospheric turbulence at potential release height(s) from the existing nuclear installation. The pairing of sensor heights on the 120-m tower are 10 m and 50 m, and 10 m and 120 m. The reference height for ambient air temperature measurement is typically 2 m above ground level (***American National Standard, 2015***). An additional monitoring campaign was therefore also established for a three-year period from January 2009 to December 2011 at a location near the 120-m tower. Ambient temperature measurement at 2 m was continued from October 2017 at the Duynefontyn WS. In addition, ambient temperature was also measured at 8 m above ground level.

Long-term dry bulb air temperature observations at the 120-m tower, at the 10 m level, over the period 1997 to 2023 (Eskom, 2023a) recorded the following:

- mean of the daily maximum: 20.1 °C (***Table 5.8.22***);
- mean of the daily minimum: 13.1 °C (***Table 5.8.23***);
- the month with the highest mean daily maximum temperature of 24.1 °C is February (***Table 5.8.22***);
- the month with the lowest mean daily maximum temperature of 16.9 °C is August (***Table 5.8.22***);
- the month with the highest mean daily minimum temperature of 16.8 °C is February (***Table 5.8.23***);
- the month with the lowest mean daily minimum temperature of 9.6 °C is July (***Table 5.8.23***).

Observations at 2 m above ground level were for the periods (a) January 2009 to December 2011 (Koeberg WS) and (b) October 2017 to February 2022 (Duynefontyn WS) recorded the following statistics:

- mean of the daily maximum: (a) 22.6 °C and (b) 20.7 °C (***Table 5.8.22***);
- mean of the daily minimum: (a) 12.5 °C and (b) 12.6 °C (***Table 5.8.23***);

- the months with the highest mean daily maximum temperature of (a) 27.2 °C and (b) 24.5 °C are January and February, respectively (***Table 5.8.22***);
- the months with the lowest mean daily maximum temperature of (a) 18.5 °C and (b) 17.0 °C are June/August and August, respectively (***Table 5.8.22***);
- the month with the highest mean daily minimum temperature of a) 17.1 °C and (b) 16.6 °C is February and January, respectively (***Table 5.8.23***);
- the month with the lowest mean daily minimum temperature of (a) 8.2 °C and (b) 8.4 °C is July/August and August, respectively (***Table 5.8.23***).

Means of the daily maximums and minimums at 8 m above ground level at the Duynefontyn WS were:

- mean of the daily maximum: 19.9 °C (***Table 5.8.22***);
- mean of the daily minimum: 12.7 °C (***Table 5.8.23***).

Table 5.8.22
Mean Daily Maximum Ambient Air Dry Bulb Temperature at the Duynefontyn site

Month	**Temperature (°C) at Height above Ground Level**						
	Koeberg WS (2009-2013) (1)	**Duynefontyn WS (2017-2022) (2)**		**120-m Tower (1997-2023) (3)**			
	2 m	**2 m**	**8 m**	**10 m**	**50 m**	**85 m**	**120 m**
January	27.2	23.9	23.3	22.9	22.3	22.1	22.1
February	27.1	24.5	23.5	24.1	23.6	23.5	23.5
March	26.3	22.2	21.2	22.2	21.9	21.9	22.0
April	23.4	21.0	20.2	20.9	20.8	20.9	21.2
May	19.8	19.4	18.8	18.7	18.6	18.7	18.4
June	18.5	18.7	18.1	17.5	17.2	17.1	17.1
July	18.9	18.2	17.6	17.1	16.7	16.6	16.6
August	18.5	17.0	16.2	16.8	16.4	16.2	16.2
September	19.6	18.9	17.9	17.8	17.2	16.1	16.7
October	22.0	20.8	19.8	19.8	19.3	18.5	18.5
November	23.6	21.3	20.3	20.9	20.2	19.2	19.2
December	26.1	22.5	21.6	22.5	21.8	21.6	21.7
Annual	22.6	20.8	19.9	20.1	19.6	19.4	19.4

Notes:

(1) The statistics included 1 January 2009 to 30 September 2013 period.
(2) The statistics included 1 October 2017 to 28 February 2022 period.
(3) The statistics included 1 October 1997 to 31 September 2023 period.

Table 5.8.23
Mean Daily Minimum Ambient Air Dry Bulb Temperature at the Duynefontyn site

Month	Temperature (°C) at Height above Ground Level						
	Koeberg WS (2009-2013) (1)	Duynefontyn WS (2017-2022) (2)		120-m Tower (1997-2023) (3)			
	2 m	2 m	8 m	10 m	50 m	85 m	120 m
January	16.9	16.5	16.4	16.1	16.5	16.5	16.7
February	17.1	16.8	16.5	16.9	17.3	17.4	17.6
March	16.0	15.3	15.1	15.3	16.0	16.1	16.4
April	13.1	13.0	13.1	13.8	14.8	14.9	15.4
May	10.6	11.3	11.4	11.9	13.3	13.6	13.5
June	9.2	10.4	10.4	10.3	12.1	12.5	12.7
July	8.2	9.0	9.0	9.6	11.4	11.7	12.0
August	8.2	8.4	8.4	9.8	11.3	11.5	11.7
September	9.3	10.2	10.4	10.9	11.9	11.5	12.1
October	11.8	11.8	12.1	12.7	13.5	13.1	13.2
November	13.3	14.0	14.0	14.1	14.7	14.1	14.2
December	15.9	15.2	15.2	15.8	16.2	16.2	16.4
Annual	12.5	12.8	12.6	13.1	14.1	14.1	14.3

Notes:

(1) The statistics included 1 January 2009 to 30 September 2013 period.
(2) The statistics included 1 October 2017 to 28 February 2022 period.
(3) The statistics included 1 October 1997 to 31 September 2023 period.

More temperature statistics for Duynefontyn WS, the 120-m tower, Bok Point, Robben Island, Rondekuil, Atlantis and Milnerton are given in the tables below (***Table 5.8.24*** to ***Table 5.8.31***).

The most extreme hourly average temperatures recorded at the 120-m tower (10 m level) over the 1997 to 2023 period were 3.0 °C (August 2021) and 38.8 °C (March 2015). The extreme hourly temperatures observed at the 2 m level near the 120-m tower were 1.8 °C (August 2011) and 40.2 °C (February 2010), over the period 2009 to 2012. The extreme hourly temperatures at the Duynefontyn WS (2 m level) over the 2017-2022 period were 2.7 °C (August 2020) and 37.8 °C (February 2018) (Eskom, 2023a). The most extreme hourly average temperatures recorded at the Bok Point WS (1998 to 2019) were 5.5 °C (August 2003) and 36.8 °C (November 2000). At the Milnerton WS over the 1998 to 2022 period (2020 only October, January 2021 to June 2022) the extreme hourly average temperatures were 0.9 °C (July 2011) and 40.8 °C (January 2000). The most extreme hourly average temperatures recorded at the Rondekuil WS over the 1998 to 2023 period were 1.3 °C (July 2003) and 41.0 °C (March 2015) and the most extreme hourly average temperatures recorded at the Robben Island WS over the 1998 to 2023 period were 6.5 °C (August 2023) and 38.3 °C (March 2015). The most extreme hourly average temperatures recorded at the Atlantis WS over the 1998 to 2023 period were 0.9 °C (July 2011) and 41.0 °C (March 2015).

The average number of days which were above or below selected maximum and minimum temperatures are also provided in the tables. Days with maximum hourly temperatures above 30 °C and 35 °C and with minimum hourly temperatures below 10 °C and 5 °C were used in the analyses. Atlantis recorded the highest average number of days with hourly temperatures above 35 °C, i.e. 1.6 days, and this was for February and 1.5 days for March (***Table 5.8.30***). Rondekuil WS recorded the second highest average number of days with hourly temperatures above 35 °C, i.e. 1.5 days, and this was for February (***Table 5.8.29***). Milnerton WS recorded 0.3 days above 35 °C, whereas Bok Point did not record any.

Rondekuil WS recorded a maximum of 7.5 days with hourly average temperatures above 30 °C. Atlantis WS recorded more days with hourly average temperatures above 30 °C, i.e. 7.7 days. Both sites recorded these days during January. Milnerton WS recorded the 2.8 days above 30 °C (February). The lowest average number of days for these temperatures were recorded at Robben Island WS (maximum of 1.2 days) and Bok Point WS a maximum of 0.3 days.

The highest average number of days with temperatures above 35 °C and 30 °C recorded at the Duynefontyn WS were 0.4 days (October) and 1.2 days (October), respectively (***Table 5.8.24***). However, the monitoring period was only for 2017 to 2022. The average number of days with temperatures above 35 °C and 30 °C recorded at the 120-m tower (10 m level) were 0.2 days (February and April) and 2.6 days (January), respectively (***Table 5.8.26***).

The highest average number of days with temperatures below 10 °C and 5 °C were recorded at the Duynefontyn WS, i.e. 22.8 days (August) and 3.0 days (August), respectively (***Table 5.8.24***). The highest average number of days with temperatures below 10 °C and 5 °C recorded at the 120-m tower (10 m level) were 15.9 days (July) and 0.4 days (July), respectively (***Table 5.8.26***). Bok Point WS (***Table 5.8.27***) recorded 5.3 days, Robben Island WS (***Table 5.8.28***) 1.3 days, Atlantis WS (***Table 5.8.30***) 16.5 days and 9.0 days at the Milnerton WS (***Table 5.8.31***). Rondekuil WS recorded the highest number of 21.4 days below 10°C, and 3.6 days below 5 °C.

The corresponding wet-bulb temperature[7] statistics during the second campaign were estimated as follows:

- mean of the daily maximum: 16.2 °C;
- mean of the daily minimum: 11.0 °C;
- the month with the highest mean daily maximum temperature of 19.1 °C is February;
- the month with the lowest mean daily maximum temperature of 13.5 °C is August;
- the month with the highest mean daily minimum temperature of a) 14.8 °C is February;
- the month with the lowest mean daily minimum temperature of 7.1 °C is August.

The lowest and highest hourly average wet-bulb temperature was 1.2 °C (August 2018) and 23.8 °C (January 2020), respectively.

---

[7] An equation for wet-bulb temperature as a function of air temperature and relative humidity at standard sea level pressure was derived by Stull (Stull, 2011):

$$T_W = T \operatorname{atan}\left(0.151977\sqrt{RH\% + 8.313659}\right) + \operatorname{atan}(T + RH\%) - \operatorname{atan}(RH\% - 1.676331) \\ + 0.00391838(RH\%)^{\frac{3}{2}} \operatorname{atan}(0.023RH\%) - 4.686035$$

Where T_W = Wet-bulb temperature [°C]
T = Dry-bulb temperature [°C]
$RH\%$ = Relative humidity [per cent]
$\operatorname{atan}()$ = arctangent function [radians]

The errors between the equation estimate and the T_W values used to develop the equation had a mean error of -0.00528°C, a median error of 0.0268°C, and a mean absolute error is 0.288°C, and the fraction of variance (r^2) explained by the regression of 99.95 per cent.

To illustrate its usage, plugging $T = 20\,°C$ and $RH\% = 50\ per\ cent$into the equation gives:

$$T_W = 20 \operatorname{atan}\left(0.151977\sqrt{50 + 8.313659}\right) + \operatorname{atan}(20 + 50) - \operatorname{atan}(50 - 1.676331) + 0.00391838(50)^{\frac{3}{2}} \operatorname{atan}(0.023\ x\ 50) \\ - 4.686035 = 13.7°C$$

Table 5.8.24
Ambient Air Dry Bulb Temperature at Duynefontyn WS (2 m Level) (October 2017 to February 2022)

Month	Daily Mean		95% Confidence Interval of Mean	Daily Median	Percentiles		Maximums and Minimums						A#DDMxT		A#DDMnT	
	MDT	StdDev			25%	75%	MnMDT	MxMDT	TMn	TMx	MDMnT	MDMxT	>35.0	>30.0	<10.0	<5.0
1	20.1	2.1	±4.07	19.8	18.2	21.7	16.0	25.4	10.6	32.8	16.6	24.0	0.0	1.8	0.0	0.0
2	20.3	2.0	±3.86	20.1	18.2	21.8	16.1	25.4	11.7	35.4	16.5	24.4	0.2	1.8	0.0	0.0
3	18.5	1.8	±3.58	18.3	16.7	20.1	14.7	23.1	9.5	31.5	15.2	22.1	0.0	0.5	0.5	0.0
4	17.0	1.9	±3.82	16.8	15.1	18.9	12.1	21.7	8.2	37.4	13.2	21.2	0.3	0.3	2.8	0.0
5	15.2	2.1	±4.19	15.1	12.8	17.3	11.2	21.3	6.1	32.4	11.3	19.4	0.0	0.5	8.5	0.0
6	14.4	2.2	±4.22	14.2	11.8	16.6	10.8	23.3	5.3	29.7	10.4	18.7	0.0	0.0	11.8	0.0
7	13.5	2.2	±4.39	13.2	10.9	15.8	8.7	22.6	3.7	30.7	9.1	18.2	0.0	0.3	19.5	1.3
8	12.9	1.6	±3.15	13.2	10.7	15.4	8.4	16.3	2.7	26.9	8.4	17.0	0.0	0.0	22.8	3.0
9	14.8	2.2	±4.30	14.5	13.0	16.7	10.4	22.7	3.6	36.3	10.2	18.9	0.3	1.0	13.3	0.5
10	16.5	2.4	±4.76	16.1	14.3	18.3	11.1	26.3	4.3	37.8	11.9	20.8	0.4	1.2	6.8	0.2
11	17.7	1.9	±3.72	17.5	15.9	19.3	13.7	23.7	7.8	32.2	14.0	21.3	0.0	0.4	2.4	0.0
12	18.8	2.0	±3.90	18.2	16.8	20.4	14.7	26.1	10.1	34.2	15.2	22.5	0.0	0.4	0.0	0.0

MDT - Mean daily temperature: mean of the temperatures observed at 24 equidistant times in the course of a continuous 24-hour period (midnight to midnight).
StdDev – Standard deviation.
MnMDT - Minimum of mean daily temperature for a month: minimum of the mean daily temperatures.
MxMDT - Maximum of mean daily temperature for a month: maximum of the mean daily temperatures.
TMn - Minimum hourly temperature: minimum of the temperatures observed at 24 equidistant times in the course of a continuous 24-hour period
TMx - Maximum hourly temperature: maximum of the temperatures observed at 24 equidistant times in the course of a continuous 24-hour period
MDMxT - Mean daily maximum temperature for a month: mean of the daily maximum temperatures.
MDMnT - Mean daily minimum temperature for a month: mean of the daily minimum temperatures.
A#DDMxT - average number of days with maximum hourly temperature above.
A#DDMnT - average number of days with minimum hourly temperature below.

Table 5.8.25
Ambient Air Dry Bulb Temperature near 120-m tower (2 m Level) (January 2009 to September 2013)

Month	Daily Mean		95% Confidence Interval of Mean	Daily Median	Percentiles		Maximums and Minimums						A#DDMxT		A#DDMnT	
	MDT	StdDev			25%	75%	MnMDT	MxMDT	TMn	TMx	MDMnT	MDMxT	>35.0	>30.0	<10.0	<5.0
1	21.7	4.5	±8.76	19.5	16.9	22.4	17.0	29.0	10.9	38.5	16.9	27.2	0.2	1.4	0.0	0.0
2	21.8	4.1	±7.96	20.9	18.5	23.4	17.3	28.9	10.2	40.2	17.1	27.1	0.3	1.5	0.0	0.0
3	20.8	4.1	±8.08	21.3	19.2	24.3	15.8	28.7	8.6	37.0	16.0	26.3	0.3	1.3	0.2	0.0
4	17.8	4.3	±8.42	21.4	19.0	24.1	7.8	27.1	5.4	38.0	13.1	23.4	0.1	0.3	1.0	0.0
5	15.1	4.3	±8.35	19.4	17.0	22.0	10.7	21.6	4.1	30.3	10.6	19.8	0.0	0.0	2.7	0.0
6	13.6	4.0	±7.91	16.1	13.9	18.4	9.3	20.6	3.6	30.3	9.2	18.5	0.0	0.0	3.7	0.6
7	13.3	3.9	±7.62	14.7	12.2	16.8	7.6	18.7	2.0	28.5	8.2	18.9	0.0	0.0	4.3	0.9
8	13.2	4.1	±8.05	13.4	10.7	15.6	8.9	19.1	1.8	29.4	8.2	18.4	0.0	0.0	4.3	0.8
9	14.4	4.4	±8.62	13.3	10.4	15.7	10.2	19.5	2.9	32.6	9.3	19.4	0.0	0.1	3.3	0.4
10	17.0	4.0	±7.89	13.7	11.2	16.2	12.6	22.0	5.1	31.2	11.8	22.0	0.0	0.1	1.4	0.0
11	18.5	4.0	±7.78	15.3	13.1	17.9	14.0	24.9	6.0	36.2	13.3	23.6	0.0	0.5	0.5	0.0
12	20.8	4.0	±7.78	17.1	14.9	19.7	14.9	27.5	6.7	36.0	15.9	26.1	0.1	0.9	0.1	0.0

MDT - Mean daily temperature: mean of the temperatures observed at 24 equidistant times in the course of a continuous 24-hour period (midnight to midnight).
StdDev – Standard deviation.
MnMDT - Minimum of mean daily temperature for a month: minimum of the mean daily temperatures.
MxMDT - Maximum of mean daily temperature for a month: maximum of the mean daily temperatures.
TMn - Minimum hourly temperature: minimum of the temperatures observed at 24 equidistant times in the course of a continuous 24-hour period
TMx - Maximum hourly temperature: maximum of the temperatures observed at 24 equidistant times in the course of a continuous 24-hour period
MDMxT - Mean daily maximum temperature for a month: mean of the daily maximum temperatures.
MDMnT - Mean daily minimum temperature for a month: mean of the daily minimum temperatures.
A#DDMxT - average number of days with maximum hourly temperature above.
A#DDMnT - average number of days with minimum hourly temperature below.

Table 5.8.26
Ambient Air Dry Bulb Temperature at the 120-m Tower (10 m Level) (October 1997 to September 2023)

Month	Daily Mean		95% Confidence Interval of Mean	Daily Median	Percentiles		Maximums and Minimums						A#DDMxT		A#DDMnT	
	MDT	StdDev			25%	75%	MnMDT	MxMDT	TMn	TMx	MDMnT	MDMxT	>35.0	>30.0	<10.0	<5.0
1	20.1	2.3	±4.50	19.7	18.0	21.6	14.4	28.9	11.7	37.3	16.1	22.9	0.1	2.6	1.2	1.2
2	20.2	2.2	±4.34	19.9	18.1	21.6	14.5	28.1	10.2	36.4	16.9	24.1	0.2	2.2	0.0	0.0
3	18.9	2.3	±4.52	18.6	16.8	20.4	11.2	27.4	8.7	38.8	15.3	22.2	0.1	1.5	0.7	0.6
4	17.1	2.5	±4.84	16.8	14.9	18.7	11.1	29.2	7.1	36.1	13.8	20.9	0.2	0.8	1.4	0.0
5	15.1	2.2	±4.27	14.9	13.2	16.7	6.5	23.8	4.9	32.1	11.9	18.7	0.0	0.4	5.7	0.1
6	13.7	2.1	±4.09	13.5	11.7	15.4	8.6	23.0	4.6	30.6	10.3	17.5	0.0	0.0	13.2	0.1
7	13.2	2.1	±4.12	12.9	11.1	14.9	7.9	22.2	3.2	30.6	9.6	17.1	0.0	0.0	17.5	0.5
8	13.3	2.0	±3.91	13.1	11.4	14.9	8.1	23.8	3.0	32.1	9.8	16.8	0.0	0.1	15.9	0.4
9	14.3	2.0	±3.91	14.1	12.5	15.8	9.8	24.2	4.2	35.9	10.9	17.8	0.1	0.4	10.2	0.1
10	16.1	2.3	±4.57	15.8	14.1	17.6	10.0	27.2	5.0	37.1	12.7	19.8	0.1	0.6	3.9	0.0
11	17.4	2.1	±4.15	17.1	15.4	18.8	11.8	26.5	6.7	36.7	14.1	20.9	0.0	0.7	0.6	0.0
12	19.0	2.2	±4.36	18.7	17.0	20.5	13.1	27.9	8.4	36.6	15.8	22.5	0.0	1.4	0.1	0.0

MDT - Mean daily temperature: mean of the temperatures observed at 24 equidistant times in the course of a continuous 24-hour period (midnight to midnight).
StdDev – Standard deviation of daily mean temperatures.
MnMDT - Minimum of mean daily temperature for a month: minimum of the mean daily temperatures.
MxMDT - Maximum of mean daily temperature for a month: maximum of the mean daily temperatures.
TMn - Minimum hourly temperature: minimum of the temperatures observed at 24 equidistant times in the course of a continuous 24-hour period
TMx - Maximum hourly temperature: maximum of the temperatures observed at 24 equidistant times in the course of a continuous 24-hour period
MDMxT - Mean daily maximum temperature for a month: mean of the daily maximum temperatures.
MDMnT - Mean daily minimum temperature for a month: mean of the daily minimum temperatures.
A#DDMxT - average number of days with maximum hourly temperature above.
A#DDMnT - average number of days with minimum hourly temperature below.

Table 5.8.27
Ambient Air Dry Bulb Temperature at the Bok Point WS (10 m Level) (January 1998 to June 2019)

Month	Daily Mean		95% Confidence Interval of Mean	Daily Median	Percentiles		Maximums and Minimums						A#DDMxT		A#DDMnT	
	MDT	StdDev			25%	75%	MnMDT	MxMDT	TMn	TMx	MDMnT	MDMxT	>35.0	>30.0	<10.0	<5.0
1	18.1	1.8	±3.44	17.8	16.6	19.2	14.7	29.6	12.0	35.5	16.0	20.5	0.0	0.2	0.0	0.0
2	18.4	1.9	±3.64	18.0	16.7	19.5	14.2	26.7	11.0	33.1	16.1	20.9	0.0	0.3	0.0	0.0
3	17.4	1.9	±3.79	17.1	15.7	18.6	12.3	26.7	8.1	32.4	15.0	20.0	0.0	0.3	0.1	0.0
4	16.5	2.2	±4.27	16.1	14.7	17.8	10.8	30.7	7.8	35.5	14.0	19.3	0.0	0.2	0.5	0.0
5	15.5	2.0	±3.92	15.1	13.8	16.5	11.6	25.5	8.0	33.0	13.0	18.2	0.0	0.3	0.9	0.0
6	14.5	2.0	±3.97	14.2	12.8	15.7	10.3	23.1	6.9	29.3	12.0	17.3	0.0	0.0	3.2	0.0
7	14.1	2.2	±4.35	13.7	12.3	15.4	9.2	23.8	7.2	30.8	11.5	17.0	0.0	0.0	5.3	0.0
8	13.9	1.8	±3.45	13.7	12.3	15.1	9.0	24.0	5.5	29.6	11.4	16.4	0.0	0.0	4.9	0.0
9	14.5	1.7	±3.24	14.4	13.1	15.7	10.5	23.5	7.3	30.9	12.1	17.0	0.0	0.2	2.5	0.0
10	15.7	1.8	±3.54	15.6	14.2	17.0	11.0	25.9	6.8	33.4	13.3	18.2	0.0	0.2	0.9	0.0
11	16.4	1.6	±3.18	16.3	15.0	17.6	12.1	24.6	8.8	36.8	14.2	18.6	0.0	0.0	0.1	0.0
12	17.6	1.7	±3.31	17.4	16.1	18.7	13.5	24.2	10.1	30.7	15.4	19.8	0.0	0.1	0.0	0.0

MDT - Mean daily temperature: mean of the temperatures observed at 24 equidistant times in the course of a continuous 24-hour period (midnight to midnight).
StdDev – Standard deviation.
MnMDT - Minimum of mean daily temperature for a month: minimum of the mean daily temperatures.
MxMDT - Maximum of mean daily temperature for a month: maximum of the mean daily temperatures.
TMn - Minimum hourly temperature: minimum of the temperatures observed at 24 equidistant times in the course of a continuous 24-hour period
TMx - Maximum hourly temperature: maximum of the temperatures observed at 24 equidistant times in the course of a continuous 24-hour period
MDMxT - Mean daily maximum temperature for a month: mean of the daily maximum temperatures.
MDMnT - Mean daily minimum temperature for a month: mean of the daily minimum temperatures.
A#DDMxT - average number of days with maximum hourly temperature above.
A#DDMnT - average number of days with minimum hourly temperature below.

Table 5.8.28
Ambient Air Dry Bulb Temperature at the Robben Island WS (10 m Level) (January 1998 to September 2023)

Month	Daily Mean		95% Confidence Interval of Mean	Daily Median	Percentiles		Maximums and Minimums						A#DDMxT		A#DDMnT	
	MDT	StdDev			25%	75%	MnMDT	MxMDT	TMn	TMx	MDMnT	MDMxT	>35.0	>30.0	<10.0	<5.0
1	19.7	1.7	±3.38	19.5	17.7	21.2	15.2	27.1	12.4	35.8	16.6	23.5	0.0	1.2	0.0	0.0
2	19.7	1.7	±3.32	19.6	17.8	21.2	14.9	25.9	12.1	34.5	16.7	23.6	0.0	1.2	0.0	0.0
3	18.3	2.0	±3.93	18.3	16.4	19.9	12.5	26.8	8.2	38.3	15.6	21.9	0.1	1.1	0.0	0.0
4	17.0	2.0	±3.92	16.8	15.1	18.4	11.9	25.8	9.3	34.6	14.6	20.3	0.0	0.4	0.0	0.0
5	15.6	1.6	±3.20	15.4	14.1	16.6	12.3	21.5	9.9	30.6	13.6	18.2	0.0	0.0	0.0	0.0
6	14.9	1.5	±2.86	14.7	13.6	15.8	11.0	20.6	8.9	28.2	13.0	17.2	0.0	0.0	0.2	0.0
7	14.5	1.6	±3.13	14.3	13.2	15.5	10.5	20.7	8.6	29.1	12.7	16.9	0.0	0.0	0.8	0.0
8	14.4	1.5	±2.97	14.3	13.1	15.4	8.7	21.2	6.5	28.5	12.6	16.7	0.0	0.0	1.0	0.0
9	15.2	1.6	±3.14	15.1	13.9	16.2	10.5	23.0	8.4	32.5	13.3	17.6	0.0	0.1	0.3	0.0
10	16.6	1.8	±3.44	16.4	15.0	17.9	11.5	24.4	8.7	33.0	14.3	19.6	0.0	0.2	0.1	0.0
11	17.6	1.7	±3.34	17.4	15.8	18.9	13.0	25.6	11.2	34.8	15.0	20.7	0.0	0.2	0.0	0.0
12	18.9	1.7	±3.38	18.8	17.0	20.5	13.6	25.4	10.7	35.1	16.1	22.3	0.0	0.6	0.0	0.0

MDT - Mean daily temperature: mean of the temperatures observed at 24 equidistant times in the course of a continuous 24-hour period (midnight to midnight).
StdDev – Standard deviation.
MnMDT - Minimum of mean daily temperature for a month: minimum of the mean daily temperatures.
MxMDT - Maximum of mean daily temperature for a month: maximum of the mean daily temperatures.
TMn - Minimum hourly temperature: minimum of the temperatures observed at 24 equidistant times in the course of a continuous 24-hour period
TMx - Maximum hourly temperature: maximum of the temperatures observed at 24 equidistant times in the course of a continuous 24-hour period
MDMxT - Mean daily maximum temperature for a month: mean of the daily maximum temperatures.
MDMnT - Mean daily minimum temperature for a month: mean of the daily minimum temperatures.
A#DDMxT - average number of days with maximum hourly temperature above.
A#DDMnT - average number of days with minimum hourly temperature below.

Table 5.8.29

Ambient Air Dry Bulb Temperature at the Rondekuil WS (10 m Level) (January 1998 to September 2023)

Month	Daily Mean		95% Confidence Interval of Mean	Daily Median	Percentiles		Maximums and Minimums						A#DDMxT		A#DDMnT	
	MDT	StdDev			25%	75%	MnMDT	MxMDT	TMn	TMx	MDMnT	MDMxT	>35.0	>30.0	<10.0	<5.0
1	22.1	2.6	±5.16	21.7	18.9	24.5	14.3	31.3	11.9	39.7	17.5	27.1	1.3	7.5	0.0	0.0
2	22.2	2.5	±4.93	22.1	19.1	24.7	15.5	30.0	11.5	40.2	17.6	27.5	1.5	7.4	0.0	0.0
3	20.4	2.9	±5.72	20.1	17.3	22.8	11.8	30.3	5.1	41.0	15.9	25.7	1.0	5.4	0.7	0.0
4	18.1	2.9	±5.75	17.9	15.0	20.6	10.4	30.1	4.6	38.0	13.7	23.8	0.4	3.2	2.2	0.1
5	15.5	2.4	±4.76	15.1	12.9	17.5	9.3	24.6	4.8	33.5	11.4	20.6	0.0	1.0	8.5	0.1
6	13.3	2.2	±4.26	13.1	11.0	15.3	7.7	21.7	2.4	30.6	9.3	18.1	0.0	0.1	15.7	1.9
7	12.6	2.1	±4.14	12.4	10.0	14.7	7.5	22.6	1.3	32.6	8.3	17.6	0.0	0.1	20.6	3.6
8	12.6	2.0	±3.96	12.4	10.2	14.6	6.6	22.4	1.9	30.3	8.3	17.3	0.0	0.0	21.4	3.5
9	14.0	2.4	±4.62	13.8	11.5	16.1	7.8	23.8	2.5	35.9	9.6	19.0	0.1	0.5	15.6	1.2
10	17.0	2.9	±5.63	16.6	13.8	19.3	9.8	29.1	4.4	38.3	12.1	22.3	0.4	2.2	5.9	0.1
11	18.7	2.7	±5.23	18.6	15.8	21.0	11.4	29.5	6.5	37.3	14.2	23.6	0.1	3.0	1.4	0.0
12	20.8	2.6	±5.02	20.5	17.8	23.2	13.6	31.3	9.5	38.9	16.4	25.5	0.3	4.6	0.0	0.0

MDT - Mean daily temperature: mean of the temperatures observed at 24 equidistant times in the course of a continuous 24-hour period (midnight to midnight).
StdDev – Standard deviation.
MnMDT - Minimum of mean daily temperature for a month: minimum of the mean daily temperatures.
MxMDT - Maximum of mean daily temperature for a month: maximum of the mean daily temperatures.
TMn - Minimum hourly temperature: minimum of the temperatures observed at 24 equidistant times in the course of a continuous 24-hour period
TMx - Maximum hourly temperature: maximum of the temperatures observed at 24 equidistant times in the course of a continuous 24-hour period
MDMxT - Mean daily maximum temperature for a month: mean of the daily maximum temperatures.
MDMnT - Mean daily minimum temperature for a month: mean of the daily minimum temperatures.
A#DDMxT - average number of days with maximum hourly temperature above.
A#DDMnT - average number of days with minimum hourly temperature below.

Table 5.8.30
Ambient Air Dry Bulb Temperature at the Atlantis (10 m Level) (January 1998 to September 2023)

Month	Daily Mean		95% Confidence Interval of Mean	Daily Median	Percentiles		Maximums and Minimums						A#DDMxT		A#DDMnT	
	MDT	StdDev			25%	75%	MnMDT	MxMDT	TMn	TMx	MDMnT	MDMxT	>35.0	>30.0	<10.0	<5.0
1	21.7	2.7	±5.35	21.2	18.2	24.5	14.3	31.4	10.4	40.4	16.8	27.2	1.3	7.7	0.0	0.0
2	21.8	2.6	±5.19	21.3	18.2	24.6	15.3	30.3	11.4	40.9	16.9	27.5	1.6	7.3	0.0	0.0
3	20.1	2.9	±5.73	19.7	16.7	22.8	12.1	30.7	9.4	41.0	15.5	25.9	1.5	5.3	0.1	0.0
4	18.2	3.1	±6.11	17.7	14.8	20.8	10.8	30.5	6.6	38.4	13.9	24.2	0.8	4.0	1.6	0.0
5	15.9	2.6	±5.12	15.4	13.1	17.9	9.2	25.4	6.2	33.5	12.2	21.0	0.0	1.3	4.0	0.0
6	14.0	2.5	±4.99	13.5	11.5	15.8	8.8	24.7	3.0	30.6	10.6	18.6	0.0	0.2	11.2	0.0
7	13.5	2.6	±5.03	13.0	10.8	15.5	8.1	25.4	0.9	32.4	9.8	18.3	0.0	0.1	16.5	0.3
8	13.4	2.4	±4.71	13.1	10.8	15.2	6.3	24.9	3.5	31.7	9.9	18.0	0.0	0.2	15.9	0.2
9	14.5	2.6	±5.07	14.1	11.8	16.5	8.1	26.4	4.1	38.6	10.6	19.6	0.1	0.8	11.2	0.1
10	17.0	3.0	±5.87	16.5	13.7	19.4	9.1	29.4	3.9	37.5	12.4	22.5	0.2	2.9	4.8	0.0
11	18.4	2.7	±5.36	18.1	15.2	20.9	8.3	29.4	5.8	38.1	13.7	23.7	0.3	3.0	1.4	0.0
12	20.4	2.6	±5.07	20.0	17.0	23.1	13.6	31.6	8.9	40.6	15.6	25.6	0.7	4.5	0.1	0.0

MDT - Mean daily temperature: mean of the temperatures observed at 24 equidistant times in the course of a continuous 24-hour period (midnight to midnight).
StdDev – Standard deviation of daily mean temperatures.
MnMDT - Minimum of mean daily temperature for a month: minimum of the mean daily temperatures.
MxMDT - Maximum of mean daily temperature for a month: maximum of the mean daily temperatures.
TMn - Minimum hourly temperature: minimum of the temperatures observed at 24 equidistant times in the course of a continuous 24-hour period
TMx - Maximum hourly temperature: maximum of the temperatures observed at 24 equidistant times in the course of a continuous 24-hour period
MDMxT - Mean daily maximum temperature for a month: mean of the daily maximum temperatures.
MDMnT - Mean daily minimum temperature for a month: mean of the daily minimum temperatures.
A#DDMxT - average number of days with maximum hourly temperature above.
A#DDMnT - average number of days with minimum hourly temperature below.

Table 5.8.31
Ambient Air Dry Bulb Temperature at the Milnerton WS (10 m Level) (January 1998 to June 2022)

Month	Daily Mean		95% Confidence Interval of Mean	Daily Median	Percentiles		Maximums and Minimums						A#DDMxT		A#DDMnT	
	MDT	StdDev			25%	75%	MnMDT	MxMDT	TMn	TMx	MDMnT	MDMxT	>35.0	>30.0	<10.0	<5.0
1	21.4	2.1	±4.11	21.3	19.2	23.2	15.0	29.6	12.9	40.8	18.1	25.5	0.3	2.1	0.0	0.0
2	21.5	2.1	±4.06	21.4	19.2	23.2	15.9	28.7	12.9	39.0	18.2	25.6	0.2	2.8	0.0	0.0
3	19.9	2.5	±4.86	19.8	17.6	21.7	12.9	29.6	8.1	39.0	16.7	24.0	0.2	2.0	0.1	0.0
4	18.1	2.5	±4.95	18.1	15.8	19.9	11.6	28.6	7.8	37.1	15.0	22.4	0.2	1.3	0.6	0.0
5	16.1	2.0	±4.01	15.8	14.2	17.4	10.9	24.4	6.3	33.1	13.1	19.7	0.0	0.5	2.2	0.0
6	14.5	1.9	±3.64	14.4	12.7	16.1	9.7	22.7	4.9	31.7	11.4	18.3	0.0	0.1	6.8	0.0
7	14.2	2.0	±3.92	14.1	12.3	15.7	8.9	22.6	4.6	31.3	11.0	18.0	0.0	0.1	9.0	0.1
8	14.2	1.9	±3.66	14.1	12.4	15.7	8.4	21.4	4.8	30.3	11.1	17.8	0.0	0.0	7.6	0.0
9	15.4	2.0	±3.99	15.1	13.5	16.8	10.3	24.6	5.6	38.5	12.2	19.0	0.0	0.4	3.5	0.0
10	17.4	2.3	±4.59	17.0	15.2	18.9	10.7	27.6	7.3	37.4	14.2	21.2	0.2	0.7	1.0	0.0
11	18.7	2.2	±4.29	18.6	16.5	20.4	12.3	28.9	8.1	38.8	15.5	22.4	0.0	0.8	0.1	0.0
12	20.5	2.1	±4.09	20.3	18.3	22.3	14.1	29.1	10.7	36.6	17.3	24.3	0.2	1.7	0.0	0.0

MDT - Mean daily temperature: mean of the temperatures observed at 24 equidistant times in the course of a continuous 24-hour period (midnight to midnight).
StdDev – Standard deviation.
MnMDT - Minimum of mean daily temperature for a month: minimum of the mean daily temperatures.
MxMDT - Maximum of mean daily temperature for a month: maximum of the mean daily temperatures.
TMn - Minimum hourly temperature: minimum of the temperatures observed at 24 equidistant times in the course of a continuous 24-hour period
TMx - Maximum hourly temperature: maximum of the temperatures observed at 24 equidistant times in the course of a continuous 24-hour period
MDMxT - Mean daily maximum temperature for a month: mean of the daily maximum temperatures.
MDMnT - Mean daily minimum temperature for a month: mean of the daily minimum temperatures.
A#DDMxT - average number of days with maximum hourly temperature above.
A#DDMnT - average number of days with minimum hourly temperature below.

The temperature persistence (in hours) at the monitoring sites is summarised in ***Table 5.8.32***. The recorded 6-hour duration maximum hourly temperature at the 120-m tower was 36.1 °C. The maximum temperature for the same duration at the Duynefontyn WS was 30.5 °C. The maximum temperatures varied between 32.5 °C and 39.0 °C at the offsite Eskom AWS (Bok Point, Robben Island, Rondekuil, Atlantis and Milnerton). The recorded 3-hour duration maximum hourly temperatures at the 120-m tower and Duynefontyn WS were 37.0 °C and 38.0 °C, respectively. The maximum temperatures at the other weather stations varied between 35.1 °C and 40.0 °C at the other weather stations.

The recorded 6-hour and 3-hour sustained minimum hourly temperatures at the 120-m tower were 4.8 °C and 4.5 °C, respectively. The minimum temperatures for the same durations at the Duynefontyn WS were 4.0 °C and 3.0 °C. The lowest minimum temperatures at the offsite Eskom AWS for the 6- and 3-hour durations were 3.7 °C and 7.2 °C, respectively at Rondekuil WS.

Table 5.8.32
Maximum and Minimum Ambient Air Dry Bulb Temperature for Sustained 3 and 6 Hours

Weather Station	Sustained Maximum Temperature (°C) for		Sustained Minimum Temperature (°C) for	
	6 hours	3 hours	6 hours	3 hours
120-m tower (10 m)(1)	36.1	37.0	4.8	4.5
2m located near 120-m tower(2)	36.0	38.0	3.5	2.5
Duynefontyn WS(3)	30.5	34.1	4.0	3.0
Bok Point WS(4)	34.0	35.0	6.5	5.5
Robben Island WS(5)	32.5	35.1	8.5	7.3
Rondekuil WS(5)	39.0	40.0	3.7	2.2
Atlantis WS(5)	38.8	39.5	4.3	4.1
Milnerton WS(4)	36.0	38.0	5.2	4.7

Notes:

(1) The statistics included October 1997 to 31 September 2023 period.
(2) The statistics included 1 January 2009 to 31 December 2011 period.
(3) The statistics included 1 October 2017 to 28 February 2022 period.
(4) The statistics included January 1998 to 30 June 2019 period.
(5) The statistics included January 1998 to 31 September 2023 period.

The dewpoint is the temperature at which the air is saturated with respect to water vapour over a liquid surface. When the temperature is equal to the dewpoint then the relative humidity is 100 per cent. The three mechanisms for relative humidity to be 100 per cent are to (a) cool the air to the dewpoint, (b) evaporate moisture into the air until the air is saturated, or (c) lift the air until it cools to the dewpoint.

Dew forms when the temperature becomes equal to the dewpoint. The favourable weather elements for dew include clear skies, light wind, adequate soil moisture, and low night-time dewpoint depressions. When the dry-bulb temperatures drop below freezing and the temperature reaches the dewpoint temperature, the ice formed on the ground surface is termed frost. Frost can form in two ways, namely by deposition or freezing of dew. Depositional frost occurs when the dewpoint is below freezing. When this frost forms, the water vapour goes directly to the solid state. Frost that forms due to the freezing of liquid water (i.e. dew) is best referred to as frozen dew. Initially, both the dewpoint and temperature are above freezing when dew forms. Longwave radiational cooling gradually lowers the temperature to or below freezing during the night. Cold air advection can also initiate freezing (e.g. cold air moving through in the middle of the night after dew has formed). Once the temperature falls to freezing, the condensed dew droplets freeze.

The corresponding dewpoint temperature[8] statistics during the second campaign were estimated as follows:

- mean of the daily maximum: 14.7 °C;
- mean of the daily minimum: 9.7 °C;
- the month with the highest mean daily maximum temperature of 17.5 °C is January;
- the month with the lowest mean daily maximum temperature of 12.3 °C is August;
- the month with the highest mean daily minimum temperature of 13.3 °C is February;

---

[8] The dew point temperature (T_d) is calculated using the Magnus formula (Alduchov & Eskridge, 1996) :

$$T_d = \frac{b}{\left[\frac{a}{ln(RH\%/100) + \frac{aT}{b+T}} - 1\right]}$$

Where T_d = Dewpoint temperature [°C]
T = Dry-bulb temperature [°C]
$RH\%$ = Relative humidity [per cent
a = constant, 17.625 [unitless]
b = constant, 243.04 [°C]
$\ln()$ = natural logarithm [unitless]

The errors between the equation estimate and the T_d values used to develop the equation had a maximum relative error of less than 0.384 per cent over a temperature range of -40°C to 50°C. To illustrate its usage, plugging $T = 20\ °C$ and $RH\% = 50\ per\ cent$ into the equation gives:

$$T_d = \frac{243.04}{\left[\frac{17.625}{ln(50/100) + \frac{17.625T}{243.04+20}} - 1\right]} = 9.26\ °C$$

- the month with the lowest mean daily minimum temperature of 6.2 °C is August.

The lowest and highest hourly average dewpoint temperature was calculated to be -2.8 °C (August 2018) and 31.2 °C (January 2022), respectively.

Albeit both relatively short monitoring periods at the Duynefontyn WS and the 2 m above ground level measurement near the 120-m tower, the observed air temperatures did not drop below 1.8°C. It is therefore expected that frost would be a rare occurrence at the site.

A measure of the vertical temperature difference (United States Nuclear Regulatory Commission, 2007c) allows the calculation of atmospheric turbulence, i.e. 'delta-T' method. This is discussed in ***Subsection 5.8.6.1.8.*** The alternative method of using the direct measurement of wind fluctuations, i.e. the 'sigma-theta' method (International Atomic Energy Agency, 2002), is also discussed and compared in ***Subsection 5.8.6.1.8.***

5.8.6.1.3 Precipitation

Types of precipitation include hail, sleet, snow, rain, and drizzle. Frost and dew are not classified as precipitation because they form directly on solid surfaces. The formation of precipitation may occur at temperatures above or below freezing. Since the rainfall measurements are done automatically, it is not currently possible to determine the details of the type of precipitation. Instead, a constant precipitation type ('showers') most common to the area is used to evaluate the impact of precipitation on airborne concentrations of contaminants and on ground contamination. No records could be obtained that quantified the occurrence of freezing precipitation at the site. However, given the relatively high wet-bulb temperatures recorded at the site (lowest of 1.2 °C for 2017 to 2022 at the Duynefontyn WS), the likelihood of freezing precipitation is expected to be low.

The site area is classified as winter rainfall (Preston-Whyte & Tyson, 1988; Schulze, 1986). Historically (Schulze, 1997), the Mean Annual Precipitation (MAP) was reported to be between 400.0 mm and 600.0 mm, as shown in ***Figure 5.8.13***. However, the rainfall measurement at the site over the 43-year period from 1980 to 2022 observed a MAP of 373.1 mm, with a maximum of 640.4 mm (1987) and a minimum of 218.0 mm (2015) (Eskom, 2023a), as shown in ***Figure 5.8.14***.

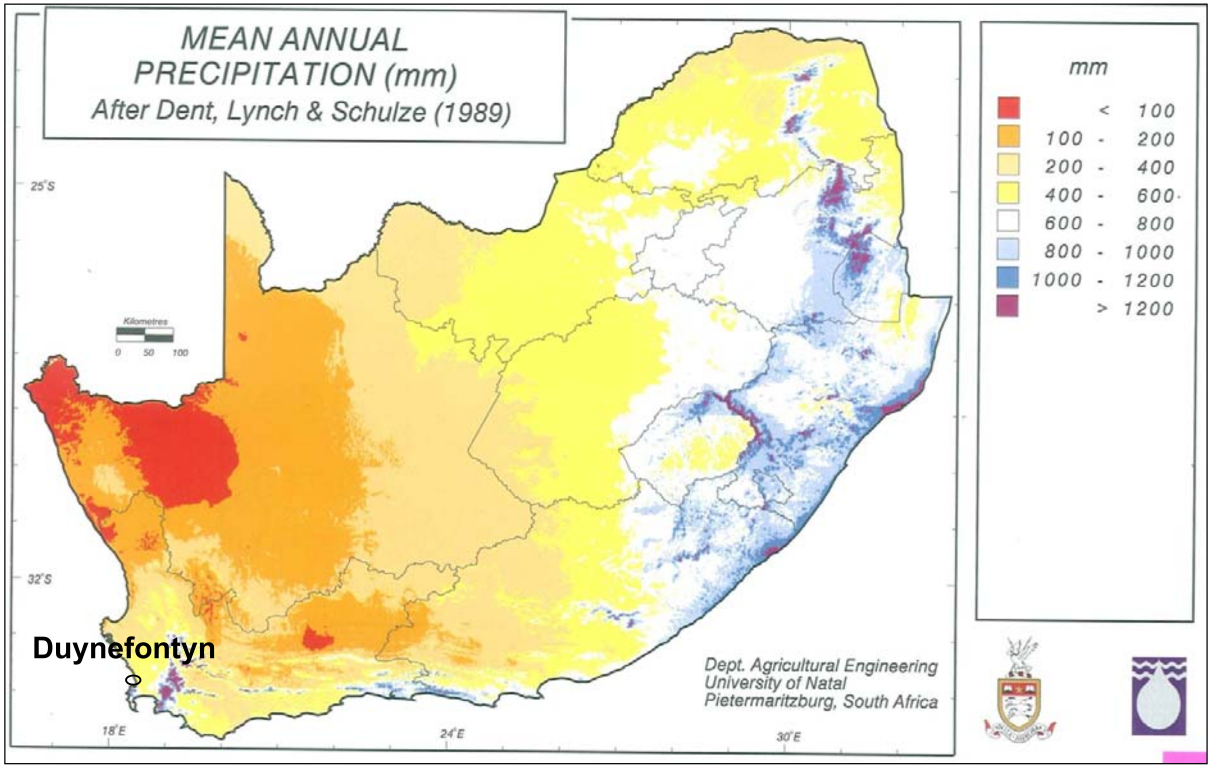

Figure 5.8.13
Mean Annual Precipitation for South Africa (Schulze, 1997)

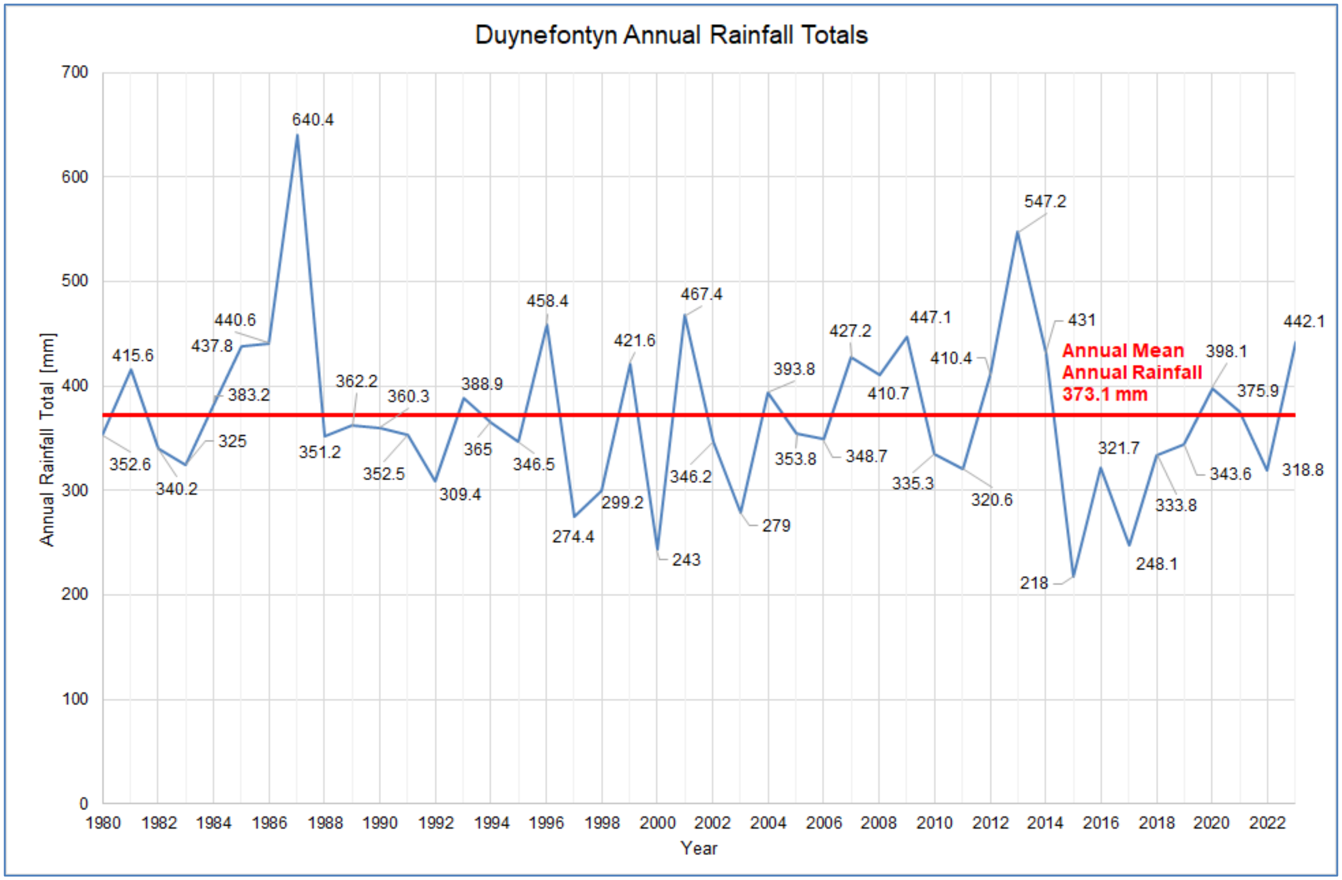

Figure 5.8.14
Annual Rainfall Totals at the Site

Reference and comparison to other weather stations in the vicinity of the site is also made (International Atomic Energy Agency, 2011). Existing rainfall data with the required reliability and length of record were also extracted from the Daily Rainfall Data Extraction Utility (Institute for Commercial Forestry Research, 2003) using surrounding SAWS stations is summarised in ***Table 5.8.33***. Long-term rainfall observations made at the SAWS stations at Atlantis Reservoir (0020846 4) over the period 1979 to 2019 recorded a MAP of 443.6 mm (Eskom, 2023a) and at CTIA (0021178A3 & 0021178B8) over the period 1961 to 2019 recorded a MAP of 501.0 mm (South African Weather Services, 2020a). The MAP for Atlantis Reservoir, albeit higher annual totals, correlates better with the site than observations at CTIA. Long-term records of rainfall are also available for Robben Island (0020649 03), Vanschoorsdrift (0021130) and Burgherspost (0041060) that recorded MAPs of 584 mm, 347 mm and 584 mm, respectively (Eskom, 2023a).

Table 5.8.33
Summary of Long-Term Mean Annual Precipitation (MAP) at Nearest Weather Stations in Comparison with Koeberg WS

Station	Years of Record	Distance from Site (km)	Elevation (m amsl)	MAP (mm)
SAWS CTIA	60 (1960-2019)	35.0	42	501
SAWS Atlantis Reservoir	41(1979-2019)	9.0	149	443
SAWS Robben Island	151 (1850-2019)	17.7	18	584
SAWS Vanschoorsdrift(1)	141 (1860-2011)	16.2	42	347
SAWS Burgherspost (1)	143 (1858-2011)	21.1	180	584
120-m Tower	44 (1980-2023)	-	24	372

Note: (1) Monitoring stations decommissioned.

The results presented in ***Table 5.8.34*** and ***Figure 5.8.15*** indicate significant differences in the monthly precipitation values for the site when compared with the long-term data set at CTIA; the latter receiving more rainfall. A comparison with the Atlantis Reservoir shows better correlation, albeit slightly higher rainfall per month. Normal monthly rainfall peaks during the winter months of June to August, with the observations at the site as follows:

- the highest monthly averages of 72.0 mm and 63.7 mm occurring in June and July, respectively;
- the lowest monthly average of 7.4 mm in February.

The highest monthly rainfall at Atlantis Reservoir during the period 1980 to 2019 of 162.4 mm occurred in July 2001. The lowest monthly rainfall of 0 mm occurred twice in January, five times in February and three times in March over this monitoring period (Eskom, 2023a).

Table 5.8.34
Average, Highest and Lowest Monthly Rainfall for CTIA, Atlantis and the Site (120-m Tower and Duynefontyn WS)

Month	Average Monthly (mm)				Highest Monthly (mm)				Lowest Monthly (mm)			
	CTIA	Atlantis	Duynefontyn WS	120-m Tower	CTIA	Atlantis	Duynefontyn WS	120-m Tower	CTIA	Atlantis	Duynefontyn WS	120-m Tower
	(1961-1990)	(1979-2019)	(Oct 2017-Feb 2022)	(1980-2023)	(1961-1990)	(1979-2019)	(Oct 2017-Feb 2022)	(1980-2023)	(1961-1990)	(1979-2019)	(Oct 2017- Feb 2022)	(1980-2023)
Jan	15	11.3	4.1	8.2	59	65.0	17.2	67.6	0	0.0	0.2	0.0
Feb	17	8.8	6.9	7.4	53	45.3	16.4	42.0	0	0.0	0.3	0.0
Mar	20	13.3	22.3	14.1	73	49.6	34.6	49.9	1	0.0	7.8	0.0
Apr	41	35.7	16.3	30.2	142	119.2	38.6	107.8	5	1.7	2.8	2.8
May	69	58.6	45.7	43.5	144	131.0	75.7	98.2	14	5.2	29.4	1.3
Jun	93	76.5	71.8	72.0	225	189.2	100.9	157.4	23	11.3	38.7	12.0
Jul	82	80.7	54.7	63.7	169	185.0	90.2	162.4	18	27.0	20.6	22.8
Aug	77	65.5	51.8	55.`	215	145.7	65.2	160.7	31	19.7	37.5	12.8
Sep	40	43.2	23.1	32.9	91	91.5	46.3	90.4	9	4.7	0.2	2.5
Oct	30	23.6	17.7	17.3	107	92.9	41.6	114.8	4	0.7	4.6	0.6
Nov	14	18.4	14.3	16.6	63	92.2	28.6	67.8	0	0.0	0.6	0.4
Dec	17	14.9	6.0	12.7	71	42.0	15.2	52.8	2	0.0	0.5	0.3
Annual Total	515	453.3	318.1	372.4	751	567.4	295.3	640.4	362	266.5	269.1	218.0

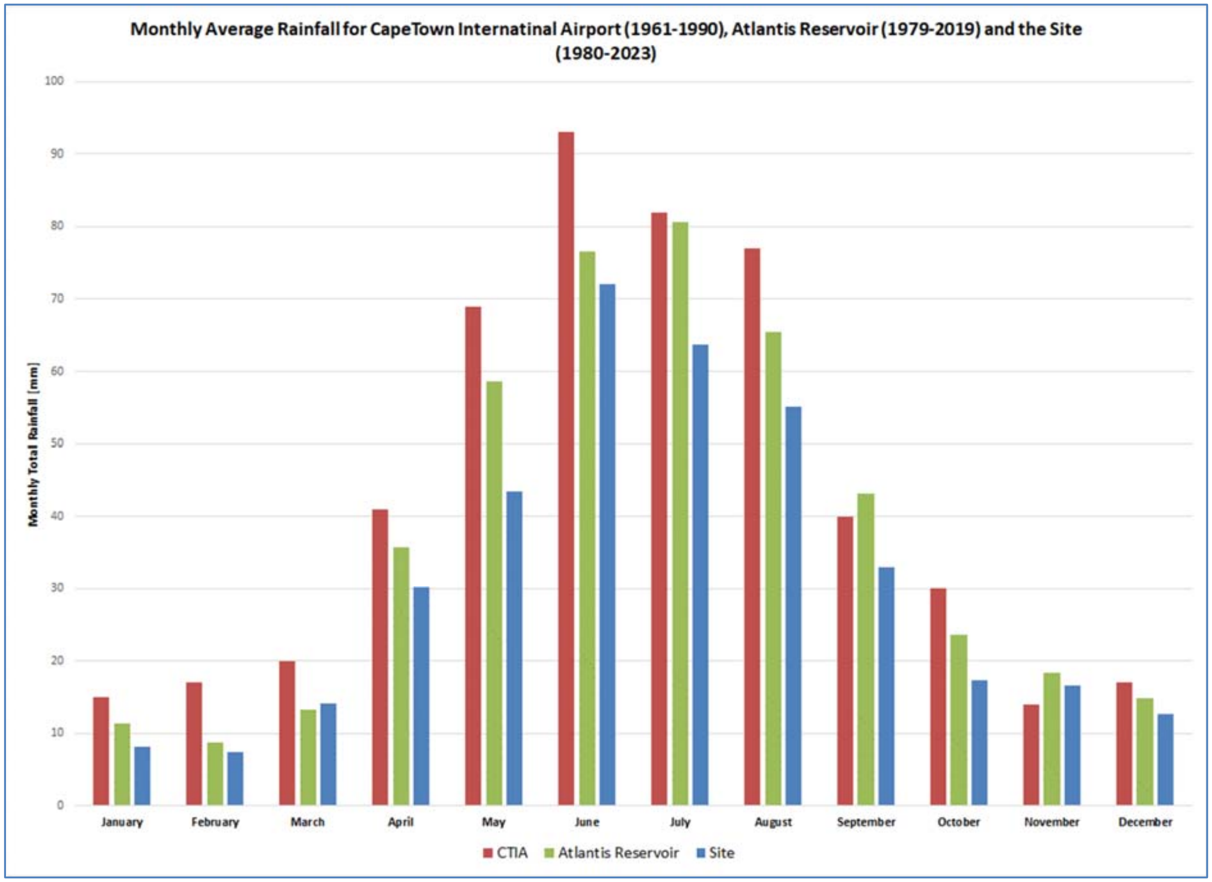

Figure 5.8.15
Monthly Rainfall Data at CTIA, Atlantis Reservoir and the Site

Only monthly rainfall totals for the period 1980 to 1997 were available for the site, whereas hourly data were available for October 1997 to September 2023 (Eskom, 2023a). The measurements of maximum 24-hour rainfall rates for CTIA are slightly higher when compared with the observations at Atlantis Reservoir and the site (see ***Table 5.8.35***) (Eskom, 2023a). The latter two stations observed very similar 24-hour rainfall rates. Whilst the highest 24-hour rainfall of 70.0 mm was recorded during July 1994 at the site and Atlantis Reservoir, the recorded highest 24-hour rainfall at the CTIA of 65.0 mm occurred in May 1974 (South African Weather Services, 2011; South African Weather Services, 2020a).

Table 5.8.35
Maximum 24-hour Rainfall for CTIA, Atlantis Reservoir and the Site

Month	CTIA (mm)		Atlantis (mm)	Duynefontyn WS (mm)	120-m tower (mm)
	(1938-1972)(1)	(1961-1990)(2)	(1979-2019)(3)	(Oct 2017- Feb 2022)	(1980-2023)(4)
January	22.9	41.0	56.0	7.9	57.4
February	32.8	27.0	23.5	8.7	26.4
March	21.1	42.0	30.0	20.3	33.8
April	44.5	39.0	63.5	14.8	62.0
May	61.7	65.0	45.0	42.1	49.3
June	58.1	58.0	45.9	36.5	58.2
July	48.8	61.0	70.0	31.7	70.0
August	47.5	56.0	44.0	27.8	57.6
September	45.5	29.0	34.0	23.5	34.6
October	48.8	53.0	46.0	30.8	50.4
November	15.5	30.0	26.0	17.0	35.7
December	7.5	21.0	25.6	9.3	19.2
Annual	61.7	65.0	70.0	42.1	70.0

Notes:
(1) (Le Roux, 1983)
(2) (South African Weather Bureau, 1996)
(3) (South African Weather Services, 2020a)
(4) (Eskom, 2023a)

The highest hourly rainfall rates at the 120-m tower and at the Duynefontyn WS are summarised in ***Table 5.8.36*** and compared with the rainfall rates recorded at CTIA. Apart from October, hourly rainfall rates at CTIA have been considerably higher than at the site. The highest and second highest hourly rainfall at the 120-m tower during the 1997 to 2023 period were 23.6 mm and 23.2 mm recorded on 6 October 2004 at 21h00 and on 15 August 2013 at 09h00, respectively. The third, fourth and fifth highest hourly rainfall were all similar and considerably lower at 15.0 mm

(2 August 2016)[9], 14.8 mm (14 June 2016), and 14.8 mm (21 November 2010), respectively.

Table 5.8.36
Highest 1 hour Rainfall for CTIA and the Site

Month	CTIA (mm)	Duynefontyn WS	120-m tower (mm)
	(1938-1972)$^{(1)}$	(Oct 2017-Feb 2022)	(1997-2023)$^{(2)}$
January	8.6	5.1	10.8
February	18.8	4.7	7.8
March	14.6	11.9	9.6
April	39.1	11.6	10.6
May	27.9	15.8	11.5
June	22.1	12.6	14.8
July	24.9	11.1	14.6
August	20.1	8.2	23.2
September	28.8	8.1	12.1
October	20.3	7.5	23.6
November	14.9	5.2	14.8
December	13.5	4.4	14.0

Notes:
(1) (Le Roux, 1983)
(2) Rainfall for 2023 up to September (Eskom, 2023a)

5.8.6.1.4 Droughts and Wet Years

The SAWS defines drought on the basis of two indices. The first index is based on the degree of dryness in comparison to normal or average amounts of rainfall for a particular area or place and the duration of the dry period. This is what is termed a meteorological drought, and the normal year would be calculated over a 30-year period.

Less than 75 per cent of normal rainfall is regarded as a severe meteorological drought but a shortfall of 80 per cent of normal rainfall will cause crop and water shortages. A wet year has 25 per cent more rainfall than the normal year (i.e. 125 per cent).

The drought and wet years during the period 1980 to September 2023 are provided in and ***Figure 5.8.16*** using the observations at the 120-m tower. During this period three wet years (1987, 2001 and 2013) and five drought years (1997, 2000, 2003, 2015 and 2017) were observed. However, the disadvantage of this index is that it compares the rainfall deficit in the current

---

[9] Not included in ***Table 5.8.36*** since the overall maximum for August was 23.2 mm.

month with rainfall for the same month in the history of the station and does not consider the cumulative effect of rainfall deficit.

The Standardised Precipitation Index (SPI) has been introduced an attempt to alleviate this shortcoming and is based on the probability of rainfall for any time scale (or moving averaging window). The SPI calculation is based on the distribution of rainfall over long time periods (preferably more than 50 years). The long-term rainfall record is fitted to a probability distribution, which is then normalised so that the mean (average) SPI for any place and time period is zero. SPI values above zero indicate wetter periods and values less than 0 indicate drier periods.

The SPI values adopted at the SAWS (***Table 5.8.37***) are the same as those developed used by the World Meteorological Organization (WMO) (World Meteorological Organization, 2012). A drought event occurs any time the SPI is continuously negative and reaches an intensity of -1.0 or less. The event ends when the SPI becomes positive. Each drought event, therefore, has a duration defined by its beginning and end, and an intensity for each month that the event continues. The positive sum of the SPI for all the months within a drought event can be termed the drought's "magnitude".

Table 5.8.37
SAWS and WMO Adopted SPI Values

SPI	Description
2.0 and more	Extremely wet
1.50 to 1.99	Very wet
1.00 to 1.49	Moderately wet
-0.99 to 0.99	Near normal
-1.00 to -1.49	Moderately dry
-1.50 to -1.99	Severely dry
-2.00 and less	Extremely dry

The timescales employed in the calculation reflect the impacts of drought on the needs of different water resources. Meteorological and soil moisture conditions (agriculture) respond to precipitation anomalies on relatively short timescales, for example 1-6 months, whereas streamflow, reservoirs, and groundwater respond to longer-term precipitation anomalies of the order of 6 months up to 24 months or longer.

The National Drought Mitigation Center-UNL developed the SPI Generator (NDMC, 2021), which allows the calculation of SPI for a given historical rainfall data set. Using the monthly rainfall totals for the 43-year period from 1980 to 2022 (since 2023 did not include a full year, this period was excluded from the analysis), the 12-month timescale SPIs were calculated using the SPI Generator and summarised in ***Figure 5.8.17***. A 12-month SPI is a comparison of the precipitation for 12 consecutive months with that recorded in the same 12 consecutive months in all previous years of available data. Because these timescales are the cumulative result of shorter periods that may be above or below normal, the longer SPIs tend to gravitate toward zero unless a distinctive wet or dry trend is taking place.

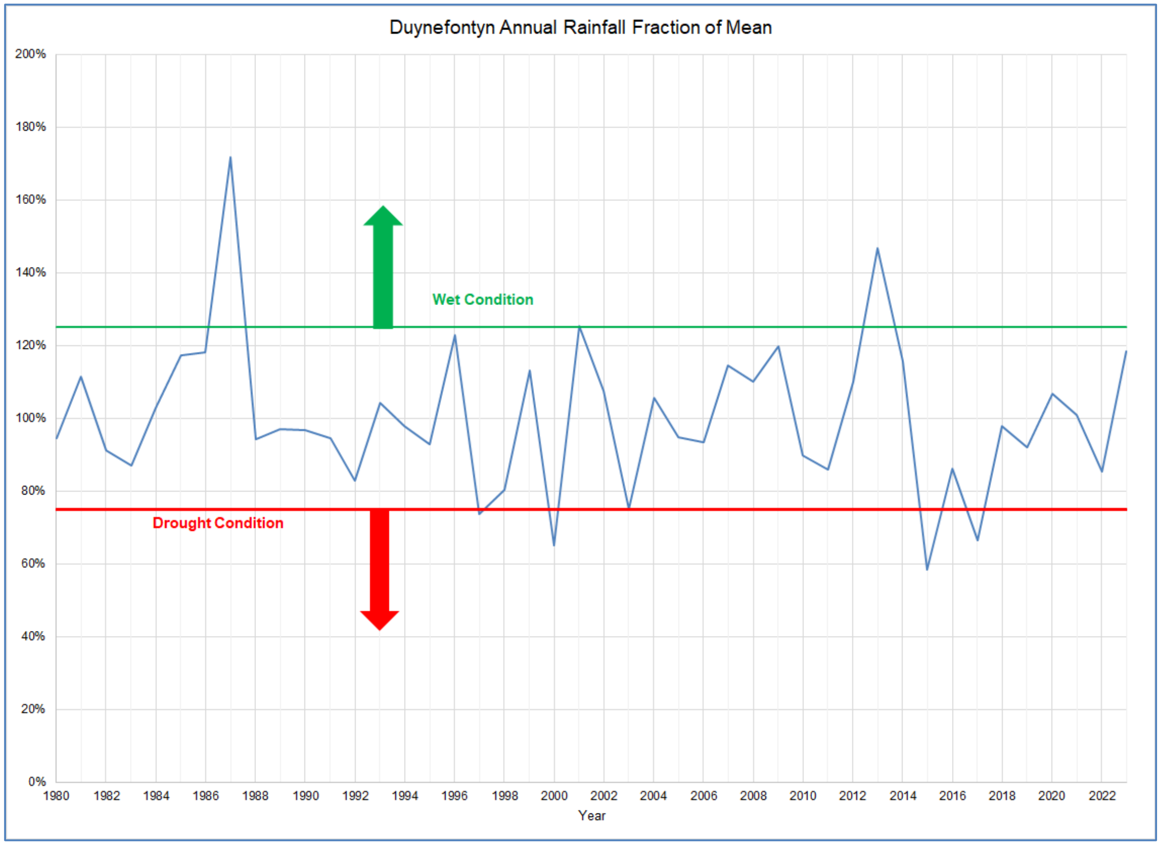

Figure 5.8.16
Dry and Wet Rainfall Periods at the Site

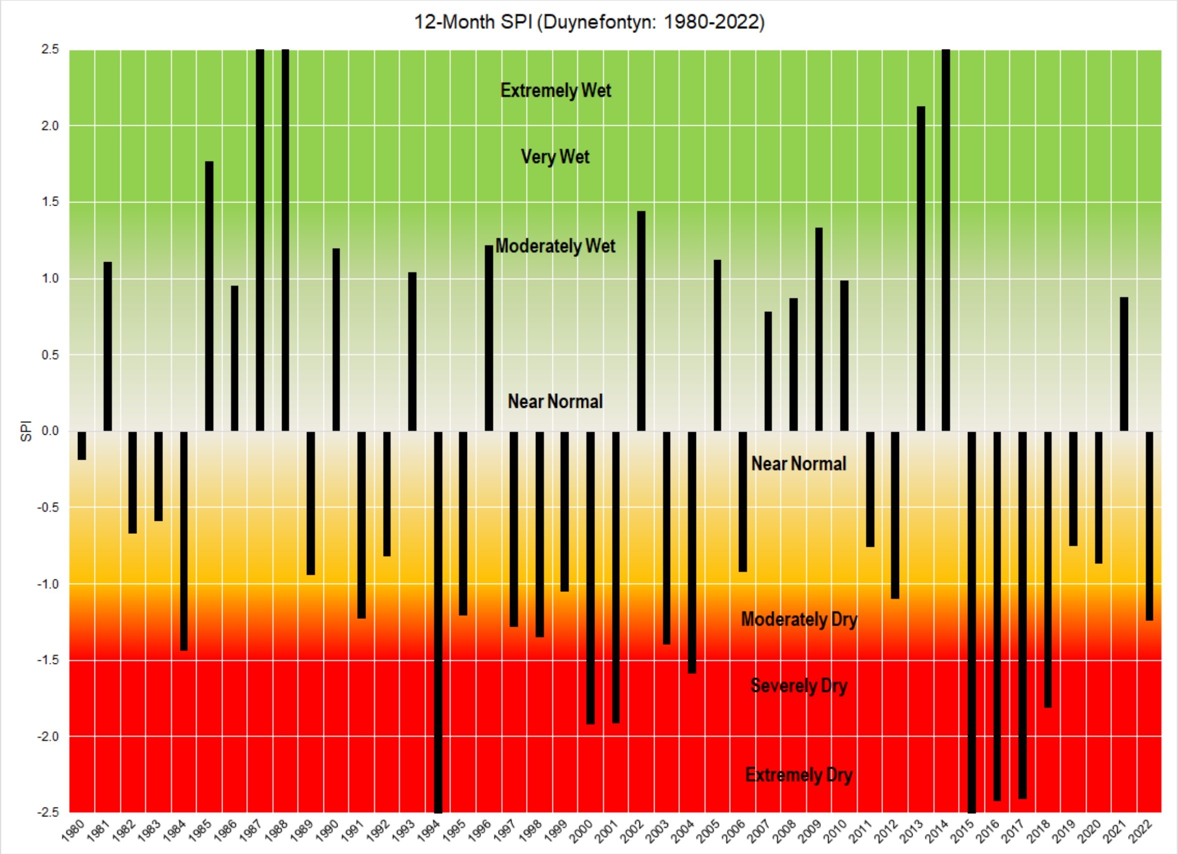

Figure 5.8.17
Dry and Wet Rainfall Periods at the Site

During the 43-year historical period, four “extremely dry” years (1994, 2015, 2016 and 2017) were observed with four “extremely wet” years (1987, 1988, 2013 and 2014). “Near normal” rain years account for 33% (14 years) of the historical period, followed by “moderately dry” years (21%, i.e., 9 years), “moderately wet” years (16%, i.e., 7 years), and “moderately dry” years (21%, i.e., 9 years). “Severely dry”, “extremely dry” and “extremely wet” years account for 9% (4 years each), respectively. The SPI indicate one “very wet” year only.

5.8.6.1.5 Thunder, Hail, Snow and Fog

Although thunder, hail, snow and fog occurrences have been recorded at the Atlantis Reservoir, data for only a six-year period could be obtained from the SAWS (Schulze, 1986). According to this information, there were no days with thunder, hail, or snow. An annual average of three days with fog was recorded.

Climate data for CTIA (1961-2010) were also used to estimate the average number of days that thunder, hail, snow and fog occur (South African Weather Bureau, 1996; South African Weather Services, 2011). This information is summarised in ***Table 5.8.38*** and the following are observed:

- thunder – The occurrence of thunder shows no particular preference towards a season or month; however the likelihood is lowest during January and December.
- hail – Hail tends to occur mainly during the winter months, with the highest likelihood during July.
- snow – The annual average number of days with snowfall for the period 1961 – 1990, was 3, with the highest likelihood during July and August. The most recent 30-year period from 1991 to 2010, recorded an annual average of 0.0.
- avalanches – Since the site is on a flat terrain, avalanches would not occur.
- blizzards – There are no record of blizzards occurring at the site.
- ice and ice cover – Since the air and sea temperatures never reach freezing point, no ice and ice covers have been reported.
- fog – Fog appears to occur significantly more at the CTIA station than at Atlantis Reservoir. Recognising the short duration of observations at the latter station, it is expected that fog occurrences at the site may be less than at CTIA.

Table 5.8.38
Average Number of Days with Thunder, Hail, Snow and Fog at CTIA (1961-2010)

Month	Thunder		Hail		Snow		Fog	
	1961-1990	1991-2010	1961-1990	1991-2010	1961-1990	1991-2010	1961-1990	1991-2010
January	0.1	0.4	0.0	0.1	0.0	0.0	1.3	3.8
February	0.5	0.8	0.1	0.0	0.0	0.0	3.3	4.2
March	0.8	0.8	0.0	0.0	0.0	0.0	5.7	6.0
April	0.7	1.8	0.2	0.0	0.0	0.0	8.0	7.6
May	0.9	1.3	0.1	0.0	0.0	0.0	9.1	10.3
June	0.8	1.1	0.1	0.1	0.2	0.0	7.1	8.3
July	0.5	1.8	0.3	0.2	1.3	0.0	7.9	5.9
August	0.7	1.1	0.0	0.3	1.3	0.0	5.3	4.8
September	0.3	0.8	0.0	0.0	0.0	0.0	4.2	4.3
October	0.5	1.4	0.1	0.1	0.1	0.1	2.5	2.5
November	0.6	0.9	0.0	0.0	0.0	0.0	1.8	1.8
December	0.2	1.0	0.0	0.0	0.0	0.0	2.2	4.1
Annual	6	7	1	1	3	0	58	60

5.8.6.1.6 Atmospheric Moisture

Measurements of relative humidity were performed for the period January 2009 to December 2011 at the site near the 120-m tower and for the period October 2017 to April 2022 at the Duynefontyn WS. A summary of the monthly and annual statistics is provided in ***Table 5.8.39.*** As a comparison, data from the SAWS weather station at Geelbek, approximately 60.5 km along the coast and north of the site, for the period 2005 to 2011 is also included in the table.

The lowest daily average relative humidity recorded at the 120-m tower and Geelbek were during December (71.9 per cent at Geelbek and 67.5 per cent at 120-m tower), whereas the lowest at the Duynefontyn WS was 60.4 per cent for February. These are followed by 72.9 per cent at Geelbek, 67.7 per cent at 120-m tower and 61.9 per cent for Duynefontyn WS. The highest daily average relative humidity at Geelbek was recorded during June (82.3 per cent) and during May at the 120-m tower (81.3 per cent) and at the Duynefontyn WS (83.9 per cent). The highest average of the daily maximum relative humidity at Geelbek WS was in May (94.9 per cent), at the 120-tower in June (92.6 per cent) and at the Duynefontyn WS in July (95.9 per cent). The lowest average of the daily minimum relative humidity at Geelbek WS and at the 120-m tower was in April with 41.6 per cent and 36.2 per cent respectively. The lowest average of the daily minimum relative humidity at Duynefontyn WS occurred in July with 49.5 per cent. The annual average relative humidity recorded was 76.8 per cent at Geelbek WS, 73.2 per cent at the 120-m tower and 74.4 per cent at the Duynefontyn WS.

Table 5.8.39
Daily Average and Mean of Daily Maximum and Minimum Relative Humidity for Geelbek (2005-2011), at the 120-m Tower (January 2009-October 2013) and the Duynefontyn WS (October 2017-Feb 2022)

Month	**Geelbek (2005-2011)**			**120-m Tower (2009-2013)**			**Duynefontyn WS (2017-2022**		
	Ave	**Min**	**Max**	**Ave**	**Min**	**Max**	**Ave**	**Min**	**Max**
January	72.9	53.9	85.7	67.7	48.7	82.3	61.9	50.1	89.3
February	74.8	50.2	90.1	69.0	45.8	85.9	60.4	52.1	99.6
March	72.5	41.8	89.1	70.9	46.9	88.2	79.0	58.5	93.5
April	76.8	41.6	93.1	70.7	36.2	91.0	78.1	55.2	93.2
May	82.1	50.7	94.9	81.3	59.6	92.3	83.9	60.5	95.4
June	82.3	55.4	94.2	81.0	58.5	92.6	80.0	56.1	94.2
July	82.2	50.2	94.4	77.7	55.4	92.0	79.7	49.5	95.9
August	81.7	61.6	92.0	77.2	52.5	89.6	80.5	58.4	94.0
September	78.2	55.4	92.8	76.3	55.6	88.3	75.7	50.5	93.3
October	73.5	50.7	87.7	71.3	56.9	83.9	73.8	45.7	91.2
November	73.0	49.2	88.6	69.1	48.4	87.1	73.3	48.6	88.0
December	71.9	54.0	87.7	67.5	45.7	83.4	66.4	48.4	90.4
Annual	76.8	41.6	94.9	73.2	36.2	92.6	74.4	45.7	99.6

5.8.6.1.7 Barometric Pressure

A summary of the barometric pressure measured at the site (October 1997 to September 2023) is provided in ***Table 5.8.40*** (daily average and average of daily maximum and minimum) and ***Table 5.8.41*** (maximum and minimum hourly) and mean sea level barometric pressure is provided in ***Table 5.8.42*** (daily average and average of daily maximum and minimum) and ***Table 5.8.43*** (maximum and minimum hourly).

Summer coastal lows are clearly observed with monthly average barometric pressures at the 120-m tower (***Table 5.8.40***) of 1009.3 hPa (December), 1008.3 hPa (January) and 1008.5 hPa (February), and mean sea level barometric pressures (***Table 5.8.42***) of 1012.4 hPa (December), 1011.4 hPa (January) and 1011.6 hPa (February). Conversely, winter stagnant high pressures are observed with monthly average barometric pressures at the 120-m tower (***Table 5.8.40***) of 1019.9 hPa (June), 1018.5 hPa (July) and 1016.8 hPa (August), and mean sea level barometric pressures (***Table 5.8.42***) of 1020.0 hPa (June), 1021.7 hPa (July) and 1019.9 hPa (August).

During spring and autumn, the barometric pressures are similar with the lower pressures at the end of spring (monthly average barometric pressure of 1011.2 hPa for November) and the start of autumn (monthly average barometric pressure of 1010.5 hPa for March). Conversely, barometric pressures are higher at the beginning of spring (monthly average barometric pressure of 1015.6 hPa for September) and the end of autumn (monthly average barometric pressure of 1014.6 hPa for May). Mid spring and autumn are similar, i.e. monthly average barometric pressure of 1013.4 hPa for October and 1016.8 hPa for August.

Table 5.8.40

Daily Average and Mean of Daily Maximum and Minimum Barometric Pressure (hPa) for the Duynefontyn WS (October 2017- Feb 2022) and the 120-m Tower (October 1997- September 2023)

Month	Duynefontyn WS (2017-2022)			120-m Tower (1997-2023)		
	Average (hPa)	Minimum (hPa)	Maximum (hPa)	Average (hPa)	Minimum (hPa)	Maximum (hPa)
January	1013.5	1010.0	1018.5	1008.3	985.6	1018.7
February	1013.0	1008.8	1017.9	1008.5	994.8	1016.8
March	1013.6	1010.5	1016.8	1010.5	997.2	1019.2
April	1016.0	1012.6	1019.1	1013.0	1001.1	1025.2
May	1016.5	1014.3	1022.5	1014.6	997.9	1027.1
June	1018.6	1014.7	1022.7	1016.9	1000.1	1031.6
July	1021.4	1016.5	1026.7	1018.5	1000.5	1036.9
August	1020.9	1016.7	1024.9	1016.8	999.9	1035.2
September	1018.4	1015.4	1021.9	1015.6	907.8	1031.7
October	1016.1	1012.9	1020.0	1013.4	1001.3	1029.5
November	1015.0	1011.0	1018.4	1011.2	992.7	1025.5
December	1013.0	1010.6	1016.5	1009.3	996.6	1019.9
Annual	1010.4	1008.8	1026.7	1014.3	907.8	1036.9

Table 5.8.41

Hourly Maximum and Minimum Barometric Pressure (hPa) for the Duynefontyn WS (October 2017- Feb 2022) and the 120-m Tower (October 1997- September 2023)

Month	Duynefontyn WS (2017-2022)		120-m Tower (1997-2023)	
	Minimum (hPa)	Maximum (hPa)	Minimum (hPa)	Maximum (hPa)
January	1003.6	1024.1	991.8	1020.9
February	1001.9	1019.9	990.1	1018.9
March	1005.1	1021.1	995.6	1023.0
April	1007.0	1024.6	997.7	1027.0
May	1005.5	1028.0	987.4	1028.7
June	1003.6	1033.3	996.1	1033.1
July	1001.1	1036.8	929.6	1043.6
August	1005.0	1036.1	994.6	1039.6
September	1005.9	1031.8	931.8	1034.8
October	1004.4	1029.3	997.9	1031.0
November	1004.7	1029.0	989.6	1027.2
December	1005.1	1025.1	992.8	1023.0
Annual	1001.1	1036.8	929.6	1043.6

Table 5.8.42

Daily Average and Mean of Daily Maximum and Minimum Mean Sea Level Barometric Pressure (hPa) for the Duynefontyn WS (October 2017- April 2022) and the 120-m Tower (October 1997-September 2022)

Month	Duynefontyn WS (2017-2022)			120-m Tower (1997-2023)		
	Average (hPa)	Minimum (hPa)	Maximum (hPa)	Average (hPa)	Minimum (hPa)	Maximum (hPa)
January	1014.9	1011.4	1019.9	1011.4	988.6	1021.8
February	1014.4	1010.2	1019.3	1011.6	997.8	1019.9
March	1015.1	1011.9	1018.2	1013.6	1000.2	1022.3
April	1017.5	1014.1	1020.5	1016.0	1004.1	1028.3
May	1017.9	1015.7	1023.9	1017.8	1001.0	1030.3
June	1020.5	1016.2	1024.1	1020.0	1003.2	1034.9
July	1022.9	1017.9	1028.1	1021.7	1003.6	1040.1
August	1022.4	1018.2	1026.4	1019.9	1003.0	1038.4
September	1019.9	1016.8	1023.4	1018.7	910.6	1034.9
October	1017.5	1014.3	1021.4	1016.5	1004.4	1032.7
November	1015.7	1005.5	1019.8	1014.3	995.6	1028.6
December	1014.5	1011.5	1018.0	1012.4	999.6	1023.1
Annual	1011.9	1005.5	1028.1	1017.4	910.6	1040.1

Table 5.8.43

Hourly Maximum and Minimum Mean Sea Level Barometric Pressure (hPa) for the Duynefontyn WS (October 2017- April 2022) and the 120-m Tower (October 1997- September 2022)

Month	Duynefontyn WS (2017-2022)		120-m Tower (1997-2023)	
	Minimum (hPa)	Maximum (hPa)	Minimum (hPa)	Maximum (hPa)
January	1004.9	1025.5	994.8	1024.1
February	1003.3	1021.4	993.0	1022.0
March	1006.5	1022.5	998.6	1026.1
April	1008.4	1026.1	1000.6	1030.2
May	1006.9	1029.5	990.3	1031.8
June	1000.1	1034.8	999.2	1036.4
July	1002.5	1038.3	932.5	1046.9
August	1006.4	1037.5	997.7	1042.8
September	1007.3	1033.3	934.7	1038.0
October	1005.8	1030.8	1000.9	1034.2
November	1006.1	1030.4	992.4	1030.4
December	1006.5	1026.6	995.9	1026.1
Annual	1000.1	1038.3	932.5	1046.9

5.8.6.1.8 Solar Radiation

Systematic solar radiation measurements in southern Africa started in the 1950s (Clemence, 1992). Based on this work a solar radiation atlas for South Africa was developed (Schulze, 1997). According to this atlas, the site should typically experience solar radiation with:

- a maximum value of about 33.9 MJ/m^2.day in December;
- a minimum value of about 12.5 MJ/m^2.day in June.
- The actual solar radiation readings near the 120-m tower for January 2009 to December 2011 observed slightly lower values (Eskom, 2023a), as shown in ***Table 5.8.44***. The average daily total solar radiation measurement for December was 26.8 MJ/m^2.day and 8.4 MJ/m^2.day for June.
- Similarly, the actual solar radiation readings at the Duynefontyn WS for October 2017 to February 2022 also observed slightly lower values (Eskom, 2023a), as shown in ***Table 5.8.44***. The average daily total solar radiation measurement for December was 28.1 MJ/m^2.day and 9.2 MJ/m^2.day for June.
-
- The highest daily solar radiation was recorded in December with 30.3 MJ/m^2.day near the 120-m tower (January 2009 to December 2011) and 30.9 MJ/m^2.day at the Duynefontyn WS.
- The lowest daily solar radiation day near the 120-m tower (January 2009 to December 2011) occurred during May and June, which recorded 1.6 MJ/m^2.day.
- The lowest daily solar radiation was recorded in June with 1.6 MJ/m^2.day near the 120-m tower (January 2009 to December 2011) and 8.3 MJ/m^2.day at the Duynefontyn WS.

Table 5.8.44
Solar Radiation at the 120-m Tower (January 2009 to December 2011) and Duynefontyn WS (October 2017 to February 2022) Compared with Schulze’s Atlas for the Duynefontyn Region

Month	Average Daily Total (MJ/m^2.day)			Highest Daily Total (MJ/m^2.day)		Lowest Daily Total (MJ/m^2.day)	
	Schulze’s Atlas(1)	120-m tower (2008-2013)(2)	Duynefontyn WS (2017-2022)(3)	120-m tower (2008-2013)(2)	Duynefontyn WS (2017-2022)(3)	120-m tower (2008-2013)(2)	Duynefontyn WS (2017-2022)(3)
January	33.6	24.2	26.8	29.3	29.6	14.3	22.3
February	30.4	23.6	23.8	26.9	27.0	12.2	21.1
March	25.2	19.6	19.5	23.5	22.1	8.7	17.7
April	19.6	11.7	15.8	14.6	17.0	3.5	14.1
May	14.8	9.8	11.3	14.2	11.9	1.6	10.7
June	12.5	8.4	9.2	11.4	10.2	1.6	8.3
July	13.3	9.6	10.5	13.7	11.9	2.8	8.6
August	16.8	11.6	13.3	16.4	14.1	2.3	12.3
September	22.0	11.4	17.7	17.0	19.6	3.9	16.3
October	27.9	22.6	22.6	26.7	24.0	11.5	20.8
November	32.1	25.4	25.7	28.9	27.6	11.6	23.6
December	33.9	26.8	28.1	30.3	30.9	9.5	26.5

Notes:
(1) (Schulze, 1997)
(2) (Eskom, 2023a)
(3) Meteorological monitoring database

5.8.6.1.9 Atmospheric Stability

The atmospheric boundary layer includes the first few hundred metres of the atmosphere. This layer is directly affected by the earth’s surface, either through the retardation of flow due to the frictional drag of the earth’s surface, or as result of the heat and moisture exchanges that take place at the surface (Stull, 1997).

During the daytime, the atmospheric boundary layer is characterised by thermal turbulence due to the heating of the earth’s surface and the extension of the mixing layer to the lowest elevated inversion. Radiative flux divergence during the night usually results in the establishment of ground-based inversions. Night-time is characterised by weak vertical mixing and the predominance of a stable layer. These conditions are normally associated with low wind speeds, hence less dilution potential (Stull, 1997).

The mixed layer ranges in depth from a few metres (i.e. stable or neutral layers) during night-time to the base of the lowest-level elevated inversion during unstable, day-time conditions. Elevated inversions may occur for a variety of reasons and on some occasions as many as five may occur in the first 1 000 m above the surface (Tyson , et al., 1976).

The southern and western coastal areas experience a persistent low-level subsidence inversion, termed the sub-escarpment layer, with its base at approximately 500 m and a thickness of about 600 m. This layer is due to the predominance of the South Atlantic High Pressure (HP) system, and represents the boundary between the dry, subsided upper air and the moist influx of maritime air. The height above ground surface of this layer is related to the thickness of the sea breeze system and the intensity of subsidence in the upper air. The strength of the inversion has been shown to vary between an average of 7°C in summer and 5.2°C in winter (Tyson , et al., 1976; Preston-Whyte, et al., 1977). The sub-escarpment inversion is stronger and occurs more frequently during the summer (51 per cent) due to the South Atlantic HP reaching its most easterly position during December (Tyson , et al., 1976). Based on the temperature gradient between the 10 m and 120-m tower heights for the period October 1997 to July 2020, surface inversions occur for approximately 36 per cent over the year (Eskom, 2023a), being most prevalent during winter months with a 42 per cent frequency of occurrence (Eskom, 2023a). Summer occurrences are 30 per cent (Eskom, 2023a).

Eskom Standard 238-52 (Eskom, 2017) requires that the atmosphere be classified into one of seven atmospheric stability classes suggested by Pasquill in 1961 (Pasquill, 1961) and later modified by Gifford in 1962 (Gifford, 1961). The seven stability classes are described as follows:

A: Very unstable or convective conditions. Calm wind, clear skies and hot day-time conditions.

B: Moderately unstable. Clear skies, day-time conditions.

C: Unstable conditions. Moderate wind, slightly overcast day-time conditions.

D: Neutral atmospheres. Strong winds or cloudy days and nights.

E: Stable conditions. Moderate wind and slightly overcast night-time conditions.

F: Moderately stable conditions. Low winds, clear skies, cold night-time conditions.

G: Very stable conditions. Calm winds, clear skies, cold night-time conditions.

The frequencies of atmospheric stability classes were calculated according to the Eskom Standard 238-52 (Eskom, 2017) . The 120-m tower vertical temperature difference between levels 120 m and 10 m were used to calculate the vertical stability classes and the 50 m standard deviations of the wind direction ('sigma-theta method') were used to calculate the horizontal stability classes. The results for the period October 1997 to September 2023 are summarised in ***Table 5.8.45*** to ***Table 5.8.47***. ***Table 5.8.45*** corresponds to the classification using the vertical temperature difference, whereas ***Table 5.8.46*** and ***Table 5.8.47*** correspond to the classification using the sigma-theta method. The reference wind direction in ***Table 5.8.45*** and ***Table 5.8.46*** are as measured at the 50 m level on the 120-m tower and in ***Table 5.8.47*** the wind direction as measured at the 10 m level. The latter is included for comparison to the classifications at the Duynefontyn and five Koeberg AWSs (Bok Point, Robben Island, Rondekuil, Atlantis and Milnerton). The most prevalent atmospheric condition in both the vertical and horizontal was observed to be slightly stable (stability class E), with 37.39 per cent in the vertical and 49.00 per cent in the horizontal planes. This is followed by neutral conditions (stability class D), with 33.60 per cent in the vertical plane and 15.65 per cent in the horizontal plane.

Both the temperature gradient and sigma-theta methods (Eskom, 2017) were used to calculate the stability classes using the 8 m/2 m temperature difference (***Table 5.8.48***) and the standard deviation of wind direction at 9 m (***Table 5.8.49***) observed at the Duynefontyn WS. Using the sigma-theta methods, the most prevalent atmospheric condition at the Duynefontyn WS was observed to be slightly stable (stability class E) with 49.74 per cent which is similar to the 120-m tower classification of 49.01 per cent. The 120-m tower using the temperature gradient method with the temperature difference between levels 10 m and 120 m, resulted in a slightly lower frequency of 37.44 per cent for E- stability class. Similarly, the second highest frequency at both the Duynefontyn WS and the 120-m tower using the sigma-theta method was for neutral conditions (stability class D) with 22.26 per cent and 15.69 per cent, respectively. Using the temperature gradient method, D-stability class was calculated to be 33.86 per cent.

The temperature difference method for the Duynefontyn WS resulted in very different classifications. This is primarily due to the steep temperature gradient normally observed close to the ground – hence the requirement for additional temperature measurements in the surface layer depth (such as the case using the 120-m tower). The sigma-theta method is therefore more suitable for stability classification at the Duynefontyn WS.

Table 5.8.45

Joint Frequency Distribution of Pasquill-Gifford Stability Classes with Wind Direction: 120-Tower

(Delta-T Method [120m/10m] & Wind Direction at 50 m – (Eskom, 2017))

Wind Direction	**Stability Classification**							
	A	**B**	**C**	**D**	**E**	**F**	**G**	**Total**
N	0.03%	0.03%	0.08%	2.23%	1.93%	0.80%	0.17%	5.25%
NNE	0.02%	0.01%	0.03%	0.77%	1.06%	0.71%	0.25%	2.85%
NE	0.00%	0.00%	0.02%	0.25%	0.70%	0.81%	0.57%	2.36%
ENE	0.00%	0.00%	0.01%	0.27%	0.64%	0.93%	1.01%	2.87%
E	0.01%	0.01%	0.03%	0.32%	0.61%	0.90%	1.04%	2.94%
ESE	0.04%	0.04%	0.10%	0.55%	1.31%	1.80%	0.75%	4.58%
SE	0.05%	0.07%	0.21%	3.43%	7.07%	3.43%	0.32%	14.59%
SSE	0.55%	0.87%	1.19%	8.56%	4.94%	0.86%	0.06%	17.03%
S	0.11%	0.17%	0.26%	1.76%	2.95%	0.92%	0.18%	6.35%
SSW	0.06%	0.08%	0.13%	1.77%	3.23%	1.21%	0.29%	6.77%
SW	0.17%	0.18%	0.29%	2.06%	2.28%	0.71%	0.16%	5.85%
WSW	0.15%	0.16%	0.23%	1.79%	1.58%	0.46%	0.07%	4.44%
W	0.12%	0.14%	0.19%	1.77%	1.53%	0.45%	0.07%	4.27%
WNW	0.11%	0.12%	0.23%	2.44%	1.92%	0.53%	0.09%	5.43%
NW	0.10%	0.10%	0.22%	3.39%	2.91%	0.90%	0.12%	7.74%
NNW	0.04%	0.03%	0.07%	2.51%	2.79%	1.10%	0.15%	6.68%
Total	1.55%	2.02%	3.28%	33.86%	37.44%	16.54%	5.30%	100%

Table 5.8.46
Joint Frequency Distribution of Pasquill-Gifford Stability Classes with Wind Direction: 120-Tower (Sigma-Theta Method [50 m] & Wind Direction at 50 m – (Eskom, 2017))

Wind Direction	Stability Classification							
	A	B	C	D	E	F	G	Total
N	0.49%	0.17%	0.33%	0.92%	2.86%	0.39%	0.07%	5.24%
NNE	0.38%	0.13%	0.22%	0.39%	1.12%	0.50%	0.10%	2.84%
NE	0.35%	0.09%	0.15%	0.33%	0.73%	0.46%	0.24%	2.35%
ENE	0.32%	0.11%	0.23%	0.48%	1.06%	0.52%	0.13%	2.85%
E	0.43%	0.20%	0.36%	0.73%	0.98%	0.19%	0.03%	2.92%
ESE	0.52%	0.20%	0.42%	1.00%	1.94%	0.47%	0.01%	4.56%
SE	0.57%	0.26%	0.50%	1.53%	8.17%	3.40%	0.09%	14.53%
SSE	0.69%	0.34%	0.71%	1.91%	11.73%	1.61%	0.03%	17.02%
S	0.79%	0.37%	0.72%	1.38%	2.49%	0.63%	0.03%	6.41%
SSW	0.58%	0.22%	0.43%	0.94%	2.59%	1.78%	0.24%	6.78%
SW	0.52%	0.19%	0.39%	0.89%	2.26%	1.40%	0.25%	5.89%
WSW	0.55%	0.24%	0.46%	1.10%	1.68%	0.42%	0.03%	4.47%
W	0.60%	0.23%	0.49%	1.14%	1.61%	0.20%	0.02%	4.29%
WNW	0.59%	0.23%	0.41%	0.96%	2.71%	0.54%	0.01%	5.45%
NW	0.57%	0.23%	0.45%	1.05%	3.93%	1.48%	0.03%	7.73%
NNW	0.57%	0.24%	0.40%	0.94%	3.14%	1.24%	0.12%	6.66%
Total	8.51%	3.46%	6.66%	15.69%	49.01%	15.24%	1.43%	100%

Table 5.8.47

Joint Frequency Distribution of Pasquill-Gifford Stability Classes with Wind Direction: 120-Tower (Sigma-Theta Method [50 m] & Wind Direction at 10 m – (Eskom, 2017))

Wind Direction	Stability Classification							
	A	B	C	D	E	F	G	Total
N	0.50%	0.16%	0.29%	0.80%	2.74%	0.59%	0.06%	5.13%
NNE	0.65%	0.17%	0.29%	0.58%	1.81%	0.69%	0.10%	4.28%
NE	0.93%	0.28%	0.45%	0.79%	1.43%	0.65%	0.21%	4.75%
ENE	0.76%	0.36%	0.59%	1.26%	2.27%	0.85%	0.24%	6.32%
E	0.50%	0.22%	0.47%	0.97%	1.71%	0.49%	0.05%	4.40%
ESE	0.34%	0.16%	0.34%	0.92%	2.51%	1.29%	0.05%	5.62%
SE	0.28%	0.14%	0.29%	1.01%	7.19%	2.48%	0.07%	11.46%
SSE	0.31%	0.18%	0.39%	1.20%	8.98%	1.14%	0.03%	12.23%
S	0.41%	0.24%	0.56%	1.18%	2.92%	0.38%	0.01%	5.71%
SSW	0.42%	0.19%	0.39%	0.86%	2.26%	1.32%	0.08%	5.52%
SW	0.43%	0.18%	0.36%	0.83%	2.31%	1.75%	0.35%	6.21%
WSW	0.55%	0.24%	0.48%	1.16%	2.15%	0.72%	0.08%	5.38%
W	0.72%	0.32%	0.62%	1.42%	2.02%	0.36%	0.02%	5.47%
WNW	0.64%	0.24%	0.44%	1.03%	2.81%	0.53%	0.01%	5.69%
NW	0.57%	0.22%	0.40%	0.87%	3.42%	1.20%	0.01%	6.69%
NNW	0.51%	0.17%	0.31%	0.79%	2.49%	0.82%	0.04%	5.13%
Total	8.51%	3.46%	6.66%	15.69%	49.01%	15.24%	1.43%	100%

Table 5.8.48
Joint Frequency Distribution of Pasquill-Gifford Stability Classes with Wind Direction: Duynefontyn WS
(Delta-T Method [8m/2m] – (Eskom, 2017))

Wind Direction	Stability Classification							
	A	**B**	**C**	**D**	**E**	**F**	**G**	**Total**
N	3.50%	0.03%	0.04%	0.14%	0.32%	0.31%	0.97%	5.29%
NNE	1.92%	0.03%	0.04%	0.17%	0.45%	0.32%	1.60%	4.53%
NE	2.42%	0.04%	0.08%	0.24%	0.65%	0.66%	2.57%	6.66%
ENE	1.56%	0.03%	0.06%	0.13%	0.39%	0.34%	1.73%	4.25%
E	1.21%	0.03%	0.05%	0.12%	0.33%	0.25%	0.97%	2.96%
ESE	3.22%	0.05%	0.05%	0.23%	0.63%	0.32%	1.07%	5.58%
SE	7.98%	0.05%	0.08%	0.25%	0.88%	0.40%	1.15%	10.80%
SSE	8.92%	0.05%	0.04%	0.22%	0.68%	0.32%	0.77%	11.00%
S	6.50%	0.01%	0.02%	0.10%	0.44%	0.12%	0.27%	7.47%
SSW	6.32%	0.01%	0.05%	0.08%	0.30%	0.12%	0.27%	7.17%
SW	4.39%	0.02%	0.01%	0.08%	0.27%	0.11%	0.29%	5.17%
WSW	4.00%	0.01%	0.02%	0.07%	0.25%	0.13%	0.30%	4.78%
W	4.83%	0.03%	0.04%	0.08%	0.29%	0.11%	0.31%	5.69%
WNW	6.11%	0.02%	0.02%	0.09%	0.42%	0.14%	0.34%	7.13%
NW	4.91%	0.02%	0.02%	0.06%	0.28%	0.11%	0.36%	5.76%
NNW	4.76%	0.02%	0.02%	0.10%	0.25%	0.16%	0.44%	5.75%
Total	72.57%	0.47%	0.66%	2.16%	6.82%	3.93%	13.39%	100%

Table 5.8.49
Joint Frequency Distribution of Pasquill-Gifford Stability Classes with Wind Direction: Duynefontyn WS (Sigma-Theta Method [9 m] – (Eskom, 2017))

Wind Direction	Stability Classification							
	A	B	C	D	E	F	G	Total
N	0.80%	0.26%	0.38%	2.44%	1.24%	0.02%	0.02%	5.16%
NNE	0.69%	0.22%	0.42%	0.72%	1.77%	0.60%	0.01%	4.42%
NE	0.80%	0.38%	0.60%	1.25%	2.87%	0.58%	0.00%	6.49%
ENE	0.74%	0.24%	0.46%	0.83%	1.77%	0.13%	0.00%	4.16%
E	0.60%	0.29%	0.40%	0.81%	0.82%	0.02%	0.00%	2.93%
ESE	0.61%	0.39%	0.63%	1.28%	2.64%	0.03%	0.00%	5.57%
SE	0.65%	1.50%	0.64%	1.98%	6.28%	0.01%	0.01%	11.07%
SSE	0.75%	1.36%	0.75%	1.69%	6.64%	0.00%	0.01%	11.21%
S	0.63%	0.38%	0.76%	1.13%	4.66%	0.01%	0.00%	7.57%
SSW	0.57%	0.29%	0.62%	1.01%	4.70%	0.01%	0.00%	7.20%
SW	0.47%	0.29%	0.44%	0.89%	3.06%	0.01%	0.00%	5.17%
WSW	0.55%	0.20%	0.36%	1.18%	2.45%	0.04%	0.00%	4.78%
W	0.55%	0.35%	0.48%	1.19%	3.12%	0.03%	0.00%	5.71%
WNW	0.61%	0.49%	0.75%	1.02%	4.32%	0.00%	0.00%	7.19%
NW	0.72%	0.56%	0.39%	2.12%	1.95%	0.00%	0.00%	5.74%
NNW	0.79%	0.37%	0.29%	2.72%	1.45%	0.00%	0.00%	5.62%
Total	10.52%	7.57%	8.36%	22.26%	49.74%	1.49%	0.06%	100%

The stability classes were also calculated using the sigma-theta method for the observations from the AWSs located at Bok Point (***Table 5.8.50***), Robben Island (***Table 5.8.51***), Rondekuil (***Table 5.8.52***), Atlantis (***Table 5.8.53***) and Milnerton (***Table 5.8.54***).

The atmospheric stability changes per hour of day depending on the thermal and mechanical turbulence. The delta-T method is preferred for establishing the vertical atmospheric stability, but only if the two temperatures adequately represent the conditions in the surface layer. The two temperatures at 10 m and 120 m on the 120-m tower are considered to be adequate for the delta-T method, whereas the temperature measurements at 2 m and 8 m on the Duynefontyn WS mast only observe a small part of the surface layer, i.e. the section with the steepest vertical temperature gradient. In this case, it is therefore more advisable to utilise the sigma-theta method, or the solar radiation/delta-T (SRDT) method as recommended by the US EPA (United States Environmental Protection Agency, 2000) and ANS (American National Standard, 2015). Measured solar radiation and delta temperature data, in combination with wind speed, provide a more complete characterisation of the physical forces affecting turbulence intensity in the atmospheric boundary layer (American National Standard, 2015). This method of determining the stability classes is based on values of solar radiation and wind speed during the day and a temperature measurement between two observation levels (e.g., between 8 m and 2 m) and wind speed at night. The SRDT method is not included in this report since it was not included in the Eskom Standard 238-52 (Eskom, 2017).

Given the different stability calculation results, it is recommended to utilise the results from the delta-T method with temperature difference between levels 10 m and 120 m on the 120-m tower (***Table 5.8.45***).

The vertical component of dispersion is a function of the extent of thermal turbulence and the depth of the surface-mixing layer. Unfortunately, the mixing layer is not easily measured as this requires measurements up to 1 km to 2 km above surface. Since the 120-m tower provides only meteorological observations for the lower part of the boundary layer (120 m and less), the mixing layer depths for the dispersion model were estimated using prognostic models that derive the depth from other parameters including solar radiation, wind speed, dry bulb temperature and atmospheric turbulence that are routinely measured (see (International Atomic Energy Agency, 2011)). (Estimates of inversion layers and mixing layer depths can be obtained with the aid of a Doppler Acoustic Sodar[10]).

---

[10] The Doppler Acoustic Sodar system is an acoustic measurement system, which has a minimum of three sound sources in different measuring directions. In each direction, the air velocity in the measuring beam direction is

Table 5.8.50
Joint Frequency Distribution of Pasquill-Gifford Stability Classes with Wind Direction: Bok Point WS
(Sigma-Theta Method [10 m] – (Eskom, 2017))

Wind Direction	Stability Classification							
	A	B	C	D	E	F	G	Total
N	1.12%	0.90%	1.41%	2.74%	3.90%	0.76%	0.12%	10.94%
NNE	0.14%	0.12%	0.22%	0.47%	1.58%	0.91%	0.30%	3.75%
NE	0.12%	0.11%	0.15%	0.21%	0.50%	0.22%	0.04%	1.34%
ENE	0.12%	0.12%	0.16%	0.25%	0.70%	0.41%	0.04%	1.81%
E	0.17%	0.15%	0.30%	0.63%	2.15%	1.57%	0.04%	5.01%
ESE	0.18%	0.21%	0.43%	1.15%	4.58%	2.37%	0.03%	8.96%
SE	0.17%	0.23%	0.57%	1.47%	4.17%	1.19%	0.00%	7.81%
SSE	0.19%	0.27%	0.74%	1.91%	5.08%	4.70%	0.00%	12.89%
S	0.19%	0.26%	0.72%	1.48%	3.77%	3.46%	0.00%	9.89%
SSW	0.16%	0.21%	0.56%	1.03%	3.42%	2.89%	0.00%	8.26%
SW	0.14%	0.14%	0.35%	0.81%	2.11%	1.06%	0.00%	4.61%
WSW	0.13%	0.12%	0.30%	0.78%	1.86%	0.19%	0.00%	3.38%
W	0.12%	0.14%	0.26%	0.84%	1.88%	0.08%	0.01%	3.33%
WNW	0.13%	0.13%	0.25%	0.81%	3.23%	0.15%	0.00%	4.71%
NW	0.13%	0.14%	0.29%	1.02%	3.67%	0.07%	0.00%	5.32%
NNW	0.22%	0.26%	0.60%	1.54%	5.13%	0.24%	0.01%	8.00%
Total	3.42%	3.50%	7.31%	17.14%	47.73%	20.29%	0.61%	100%

---

determined with the aid of the Doppler phenomenon. Combining measurements conducted in different directions, the system determines the wind components of the mixing layer at intervals of at least 50 m in the vertical direction, up to the highest possible height in each weather situation. The wind direction and velocity, deviation of the wind direction as well as the deviation parameters and the height of the potential inversion layer, necessary for dispersion calculations, are determined on the basis of the measurement results.

Table 5.8.51

Joint Frequency Distribution of Pasquill-Gifford Stability Classes with Wind Direction: Robben Island WS (Sigma-Theta Method [10 m] – (Eskom, 2017))

Wind Direction	Stability Classification							
	A	B	C	D	E	F	G	Total
N	0.21%	0.23%	0.74%	2.89%	4.95%	0.92%	0.01%	9.95%
NNE	0.17%	0.17%	0.30%	0.64%	2.06%	1.48%	0.01%	4.84%
NE	0.14%	0.14%	0.20%	0.34%	0.81%	0.63%	0.01%	2.26%
ENE	0.14%	0.11%	0.20%	0.27%	0.32%	0.05%	0.01%	1.09%
E	0.15%	0.12%	0.20%	0.30%	0.43%	0.11%	0.00%	1.31%
ESE	0.19%	0.15%	0.25%	0.48%	1.36%	1.41%	0.02%	3.86%
SE	0.27%	0.26%	0.45%	1.11%	5.29%	3.36%	0.01%	10.75%
SSE	0.46%	0.50%	0.97%	2.30%	14.56%	0.79%	0.00%	19.59%
S	0.42%	0.42%	0.79%	1.44%	0.82%	0.02%	0.00%	3.92%
SSW	0.32%	0.30%	0.65%	3.38%	1.07%	0.04%	0.00%	5.77%
SW	0.31%	0.25%	0.57%	4.86%	1.74%	0.09%	0.01%	7.82%
WSW	0.27%	0.25%	0.75%	2.70%	0.55%	0.05%	0.00%	4.58%
W	0.26%	0.24%	0.98%	1.86%	0.27%	0.02%	0.00%	3.63%
WNW	0.24%	0.25%	0.72%	2.45%	0.47%	0.04%	0.00%	4.17%
NW	0.24%	0.24%	0.58%	1.90%	3.26%	0.06%	0.00%	6.28%
NNW	0.24%	0.24%	0.48%	1.44%	6.10%	1.68%	0.00%	10.17%
Total	4.04%	3.87%	8.84%	28.33%	44.07%	10.75%	0.09%	100.0%

Table 5.8.52
Joint Frequency Distribution of Pasquill-Gifford Stability Classes with Wind Direction: Rondekuil WS
(Sigma-Theta Method [10 m] – (Eskom, 2017))

Wind Direction	Stability Classification							
	A	B	C	D	E	F	G	Total
N	0.55%	0.44%	0.86%	2.45%	3.47%	0.07%	0.02%	7.85%
NNE	0.69%	0.56%	1.04%	2.50%	4.03%	0.28%	0.04%	9.14%
NE	0.57%	0.49%	0.89%	2.19%	2.78%	0.21%	0.01%	7.14%
ENE	0.42%	0.32%	0.57%	1.11%	1.42%	0.11%	0.00%	3.95%
E	0.36%	0.22%	0.31%	0.41%	0.44%	0.06%	0.00%	1.80%
ESE	0.36%	0.22%	0.29%	0.39%	0.64%	0.10%	0.01%	2.01%
SE	0.44%	0.29%	0.40%	0.56%	1.13%	0.27%	0.01%	3.12%
SSE	0.62%	0.47%	0.72%	1.18%	3.26%	0.31%	0.01%	6.56%
S	0.71%	0.57%	1.01%	2.71%	7.24%	0.13%	0.00%	12.37%
SSW	0.93%	0.75%	1.27%	2.41%	2.79%	0.04%	0.00%	8.20%
SW	1.23%	1.07%	1.92%	4.06%	4.06%	0.15%	0.00%	12.50%
WSW	1.04%	0.87%	1.55%	3.88%	4.15%	0.05%	0.00%	11.55%
W	0.60%	0.35%	0.58%	1.51%	1.56%	0.03%	0.00%	4.65%
WNW	0.41%	0.20%	0.29%	0.76%	1.36%	0.02%	0.00%	3.05%
NW	0.34%	0.20%	0.26%	0.54%	1.36%	0.00%	0.00%	2.70%
NNW	0.43%	0.24%	0.33%	0.72%	1.67%	0.03%	0.00%	3.42%
Total	9.71%	7.29%	12.28%	27.39%	41.36%	1.87%	0.11%	100.0%

Table 5.8.53

Joint Frequency Distribution of Pasquill-Gifford Stability Classes with Wind Direction: Atlantis WS (Sigma-Theta Method [10 m] – (Eskom, 2017))

Wind Direction	Stability Classification							
	A	**B**	**C**	**D**	**E**	**F**	**G**	**Total**
N	0.35%	0.45%	2.72%	4.02%	1.35%	0.17%	0.03%	9.10%
NNE	0.35%	0.45%	1.25%	1.27%	0.95%	0.15%	0.02%	4.45%
NE	0.37%	0.41%	0.53%	1.09%	1.35%	0.17%	0.00%	3.92%
ENE	0.34%	0.37%	0.69%	1.60%	1.17%	0.04%	0.00%	4.20%
E	0.42%	0.39%	0.93%	1.80%	0.71%	0.01%	0.00%	4.25%
ESE	0.52%	0.57%	1.36%	1.74%	0.17%	0.00%	0.00%	4.36%
SE	0.60%	0.63%	1.37%	1.89%	0.26%	0.01%	0.00%	4.75%
SSE	0.59%	0.67%	2.80%	4.92%	0.48%	0.01%	0.00%	9.48%
S	0.53%	0.70%	3.23%	6.15%	0.49%	0.01%	0.00%	11.10%
SSW	0.56%	0.74%	3.05%	3.72%	0.30%	0.01%	0.00%	8.38%
SW	0.53%	0.78%	3.63%	2.40%	0.17%	0.00%	0.00%	7.52%
WSW	0.44%	0.79%	3.59%	1.65%	0.16%	0.00%	0.00%	6.64%
W	0.37%	0.62%	2.17%	1.09%	0.09%	0.00%	0.00%	4.34%
WNW	0.31%	0.51%	1.94%	1.26%	0.11%	0.00%	0.00%	4.12%
NW	0.29%	0.36%	1.43%	2.26%	0.49%	0.02%	0.00%	4.85%
NNW	0.31%	0.36%	1.52%	4.94%	1.30%	0.10%	0.01%	8.54%
Total	6.87%	8.80%	32.20%	41.80%	9.56%	0.69%	0.08%	100.0%

Table 5.8.54
Joint Frequency Distribution of Pasquill-Gifford Stability Classes with Wind Direction: Milnerton WS
(Sigma Theta Method [10 m] – (Eskom, 2017))

Wind Direction	Stability Classification							
	A	**B**	**C**	**D**	**E**	**F**	**G**	**Total**
N	1.36%	0.76%	2.05%	1.28%	0.12%	0.00%	0.00%	5.58%
NNE	0.56%	0.48%	0.87%	0.71%	0.15%	0.01%	0.00%	2.80%
NE	0.23%	0.16%	0.23%	0.20%	0.09%	0.01%	0.01%	0.93%
ENE	0.16%	0.11%	0.15%	0.17%	0.11%	0.01%	0.01%	0.72%
E	0.16%	0.11%	0.18%	0.27%	0.29%	0.02%	0.00%	1.02%
ESE	0.18%	0.15%	0.34%	1.66%	1.45%	0.05%	0.00%	3.83%
SE	0.23%	0.26%	1.84%	6.63%	0.94%	0.01%	0.00%	9.91%
SSE	0.32%	0.69%	18.49%	13.44%	0.46%	0.01%	0.00%	33.40%
S	0.27%	0.50%	4.10%	1.76%	0.09%	0.00%	0.00%	6.73%
SSW	0.23%	0.27%	0.35%	0.25%	0.09%	0.00%	0.00%	1.19%
SW	0.19%	0.21%	0.32%	0.37%	0.18%	0.00%	0.00%	1.28%
WSW	0.22%	0.22%	0.46%	1.54%	0.67%	0.01%	0.00%	3.12%
W	0.22%	0.25%	0.61%	4.52%	1.95%	0.01%	0.00%	7.58%
WNW	0.26%	0.28%	0.91%	5.20%	0.35%	0.00%	0.00%	7.01%
NW	0.34%	0.42%	1.08%	5.69%	0.80%	0.00%	0.00%	8.34%
NNW	0.83%	0.83%	1.59%	3.13%	0.16%	0.00%	0.00%	6.55%
Total	5.76%	5.71%	33.59%	46.82%	7.93%	0.16%	0.04%	100.0%

5.8.6.1.10 Evapotranspiration Rate

Evapotranspiration rates were calculated for the January 2009 to December 2011 monitoring period (monitored near the 120-m tower) and for the October 2017 to February 2022 monitoring period at the Duynefontyn WS using the Penman[11] and Penman-Monteith[12] methods for open water and crop evaporation (see ***Table 5.8.55***). These methods require data on dry bulb temperature, relative humidity, solar radiation and wind speed as discussed in ***Appendix 5.8.C***).

Estimates from the atlas of potential evapotranspiration rates[13] for South Africa (Schulze, 1997) have also been included (see ***Table 5.8.55***) to enable a comparison of these regional values with the calculated values using the site data. The evapotranspiration rates calculated using Penman-Monteith method are generally lower, and using the Penman method generally higher than Schulze's estimates, but the same monthly trends and values are observed, with:

- the maximum evapotranspiration rates during November and December at the site;
- the minimum evapotranspiration rate during June at the site.

---

[11] In 1948, Penman combined an energy balance with a mass transfer method and derived an equation to compute the evaporation from an open water surface from standard climatological records of sunshine, temperature, humidity and wind speed.

[12] The Penman method was further developed by many researchers and extended to cropped surfaces by introducing resistance factors. The Penman-Monteith equation is one such method and predicts the crop evapotranspiration at a location using daily mean temperature, wind speed, relative humidity, and solar radiation.

[13] The rate of evapotranspiration from a hypothetical crop with an assumed crop height of 0.12 m, a fixed canopy resistance of 70.00 s/m and an albedo of 0.23, which would closely resemble evapotranspiration from an extensive surface of green grass of uniform height, actively growing, completely shading the ground and not short of water.

Table 5.8.55
Monthly Total Potential Evapotranspiration Rates

Month	Schulze's Atlas[1]	120-m Tower[2] (January 2009- December 2011)		Duynefontyn WS (October 2017- February 2022)	
	(mm)	(mm)		(mm)	
	Penman-Monteith	Penman-Monteith	Penman	Penman-Monteith	Penman
January	210	154.5	243.2	167.2	209.8
February	168	135.9	209.8	167.7	214.1
March	146	126.8	191.4	149.9	187.5
April	99	75.5	111.1	101.5	116.2
May	72	52.5	77.3	85.3	103.9
June	54	46.5	68.6	68.7	76.3
July	58	58.8	85.9	84.0	104.5
August	75	58.4	85.8	91.0	117.9
September	102	51.4	76.2	117.2	150.9
October	143	98.9	150.8	163.5	210.7
November	172	120.1	185.4	180.7	237.0
December	205	151.1	235.6	179.6	231.6

Notes:
(1) (Schulze, 1997)
(2) (Eskom, 2023a)

The high evaporation rates observed during the summer months (***Table 5.8.55***) are further exacerbated through the coincidence of the summer dry season. Windy conditions during the summer are therefore more conducive to episodes of windblown dust than during the winter.

5.8.6.1.11 Corrosivity

(a) Abrasive Effects by Sand and Dust

Since strong winds are evident at the site, large exposed sandy areas could be prone to the development of windblown dust. They occur when wind forces exceed the threshold value at which loose sand and dust are removed from a dry surface and become airborne. The term 'dust storm' is most often used when fine particles are blown long distances, whereas the term 'sandstorm' is more likely to be used when, in addition to fine particles obscuring visibility, a considerable amount of larger sand particles become airborne and are mobilised, but closer to the surface. The vegetation found on the site, however, acts as a natural mitigation measure. Dust mobilisation occurs only for wind velocities higher than a threshold value and is not linearly dependent on the wind friction and velocity. Typically, wind speeds that exceed 5.4 m/s near the surface (United States Environmental Protection Agency , 1992) could initiate dust mobilisation from disturbed land surfaces. The IAEA (International Atomic Energy Agency, 2011) suggests 5.8 m/s for this threshold. An alternative form to describe the mobilisation threshold is by using a threshold friction velocity. The threshold friction velocity, defined as the minimum friction velocity required for the initiation of particle motion, is dependent on the size of the erodible particles and the effect of the wind shear stress on the surface. The threshold friction velocity decreases with a decrease in the particle diameter, for particles with diameters >60 µm. Particles with a diameter <60 µm result in increasingly high threshold friction velocities, due to the increasingly strong cohesion forces linking such particles to each other (Marticorena & Bergametti, 1995). Duynefontyn is characterised by aeolian sands with particle size ranges from 283µm to 496µm (***Appendix 5.8.H***). The friction velocity is therefore estimated to be about 0.3 m/s to 0.4 m/s (Marticorena & Bergametti, 1995).

(Hsu, 1977) established a relationship for the friction velocity in terms of wind speeds measured at 2 m above the surface:

$$u_* = au_{2m}$$

where the constant *a* varies between 0.037 to 0.099, as shown below:

Tidal flat	a = 0.037
Beaches	a = 0.044
Low dune field (<50cm)	a = 0.048
Dune (scarp)	a = 0.050
Swale	a = 0.058
Dune top (<45 m)	a = 0.070
Dune lee	a = 0.099

Assuming the constant representing dunes of 0.050, the threshold velocity is estimated at 6.0 m/s at 2 m measurement height or 7.5 m/s by extrapolating to 9 m height.

According to the IAEA (International Atomic Energy Agency, 2011), the frequency of dust storms and sandstorms can be identified through hourly weather observations when visibility is 10 kilometres or less, the wind speed exceeds a threshold value (i.e. 7.5 m/s), and relative humidity is below a threshold value (i.e. less than 70 per cent) (International Atomic Energy Agency, 2011).

On analysis of the Duynefontyn WS data (January 2018 to April 2022), the highest number of hours of windblown dust occurred during the summer months, with January experiencing the highest occurrence. The lowest dust conditions occurred during May. These results are summarised in ***Figure 5.8.18***.

The IAEA (2011) further proposes that appropriate values of dust or sand concentration should be computed on the basis of empirical relationships using visibility observations. The need to understand the relationship between visibility and dust concentration as part of wind erosion research has long been recognised (e.g. (Chepil & Woodruff, 1957; Patterson & Gillette, 1977; Ette & Olorode, 1988; Ackerman & Cox, 1989). In a relatively recent study by Baddock *et al* (Baddock, et al., 2014), several empirical correlations were analysed and that led to a new correlation that was based on an outcome of an ongoing, long term, synergistic dust monitoring programme in rural New South Wales, Australia. The general form of these correlations is as follows:

$$C_{VTSD} = bVis^{n}$$

Where C_{VTSD} is the total suspended dust concentration (mg/m³), Vis is the visibility (km) and *b* and *n* are experimentally derived constants. Baddock *et al* (Baddock, et al., 2014) derived the following values for the constants:

$$b = 4.050 \text{ and } n = -1.016$$

As recommended by the IAEA (International Atomic Energy Agency, 2011), the results of the assessment are to be expressed as total dust or sand loading (mg-h/m³), duration (h), and average dust or sand loading (mg/m³) for the historic dust storm or sandstorm that had the largest calculated time integrated dust or sand loading. The dust loadings were calculated using the IAEA (International Atomic Energy Agency, 2011) methodology and the concentrations estimated as indicated in the above equation.

The highest dust loading during the monitoring period occurred from 09h00 to 22h00 on 17 December 2020. The time integrated dust loading for this period was calculated to be 64.9 mg-h/m³ and the duration, 14 hours. The average dust concentration during this period was 4.63 mg/m³. The average wind speed for the 14-hour period was 9.8 m/s which occurred from the south, with maximum gusts up to 17.3 m/s, maximum 10-minute average wind speeds up to 12.6 m/s and maximum hourly average wind speed of 9.9 m/s.

Based on the observed frequency of dust events (***Figure 5.8.18***), January, February and November are the months most likely to experience dust storms, whereas May to August are the months least likely to experience dust storms. It is likely that the summer season is likely to have about 10 days of dust events in total.

(b) Freeze-Thaw

There are two ways that the phenomenon of freeze-thaw occurs in nature. The first is through the repeated cycle of melting and freezing of water on the natural cracks and grooves of rocks, or concrete building structures. The second phenomenon occurs when the surface layer of rock or concrete is baked by direct sunlight causing the top layer to expand and contract repeatedly, causing distress and eventually, cracks. Both phenomena require extreme daily temperature variations. Concrete can better withstand the effects of both phenomena with the addition of additives. Freeze-thaw occurs when concrete (or rocks) is saturated with water and the temperature drops, freezing the water molecules. The frozen water expands 9 per cent of its original volume. Whilst there are many theories (Guo, et al., 2022)as to the damage mechanisms in concrete, the simple view Is that the increase in volume produces increased pressure in the pores of the concrete. Tiny cracks will form where this pressure exceeds the tensile strength of the concrete. Increased frequency of freeze-thaw cycles will result in more stress on the concrete structure. However, besides the frequency of freeze–thaw cycles, the frost intensity should also play an important role. The frost intensity describes how long and to what extent the temperature falls below the 0°C transition. According to (Walder & Hallet , 1985), most of the damage potential can be assumed for a temperature of -10°C.

However, this temperature range has not been observed at the Duynefontyn site with the recorded lowest hourly average of 3.2°C. The 10 000-year return period projects a temperature below 0°C, i.e. -0.5°C. Even the projected 100 000 000-year return period estimate of -6.0 ± 3.4°C does not reach -10°C. The possibility of freeze-thaw from frozen water in the pores is therefore not likely at the site; estimated to be 1 in 10 000 years chance, and hence freezing thaw phenomenon is not an issue. Additionally, regarding the possibility of ice occurring in the sea surrounding the site, the lowest seawater temperature measured in all the data sets described in ***Section 5.9*** is 8.12°C, and an extreme value analysis of the minimum measured temperatures at Site C (-3m msl) was above 0°C at an exceedance of 1x10-8 per year. On this basis ice is not anticipated to form in the sea at the site.

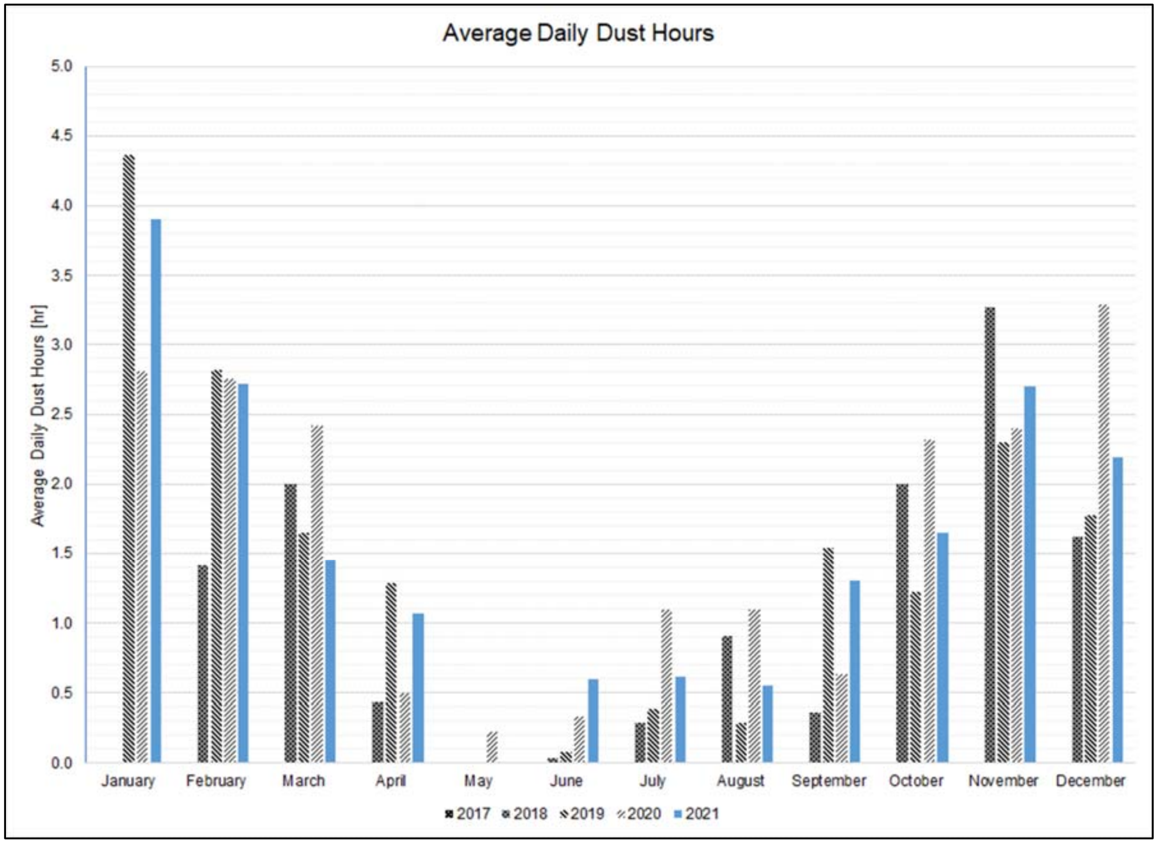

Figure 5.8.18
Average Durations (Hours) of Dust Conditions per Day Per Month

(c) Atmospheric Corrosion

Metal components exposed to weather elements and sea mist will inevitably experience damage due to atmospheric corrosion. The severity of the corrosion and the rate at which corrosion will take place are dependant primarily upon the properties of the surface formed electrolytes, which in turn are dependent upon factors such as the humidity and pollution levels in the atmosphere.

Three relatively common methods to assess the corrosivity of a particular atmosphere include:

- The coupon-based method (CLIMAT). This method involves the exposure of metallic coupons which may include steel, zinc, copper and aluminium to the environment and classifying the resultant corrosion. Flat panels exposed on exposure racks are a common coupon-type device for atmospheric corrosivity measurements (ISO Standard 9226, (International Organisation of Standardisation, 2012d)). ISO 9226 also provides the open helix specimens as an alternative. The ‘wire-on-bolt’[14] is a slight modification of this version. Various other specimen configurations may also be used, including stressed U-bend or C-ring specimens for stress corrosion cracking studies.
- Different from the coupon method, the exposure programme provides actual corrosion rates of materials. The corrosion rates are calculated from the weight loss because of corrosion over the test period. The test period is however considerably longer than for the CLIMAT testing, with panels being removed for evaluation only once a year. Typically, a number of test panels for each material would be exposed so that as the panels are removed, the corrosion rates for exposure times of one year, two year, three years etc. can be determined. This provides information as to whether the corrosion rate of a material increases or decreases with time.
- The third method (ISO Standard 9223, (International Organisation for Standardisation, 2012a)) involves measuring meteorological parameters (temperature and relative humidity) and the deposition rate of sulfur dioxide and airborne salinity and classifying the atmosphere according to standardised measurements.

Four campaigns of corrosion monitoring have been completed. The first campaign employed the coupon-based and exposure methods

---

[14] With the ‘wire on bolt’ technique, the CLIMAT unit consists of three bolts of different materials around which are wound aluminium wires of known mass. The bolt materials used are nylon, steel and copper to determine the atmospheric, marine and industrial corrosivities, respectively.

(January 1991 to February 1993) (Gross & Nixon, 1993), with the second, third and fourth campaigns based on the monitoring of sulfur dioxide fallout, airborne salinity and meteorological parameters. The second campaign occurred during the period 17 May 2008 to 25 January 2009, the third campaign from 10 October 2012 to 12 September 2013 and the fourth campaign from 10 October 2017 to 10 March 2022 (Burger, 2022). The results from these campaigns are discussed below.

(i) Coupon-Based Corrosion Monitoring

Two CLIMAT units were placed at two locations on the site (Gross & Nixon, 1993). The first site is situated approximately 50 m from the high tide mark and is at an elevation of 1.5 m above ground. The test period reported includes the results from June 1991 to January 1993. The second test site is situated at the Koeberg WS, approximately 740 m[15] from the high tide mark. The corrosivities were evaluated over the period August 1991 to September 1992. CLIMAT units were attached to the 120-m tower at elevations of 12 m, 48 m, 84 m and 120 m above the tower base, which is at about 24 m amsl. The coupons were exposed for approximately 90 days where after the weight loss of the exposed materials were measured and from this the corrosivity was calculated.

Marine corrosion is the controlling form of corrosion (Gross & Nixon, 1993), followed by atmospheric corrosivity and the much less significant industrial corrosivity. The corrosivities are expressed in terms of degrees of severity and are divided into five levels depending upon the average per cent mass loss measured. The definitions of these levels are provided in ***Table 5.8.56***. The *Negligible* range would indicate that the corrosion rates are very low and only minimal corrosion protection would be required. The corrosion would become significant in the *Moderate* range increasing up to the *Very Severe* range where corrosion would be expected to be a major problem requiring comprehensive corrosion protection.

Table 5.8.56
Classification of Marine Atmospheres Based on the Per Cent Mass Loss

Classification	% Mass Loss	Significance
Negligible (N)	0% to 2%	Average Habitable Area
Moderate (M)	2% to 5%	Seaside
Moderately Severe (MS)	5% to 10%	Seaside and Exposed
Severe (S)	10% to 20%	Very Exposed
Very Severe (VS)	above 20%	Very Exposed, Wind and Sand Swept

---

[15] The original report states “approximately 1000m”, however, when this was reviewed it is estimated to be closer to 740 m from the high tide mark.

Averages of the marine corrosivity values measured at the two sites over the respective test periods are summarised in ***Table 5.8.57*** (Gross & Nixon, 1993) for the period January 1991 to February 1993. The marine corrosivity results at the test site closest to the ocean can be seen to be in the very severe range. The highest result recorded was for the period October 1992 to January 1993.

In comparison, the results on the 120-m tower were all in the severe range with the exception of a single value in the very severe range at 12 m. This high value was recorded during the period May 1992 to September 1992. This coincides with the second highest value recorded at the test site. Increases in the height above the tower base did not significantly reduce the corrosivities. The report concluded that the site experiences severe marine corrosion, but that there is a reduction as the distance from the high-tide mark increases.

Table 5.8.57
Average Marine Corrosivity at the Site (Gross & Nixon, 1993)

	Distance from High Tide Mark	Height above Ground Level	Corrosivity (% Mass Loss)	
Test site	50 m	1.5 m	34.4%	June 1991 to January 1993
120-m Tower	740 m	12 m	25.2%	August 1991 to September 1992.
		48 m	17.4%	
		84 m	16.9%	
		120 m	16.3%	

Note: Samples were located on 3-month, back-to-back cycles for the indicated periods

(ii) Metal Exposure Corrosion Monitoring

Annual corrosion rates were also determined for the first year's exposure (1991) of metals to the atmosphere at the test site. The exposed metals included mild steel, galvanised steel, stainless steel (grades 3CR12[16] and AISI 316L[17]), copper, aluminium, and zinc. The results are provided in ***Table 5.8.58*** (Gross & Nixon, 1993). The highest corrosion rate was recorded for mild steel of 0.38 mm/year. The corrosion rate for 3CR12 steel of 0.11 mm/year indicates very high corrosion conditions (Gross & Nixon, 1993). Aluminium and AISI 316L showed no mass loss (0.000 mm/year) and no pitting or localised corrosion attack was identified.

---

[16] 3CR12 is a 11 to 12 per cent chromium containing corrosion resisting ferritic steel.

[17] AISI 316L is a low carbon (less than or equal to 0.03 per cent) stainless steel

Table 5.8.58
Observed Corrosion Rate Values for Various Metals and Exposure Periods (Gross & Nixon, 1993)

Metal	Corrosion Rate (µm/a) for First Year
Mild Steel	380
Galvanised Mild Steel	7
3CR12 corrosion resisting steel	110
AISI 316L stainless steel	0
Aluminium	0
Copper	5
Zinc	5

(iii) Measurement of Pollutants Corrosion Monitoring

The more recent corrosion tests were completed based on the ISO 9223 International Standard (International Organisation for Standardisation, 2012a) methodology including the periods from 11 April 2008 to 10 April 2009, 10 October 2012 to 12 September 2013 and 10 October 2017 to 10 March 2022 (Burger, 2022).

Marine atmospheric corrosion is primarily catalysed by moisture and oxygen, but is accentuated by contaminants such as sulfur compounds and salt spray. The prediction of atmospheric corrosion rates therefore contains a term for ‘time of wetness’, which is a function of the ambient air temperature and relative humidity, and the quantity of pollutants in the air, specifically sulfur dioxide and sodium chloride. The ISO 9223 International Standard (International Organisation for Standardisation, 2012a) specifies the key factors in the atmospheric corrosion of metals and alloys and provides the methods for determining these.

The International Standard provides a corrosion classification scheme that can directly be used for technical and economic analyses of corrosion damage and for the rational choice of protection measures. According to this classification scheme, corrosion rates (r_{corr}) are provided (***Table 5.8.60)*** corresponding to the six categories (*C1* to *C5* and *CX*), ranging from very low to very high and extreme (***Table 5.8.59***). Based on this classification and the corrosion rates measured during the 1991-1993 monitoring campaign ***Table 5.8.58*** (Gross & Nixon, 1993) the site falls within category C5, i.e., “very high” severity (***Table 5.8.59***), with respect to 3CR12 corrosion resisting steel, copper and zinc. For mild steel the corrosion potential is extremely high (CX), however, for AISI 316L stainless steel and galvanised mild steel, the classifications are C1 and C2, respectively. It should be noted that only the classification scheme is applied here for indicative comparisons and not the method of determining the corrosion rates.

As per the ISO 9223 International Standard these corrosion rates may also be estimated from a combination of the annual average temperature, relative humidity, and sulfur dioxide[18] and chloride deposition rates.

Table 5.8.59
ISO 9223:2012 Categories of Corrosivity of the Atmosphere

Category	Corrosivity	Typical Environment Examples
C1	Very low	Dry or cold zone, atmospheric environment with very low pollution and time of wetness, e.g. certain deserts, Central Arctic/Antarctica
C2	Low	Temperate zone, atmospheric environment with low pollution (annual average sulfur dioxide less than 5 µg/m³), e.g. rural areas, small towns Dry or cold zone, atmospheric environment with short time of wetness, e.g. deserts, subarctic areas
C3	Medium	Temperate zone, atmospheric environment with medium pollution (annual average sulfur dioxide 5 µg/m³ to 30 µg/m³) or some effect of chlorides, e.g. urban areas, coastal areas with low deposition of chlorides Subtropical and tropical zone, atmosphere with low pollution
C4	High	Temperate zone, atmospheric environment with high pollution (annual average sulfur dioxide 30 µg/m³ to 90 µg/m³) or substantial effect of chlorides, e.g. polluted urban areas, industrial areas, coastal areas without spray of salt water or, exposure to strong effect of de-icing salts. Subtropical and tropical zone, atmosphere with medium pollution
C5	Very high	Temperate and subtropical zone, atmospheric environment with very high pollution (annual average sulfur dioxide 90 µg/m³ to 250 µg/m³) and/or significant effect of chlorides, e.g. industrial areas, coastal areas, sheltered positions on coastline
CX	Extreme	Subtropical and tropical zone (very high time of wetness), atmospheric environment with very high sulfur dioxide pollution (annual average higher than 250 µg/m³) including accompanying and production factors and/or strong effect of chlorides, e.g. extreme industrial areas, coastal and offshore areas, occasional contact with salt spray.

---

[18] The sulfur dioxide deposition rate is calculated from the measured air concentration according to the method provided in the International Standard (ISO 9225 (International Organisation for Standardisation, 2012c)).

Table 5.8.60
ISO 9223:2012 Corrosion rates, r_{corr}, for the First Year of Exposure for the Different Corrosivity Categories

Corrosivity category	**Corrosion rates of metals** r_{corr}				
	Unit	**Carbon steel**	**Zinc**	**Copper**	**Aluminium**
C1	g/m²-annum	$r_{corr} \le 10$	$r_{corr} \le 0.7$	$r_{corr} \le 0.9$	negligible
	µm/annum	$r_{corr} \le 1.3$	$r_{corr} \le 0.1$	$r_{corr} \le 0.1$	—
C2	g/m²-annum	$10 < r_{corr} \le 200$	$0.7 < r_{corr} \le 5$	$0.9< r_{corr} \le 5$	$r_{corr} \le 0.6$
	µm/annum	$1.3 < r_{corr} \le 25$	$0.1 < r_{corr} \le 0.7$	$0.1 < r_{corr} \le 0.6$	—
C3	g/m²-annum	$200 < r_{corr} \le 400$	$5 < r_{corr} \le 15$	$5 < r_{corr} \le 12$	$0.6 < r_{corr} \le 2$
	µm/annum	$25 < r_{corr} \le 50$	$0.7 < r_{corr} \le 2.1$	$0.6 < r_{corr} \le 1.3$	—
C4	g/m²-annum	$400 < r_{corr} \le 650$	$15 < r_{corr} \le 30$	$12 < r_{corr} \le 25$	$2 < r_{corr} \le 5$
	µm/annum	$50 < r_{corr} \le 80$	$2.1 < r_{corr} \le 4.2$	$1.3 < r_{corr} \le 2.8$	—
C5	g/m²-annum	$650 < r_{corr} \le 1\ 500$	$30 < r_{corr} \le 60$	$25 < r_{corr} \le 50$	$5 < r_{corr} \le 10$
	µm/annum	$80 < r_{corr} \le 200$	$4.2 < r_{corr} \le 8.4$	$2.8 < r_{corr} \le 5.6$	—
CX	g/m²-annum	$1\ 500 < r_{corr} \le 5\ 500$	$60 < r_{corr} \le 180$	$50 < r_{corr} \le 90$	$r_{corr} > 10$
	µm/annum	$200 < r_{corr} \le 700$	$8,4 < r_{corr} \le 25$	$5,6 < r_{corr} \le 10$	—

Notes

- The classification criterion is based on the methods of determination of corrosion rates of standard specimens for the evaluation of corrosivity (see ISO 9226).
- The corrosion rates, expressed in grams per square metre per year [g/(m²-annum)], are recalculated in micrometres per year(µm/annum) and rounded.
- The standard metallic materials are characterized in ISO 9226.
- Aluminium experiences uniform and localized corrosion. The corrosion rates shown in this table are calculated as uniform corrosion. Maximum pit depth or number of pits can be a better indicator of potential damage. It depends on the final application. Uniform corrosion and localized corrosion cannot be evaluated after the first year of exposure due to passivation effects and decreasing corrosion rates.
- Corrosion rates exceeding the upper limits in category C5 are considered extreme. Corrosivity category CX refers to specific marine and marine/industrial environments

Sulfur Dioxide Deposition

Sulfate ions are formed in the surface moisture layer by the oxidation of sulfur dioxide and their formation is considered to be the main corrosion accelerating effect from sulfur dioxide. Sulfur dioxide may be expressed either in terms of a deposition rate or an airborne concentration. The method of determining the deposition rate in this instance followed the ISO 9225 Sulfation Plate Method (International Organisation for Standardisation, 2012c).

The average sulfate deposition rate observed at the 120-m tower for the period 17 May 2008 to 25 January 2009 was 0.16 mg/m²-day, with monthly deposition rates ranging from 0.07 mg/m²-day to 0.30 mg/m²-day. The average sulfate deposition rate observed during the second campaign

(10 October 2012 to 12 September 2013) was 1.28 mg/m²-day and ranged from 0.11 mg/m²-day to 2.88 mg/m²-day per month.

Similarly, the average sulfate deposition rate observed at the Duynefontyn WS (265 m from the highwater mark) for the period October 2017 to March 2022 was 1.04 mg/m²-day, with monthly deposition rates ranging from 0.03 mg/m²-day to 5.36 mg/m²-day.

Chlorine Deposition

Airborne salinity was evaluated and recorded in accordance with ISO 9225 (International Organisation for Standardisation, 2012c). The average chloride deposition rate observed at the 120-m tower for the period 17 May 2008 to 25 January 2009 was 51.0 mg/m²-day (ranging from 11.1 mg/m²-day to 215.5 mg/m²-day). For the period October 2010 to September 2013, the average chloride deposition rate was 119.6 mg/m²-day that ranged from 25.0 mg/m²-day to 676.3 mg/m²-day.

The average chloride deposition rate observed at the Duynefontyn WS for the period October 2017 to March 2022 was 279.2 mg/m²-day that ranged from 80.3 mg/m²-day to 863.5 mg/m²-day.

Atmospheric Corrosivity Dose Response Functions

In the International Standard (ISO 9223:2012, (International Organisation for Standardisation, 2012a)), the corrosion rate for steel, zinc, copper and aluminium is calculated using dose-response functions. Dose-response functions for these standard metals are given, describing the corrosion attack after the first year of exposure in open air as a function of sulfur dioxide dry deposition, chloride dry deposition, temperature and relative humidity. The functions are based on results of worldwide corrosion field exposures and cover climatic earth conditions and pollution situations within the scope of the Standard. The general form of the dose-response function is as follows:

$$r_{corr} = c_1 P_d^{c_2} \exp(c_3 RH + c_4[T - 10]) + c_5 S_d^{c_6} \exp(c_7 RH + c_8 T)$$

where:

r_{corr} = first-year corrosion rate of metal, expressed in µm/annum

RH = annual average relative humidity, expressed as a percentage [%]

T = annual average temperature, expressed in degrees Celsius [°C]

P_d = annual average SO_2 deposition, expressed in mg/m²-day

S_d = annual average chloride deposition, expressed in mg/m²-day

c_1 to c_8 = are constants as defined in ***Table 5.8.61***.

Table 5.8.61
Constants for Dose-Response Function to Estimate Corrosion Attack Rates (ISO 9223:2012)

Constant		Steel	Zinc	Copper	Aluminium
c1		1.77	0.0129	0.0053	0.004
c2		0.52	0.44	0.26	0.73
c3		0.020	0.046	0.059	0.025
c4	*T≤10*	0.150	0.038	0.126	0.004
	T>10	-0.054	-0.071	-0.080	-0.043
c5		0.013	0.017	0.010	0.0018
c6		0.62	0.57	0.27	0.60
c7		0.033	0.008	0.036	0.020
c8		0.040	0.085	0.049	0.094

A summary of the calculated corrosion rates for carbon steel, zinc, copper and aluminium using the above relationship is provided in ***Table 5.8.62***. Estimated levels of uncertainty for assessment of the corrosivity category based on the dose-response function according to ISO 9223 for carbon steel, zinc and copper -33% to +50% and -50% to 100% for aluminium (International Organisation for Standardisation, 2012a). The estimated corrosion rate range based on these levels of uncertainty is also included in the table. The annual average relative humidity and temperature used in the relationship were 77 per cent and 16.7°C, respectively. Annual average sulfur dioxide and chloride deposition rates of 1.50 mg/m²-day and 293.3 mg/m²-day were used, respectively. Considering the levels of uncertainty of the estimation method, the site is therefore considered to have a high (C4) to very high (C5) corrosion potential (***Table 5.8.59***). This conclusion is in line with the results obtained with the Metal Exposure Corrosion Monitoring (see ***Table 5.8.58***).

Table 5.8.62
ISO 9224:2012 calculated corrosion rate values for various metals and exposure periods

Metal	First Year Corrosion Rate	
	Corrosion Rate [µm/annum]	**Corrosivity category (from *Table 5.8.60*)**
Carbon Steel	85.8 (74.1;105.3) (1)	C5 (C4 to C5) (1)
Zinc	3.4 (3.0;4.1) (1)	C4 (C4 to C5) (1)

Metal	First Year Corrosion Rate	
	Corrosion Rate [µm/annum]	Corrosivity category (from ***Table 5.8.60***)
Copper	1.9 (1.8;2.1) (1)	C4 (C4 to C5) (1)
Aluminium	1.2 (1.0;1.4) (1)	(2)

Notes
1. Values in brackets represent level of uncertainty
2. Aluminium is not categorised by penetration rate (µg/m²) in ***Table 5.8.60*** because aluminium alloys corrode by a pitting mechanism. The corrosion category was therefore not established.

The International Standard (ISO 9224:2012 (International Organisation for Standardisation, 2012b)), provides a relationship that can be used to indicate that the total attack, *D*, expressed either as mass loss per unit area or penetration depth, is given as:

$$D = r_{corr} t^b$$

where

D = total attack, expressed as penetration depth [µm]

r_{corr} = first-year corrosion rate of metal, expressed in µm/annum

t = exposure time, expressed in years

b = metal-environment-specific time exponent (***Table 5.8.63***)

Table 5.8.63
Constant (*b*) for attack depth function (ISO 9224:2012)

Applicable Estimate	Steel	Zinc	Copper	Aluminium
Average Estimate	0.523	0.813	0.667	0.728
Conservative Estimate	0.575	0.873	0.726	0.807

The attack depth was calculated using the onsite parameters and the average estimate is illustrated in ***Figure 5.8.19*** for the first 20 years of exposure.

The change in corrosivity as a function of distance from the sea was discussed in the Coupon-based Corrosion Monitoring section. From the average rate of change, based on readings at 50 m and 740 m from the high tide mark (***Table 5.8.57***), the corrosion rates closer to the sea can be extrapolated. The applicable ratio for extrapolation is estimated to be 1.36 at 50 m. For example, using the values in ***Table 5.8.63***, the extrapolated average rates for carbon steel at 50 m from the high tide mark are estimated to be approximately 126 µg/year. The corrosivity at the site, based on the marine and atmospheric corrosion calculations, is considered to vary between severe and very severe (50 m from high water mark).

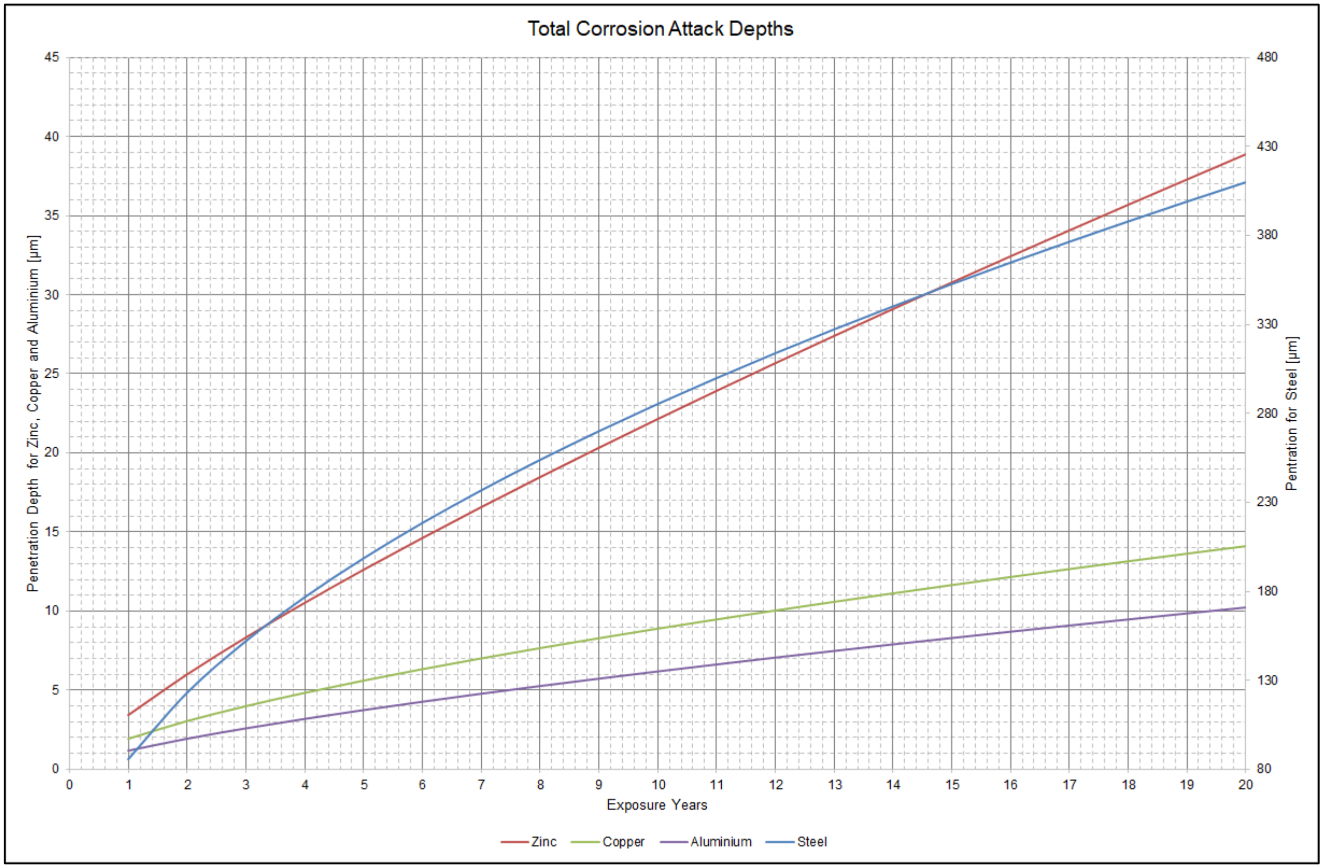

Figure 5.8.19
Calculated corrosion attack depths as a function of time using the ISO 9224:2012 methodology

5.8.6.2 Extreme, Severe and Rare Phenomena

5.8.6.2.1 Severe and Rare Phenomena

The IAEA standards state that rare meteorological phenomena (International Atomic Energy Agency, 2011) occur infrequently. Thus, at any station, the instruments used for routine measurements would rarely register characteristics of these phenomena. Rare meteorological phenomena, which are highly complex, are usually scaled in terms of their intensity. These intensity values may be expressed in terms of either a qualitative characteristic such as damage or a quantitative physical parameter such as wind speed.

The paucity of detailed studies on severe storm and climate hazards in the Duynefontyn region has made it difficult to analyse and synthesise information for the purposes of quantifying the frequency of occurrence. As a result, for the purpose of this SSR it was necessary to use information from weather observations made by the SAWS at CTIA. Although it is not possible to quantify an uncertainty in this approach, it is expected that similar weather patterns would be exhibited. This is expected because of the proximity of the site and the weather office at CTIA and because these locations are affected by the same synoptic scale systems (Preston-Whyte & Tyson, 1988).

(a) Severe Weather

The southwestern coast of South Africa is subject to large synoptic scale systems that drive the local weather conditions in any given area. As described in the South African Weather Bureau Report WB40 (Schulze, 1986), these local weather conditions are normally characterized by low level stratus clouds and not by towering convective storms that produce hail and thunder showers. Severe weather is more closely associated with severe wind conditions. Four main wind producing systems have been identified (Preston-Whyte & Tyson, 1988):

- coastal low buster;
- cut-off lows;
- shallow southeasterlies;
- mid-latitude lows.

The last two systems are the most significant in terms of wind speed. Winds in these systems can produce speeds at ground level of up to 35 m/s (126 km/h), which can cause considerable damage to buildings that are not designed to withstand these conditions.

The site can potentially experience severe weather in the form of thunderstorms, hail, hurricane force winds and possibly tornadoes. Many of the severe storms occurring in the Western Cape are compound, producing various combinations of hail, wind, tornado, lightning and flash flooding. Damaging winds associated with severe thunderstorms include tornadoes, downbursts (macrobursts or microbursts)[19], straight-line winds[20], gust fronts and derechoes[21]. These are discussed later below.

Historical records, covering a period of about 300 years of severe weather events in the region, lists 160 severe wind events and 11 tornadoes up to 2020 (South African Weather Service, 1991) and (South African Weather Services, 2020b). The same record also lists 36 severe rain and 146 flood events. ***Appendix 5.8.I*** summarises the most severe of these events, also including extreme cold and hot, dense fog, snow, frost, hail and fires (South African Weather Service, 1991). The events in a radius of 100 km were included in the summary.

(b) Tropical Cyclones

Nuclear power plants must be designed so that they remain in a safe condition under extreme meteorological events, including those that could result in the most extreme wind events (cyclones/hurricanes[22] and tornadoes) that could reasonably be predicted to occur at the site. The maximum probable wind speed at the site must therefore be considered in determining the acceptability of the site for a nuclear installation(s). Furthermore, site parameters must be established such that potential threats from such strong winds will pose no undue risk to the proposed and existing nuclear installation(s).

It is important to note the difference between a hurricane and hurricane force winds. The latter refers to a wind speed scale described by the Beaufort Scale as winds with speeds above 118 km/h (32.8 m/s). This wind speed (as a gust) has been exceeded 5 times (1986, 1987, 1993, 1994 and 2002) over the 40-year monitoring period at the site. The hourly average has never

---

[19] A downburst is created by an area of significantly rain-cooled air that, after hitting ground level, spreads out in all directions producing strong winds. Microbursts and macrobursts are downbursts at very small and larger scales, respectively. Most downbursts are less than 4 km in extent: these are called microbursts. Downbursts larger than 4 km in extent are sometimes called macrobursts (Eskom, 2023a).

[20] Straight-line winds are common with the gust front of a thunderstorm or originate with a downburst from a thunderstorm. If these winds meet or exceed 93 km/h then the storm is classified as severe (Eskom, 2023a).

[21] The term ‘derecho’ is used to describe larger scale straight-line winds advancing very quickly ahead of a well organised, long-lasting squall line or a large-scale multiple cell storm (International Atomic Energy Agency, 2011).

[22] Depending on its location and strength, a tropical cyclone is referred to by different names, including hurricane, typhoon, tropical storm, cyclonic storm, tropical depression, or simply cyclone. A hurricane is a tropical cyclone that occurs in the Atlantic Ocean and northeastern Pacific Ocean, and a typhoon occurs in the northwestern Pacific Ocean; in the south Pacific or Indian Ocean, comparable storms are referred to simply as "tropical cyclones" or "severe cyclonic storms".

exceeded this speed for this monitoring period. The highest gust of 38.8 m/s occurred during May 1987.

The Duynefontyn region is not on a hurricane (tropical cyclone) track or adjacent to a warm ocean. Therefore, it is not expected that the site will experience a cyclone, or at least there is a very low probability. Tropical cyclones are generated in areas, where the ocean surface temperature is greater than 27°C and between latitudes 5°S to 30°S. The site is located south of 33°S and is therefore not subject to tropical cyclones. It is not clear how climate change will affect the occurrence of cyclones and it has not been presented in the 5th Assessment Report of the Intergovernmental Panel on Climate Change (IPCC) (Intergovernmental Panel on Climate Change, 2013).

To ensure the safety of nuclear installation(s) in the event of a hurricane strike, NRC regulations (United States Nuclear Regulatory Commission, 2011) require that nuclear installation(s) designs consider the impact of hurricane-generated missiles, in addition to the direct action of the hurricane wind. The two basic approaches used to characterise hurricane-generated missiles are (United States Nuclear Regulatory Commission, 2010):

(1) A standard spectrum of hurricane missiles – protection from a spectrum of missiles (ranging from a massive missile that deforms on impact to a rigid penetrating missile) provides assurance that the necessary structures, systems, and components will be available to mitigate the potential effects of a hurricane on plant safety. Given that the design basis hurricane windspeed has a very low frequency of occurrence, to be credible, the representative missiles must be common items around the plant site and must have a reasonable probability of becoming airborne within the hurricane wind field.

(2) A site-specific probabilistic assessment of the hurricane hazard – no definitive guidance has been developed for use in applying hazard probability methods to characterise site dependent hurricane-generated missiles. Damage to safety-related structures by hurricanes or other wind generated missiles implies that a sequence of random events has occurred. That event sequence typically includes an occurrence of a hurricane in the plant vicinity, existence, and availability of missiles in the area, injection of missiles into the wind field, suspension and flight of those missiles, impact of the missiles on safety-related structures, and resulting damage to critical equipment.

(3) To ensure the safety of nuclear power plants in the event of a tornado or hurricane strike in the Unites States the NRC regulations require that nuclear power plant designs consider the impact of tornado or hurricane-generated missiles in addition to the direct action of the wind (United States

Nuclear Regulatory Commission , 2007b; United States Nuclear Regulatory Commission, 2011). As per these NRC regulations the wind speeds used to determine the wind gust are nominal 3-second peak-gust values corresponding to an exceedance frequency of 10^{-7} per year measured at a height of 10 m in flat open terrain. From an analysis of wind gusts observed at the 10 m level of the 120-m tower for the period 1980 to 2023, the wind gust corresponding to an exceedance frequency of 10^{-7} per year is 90.7 m/s (see **Subsection 5.8.6.2.2**).

(c) Tornadoes

Tornadoes are amongst the most violent and destructive of all extreme weather phenomena. A tornado, from the Latin *tornare* (‘to turn’), is a violent rotating column of air extending from a thunderstorm. Tornadoes in South Africa are typically associated with very hot air masses and severe thunderstorms (Goliger, et al., 1997). There are several different methods of classifying tornadoes. Historically, South Africa used the ‘Fujita-Pearson scale classification’ (Goliger, et al., 1997) to record tornado occurrences. This system classifies tornadoes in six intensities, ranging from F0 (no damage) to F5 (incredible damage). The intensity is based on the apparent damage to structures, the extent of the path and other descriptors from which wind speeds are then inferred. About 65 per cent of the South African tornadoes (Goliger, et al., 1997) are classified as F0 or F1 (light damage), while more than 90 per cent are classified as F0, F1 or F2 (considerable damage, with maximum wind speeds of up to 70 m/s). Only about 8 per cent of the documented tornadoes were F3, i.e. severe damage, with maximum wind speeds of up to 90 m/s. The tornado which occurred in Mount Ayliff (Eastern Cape Province) in January 1999 was seemingly the most severe ever reported, with a classification of F4. The Fujita Scale has been replaced in some countries by the updated Enhanced Fujita Scale (EF-Scale). As with the Fujita Scale, the EF-Scale still is a set of wind estimates (not measurements) based on damage. It uses three-second gusts estimated at the point of damage based on a judgment of 8 levels of damage to a set of 28 indicators ranging from damage to small barns and farm outbuildings (indicator 1) to destruction of soft-wood trees (indictor 28). These estimates vary with height and exposure. The EF Scale more accurately matches wind speeds to the severity of damage, as opposed to the Fujita scale that classifies only on a scale of damage. The EF Scale was formulated due to research which suggested that the wind speeds required to inflict damage by intense tornadoes on the Fujita Scale are greatly overestimated. A process of expert elicitation with top engineers and meteorologists developed a correlation between the original Fujita Scale and the EF Scale wind speeds for the historical Fujita Scale database to be preserved. By correlating the Fujita Scale wind speeds with the EF Scale wind speeds, a tornado rated according to the Fujita Scale will have the same “F-Number” in the EF Scale, e.g. F3 translates into EF3, although the wind speed ranges are different. The wind speeds based on the equivalent EF Scale are summarised in ***Table 5.8.64*** (McDonald & Mehta, 2006).

Table 5.8.64
EF-Scale Wind Speed Ranges Derived from Fujita-Scale Wind Speed Ranges (McDonald & Mehta, 2006)

Enhanced Fujita Scale (Fujita Scale)	3-Second Gust Estimate	Fujita-Scale Description
EF0 (F0)	105 to 137 km/hr 29 to 38 m/s	Light damage. Some damage to chimneys; branches broken off trees; shallow-rooted trees pushed over; sign boards damaged.
EF1 (F1)	138 to 177 km/hr 39 to 49 m/s	Moderate damage. The lower limit is the beginning of hurricane wind speed; peels surface off roofs; mobile homes pushed off foundations or overturned; moving vehicles pushed off the roads; attached garages may be destroyed.
EF2 (F2)	178 to 217 km/hr 50 to 60 m/s	Significant damage. Roofs torn off frame houses; mobile homes demolished; boxcars overturned; large trees snapped or uprooted; high-rise windows broken and blown in; light-object missiles generated
EF3 (F3)	218 to 269 km/hr 61 to 75 m/s	Severe damage. Roofs and some walls torn off well-constructed houses; trains overturned; most trees in forests uprooted; heavy cars lifted off the ground and thrown.
EF4 (F4)	270 to 322 km/hr 76 to 89 m/s	Devastating damage. Well-constructed houses levelled; structures with weak foundations blown away some distance; cars thrown, and large missiles generated.
EF5 (F5)	>322 km/hr >89 m/s	Incredible damage. Strong frame houses lifted off foundations and carried considerable distances to disintegrate; automobile-sized missiles fly through the air farther than 100 metres; trees debarked; steel-reinforced concrete structures badly damaged and skyscrapers toppled

Table 5.8.65
Summary of Tornado Phenomena Recorded Around Duynefontyn Area (1905-2020) ((Goliger, et al., 1997) and (South African Weather Services, 2020a))

Location	Date	F-Scale	Distance from Site (km)
Malmesbury	29/09/1925	F2	36.9
Malmesbury	01/05/1952	F0	36.9
Bredasdorp	19/02/1963	F0	175.4
Cape-Valley	09/11/1964	F1	31.0
Rawsonville	24/01/1987	F0	82.0
Saldanha Bay	12/09/1987	F1	77.0
Strandfontein	15/09/1987	F0	60.0
Cape Town	29/08/1999	F1	31.0
Cape Town	04/10/2002	F1	31.0
Ladismith	11/11/2003	F1	264.0
Cape Town	30/08/2008	F0	31.0
Darling (1)	02/04/2014	F? (2)	34.0
Bonteheuwel (1)	25/10/2016	F? (2)	33.0
Suurbraak (1)	25/01/2017	(3)	211.8
Klapmuts (1)	19/07/2019	(3)	46.0

Notes
(1) Not included in SAWS database but listed in https://sawx.co.za/resources/history-tornadoes-south-africa/.
(2) Listed in as a tornado but the F Scale is unknown (https://sawx.co.za/resources/history-tornadoes-south-africa/)
(3) Listed in as a possible tornado but the F Scale is unknown (https://sawx.co.za/resources/history-tornadoes-south-africa/)

On the basis of the available tornado occurrences from 1905 to 2020 (Goliger, et al., 1997; South African Weather Services, 2020a) an estimate of tornado frequency for the site was made by spatial analyses of location and corresponding intensities of all tornado recordings listed by the SAWS as well as those in ***Table 5.8.65***. The table includes tornadoes witnessed up to a maximum distance of about 300 km from the site, which corresponds to the Duynefontyn region used in the Seismic Study. Since no recordings of waterspouts could be sourced, the area west of the site could not be included in the analysis.

The likelihood of a tornado striking a specific region can be expressed in terms of the number of tornadoes over a given period of time reported within a specific unit area (Goliger, et al., 1997). The frequency of tornadoes listed by the SAWS for this area is 11 over a period of 116 years (***Table 5.8.65***), therefore a frequency of about 0.09 per year. Using the distances from the site to the reported locations of the tornadoes (***Table 5.8.65***), and calculating the area included by these radiuses, the average tornado strike frequency (irrespective of the severity) was calculated to be 9.5×10^{-6} per year per km², with a minimum estimate of 5.9x10^{-7} per year per km² and a maximum estimate of 2.4x10^{-5} per year per km². This confirms the result obtained by Goliger *et al* (Goliger, et al., 1997), as displayed in (***Figure 5.8.20***), which indicates that the frequency is 10^{-5} or less per year per km². Using the estimated probabilities for the various tornado severities, discussed above, it is estimated that the frequencies are 4.3x10^{-6} per year per km² for F1, 7.6x10^{-7} per year per km² for F2, and 8.5x10^{-8} per year per km² for F3.

From ***Table 5.8.65*** it is evident that tornado activity has increased since 1987 within an 80 km radius from the site. Whilst climate change may have contributed to increases in tornado frequencies, it may also simply be that the reporting of tornadoes has increased due to population spread as well as the associated damage to property. Nevertheless, considering the past 34 years' tornado history in ***Table 5.8.65***, the number of tornadoes were 7 and therefore the probability of a tornado increases to 0.21 per year. The average tornado strike frequency estimate would then increase to 2.1x10^{-5} per year per km², and the frequencies per severity increase to 9.3x10^{-6} per year per km² for F1, 1.7x10^{-6} per year per km² for F2, and less than 1.8x10^{-7} per year per km² for F3.

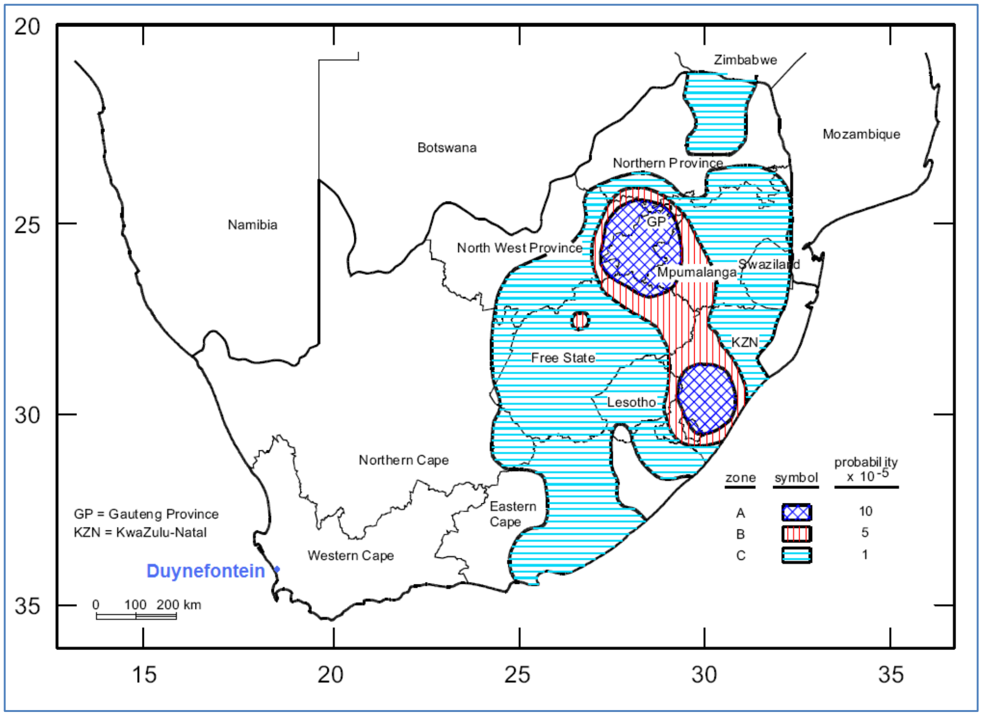

Figure 5.8.20
Mean Annual Rate of Occurrence of Tornadoes (Excluding Events with an Intensity of F0 on Fujita Scale) (Goliger, et al., 1997)

In the second approach, all recorded tornadoes were included in the analysis and a spatial interpolation applied to estimate the frequency over South Africa, as per Goliger *et al* (Goliger, et al., 1997). The locations of these tornadoes and Fujita-Scales for the period 1905 to 2020 are shown in ***Figure 5.8.21***. The inter-distance between all tornadoes were used to establish optimal spatial clusters that would be representative of tornado bins. A large cluster would incorporate more tornado occurrences; however, the larger area would reduce the frequency spatially (i.e. per km²). On the other hand, a smaller cluster would have a lower number of tornadoes, however, the smaller area may increase the spatial value. Based on an analysis of the 222 tornadoes, it was calculated that by grouping tornadoes into regions represented by circles with a radius of 120 km, the tornado frequency per km² estimate would reach a maximum. The number of tornadoes per cluster and per Fujita-Scale was therefore determined for the 116-year period and these totals divided by the cluster area (i.e. area of circle with radius 120 km = 45 239 km²). The resulting tornado frequency distributions for South Africa for the four Fujita Scales are shown in ***Figure 5.8.22*** to ***Figure 5.8.25***.

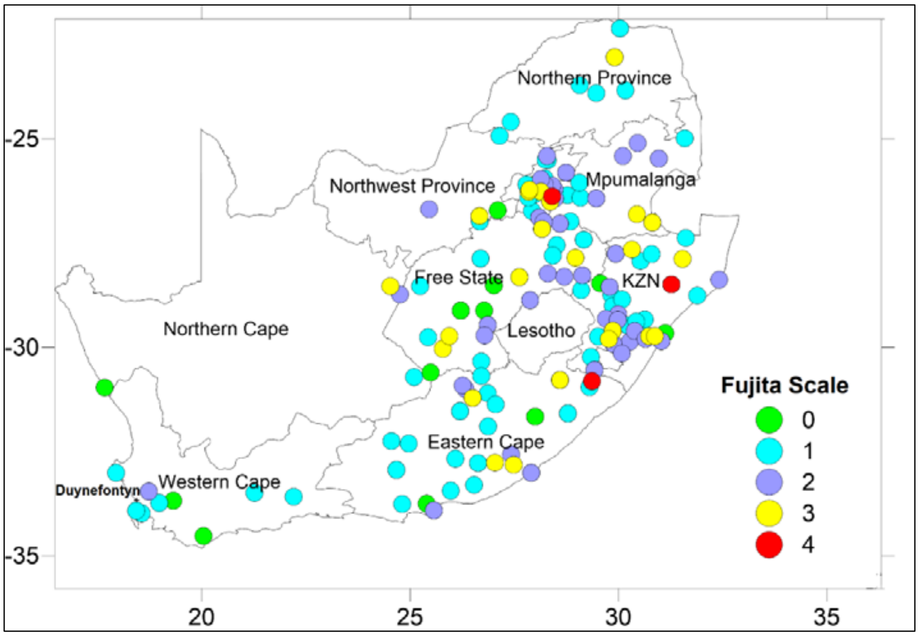

Figure 5.8.21
Occurrence of Tornadoes for Period from 1905 to 2020

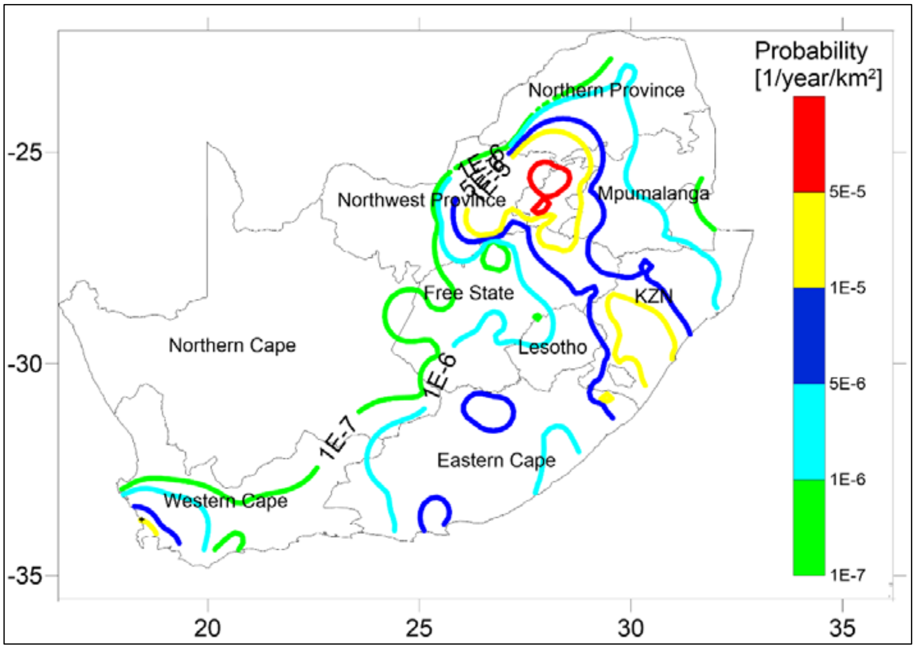

Figure 5.8.22
Mean Annual Rate of Occurrence of F1 Tornadoes (1905 to 2020)

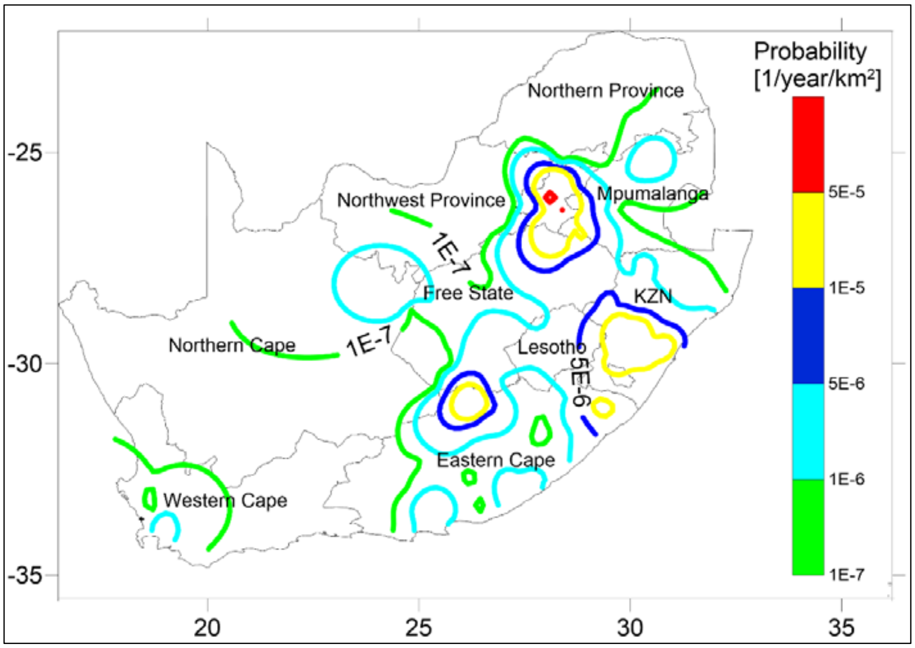

Figure 5.8.23
Mean Annual Rate of Occurrence of F2 Tornadoes (1905 to 2020)

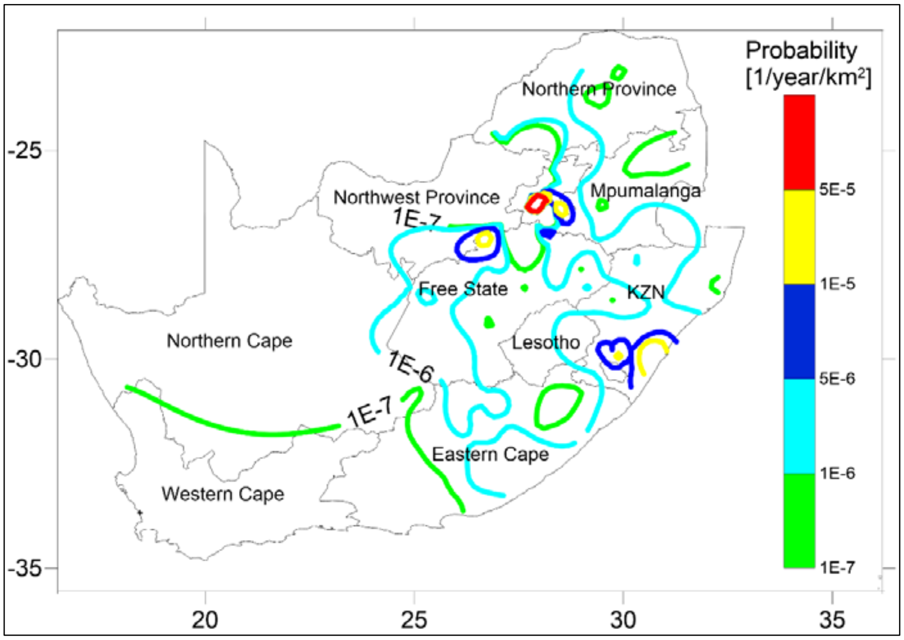

Figure 5.8.24
Mean Annual Rate of Occurrence of F3 Tornadoes (1905 to 2020)

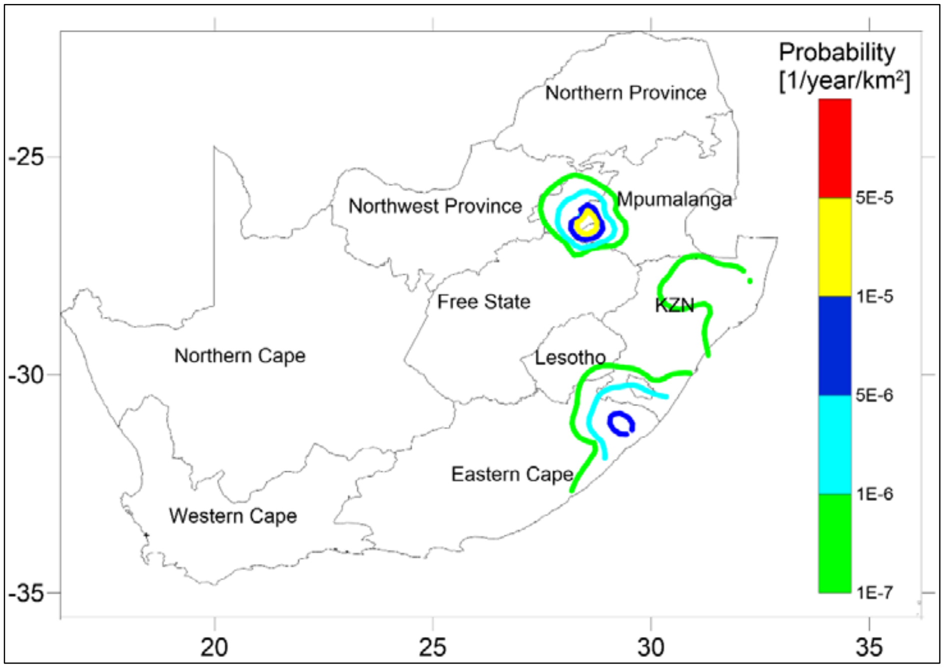

Figure 5.8.25
Mean Annual Rate of Occurrence of F4 Tornadoes (1905 to 2020)

Using the calculated probabilities for the various tornado severities, discussed above, it is estimated that the average tornado strike frequency for the site region (irrespective of the severity) was calculated to be $1.0x10^{-5}$ per year per km². The frequencies per severity are $7.0x10^{-6}$ per year per km² for F0, $2.4x10^{-6}$ per year per km² for F1, $5.6x10^{-7}$ per year per km² for F2, and less than $1.0x10^{-8}$ per year per km² for F3. Adjusting these results to account for the observed recent increases in tornado observations over the past 34 years, the average tornado strike frequency estimate increases to $2.2x10^{-5}$ per year per km², and the frequencies per severity increase to $1.7x10^{-5}$ per year per km² for F0, $5.2x10^{-6}$ per year per km² for F1, $1.2x10^{-6}$ per year per km² for F2, and less than $2.2x10^{-8}$ per year per km² for F3.

As concluded by Goliger *et al* (Goliger, et al., 1997), it is extremely difficult to obtain direct and reliable wind speed records from a tornado and this necessitated the use of indirect methods of estimating the tornado wind speeds, such as those used in the EF Scale. According to the above analysis, EF2 tornadoes at the site have an expected probability that is above 10^{-7} per year and EF3 tornadoes well below 10^{-7} per year. Using the EF Scale, the estimated maximum tornado wind speeds are estimated to be 61 m/s to 75 m/s (***Table 5.8.64***) (McDonald & Mehta, 2006).

As an alternative, the frequency may be based on the affected area of the tornado path assuming uniformly distributed strikes within the area of interest (i.e., 300 m radius) used above. This approach requires knowledge of tornado path length and width, and for the current purposes used the path length and widths which are associated with the Enhanced-Fujita Scale as determined by and summarised in (***Table 5.8.66***). Using the number of recorded tornadoes of 11 in the area of interest over a period of 116 years, total area in the tornado path is calculated as 2.618 km² (***Table 5.8.67***).

Table 5.8.66
Tornado Path Length and Width Correlated to Enhanced-Fujita Scales (Elsner, et al., 2014)

Scale	Path Length [km]				Path Width [m]			
	Range		Median	Average	Range		Median	Average
	Lower Quartile	Upper Quartile			Lower Quartile	Upper Quartile		
EF0	0.29	2.7	0.8	2.27	22.9	68.6	45.7	54.9
EF1	1.77	9.33	4.4	7.1	68.6	182.9	91.4	163.8
EF2	4.53	19.25	10	14.3	137.2	402.3	228.6	344.1
EF3	12.38	36.34	23	29.1	339.5	1005.8	548.6	736.3
EF4	17.07	64.63	35	52.6	603.5	1207	804.7	997.9
EF5	45.51	65.93	59	72	1207	1609.3	1920.2	1635.8

Table 5.8.67
Calculated Tornado Path Areas (1905-2020)

Scale	Tornado Path								
	Length [km]	Width [m]	Area [km²]	Number Recorded		Total Area [km²]		Total Length [km]	
				1905 - 2020	1987-2020	1905 - 2020	1987-2020	1905 - 2020	1987-2020
F0	2.27	54.9	0.1	5	2	0.623	0.249	11.4	4.54
F1	7.1	163.8	1.2	5	4	5.815	4.652	35.5	28.4
F2	14.29	344.1	4.9	1	0	4.917	0	14.3	0
F3	29.09	736.3	21.4	0	0	0	0	0	0
F4	52.55	997.9	52.4	0	0	0	0	0	0
F5	71.95	1635.8	117.7	0	0	0	0	0	0
TOTAL				11	6	11.355	4.901	61.1	32.94

As per (Ramsdell, J. V.,Jr; Rishel, J. P.;, 2007), the annual strike frequency would then be:

$$P_p = \frac{A_t}{NA_r}$$

Where, A_t is the total tornado path area in the region of interest, A_r, and N is the number of years of record of tornado strikes. The inherent assumption is that tornado strikes within the area of interest A_r are uniformly distributed. With $A_t = 11.355$ km², $A_r = 282743.3$ km² $(A_r = \pi R^2 = \pi\ 300^2 =$ 282743.3), and $N = 116$, the annual strike frequency is calculated to be 3.5x10^{-7}. Or, if only half of the area is considered to be land-based, the annual strike frequency is calculated to be 6.9x10^{-7}. If the tornado numbers for the latest 34 years are used, the annual strike frequency is calculated to be 5.1x10^{-7} (full area) and 1.06x10^{-6} (half area).

To estimate the additional probability of a tornado striking a large structure, it is necessary to determine a characteristic dimension of the structure and the expected length of the tornados. The additional annual strike frequency is given by (Ramsdell, J. V.,Jr; Rishel, J. P.;, 2007)

$$P_{ps} = \frac{w_s L_t}{NA_r}$$

Where the impacted area is the product of a characteristic dimension of the structure w_s and the total length of the tornado paths, L_t. Assuming for illustrative purposes, $w_s = 1\,000$ m , the additional annual strike frequency based on the 116 years' data is calculated to be 1.6x10^{-6} (3.7x10^{-6} half area) and the total annual strike frequency therefore 2.2x10^{-6} (4.4x10^{-6} half area).

The additional annual strike frequency based on the 34 years' data is calculated to be 3.4x10^{-6} (6.9x10^{-6} half area) and the total annual strike frequency therefore 3.9x10^{-6} (7.9x10^{-6} half area). It is noted that these calculated probabilities are significantly lower than the values obtained with the previous two methods, i.e. 2.1x10^{-5} per year per km² and 2.2x10^{-5} per year per km², respectively.

(d) Severe thunderstorms

Given the low likelihood of tornadoes in the region, as discussed in the previous section, the majority of severe thunderstorms are therefore most probably non-tornadic. Downbursts and straight-line winds, as opposed to tornadic winds, would mostly be accountable for damage to property and livelihoods at the site. A downburst is an exceptionally energetic downdraft that exits at the base of a thunderstorm and spreads out at the earth's surface as strong and gusty horizontal winds that may cause property damage (Greer, 1996). Winds may reach 280 km/h in exceptionally powerful events (Geer, 1996). Gust fronts, straight-line winds and derechoes develop along the leading edge or outflow boundary of an advancing thunderstorm. Straight-line winds, usually blowing from one direction, as distinct from rotational winds in tornadoes, develop in association with gust fronts and may cause considerable damage, with winds of up to 160 km/h. The highest wind speed (gust) on record (1980 to September 2023) for the site for is 38.8 m/s (140 km/h) (***Table 5.8.5***).

As given in ***Subsection 5.8.6.1.4***, it is estimated, based on observations at CTIA, that the number of thunder days at the site is 6 per year. There appears to be no preference to a specific season or month; however, the likelihood is lowest during January and December.

(e) Hail

The average number of days with hail at the site is estimated to be 1 per year (***Subsection 5.8.6.1.5*** and (Schulze, 1986)).

(f) Lightning

A Lightning Detection Network (LDN) was set up in 2006 by the SAWS in South Africa. The annual average lightning stroke/flash ratio was found to be 2.4 (Gijben, 2021). The annual CG flash density for South Africa according to the LDN observations for the period 2006 to 2018 is shown in ***Figure 5.8.26*** (Gijben, 2021). From this observation, the cloud to ground flash density for the site is <1 lightning flash per year per km². The highest peak current recorded during the period was 166 kA with a median peak of cloud-to-ground of 15 kA and of positive cloud-to-ground of 25 kA (Gijben, 2021).

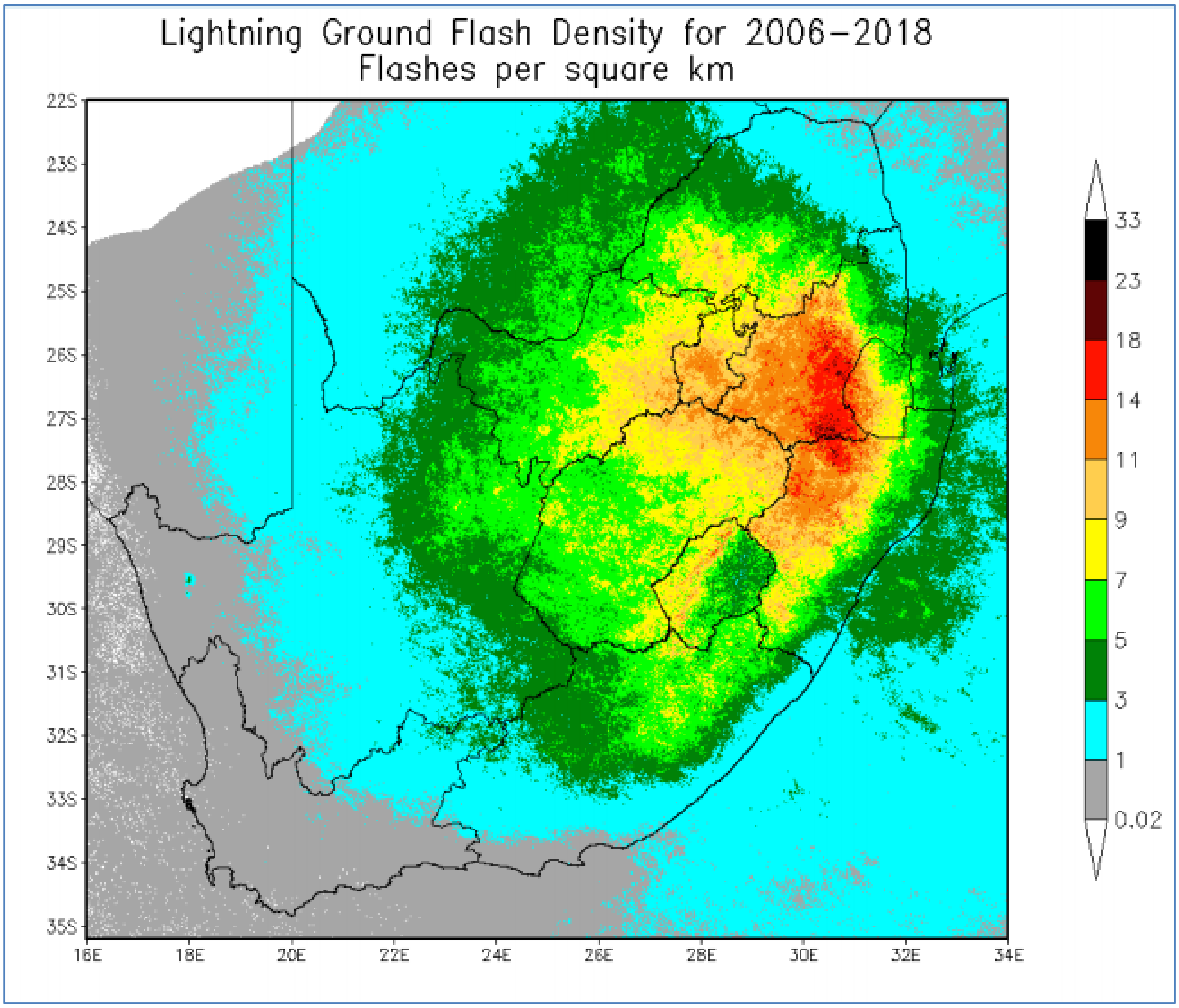

Figure 5.8.26
Mean Annual Ground Flash Density (flashes/km²) for 2006 to 2018 (Gijben, 2021)

Lightning activities were also measured at the Duynefontyn WS from October 2017 to February 2022. The average annual number of lightning strokes measured at the Duynefontyn WS was 18123 strokes. The number of flashes has been estimated assuming a minimum of 2.5 strokes per flash (Gijben, 2021) as the Upper Estimate (7 928 flashes), 25 strokes per flash as the Lower Estimate (793 flashes) (Gill, 2009) and 13.75 strokes per flash (mid value) as the Middle Estimate (1 441 flashes)[23]. The flash density for the monitoring period is therefore estimated to be between 0.2 and 1.6 flashes per km², with a mid-value of 0.3 flashes per km², which is similar to the SAWS LDN observations.

5.8.6.2.2 Extreme Meteorological Variables

Extreme values of meteorological variables (International Atomic Energy Agency, 2019), such as air temperature and wind speed need to be considered in the development of the nuclear installation(s). These variables are measured routinely over a network of fixed stations. These measurements are normalized e.g. data collected on wind speed are normalised to given heights. The extreme values, associated with the annual probabilities of being exceeded, have been derived from the measurements. The following three extreme variables are considered of importance for the nuclear installation(s) on the site:

- extreme rainfall;
- extreme air ambient temperature;
- extreme wind.

The meteorological data collected at the site for the period October 1980 to September 2023 are considered to provide reasonable estimates of the extreme values for rainfall, temperature and wind speed. The confidence in the statistically expected extremes and return periods improve with the timeframe of the data record; this is addressed further in the section on uncertainty. Use has been made of data from the SAWS stations in the region that have been gathered over longer timeframes to supplement and support the data collected at the site, see (***Table 5.8.1***).

Extreme value analysis was performed by fitting an extreme distribution (i.e. Gumbel) using Method of Moments, Method of L-Moments, Method of Maximum Likelihood, Gumbel's Fitting Method and the Method of Least Squares (see ***Appendix 5.8.B***). The highest peaks (e.g. wind gust, extreme minimum and maximum temperatures) per year were used in the analysis. The uncertainty was calculated using a Jackknife resampling method. The Jackknife samples are computed by leaving out one observation from the set of observations at a time. Each Jackknife sample is then used to evaluate the mean and standard deviation of the estimate. For each annual

---

[23] A flash consists of one or perhaps as many as 25 return strokes (Rakov, 2007; Gill, 2009). International studies done on stroke multiplicity in cloud to ground (CG) lightning flashes found that the average negative stroke multiplicity is 4.6, 6.4, 3.4 and 4.5 for Florida, New Mexico, Sweden and Sri-Lanka respectively (Rakov & Huffines, 2003). Similar CG stroke multiplicity of 4.2 was found in South Africa by (Schonland, 1956)and 3.5 by (Malan,, 1956).

probability of exceedance, the 95 per cent confidence interval is calculated assuming a normal distribution, i.e. 1.96 × standard deviation.

(a) Extreme Rainfall

Rainfall has been measured at the site since 1980 and provides 43 years data to support long-term projections. From the analysis of site rainfall data for the 1980-2022 period (***Subsection 5.8.6.1.3***) the highest hourly, 24-hourly, monthly and annual precipitation was 23.6 mm, 70.0 mm, 295.3 mm and 640.4 mm, respectively. Extreme value analyses were performed on the observed annual and 24-hour totals for this 43-year period. The statistical approach which was followed in the analyses is discussed in ***Appendix 5.8.B***. Extreme values for probabilities ranging from “1-in-10” to “1-in-100 000 000” (or $1x10^{-1}$ to $1x10^{-8}$ or return periods of 10 to 100 000 000 years) were calculated by fitting observed rainfall totals to a Gumbel distribution function. The results from the analysis for annual totals and 24-hour storms are given in ***Table 5.8.68*** and ***Table 5.8.69***, respectively.

Table 5.8.68
Expected Annual Total Rainfall in Return Periods of 10 to 100 000 000 Years at the Site (43 Years)

Return Periods	**Rainfall (mm)**	
	Annual	**95th Confidence Interval**
10	471.1	± 45.3
100	611.9	± 85.7
1 000	750.1	± 127.0
10 000	888.1	± 168.7
100 000	1026.1	± 210.5
1 000 000	1164.1	± 252.4
10 000 000	1302.1	± 294.4
100 000 000	1440.1	± 336.4

Table 5.8.69
Expected Maximum 24-hour Total Rainfall in Return Periods of 10 to 100 000 000 Years at the Site (43 Years)

Return Periods	**24-Hour Storm (mm)**	
	Annual	**95th Confidence Interval**
10	49.0	± 7.3
100	69.0	± 12.8
1 000	88.6	± 18.3
10 000	108.1	± 23.7
100 000	127.7	± 29.2
1 000 000	147.2	± 34.7
10 000 000	166.7	± 40.2

100 000 000	186.3	± 45.7

According to the latest climate change projections (5th Assessment Report the IPCC (Intergovernmental Panel on Climate Change, 2013) (ARP5), both increases and decreases in heavy precipitation are predicted over southern Africa, depending on the region and precipitation statistical parameter examined. Changes in wet-day intensity and in the fraction of days with rainfall higher than 10 mm are expressed in units of standard deviations. Accordingly, the projections show a decrease of up to 0.4 standard deviations for the former and a decrease up to 0.6 for the latter for the Site. Changes in percentages of days with precipitation above the 95 per cent quantile are projected to be reduced by up to 1 per cent in the Western Cape in both the near-future (typically 2050) and far-future (typically 2100). Downscaled climate change models have been prepared for South Africa by SAWS (South African Weather Service, 2017) and the Council for Scientific and Industrial Research (CSIR) ((Engelbrecht, et al., 2019) and (CSIR, 2021)). The two CSIR studies differed in that the former (Engelbrecht, et al., 2011) provided projections for near (2021-2050) and far (2071-2099) horizons, whereas the latter (CSIR, 2021) provided projections for specific years, namely 2044, 2064, 2110 and 2130.

In order to accommodate the uncertainties in future greenhouse gas (GHG – most importantly, carbon dioxide (CO_2) methane (CH_4) and nitrous oxide (N_2O)) emission scenarios, a standard set of scenarios were used in ARP5 to ensure that the starting conditions, historical data, and projections employed by the different groups are complementary, comparable and consistent across the various branches of climate science. These scenarios are called Representative Concentration Pathways (RCPs) that describe alternative assumptions about selected approximate total radiative forcing values for the year 2100 relative to 1750 (Intergovernmental Panel on Climate Change, 2013). RCPs are scenarios depicting the evolution of emissions and concentrations of the most important GHGs, aerosols, chemically active gases and those related to changes in land use and land cover resulting in specified levels of radiative forcing. For each category of emissions, an RCP contains a set of starting values and the estimated emissions up to 2100, based on assumptions about economic activity, energy sources, population growth and other socio-economic factors. There are four pathways, namely RCP8.5, RCP6, RCP4.5 and RCP2.6, with each numerical referring to the radiative forcing in W/m^2. Therefore RCP8.5 implies radiative forcing higher than 8.5 W/m^2 by 2100, whereas radiative forcing stabilises at approximately 6 W/m^2, 4.5 W/m^3 and 2.6 W/m^3 after 2100 in the RCP6, RCP4.5 and RCP2.6 pathways, respectively. The worse-case pathway is RCP 8.5, which is representative of scenarios in the literature that lead to high GHG levels (Riahi, et al., 2007).

Based on the downscaled simulations performed by the CSIR (CSIR, 2021), the projected annual total rainfall changes, averaged over an area of 100 km by 100 km (centred around the site) for the RCP8.5 scenario are as follows:

- year 2044 : -54.1 (-45.7; -62.8) mm;
- year 2064 : -72.0 (-59.6; -73.7) mm;
- year 2110 : -117.7 (-112.1; -119.6) mm;
- year 2130 : -142.7 (-142.1; -143.8) mm.

The values in brackets represent the 5th and 95th percentiles.

Although the CSIR (CSIR, 2021) results did not provide 24-hour storm projections, the earlier CSIR (Engelbrecht, et al., 2019) results indicated a decrease in the number of extreme rainfall events, i.e.:

- near-horizon (2021-2050) : -1 (-3,-1) day;
- far horizon (2071-2099) : -3 (-4,-2) days.

An extreme rainfall event is defined as 20 mm of rain occurring within 24 hours over an area of 64 km². The values in brackets represent the 10th and 90th percentiles.

In a 2011 perspective on climate change and the South African water sector, (Schulze, 2011) concluded that for short duration rainfall events (i.e. 5 minutes to 24 hours) design rainfall for a given location can be estimated as:

- Overall across South Africa an increase up to 10 per cent in short duration design rainfalls may be expected, but with patches south of 32 °S and north of 27 °S where the models show no discernible change from the present.
- Of note is the high projected change in short duration design rainfall in the area transitional between the summer and winter rainfall areas, where increases of up to 40 per cent are projected.

For the site in particular, the average ratio of changes for short duration design rainfall (all return periods) were estimated by Schultze (Schulze, 2011) to be “no-change” for the near future (2046-2065) and a unitless ratio of change between 1.0 and 1.1, for the far future (2081-2100) scenarios. Given the projected decrease in annual total rainfall due to climate change factors, the extreme estimates in ***Table 5.8.68*** are expected to represent the upper rainfall levels. Although the climate change projections indicate a decrease in the number of extreme rainfall events, it would be conservative to assume the extreme values estimated in ***Table 5.8.69*** for 24-hour storm events.

(b) Extreme Ambient Air Temperature

A relatively long record of ambient air temperature is available for the site (October 1997-September 2023), but at 10 m above ground level (and higher) only. The ambient air temperature measurements at the standard height of at 2 m are only available for a period of seven (non-consecutive) years (January 2009 to September 2013 and October 2017 to February 2022) (Eskom, 2023a).

The extreme minimum and hourly average temperatures for the site were based on the extreme values recorded at the 10-m level of the 120-m tower due to the length of available observations. The expected ambient air temperatures for this station are summarised in ***Table 5.8.70***. Details of the methodology for calculating the return period temperatures are provided in ***Appendix 5.8.B***.

Table 5.8.70

Expected Minimum and Maximum Hourly Average Temperature (°C) in Return Periods of 10 to 100 000 000 Years at the Site (25 Years)

Return Period	Minimum Hourly Average Temperature (°C)		Maximum Hourly Average Temperature (°C)	
	Minimum	95th Confidence Interval	Maximum	95th Confidence Interval
10	3.5	± 0.5	37.5	± 0.9
100	1.6	± 1.0	40.4	± 2.0
1 000	-0.2	± 1.5	43.3	± 3.2
10 000	-2.1	± 2.0	46.2	± 4.3
100 000	-3.9	± 2.5	49.1	± 5.5
1 000 000	-5.8	± 3.0	52.0	± 6.7
10 000 000	-7.6	± 3.5	54.9	± 7.9
100 000 000	-9.5	± 4.0	57.8	± 9.0

The IAEA (International Atomic Energy Agency, 2011) considers the temperature increase by 2100 relative to 2000 to be 1.8–4.0°C (best estimate) and 1.1–6.4°C (including the likely uncertainty range for each of the scenarios considered owing to different responses of the climate models (***Subsection 5.8.9.2***)). The projections from the CSIR downscaled models (CSIR, 2021), provided the following minimum, mean and maximum daily temperatures changes averaged over an area of 100 km by 100 km (centred around the Site) for the RCP8.5 scenario:

- Daily Minimum Temperature Change (°C):

- year 2044 : +0.9 (+0.5,+1.4);
- year 2064 : +1.6 (+1.2,+2.1);
- year 2110 : +3.5 (+2.9,+3.5);
- year 2130 : +4.6 (+3.8,+5.3).

- Daily Mean Temperature Change (°C):
  - year 2044 : +0.9 (+0.6,+1.4);
  - year 2064 : +1.6 (+1.2,+2.1);
  - year 2110 : +3.5 (+3.0,+4.1);
  - year 2130 : +4.4 (+3.9,+5.2).
- Daily Maximum Temperature Change (°C):
  - year 2044 : +1.0 (+0.6,+1.5);
  - year 2064 : +1.7 (+1.3,+2.2);
  - year 2110 : +3.6 (+3.2,+4.1);
  - year 2130 : +4.7 (+4.3,+5.2).

The values in brackets represent the 5th and 95th percentiles (this corresponds to the 90 per cent confidence interval).

The *Special Report on Managing the Risks of Extreme Events and Disasters to Advance Climate Change Adaptation* (SREX) (Intergovernmental Panel on Climate Change, 2012) has been jointly coordinated by Working Groups I (WGI) and II (WGII) of the IPCC. The SREX report focuses on the relationship between climate change and extreme weather and climate events, the impacts of such events, and the strategies to manage the associated risks. A changing climate leads to changes in the frequency, intensity, spatial extent, duration, and timing of extreme weather and climate events. The SREX report approaches the topic by assessing the scientific literature on issues that range from the relationship between climate change and extreme weather and climate events (‘climate extremes’) to the implications of these events for society and sustainable development. Projections of extremes in any of the meteorological parameters are difficult to determine. Based on the SREX report, the approach to adjusting maximum temperature extremes for climate change is to apply a reduction in the return period of the predicted extreme value. So, a 10-fold reduction would mean that an extreme value calculated for a 1 000-year return period (unadjusted for climate change) would instead be for a 100-year return period. Based on this approach, and based on the ARP5 results, the return periods for the extreme hourly maximum temperatures should be reduced by 7-fold for 2044, 8-fold for 2064, 11-fold for 2110 and 12-fold for 2130, respectively. As a conservative estimate, the hourly minimum temperature extremes will assume the unadjusted projections, but with adjusted 95 per cent confidence interval. The expected extreme temperature ranges due to this temperature increase predictions are included in ***Table 5.8.71*** and ***Table 5.8.72***.

(c) Extreme Wind Speed

Operating experience globally of nuclear installations has shown that extreme winds mainly affect the power supply and availability of the electricity grid. However, sometimes damage is sustained to the switchyards. Recorded accidents typically evolve into turbine trip and loss of off-site power. In a few cases, the pressure differential creates some false signals to nuclear installation instrumentation.

Table 5.8.71
Minimum Hourly Average Temperatures Including Climate Change Projections at the Site

Return Periods	Hourly Minimum Temperatures [°C]							
	2044		2064		2110		2130	
	Extreme	95% Confidence Interval	Extreme	95 % Confidence Interval	Extreme	95% Confidence Interval	Extreme	95% Confidence Interval
10	3.5	± 0.5	3.5	± 0.6	3.5	± 0.6	3.5	± 0.7
100	1.6	± 1.1	1.6	± 1.1	1.6	± 1.3	1.6	± 1.3
1 000	-0.2	± 1.6	-0.2	± 1.7	-0.2	± 1.9	-0.2	± 2.0
10 000	-2.1	± 2.1	-2.1	± 2.2	-2.1	± 2.5	-2.1	± 2.7
100 000	-3.9	± 2.7	-3.9	± 2.8	-3.9	± 3.2	-3.9	± 3.3
1 000 000	-5.8	± 3.2	-5.8	± 3.4	-5.8	± 3.8	-5.8	± 4.0
10 000 000	-7.6	± 3.7	-7.6	± 3.9	-7.6	± 4.4	-7.6	± 4.7
100 000 000	-9.5	± 4.3	-9.5	± 4.5	-9.5	± 5.1	-9.5	± 5.4

Table 5.8.72
Expected Maximum Hourly Average Temperatures Including Climate Change Projections at the Site

Return Periods	Hourly Maximum Temperatures [°C]							
	2044		2064		2110		2130	
	Extreme	95% Confidence Interval	Extreme	95 % Confidence Interval	Extreme	95% Confidence Interval	Extreme	95% Confidence Interval
10	39.4	± 0.9	40.7	± 1.0	44.2	± 1.1	46.1	± 1.1
100	42.5	± 2.1	43.9	± 2.2	47.7	± 2.4	49.7	± 2.5
1 000	45.5	± 3.4	47.0	± 3.5	51.1	± 3.8	53.3	± 3.9
10 000	48.6	± 4.5	50.2	± 4.7	54.5	± 5.1	56.8	± 5.3
100 000	51.6	± 5.8	53.3	± 6.0	57.9	± 6.5	60.4	± 6.8
1 000 000	54.6	± 7.0	56.4	± 7.3	61.3	± 7.9	63.9	± 8.2
10 000 000	57.7	± 8.3	59.6	± 8.6	64.7	± 9.3	67.4	± 9.7
100 000 000	60.7	± 9.5	62.7	± 9.8	68.1	± 10.6	71.0	± 11.1

At sites close to the marine environment, heavy salt sprays from the sea in the form of a precipitation during the most violent phases created electrical shorts in exposed electrical equipment (bushings and switchgears) and, later, deep corrosion and malfunctions (International Atomic Energy Agency, 2021). As a result of the high occurrence of strong wind speeds, such incidents may be likely to occur at the site.

From the analysis of site wind speed data for the 1980-2022 period (***Subsection 5.8.6.1.1***) the highest gust, hourly and monthly wind speeds were 38.8, 17.2 and 6.8 m/s, respectively. Extreme value analyses were performed on the observed maximum hourly and gusts for this 40-year period (***Appendix 5.8.B***). The expected extreme wind speeds for the site are summarised in ***Table 5.8.73***.

Table 5.8.73
Extreme Highest Hourly Average Wind Speed and Wind Gust (m/s) for the Site (1980-2022)

Return Period	Maximum Hourly Average Wind Speed (m/s)		Wind Gust (m/s)	
	Mean	95th Confidence Interval	Mean	95th Confidence Interval
10	16.9	± 1.0	33.8	± 2.7
100	21.6	± 1.5	43.3	± 4.8
1 000	26.3	± 2.2	52.7	± 6.8
10 000	30.9	± 2.8	62.0	± 8.9
100 000	35.5	± 3.5	71.4	± 11.0
1 000 000	40.2	± 4.2	80.8	± 13.1
10 000 000	44.8	± 4.8	90.1	± 15.2
100 000 000	49.4	± 5.5	99.5	± 17.3

The South African National Standards (SANS) issued a national design code for wind loadings on buildings and structures, SANS 10160-Part 3 (South African National Standards, 2019), which provides regional basic 3-second wind speeds for a 50-year return period. ***Figure 8.8.27*** (South African National Standards, 2019) illustrates the map contained in the national design code of the SANS standard.

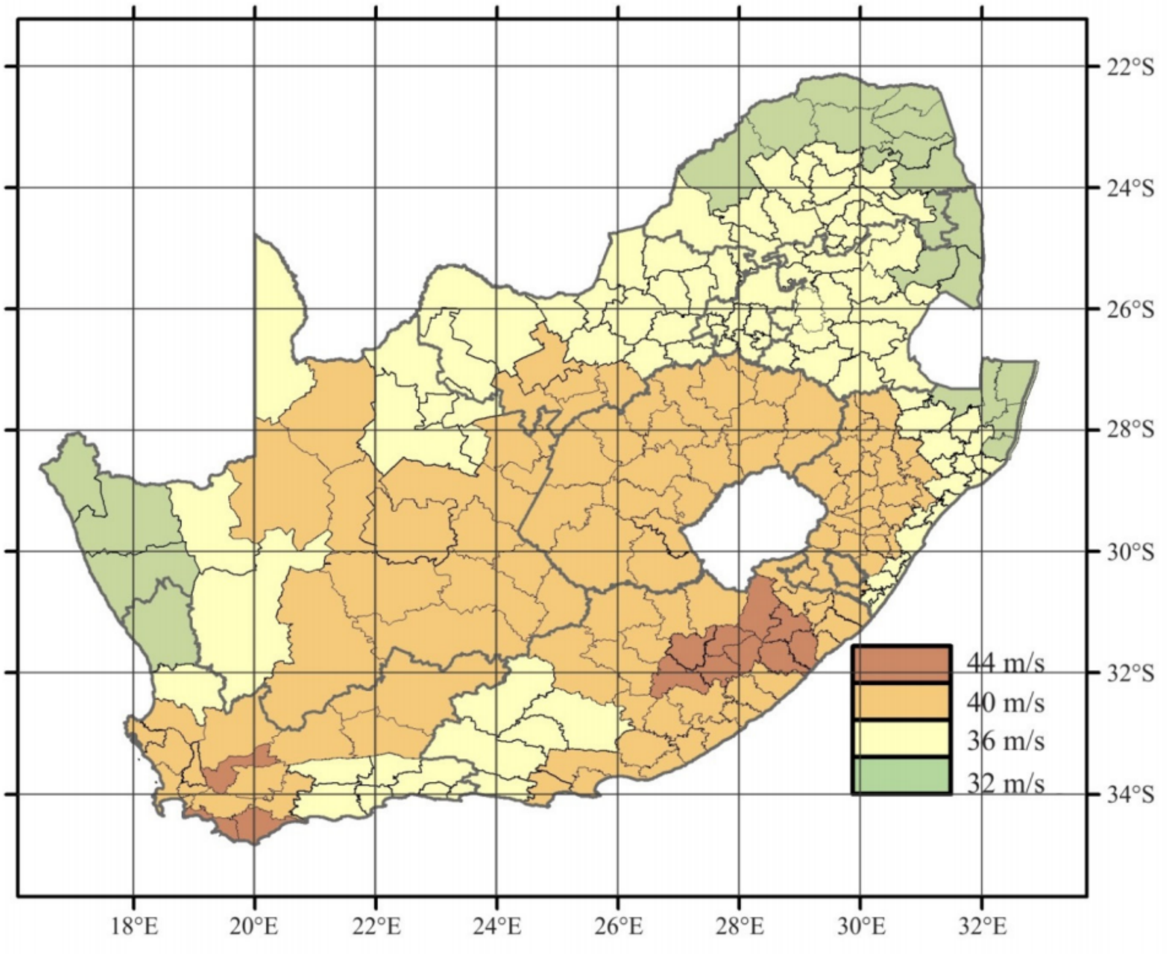

Figure 5.8.27
Map of Fundamental Value of Basic 3-s Gust Wind Speed (50 Year Return Period) (South African National Standards, 2019)

According to this code, the 50-year return period regional basic wind speed 3-s gust is 40 m/s. Although not given in ***Table 5.8.73***, the calculated 50-year return 3-s gust for the site is calculated to be 40.7 m/s. These values are very similar. It is stated in the NNR position paper (NNR PP-0014) on external events that should be considered in assessing sites, that the extreme value cannot be lower than the value provided by the national design code for the same region.

Extreme winds are often considered in the context of the extreme phenomena with which they are associated such as cyclones, thunderstorm downbursts, and tornadoes. Changes in wind extremes may arise from changes in the intensity or location of their associated phenomena (e.g. a change in local convective activity) or from other changes in the climate system such as the movement of large-scale circulation patterns. The SREX report (Intergovernmental Panel on Climate Change, 2012) states that there is evidence to suggest an increase in extreme winds from tropical cyclones in the future. Furthermore, an increase in atmospheric GHG concentrations may cause some of the atmospheric conditions conducive to tornadoes such as atmospheric instability to increase due to increasing temperature and humidity, while others such as vertical shear to decrease due to a reduced pole-to-equator temperature gradient, but the literature on these phenomena is extremely limited. There is thus low confidence in projections of changes in such small-scale systems because of limited studies, inability of climate models to resolve these phenomena and possible competing factors affecting future changes. Confidence in the extreme wind changes is therefore lower in the regions most influenced by these phenomena irrespective of whether there is high agreement between simulation models on the direction (i.e., increase or decrease) of the wind speed change. Based on the downscaled simulations performed by the CSIR (CSIR, 2021), the mean projected maximum hourly average wind speed and gusts, averaged over an area of 100 km by 100 km (centred around the site) for the RCP8.5 scenario are as follows (expressed as percentage change):

	Highest Hourly Average	Gust
• year 2044	+2.28 (-2.37,+6.29)	+0.92 (-0.55,+2.29)
• year 2064	+3.85 (-1.21,+8.69)	+1.44 (-0.16,+3.05)
• year 2110	+8.04 (+2.37,+13.30)	+3.10 (+1.34,+4.82)
• year 2130	+10.29 (+4.13,+15.73)	+3.98 (+2.09,+5.75)

The values in brackets represent the 5th and 95th percentiles (90 per cent confidence interval).

It is stated in the SREX report that changes in extremes may be directly related to changes in mean climate, because mean future conditions in some variables are projected to lie within the tails of present-day condition probability distributions. It was therefore assumed that the predicted extreme winds in ***Table 5.8.73*** will similarly increase according to these projections, i.e. using the fractional increases. The predicted extreme winds for the four time horizons and return periods are summarised in ***Table 5.8.74*** for the maximum hourly average wind speeds and in ***Table 5.8.75*** for gusts. The confidence intervals were assumed to remain the same as for the original extreme value analysis.

Wind direction changes were not provided as part of the downscaled model outputs. Instead, the study by (Herbst & Rautenbach, 2015) which attempted to quantify the projected changes in seasonal daily mean wind speeds and directions for South Africa around the mid-21st century (2051-2075) was consulted. The following seasonal changes were projected:

March-April-May	an easterly wind shift;
June-July-August	a southerly wind shift;
September-October-November	a southeasterly wind shift;
December-January-February	an easterly wind shift.

Table 5.8.74

Expected Maximum Hourly Average Wind Speeds Including Climate Change Projections at the Site

Return Periods	Maximum Hourly Average Wind Speed [m/s]							
	2044		2064		2110		2130	
	Extreme	95% Confidence Interval	Extreme	95 % Confidence Interval	Extreme	95% Confidence Interval	Extreme	95% Confidence Interval
10	17.3	± 1.0	17.6	± 1.0	18.3	± 1.0	18.7	± 1.0
100	22.1	± 1.5	22.5	± 1.5	23.4	± 1.5	23.9	± 1.5
1 000	26.9	± 2.2	27.3	± 2.2	28.4	± 2.2	29.0	± 2.2
10 000	31.6	± 2.8	32.1	± 2.8	33.4	± 2.8	34.1	± 2.8
100 000	36.4	± 3.5	36.9	± 3.5	38.4	± 3.5	39.2	± 3.5
1 000 000	41.1	± 4.2	41.7	± 4.2	43.4	± 4.2	44.3	± 4.2
10 000 000	45.8	± 4.8	46.5	± 4.8	48.4	± 4.8	49.4	± 4.8
100 000 000	50.5	± 5.5	51.3	± 5.5	53.4	± 5.5	54.5	± 5.5

Table 5.8.75
Expected Wind Gust Speeds Including Climate Change Projections at the Site

Return Periods	Maximum Hourly Average Wind Speed [m/s]							
	2044		2064		2110		2130	
	Extreme	95% Confidence Interval	Extreme	95 % Confidence Interval	Extreme	95% Confidence Interval	Extreme	95% Confidence Interval
10	34.1	± 2.7	34.2	± 2.7	34.8	± 2.7	35.1	± 2.7
100	43.7	± 4.8	43.9	± 4.8	44.6	± 4.8	45.0	± 4.8
1 000	53.2	± 6.8	53.4	± 6.8	54.3	± 6.8	54.8	± 6.8
10 000	62.6	± 8.9	62.9	± 8.9	64.0	± 8.9	64.5	± 8.9
100 000	72.1	± 11.0	72.4	± 11.0	73.6	± 11.0	74.2	± 11.0
1 000 000	81.5	± 13.1	81.9	± 13.1	83.3	± 13.1	84.0	± 13.1
10 000 000	90.9	± 15.2	91.4	± 15.2	92.9	± 15.2	93.7	± 15.2
100 000 000	100.4	± 17.3	100.9	± 17.3	102.6	± 17.3	103.4	± 17.3

5.8.7 Atmospheric Dispersion Modelling

5.8.7.1 Dispersion Model

The IAEA recognises Gaussian-plume models (International Atomic Energy Agency, 2001) to be well suited for use in radiological assessment activities and specifically near-field (typically <50 km) applications where the steady-state meteorology assumption is most likely to apply.

Perhaps the most widely used Gaussian dispersion model internationally that requires stability classes as input has been the US Environmental Protection Agency (US EPA) AERMET/AERMOD model suite (Cimorelli, et al., 2004). It is stated in *Section 1* of RG-0016 that *"All calculation models and/or evaluation models used in safety analyses are designed, developed, verified and validated, implemented, used and controlled in accordance with recognised nuclear industry standards and/or practices."* The details of the model selection, validation and verification is provided in the Validation and Verification Report (V&V Report) (Burger, 2021). In the V&V Report, it was concluded that the US EPA AERMOD atmospheric model satisfy the requirements for simulation atmospheric dispersion from nuclear installations for the purposes of the SSR.

AERMET is a meteorological pre-processor for AERMOD. Input data can come from hourly cloud cover observations, surface meteorological observations and twice-a-day upper air soundings. As applied in this instance, onsite hourly average wind speed, dry bulb temperature, solar radiation and rainfall were used as input into the model. The wind speed and temperature were taken from the different levels on the 120-m tower. The input files are contained in ***Appendix 5.8.N*** (surface meteorological data) and ***Appendix 5.8.O*** (profile data).

AERMAP is a terrain pre-processor designed to simplify and standardize the input of terrain data for AERMOD. Input data include receptor terrain elevation data. The model input file is provided in ***Appendix 5.8.P.*** The model results are expressed as concentrations (normally at ground level) and deposition rates over different periods of exposure.

5.8.7.2 Dispersion Factor

The dispersion factor was calculated using the AERMOD model and provided as the effluent concentration (χ) and deposition (D) normalised by the source strength (Q). This was calculated using hourly averaged meteorological data obtained from the site for a five-year period 2015 to 2019).

To simulate worst-case postulated accidents, the following assumptions were made:

- there is no building wake effect;
- the effective release is from 1.5 m above ground level;
- exit gas velocity assumed 0 m/s;
- stack diameter of 2 m;
- exit gas temperature assumed 298 K;
- the receptor height is 1.5m;
- modelling domain includes an area of 40 km by 40 km, with the nuclear installation(s) located at the centre of the modelling domain;
- the grid resolutions:
  - 100 m by 100 m for a 5 km by 5 km domain;
  - 200 m by 200 m for 40 km by 40 km domain.

The hourly average meteorological surface and tower data are used to simulate a release event and the concentrations/depositions for that hour are calculated at each of the regular grid locations (receptors). The concentrations/depositions for each of the simulation hours are individually compared at a receptor and the 99.9th (2nd highest) and 95th percentile concentrations/depositions stored for the preparation of the spatial and directional plots given below.

The normalised deposition rate includes rain washout as well as dry deposition.

The figures below represent the following dispersion factors:

- concentration:
  - 2nd highest hourly average:
    - 5 km by 5 km : ***Figure 5.8.28***
    - 40 km by 40 km : ***Figure 5.8.29***
  - 95th percentile hourly average:
    - 5 km by 5 km : ***Figure 5.8.30***
    - 40 km by 40 km : ***Figure 5.8.31***
  - 2nd Highest 3-hourly average:
    - 5 km by 5 km : ***Figure 5.8.32***

    - 40 km by 40 km : ***Figure 5.8.33***
  - 2nd Highest 8-hourly average:
    - 5 km by 5 km : ***Figure 5.8.34***
    - 40 km by 40 km : ***Figure 5.8.35***
  - 2nd Highest 24-hourly (daily) average:
    - 5 km by 5 km : ***Figure 5.8.36***
    - 40 km by 40 km : ***Figure 5.8.37***
  - Highest monthly average:
    - 5 km by 5 km : ***Figure 5.8.38***
    - 40 km by 40 km : ***Figure 5.8.39***
  - Highest Annual average:
    - 5 km by 5 km : ***Figure 5.8.40***
    - 40 km by 40 km : ***Figure 5.8.41***
- deposition:
  - 2nd highest hourly total:
    - 5 km by 5 km : ***Figure 5.8.42***
    - 40 km by 40 km : ***Figure 5.8.43***
  - 95th percentile hourly total:
    - 5 km by 5 km : ***Figure 5.8.44***
    - 40 km by 40 km : ***Figure 5.8.45***
  - 2nd Highest 3-hour total:
    - 5 km by 5 km : ***Figure 5.8.46***
    - 40 km by 40 km : ***Figure 5.8.47***
  - 2nd Highest 8-hour total:
    - 5 km by 5 km : ***Figure 5.8.48***
    - 40 km by 40 km : ***Figure 5.8.49***
  - 2nd Highest 24-hour total:
    - 5 km by 5 km : ***Figure 5.8.50***
    - 40 km by 40 km : ***Figure 5.8.51***
  - Highest monthly total:
    - 5 km by 5 km : ***Figure 5.8.52***

  - 40 km by 40 km : ***Figure 5.8.53***
- Highest annual total:
  - 5 km by 5 km : ***Figure 5.8.54***
  - 40 km by 40 km : ***Figure 5.8.55***

Figure 5.8.56 to ***Figure 5.8.63*** are summaries of the א/Q values of the 2nd highest hourly, 3-hourly, 8-hourly, 24-hourly, and highest monthly and annual averages, grouped into the 16 cardinal wind directions at 800 m, 3 km and 8 km, downwind of the nuclear installation(s).

The data used to develop these figures are summarised in ***Table 5.8.76*** and ***Table 5.8.77***.

Similarly, ***Figure 5.8.64*** to ***Figure 5.8.72*** are summaries of the D/Q values of the 2nd highest hour, 3-hour, 8-hour, 24-hour and highest month and annual totals, grouped into the 16 cardinal wind directions at 800 m, 3 km and 8 km, downwind of the nuclear installation(s).

The data used to develop these figures are summarised in ***Table 5.8.78*** and ***Table 5.8.79***.

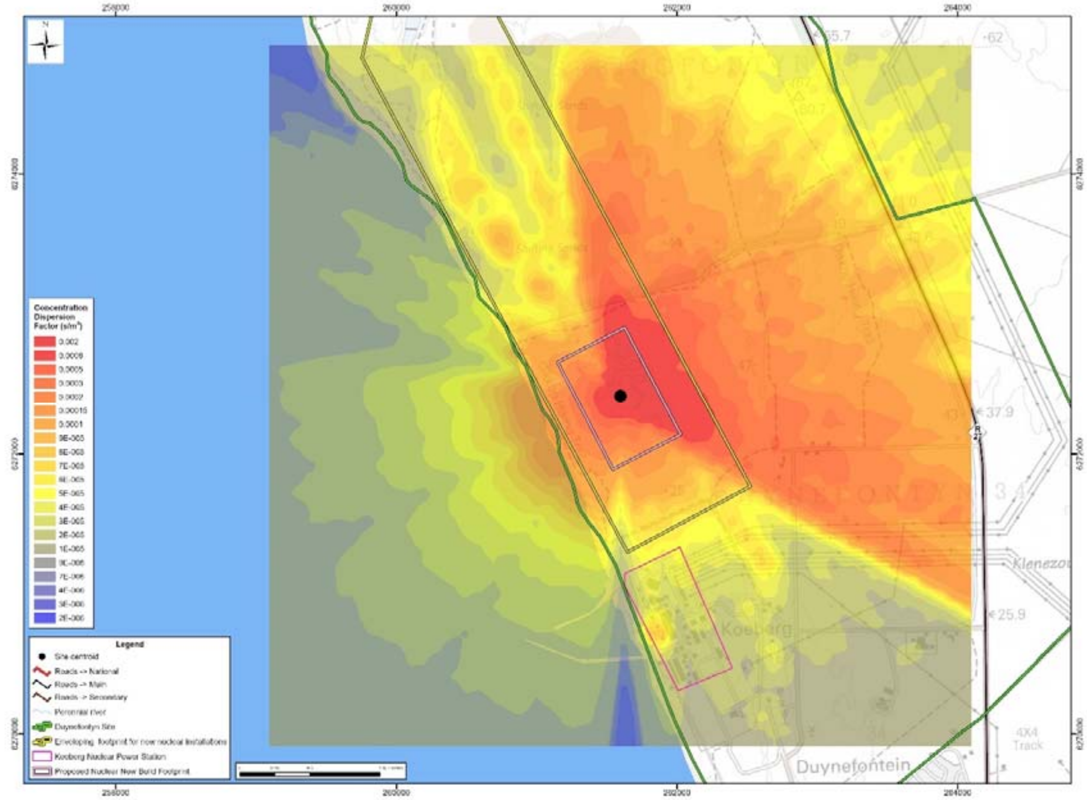

Figure 5.8.28
The Predicted 2nd Highest Hourly Average Ground Level Concentration Dispersion Factor (א/Q) for a 5 km by 5 km area

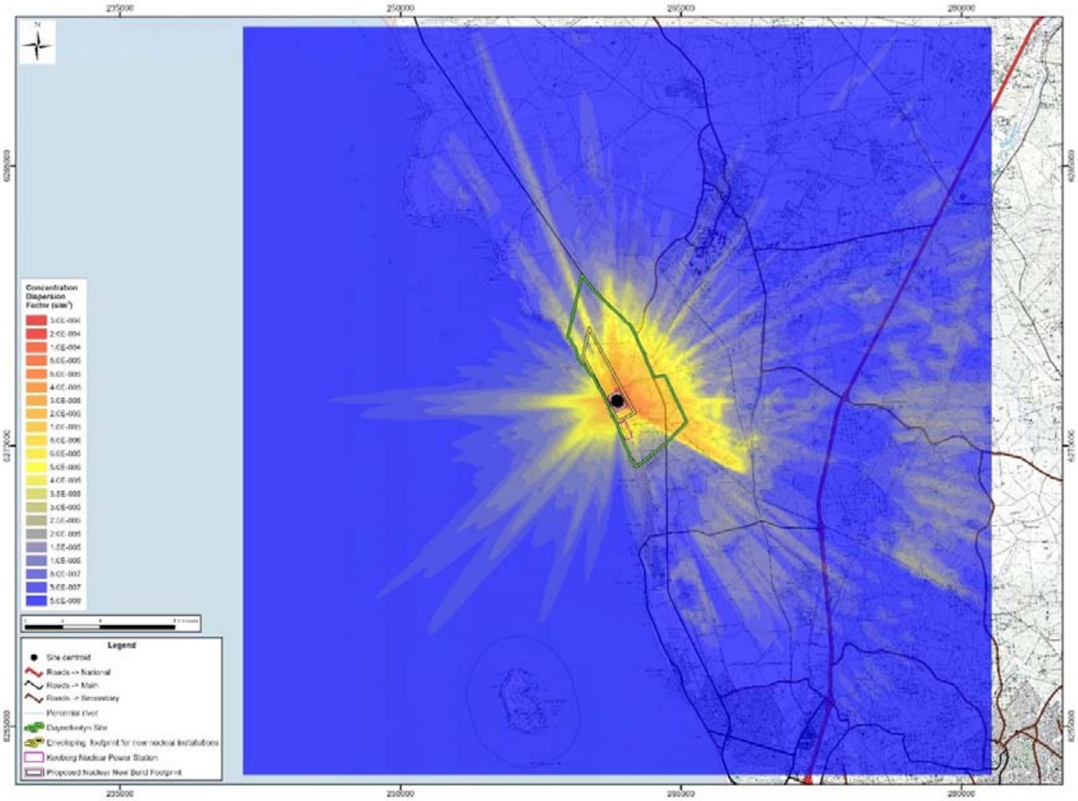

Figure 5.8.29
The Predicted 2nd Highest Hourly Average Ground Level Concentration Dispersion Factor (א/Q) for a 40 km by 40 km area

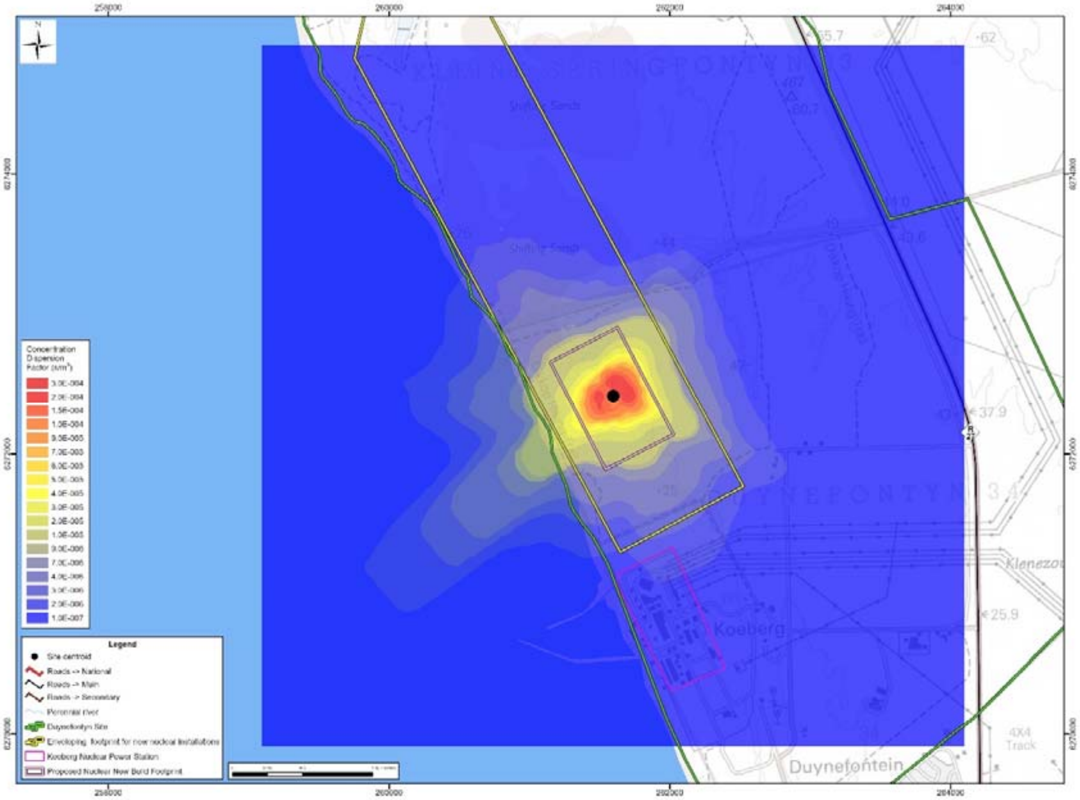

Figure 5.8.30
The Predicted 95th Percentile Ground Level Concentration Dispersion Factor (א/Q) for a 5 km by 5 km area

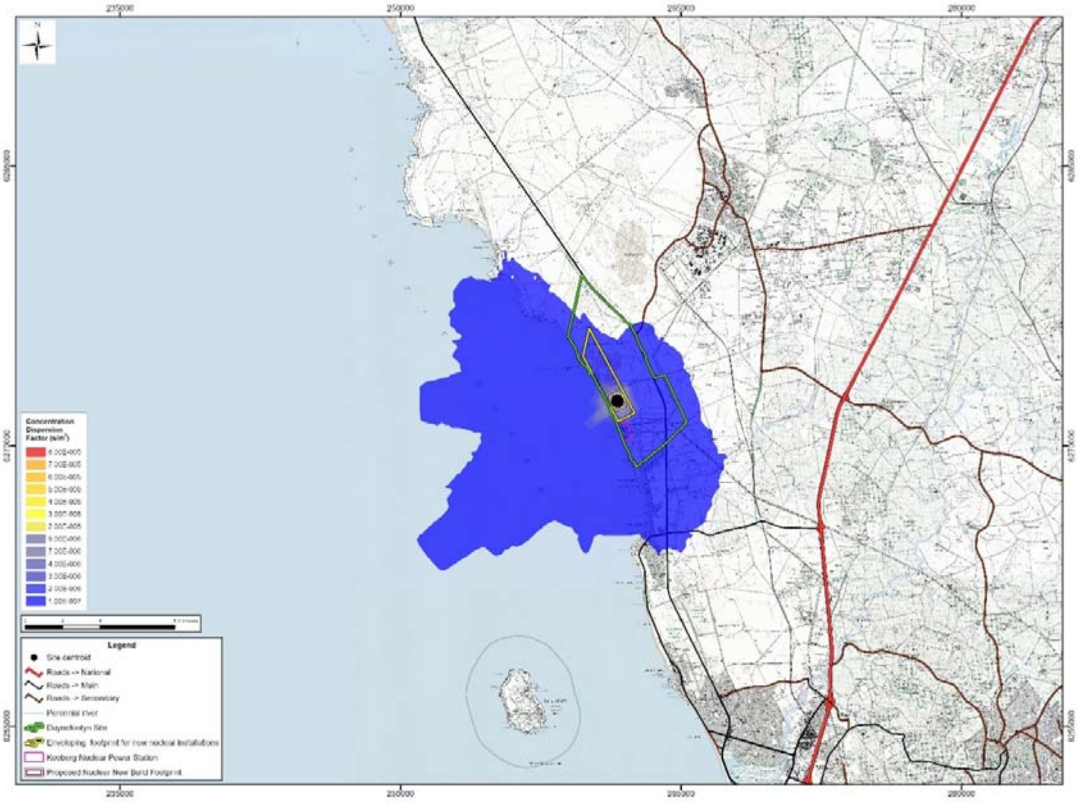

Figure 5.8.31

The Predicted 95th Percentile Ground Level Concentration Dispersion Factor (ꭓ/Q) for a 40 km by 40 km area

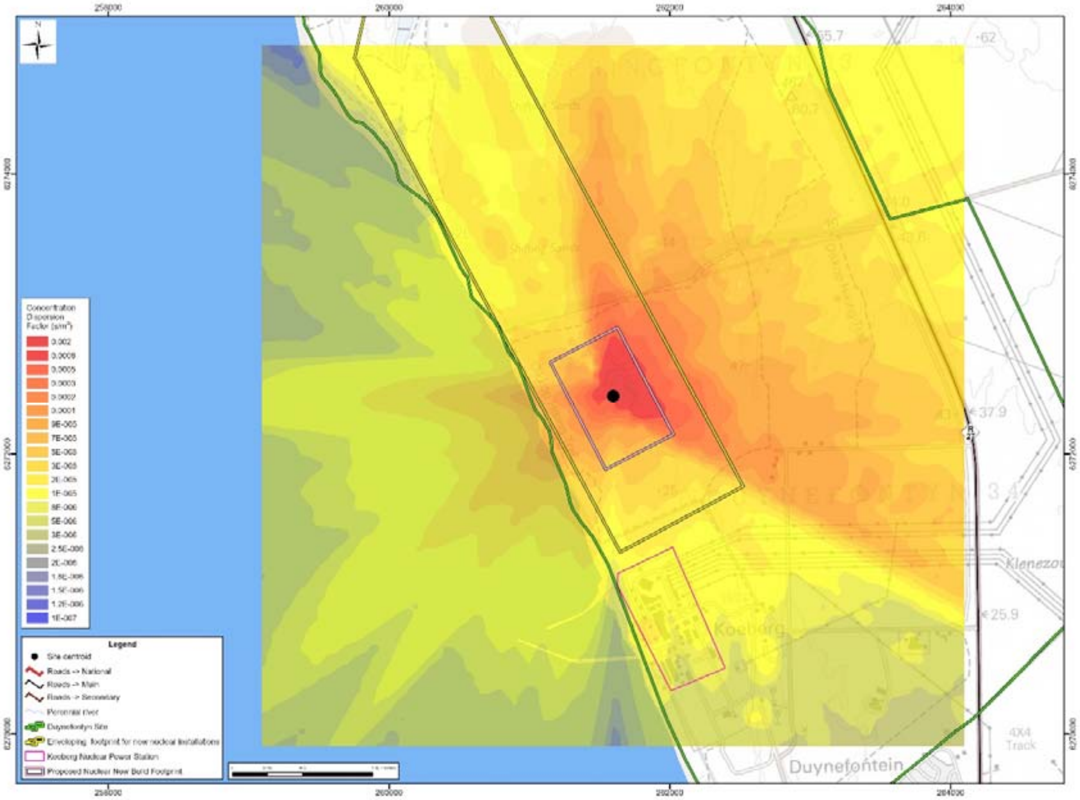

Figure 5.8.32
The Predicted 2nd Highest 3-Hourly Average Ground Level Concentration Dispersion Factor (ϰ/Q) for a 5 km by 5 km area

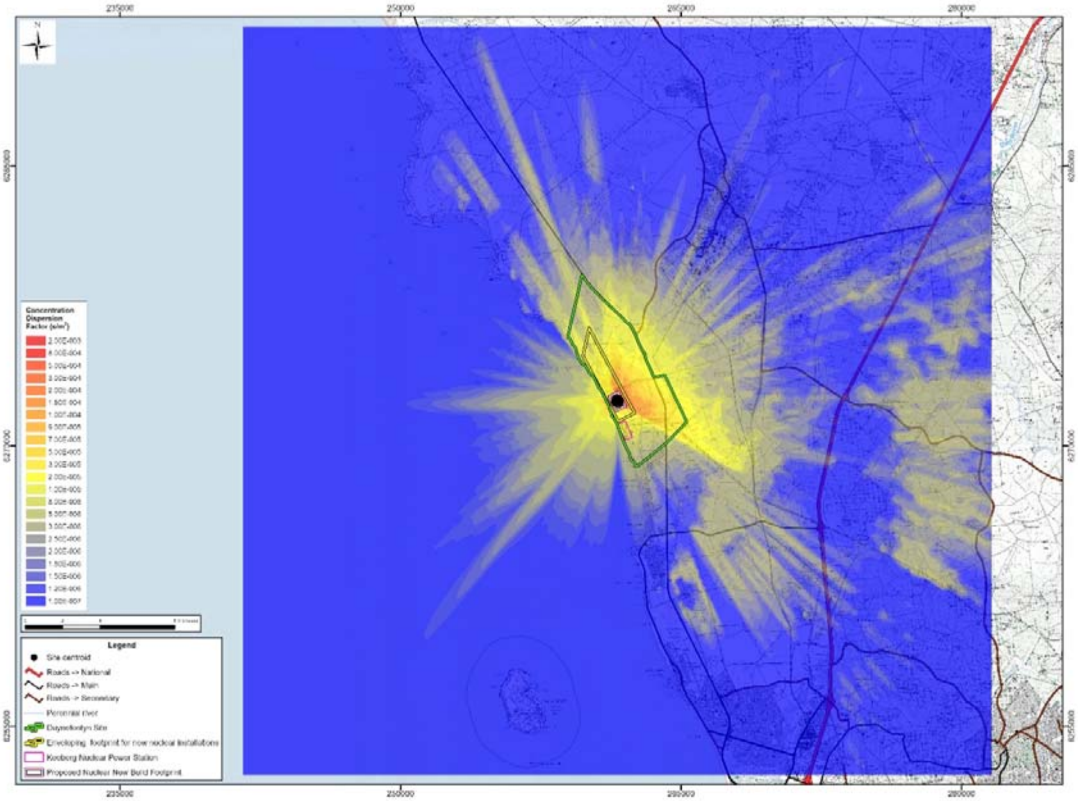

Figure 5.8.33
The Predicted 2nd Highest 3-Hourly Average Ground Level Concentration Dispersion Factor (ӽ/Q) for a 40 km by 40 km area

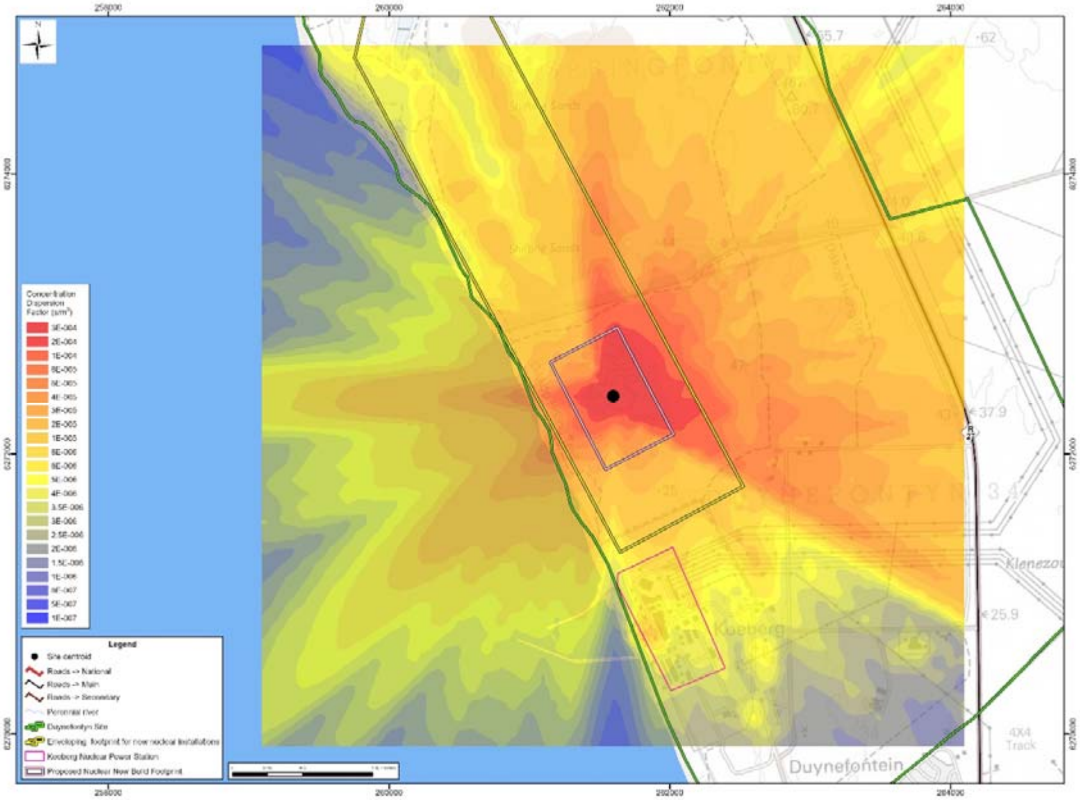

Figure 5.8.34
The Predicted 2nd Highest 8-Hourly Average Ground Level Concentration Dispersion Factor (χ/Q) for a 5 km by 5 km area

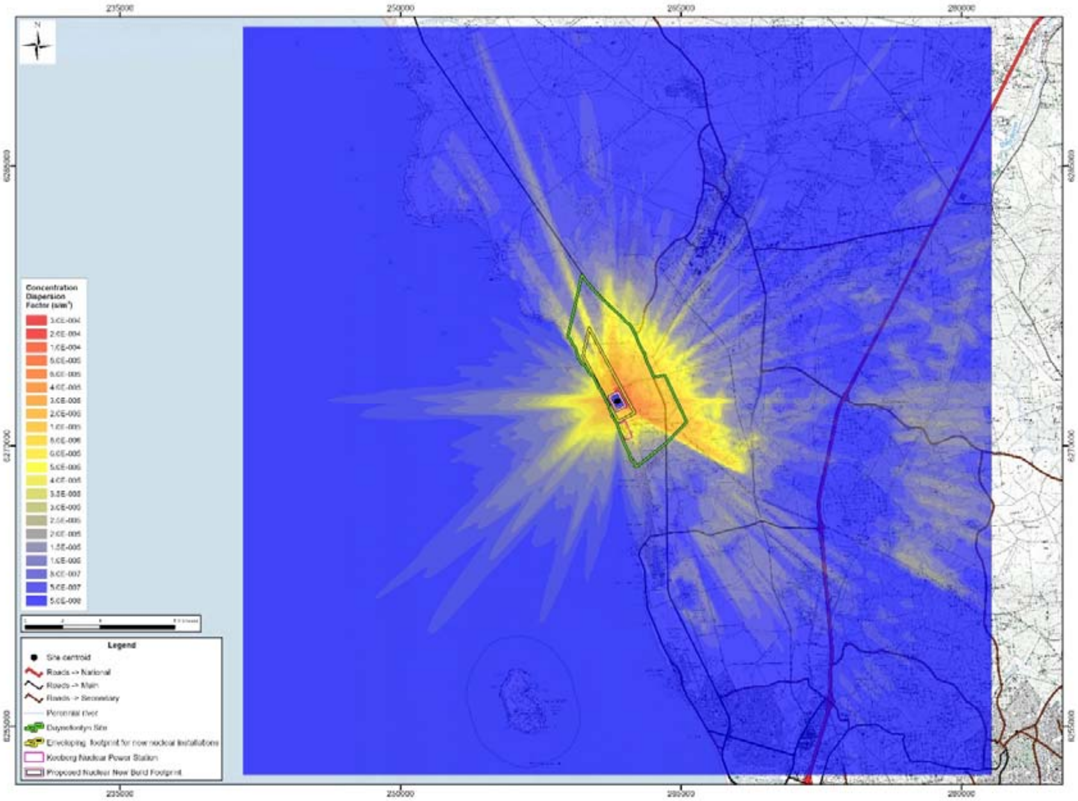

Figure 5.8.35
The Predicted 2nd Highest 8-Hourly Average Ground Level Concentration Dispersion Factor (א/Q) for a 40 km by 40 km area

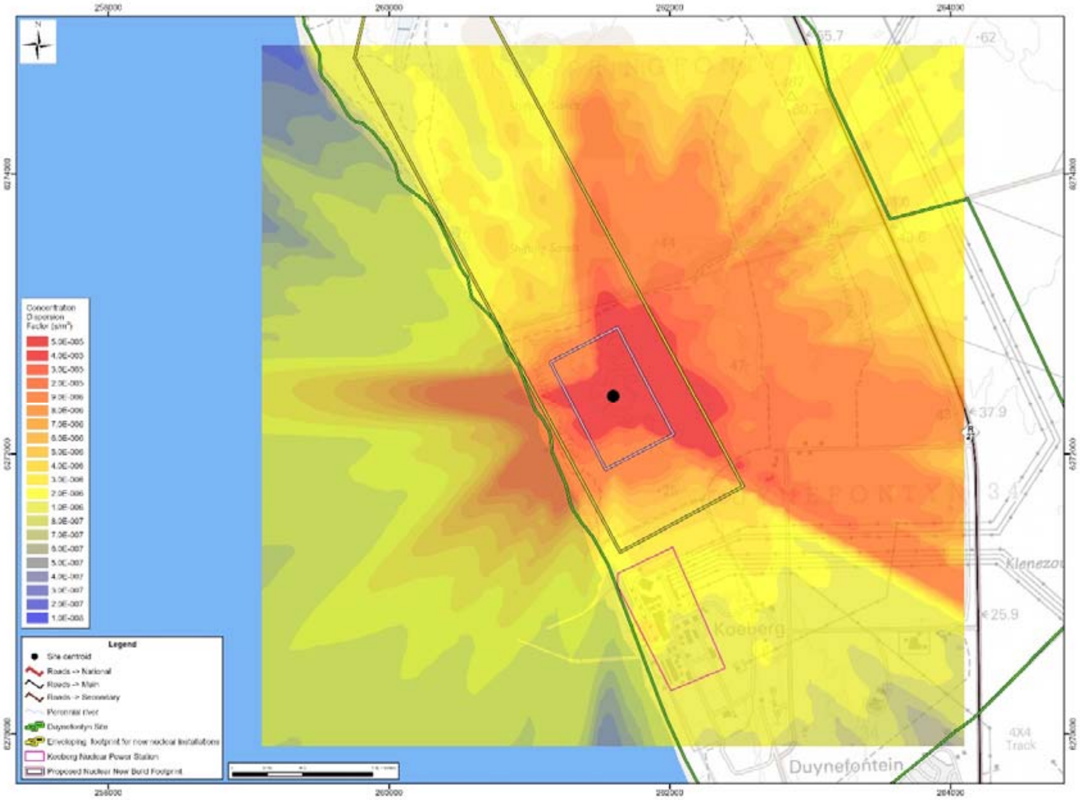

Figure 5.8.36
The Predicted 2nd Highest 24-Hourly Average Ground Level Concentration Dispersion Factor (א/Q) for a 5 km by 5 km area

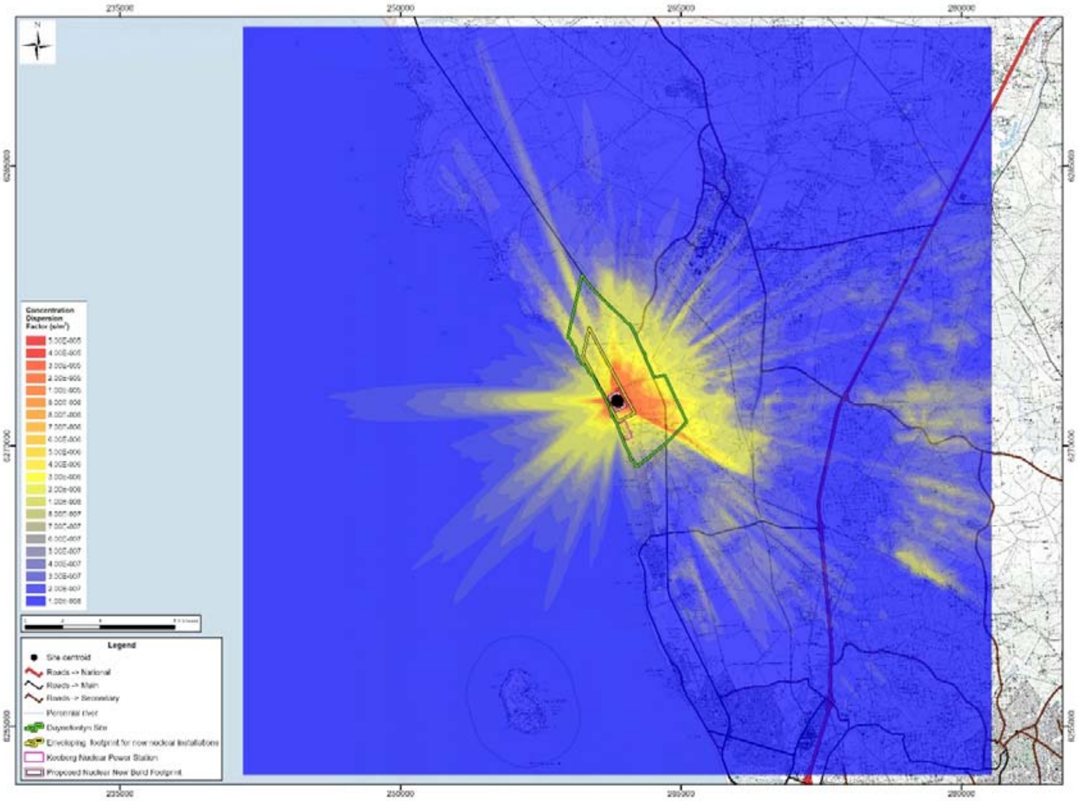

Figure 5.8.37
The Predicted 2nd Highest 24-Hourly Average Ground Level Concentration Dispersion Factor (א/Q) for a 40 km by 40 km area

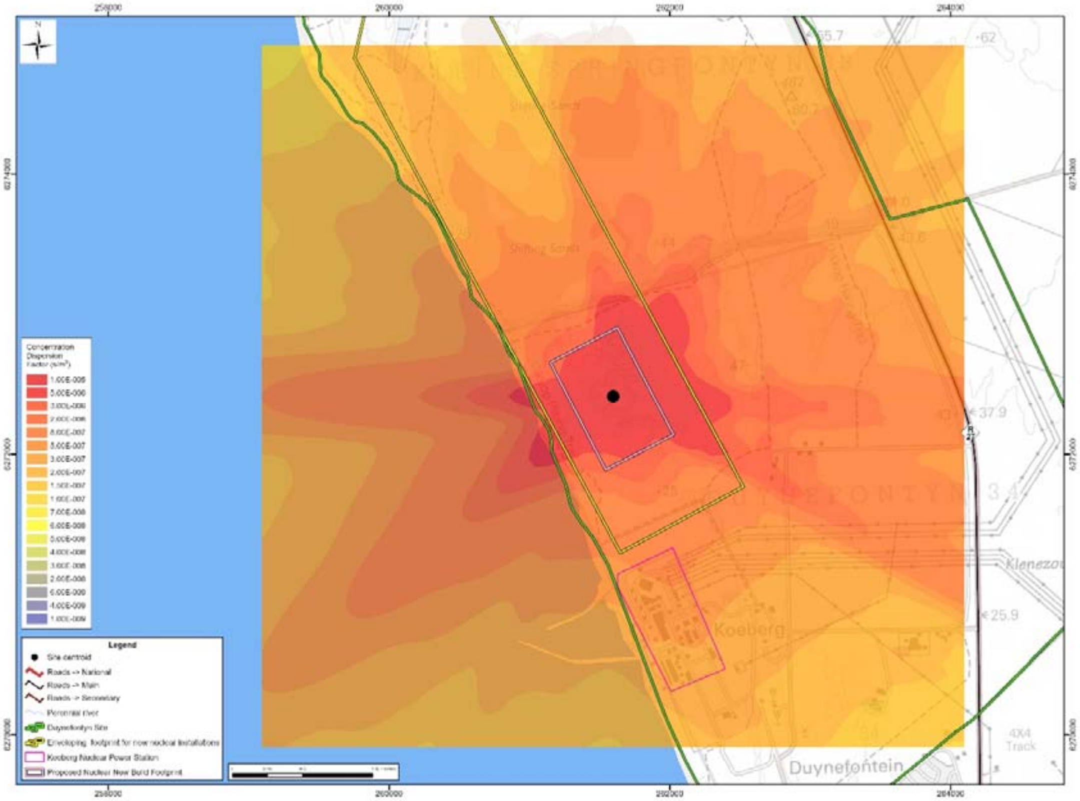

Figure 5.8.38
The Predicted Highest Monthly Average Ground Level Concentration Dispersion Factor (ϰ/Q) for a 5 km by 5 km area

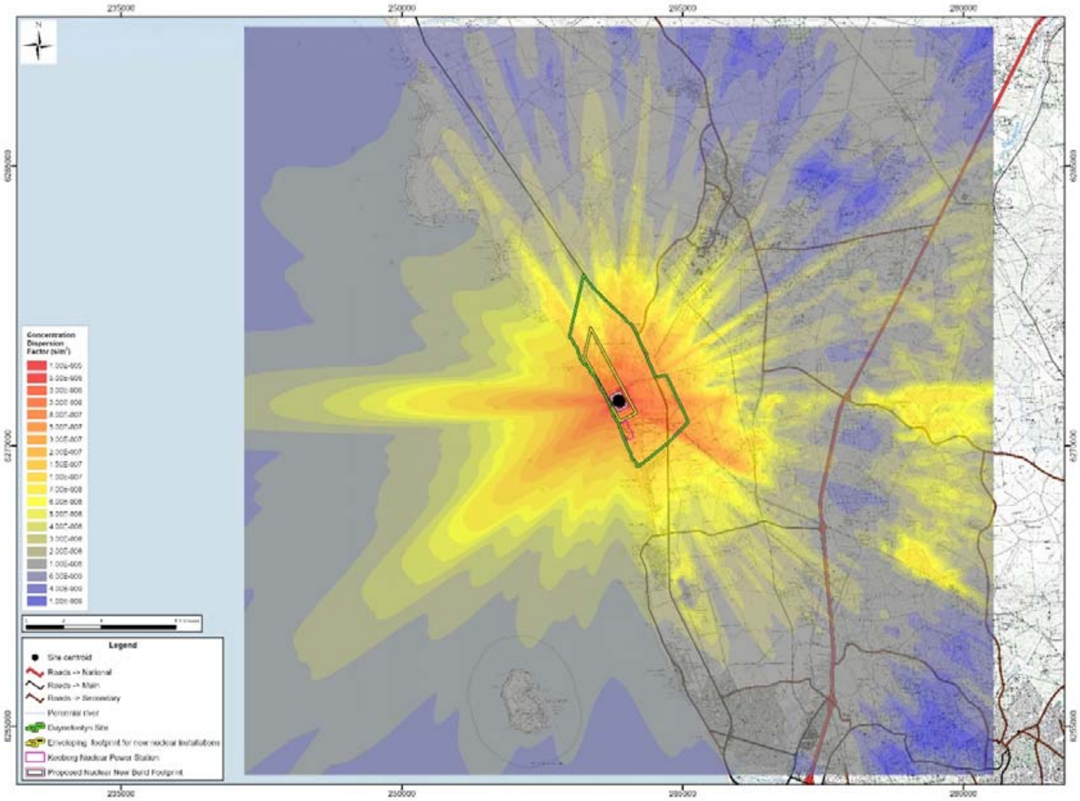

Figure 5.8.39
The Predicted Highest Monthly Average Ground Level Concentration Dispersion Factor (χ/Q) for a 40 km by 40 km area

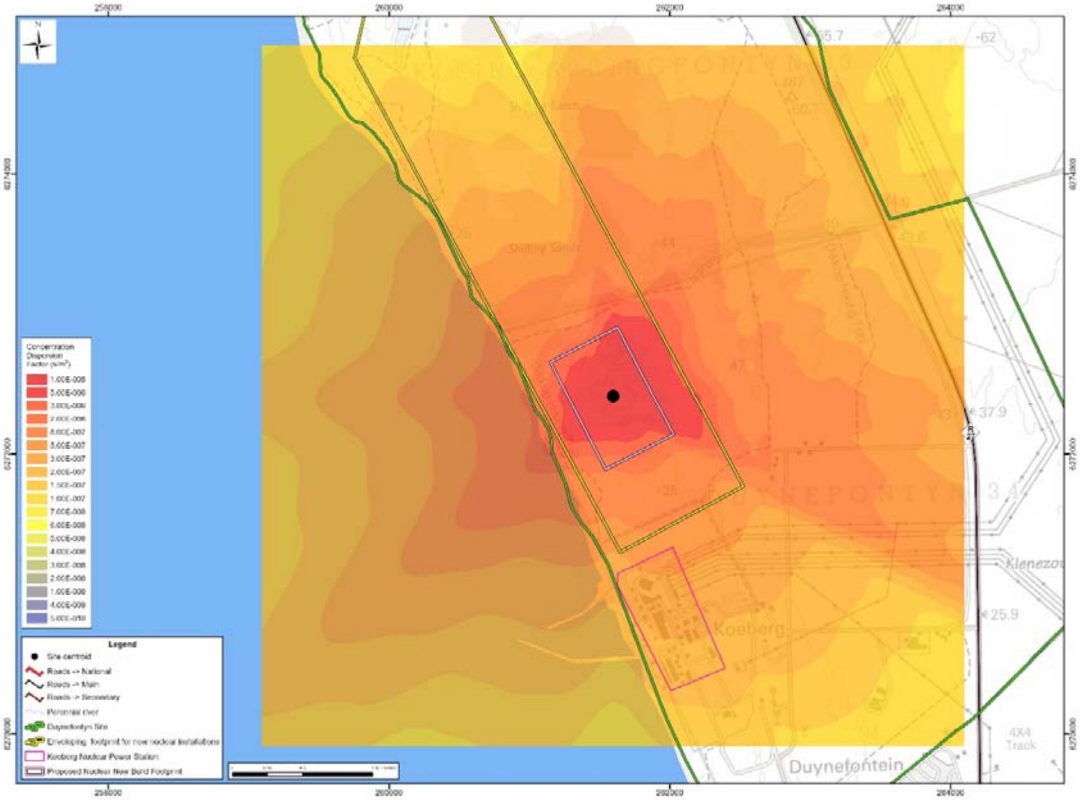

Figure 5.8.40
The Predicted Highest Annual Average Ground Level Concentration Dispersion Factor (א/Q) for a 5 km by 5 km area

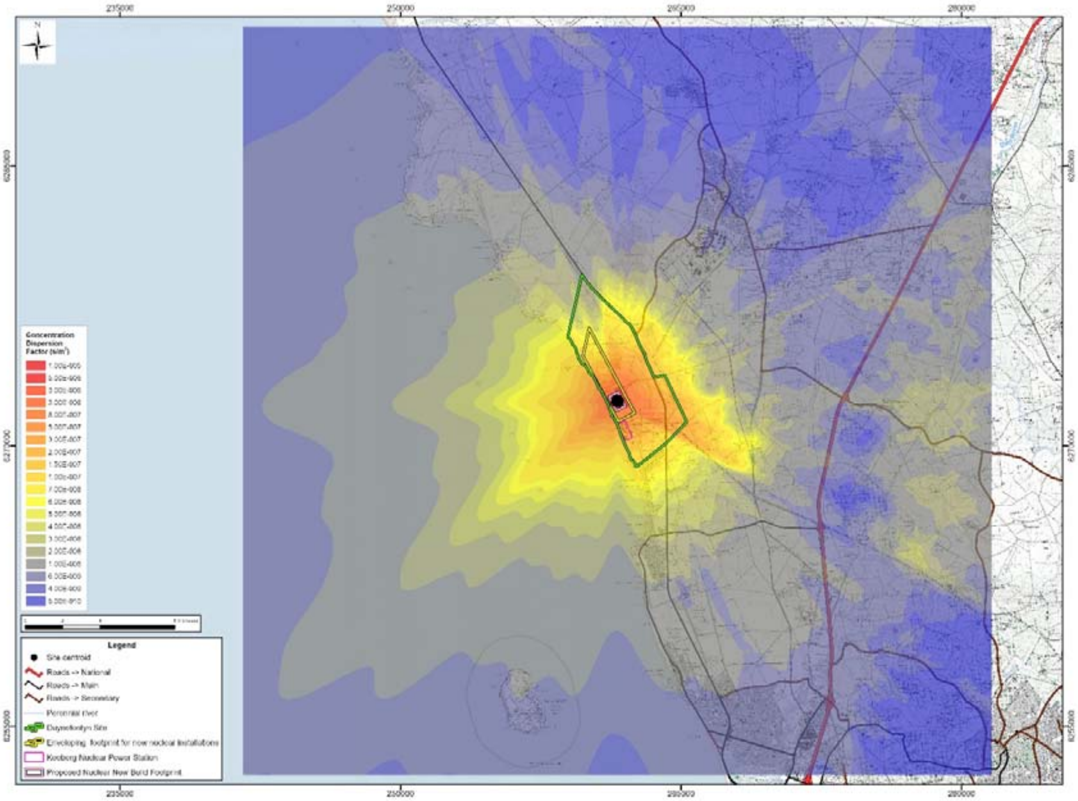

Figure 5.8.41
The Predicted Highest Annual Average Ground Level Concentration Dispersion Factor (א/Q) for a 40 km by 40 km area

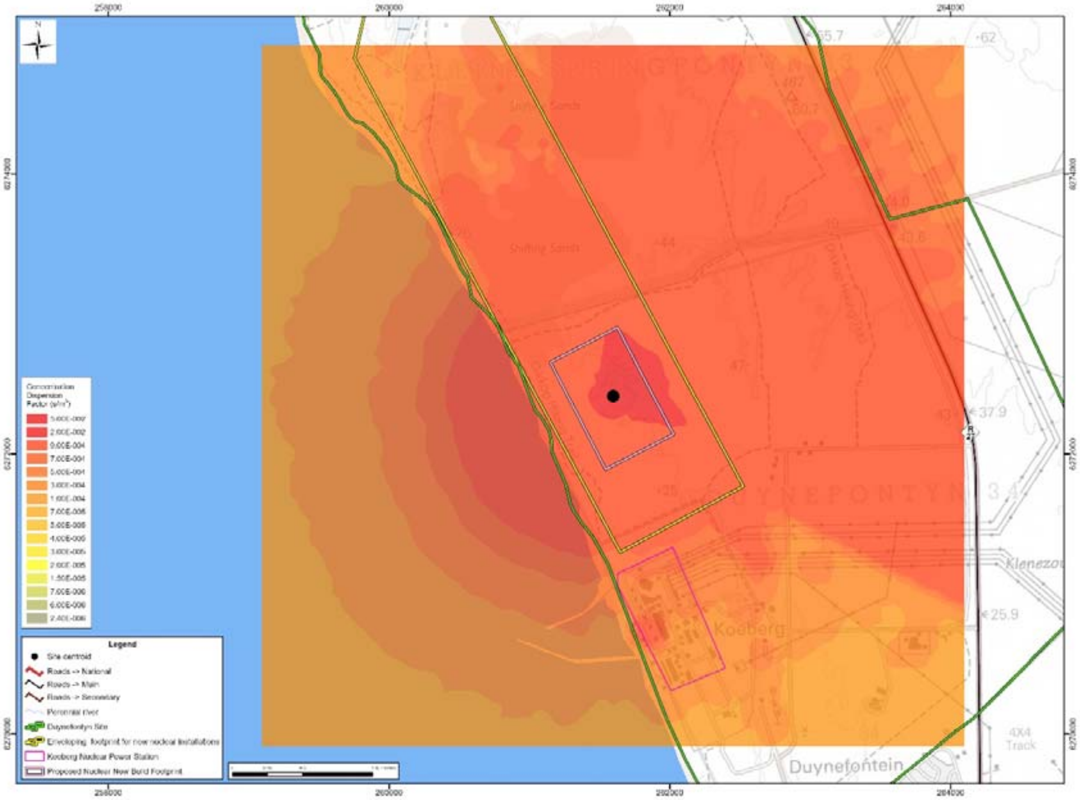

Figure 5.8.42
The Predicted 2nd Highest Hourly Total Deposition Dispersion Factor (*D/Q*) for a 5 km by 5 km area

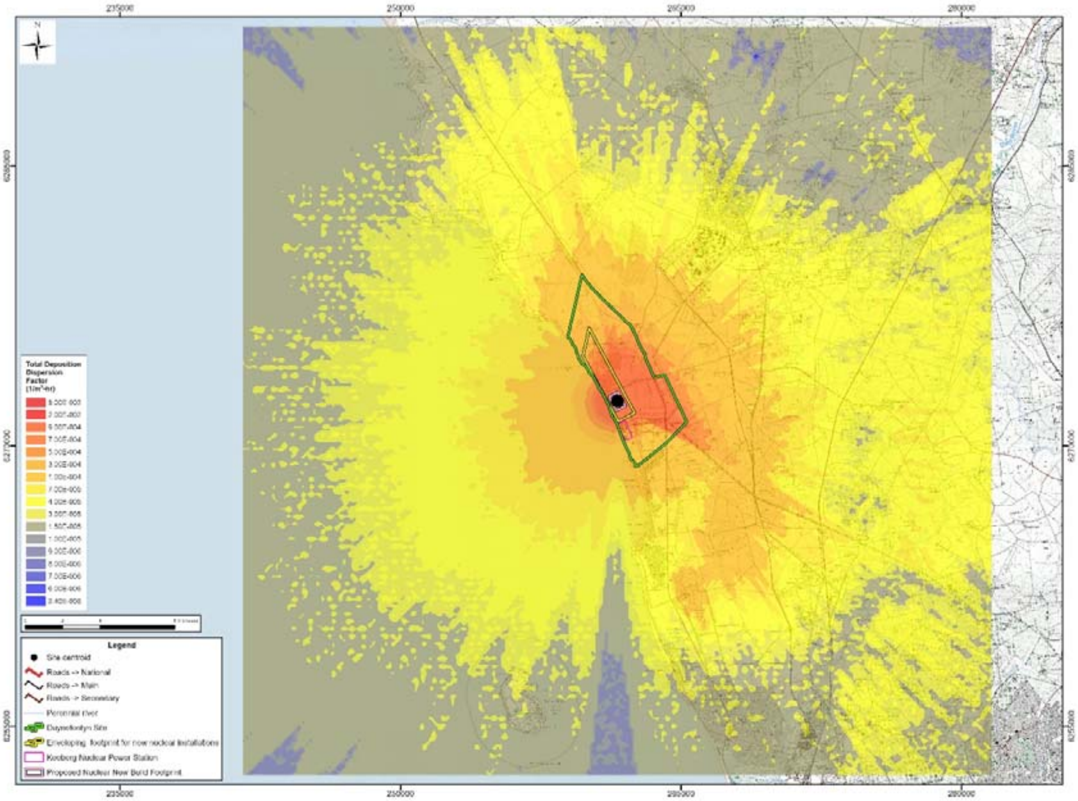

Figure 5.8.43
The Predicted 2nd Highest Hourly Total Deposition Dispersion Factor (*D/Q*) for a 40 km by 40 km area

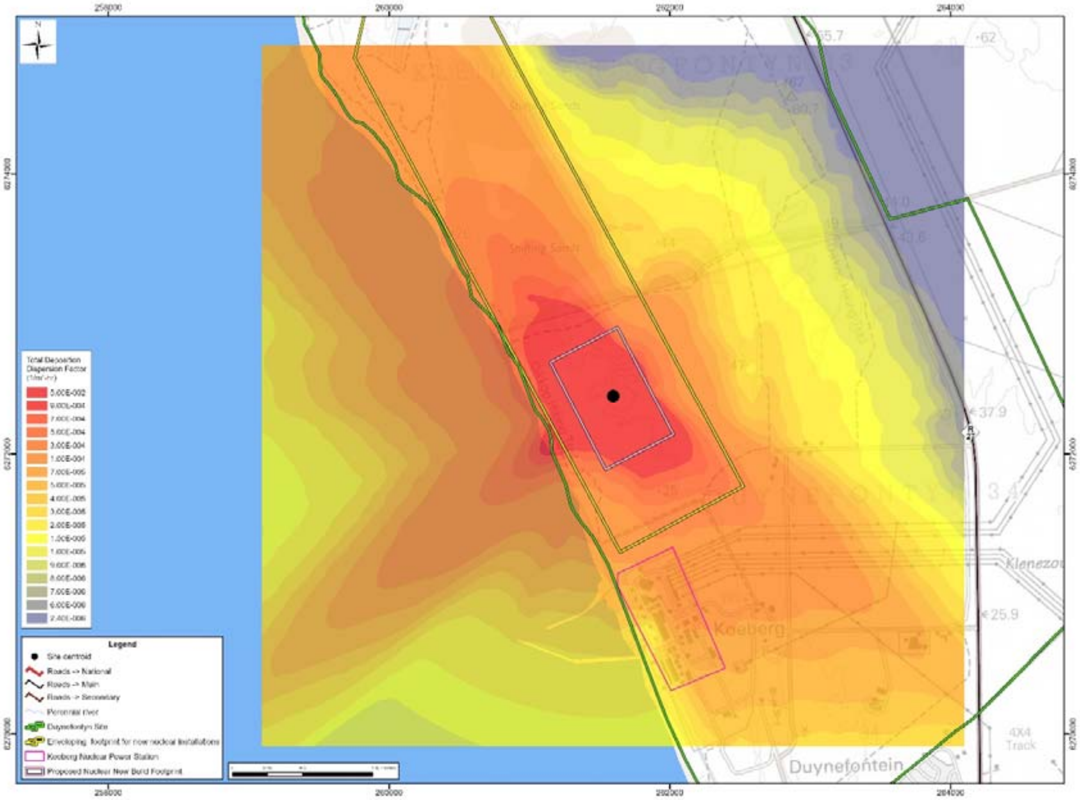

Figure 5.8.44
The Predicted 95th Percentile Hourly Total Deposition Factor (*D/Q*) for a 5 km by 5 km area

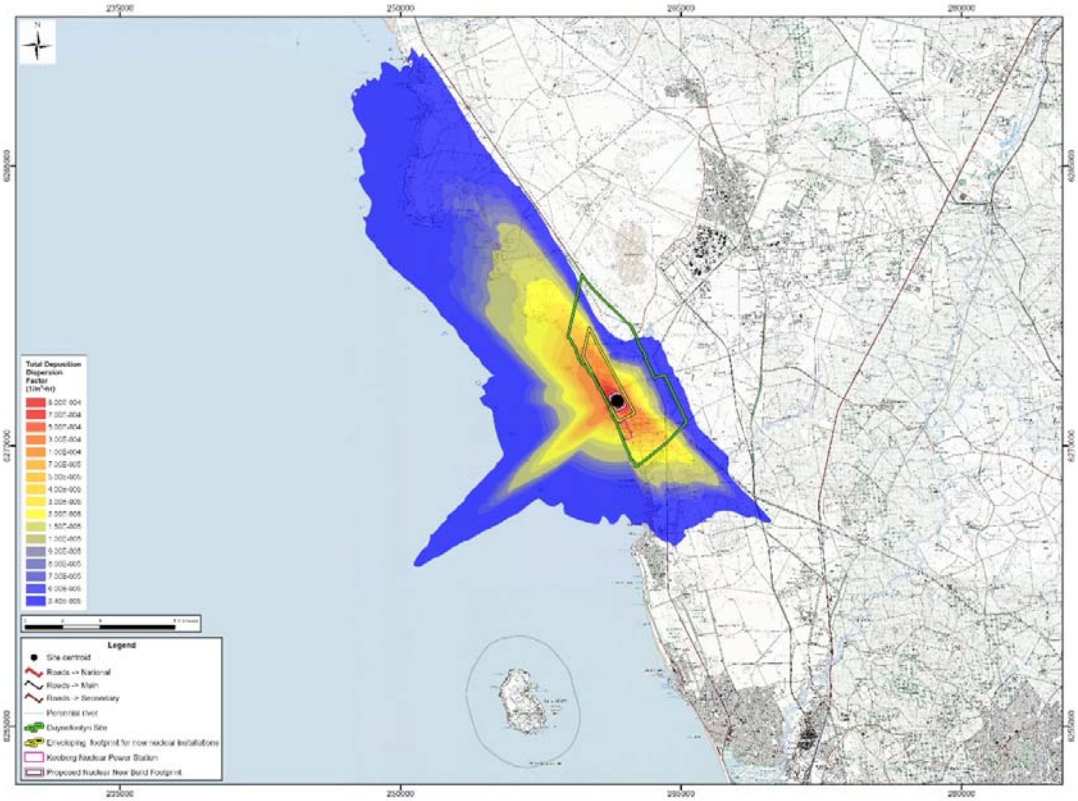

Figure 5.8.45
The Predicted 95th Percentile Hourly Total Deposition Factor (*D/Q*) for a 40 km by 40 km area

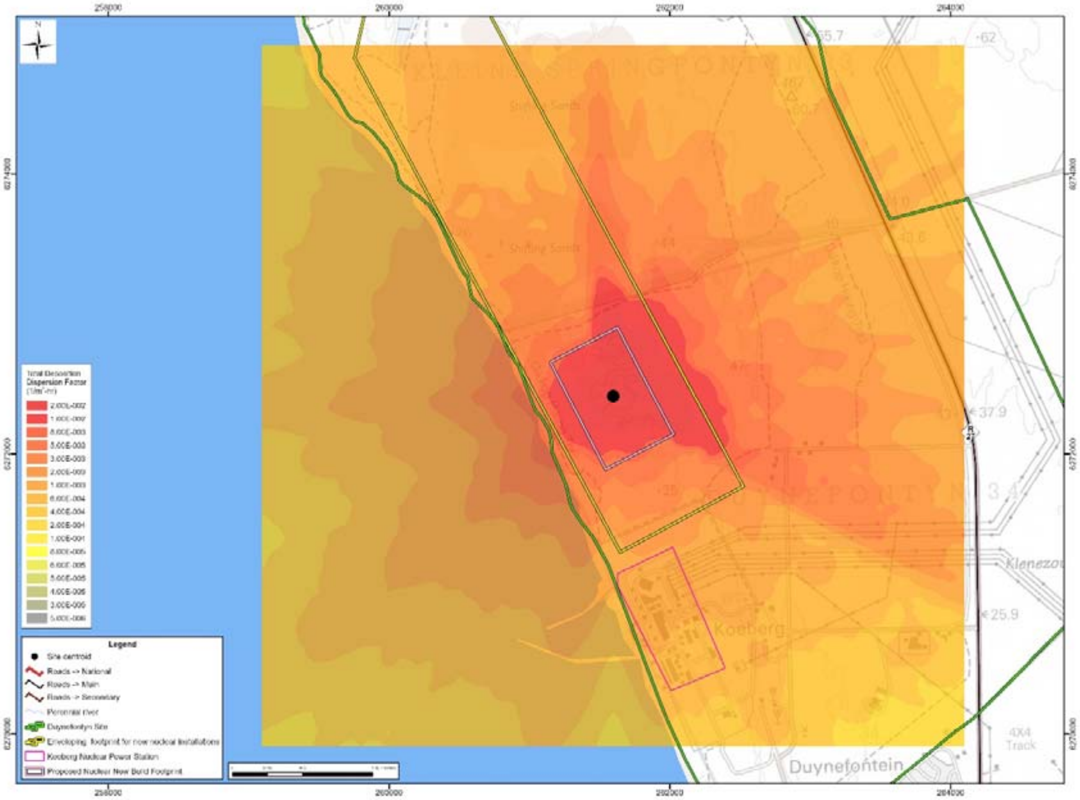

Figure 5.8.46
The Predicted 2nd Highest 3-Hour Total Deposition Factor (*D/Q*) for a 5 km by 5 km area

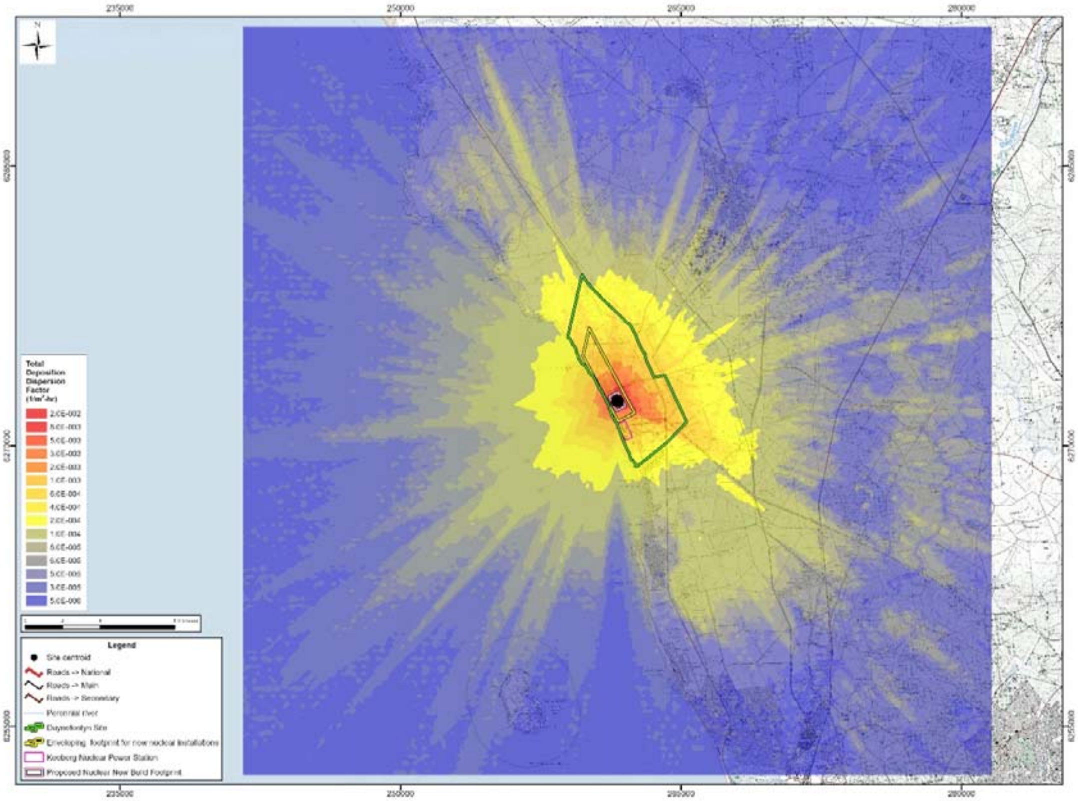

Figure 5.8.47
The Predicted 2nd Highest 3-Hour Total Deposition Factor (*D/Q*) for a 40 km by 40 km area

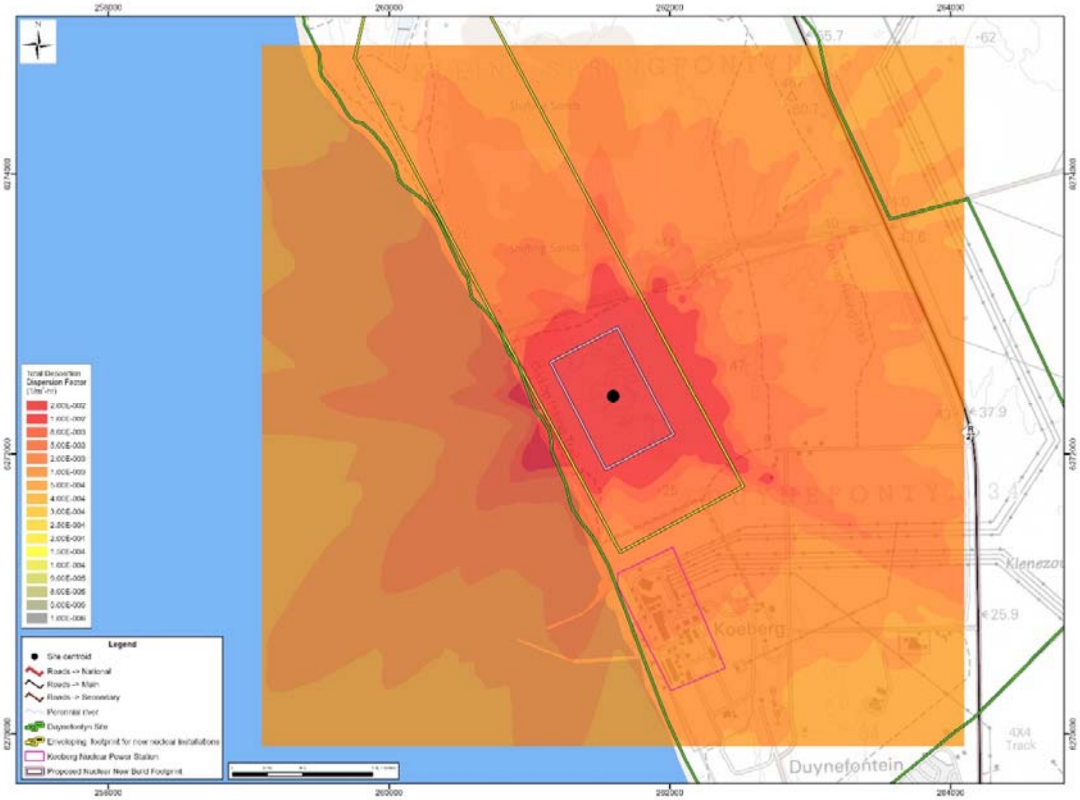

Figure 5.8.48
The Predicted 2nd Highest 8-Hour Total Deposition Factor (*D/Q*) for a 5 km by 5 km area

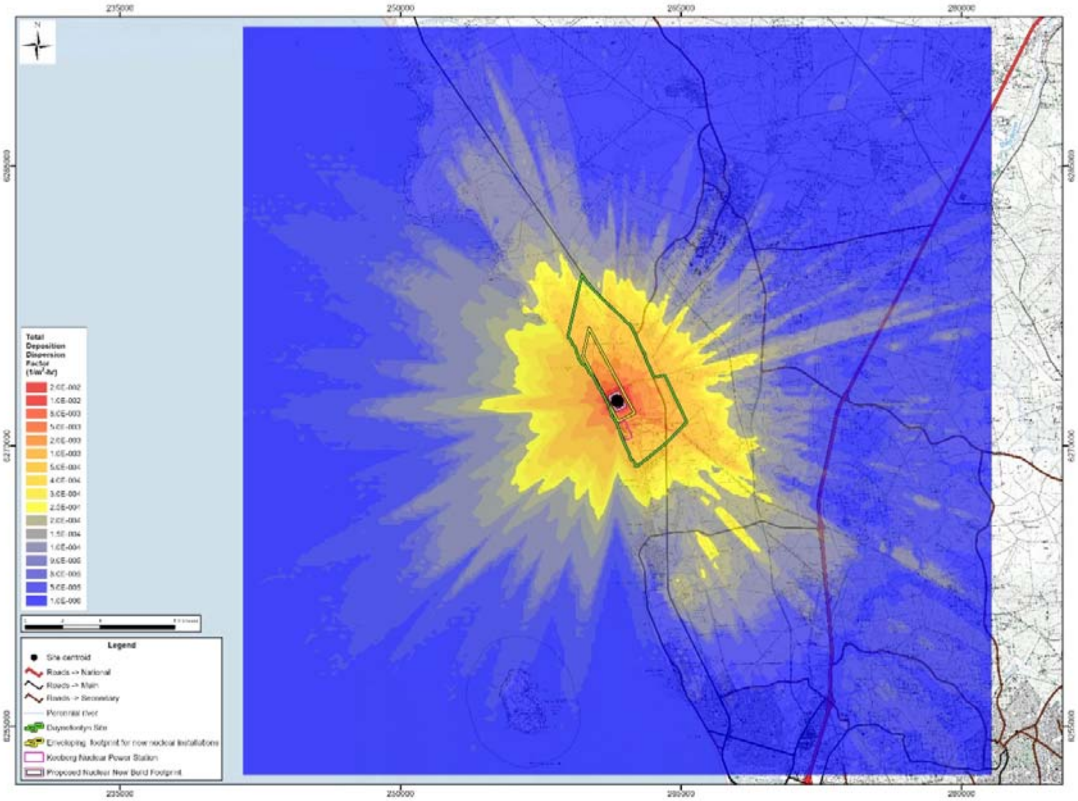

Figure 5.8.49
The Predicted 2nd Highest 8-Hour Total Deposition Factor (*D/Q*) for a 40 km by 40 km area

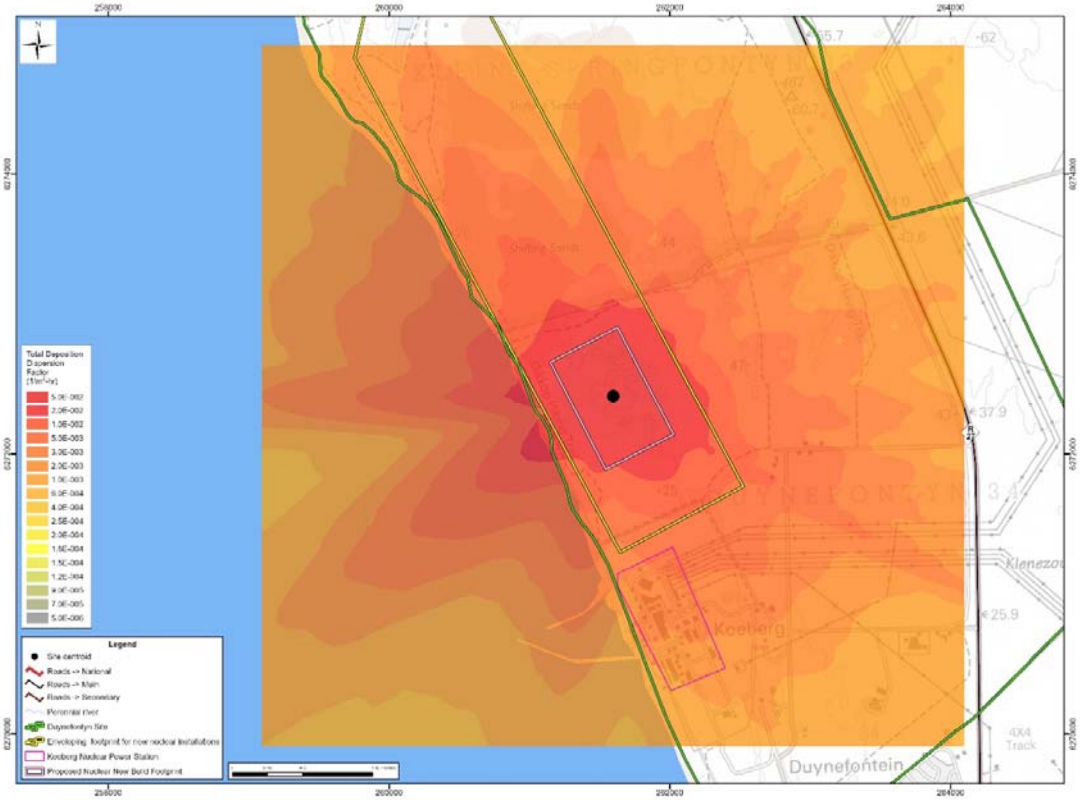

Figure 5.8.50
The Predicted 2nd Highest 24-Hour Total Deposition Factor (*D/Q*) for a 5 km by 5 km area

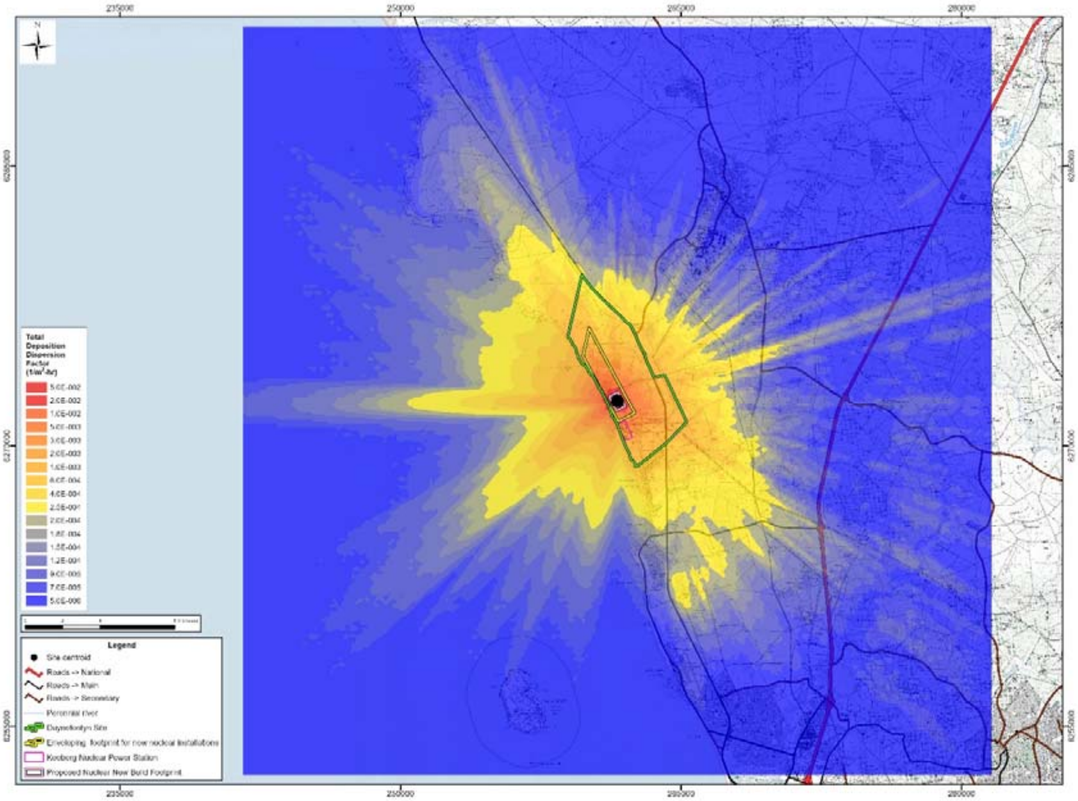

Figure 5.8.51
The Predicted 2nd Highest 24-Hour Total Deposition Factor (*D/Q*) for a 40 km by 40 km area

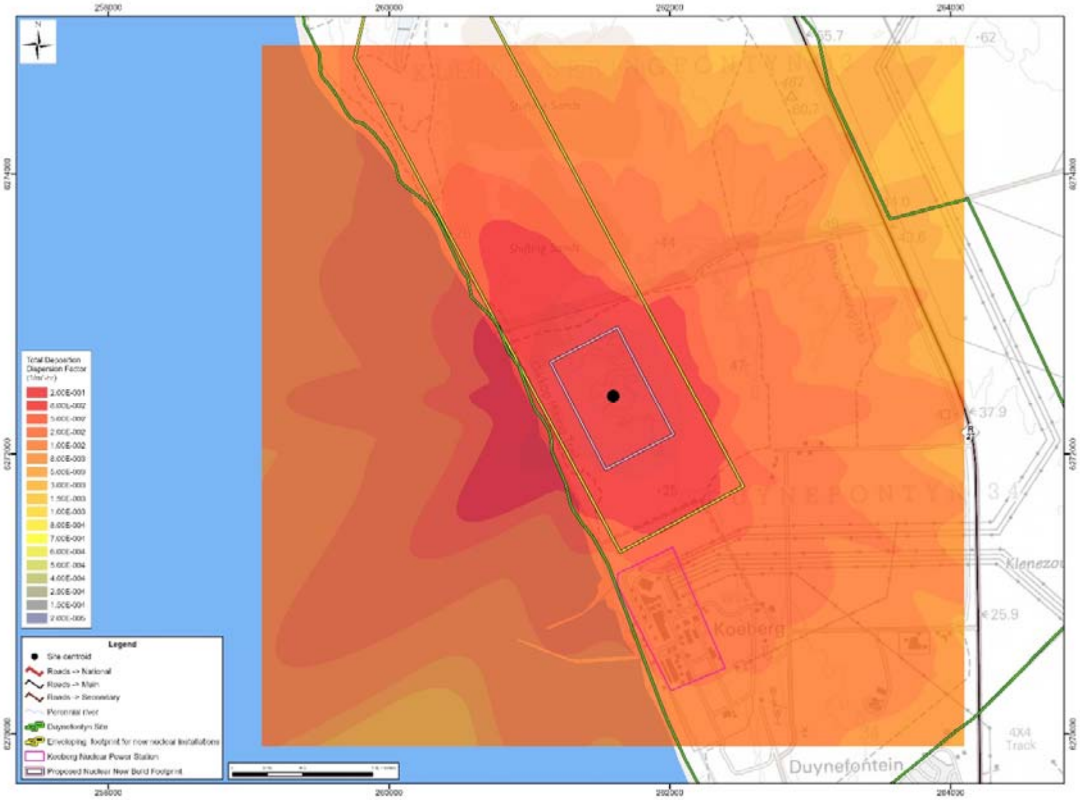

Figure 5.8.52
The Predicted Highest Monthly Total Deposition Factor (*D/Q*) for a 5 km by 5 km area

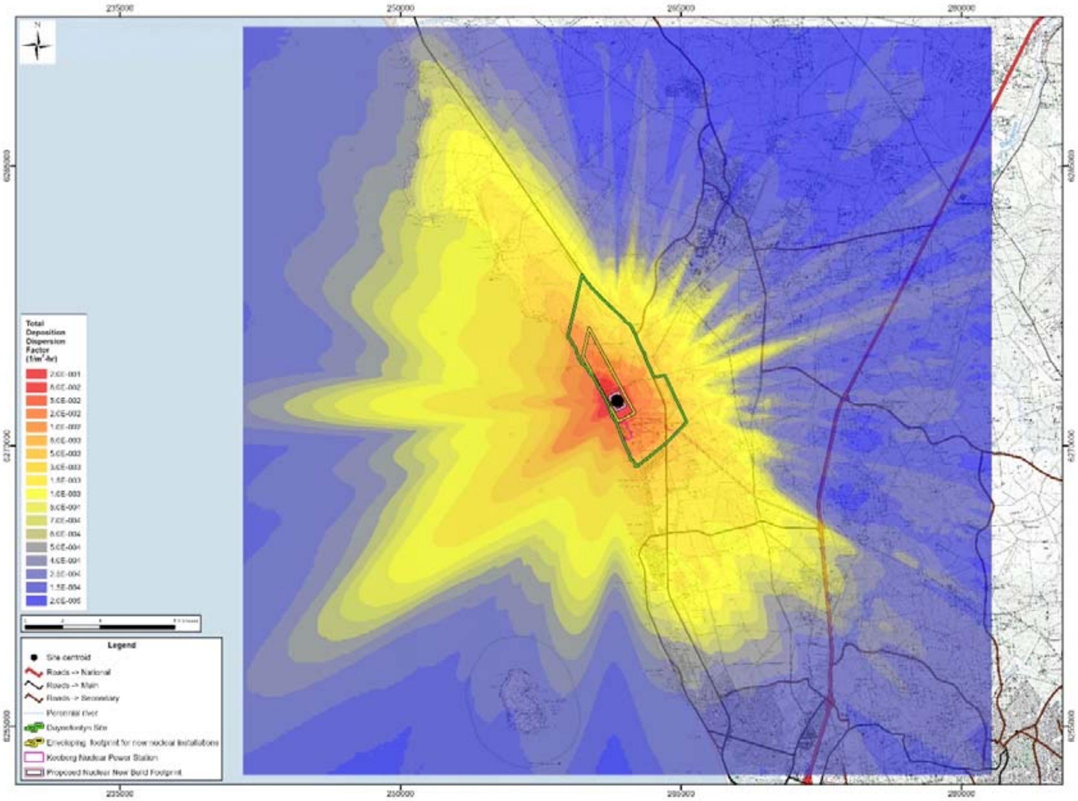

Figure 5.8.53
The Predicted Highest Monthly Total Deposition Factor (*D/Q*) for a 40 km by 40 km area

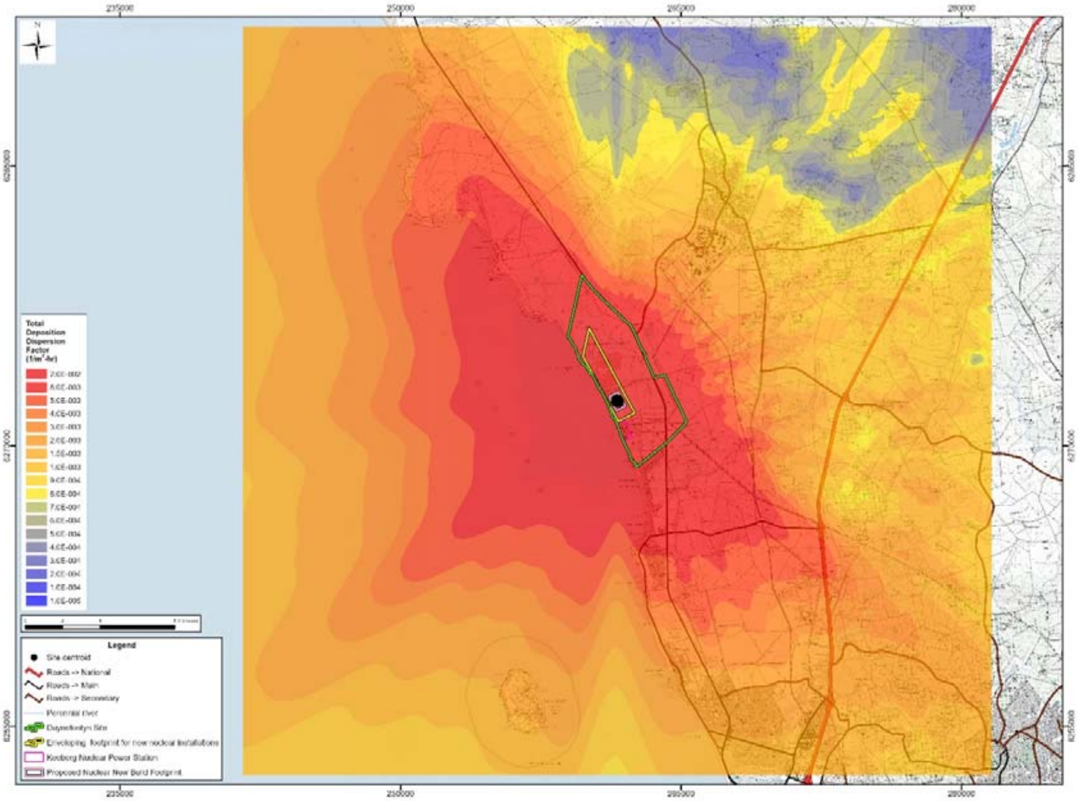

Figure 5.8.54
The Predicted Highest Annual Total Deposition Factor (*D/Q*) for a 5 km by 5 km area

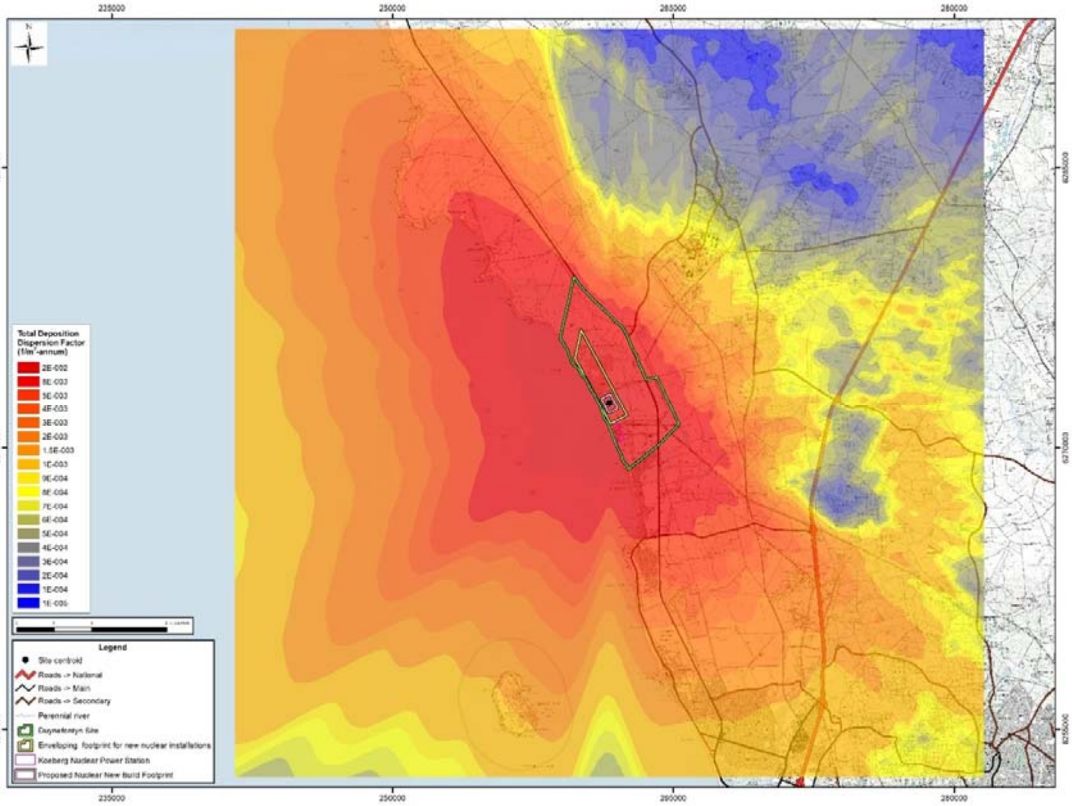

Figure 5.8.55
The Predicted Highest Annual Total Deposition Factor (*D/Q*) for a 40 km by 40 km area

Table 5.8.76

Dispersion Factors based on 2nd Highest Hourly, 3-Hourly, 8-Hourly and 24-hourly Average Predictions at 800 m, 3 km and 8 km Downwind of the Nuclear Installation(s) for Different Wind Directions

Distance (m)	Highest Hourly			Highest 3-Hourly			Highest 8-Hourly			Highest 24-Hourly		
	800	3000	8000	800	3000	8000	800	3000	8000	800	3000	8000
N	6.74E-04	6.67E-05	7.52E-06	2.52E-04	4.55E-05	2.90E-06	1.18E-04	1.80E-05	1.10E-06	3.97E-05	6.02E-06	3.69E-07
NNE	5.76E-04	4.85E-05	5.77E-06	1.92E-04	2.02E-05	3.08E-06	9.01E-05	7.60E-06	1.23E-06	3.27E-05	2.69E-06	4.22E-07
NE	5.28E-04	4.93E-05	7.18E-06	1.88E-04	2.44E-05	3.13E-06	7.45E-05	1.13E-05	1.53E-06	3.38E-05	3.78E-06	5.11E-07
ENE	4.34E-04	5.73E-05	9.17E-06	1.72E-04	2.63E-05	3.59E-06	8.49E-05	1.01E-05	1.44E-06	2.85E-05	3.37E-06	4.86E-07
E	6.16E-04	1.16E-04	1.42E-05	2.68E-04	3.98E-05	4.76E-06	1.12E-04	1.57E-05	2.27E-06	4.32E-05	6.53E-06	7.82E-07
ESE	7.49E-04	1.62E-04	1.52E-05	2.58E-04	5.72E-05	5.71E-06	1.31E-04	2.73E-05	2.31E-06	6.25E-05	1.39E-05	8.53E-07
SE	1.07E-04	2.15E-05	1.50E-05	4.10E-05	8.09E-06	5.00E-06	1.81E-05	3.21E-06	2.15E-06	8.09E-06	1.13E-06	6.54E-07
SSE	1.01E-04	1.45E-05	8.59E-06	3.67E-05	5.17E-06	2.89E-06	1.83E-05	2.38E-06	1.29E-06	7.67E-06	8.58E-07	4.55E-07
S	9.55E-05	1.45E-05	3.48E-06	3.53E-05	5.09E-06	1.26E-06	1.71E-05	2.38E-06	6.51E-07	7.20E-06	9.52E-07	2.38E-07
SSW	1.02E-04	1.53E-05	3.52E-06	4.73E-05	5.43E-06	1.28E-06	2.39E-05	2.69E-06	9.01E-07	1.30E-05	1.16E-06	3.33E-07
SW	9.85E-05	1.51E-05	6.19E-06	6.09E-05	9.62E-06	2.63E-06	3.54E-05	5.17E-06	1.18E-06	1.43E-05	1.84E-06	4.09E-07
WSW	1.07E-04	1.53E-05	3.42E-06	5.59E-05	7.02E-06	1.43E-06	3.01E-05	3.05E-06	6.56E-07	1.19E-05	1.12E-06	2.47E-07
W	9.45E-05	1.49E-05	3.53E-06	6.20E-05	9.20E-06	2.17E-06	3.95E-05	5.15E-06	1.19E-06	1.97E-05	2.54E-06	5.21E-07
WNW	1.14E-04	1.38E-05	3.51E-06	4.34E-05	5.09E-06	1.24E-06	1.96E-05	2.31E-06	5.91E-07	7.03E-06	8.02E-07	1.98E-07
NW	6.69E-05	4.44E-05	7.70E-06	2.66E-05	1.49E-05	2.65E-06	1.38E-05	6.44E-06	1.07E-06	5.57E-06	2.16E-06	3.59E-07
NNW	2.77E-04	4.43E-05	1.53E-05	1.01E-04	1.74E-05	5.75E-06	3.81E-05	8.32E-06	2.93E-06	1.31E-05	2.79E-06	8.75E-07

Table 5.8.77

Dispersion Factors based on Highest Averages of 3-Daily, Monthly, Annual and 95th Percentile Predictions at 800 m, 3 km and 8 km Downwind of the Nuclear Installation(s) for Different Wind Directions

Distance (m)	**Highest 3-Daily**			**Highest Monthly**			**Highest Annual**			**95th Percentile**		
	800	**3000**	**8000**	**800**	**3000**	**8000**	**800**	**3000**	**8000**	**800**	**3000**	**8000**
N	3.30E-05	5.00E-06	3.06E-07	4.16E-06	4.76E-07	5.46E-08	2.67E-06	2.21E-07	1.80E-08	3.24E-06	1.60E-07	2.29E-08
NNE	2.72E-05	2.23E-06	3.50E-07	6.54E-06	3.68E-07	4.70E-08	3.28E-06	1.76E-07	1.67E-08	6.19E-06	2.26E-07	1.97E-08
NE	2.80E-05	3.14E-06	4.24E-07	4.01E-06	4.08E-07	5.57E-08	2.48E-06	1.69E-07	1.60E-08	4.83E-06	2.11E-07	2.15E-08
ENE	2.37E-05	2.80E-06	4.03E-07	3.77E-06	3.61E-07	5.27E-08	2.12E-06	1.62E-07	1.88E-08	3.48E-06	1.91E-07	2.78E-08
E	3.58E-05	5.42E-06	6.49E-07	5.64E-06	8.87E-07	8.87E-08	2.62E-06	3.19E-07	3.49E-08	3.62E-06	2.10E-07	3.86E-08
ESE	5.19E-05	1.16E-05	7.08E-07	5.54E-06	1.26E-06	1.33E-07	3.79E-06	5.19E-07	5.41E-08	7.00E-06	5.44E-07	4.50E-08
SE	6.72E-06	9.42E-07	5.43E-07	1.67E-06	2.18E-07	6.87E-08	1.30E-06	1.37E-07	3.18E-08	4.91E-06	6.09E-07	9.59E-08
SSE	6.37E-06	7.12E-07	3.78E-07	2.14E-06	2.35E-07	5.16E-08	1.47E-06	1.40E-07	3.07E-08	5.70E-06	6.17E-07	1.22E-07
S	5.98E-06	7.90E-07	1.97E-07	1.53E-06	1.73E-07	3.84E-08	1.01E-06	1.14E-07	2.78E-08	3.90E-06	3.94E-07	9.70E-08
SSW	1.08E-05	9.67E-07	2.76E-07	2.81E-06	2.11E-07	4.87E-08	1.61E-06	1.40E-07	3.07E-08	6.06E-06	5.01E-07	1.31E-07
SW	1.19E-05	1.53E-06	3.39E-07	4.42E-06	5.45E-07	1.13E-07	2.13E-06	2.54E-07	5.50E-08	1.04E-05	1.18E-06	2.31E-07
WSW	9.90E-06	9.26E-07	2.05E-07	4.86E-06	3.74E-07	8.89E-08	2.11E-06	1.92E-07	4.17E-08	1.18E-05	9.85E-07	2.15E-07
W	1.63E-05	2.11E-06	4.32E-07	4.62E-06	6.06E-07	1.25E-07	1.43E-06	1.73E-07	3.73E-08	5.83E-06	6.25E-07	1.40E-07
WNW	5.84E-06	6.66E-07	1.64E-07	2.21E-06	1.98E-07	4.55E-08	1.54E-06	1.37E-07	3.00E-08	6.01E-06	5.87E-07	1.41E-07
NW	4.62E-06	1.79E-06	2.98E-07	1.56E-06	2.57E-07	5.29E-08	1.33E-06	1.35E-07	2.92E-08	5.05E-06	6.42E-07	1.41E-07
NNW	1.09E-05	2.31E-06	7.27E-07	2.06E-06	2.82E-07	6.51E-08	1.42E-06	1.28E-07	2.79E-08	5.33E-06	4.39E-07	1.06E-07

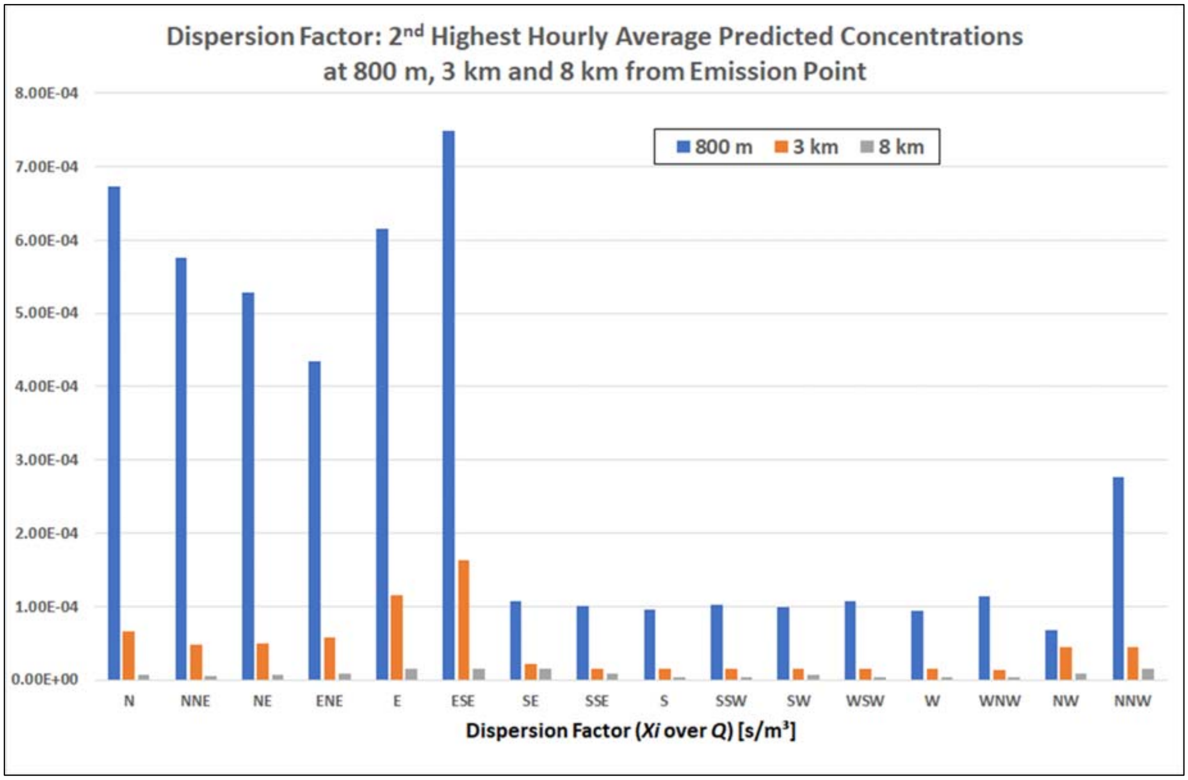

Figure 5.8.56
Dispersion Factors (א/Q) based on the 2nd Highest Hourly Average Predictions at 800 m, 3 km and 8 km Downwind of the Nuclear Installation(s) for Different Wind Directions

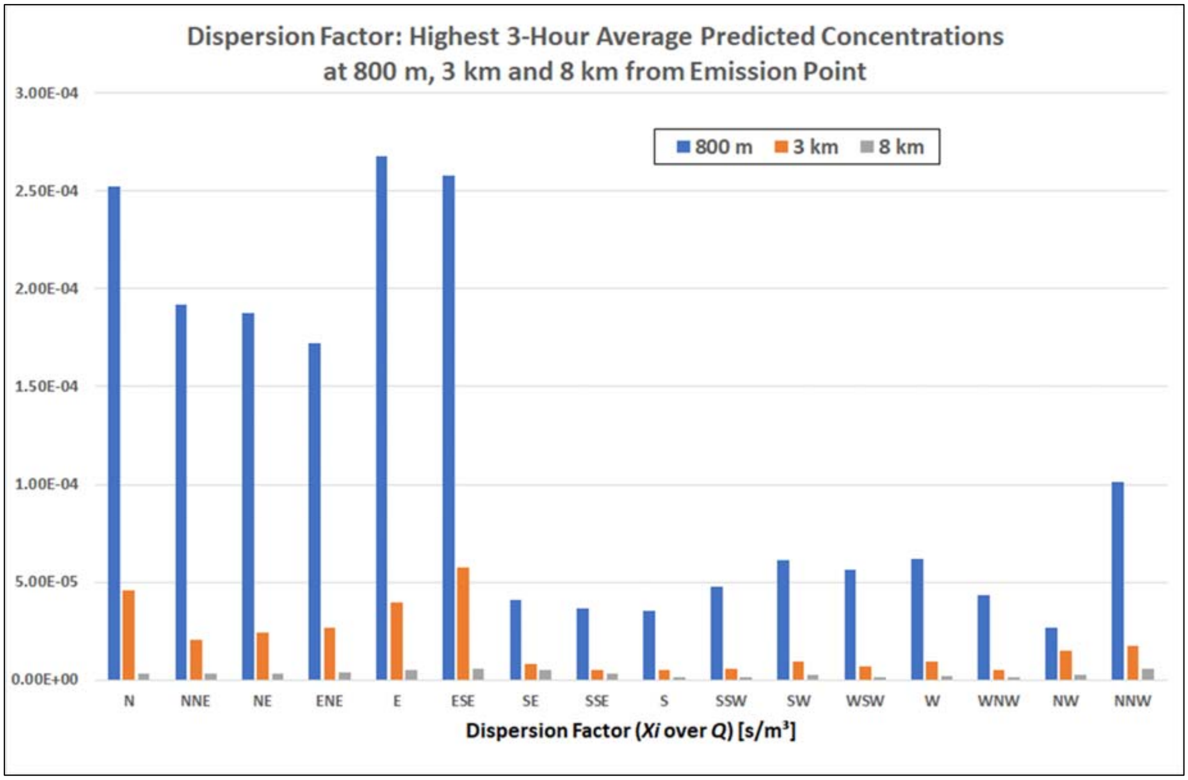

Figure 5.8.57
Dispersion Factors (ϰ/Q) based on the Highest 3-Hourly Average Predictions at 800 m, 3 km and 8 km Downwind of the Nuclear Installation(s) for Different Wind Directions

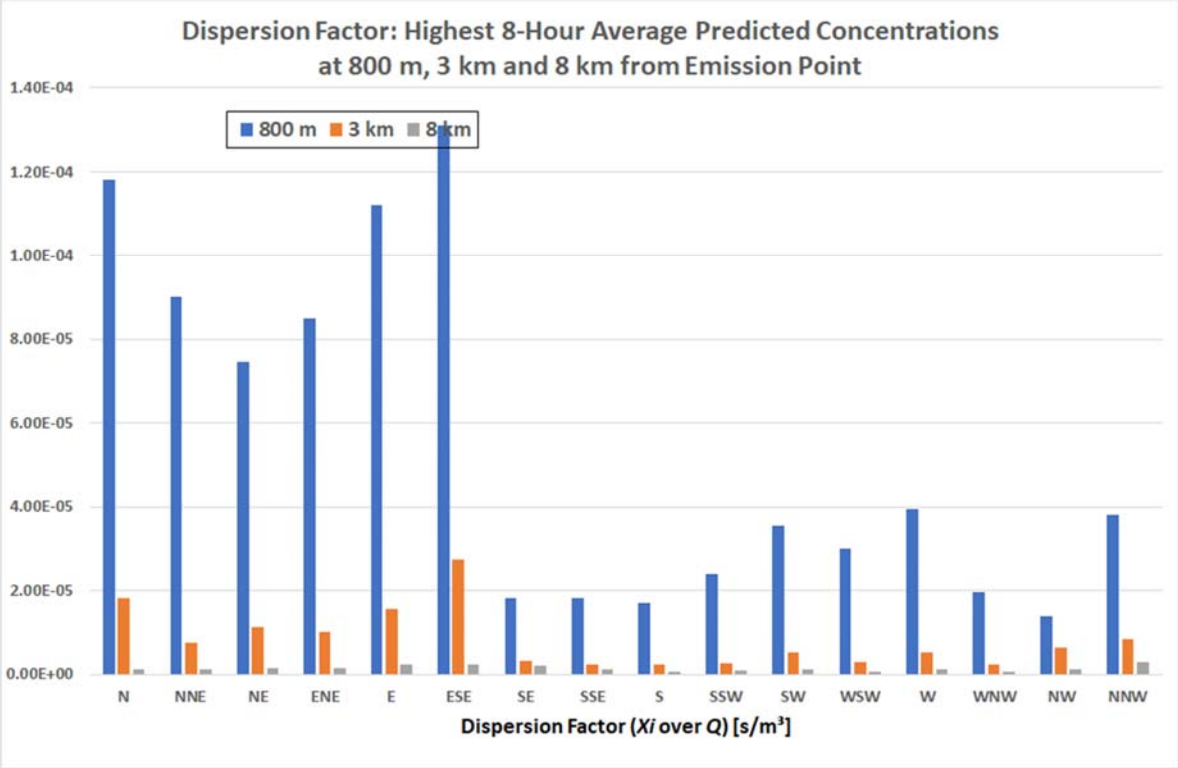

Figure 5.8.58
Dispersion Factors (א/Q) based on the Highest 8-Hourly Average Predictions at 800 m, 3 km and 8 km Downwind of the Nuclear Installation(s) for Different Wind Directions

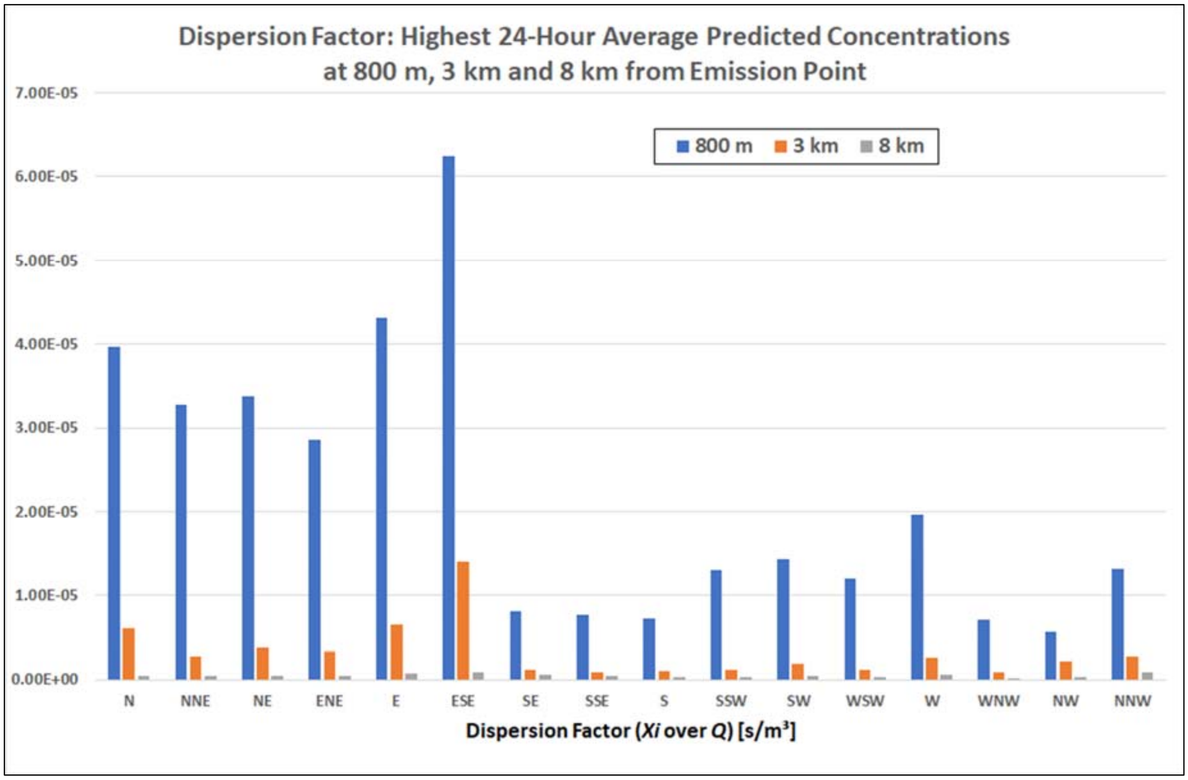

Figure 5.8.59
Dispersion Factors (ϰ/Q) based on the Highest 24-Hourly Average Predictions at 800 m, 3 km and 8 km Downwind of the Nuclear Installation(s) for Different Wind Directions

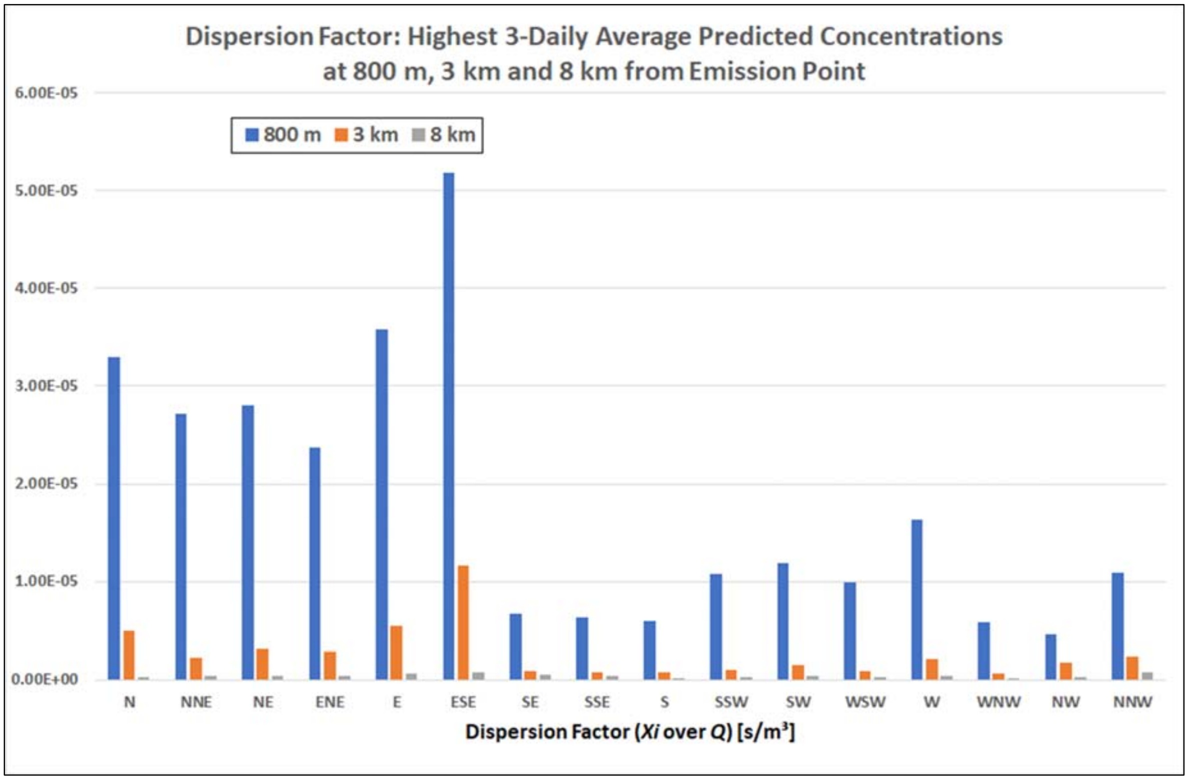

Figure 5.8.60
Dispersion Factors (ϰ/Q) based on the Highest 3-Daily Average Predictions at 800 m, 3 km and 8 km Downwind of the Nuclear Installation(s) for Different Wind Directions

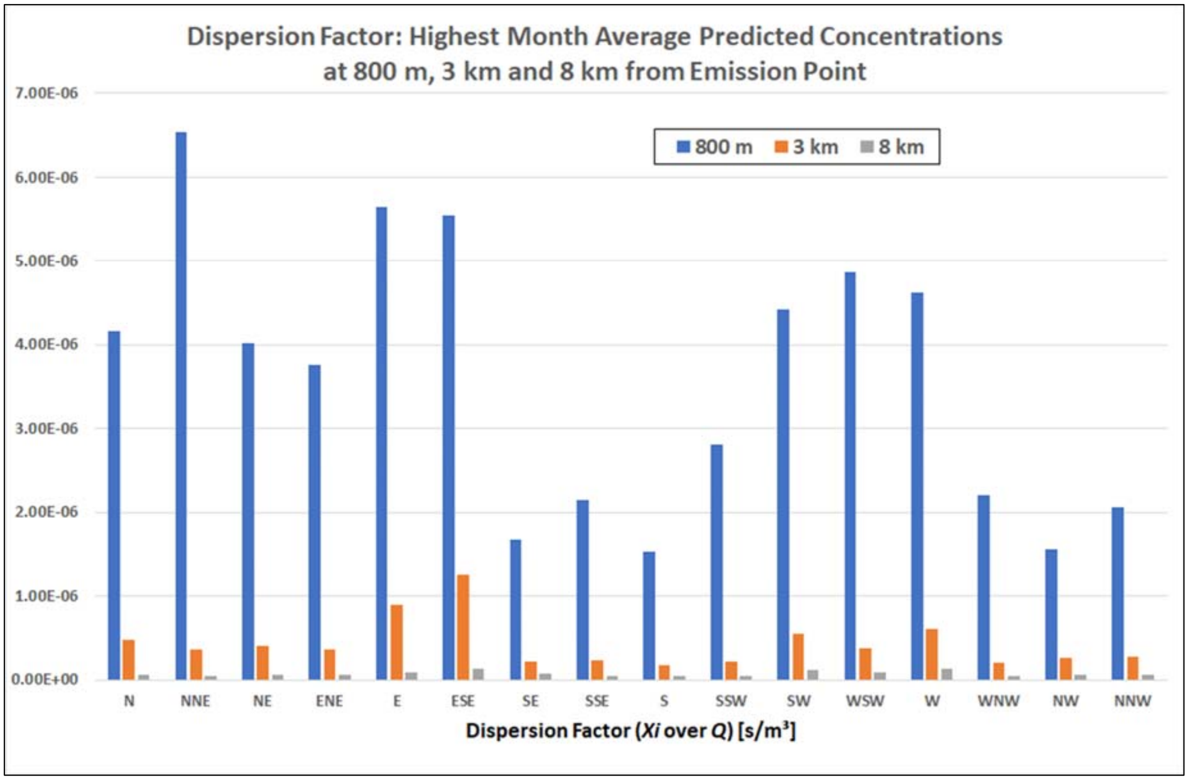

Figure 5.8.61
Dispersion Factors (ϰ/Q) based on the Highest Monthly Average Predictions at 800 m, 3 km and 8 km Downwind of the Nuclear Installation(s) for Different Wind Directions

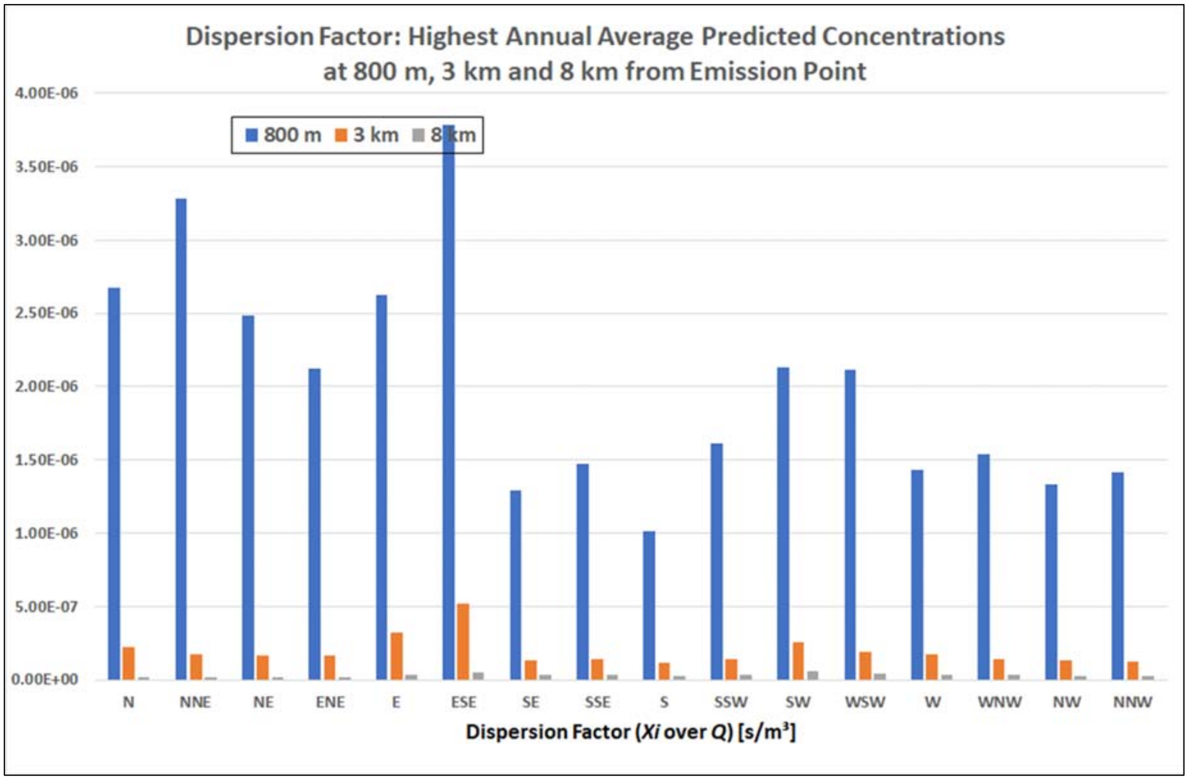

Figure 5.8.62
Dispersion Factors (ϰ/Q) based on the Highest Monthly Average Predictions at 800 m, 3 km and 8 km Downwind of the Nuclear Installation(s) for Different Wind Directions

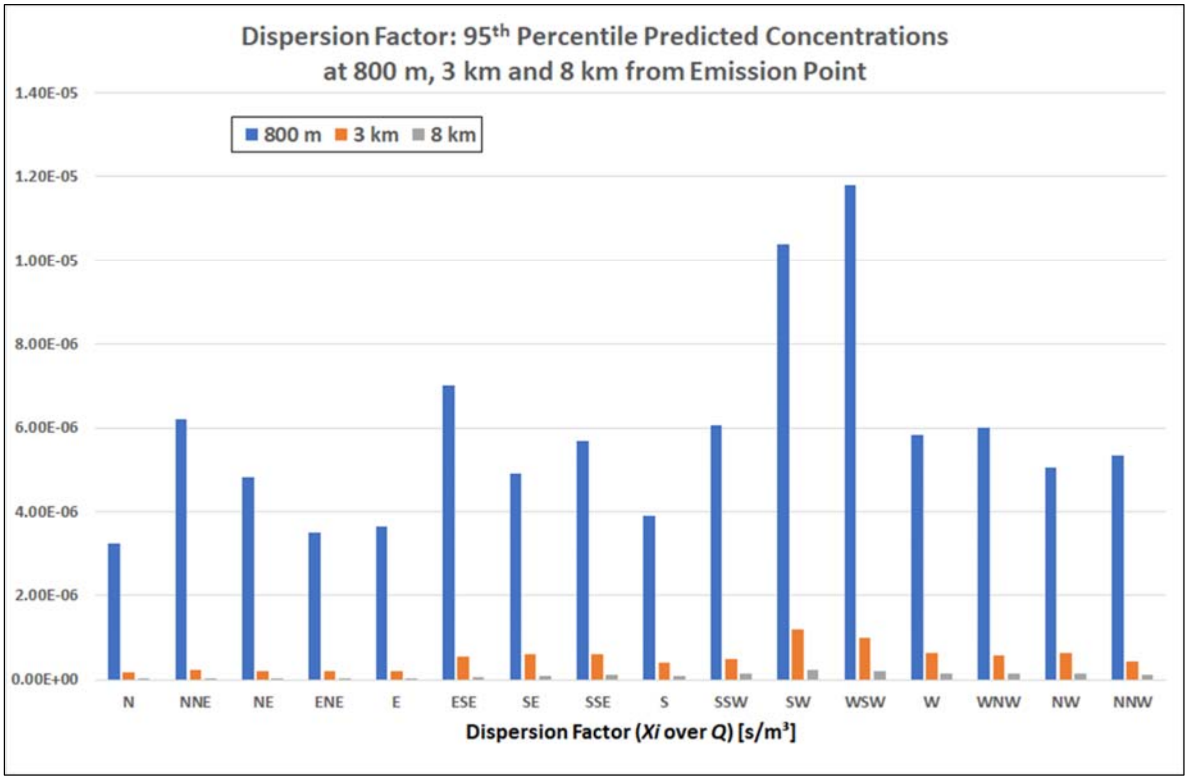

Figure 5.8.63
Dispersion Factors (ϰ/Q) Based on the 95th Percentile of the Hourly Average Predictions at 800 m, 3 km and 8 km Downwind of the Nuclear Installation(s) for Different Wind Directions

Figure 5.8.64 is a summary of the ϰ/Q values of 2nd highest hourly averages for different downwind distances and averaging periods.

Figure 5.8.65 to ***Figure 5.8.72*** summarise the D/Q values given as the total deposition over the period of interest (i.e. 3-hour, 8-hour, 1-day, 3-days, month, year and 95th percentile) for different downwind distances and averaging periods.

Figure 5.8.73 is a summary of the D/Q values given as the total deposition over the period of interest (i.e. 1-hour, 1-day, month, year) for different downwind distances and averaging periods.

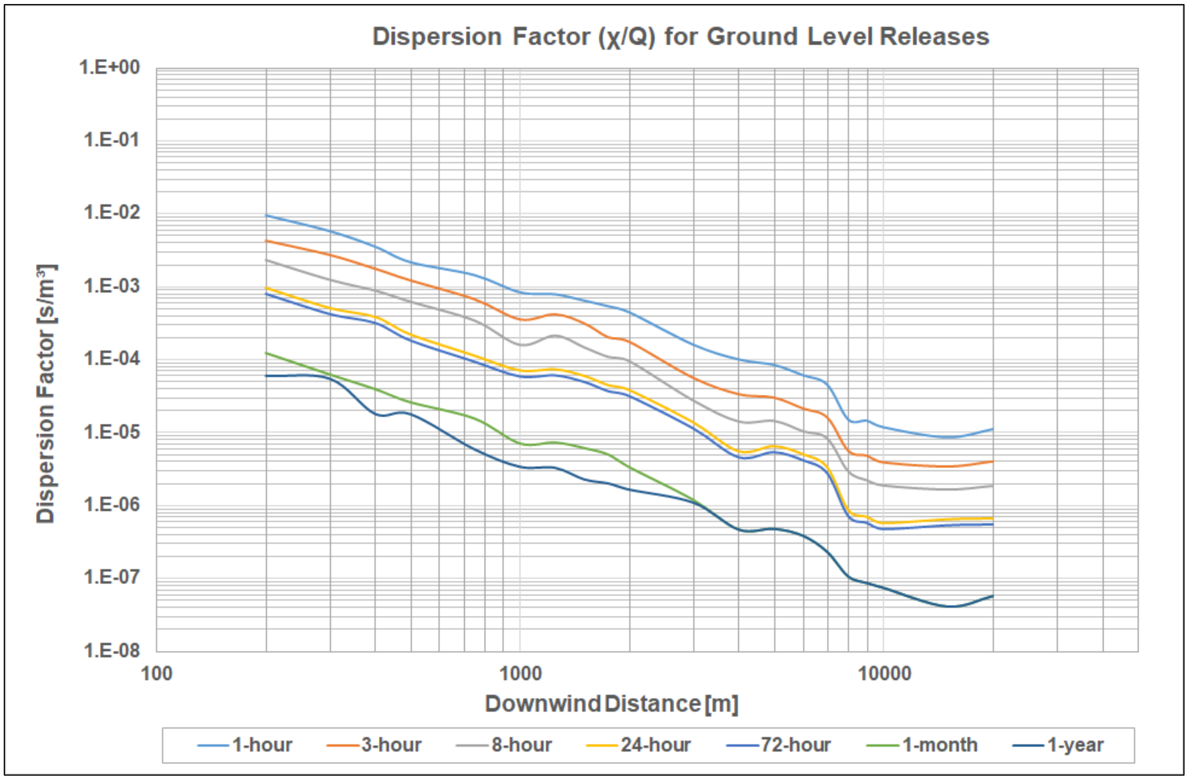

Figure 5.8.64
Dispersion Factors (ϰ/Q) Based on Concentration Predictions at Various Downwind Distances and Averaging Periods

Table 5.8.78

Fallout Factors based on 2nd Highest Hour, 3-Hour, 8-Hour and 24-hour Total Deposition Predictions at 800 m, 3 km and 8 km Downwind of the Nuclear Installation(s) for Different Wind Directions

Distance (m)	Highest Hourly			Highest 3-Hourly			Highest 8-Hourly			Highest 24-Hourly		
	800	3000	8000	800	3000	8000	800	3000	8000	800	3000	8000
N	8.36E-03	9.40E-04	1.30E-04	1.13E-02	1.72E-03	1.30E-04	1.50E-02	2.19E-03	1.50E-04	1.52E-02	2.25E-03	1.60E-04
NNE	8.01E-03	7.70E-04	1.00E-04	9.38E-03	1.03E-03	1.70E-04	1.18E-02	1.03E-03	1.70E-04	1.45E-02	1.14E-03	1.80E-04
NE	8.31E-03	7.20E-04	1.50E-04	9.06E-03	1.28E-03	1.70E-04	1.05E-02	1.63E-03	2.30E-04	1.32E-02	1.64E-03	2.70E-04
ENE	6.92E-03	8.10E-04	1.30E-04	9.43E-03	1.19E-03	1.70E-04	9.90E-03	1.55E-03	2.50E-04	1.05E-02	1.72E-03	3.30E-04
E	7.96E-03	1.11E-03	1.60E-04	1.03E-02	1.17E-03	1.90E-04	1.19E-02	1.23E-03	1.90E-04	1.65E-02	1.55E-03	2.00E-04
ESE	1.00E-02	1.41E-03	2.00E-04	1.23E-02	1.92E-03	2.30E-04	2.11E-02	2.95E-03	3.50E-04	2.16E-02	2.99E-03	3.60E-04
SE	1.83E-03	2.70E-04	1.50E-04	4.14E-03	4.90E-04	2.30E-04	7.92E-03	8.30E-04	2.70E-04	1.68E-02	1.46E-03	3.60E-04
SSE	1.83E-03	2.10E-04	1.10E-04	4.12E-03	4.30E-04	1.40E-04	8.54E-03	8.70E-04	2.10E-04	1.96E-02	1.33E-03	2.90E-04
S	1.55E-03	2.10E-04	7.00E-05	3.74E-03	4.20E-04	9.00E-05	8.08E-03	8.90E-04	1.70E-04	1.03E-02	1.05E-03	1.90E-04
SSW	1.92E-03	2.10E-04	8.00E-05	4.15E-03	4.40E-04	1.10E-04	7.61E-03	8.50E-04	1.60E-04	1.10E-02	1.07E-03	1.90E-04
SW	1.73E-03	2.20E-04	8.00E-05	4.76E-03	5.60E-04	1.30E-04	1.11E-02	1.14E-03	2.20E-04	1.74E-02	1.83E-03	3.40E-04
WSW	1.94E-03	2.20E-04	8.00E-05	4.78E-03	4.50E-04	1.00E-04	1.14E-02	8.50E-04	1.80E-04	2.34E-02	1.86E-03	2.90E-04
W	1.65E-03	2.20E-04	8.00E-05	4.39E-03	5.00E-04	1.10E-04	9.29E-03	1.10E-03	2.30E-04	1.96E-02	2.22E-03	4.30E-04
WNW	1.85E-03	2.20E-04	8.00E-05	4.78E-03	4.70E-04	1.10E-04	1.04E-02	1.00E-03	2.10E-04	1.86E-02	1.55E-03	2.90E-04
NW	1.64E-03	5.00E-04	9.00E-05	4.06E-03	9.70E-04	1.70E-04	8.42E-03	1.44E-03	2.50E-04	1.83E-02	2.66E-03	4.10E-04
NNW	3.49E-03	6.10E-04	1.60E-04	4.54E-03	1.00E-03	2.70E-04	9.75E-03	1.60E-03	2.90E-04	2.22E-02	2.70E-03	4.50E-04

Table 5.8.79

Fallout Factors based on Hourly, 3-Day, Month, Annual and 95th Percentile Total Deposition Predictions at 800 m, 3 km and 8 km Downwind of the Nuclear Installation(s) for Different Wind Directions

Distance (m)	**Highest 3-Daily**			**Highest Monthly**			**Highest Annual**			**95th Percentile**		
	800	**3000**	**8000**	**800**	**3000**	**8000**	**800**	**3000**	**8000**	**800**	**3000**	**8000**
N	3.79E-02	5.60E-03	3.98E-04	8.74E-02	5.34E-03	7.10E-04	6.96E-01	3.96E-02	5.13E-03	2.40E-04	4.30E-06	5.28E-07
NNE	3.61E-02	2.84E-03	4.48E-04	8.37E-02	4.26E-03	5.40E-04	6.47E-01	3.16E-02	3.34E-03	1.32E-04	4.39E-06	5.97E-07
NE	3.29E-02	4.08E-03	6.72E-04	6.40E-02	4.48E-03	5.40E-04	4.95E-01	3.01E-02	3.21E-03	1.02E-04	4.22E-06	5.99E-07
ENE	2.61E-02	4.28E-03	8.22E-04	5.66E-02	4.48E-03	6.60E-04	4.39E-01	2.88E-02	3.56E-03	8.78E-05	3.77E-06	5.49E-07
E	4.10E-02	3.86E-03	4.98E-04	5.37E-02	5.14E-03	6.50E-04	4.81E-01	4.15E-02	4.63E-03	8.94E-05	4.70E-06	6.48E-07
ESE	5.38E-02	7.45E-03	8.97E-04	1.10E-01	1.00E-02	1.27E-03	9.66E-01	8.71E-02	1.15E-02	7.95E-04	3.77E-05	1.50E-06
SE	4.17E-02	3.64E-03	8.97E-04	1.20E-01	9.31E-03	1.82E-03	8.70E-01	7.25E-02	1.52E-02	8.14E-04	6.24E-05	6.37E-06
SSE	4.88E-02	3.31E-03	7.22E-04	1.50E-01	1.02E-02	1.82E-03	9.85E-01	6.53E-02	1.15E-02	7.29E-04	3.60E-05	2.95E-06
S	2.56E-02	2.62E-03	4.73E-04	7.80E-02	6.54E-03	1.22E-03	5.72E-01	4.79E-02	9.04E-03	2.80E-04	1.19E-05	1.69E-06
SSW	2.74E-02	2.66E-03	4.73E-04	9.11E-02	7.97E-03	1.28E-03	7.03E-01	5.42E-02	8.93E-03	3.10E-04	1.26E-05	1.70E-06
SW	4.34E-02	4.56E-03	8.47E-04	1.31E-01	1.20E-02	2.23E-03	8.77E-01	7.98E-02	1.46E-02	6.68E-04	5.55E-05	9.07E-06
WSW	5.82E-02	4.63E-03	7.22E-04	1.28E-01	8.05E-03	1.45E-03	9.46E-01	6.54E-02	1.20E-02	6.99E-04	3.48E-05	4.53E-06
W	4.89E-02	5.53E-03	1.07E-03	8.55E-02	6.71E-03	1.24E-03	6.77E-01	5.71E-02	9.76E-03	4.12E-04	1.95E-05	1.91E-06
WNW	4.62E-02	3.86E-03	7.22E-04	1.68E-01	1.13E-02	1.82E-03	1.38E+00	8.94E-02	1.47E-02	1.01E-03	7.43E-05	1.14E-05
NW	4.56E-02	6.62E-03	1.02E-03	1.76E-01	2.13E-02	3.19E-03	1.39E+00	1.46E-01	2.24E-02	9.30E-04	1.28E-04	1.95E-05
NNW	5.52E-02	6.72E-03	1.12E-03	2.03E-01	2.15E-02	3.42E-03	1.56E+00	1.45E-01	2.32E-02	1.05E-03	1.29E-04	1.93E-05

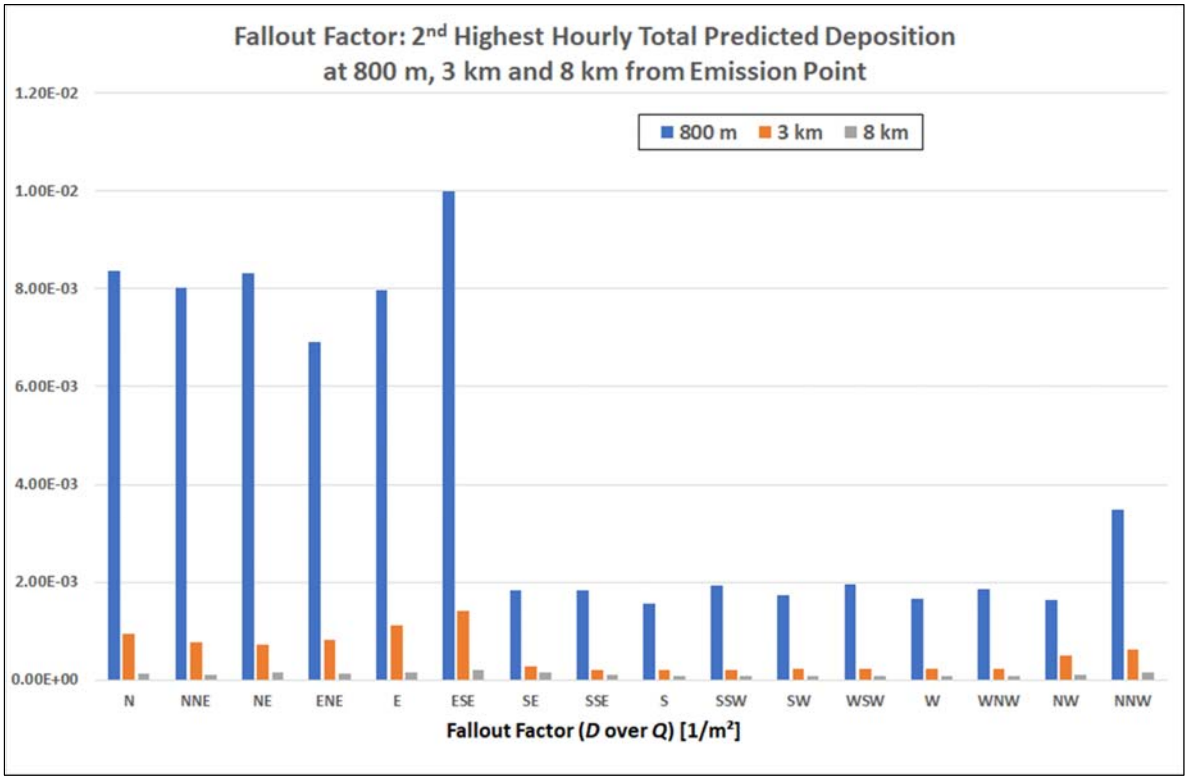

Figure 5.8.65
Fallout Factors D/Q) based on the 2nd Highest Hourly Total Predictions at 800 m, 3 km and 8 km Downwind of the Nuclear Installation(s) for Different Wind Directions

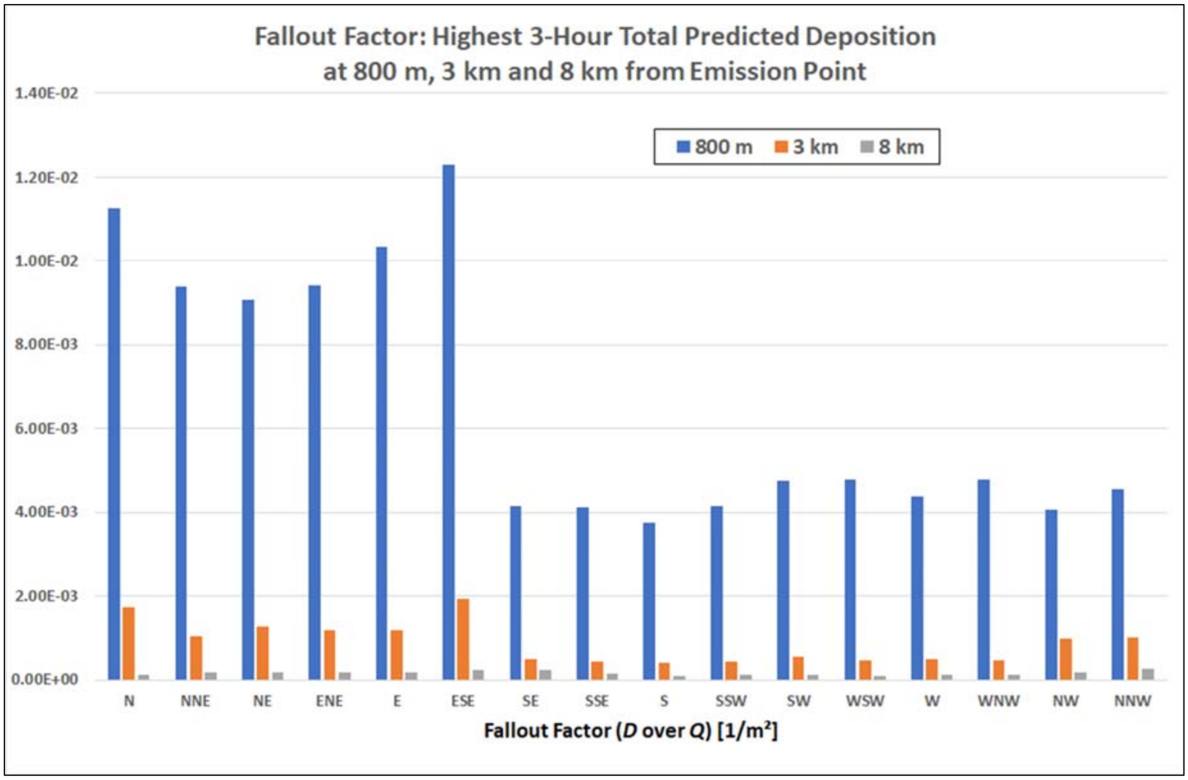

Figure 5.8.66
Fallout Factors (*D/Q*) based on the Highest 3-Hourly Total Predictions at 800 m, 3 km and 8 km Downwind of the Nuclear Installation(s) for Different Wind Directions

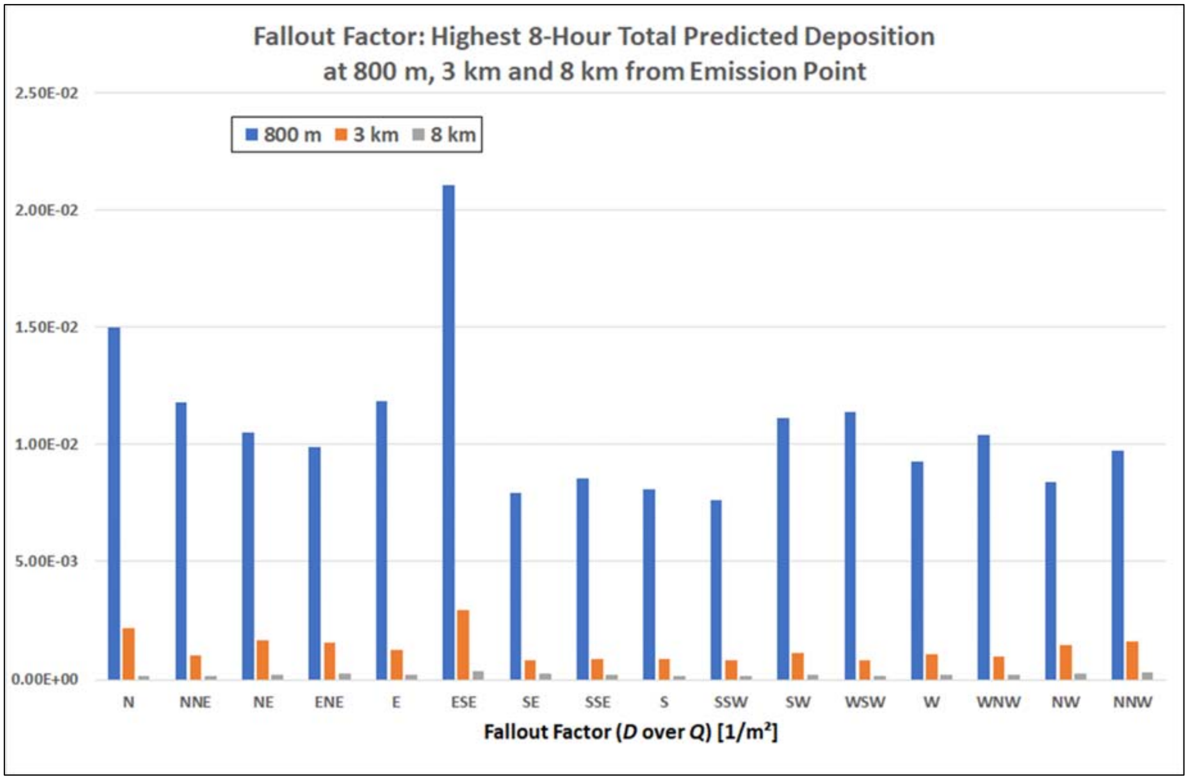

Figure 5.8.67
Fallout Factors (*D/Q*) based on the Highest 8-Hourly Total Predictions at 800 m, 3 km and 8 km Downwind of the Nuclear Installation(s) for Different Wind Directions

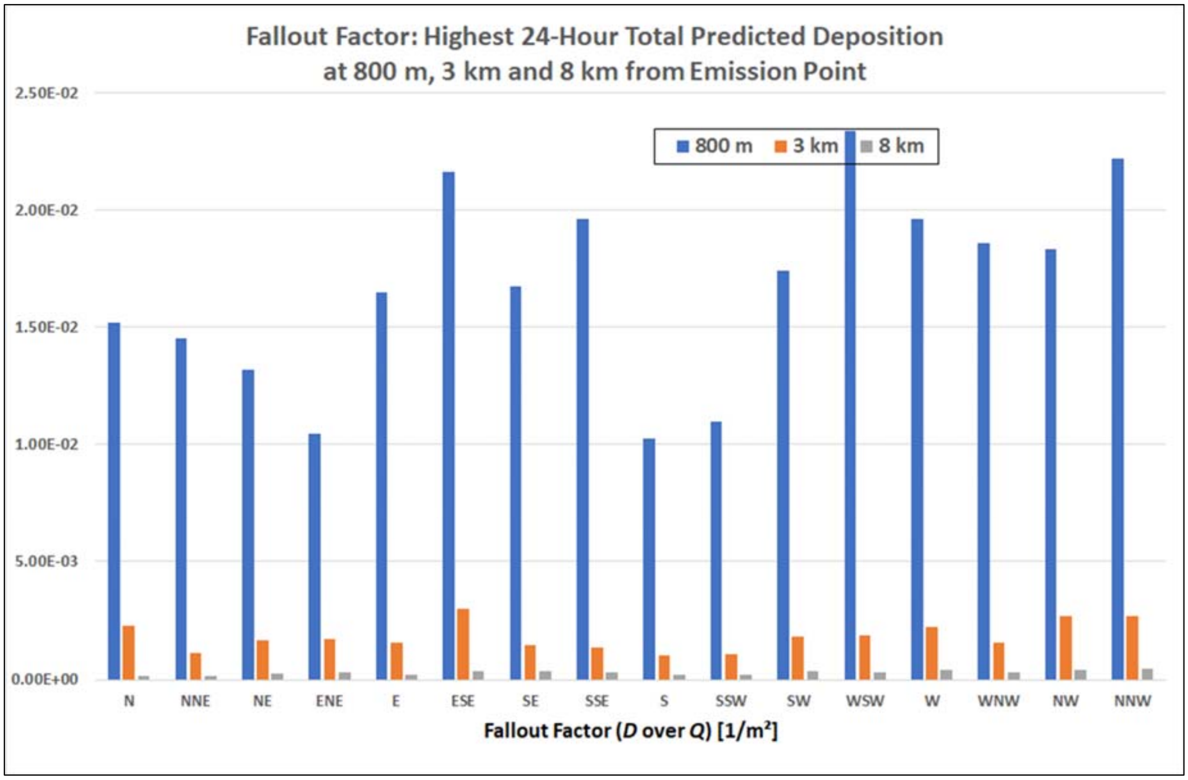

Figure 5.8.68
Fallout Factors (*D/Q*) based on the Highest 24-Hourly Total Predictions at 800 m, 3 km and 8 km Downwind of the Nuclear Installation(s) for Different Wind Directions

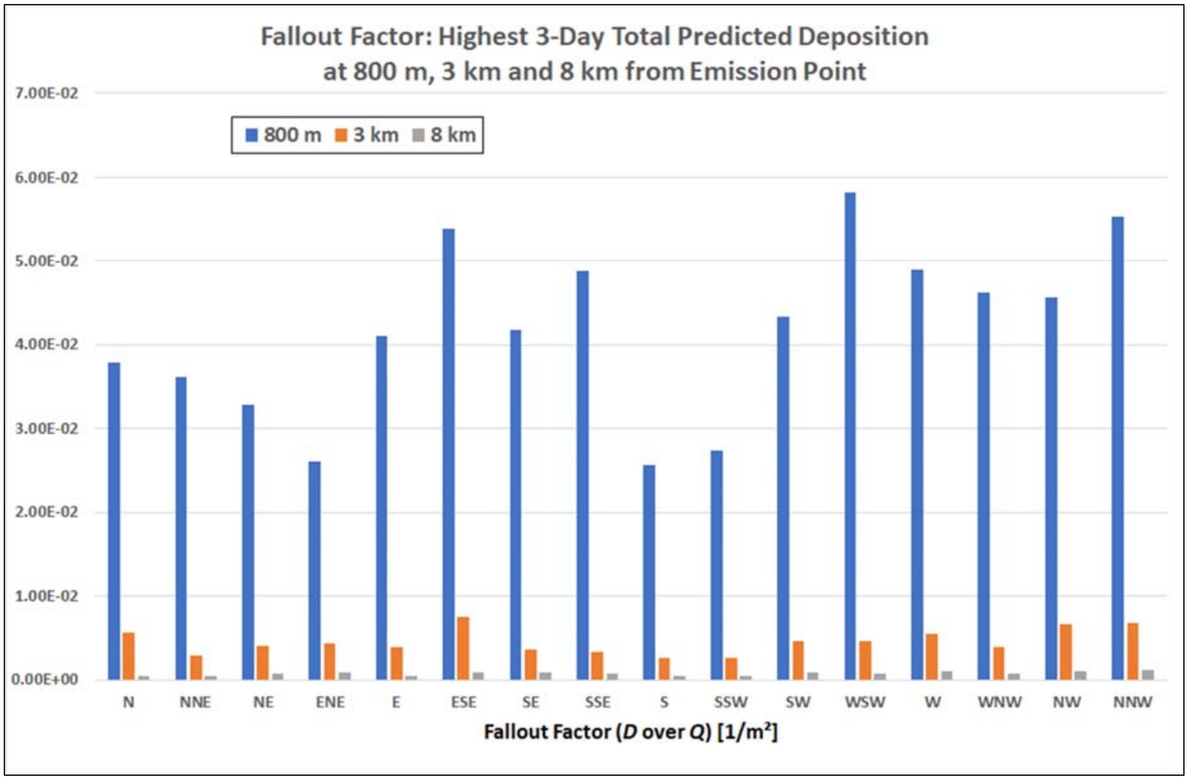

Figure 5.8.69
Dispersion Factors (א/Q) based on the Highest 3-Daily Average Predictions at 800 m, 3 km and 8 km Downwind of the Nuclear Installation(s) for Different Wind Directions

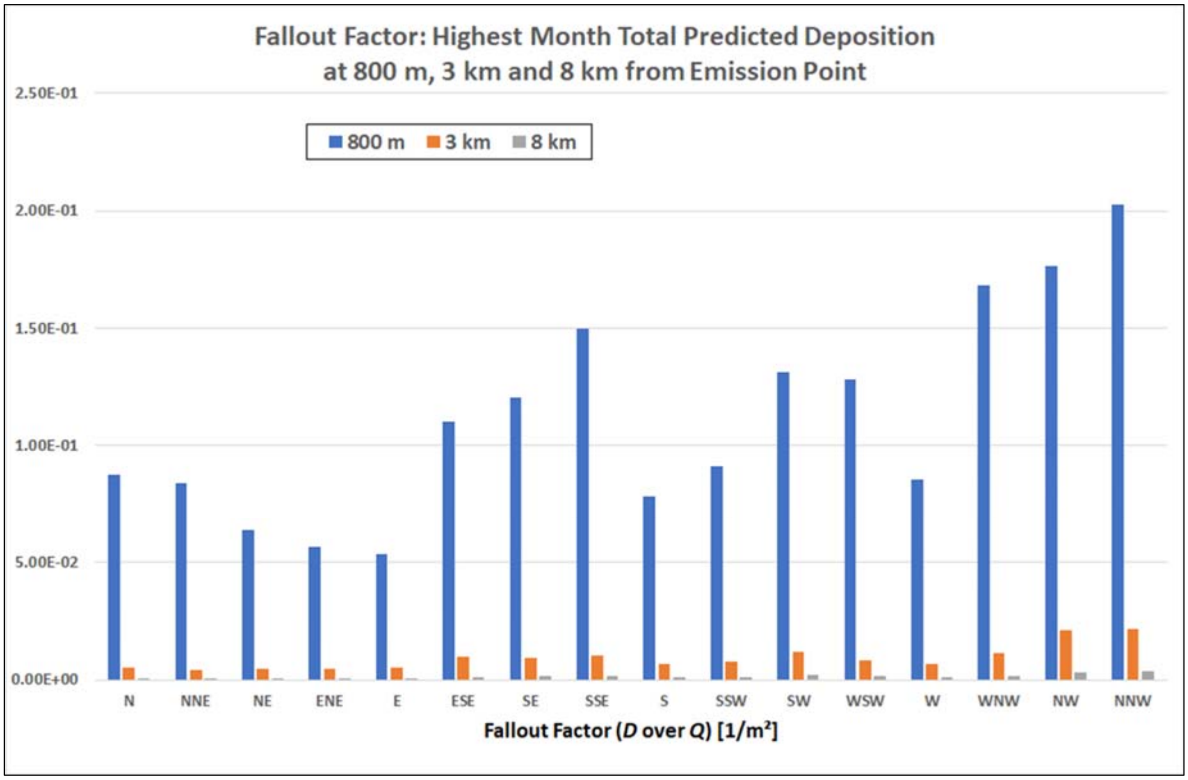

Figure 5.8.70
Fallout Factors (*D/Q*) based on the Highest Monthly Total Predictions at 800 m, 3 km and 8 km Downwind of the Nuclear Installation(s) for Different Wind Directions

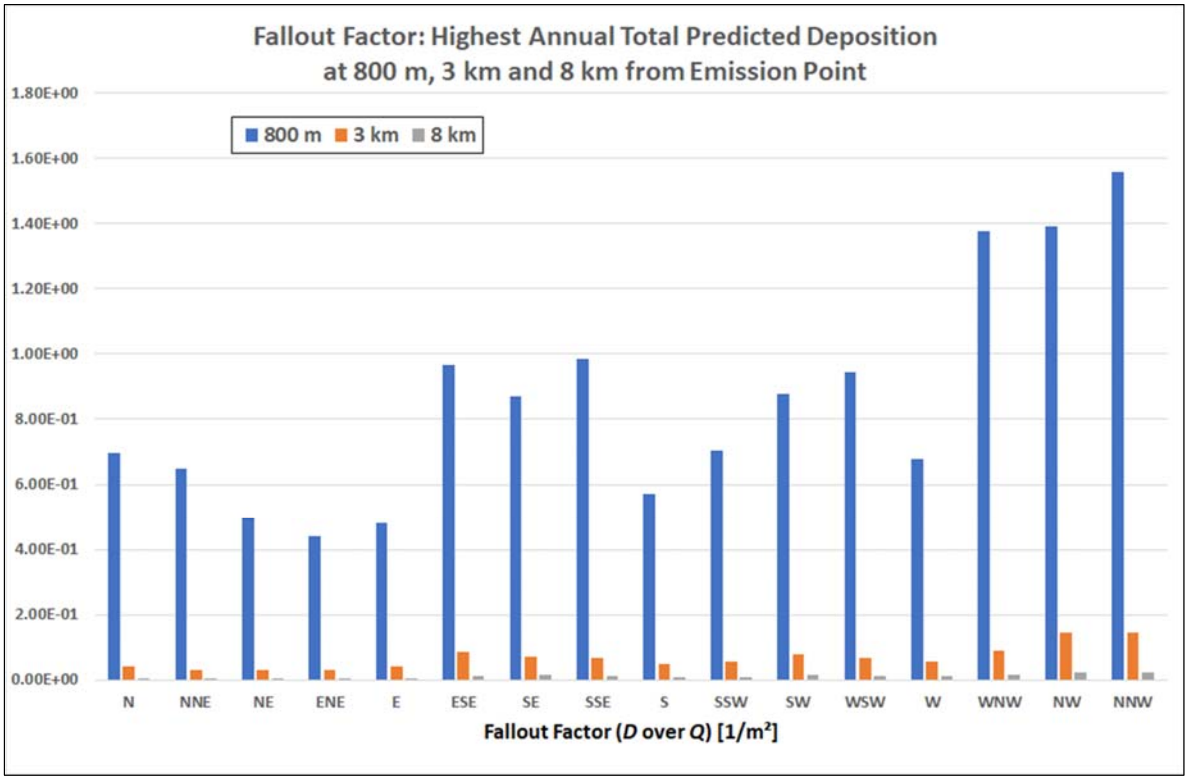

Figure 5.8.71
Fallout Factors (*D/Q*) based on the Highest Annual Total Predictions at 800 m, 3 km and 8 km Downwind of the Nuclear Installation(s) for Different Wind Directions

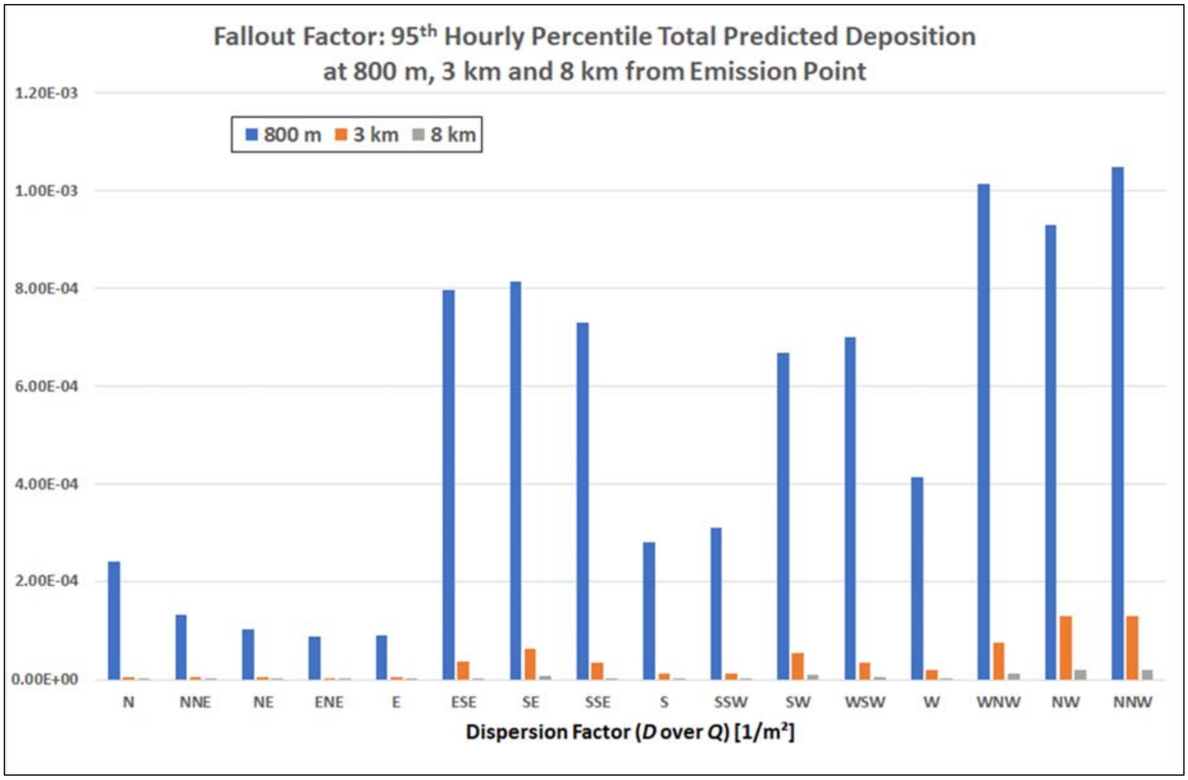

Figure 5.8.72
Fallout Factors (*D/Q*) Based on the 95th Percentile of the Hourly Total Predictions at 800 m, 3 km and 8 km Downwind of the Nuclear Installation(s) for Different Wind Directions

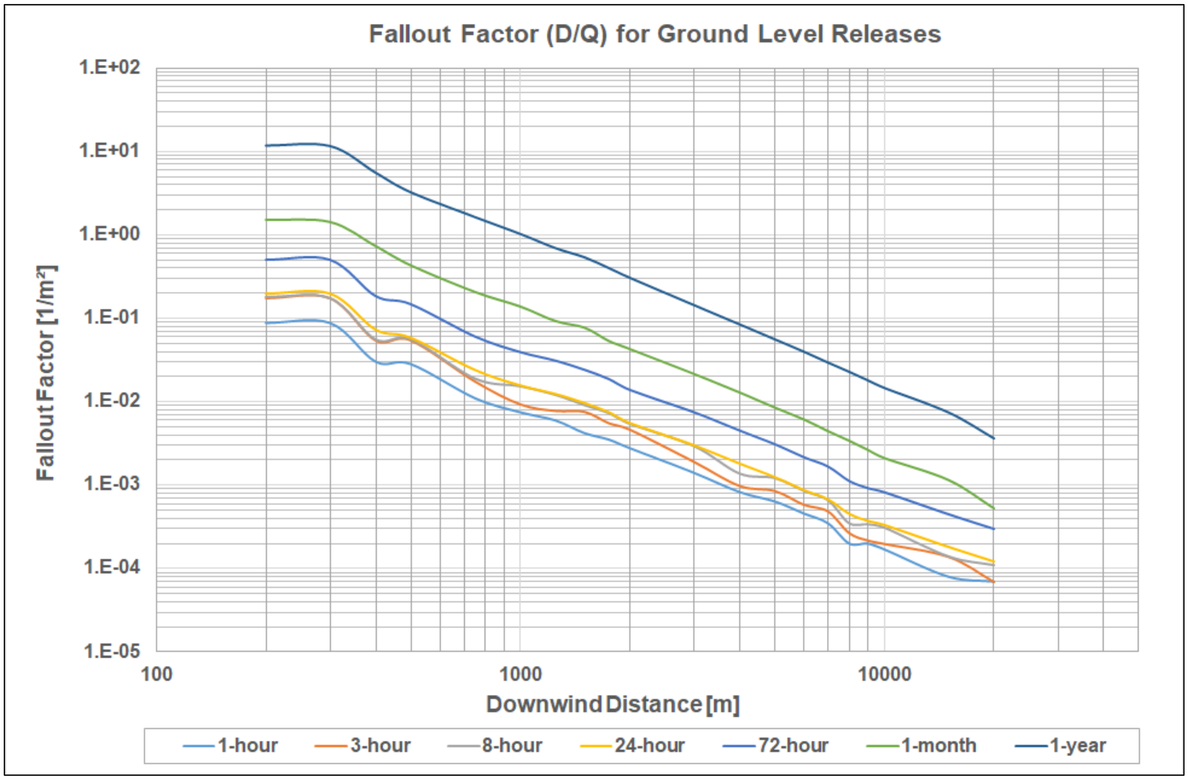

Figure 5.8.73
Fallout Factors (D/Q) Based on the 2nd Highest Hourly Average Deposition Predictions at Various Downwind Distances and Averaging Periods

5.8.8 Monitoring Programme

Meteorological parameters were monitored to characterise the atmospheric conditions at the proposed site and to enable, *inter alia*, an assessment of the magnitude and recurrence probability of extreme events/external hazards. The analysis made use of both on- and off-site monitoring data; the latter mainly due to the relatively short duration of on-site information to enable long term analysis.

5.8.8.1 On-Site Monitoring

International standards for nuclear installation site applications (International Atomic Energy Agency, 2011) and (United States Nuclear Regulatory Commission, 2007c) require consideration of the meteorological characteristics of the site that are necessary for safety analysis or that may have an impact on plant design. They also require the evaluation of atmospheric dispersion characteristics and the establishment of dispersion parameters, as atmospheric dispersion estimates are significant inputs to safety assessment. (see ***Subsection 5.8.3***). These assessments are needed for design and licensing purposes (International Atomic Energy Agency, 2011).

For these reasons, a meteorological monitoring programme has been implemented and will be continued at the site and the region in order to evaluate regional and site-specific meteorological parameters during the nuclear installation lifetime.

5.8.8.1.1 Prior to Nuclear Installation Operation

The historical meteorological data are planned to be continuously compared with on-site data collected after the new nuclear installations are designed and constructed (but before operation), to assist with confirmation of the acceptability of the as built plant and confirm assumptions made in the calculation models (International Atomic Energy Agency, 2002) and (United States Environmental Protection Agency, 2000)). The meteorological parameters included in the monitoring programme are:

- wind direction (degrees) and derived standard deviation of wind direction (degrees);
- wind speed (m/s) including wind gusts (m/s);
- ambient temperature (°C) (including temperature differences between height levels (°C);
- relative humidity (per cent);
- precipitation (mm);
- solar radiation (kW/m^2);
- barometric pressure (hPa).

The instrument specifications, tower height, instrument placements at different heights on the tower, sampling intervals and averaging periods, data recording and storage will be as per ANSI/ANS-3.11 Standard (American National Standard, 2015) and Eskom Standard 238-52 (Eskom, 2017) for meteorological requirements for nuclear installations. Evapotranspiration and atmospheric stabilities are derived from these parameters, as discussed in ***Subsection 5.8.6.1.8*** and ***Subsection 5.8.6.1.9***, respectively.

Corrosion monitoring will also be repeated to build up a longer history. Although the existing observations are adequate to determine the current corrosivity at the site, a long-term history will identify any changes that might occur.

5.8.8.1.2 During Nuclear Installation, Operation and Decommissioning

All meteorological data parameters, as listed in the previous section, will continuously be collected and evaluated to:

- confirm the design bases for the nuclear installation(s);
- enable calculations of atmospheric dispersion and statistical analyses;
- demonstrate the on-going feasibility of the emergency plan;
- meet the requirements for a safe nuclear installation operation.

More specifically, the programme will be developed to provide the relevant meteorological information needed for the following assessments (United States Nuclear Regulatory Commission, 2007c; Eskom, 2017; National Nuclear Regulator, 2016a):

- an assessment of the annual radiation dose to the public resulting from the routine discharges to demonstrate compliance with regulatory requirements; an assessment of atmospheric dispersion immediately following an accidental release of airborne radioactive materials to provide input to the evaluation of the consequences of radioactive releases to the atmosphere and to aid in the implementation of emergency response decisions in accordance with the NNR requirements;
- a periodic assessment of natural phenomena being experienced or projected beyond usual levels (e.g. high winds) for the purposes of emergency planning;
- a periodic assessment of the potential dispersion of radioactive materials from, and the radiological consequences of, a spectrum of accidents to aid in evaluating the environmental risk posed by the nuclear installation(s).

Periodic assessment of meteorological instruments and information requirements will identify the need for new or enhanced instrumentation, for example, on-line real-time atmospheric dispersion modelling for use during emergency conditions.

While the nuclear facility is being decommissioned, the continued need for onsite meteorological data should be evaluated based on the potential impacts of the remaining hazard footprint (American National Standard, 2015).

5.8.8.2 Off-Site Monitoring

Whilst still building up a history of on-site meteorological data, long-term data from weather stations in the vicinity of the site will be analysed to support estimating extreme weather conditions. These include data from the offsite Eskom meteorological stations already in operation as part of Koeberg's emergency preparedness and response will be collected and analysed.

5.8.9 Management of Uncertainties

5.8.9.1 Measurement and Analyses

The uncertainties associated with the establishment of a meteorological baseline for the site will be introduced through the following activities:

- observation of meteorological parameters:
  - onsite measurements;
  - use of other sources (e.g. SAWS);
- data analyses:
  - statistical methods;
  - derived meteorological parameters;
  - atmospheric dispersion calculations.

The factors that influence the uncertainty of data from the onsite monitoring station include:

- sufficient instrumentation to monitor relevant parameters;
- instrumentation accuracy;
- location (macro and micro);
- timeframe of monitoring database.

Instrumentation has been provided to monitor the main meteorological parameters that can be measured without observation i.e. not including mist, fog, cloud cover, cloud type. These parameters include the wind vector, ambient air, dry bulb temperature, relative humidity, atmospheric pressure, solar radiation and precipitation. Other meteorological parameters can be derived from these and typically include atmospheric stability, wet-bulb temperature, dew point and evapotranspiration.

The methodologies used to derive the latter parameters are based on first principles (e.g. wet-bulb temperature and dew point) and empirical correlations (e.g. atmospheric turbulence and evapotranspiration). The uncertainties associated with parameters obtained from empirical correlations are expected to be greater than those from first principles, by pure nature that the former methods are derived from experimentation with inherent uncertainties, whereas the latter are inter-related meteorological relationships. Atmospheric stability classes are estimated using either the vertical temperature gradient or from a measure of the change in wind direction (‘sigma theta’). Whilst both methods aim to define the same atmospheric stability classes, different results were shown to be obtained at the same site (see ***Tables 5.8.45***, ***5.8.46*** and ***5.8.47***). A comparison of the two methods provided in the Eskom Standard 238-52 (Eskom, 2017) is given in ***Tables 5.8.80***. The delta-T method refers to the 120-m tower vertical temperature difference between 120 m and 10 m measurement levels, and the Sigma-Theta method refers to the standard deviations of the wind direction at the 50 m measurement level. According to the classification results, there is a bias towards more unstable conditions (classes A, B and C) with the horizontal classification (Sigma-Theta method) compared with the vertical classification (delta-T method), i.e. 18.63 per cent compared with 6.85 per cent. Furthermore, very stable conditions (G-class) are more pronounced with the vertical classification (5.30 per cent) compared with the horizontal classification (1.43 per cent). Neutral conditions (D-class) are also more pronounced with the vertical classification (33.86 per cent) compared with the horizontal classification (15.69 per cent).

Table 5.8.80
Comparison of Atmospheric Stability Classification Schemes for the Site (1997-2023)

Atmospheric Stability Class	Atmospheric Stability Frequency of Occurrence	
	Delta-T Method [120m/10m] Vertical Stability	Sigma-Theta Method [50 m] Horizontal Stability
A	1.55%	8.51%
B	2.02%	3.46%
C	3.28%	6.66%
D	33.86%	15.69%
E	37.44%	49.01%
F	16.54%	15.24%
G	5.30%	1.43%

As shown in ***Table 5.8.45***, according to the Delta-T method (vertical classification), very stable conditions (G-class) were observed during winds originating from the NNE, NE, ENE, E and ESE wind directions. This was similarly observed for the F-class stabilities, i.e. N, NNE, NE, ENE, E, ESE and SE wind directions. Although neutral conditions (D-class) occurred most frequently from the western sector, observations were also made during winds from the SSE. The Sigma-Theta method exhibited similar stability-wind direction preferences; however, E-class frequencies dominated the distribution significantly more than with the Delta-T method. The Sigma-Theta method classified most unstable observations from the E, W, S and WSW, whereas the Delta-T method observed unstable conditions mainly from the SE, SSE, NW and SSW, as shown in ***Table 5.8.46***.

However, since the estimation of atmospheric turbulence is very important for the calculation of atmospheric dispersion, the most recently accepted methodologies have been adopted for use directly in the atmospheric dispersion model. The AERMOD dispersion model does not require the specification of atmospheric stability classes; instead, the boundary layer structure is estimated using direct measurements, in this wind speed and temperature measurements from the 120-m tower.

There will always be some error in any mathematical model, but it is desirable to structure the model in such a way to minimise the total error. Essentially, the dispersion model represents the most likely outcome of an ensemble of experimental results. The total uncertainty can be thought of as the sum of three components: the uncertainty due to errors in the model physics; the uncertainty due to data errors; and the uncertainty due to stochastic processes (turbulence) in the atmosphere.

The stochastic uncertainty includes all errors or uncertainties in data such as source variability, observed concentrations, and meteorological data. Even if the field instrument accuracy is excellent, there can still be large uncertainties due to unrepresentative placement of the instrument (or taking of a sample for analysis). Model evaluation studies suggest that the data input error term is often a major contributor to total uncertainty. Even in the best tracer studies, the atmospheric emission rates are known only with an accuracy of ±5 per cent, which translates directly into a minimum error of that magnitude in the model predictions. It is also well known that wind direction errors are the major cause of poor agreement, especially for relatively short-term predictions (minutes to hourly) and long downwind distances. All of the above factors contribute to the inaccuracies not even associated with the mathematical models themselves.

The AERMOD model has been shown to be an improvement on the older generation dispersion models that utilise discrete diffusion parameters (e.g. Pasquill-Gifford), especially short-term predictions (Hanna, et al., 1999; Perry, et al., 2004). However, the range of uncertainty of the model predictions is still regarded to be within a factor of two (Perry, et al., 2004). The accuracy improves with fairly strong wind speeds and during neutral atmospheric conditions (Perry, et al., 2004). Vamsidhar *et al* (Vamsidhar , et al., 2010) presented a comprehensive review of the uncertainty and sensitivity analyses associated with prediction of ground level pollutant concentrations using the US EPA's AERMOD equations for point sources. Both stable and unstable (convective) boundary layer conditions were studied. The parameters considered for these analyses included emission rate, stack exit velocity, stack exit temperature, wind speed, lateral dispersion parameter, vertical dispersion parameter, weighting coefficients for both updraft and downdraft, total horizontal distribution function, cloud cover, ambient temperature, and surface roughness length A roughness length of 0.36 m was estimated using the 120-m Tower wind speed measurements[24]. The corresponding probability distribution functions, depending on the measured or practical values are assigned to perform uncertainty and sensitivity analyses in both unstable and stable atmospheric cases. The results for uncertainty in predicting ground level concentrations at different downwind distances during unstable conditions varied between 67 per cent and 75 per cent, while it ranged between 40 per cent and 47 per cent in stable boundary layer. The sensitivity analysis showed that vertical dispersion parameter and total horizontal distribution function have contributed to 82 per cent and 15 per cent variance in predicting concentrations in the unstable boundary layer. In the stable boundary layer, vertical dispersion parameter and total horizontal distribution function have contributed about 10 per cent and 75 per cent to variance in predicting concentrations respectively. Wind speed had a negative contribution to variance and the other parameters had a negligent or zero contribution to variance.

Table 5.8.2 provides the required accuracies of the measuring instruments. These accuracies equal or better the requirements of ANSI/ANS-311-2015 (ANS 2015) and (Eskom, 2017), and have been maintained through the adopted quality assurance programme of calibration and maintenance. The instrument uncertainties were calculated using the methodology contained in *Guidelines for Evaluating and Expressing the Uncertainty of NIST Measurement Results* published by the United States Department of Commerce, Technology Administration National Institute of Standards and Technology (NIST) (Barry & Kuyatt, 1994). The calculated expanded uncertainties associated with the meteorological instrumentation are as follows:

---

[24] The aerodynamic roughness length is a theoretical height that must be determined from the wind speed profile. The roughness height was estimated using hourly average wind speeds at all four levels on the 120-m Tower. There has also been some success at relating this height to the arrangement, spacing, and physical height of individual roughness elements such as vegetation or houses. As an approximation, the roughness length is approximately one-tenth of the height of the surface roughness elements. The average height of the vegetation in the surrounding area ranges between 2 m and 4 m, which agrees with the estimate of 0.36 m from measurement of the wind speed at the 120-m Tower.

Wind direction (0 to 360) : 1 degree

Wind direction (True North) : 5 degrees

Wind speed (200 to 6200 rpm) : 6 rev. per minute

Wind speed (starting threshold) : 100 µNewton-metre

Barometric pressure (800 to 1100 hPa) : 1 hPa

Temperature (0°C to 40°C) : 0.2 °C

Solar Irradiance (0 to 1200 W/m²) : 60 W/m²

Rain gauge (2.5 to 5 millilitres) : 0.1 millilitres

Humidity (11 to 75 per cent) : 4 per cent

These uncertainties are being managed through bi-annual calibration checks on all meteorological monitoring instrumentation.

Both short- and long-term analyses are required from the meteorological data collected on site. Short-term analyses would typically include hourly average dispersion calculations, whereas long-term analyses would be required to establish extremes and rare phenomena. The 43-year monitoring data collected on site have provided adequate information to determine both average and extreme observations; however, the accuracy of forecasting future extreme weather events would only improve with increased historical information. The IAEA recommends (International Atomic Energy Agency, 2011) that the long-term data used to evaluate extreme values of meteorological variables should cover a period proportionate with the return period used for assessing the corresponding design basis, i.e. not greater than four times the duration of the sample. Notwithstanding the above recommendation, wind gusts, extreme minimum and maximum temperatures and rainfall rates, for return years of up to 100 000 000 have been calculated (see **Subsection 5.8.6.2.2**), as required by the Technical Specification for this section (Eskom, 2022). Wind speed and rainfall extremes are based on measured data sets covering a period of 43 years (1980 to 2022, excluding 9 months in 2023), and temperature a period of 23 years (1997 to 2019), which implies that values for return periods more than 100 years need to be interpreted with caution. This is demonstrated by the increasing 95th confidence interval estimates for increasing return years in **Subsection 5.8.6.2.2**. The conservative approach would be to apply the upper estimate of the interval, rather than the mean.

5.8.9.2 Uncertainties due to Climate Change

Climate change is a key area of uncertainty that will affect the meteorology of the site. The key aspects here are greater variations in extreme temperature, wind speed and rainfall events. All key climate indicators reflect trends consistent with a warming climate, including land and ocean temperatures, sea level and greenhouse gas (GHG) concentrations in the atmosphere, which all surpassed the records set just in the preceding year. The following global changes have been observed:

- from 1880 to 2012, globally averaged surface temperature increased by 0.85°C;
- the past 5 years are collectively the warmest years in modern record;
- Northern Hemisphere (NH): 2016 warmest year with +1.27°C;
- Southern Hemisphere (SH): 2016 warmest year with +0.71°C;
- the global mean sea level rose by 0.19 m between 1901 and 2010;
- the upper few metres of the ocean are warming - Data from the US National Oceanic and Atmospheric Administration (NOAA) show an increase of *c.* 0.13°C per decade over the past 100 years.
- the greatest ocean warming is occurring in the SH and contributing to the subsurface melting of Antarctic ice shelves.

Assessments of historical trends of measured surface temperature in South Africa have all shown a general upward trend, in both mean and extreme values, over recent decades (Kruger & Nxumalo, 2016). In addition, some regional differences in trends have been identified. However, these observations indicate that South Africa is warming at a slower rate than most other continental parts of the world, i.e. mostly less than 0.1°C per decade. This may be due to the buffering effect of the surrounding oceans. Using a data homogenisation procedure enabled the combination of stations from different time series from which trend analysis could be applied, to a common analysis period back to around 1931. The analyses show the general warming trend with a general increase in extreme warm events, and a general decrease in extreme cold events across South Africa. The analysis of seasonal trends shows that, while there are noteworthy differences on a regional basis, austral summer shows on average the strongest warming, followed by autumn, winter and spring. However, the central interior shows non-significant or similar trends when compared to the other parts of South Africa. There is no countrywide acceleration in the warming trends, but some regional consistencies in the temporal changes in trends could be determined, i.e. increases in trends in the central interior and decreases in trends along most of the coastal region.

A rainfall trend analysis for South Africa was completed by Kruger and Nxumalo (Kruger & Nxumalo, 2017) through optimizing district rainfall and individual rainfall station data sets for the longest possible period of analysis (i.e. 1921–2015). Two interlinked data sets were used for the trend analyses, namely, daily time series of 60 individual rainfall stations and the daily district rainfall of 88 of 94 rainfall districts. In general, the results show an increase in rainfall for most rainfall stations in the southern interior of South Africa, and indications of decreases in rainfall in the far northern and northeastern parts. The increase in the annual rainfall in the south is reflected in the seasonal trends, where summer rainfall shows a similar increase, but also extends into the central interior. For other seasons, most of the country shows no significant historical trend changes in annual total rainfall. Decreases in rainfall from wet spells were noted in most places over the east and northeast, while the southern and eastern parts along the escarpment experienced shorter annual dry spells. From the extreme rainfall analyses, an increase in daily rainfall extremes in the southern to western interior is apparent, but apart from summer rainfall regions, the other areas do not show spatially coherent statistically significant results. Mixed indications were observed in the updated analysis of the trends in extreme rainfall for South Africa (1931 to 2019) (South African Weather Services, 2020a). The annual maximum daily and five-daily rainfalls show significant increases in the central and southern interior, whereas trends in the intensity of rainfall on rainy days show mixed signals, but there are clear decreases in the far northeastern interior and increases in the central and southeastern parts. In the case of the 25 mm rainfall threshold, increases are apparent over the central and southern interior and spreading eastwards, while decreases are only apparent in the far north.

In the research article by (Wright & Grab, 2017) of wind speed characteristics and implications for wind power generation in the Northern, Western and Eastern Cape provinces, data from 19 weather stations with high-resolution wind records between 1995 and 2014 were evaluated. The closest weather station in the analysis to the Duynefontyn study area was at Langebaan. Although a 20-year period is insufficient to establish conclusive changes in wind associated with climate change, the record is nevertheless able to provide tentative comparison of the data sets and indicate mean wind speed variance and trends over the last 20 years for the Cape regions. The most significant findings were:

- Most stations (79 per cent) recorded a decrease in mean annual wind speed over the study period.
- The mean rate of decrease across all stations over the 20-year period equates to -1.25 per cent.
- The largest seasonal decline of -0.15 per cent per annum was recorded in summer.
- Statistically significant declines in mean annual wind speed are somewhat more pronounced for the coastal zone (-0.08 per cent per annum) than over interior regions (-0.06 per cent per annum) for the study period.

It is noted that these observed reductions in wind speed is in contrast with the findings of the simulated downscaled models discussed in ***Subsection 5.8.6.2.2(c)***. The projected changes due to climate change indicate increased wind speed by 2044 (+2.28 per cent), 2064 (+3.85 per cent), 2110 (8.04 per cent) and 2130 (+10.29 per cent) (CSIR, 2021). This difference in comparison reflects the low confidence in the projections of wind change projections.

Climate change over southern Africa may be anticipated to be closely linked to changes in the dynamics of the regional Hadley cell. High- and low-pressure systems are projected to change in response to the expansion of the Hadley cell in a warmer world (Seidel, et al., 2008). Over southern Africa, the strengthening and expanding subtropical high-pressure belt is, under climate change, projected to contribute to the southward displacement (or blocking) of frontal systems bringing rainfall over southern Africa. As per AR5, the mean sea level pressure is therefore projected to decrease.

As discussed in ***Subsection 5.8.2.6.6*** the IPCC has prepared four scenarios that assume the stabilization of anthropogenic forcing of the climate system at different levels. The treatment of climate change for the study area is based on downscaled model simulations completed by the CSIR (Engelbrecht, et al., 2019; CSIR, 2021) and the SAWS (South African Weather Service, 2017) for South Africa for two RCPs, namely RCP4.5 and RCP8.5. The CSIR data consisted of three data sets and reports. Two of these were specifically produced for the two future horizons of 2012-2050 and 2071-2099 (Engelbrecht, et al., 2019) and the third data set consists of annual means from 1960 to 2099 (CSIR, 2021). The first two data sets were provided on a 50 km and 8 km model grid resolution, respectively. The third data set was provided as a spatial average for an area of 100 km by 100 km with the site at the centre. The SAWS simulations were also for two future horizons, i.e. 2036-2065 and 2066-2095, and covered a 0.44° (approximately 45 km) spatial resolution. Where the required information could not be obtained from these downscaled models, the analysis was supplemented with information extracted from the ARP5. Although the downscaled simulations included both gradual climate change (GCC) and extreme weather events (EWE) the latter treatments were only focussed on extreme rainfall days, hot and heatwave days (Engelbrecht, et al., 2019). No attempt was made in the downscaled models to forecast extreme temperatures, wind gusts and rainfall events. Instead, the SREX reports (Intergovernmental Panel on Climate Change, 2012) treatment of risks of extreme events was consulted in combination with the downscaled CSIR results. The projections based on RCP8.5 were adopted for inclusion in the SSR due to the uncertainty on whether any of the mitigation emissions would be achieved.

Wind direction changes were not provided as part of the downscaled model outputs. Instead, the study by Herbst and Rautenbach (Herbst & Rautenbach, 2015) which attempted to quantify the projected changes in seasonal daily mean wind speeds and directions for South Africa around the mid-21st century (2051-2075) was consulted. Small scale rare weather events such as thunder, lightning and hail events have not been simulated in any of the global climate models (GCMs). Projections of extremes in any of the meteorological parameters are difficult to determine. Extreme rainfall events are mostly caused by intense thunderstorms, which are often also the cause of lightning, hail, damaging winds and flash floods. That is, the climate change projections analysed with these models are indicative that decreases in these hazardous rainfall events are plausible over the study area. The more conservative approach would therefore be to assume the historical statistics rather than to reduce any frequencies of these events. Similarly, none of the models simulate the occurrence of tornadoes.

Based on the SREX report (Intergovernmental Panel on Climate Change, 2012), the approach to adjusting temperature extremes for climate change is to apply a reduction in the return period of the predicted extreme value. For wind speeds and rainfall, it is recommended to adopt the projected changes in the GCC.

In summary, the projected fractional changes in rainfall, temperature wind speed and atmospheric pressure due to climate change are given in ***Table 5.8.81***. The absolute values for these meteorological parameters are summarised in ***Table 5.8.82***

Table 5.8.81
Fractional Climate Change Projections for Rainfall, Temperature, Wind Speed and Atmospheric Pressure

Parameter	Period	Baseline (1997-2019)	Statistic	Horizon Projected Fractional Change (per cent)			
				2044	2064	2110	2130
Rainfall	Annual Average	372.1 mm	95th Percentile	-16.89%	-19.81%	-32.13%	-38.64%
			Mean	-14.54%	-19.36%	-31.62%	-38.35%
			5th Percentile	-12.28%	-16.01%	-30.13%	-38.19%
	24-Hour Maximum	70.0 mm	95th Percentile	0.00%	3.72%	12.19%	15.76%
			Mean	0.00%	3.64%	12.00%	15.64%
			5th Percentile	0.00%	3.01%	11.43%	15.57%
Temperature	Min Daily	13.2 °C	95th Percentile	10.51%	16.12%	31.93%	40.32%
			Mean	7.01%	12.24%	26.48%	33.97%
			5th Percentile	3.89%	8.74%	21.70%	28.44%
	Mean Daily	16.5 °C	95th Percentile	8.49%	12.78%	24.80%	31.27%
			Mean	5.74%	9.84%	20.97%	26.90%
			5th Percentile	3.43%	7.43%	18.01%	23.70%
	Max Daily	20.3 °C	95th Percentile	7.42%	11.07%	20.43%	25.57%
			Mean	5.09%	8.53%	17.87%	22.92%
			5th Percentile	2.97%	6.53%	15.94%	21.14%
Wind Speed	Hour Average	4.1 m/s	95th Percentile	6.29%	8.69%	13.30%	15.73%
			Mean	2.28%	3.85%	8.04%	10.29%
			5th Percentile	-2.37%	-1.21%	2.37%	4.13%
	Average of Hour Maximums	13.5 m/s	95th Percentile	2.29%	3.05%	4.82%	5.75%
			Mean	0.92%	1.44%	3.10%	3.98%
			5th Percentile	-0.55%	-0.16%	1.34%	2.09%
	Peak Hourly Maximum	17.2 m/s	95th Percentile	2.33%	2.91%	4.65%	5.81%
			Mean	1.16%	1.74%	2.91%	4.07%
			5th Percentile	-0.58%	0.00%	1.16%	2.33%
	Gust	38.8 m/s	95th Percentile	2.29%	3.05%	4.82%	5.75%

Parameter	Period	Baseline (1997-2019)	Statistic	Horizon Projected Fractional Change (per cent)			
				2044	2064	2110	2130
			Mean	0.92%	1.44%	3.10%	3.98%
			5th Percentile	-0.55%	-0.16%	1.34%	2.09%
MSL Pressure	Extreme Lower (Hourly)	932.1 hPa	95th Percentile	0.00%	0.00%	-0.05%	-0.07%
			Mean	-0.02%	-0.04%	-0.08%	-0.11%
			5th Percentile	-0.05%	-0.07%	-0.12%	-0.15%
	Mean Annual	1013.8 hPa	95th Percentile	0.01%	0.00%	-0.05%	-0.07%
			Mean	-0.02%	-0.04%	-0.08%	-0.11%
			5th Percentile	-0.05%	-0.07%	-0.12%	-0.15%
	Extreme Upper (Hourly)	1045.4 hPa	95th Percentile	0.01%	0.00%	0.00%	0.00%
			Mean	0.00%	0.00%	0.00%	0.00%
			5th Percentile	0.00%	0.00%	0.00%	0.00%

Table 5.8.82

Climate Change Projections for Rainfall, Temperature, Wind Speed and Atmospheric Pressure at the Site

Meteorological Parameter	Period	Baseline (1997-2019)	Statistic	Horizon Projected Absolute Values			
				2044	**2064**	**2110**	**2130**
Rainfall [mm]	Annual Average	372.1	95th Percentile	309.3	298.4	252.5	228.3
			Mean	318.0	300.1	254.4	229.4
			5th Percentile	326.4	312.5	260.0	230.0
	24-Hour Maximum	70.0	95th Percentile	70.0	72.6	78.5	81.0
			Mean	70.0	72.5	78.4	80.9
			5th Percentile	70.0	72.1	78.0	80.9
Temperature [°C]	Min Daily	13.2	95th Percentile	14.6	15.3	17.4	18.5
			Mean	14.1	14.8	16.7	17.7
			5th Percentile	13.7	14.4	16.1	17.0
	Mean Daily	16.5	95th Percentile	17.9	18.6	20.6	21.7
			Mean	17.4	18.1	20.0	20.9
			5th Percentile	17.1	17.7	19.5	20.4
	Max Daily	20.3	95th Percentile	21.8	22.5	24.4	25.5
			Mean	21.3	22.0	23.9	25.0
			5th Percentile	20.9	21.6	23.5	24.6
Wind Speed [m/s]	Hour Average	4.1	95th Percentile	4.4	4.5	4.6	4.7
			Mean	4.2	4.3	4.4	4.5
			5th Percentile	4.0	4.1	4.2	4.3
	Average of Hour Maximums	13.5	95th Percentile	13.8	13.9	14.2	14.3
			Mean	13.6	13.7	13.9	14.0
			5th Percentile	13.4	13.5	13.7	13.8
	Peak Hourly Maximum	17.2	95th Percentile	17.6	17.7	18.0	18.2
			Mean	17.4	17.5	17.7	17.9
			5th Percentile	17.1	17.2	17.4	17.6
	Gust	38.8	95th Percentile	39.7	40.0	40.7	41.0
			Mean	39.2	39.4	40.0	40.3

Meteorological Parameter	Period	Baseline (1997-2019)	Statistic	Horizon Projected Absolute Values			
				2044	2064	2110	2130
			5th Percentile	38.6	38.7	39.3	39.6
MSL Pressure [hPa]	Extreme Lower (Hourly)	932.1	95th Percentile	932.1	932.1	931.7	931.4
			Mean	931.9	931.8	931.3	931.1
			5th Percentile	931.6	931.4	931.0	930.7
	Mean Annual	1013.8	95th Percentile	1013.9	1013.8	1013.3	1013.1
			Mean	1013.6	1013.4	1013.0	1012.7
			5th Percentile	1013.3	1013.1	1012.6	1012.3
	Extreme Upper (Hourly)	1045.4	95th Percentile	1045.5	1045.4	1045.4	1045.4
			Mean	1045.4	1045.4	1045.4	1045.4
			5th Percentile	1045.4	1045.4	1045.4	1045.4

5.8.10 Management System

The appropriate grading for safety classification in terms of RD-0034 following Eskom's classification procedure (National Nuclear Regulator, 2008) has been determined as Safety Class C, i.e. not important to nuclear safety, and in terms of the procedure, compliance with an ISO 9001 or equivalent system is required. Supporting information can be found in ***Chapter 10*** (Management System).

A quality assurance programme has been followed that includes the minimum meteorological parameters to sample, minimum specifications for meteorological instrumentation and siting criteria, data collection and validation procedures, instrument maintenance procedures, methods of analyses and archiving procedures. (Refer to ***Chapter 10***).

The collection of meteorological data from the monitoring station at the site is done every two weeks. These data are stored on two computer servers (mirrored) in two separate fire-proof strong rooms. Detailed records are kept of the work carried out, calculations made and databases established. These include:

- raw monitoring database;
- processed monitoring database;
- dispersion model input files;
- dispersion model output files;
- dispersion factor database (short- and long-term simulations);
- meteorological instrumentation calibration certificates.

Electronic records are stored in a secure central repository with regular off-site back-ups.

Whereas the monitoring of meteorological parameters can be verified by inspectors, dispersion modelling and further processing of meteorological parameters do not lend themselves to direct verification or tests that can be precisely defined and controlled. Peer review of these evaluations is essential and was done by a suitably qualified and experienced person, independent from those who did the work.

It is stated in *Section 1* of RG-0016 that *"All calculation models and/or evaluation models used in safety analyses are designed, developed, verified and validated, implemented, used and controlled in accordance with recognised nuclear industry standards and/or practices."* The Verification and Validation report (Burger, 2021) was completed with the following objectives:

- to identify, describe and understand the different physical processes being simulated;
- to demonstrate the capabilities and limitations of the mathematical formulations, utilised in the selected software, in simulating the identified physical processes;
- to verify the software input pre-processing and the output post-processing;
- to define and demonstrate the minimum qualifications required to use the software and the models.

In the V&V Report, it was concluded that the US EPA AERMOD atmospheric model satisfy the requirements for simulation atmospheric dispersion from nuclear installations for the purposes of the SSR. The following documentation has been included as appendices to this SSR:

- dispersion model input files (***Appendix 5.8.J*** to ***Appendix 5.8.P***);
- dispersion model output files (***Appendix 5.8.Q*** to ***Appendix 5.8.T***);
- meteorological instrumentation calibration certificates. (***Appendix 5.8.F***).

The RG 011 regulatory compliance matrix is provided in ***Table 5.8.83***, that lists the relevant clauses and the specific sections/regulations referred to and in which sections of this SSR they have been addressed.

Table 5.8.83
Regulatory Compliance Matrix

RG 0011 clause	RG 0011 sub clause	Issue	Section where Covered
Assessment of hazards associated with external natural and human-induced events	7.1 General approach for External Events	(2) Adequately investigated with respect to all characteristics that could affect safety in relation to natural and human-induced events	5.8
		(3) Hazards associated with external events, which are to be considered in the design of the nuclear facility, must be determined. For an external event (or a combination of events), the parameters and the values of those parameters used to characterise the hazards must be chosen so that they can be used readily in the design of the nuclear facility.	5.8.12
		(5) Prehistorical, historical and instrumental information and records, as applicable, on the occurrences and severity of those important natural phenomena or human-induced situations/activities should be collected for the region and carefully analysed for reliability, accuracy and completeness	5.8.5
		(6) Appropriate methodologies should be adopted for establishing the hazards from important external phenomena	5.8.4 & 5.8.5
		(7) Methodologies used should be the current and state of the art, and should be justified as being compatible with the characteristics of the region.	5.8.4 & 5.8.5, V & V Report
		(8) Preferential consideration should be given to applicable probabilistic methodologies	Appendix 5.8.B
		(10) The size of the region, to which a method for establishing the hazards associated with major external phenomena is to be applied, should be large	5.8.6.1 (a) & (b), 5.8.6.2.1 (b) & (c), 5.8.7, 5.8.10

RG 0011 clause	RG 0011 sub clause	Issue	Section where Covered
		enough to include all features and areas that could be of significance in the determination of the event.	
		(12) If data for a particular type of natural phenomenon are incomplete for the region, then data from other regions having sufficiently similar characteristics should be used, with proper justification, in evaluation of the design basis event.	5.8.6.1.1, 5.8.6.1.2, 5.8.6.1.3,& 5.8.6.1.5
	7.2 Natural Events 7.2.2 Meteorological Events	(1) Meteorological and climatological characteristics for the region around the site should be investigated and evaluated to ensure the safety of nuclear facility. Meteorological events/parameters to be considered for evaluation of design bases include:	
		- Wind	5.8.6.1.1 &5.8.6.2.2(c)
		- Precipitation	5.8.6.1.3 & 5.8.6.2.2(a)
		-Storm surge	5.8.6.1.4 & 5.8.6.1.2(d)
		-Tropical cyclone	5.8.6.2.1(b)
		-Air temperature (dry bulb and wet bulb)	5.8.6.1.2, 5.8.6.2.2(b) & 5.8.12
		- Humidity	5.8.6.1.6
		(2) The following rare meteorological events should also be considered in the evaluation of site characteristics:	
		- Lightning	5.8.2.1(f)
		- Tornado	5.8.2.1(c)
		- Snow	5.8.6.5
		- Waterspouts	5.8.6.2.1(c)
		- Dust and sandstorms	5.8.6.11(a)
		- Hail storms	5.8.6.1.5 & 5.8.6.2.1(e)
		- Freezing precipitation	5.8.6.1.3
		- Frost	5.8.6.1.3
		- Cloud burst	5.8.6.2.1(d)

RG 0011 clause	RG 0011 sub clause	Issue	Section where Covered
		- Other phenomena	5.8.6.2
		(3) Hazards associated with all relevant meteorological phenomena should be identified and evaluated to arrive at the corresponding design basis parameter to ensure the safety of the facilities to be located at the site	5.8.10
		(4) Historical data of the event at and around the site should be utilised for evaluation of the potential of occurrence, frequency and severity of the meteorological event.	5.8.5
		(5) Historical data on persistent high winds during cyclones, tornadoes and storms occurring at and around the region should be used for static loading and wind induced missile generation, while data on short duration bursts of wind should be utilised for studies of dynamic loading. Historical data on circulating wind during tornadoes, if any, occurring at or around the region should also be collected.	5.8.5 & 5.8.6.2
		(6) Collected data should be used to generate design basis wind speeds taking into account the safety goal defined in PP-0014	5.8.6.2(c)
		(7) Site-specific design basis wind speeds should be based on sufficient and reliable data.	5.8.6.2(c)
	7.2 Natural Events 7.2.3 Flooding	4) Suitable meteorological, hydrological and topographical data, including data on relevant bodies of water, should be collected. Uncertainty and data adequacy, if any, should be taken into consideration	5.8
8 Assessment of the potential radiological	8.3 Transport and Diffusion of Effluents	(1) A meteorological investigation should be carried out to evaluate regional and site-specific meteorological parameters. Data should be collected	5.8.5

RG 0011 clause	RG 0011 sub clause	Issue	Section where Covered
impacts of the nuclear facility	Discharged into the Atmosphere 8.3.1 General Considerations	from appropriate elevations above ground in order to obtain realistic dispersion parameters.	
		(3) The type and extent of acquired and stored meteorological data should allow for reliable statistical analyses to determine the distribution of radiation exposures	5.8.5 & 5.8.6
		(4) Contamination in the air, on the ground and in water over short and long periods of time should be described in the atmospheric dispersion models, with account taken of diffusion conditions in the region.	5.8.7
		(5) Use of parameters in calculational models should be substantiated as to their appropriateness for use in estimating releases	5.8.7
		6) The atmospheric dispersion and deposition models used must be documented, described in detail and substantiated to allow a review of their accuracy and validity, source configuration, suitability of input parameters, topography, and appropriateness for the site, plant and release characteristics.	5.8.7 & Atmospheric Dispersion Modelling Verification and Validation: Numerical Atmospheric Dispersion Model
	8.3.2 Meteorological considerations	(1) A programme for meteorological investigation should be designed to collect and evaluate data continuously and should provide data for an adequate time period (for at least two full years) that are representative of the site and should continue for the lifetime of the facility. In addition, the data should be compared with data collected after the plant is constructed, but before operation, to determine whether changes are necessary to the design bases or to assumptions made in the calculation model.	5.2, 5.8.5 & 5.8.5.6
		(2) In collecting meteorological data, care should be taken to prevent local effects from unduly altering the	5.8.5

RG 0011 clause	RG 0011 sub clause	Issue	Section where Covered
		values of the parameters to be measured. It should be ensured that the data collected adequately represent local meteorological conditions	
		(3) In order to provide a description of the meteorological conditions, data on the following should be obtained concurrently:	
		a) Wind vectors (i.e. wind directions and speeds);	5.8.6.1.1
		b) Specific indicators of atmospheric turbulence;	5.8.6.1.8
		c) Precipitation;	5.8.6.1.3
		d) Air temperatures;	5.8.6.1.2
		e) Humidity; and	5.8.6.1.5
		f) Air pressure	5.8.6.1.6
	8.3.3 Instrumentation and measurements	(1) Meteorological equipment should be installed in such a way as to obtain data representing the dispersion conditions at release points. Examination of the terrain around a nuclear facility site is necessary. Topographical features of interest should be considered in the installation of equipment. Instruments should be capable of obtaining data representing the entire profile of the wind, at least up to the height of potential releases.	5.8.5.5
		(2) At sites where there is a potential for fogging or icing, due to an increase in atmospheric moisture content caused by plant operation, instrumentation should be provided for measuring the dew point (or humidity) on the tower or mast.	5.8.5.5

RG 0011 clause	RG 0011 sub clause	Issue	Section where Covered
		(3) Equipment should be properly exposed and should be positioned far enough from any obstacles to minimise their effects on measurements. The tower or mast should be sited at approximately the same elevation as finished plant grade and in an area where plant structures will have little or no influence on the meteorological measurements.	5.8.5.5
		(4) Meteorological instrumentation and systems should be shielded, maintained, serviced and calibrated on a regular basis in order to mitigate harmful environmental effects such as sun, lightning, ice, sandstorms and corrosive agents and to ensure availability and reliability of data.	5.8.5.5
		5) In assessing the accuracy of instrumentation, allowance should be made for errors due to cabling, signal conditioning, recording, solar radiation and the effects of fluctuations in environmental temperature.	5.8.5.4 & 5.8.5.5
		6) Measurements should be made at more than one location where the wind speed or direction varies significantly across the region.	5.8.5.3
		7) Measurements should be made at the following elevations in order to obtain wind data continuously: a) At an elevation of 10m in accordance with standards that have been established by the World Meteorological Organization (WMO), for purposes of comparing and correlating wind data from the site with wind data from the synoptic network of meteorological stations; and	5.8.5.3
		b) At the point representing the effective height of discharge.	5.8.5.3

RG 0011 clause	RG 0011 sub clause	Issue	Section where Covered
		(8) Measurement techniques for recording meteorological data should be in line with the standards published by the national meteorological services. The general tendency is to record average values for a given constant duration, such as 3s gusts, 60s averages or 10min averages (the averaging time is a characteristic of the database).	5.8.5
		(9) The wind vector at different elevations and temperatures should be averaged at least once per hour, while the period of integration for other variables such as solar radiation levels and precipitation levels should be one hour. Wind direction should be averaged as a vector and wind speed as a scalar over the prescribed time period.	5.8.6.1
		(10) The basic reduced data should be compiled into monthly or seasonal and annual joint frequency distributions of wind speed and wind direction by atmospheric stability class. Similar tables of joint frequency distribution should be prepared for each of the other atmospheric stability classes.	5.8.6.1
		(11) In developing site-specific diffusion models, sufficient information should be acquired on the space and time distributions of wind and temperature to be able to understand and determine the trajectory of effluents.	5.8.6 & 5.8.7
		a) Fluctuations in wind direction (sigma theta method); b) Air temperature and temperature lapse rate (delta-T method); c) Wind speed and solar radiation levels or sky cover during the daytime, and sky cover or net radiation levels at night-time (insulation method); and	5.8.6.1 & 5.8.6.1.8

RG 0011 clause	RG 0011 sub clause	Issue	Section where Covered
		d) Wind speed at different heights.	
		(13) Determination of the temperature variation for an atmospheric layer with height between at least two measurement levels should be provided. These levels should include the level at which the wind is measured.	5.8.5 & 5.8.6.1.2
		(14) The frequency, duration and time of the measurements of temperature variation with height should be concomitant with the wind data.	5.8.5 & 5.8.5.3
		(15) Precipitation and humidity should be recorded at least hourly.	5.8.5.2 & 5.8.6.1.3
		(16) A joint frequency distribution of wind direction and wind speed for each stability class (three-dimensional weather statistics) should be provided.	5.8.6.1.9
		(17) The probability of occurrence of different sets of meteorological conditions should be determined during different periods of time over the duration of, for example: An accident, in the first hours of the postulated accident, on the first day, over the first week and over the balance of the duration of the accident	5.8.7
10 nuclear security arrangements during siting	10.4 Security Plan and Measures	(11) Determination of the temperature variation for an atmospheric layer with height between at least two measurement levels should be provided. These levels should include the level at which the wind is measured.	5.8

Information from the Meteorology Section is used in a number of other sections of this SSR. ***Table 5.8.84*** is a summary of the links to different sections that requires meteorological information.

Table 5.8.84
Summary of Activities, Links and Quality Requirements

Activity	Links		Quality Requirements
	Inputs	Outputs	
Meteorological Measurement	Desk studies, Additional measurements	***Section 5.9*** (Oceanography and Coastal Engineering) – wind speed, wind direction and barometric pressure ***Section 5.10*** (Hydrology and Hydraulics) – rainfall ***Section 5.11*** (Geohydrology) - recharge and water balance calculations used in the groundwater modelling ***Chapters 6*** (Evaluation of External Events) and ***7*** (Potential Radiological Impact on the Public and the Environment) - external events ***Chapter 8*** – wind speed, stability joint frequency table	Monitoring protocol Calibration certificates Certificate of accreditation for selected laboratories
Modelling	Location and Plant perimeter envelope in ***Chapter 1*** (Introduction) Sea temperature measurements in ***Section 5.9***	***Section 5.11*** – deposition rates for input into the contaminant transport modelling ***Chapter 7*** – air concentration and deposition rates for input into the health risk calculations	Table showing rationale for selection of model code(s). International benchmarking, use and acceptability. Validation and verification of computer software codes used to comply with NNR requirements. Uncertainties and management/incorporation thereof. Sensitivity analysis. Peer Review

5.8.10.1 Maintenance and Service

Proper maintenance of weather station components is required to obtain accurate data. Thus, calibration and inspection of the instruments is done on a bi-annual basis to ensure that the equipment is in good operating condition and measurements are made according to the prescribed standards.

Routine and simple maintenance is accomplished through visual inspection of the weather station by the Koeberg Weather Station personnel. The following preventative maintenance steps are in place to ensure a properly functioning weather station:

- once a month:
  - checking of the solar radiation sensor for level and contamination and clean if necessary;
  - checking of the rain gage funnel for debris and level;
  - visual inspection of the wind sensors and radiation shield;
  - visual inspection of the anemometer at low wind speeds;
  - checking of the filter of the temperature/humidity sensors for contamination;
- bi-annually:
  - calibration of meteorological sensors and their accuracy verified;
  - replacing anemometer bearings;
  - cleaning the radiation shield;
  - replacing sensor cables as required.

In addition, general maintenance of meteorological equipment includes:

- occasional cleaning of the glass on the solar panel;
- checking of the sensor leads and cables for cracking, deterioration, proper routing and strain relief;
- checking of the tower for structural damage, proper alignment and level;
- checking of the equipment quality as part of normal operation;
- checking and control exposure of the instruments regularly;

- check of battery power;
- checking of operational mode of the data logger;
- quality control of all data recorded.

More specific maintenance such as sensor calibration, sensor performance testing and sensor component replacement is done by a skilled technician.

The date and time of the calibration, together with the name of the person who performed the calibration, is recorded on the calibration certificate for future reference.

The meteorological system aims to provide a minimum critical data availability of 80 per cent prior to operation, and 99 per cent monthly during operation of the nuclear installation(s).

5.8.10.2 Data collection and storage

As per the IAEA (International Atomic Energy Agency, 2002; International Atomic Energy Agency, 2011), the measurement of meteorological parameters should include air temperature, wind speed and wind direction, precipitation and humidity, measured at standard heights and exposure for the variables. A basic meteorological monitoring programme consists of measurements of horizontal wind speed; horizontal wind direction; air temperature, including the difference between air temperatures at two vertical levels on a tower; liquid precipitation; and any combination of additional measurements necessary to determine atmospheric stability (American National Standard, 2015).

The standard vertical location or height for horizontal wind speed and direction measurements shall be at approximately 10 m above ground level (American National Standard, 2015). Additional measurements should be made at the level representative of the most probable atmospheric release height applicable to activities involving radioactive and toxic chemical substances, considering the input data requirements of dispersion models used by the facility analysts and emergency responders. In some cases, horizontal wind speed measurements may be taken at other levels to meet specific requirements of the meteorological monitoring programme.

The monitoring level for air temperature shall be at a height applicable to programme requirements or at 2 m (American National Standard, 2015). The monitoring levels for delta temperature shall be spaced such that the profile is representative of, and characterises the magnitude of, atmospheric turbulence at any potential release height(s) from the affected facility (American National Standard, 2015). Typical pairing of sensor heights is

60 m and 10 m, or 10 m and 2 m above ground level, depending on the turbulence determination methodology (American National Standard, 2015).

Wind speed and direction is measured at a height of 9 m[25] at the Duynefontyn WS. Dry-bulb temperature is measured at 2 m above ground level and at 8 m above ground level. The data at the Duynefontyn WS are collected onsite and processed electronically using a Campbell CR10X data logger and stored in the data logger memory. Sampling of instruments is done at 10-second intervals and stored as 10-minute averages. Downloading from the data logger is done using a portable computer with an RS232 link.

All meteorological data are continuously collected on site.

Wind speed, wind direction and dry-bulb temperature are measured at heights of 10 m, 50 m, 85 m and 120 m on the 120-m tower. The data from the instruments on the 120-m tower are downloaded via cable and stored directly onto computer, as 3-second readings. These data are moved to a Microsoft database for analysis and reporting purposes.

Responsibility for management and custodianship of documents and data lies with the Eskom Nuclear Sites Project Manager (refer to ***Chapter 10***).

5.8.11 Potential Impact on the Nuclear Installation Design and Operation

External meteorological events could pose hazards that affect very specific nuclear installation systems and are not usually considered in the structural integrity evaluation of the buildings, for example low pressures during extreme wind conditions could affect roof structures, or overpressures that would be obtained from a tornado. Therefore, the following needs to be considered (International Atomic Energy Agency, 2021) in the hazard evaluation and also in the nuclear installation design:

- the impact of wind and lightning on the availability of off-site power;
- the impact of temperature, moisture and lightning on the functionality of safety related equipment, and particularly the instrumentation and control equipment;
- the corrosion potential on the structural integrity of buildings.

Experience has shown (International Atomic Energy Agency, 2021) that the damage caused by lightning could be extensive. It has mainly affected electrical equipment in recorded events, but very often has developed into

---

[25] Although the difference between 10 m and 9 m is small, a wind profile correction (typically about 1 per cent, depending on the atmospheric stability and surface roughness length) may be applied to standardise to 10 m.

transformer explosions, serious fire accidents and spurious signals to valves with consequent flooding and loss of off-site power. Special protection from lightning should be designed and implemented, with periodic assessment of a proper earthing system and regular inspections of the insulation of exposed equipment. In general, a comprehensive Faraday cage should be put in place by means of narrow mesh thin steel reinforcing in the outer skin of the building walls. Special care should be taken in the protection of conductors at short distances from each other and/or protruding from the cage protected volume.

Although it was shown that snow is unlikely to occur, if present on the site, it could induce damage to and unavailability of the power supply or the electrical grid. It could also affect ventilation intakes and discharges, structural loading, access by the operator to external safety related facilities and mobility of emergency vehicles.

Consideration should be also given to extreme low temperature that:

- may adversely affect instrumentation and control systems, which may generate spurious signals;
- created moisture condensation in closed rooms, with consequent dropping of water onto electrical equipment causing short circuits and malfunctions;
- may prevent the air ventilation system from working properly;
- may hinder proper operation of diesel generators where the fuel show separation of paraffin;
- may damage the external power supply system and limit the availability of service water.

5.8.12 Conclusions

The site-specific parameters applicable to the site are given in ***Table 5.8.85*** and ***Table 5.8.86.*** The chosen values for the rainfall, wind speed and atmospheric stabilities were based on the time covered by the database at the 120-m tower. Temperature parameters were based on both the 120-m tower (observed at 10 m height level) and the Duynefontyn WS (2 m height level). The former database was used due to the length of the observation record for predicting extreme values (return periods). An attempt was made to estimate the impact that climate change may have on these extreme projections. Although the climate change projections indicate a decrease in rainfall and possibly the number of extreme rainfall events, the assumption was made that the projections would be the same as currently experienced.

Table 5.8.85
Site Specific Parameters Part 1

Meteorological Parameter		Baseline	Climate Change Projections (Including 95% Confidence Intervals)			
			2044	**2064**	**2110**	**2130**
Annual Average		4.1	4.2 ± 0.2	4.3 ± 0.2	4.4 ± 0.2	4.5 -0.3+0.2
Hourly Maximum Wind Speed [m/s] (10 m above site ground level)	Extreme Observed & Projected	17.2	17.4 ±0.3	17.5 ±0.3	17.7 ±0.3	17.9 ±0.3
	10 Year Return	16.9 ± 1.0	17.3 ± 1.0	17.6 ± 1.0	18.3 ± 1.0	18.7 ± 1.0
	100 Year Return	21.6 ± 1.5	22.1 ± 1.5	22.5 ± 1.5	23.4 ± 1.5	23.9 ± 1.5
	1 000 Year Return	26.3 ± 2.2	26.9 ± 2.2	27.3 ± 2.2	28.4 ± 2.2	29.0 ± 2.2
	10 000 Year Return	30.9 ± 2.8	31.6 ± 2.8	32.1 ± 2.8	33.4 ± 2.8	34.1 ± 2.8
	100 000 Year Return	35.5 ± 3.5	36.4 ± 3.5	36.9 ± 3.5	38.4 ± 3.5	39.2 ± 3.5
	1 000 000 Year Return	40.2 ± 4.2	41.1 ± 4.2	41.7 ± 4.2	43.4 ± 4.2	44.3 ± 4.2
	10 000 000 Year Return	44.8 ± 4.8	45.8 ± 4.8	46.5 ± 4.8	48.4 ± 4.8	49.4 ± 4.8
	100 000 000 Year Return	49.4 ± 5.5	50.5 ± 5.5	51.3 ± 5.5	53.4 ± 5.5	54.5 ± 5.5
Wind peaks (**gusts**) [m/s] (10 m above site ground level)	Extreme Observed & Projected	38.8	39.2 -0.6+0.5	39.4± 0.6	40.0 ± 0.7	40.3 ± 0.7
	10 Year Return	33.8 ± 2.7	34.1 ± 2.7	34.2 ± 2.7	34.8 ± 2.7	35.1 ± 2.7
	100 Year Return	43.3 ± 4.8	43.7 ± 4.8	43.9 ± 4.8	44.6 ± 4.8	45.0 ± 4.8
	1 000 Year Return	52.7 ± 6.8	53.2 ± 6.8	53.4 ± 6.8	54.3 ± 6.8	54.8 ± 6.8
	10 000 Year Return	62.0 ± 8.9	62.6 ± 8.9	62.9 ± 8.9	64.0 ± 8.9	64.5 ± 8.9
	100 000 Year Return	71.4 ± 11.0	72.1 ± 11.0	72.4 ± 11.0	73.6 ± 11.0	74.2 ± 11.0
	1 000 000 Year Return	80.8 ± 13.1	81.5 ± 13.1	81.9 ± 13.1	83.3 ± 13.1	84.0 ± 13.1

Meteorological Parameter		**Baseline**	**Climate Change Projections (Including 95% Confidence Intervals)**			
			2044	**2064**	**2110**	**2130**
	10 000 000 Year Return	90.1 ± 15.2	90.9 ± 15.2	91.4 ± 15.2	92.9 ± 15.2	93.7 ± 15.2
	100 000 000 Year Return	99.5 ± 17.3	100.4 ± 17.3	100.9 ± 17.3	102.6 ± 17.3	103.4 ± 17.3
Ambient temperature [°C]	Mean daily maximum dry bulb temperature	20.1	21.1 -0.4+0.5	21.8 -0.4+0.5	23.7 -0.4+0.5	24.7 -0.4+0.5
	- coincident wet bulb temperature (a)	16.0	18.0 -0.3+0.1	18.3 -0.4+0.2	19.1 -0.5+0.2	19.4 -0.7+0.2
	Mean daily maximum wet bulb temperature (a)	16.2	18.2 -0.2+0.2	18.5 -0.2+0.4	19.3 -0.2+0.6	19.7 -0.3+0.6
	Extreme Observed & Projected dry-bulb maximum	38.8	39.8 -0.5+0.4	40.5 -0.5+0.4	42.4 -0.5+0.4	43.5 -0.5+0.4
	10 Year Return	37.5 ± 0.9	40.3 ± 1.8	41.1 ± 1.8	43.4 ± 2.0	44.5 ± 2.0
	100 Year Return	40.4 ± 2.0	42.6 ± 2.7	43.4 ± 2.8	45.6 ± 2.9	46.8 ± 3.0
	1 000 Year Return	43.3 ± 3.2	44.9 ± 3.7	45.7 ± 3.8	47.9 ± 3.9	49.1 ± 4.0
	10 000 Year Return	46.2 ± 4.3	47.1 ± 4.7	48.0 ± 4.8	50.2 ± 4.9	51.3 ± 4.9
	100 000 Year Return	49.1 ± 5.5	49.4 ± 5.7	50.2 ± 5.8	52.4 ± 5.9	53.6 ± 5.9
	1 000 000 Year Return	52.0 ± 6.7	51.7 ± 6.7	52.5 ± 6.8	54.7 ± 6.9	55.9 ± 6.9
	10 000 000 Year Return	54.9 ± 7.9	53.9 ± 7.7	54.7 ± 7.7	57.0 ± 7.9	58.1 ± 7.9
	100 000 000 Year Return	57.8 ± 9.0	56.2 ± 8.7	57.0 ± 8.7	59.2 ± 8.9	60.4 ± 8.9
	Maximum temperature of 3-hour duration (b)	37.0 Corresponding Wet Bulb Temperature 19.0	37.9 -0.5+0.3	38.6 -0.5+0.4	40.5 -0.6+0.5	41.4 -0.8+0.5
	Maximum temperature of 6-hour duration (b)	36.1	37.0 -0.5+0.3	37.7 -0.5+0.4	39.6 -0.6+0.5	40.5 -0.8+0.5

Meteorological Parameter		Baseline	Climate Change Projections (Including 95% Confidence Intervals)			
			2044	2064	2110	2130
		Corresponding Wet Bulb Temperature 18.9				
	Maximum temperature of 7-day duration (b)	18.5 Corresponding Wet Bulb Temperature 15.5	19.4 -0.5+0.3	20.1 -0.5+0.4	22.0 -0.6+0.5	22.9 -0.8+0.5
	Mean daily minimum dry bulb temperature	13.1	13.8 -0.3+0.3	14.2 -0.3+0.3	15.4 -0.3+0.3	16.1 -0.2+0.3
	- coincident wet bulb temperature (a)	11.5	12.9 -0.2+0.1	13.1 -0.2+0.1	13.7 -0.4+0.2	14.0 -0.5+0.2
	Mean daily minimum wet bulb temperature (a)	11.0	12.4 -0.1+0.2	12.6 -0.1+0.2	13.1 -0.2+0.4	13.4 -0.2+0.5
	Extreme Observed & Projected dry-bulb minimum	3.0	3.9 -0.5+0.4	4.6 -0.5+0.4	6.5 -0.7+0.6	7.5 -0.8+0.7
	10 Year Return	3.5 ± 0.5	3.4 ± 0.8	4.1 ± 0.8	5.8 ± 0.9	6.7 ± 0.9
	100 Year Return	1.6 ± 1.0	2.0 ± 1.2	2.7 ± 1.2	4.4 ± 1.3	5.3 ± 1.3
	1 000 Year Return	-0.2 ± 1.5	0.7 ± 1.6	1.3 ± 1.7	3.0 ± 1.7	3.9 ± 1.7
	10 000 Year Return	-2.1 ± 2.0	-0.7 ± 2.1	-0.1 ± 2.1	1.6 ± 2.1	2.5 ± 2.2
	100 000 Year Return	-3.9 ± 2.5	-2.1 ± 2.5	-1.5 ± 2.5	0.2 ± 2.6	1.1 ± 2.6
	1 000 000 Year Return	-5.8 ± 3.0	-3.5 ± 2.9	-2.9 ± 3.0	-1.2 ± 3.0	-0.2 ± 3.0
	10 000 000 Year Return	-7.6 ± 3.5	-4.9 ± 3.4	-4.3 ± 3.4	-2.6 ± 3.5	-1.6 ± 3.5
	100 000 000 Year Return	-9.5 ± 4.0	-6.3 ± 3.8	-5.7 ± 3.8	-4.0 ± 3.9	-3.0 ± 3.9
	Minimum temperature of 3-hour duration (b)	4.5	5.4 -0.5+0.3	6.1 -0.5+0.4	8.0 -0.6+0.5	8.9 -0.8+0.5

Meteorological Parameter		Baseline	Climate Change Projections (Including 95% Confidence Intervals)			
			2044	2064	2110	2130
		Corresponding Wet Bulb Temperature 3.6				
	Minimum temperature of 6-hour duration (b)	4.8 Corresponding Wet Bulb Temperature 4.0	5.7 -0.5+0.3	6.4 -0.5+0.4	8.3 -0.6+0.5	9.2 -0.8+0.5
	Minimum temperature of 7-day duration (b)	14.0 Corresponding Wet Bulb Temperature 12.1	14.9 -0.5+0.3	15.6 -0.5+0.4	17.5 -0.6+0.5	18.4 -0.8+0.5
Rainfall [mm]	Average Annual Total	372.4	318.3 -8.8+8.4	300.3 -1.7+12.5	254.7 -1.9+5.5	229.6 -1.1+0.6
	Extreme Annual Total	640.4	Projections indicate reduction. Worst-case assumption assumes same as baseline			
	Annual Re-occurrences:					
	10 Year Return	471.1 ± 45.3	Projections indicate reduction. Worst-case assumption assumes same as baseline			
	100 Year Return	611.9 ± 85.7				
	1 000 Year Return	750.1 ± 127.0				
	10 000 Year Return	888.1 ± 168.7				
	100 000 Year Return	1026.1 ± 210.5				
	1 000 000 Year Return	1164.1 ± 252.4				
	10 000 000 Year Return	1302.1 ± 294.4				
	100 000 000 Year Return	1440.1 ± 336.4				
	Extreme 24-hour Storm	70	Projections indicate reduction. Worst-case assumption assumes same as baseline			
	24-Hour Re-occurrences:					

Meteorological Parameter		Baseline	Climate Change Projections (Including 95% Confidence Intervals)			
			2044	2064	2110	2130
	10 Year Return	49.0 ± 7.3	Projections indicate reduction. Worst-case assumption assumes same as baseline			
	100 Year Return	69.0 ± 12.8				
	1 000 Year Return	88.6 ± 18.3				
	10 000 Year Return	108.1 ± 23.7				
	100 000 Year Return	127.7 ± 29.2				
	1 000 000 Year Return	147.2 ± 34.7				
	10 000 000 Year Return	166.7 ± 40.2				
	100 000 000 Year Return	186.3 ± 45.7				
	Extreme 1-hour Storm	23.6	Insufficient data to make projection. Assume same as baseline			
Mean Sea Level Atmospheric pressure [hPa]	Daily Minimum	910.6 (September)	Not available	Not available	Not available	Not available
	Daily Maximum	1040.0 (July)	Not available	Not available	Not available	Not available
	Extreme Lower (Hourly)	932.5	932.3 -0.3+0.2	932.1 -0.4+0.3	931.7 -0.3+0.4	930.7 -0.4+0.3
	Mean Annual	1016.2	1015.9 -0.3+0.3	1015.7 -0.3+0.4	1015.3 -0.4+0.3	1015.0 -0.4+0.4
	Extreme Upper (Hourly)	1046.9	1046.9 -0.0+0.1	1046.9 -0.0+0.0	1046.9 -0.0+0.0	1046.9 -0.0+0.0

Notes:

(a) Wet-bulb temperature projections are not part of the primary meteorological variables provided by the climate change mode used in the analyses. The projections provided in the table are based on using the daily minimum, mean and maximum temperature projected increases and assuming ±25% variation in the corresponding moisture content.

(b) Temperatures of 3-hour, 6- hour and 7-day durations assumed projected temperature increases as per the climate change model.

Table 5.8.86
Site Specific Parameters Part 2

Meteorological Parameter			Value			
Tornadoes	Tornado Probability (EF - Enhanced Fujita Scale)	Based on 116-year database 1905 -2020	All(2)	1.0×10^{-5} per year per km²		
			EF0	7.0×10^{-6} per year per km²		
			EF1	2.4×10^{-6} per year per km²		
			EF2	5.6×10^{-7} per year per km²		
			EF3	1.0×10^{-8} per year per km²		
			EF4	$<1.0 \times 10^{-8}$ per year per km²		
		Based on 34-year database 1987 - 2020 (1)	All(2)	2.2×10^{-5} per year per km²		
			EF0	1.7×10^{-5} per year per km²		
			EF1	5.2×10^{-6} per year per km²		
			EF2	1.2×10^{-6} per year per km²		
			EF3	2.2×10^{-8} per year per km²		
			EF4	$<2.2 \times 10^{-8}$ per year per km²		
	10^{-7} per year wind speed: - maximum wind speed - maximum translational - maximum rotational		 75.0 m/s 15.0 m/s 60.0 m/s			
			Lower Quartile	Upper Quartile	Median	Average
	Path Width [m]:					
	EF0 tornado (70% to 74% probability)		22.9	68.6	45.7	54.9
	EF1 tornado (23% to 24% probability)		68.6	182.9	91.4	163.8
	EF2 tornado (5% to 6% probability)		137.2	402.3	228.6	344.1
	EF3 tornado (<0.01% probability)		339.5	1005.8	548.6	736.3
	Path Length [km]					
	EF0 tornado (70% to 74% probability)		0.29	2.7	0.8	2.27
	EF1 tornado (23% to 24% probability)		1.77	9.33	4.4	7.1
	EF2 tornado (5% to 6% probability)		4.53	19.25	10	14.3
	EF3 tornado (<0.01% probability)		12.38	36.34	23	29.1
	Pressure drop for 10^{-7} per year wind speed		40 hPa			
	Maximum rate of pressure drop for 10^{-7} per year wind speed		13 hPa/s			
Atmospheric Turbulence (Delta-T Method)	Convective (A)		1.55%			
	Unstable (B)		2.02%			

Meteorological Parameter		Value	
(120-m Tower)	Moderately Unstable (C)	3.28%	
	Neutral (D)	33.86%	
	Moderately Stable (E)	37.44%	
	Stable (F)	16.54%	
	Very Stable (G)	5.30%	
Prolonged Inversions	Likelihood	Annual	22%
		Summer	14%
		Winter	30%
Snowfall (3)	Average	0.0 mm/h	
	Maximum load	0.0 N/m^3	
Lightning	Flashes/year/km^2	0.3 flashes/year/km^2 (range 0.2 to 1.6)	
	Average strokes per flash	13.75	
	Maximum strokes per flash	25	
	Average peak current	25 kA	
	Highest peak current	166 kA	
Thunder	No. days with thunder	7.0 days/year	
Hail	No. days with hail	1.0 days/year	
Frost	No. days with frost	0 days/year	
Fog	No. days with fog	60 days/year	
Relative humidity	Summer (relative humidity at 37 ºC, dry bulb)	14.6%	
	Winter (relative humidity at -25 ºC, dry bulb)	91.1% at lowest temperatures Assume 100% at -25ºC	
Solar Radiation	Lowest daily total	8.3 MJ/m^2.day (June)	
	Highest daily total	30.9 MJ/m^2.day (December)	
Penman Evapotranspiration	Monthly Total Minimum	76.3 mm (June)	
	Monthly Total Maximum	237.0 mm (December)	
Corrosivity	Rate in 1st year	Carbon steel	85.8 µm/year
		Zinc	3.4 µm/year
		Copper	1.9 µm/year
		Aluminium	1.2 µm/year
	Average rate over 20 years	Carbon steel	20.0 µm/year
		Zinc	1.9 µm/year
		Copper	0.7 µm/year

Meteorological Parameter		Value	
		Aluminium	0.5 µm/year

Notes:

(2) Tornado activity has increased since 1987 within an 80 km radius from the site. Whilst climate change may have contributed to increases in tornado frequencies, it may also simply be that the reporting of tornadoes has increased due to population spread as well as the associated damage to property.

(3) The “All” tornado entry combines all frequencies from EF0 to EF4 in the table.

(4) This reflects current observation; however extreme minimum temperatures (excluding climate change projections indicate temperatures well below freeze point for water and may result in the occurrence of snow at the site

5.8.13 References

1. Ackerman, S. A. & Cox, S. K., 1989. Surface weather observations of atmospheric dust over the Southwest Summer Monsoon Region. *Meteorology and Atmospheric Physics,* Volume 41, pp. 19-34.
2. Alduchov, O. A. & Eskridge, R. E., 1996. Improved Magnus Form Approximation of Saturation Vapor Pressure. *J. Appl. Meteor.,* Volume 35, pp. 601-609.
3. American National Standard, 2015. *Determining Meteorological Information at Nuclear Facilities, American Nuclear Society, ANSI/ANS-3.11-2015.,* s.l.: American National Standard.
4. Baddock, M. C. et al., 2014. A visibility and total suspended dust relationship. *Atmospheric Environment,* Volume 89, pp. 329-336.
5. Barry, N. T. & Kuyatt, C. E., 1994. *Guidelines for Evaluating and Expressing the Uncertainty of NIST Measurement Results, NIST Technical Note 1297,* Githersburg: , National Institute of Standards and Technology, United States Department of Commerce Technology Administration.
6. Burger, L., 2022. *Corrosion Monitoring Using ISO 9226 Method at Koeberg Weather Station: 11 April 2008 to 10 March 2022, SRK Database Archive,* Cape Town: s.n.
7. Burger, L. W., 2021. *V&V Report for Meteorology,* Halfway House: Airshed Planning Professionals.
8. Chepil, W. S. & Woodruff, N. P., 1957. Sedimentary characteristics of dust storms: II. Visibility and dust concentration. *American Journal of Science,* Volume 255, pp. 104-114.
9. Cimorelli, A. J. et al., 2004. *AERMOD: Description of Model Formulation, EPA-454/R-03-004,* Research Triangle Park, NC: U.S. Environmental Protection Agency.
10. Clemence, B. S. E., 1992. An Attempt at Estimating Solar Radiation at South African Sites Which Measure Air Temperature Only.. *South African Journal of Plant and Soil,* pp. 9, 40-42.
11. CSIR, 2021. *Eskom-CSIR 50-km Resolution Downscaled Climate Change Simulation Results, Data Bundles: 16 April 2021 Revised 28 April 2021 (“modelData_CSIR.zip”).* Pretoria: Council for Scientific and Industrial Research.
12. Department of Energy, 2011. *R.927: National Nuclear Regulator Act, 1999 (Act No. 47 OF 1999): Regulations on Licensing of Sites for New Nuclear Installations.* Pretoria: Government Gazette 34735.

13. Elsner, J. B., Jagger, T. H. & Elsner, I. J., 2014. Tornado Intensity Estimated from Damage Path Dimensions. *PLOS One,* 9(9), pp. 1-7.
14. Engelbrecht, F. et al., 2019. *Climate Change Vulnerability Projections at Ultrahigh Spatial Resolutions (8 km) over South Africa, Eskom Confidential Research Report No. RES/RR/15/1780145.,* Johannesburg: Eskom.
15. Eskom, 1997. *Monthly Hardcopy Reports: January 1980 to September 1997, Koeberg Weather Station,* Cape Town: Eskom.
16. Eskom, 2017. *Meteorological Requirements for Nuclear Installations. Standard 238-52,* Cape Town: Eskom.
17. Eskom, 2019a. *Address NNR comments on and update the Duynefontyn and Thyspunt Site Safety Reports Chapters 5, 6, 7 and 8 inclusive of extended monitoring on Meteorology and Geohydrology and data gathering. NSIP03894, 6 February 2019,* s.l.: Eskom.
18. Eskom, 2021. *Technical Specifications for the Development of Site Safety Reports. NSIP01388. Rev 1.,* Johannesburg: Eskom.
19. Eskom, 2022. *Technical Specification for Site Safety Reports. NSIP01388. Rev 2,* Cape Town: Eskom.
20. Eskom, 2023a. *Electronic Hourly Average 120-m Mast Microsoft Database: Oct1997 to Sep2023, Koeberg Weather Station,* Cape Town, SRK Database Archive, Cape Town: s.n: Eskom.
21. Eskom, 2023b. *Electronic Hourly Average Meteorology for Atlantis, Bok Point, Rondekuil, Milnerton and Robben Island: 1997 to September 2023, Koeberg Weather Station,* Cape Town: Eskom, SRK Database Archive.
22. Ette, I. I. I. & Olorode, D. O., 1988. The effects of the Harmattan dust on air conductivity and visibility at Ibadan, Nigeria. *Atmospheric Environment,* Volume 22, pp. 2625-2627.
23. Gifford, F. A., 1961. Uses of Routine Meteorological Observations for Estimating Atmospheric Dispersion. *Nuclear Safety,* Volume 2, pp. 547-51.
24. Gijben, M., 2021. *The South African Lightning Detection Network: MTG LI Mission Advisory Group Meeting, South African Weather Service..* [Online]
Available at: https://www.eumetsat.int/media/47898/The South African Lightning Detection Network.pdf
[Accessed 20 February 2021].
25. Gill, T., 2009. *Initial Steps in the Development of a Comprehensive Lightning Climatology of South Africa.* Johannesburg: Master of Science

Thesis, University of the Witwatersrand, School of Geography, Archaeology and Environmental Studies: Climatology Research Group.

26. Goliger, A. M., Milford, R. V., Adam, B. F. & Edwards, M., 1997. *Inkanyamba - Tornadoes in South Africa.* Pretoria: United Litho.
27. Greer, I. W., 1996. *Glossary of Weather and Climate with Related Oceanic and Hydrologic Terms..* Boston: American Meteorological Society.
28. Gross, C. J. & Nixon, M., 1993. *Review of Corrosion Data for the Proposed Nuclear Sites on the Eastern, Southern and Western Cape Coasts. Eskom Report No. TRR/S93/091, Project No. 7762M168U/089,* Johannesburg: Section: Materials Technology, Department: Scientific invest.
29. Guo, J. et al., 2022. Damage Mechanism and Modeling of Concrete in Freeze–Thaw Cycles: A Review.. *Buildings 2022,* Volume 12, p. 1317.
30. Hanna, S. R., Egan, B. A., Purdum, J. & Wagler, J., 1999. Evaluation of the ADMS, AERMOD, and ISC3 Dispersion Models with the Optex, Duke Forest, Kincaid, Indianapolis, and Lovett Field Data Sets. *International Journal of Environment and Pollution,* 16(1-6), p. 2001.
31. Herbst, L. & Rautenbach, H., 2015. Climate Change Impacts on Mean Wind Speeds in South Africa. *The Clean Air Journal,* 25(2).
32. Hsu, S. A., 1977. Boundary Layer Meteorological Research in the Coastal Zone,. *Geoscience and Man, H. J. Walker, ed., School of Geoscience, Louisiana State University, Baton Rouge, LA,* Volume 18, pp. 99-111.
33. Institute for Commercial Forestry Research, 2003. *Daily Rainfall Data Extraction Utility, User Manual Version 1.2. ,* Pietermaritzburg: KwaZulu-Natal University.
34. Intergovernmental Panel on Climate Change, 2012. *Managing the Risks of Extreme Events and Disasters to Advance Climate Change Adaptation. A Special Report of Working Groups I and II of the Intergovernmental Panel on Climate Change ,* Cambridge, UK and New York, USA: Cambridge University Press.
35. Intergovernmental Panel on Climate Change, 2013. *Climate Change 2013: The Physical Science Basis. Contribution of Working Group I to the Fifth Assessment Report of the Intergovernmental Panel on Climate Change,* Cambridge, UK, and New York, NY, USA: Cambridge University Pres.
36. International Atomic Energy Agency, 2001. *Generic Models for Use in Assessing the Impact of Discharge of Radioactive Substances to the*

Environment. Safety Report Series No. 19., Vienna: International Atomic Energy Agency.

37. International Atomic Energy Agency, 2002. *Dispersion of Radioactive Material in Air and Water and Consideration of Population Distribution in Site Evaluation for Nuclear Power Plants. Safety Standards Series, Safety Guide. No.NS-G-3.2,* Vienna: International Atomic Energy Agency.
38. International Atomic Energy Agency, 2011. *Meteorological and Hydrological Hazards in Site Evaluation for Nuclear Installations, Safety Standard Series, Specific Safety Guide No. SSG-18,* Vienna: International Atomic Energy Agency.
39. International Atomic Energy Agency, 2019. *Site Evaluation for Nuclear Installations. Safety Standard Series, Specific Safety Requirements No. SSR-1,* Vienna: International Atomic Energy Agency.
40. International Atomic Energy Agency, 2021. *Design of Nuclear Installations Against External Events Excluding Earthquakes. Safety Standards Series, Specific Safety Guide No. ssg-68,* Vienna: International Atomic Energy Agency.
41. International Organisation for Standardisation, 2012a. *ISO 9223 (2012), Corrosion of Metals and Alloys-Corrosivity of Atmospheres – Guiding Values for the Corrosivity Categories. 2nd Edition,* Geneva: International Organisation for Standardisation.
42. International Organisation for Standardisation, 2012b. *ISO 9224 (2012), Corrosion of Metals and Alloys-Corrosivity of Atmospheres - Guiding Values for the Corrosivity Categories. 2nd Edition.* Geneva: International Organisation for Standardisation.
43. International Organisation for Standardisation, 2012c. *ISO 9225 (2012), Corrosion of Metals and Alloys-Corrosivity of Atmospheres - Measurement of Pollution. 2nd Edition,* Geneva: International Organisation for Standardisation.
44. International Organisation of Standardisation, 2012d. *ISO 9226 (2012), Corrosion of Metals and Alloys-Corrosivity of Atmospheres - Determination of Corrosion Rate of Standard Specimens for the Evaluation of Corrosivity. 2nd Edition,* Geneva: International Organisation of Standardisation.
45. International Organisation of Standardisation, 2017. *ISO 17025 (2017), General Requirements for the Competence of Testing and Calibration Laboratories,* Geneva: International Organisation of Standardisation.
46. Johnston, P., 1983. *Variations in Albedo Among Natural and Disturbed South Western Cape Veld Types, Research Report No.46,* Cape Town: School of Environmental Studies, University of Cape Town.

47. Kruger, A. C. & Nxumalo, M. P., 2017. Historical rainfall trends in South Africa: 1921–2015. *Water SA,* 43(2), pp. 285-297.
48. Kruger, A. C. & Nxumalo, M., 2016. Surface Temperature Trends from Homogenized Time Series in South Africa: 1931–2015. *International Journal of Climatology,* 37(5), pp. 2364-2377.
49. Le Roux, J. J., 1983. *Climate of South Africa. Part 11: Extreme Values of Rainfall, Temperature and Wind for Selected Return Periods, WB 36,* Pretoria: Weather Bureau, Department of Transport..
50. Malan,, D. J., 1956. The Relation Between the Number of Strokes, Stroke Interval and the Total Duration of Lightning Discharges. *. Geofisica, Pura e Applicalo Milan,* Volume 34, pp. 224-230.
51. Marticorena, B. & Bergametti, G., 1995. Modelling the Atmospheric Dust Cycle: 1. Design of a Soil-Derived Dust Emission Scheme. *Journal of Geophysical Research,* Volume 100, pp. 16415-16430.
52. McDonald, J. & Mehta, K. C., 2006. *A Recommendation for an Enhanced Fujita Scale (EF-Scale)..* Texas: Lubbock, Texas: Wind Science and Engineering Research Center, Texas Tech University.
53. National Nuclear Regulator, 2008. *RD-0034: Quality and Safety Management Requirements for Nuclear Installations. Rev 0,* Centurion: National Nuclear Regulator.
54. National Nuclear Regulator, 2012a. *Consideration of External Events for New Nuclear Installations, Position Paper PP-0014, Rev 0,* Centurion: National Nuclear Regulator.
55. National Nuclear Regulator, 2012b. *Emergency Planning Technical Basis For New Nuclear Installations, Position Paper PP-0015, Rev 0,* Centurion: National Nuclear Regulator.
56. National Nuclear Regulator, 2016a. *Interim Guidance for the Siting of Nuclear Facilities, Regulatory Guide RG-0011 Rev0,* Centurion: National Nuclear Regulator.
57. National Nuclear Regulator, 2016b. *Guidance on the Verification and Validation of Evaluation and Calculation Models used in Safety and Design Analyses, Regulatory Guide RG-0016, Rev 0,* Centurion: National Nuclear Regulator.
58. NDMC, 2021. *Standardized Precipitation Index (SPI), Integrated Drought Management Programme.* [Online] Available at: https://drought.unl.edu/droughtmonitoring/SPI/SPIProgram.aspx
59. Pasquill, F., 1961. The Estimation of the Dispersion of Windborne Materials.. *Meteorological Magazine,* Volume 90.

60. Patterson, E. M. & Gillette, D. A., 1977. Measurements of visibility vs mass of airborne soil particles. *Atmospheric Environment,* Volume 11, pp. 193-196.
61. Penman, H. L., 1948. Natural Evaporation from open Water, Bare and Grass.. *Proc. R. Soc. Lond., Ser. A 193,* , pp. 120-145.
62. Penman, H. L., 1963. *Vegetation and Hydrology. Technical Communication no. 53,* Harpenden, England: Commonwealth Bureau of Soils.
63. Perry, S. G. et al., 2004. AERMOD: A Dispersion Model for Industrial Source Applications. Part II: Model Performance Against 17 Field Study Databases. *Journal of Applied Meteorology,* Volume 44, pp. 694-708.
64. Preston-Whyte, R. A., Diab, R. D. & Tyson, P. D., 1977. Towards an Inversion Climatology of Southern Africa: Part II, Surface Inversions.. *South African Geographical Journal,* pp. 59(1), 45-59.
65. Preston-Whyte, R. A. & Tyson, P. D., 1988. *The Atmosphere and Weather over South Africa..* Cape Town: Oxford University Press.
66. Rakov, V. A., 2007. *Lightning Phenomenology and Parameters Important for Lightning Protection.* Foz do Iguaçu, Brazil, IX International Symposium on Lightning Protection 26-30 November 2007.
67. Rakov, V. A. & Huffines, G. R., 2003. Return Stroke Multiplicity of Negative Cloud-to-Ground Lightning Flashes. *J. App. Meteor.,* Volume 42, pp. 1455-1462.
68. Ramsdell, J. V.,Jr; Rishel, J. P.;, 2007. *Tornado Climatology of the Contiguous United States, NUREG/CR-4461, Rev 2,* Washington: U.S. Nuclear Regulatory Commission.
69. Riahi, K., Grübler, A. & Nakicenovic, N., 2007. Scenarios of Long-Term Socio-Economic and Environmental Development Under Climate Stabilization. *Technol Forecast Soc Chang,* Volume 74, p. 887–935.
70. Schonland, B. F. J., 1956. The Lightning Discharge. *Handbuch, der Physik (Springer - Verlag OHG, Berlin),* Volume 22, pp. 576-628.
71. Schulze, B., 1986. *Climate of South Africa, WB 40..* Pretoria: Weather Bureau, Department of Transport.
72. Schulze, R. E., 1997. *South African Atlas of Agrohydrology and Climatology..* Pietermaritzburg: Department of Agriculture and Engineering, University of Natal.
73. Schulze, R. E., 2011. *A 2011 Perspective on Climate Change and The South African Water Sector, Report TT518/12,* Pietermaritzburg: Water Research Commission..

74. Seidel, D. J., Fu, Q., Randel, W. J. & Reichler, T., 2008. Widening of the Tropical Belt in a Changing Climate. *Nat Geosci.,* Volume 1, pp. 21-24.
75. Shuttleworth, W., 1993. Chapter 4. In: D. Maidment, ed. *Evaporation.* New York: McGraw-Hill, p. pp. 4.1–4.53 .
76. South African National Standards, 2019. *SANS 10160-3:2019 Basis of Structural Design and Actions for Buildings and Industrial Structures, Part 3: Wind Actions,* Pretoria: South African Bureau of Standards.
77. South African Weather Bureau, 1996. *The Weather and Climate of the Extreme South-Western Cape,* Pretoria: Department of Environmental Affairs and Tourism.
78. South African Weather Service, 1991. *Caelum - A History of Notable Weather Events in South Africa 1550 – 1990,* Pretoria: SA Weather Service Publication.
79. South African Weather Service, 2017. *A Climate Change Reference Atlas: Based on CMIP5 – CORDEX Downscaling,* Pretoria: South African Weather Service.
80. South African Weather Services, 2011. *National Weather Service Database,* Pretoria: South African Weather Services.
81. South African Weather Services, 2020a. *Rainfall Measurement for Atlantis, Robben Island and Cape Tow Weather Office,* Bloemfontein: South African Weather Services.
82. South African Weather Services, 2020b. *Trends in Extreme Climate Indices in South Africa: 2019, Document Reference: WCS-CLS-WMO_EXTREME_CLIMATE_INDICES_2019.1, Ver. 01,* Pretoria: South African Weather Services.
83. Stull, R., 1997. *An Introduction to Boundary Layer Meteorology. Kluwer.* Amsterdam: Academic Publishers.
84. Stull, R., 2011. Wet-Bulb Temperature from Relative Humidity and Air Temperature. *American Meteorological Society,* 50(November), pp. 2267-2269.
85. Tyson , P. D., Preston-Whyte, R. A. & Diab, R. D., 1976. Towards an Inversion Climatology of Southern Africa: Part I, Surface Inversions.. *South African Geographical Journal,* Volume 58, pp. 151-163.
86. United States Environmental Protection Agency , 1992. *Fugitive Dust Background Document and Technical Information Document for Best Available Control Measures, EPA-450/2-92-004,* Springfield, VA: U.S. Department of Commerce.
87. United States Environmental Protection Agency, 2000. *Meteorological Monitoring Guidance for Regulatory Modeling Applications. Office of Air*

Quality Planning & Standards, EPA-454/R-99-005, Durham: United States Environmental Protection Agency.

88. United States Nuclear Regulatory Commission , 2007b. *Design Basis Tornado and Tornado Missiles for Nuclear Power Plants. Regulatory Guide. 1.76, Rev 1,* Washington DC: United States Nuclear Regulatory Commission .
89. United States Nuclear Regulatory Commission, 1983. *Atmospheric Dispersion Models for Potential Accident Consequence Assessments at Nuclear Power Plants. Regulatory Guide. 1.145, Rev 1,* Washington DC: United States Nuclear Regulatory Commission.
90. United States Nuclear Regulatory Commission, 2007a. *NUREG-0800, Section 2.3.1 (Regional Climatology), 2.3.2 (Local Meteorology), 2.3.3 (Onsite Meteorological Measurements Programs) and 2.3.4 (Shortterm Dispersion Estimates for Accident Releases) Rev 3,* Washington DC: United States Nuclear Regulatory Commission.
91. United States Nuclear Regulatory Commission, 2007c. *Meteorological Monitoring Programs for Nuclear Power Plants, Regulatory Guide. 1.23, Rev 1,* Washington DC: United States Nuclear Regulatory Commission.
92. United States Nuclear Regulatory Commission, 2011. *Design-Basis Hurricane and Hurricane Missiles for Nuclear Power Plants, Regulatory Guide. 1.221, Rev 1.,* Washington DC: United States Nuclear Regulatory Commission.
93. Vamsidhar , V. P., Kumar, A. & Kadiyala, A., 2010. Estimation of Uncertainty in Predicting Ground Level Concentrations from Direct Source Releases in an Urban Area Using the USEPA’s AERMOD Model Equations. In: A. Kumar, ed. *Air Quality.* s.l.:Intech.
94. Walder, J. & Hallet , B., 1985. A theoretical model of the fracture of rock during freezing. *Geol Soc Am Bull ,* Volume 96, p. 336–346.
95. World Meteorological Organisation, 2011. *Guide to Climatological Practices, WMO-No. 100,* Geneva: World Meteorological Organisation.
96. World Meteorological Organization, 2012. *Standardized Precipitation Index User Guide, WMO-No. 1090,* Geneva, Switzerlad: World Meteorological Organization.
97. Wright, M. A. & Grab, S. W., 2017. Wind Speed Characteristics and Implications for Wind Power Generation: Cape Regions, South Africa. *South African Journal of Science,* 113(7/8).

Appendix 5.8.A: Offsite Eskom AWS Wind Data Summaries

Table 5.8.A.1
Wind Speed and Direction Categorisation at the Bok Point WS (January 1998 to June 2019)

Wind Direction	Wind Speed [m/s] at 10 m level												Total (%)
	<0.5	0.5-1.0	1.0-2.0	2.0-3.0	3.0-4.0	4.0-5.0	5.0-6.0	6.0-8.0	8.0-10.0	10.0-13.0	13.0-18.0	>18.0	
N	0.03%	0.10%	0.51%	0.86%	1.52%	2.24%	1.92%	2.06%	0.96%	0.44%	0.04%	0.00%	10.67%
NNE	0.03%	0.09%	0.35%	0.42%	0.47%	0.67%	0.85%	0.61%	0.18%	0.04%	0.00%	0.00%	3.70%
NE	0.02%	0.10%	0.36%	0.32%	0.14%	0.08%	0.07%	0.17%	0.06%	0.01%	0.00%	0.00%	1.33%
ENE	0.02%	0.09%	0.48%	0.68%	0.26%	0.10%	0.06%	0.05%	0.01%	0.00%	0.00%	0.00%	1.75%
E	0.01%	0.10%	0.65%	1.27%	1.13%	0.97%	0.47%	0.12%	0.01%	0.01%	0.00%	0.00%	4.76%
ESE	0.01%	0.09%	0.75%	1.38%	1.71%	1.89%	1.64%	0.94%	0.11%	0.06%	0.00%	0.00%	8.59%
SE	0.01%	0.08%	0.70%	1.22%	1.12%	1.09%	1.11%	1.65%	0.65%	0.22%	0.01%	0.00%	7.85%
SSE	0.01%	0.08%	0.71%	1.29%	1.19%	1.26%	1.41%	2.59%	2.43%	2.60%	0.60%	0.00%	14.16%
S	0.01%	0.08%	0.70%	1.12%	0.88%	0.93%	1.08%	2.25%	1.59%	0.91%	0.17%	0.00%	9.72%
SSW	0.01%	0.08%	0.64%	0.94%	0.80%	0.89%	1.03%	1.96%	1.10%	0.29%	0.01%	0.00%	7.77%
SW	0.00%	0.07%	0.55%	0.86%	0.74%	0.65%	0.55%	0.65%	0.19%	0.07%	0.01%	0.00%	4.35%
WSW	0.01%	0.08%	0.47%	0.88%	0.70%	0.42%	0.24%	0.22%	0.15%	0.10%	0.02%	0.00%	3.28%
W	0.01%	0.08%	0.52%	0.96%	0.74%	0.43%	0.24%	0.25%	0.18%	0.11%	0.03%	0.00%	3.55%
WNW	0.01%	0.08%	0.56%	1.07%	1.31%	0.74%	0.41%	0.39%	0.16%	0.09%	0.03%	0.00%	4.86%
NW	0.02%	0.08%	0.51%	0.78%	0.89%	0.93%	0.81%	1.02%	0.41%	0.13%	0.03%	0.00%	5.60%
NNW	0.02%	0.10%	0.54%	0.91%	1.10%	1.18%	1.10%	1.78%	0.89%	0.36%	0.04%	0.00%	8.04%
TOTAL	0.22%	1.38%	9.00%	14.97%	14.69%	14.47%	12.99%	16.72%	9.08%	5.45%	1.01%	0.00%	100.00%

Table 5.8.A.2
Wind Speed and Direction Categorisation at the Milnerton WS (January 1998 to June 2022)

Wind Direction	Wind Speed [m/s] at 10 m level												Total (%)
	<0.5	**0.5-1.0**	**1.0-2.0**	**2.0-3.0**	**3.0-4.0**	**4.0-5.0**	**5.0-6.0**	**6.0-8.0**	**8.0-10.0**	**10.0-13.0**	**13.0-18.0**	**>18.0**	
N	0.12%	0.47%	1.64%	1.64%	0.93%	0.43%	0.20%	0.13%	0.02%	0.00%	0.00%	0.00%	5.58%
NNE	0.15%	0.47%	0.91%	0.53%	0.46%	0.21%	0.06%	0.01%	0.00%	0.00%	0.00%	0.00%	2.80%
NE	0.14%	0.35%	0.34%	0.06%	0.03%	0.01%	0.01%	0.00%	0.00%	0.00%	0.00%	0.00%	0.93%
ENE	0.10%	0.28%	0.28%	0.04%	0.01%	0.00%	0.00%	0.00%	0.00%	0.00%	0.00%	0.00%	0.72%
E	0.08%	0.28%	0.50%	0.12%	0.03%	0.01%	0.01%	0.00%	0.00%	0.00%	0.00%	0.00%	1.02%
ESE	0.06%	0.26%	1.08%	1.51%	0.81%	0.10%	0.01%	0.00%	0.00%	0.00%	0.00%	0.00%	3.83%
SE	0.07%	0.25%	1.13%	2.37%	2.63%	1.76%	0.89%	0.67%	0.13%	0.01%	0.00%	0.00%	9.91%
SSE	0.06%	0.17%	0.94%	2.18%	4.19%	6.41%	7.16%	9.37%	2.69%	0.22%	0.00%	0.00%	33.40%
S	0.04%	0.13%	0.51%	0.67%	0.76%	0.97%	1.08%	1.82%	0.69%	0.06%	0.00%	0.00%	6.73%
SSW	0.04%	0.10%	0.29%	0.28%	0.20%	0.11%	0.06%	0.08%	0.03%	0.00%	0.00%	0.00%	1.19%
SW	0.04%	0.09%	0.25%	0.29%	0.24%	0.15%	0.09%	0.09%	0.03%	0.01%	0.00%	0.00%	1.28%
WSW	0.05%	0.16%	0.47%	0.63%	0.66%	0.49%	0.37%	0.23%	0.05%	0.01%	0.00%	0.00%	3.12%
W	0.06%	0.26%	0.91%	1.57%	1.83%	1.59%	0.92%	0.36%	0.06%	0.01%	0.00%	0.00%	7.58%
WNW	0.08%	0.28%	1.06%	1.56%	1.67%	1.27%	0.61%	0.39%	0.07%	0.01%	0.00%	0.00%	7.01%
NW	0.09%	0.30%	1.17%	1.46%	1.49%	1.43%	1.11%	1.07%	0.20%	0.03%	0.00%	0.00%	8.34%
NNW	0.11%	0.38%	1.29%	1.33%	0.94%	0.87%	0.68%	0.74%	0.18%	0.03%	0.00%	0.00%	6.55%
TOTAL	1.31%	4.24%	12.77%	16.23%	16.88%	15.82%	13.24%	14.98%	4.15%	0.39%	0.00%	0.00%	100.00%

Table 5.8.A.3

Wind Speed and Direction Categorisation at the Rondekuil WS (January 1998 to September 2023)

Wind Direction	**Wind Speed [m/s] at 10 m level**												**Total (%)**
	<0.5	**0.5-1.0**	**1.0-2.0**	**2.0-3.0**	**3.0-4.0**	**4.0-5.0**	**5.0-6.0**	**6.0-8.0**	**8.0-10.0**	**10.0-13.0**	**13.0-18.0**	**>18.0**	
N	0.24%	0.48%	1.16%	0.72%	0.74%	0.92%	0.95%	1.48%	0.79%	0.35%	0.03%	0.00%	7.86%
NNE	0.38%	0.76%	3.28%	2.64%	1.01%	0.60%	0.28%	0.16%	0.02%	0.01%	0.00%	0.00%	9.14%
NE	0.32%	0.68%	3.51%	2.16%	0.37%	0.07%	0.02%	0.01%	0.00%	0.01%	0.00%	0.00%	7.16%
ENE	0.16%	0.43%	1.89%	1.17%	0.23%	0.04%	0.02%	0.02%	0.00%	0.00%	0.00%	0.00%	3.97%
E	0.09%	0.21%	0.59%	0.38%	0.21%	0.12%	0.09%	0.09%	0.04%	0.01%	0.00%	0.00%	1.83%
ESE	0.07%	0.17%	0.34%	0.21%	0.19%	0.18%	0.17%	0.25%	0.22%	0.17%	0.03%	0.00%	2.01%
SE	0.06%	0.16%	0.42%	0.41%	0.46%	0.46%	0.40%	0.50%	0.19%	0.06%	0.01%	0.00%	3.11%
SSE	0.08%	0.19%	0.55%	0.74%	0.85%	0.81%	0.72%	1.15%	0.79%	0.57%	0.10%	0.00%	6.54%
S	0.12%	0.23%	0.76%	0.77%	0.77%	1.03%	1.18%	2.73%	2.23%	1.99%	0.52%	0.00%	12.33%
SSW	0.16%	0.35%	1.29%	1.10%	0.90%	0.88%	0.86%	1.37%	0.83%	0.41%	0.02%	0.00%	8.18%
SW	0.32%	0.55%	2.62%	2.95%	1.80%	1.38%	1.18%	1.43%	0.21%	0.02%	0.00%	0.00%	12.46%
WSW	0.24%	0.52%	2.08%	2.26%	1.59%	1.30%	1.22%	1.86%	0.41%	0.05%	0.00%	0.00%	11.53%
W	0.12%	0.31%	0.73%	0.51%	0.52%	0.58%	0.59%	0.90%	0.33%	0.08%	0.00%	0.00%	4.67%
WNW	0.09%	0.23%	0.38%	0.25%	0.30%	0.35%	0.36%	0.63%	0.36%	0.13%	0.01%	0.00%	3.07%
NW	0.10%	0.22%	0.33%	0.23%	0.28%	0.30%	0.31%	0.46%	0.29%	0.16%	0.02%	0.00%	2.70%
NNW	0.13%	0.31%	0.47%	0.29%	0.33%	0.36%	0.32%	0.59%	0.41%	0.20%	0.02%	0.00%	3.43%
TOTAL	2.68%	5.79%	20.41%	16.80%	10.56%	9.38%	8.67%	13.61%	7.12%	4.20%	0.77%	0.00%	100.00%

Table 5.8.A.4
Wind Speed and Direction Categorisation at the Robben Island WS (January 1998 to September 2023)

Wind Direction	Wind Speed [m/s] at 10 m level												Total (%)
	<0.5	0.5-1.0	1.0-2.0	2.0-3.0	3.0-4.0	4.0-5.0	5.0-6.0	6.0-8.0	8.0-10.0	10.0-13.0	13.0-18.0	>18.0	
N	0.06%	0.20%	1.33%	1.35%	0.89%	0.87%	0.86%	1.68%	1.32%	1.12%	0.30%	0.00%	9.97%
NNE	0.06%	0.26%	1.03%	1.11%	0.92%	0.56%	0.30%	0.31%	0.16%	0.10%	0.02%	0.00%	4.84%
NE	0.05%	0.20%	0.59%	0.48%	0.39%	0.30%	0.14%	0.08%	0.01%	0.00%	0.00%	0.00%	2.26%
ENE	0.05%	0.19%	0.44%	0.22%	0.12%	0.05%	0.02%	0.01%	0.00%	0.00%	0.00%	0.00%	1.09%
E	0.05%	0.19%	0.44%	0.29%	0.18%	0.10%	0.04%	0.02%	0.00%	0.00%	0.00%	0.00%	1.31%
ESE	0.05%	0.21%	0.59%	0.56%	0.56%	0.61%	0.45%	0.57%	0.24%	0.03%	0.00%	0.00%	3.86%
SE	0.07%	0.19%	0.88%	1.16%	1.25%	1.18%	1.03%	1.83%	1.65%	1.29%	0.19%	0.00%	10.72%
SSE	0.09%	0.17%	0.82%	1.34%	1.54%	1.37%	1.32%	2.94%	3.57%	4.75%	1.61%	0.01%	19.54%
S	0.04%	0.10%	0.57%	0.90%	0.88%	0.59%	0.35%	0.30%	0.12%	0.05%	0.00%	0.00%	3.91%
SSW	0.04%	0.09%	0.54%	1.21%	1.23%	0.98%	0.73%	0.86%	0.08%	0.00%	0.00%	0.00%	5.76%
SW	0.03%	0.12%	0.65%	1.29%	1.62%	1.56%	1.25%	1.24%	0.06%	0.00%	0.00%	0.00%	7.82%
WSW	0.04%	0.10%	0.70%	1.25%	1.19%	0.82%	0.36%	0.12%	0.02%	0.00%	0.00%	0.00%	4.58%
W	0.04%	0.10%	0.72%	1.12%	0.97%	0.41%	0.15%	0.12%	0.02%	0.00%	0.00%	0.00%	3.66%
WNW	0.04%	0.10%	0.78%	1.39%	1.04%	0.47%	0.19%	0.14%	0.04%	0.01%	0.00%	0.00%	4.18%
NW	0.04%	0.12%	0.87%	1.73%	1.44%	0.86%	0.52%	0.50%	0.16%	0.06%	0.01%	0.00%	6.29%
NNW	0.05%	0.16%	1.12%	2.01%	1.66%	1.13%	0.92%	1.49%	0.92%	0.60%	0.15%	0.00%	10.19%
TOTAL	0.80%	2.50%	12.08%	17.40%	15.88%	11.86%	8.63%	12.19%	8.37%	8.00%	2.27%	0.02%	100.00%

Table 5.8.A.5
Wind Speed and Direction Categorisation at the Atlantis WS (January 1998 to September 2023)

Wind Direction	**Wind Speed [m/s] at 10 m level**												**Total (%)**
	<0.5	**0.5-1.0**	**1.0-2.0**	**2.0-3.0**	**3.0-4.0**	**4.0-5.0**	**5.0-6.0**	**6.0-8.0**	**8.0-10.0**	**10.0-13.0**	**13.0-18.0**	**>18.0**	
N	0.19%	0.75%	1.87%	1.92%	1.57%	1.16%	0.84%	0.69%	0.09%	0.00%	0.00%	0.00%	9.10%
NNE	0.22%	0.81%	1.56%	0.87%	0.48%	0.27%	0.15%	0.08%	0.00%	0.00%	0.00%	0.00%	4.45%
NE	0.20%	0.79%	2.10%	0.70%	0.10%	0.02%	0.01%	0.00%	0.00%	0.00%	0.00%	0.00%	3.92%
ENE	0.16%	0.67%	2.29%	0.95%	0.10%	0.03%	0.00%	0.00%	0.00%	0.00%	0.00%	0.00%	4.20%
E	0.13%	0.51%	1.75%	1.42%	0.29%	0.10%	0.03%	0.01%	0.00%	0.00%	0.00%	0.00%	4.25%
ESE	0.13%	0.48%	1.30%	0.97%	0.56%	0.41%	0.31%	0.20%	0.01%	0.00%	0.00%	0.00%	4.36%
SE	0.15%	0.54%	1.54%	0.94%	0.57%	0.42%	0.34%	0.23%	0.02%	0.00%	0.00%	0.00%	4.75%
SSE	0.15%	0.57%	2.12%	2.09%	1.75%	1.27%	0.83%	0.60%	0.10%	0.00%	0.00%	0.00%	9.48%
S	0.15%	0.53%	1.78%	2.00%	1.94%	1.76%	1.35%	1.38%	0.20%	0.01%	0.00%	0.00%	11.10%
SSW	0.14%	0.51%	1.51%	1.46%	1.33%	1.29%	1.01%	0.96%	0.17%	0.00%	0.00%	0.00%	8.38%
SW	0.11%	0.41%	1.35%	1.51%	1.72%	1.52%	0.72%	0.18%	0.00%	0.00%	0.00%	0.00%	7.52%
WSW	0.08%	0.33%	1.14%	1.42%	1.65%	1.36%	0.53%	0.12%	0.00%	0.00%	0.00%	0.00%	6.64%
W	0.08%	0.28%	0.93%	0.97%	0.95%	0.79%	0.27%	0.07%	0.00%	0.00%	0.00%	0.00%	4.34%
WNW	0.08%	0.30%	1.02%	0.87%	0.78%	0.59%	0.30%	0.17%	0.01%	0.00%	0.00%	0.00%	4.12%
NW	0.09%	0.34%	1.27%	1.07%	0.78%	0.57%	0.37%	0.30%	0.05%	0.00%	0.00%	0.00%	4.85%
NNW	0.12%	0.47%	1.59%	1.65%	1.50%	1.18%	0.90%	0.94%	0.18%	0.02%	0.00%	0.00%	8.54%
TOTAL	2.18%	8.30%	25.14%	20.82%	16.07%	12.74%	7.95%	5.93%	0.83%	0.04%	0.00%	0.00%	100.00%

Table 5.8.A.6
Mean and Maximum Hourly Wind Speed per Direction at Bok Point WS (January 1998 to June 2019)

Sector-Averaged Hourly Wind Speed		Sector Maximum Hourly Wind Speed	
Wind Direction	**Wind Speed (m/s)**	**Wind Direction**	**Wind Speed (m/s)**
SSE	7.0	**ESE**	18.9
S	6.1	**SSE**	18.1
SSW	5.5	**W**	17.9
NNW	5.4	**S**	17.7
N	5.3	**NNW**	17.4
SE	4.9	**WNW**	17.2
NW	4.8	**WSW**	16.6
NNE	4.6	**NW**	16.6
SW	4.3	**SSW**	16.3
ESE	4.2	**N**	16.3
WNW	4.0	**SW**	15.8
W	4.0	**SE**	14.8
WSW	3.9	**ENE**	14.6
E	3.4	**E**	13.3
NE	3.3	**NE**	13.3
ENE	2.7	**NNE**	13.0

Table 5.8.A.7
Mean and Maximum Hourly Wind Speed per Direction at Milnerton WS (January 1998 to June 2022)

Sector-Averaged Hourly Wind Speed		Sector Maximum Hourly Wind Speed	
SSE	5.4	**NW**	13.6
S	5.2	**NNW**	13.3
NW	3.9	**SSE**	12.7
SE	3.6	**SW**	12.3
W	3.6	**S**	11.8
NNW	3.6	**WSW**	11.7
WSW	3.5	**WNW**	11.6
WNW	3.4	**W**	11.5
SW	3.2	**SE**	11.0
SSW	3.0	**N**	10.9
N	2.5	**SSW**	10.2
ESE	2.3	**ESE**	8.8
NNE	2.1	**NNE**	7.7
E	1.4	**ENE**	6.8
NE	1.2	**E**	6.3
ENE	1.1	**NE**	6.1
SSE	5.4	**NW**	13.6

Table 5.8.A.8

Mean and Maximum Hourly Wind Speed per Direction at Rondekuil WS (January 1998 to September 2023)

Sector-Averaged Hourly Wind Speed		**Sector Maximum Hourly Wind Speed**	
Wind Direction	**Wind Speed (m/s)**	**Wind Direction**	**Wind Speed (m/s)**
SSE	7.0	**W**	19.7
S	5.5	**WSW**	18.5
SE	4.9	**SSE**	17.9
NW	4.8	**WNW**	17.5
SSW	4.8	**NW**	16.9
SW	4.8	**S**	16.1
NNW	4.8	**SE**	16.0
WNW	4.7	**N**	15.9
N	4.3	**ESE**	15.6
WSW	4.3	**SW**	15.5
W	3.8	**NNW**	15.3
ESE	3.4	**NNE**	15.0
NNE	2.7	**SSW**	13.9
E	2.3	**E**	13.8
ENE	1.8	**ENE**	13.6
NE	1.8	**NE**	12.5

Table 5.8.A.9

Mean and Maximum Hourly Wind Speed per Direction at Robben Island WS (January 1998 to September 2023)

Sector-Averaged Hourly Wind Speed		Sector Maximum Hourly Wind Speed	
Wind Direction	**Wind Speed (m/s)**	**Wind Direction**	**Wind Speed (m/s)**
SSE	7.9	**SSE**	20.3
SE	6.0	**NNW**	19.9
N	5.8	**SE**	19.8
NNW	4.9	**N**	19.6
SW	4.2	**NW**	16.3
ESE	4.1	**NNE**	15.9
SSW	4.0	**S**	14.4
S	3.7	**ESE**	13.0
NW	3.7	**WNW**	11.9
NNE	3.5	**SW**	11.0
WSW	3.3	**NE**	10.9
WNW	3.1	**W**	10.7
W	3.0	**ENE**	10.6
NE	2.8	**E**	10.6
E	2.3	**WSW**	10.5
ENE	2.0	**SSW**	10.1

Table 5.8.A.10
Mean and Maximum Hourly Wind Speed per Direction at Atlantis WS (January 1998 to September 2023)

Sector-Averaged Hourly Wind Speed		Sector Maximum Hourly Wind Speed	
Wind Direction	**Wind Speed (m/s)**	**Wind Direction**	**Wind Speed (m/s)**
S	3.7	**NW**	11.8
SSW	3.6	**NNW**	11.6
NNW	3.6	**S**	11.6
SW	3.2	**N**	10.7
N	3.2	**SSE**	10.6
WSW	3.2	**SSW**	10.5
SSE	3.2	**WNW**	10.2
NW	3.0	**SE**	10.1
WNW	3.0	**E**	9.6
W	3.0	**ESE**	9.4
ESE	2.7	**NNE**	9.1
SE	2.6	**W**	8.7
NNE	2.1	**WSW**	8.4
E	1.9	**SW**	7.6
ENE	1.6	**NE**	6.8
NE	1.5	**ENE**	6.5

Table 5.8.A.11
Maximum Wind Speed per Month at the Bok Point (January 1998 to June 2019)

Wind Direction	Wind Speed [m/s] at 10 m level per Month												Annual
	Jan	Feb	Mar	Apr	May	Jun	Jul	Aug	Sep	Oct	Nov	Dec	
N	9.9	9.6	10.9	13.5	14.7	16.3	16.0	14.7	15.7	13.0	14.1	12.0	16.3
NNE	8.5	8.5	9.0	10.6	13.0	12.4	11.9	12.5	11.6	9.4	9.6	11.1	13.0
NE	4.5	10.0	12.5	9.2	11.8	10.0	10.2	10.2	8.5	13.3	8.8	10.9	13.3
ENE	6.5	8.5	7.4	9.5	9.0	8.8	12.2	7.7	9.3	14.6	8.0	10.9	14.6
E	8.9	8.7	8.1	10.8	13.2	12.5	7.4	7.3	11.1	6.9	7.0	13.3	13.3
ESE	14.0	11.9	14.2	12.0	13.0	11.5	10.2	8.7	9.4	12.4	11.1	18.9	18.9
SE	13.7	13.3	13.0	13.6	12.3	14.8	13.1	11.2	13.3	14.4	13.2	11.9	14.8
SSE	16.3	16.4	17.2	16.2	13.1	15.4	17.0	18.1	16.6	17.5	16.8	16.7	18.1
S	15.7	15.2	15.4	13.6	14.4	16.5	13.5	15.2	14.6	17.7	16.4	15.8	17.7
SSW	12.4	11.7	13.3	13.0	15.2	14.3	15.2	13.9	13.2	14.2	16.3	12.9	16.3
SW	10.3	9.2	11.5	14.0	10.4	14.0	15.8	14.8	15.3	12.2	12.2	9.3	15.8
WSW	7.3	7.3	8.7	10.1	14.6	14.9	15.4	16.6	14.7	13.0	13.1	9.4	16.6
W	8.1	6.9	8.4	8.2	14.5	16.6	14.9	17.9	13.1	12.9	11.1	11.9	17.9
WNW	9.7	9.8	10.3	9.9	14.0	16.0	15.9	16.2	17.2	12.1	11.9	10.5	17.2
NW	11.1	10.8	9.6	12.4	14.1	16.4	16.6	15.6	14.6	13.2	12.6	11.5	16.6
NNW	12.8	10.8	11.4	14.7	15.3	15.5	17.4	16.1	16.3	14.3	13.9	13.2	17.4
Maximum	16.3	16.4	17.2	16.2	15.3	16.6	17.4	18.1	17.2	17.7	16.8	18.9	18.9

Table 5.8.A.12
Maximum Wind Speed per Month at the Milnerton (January 1998 to June 2022)

Wind Direction	Wind Speed [m/s] at 10 m level per Month												Annual
	Jan	Feb	Mar	Apr	May	Jun	Jul	Aug	Sep	Oct	Nov	Dec	
N	5.5	5.1	6.2	7.6	9.5	9.6	10.8	10.1	10.9	8.2	6.4	5.0	10.9
NNE	4.6	6.0	5.4	5.5	6.7	7.7	7.1	6.5	6.4	5.4	6.2	5.0	7.7
NE	4.9	5.7	5.4	5.3	6.1	5.5	5.2	4.2	3.9	3.3	3.9	3.1	6.1
ENE	3.6	2.5	3.1	2.7	3.3	2.7	5.5	3.6	6.8	4.1	4.1	6.6	6.8
E	5.6	4.1	4.5	3.7	5.1	3.8	5.5	4.9	6.3	4.7	4.4	6.0	6.3
ESE	4.9	5.0	4.7	6.6	5.4	4.0	5.5	6.0	5.3	6.4	4.9	8.8	8.8
SE	10.8	8.7	10.0	9.8	7.1	9.5	10.1	9.2	10.4	11.0	10.6	10.3	11.0
SSE	11.7	12.0	12.6	10.7	9.3	8.8	9.7	10.7	10.4	12.7	11.4	12.3	12.7
S	11.8	11.1	10.5	10.0	9.5	6.7	7.6	7.2	8.9	10.9	10.2	11.1	11.8
SSW	9.4	10.2	10.2	9.4	7.5	7.6	6.9	6.2	5.6	6.1	7.9	9.8	10.2
SW	8.6	9.9	11.5	8.7	6.8	12.3	9.3	12.0	8.4	7.3	7.8	6.2	12.3
WSW	8.1	8.6	8.7	7.1	9.4	11.7	10.3	11.5	9.1	10.2	8.8	9.4	11.7
W	8.5	9.8	8.0	7.0	10.3	11.5	10.9	10.7	9.8	8.6	8.3	7.4	11.5
WNW	8.3	8.4	8.7	7.9	9.6	11.6	11.0	11.2	11.4	8.5	8.9	7.3	11.6
NW	9.1	8.2	8.3	9.1	11.8	11.7	13.6	11.8	11.9	11.0	10.5	10.1	13.6
NNW	9.5	6.8	8.6	11.7	11.8	10.5	13.3	11.1	12.4	9.8	9.3	9.8	13.3
Maximum	11.8	12.0	12.6	11.7	11.8	12.3	13.6	12.0	12.4	12.7	11.4	12.3	13.6

Table 5.8.A.13
Maximum Wind Speed per Month at the Rondekuil (January 1998 to September 2023)

Wind Direction	Wind Speed [m/s] at 10 m level per Month												Annual
	Jan	Feb	Mar	Apr	May	Jun	Jul	Aug	Sep	Oct	Nov	Dec	
N	13.1	15.5	13.0	12.7	15.4	16.1	14.7	14.7	14.4	12.7	15.0	11.6	16.1
NNE	13.6	12.5	17.5	9.7	10.9	10.2	9.7	10.4	9.1	8.9	8.6	10.7	17.5
NE	12.9	13.9	11.3	6.8	5.7	7.8	5.8	5.6	6.4	5.3	13.0	12.6	13.9
ENE	11.1	8.9	7.5	6.4	8.1	10.1	5.7	6.7	5.3	6.6	12.5	11.6	12.5
E	12.7	12.1	11.7	9.3	11.4	12.0	9.0	10.2	7.8	9.9	12.1	13.8	13.8
ESE	13.9	13.9	13.9	15.7	14.6	13.6	12.9	11.6	9.9	14.8	15.3	19.7	19.7
SE	15.5	12.4	12.2	13.8	10.2	13.0	11.2	9.0	10.4	14.7	14.2	15.3	15.5
SSE	17.4	15.6	17.0	15.3	13.6	12.9	17.9	16.3	12.0	14.7	14.7	16.5	17.9
S	17.3	17.5	15.9	16.3	12.0	13.3	12.2	14.0	14.2	18.5	15.9	18.0	18.5
SSW	14.9	13.9	13.1	13.3	9.3	12.5	11.9	10.7	15.9	13.4	13.4	14.9	15.9
SW	10.3	11.3	11.6	9.8	10.8	9.4	12.6	11.7	15.0	9.3	11.5	10.6	15.0
WSW	12.4	11.1	11.4	11.0	13.1	12.4	11.7	13.6	11.2	10.8	12.5	11.3	13.6
W	12.8	11.6	10.7	10.2	12.4	14.8	15.3	12.3	12.5	11.3	10.9	11.8	15.3
WNW	13.1	13.2	11.0	12.9	13.6	16.0	13.4	13.8	15.8	11.8	12.7	12.9	16.0
NW	13.9	11.7	12.4	13.0	14.3	15.6	14.7	13.5	15.3	14.1	12.7	14.3	15.6
NNW	12.9	10.0	13.7	16.0	15.5	16.9	14.8	14.3	14.5	12.8	15.2	13.3	16.9
Maximum	17.4	17.5	17.5	16.3	15.5	16.9	17.9	16.3	15.9	18.5	15.9	19.7	19.7

Table 5.8.A.14
Maximum Wind Speed per Month at the Robben Island (January 1998 to September 2023)

Wind Direction	Wind Speed [m/s] at 10 m level per Month												Annual
	Jan	Feb	Mar	Apr	May	Jun	Jul	Aug	Sep	Oct	Nov	Dec	
N	13.1	15.5	13.0	12.7	15.4	16.1	14.7	14.7	14.4	12.7	15.0	11.6	16.1
NNE	13.6	12.5	17.5	9.7	10.9	10.2	9.7	10.4	9.1	8.9	8.6	10.7	17.5
NE	12.9	13.9	11.3	6.8	5.7	7.8	5.8	5.6	6.4	5.3	13.0	12.6	13.9
ENE	11.1	8.9	7.5	6.4	8.1	10.1	5.7	6.7	5.3	6.6	12.5	11.6	12.5
E	12.7	12.1	11.7	9.3	11.4	12.0	9.0	10.2	7.8	9.9	12.1	13.8	13.8
ESE	13.9	13.9	13.9	15.7	14.6	13.6	12.9	11.6	9.9	14.8	15.3	19.7	19.7
SE	15.5	12.4	12.2	13.8	10.2	13.0	11.2	9.0	10.4	14.7	14.2	15.3	15.5
SSE	17.4	15.6	17.0	15.3	13.6	12.9	17.9	16.3	12.0	14.7	14.7	16.5	17.9
S	17.3	17.5	15.9	16.3	12.0	13.3	12.2	14.0	14.2	18.5	15.9	18.0	18.5
SSW	14.9	13.9	13.1	13.3	9.3	12.5	11.9	10.7	15.9	13.4	13.4	14.9	15.9
SW	10.3	11.3	11.6	9.8	10.8	9.4	12.6	11.7	15.0	9.3	11.5	10.6	15.0
WSW	12.4	11.1	11.4	11.0	13.1	12.4	11.7	13.6	11.2	10.8	12.5	11.3	13.6
W	12.8	11.6	10.7	10.2	12.4	14.8	15.3	12.3	12.5	11.3	10.9	11.8	15.3
WNW	13.1	13.2	11.0	12.9	13.6	16.0	13.4	13.8	15.8	11.8	12.7	12.9	16.0
NW	13.9	11.7	12.4	13.0	14.3	15.6	14.7	13.5	15.3	14.1	12.7	14.3	15.6
NNW	12.9	10.0	13.7	16.0	15.5	16.9	14.8	14.3	14.5	12.8	15.2	13.3	16.9
Maximum	17.4	17.5	17.5	16.3	15.5	16.9	17.9	16.3	15.9	18.5	15.9	19.7	19.7

Table 5.8.A.15
Maximum Wind Speed per Month at the Atlantis (January 1998 to September 2023)

Wind Direction	Wind Speed [m/s] at 10 m level per Month												Annual
	Jan	Feb	Mar	Apr	May	Jun	Jul	Aug	Sep	Oct	Nov	Dec	
N	8.8	9.8	9.6	10.0	10.2	10.7	9.9	10.0	9.2	8.9	10.5	7.7	10.7
NNE	6.6	6.2	6.4	7.1	8.1	8.1	7.7	9.1	7.5	6.8	8.7	6.2	9.1
NE	2.8	3.6	5.5	5.1	4.7	6.4	4.3	5.3	5.4	6.8	6.5	3.8	6.8
ENE	4.3	4.5	5.0	4.5	5.1	5.0	5.0	6.1	5.9	5.9	6.5	4.8	6.5
E	5.3	6.0	6.3	5.1	5.8	6.0	4.1	6.9	6.8	7.1	6.5	9.6	9.6
ESE	8.7	8.2	7.9	8.4	7.5	8.0	6.3	7.6	7.8	8.6	8.3	9.4	9.4
SE	8.0	8.2	10.1	7.9	9.0	7.5	9.2	6.6	9.2	8.5	8.9	8.6	10.1
SSE	9.8	9.6	9.8	8.4	8.7	7.3	7.6	8.5	10.0	9.2	10.1	10.6	10.6
S	10.8	9.4	10.8	9.7	6.7	8.4	9.6	11.6	10.0	9.9	10.9	10.6	11.6
SSW	10.0	10.2	9.2	9.1	7.1	7.4	7.8	7.1	8.0	9.7	10.0	10.5	10.5
SW	7.4	7.1	6.9	7.0	6.7	6.9	7.1	7.1	6.8	6.7	7.5	7.6	7.6
WSW	7.2	7.4	6.5	6.0	8.4	8.2	7.3	8.0	8.2	7.4	7.2	7.6	8.4
W	6.9	6.2	6.5	6.6	7.5	7.6	7.7	8.6	7.4	7.0	8.7	6.7	8.7
WNW	8.8	8.2	7.4	7.7	8.4	10.2	8.0	9.0	10.1	9.0	7.3	9.1	10.2
NW	9.6	9.4	8.3	7.5	8.8	10.4	11.8	9.5	9.8	8.4	9.5	9.1	11.8
NNW	7.9	7.4	9.3	10.6	10.2	11.4	10.5	10.7	11.6	10.5	8.9	8.8	11.6
Maximum	10.8	10.2	10.8	10.6	10.2	11.4	11.8	11.6	11.6	10.5	10.9	10.6	11.8

Appendix 5.8.B: Distribution of Extreme Values

The extreme rainfall, wind speed and temperature estimates are used to determine critical design which the nuclear installation(s) must withstand during its lifetime. Extreme annual values of meteorological parameters constitute samples of random variables, which may be characterized by specific probability distributions. In principle, the data set should be analysed with probability distribution functions appropriate to the data sets under study. Among these, the generalized extreme value distributions are widely used (***International Atomic Energy Agency, 2011***): Fisher–Tippett Type I (Gumbel), Type II (Fréchet) and Type III (Weibull).

Extreme meteorological conditions are defined in terms of recurrence periods, e.g. 10-, 100- , …., 100 000 000-year recurrence periods, or equivalently expressed as probabilities of 1x10^{-1}, 1x10^{-2}, …., 1x10^{-8} per year. So, for example, the 100-year wind speed is defined as the wind speed exceeded on average once in a period of 100 years, or a wind speed with a probability of 1x10^{-2} per year.

The Gumbel distribution is suitable to describe the distribution of extreme rainfall (annual totals and 24-hour storm events), wind speed (hourly means and gusts) and temperatures (minimum and maximum). The classical extreme value theory is based on three asymptotic extreme value distributions. The Generalized Extreme Value (GEV) distribution combines these three distributions into a single mathematical form with the cumulative distribution function:

$$F(x) = \exp\left\{-\exp\left(\frac{x-\xi}{\alpha}\right)\right\} F(x) = \exp\left\{-\exp\left(\frac{x-\xi}{\alpha}\right)\right\} \text{ for k} = 0$$

$$F(x) = \exp\left\{-\left[1-k\left(\frac{x-\xi}{\alpha}\right)\right]\right\}^{1/k} \text{ for k} \neq 0$$

where *k*, *α* and *ξ* are the shape, scale and location parameter, respectively, and *x* is the maximum of an epoch.

When *k* = 0, it is the Type I GEV or so-called Gumbel distribution; when *k* < 0, the GEV is called the Type II (or Frechet) distribution, which has a long right tail; when *k* > 0, it is the Type III GEV (a form of the Weibull distribution) and has a short tail. In order to determine whether or not a particular sample came from a population distribution that is Gumbel, Frechet, or Weibull, one may check a probability plot. If such a plot produces points that fall close to a straight line, then the distribution function that the plot is based upon is a reasonable model (International Atomic Energy Agency, 2011). To illustrate, the Gumbel distribution can also be written as:

$$x = \alpha \ln(-\ln[F(x)]) + \xi = \alpha u + \xi$$

So, plotting *x* against *u* gives a straight line. This property enables a visual check to be made of the extent to which a data set fits the Gumbel distribution.

There are a number of different methods available to determine the shape, scale and location parameters from a data set, including:

- Method of Moments;
- Method of L-Moments;
- Method of Maximum Likelihood;
- Gumbel's Fitting Method;
- Method of Least Squares.

In the analysis, all five methods were used. The final selection was based on the method resulting in the best fit to the observed values; identified using the Kolmogorov-Smirnov test. The Kolmogorov–Smirnov test statistic, *D*, quantifies a distance between the GEV distribution function of the sample and the cumulative distribution function of the observation:

$$D = \max\left| F(x_i) - \frac{i-1}{n}, \frac{i}{n} - F(x_i) \right|$$

where $F(x_i)$ is the calculated probability given by the GEV distribution function for an observation x_i, taken from a set of *n* values, ranked from smallest (*i* = *0*) to highest (*i* = *n*), i.e.

$$x_1 < \cdots x_i < \cdots < x_n$$

The null distribution of this statistic is calculated under the null hypothesis that the sample is drawn from the reference distribution (i.e. observations). The null hypothesis, that the GEV distribution function is an appropriate distribution function, is rejected when *D* assumes a large value. For a confidence level of 95%, under the null hypothesis, a distribution function with a *D* larger than $1.36/\sqrt{n}$ would be rejected. For *n = 40*, *D ≤ 0.21*.

Extreme Rainfall

The 40-years (1980-2019) of rainfall maxima which were observed at the Site are summarised in ***Table 5.8.B.1***. These data were used to fit an appropriate GEV using the five methods listed above. The results from the distribution fit (shape *k*, scale *α*, location *ξ* and Kolmogorov–Smirnov test statistic, *D*) are summarised in ***Table 5.8.B.2*** (24-hour storm) and ***Table 5.8.B.3*** (annual total rainfall). The tables also include the extremes for return periods 10- to 100 000 000 years. Four methods, i.e. method of moments, method of L-moments, method of maximum likelihood, and method of least squares resulted in an acceptable fit for a 95 per cent confidence interval null hypothesis test, with the method of maximum likelihood performing the best for the 24-hour storm data and the method of moments performing best for the annual rainfall data.

Table 5.8.B.1
Maximum 24-Hour and Annual Total Rainfall (the Site)

Year	Rainfall [mm]		Year	Rainfall [mm]	
	24-Hour Max	Annual		24-Hour Max	Annual
1980	29.0	352.6	2002	28.0	346.2
1981	57.4	415.6	2003	29.2	279.0
1982	23.4	340.2	2004	50.4	393.8
1983	34.6	325.0	2005	34.8	353.8
1984	19.4	383.2	2006	19.9	348.7
1985	59.4	437.8	2007	33.5	427.2
1986	24.0	440.6	2008	35.7	410.7
1987	57.6	640.4	2009	38.8	447.1
1988	35.0	351.2	2010	27.5	335.3
1989	26.5	362.2	2011	26.2	320.6
1990	36.2	360.3	2012	27.6	410.4
1991	30.6	352.5	2013	46.4	547.2
1992	29.2	309.4	2014	22.7	431.0
1993	62.0	388.9	2015	21.6	218.0
1994	70.0	365.0	2016	26.7	321.7
1995	28.0	346.5	2017	26.2	248.1
1996	58.2	458.4	2018	32.7	333.8
1997	31.2	280.4	2019	30.3	343.6
1998	28.6	299.2	2020	36.9	398.1
1999	34.6	421.6	2021	35.5	375.9
2000	24.2	243.0	2022	39.8	318.8
2001	46.4	467.4			

These distribution functions are also illustrated in ***Figure 5.8.B.1*** (24-hour storm) and ***Figure 5.8.B.2*** (annual total rainfall).

Table 5.8.B.2
Comparison of Methods to Determine Extreme 24-Hour Storms (the Site)

Return Period	24-Hour Maximum Rainfall [mm]				
	Method of Moments	Method of L-Moments	Method of Maximum Likelihood	Gumbel's Fitting Method	Method of Least Squares
10	51.6	51.4	49.0	53.6	52.2
100	74.4	74.0	69.0	78.8	75.8
1000	96.8	96.2	88.6	103.6	99.0
10000	119.2	118.3	108.1	128.3	122.1
100000	141.6	140.5	127.7	153.1	145.2
1000000	164.0	162.6	147.2	177.8	168.3
10000000	186.4	184.8	166.7	202.5	191.3
100000000	208.8	206.9	186.3	227.2	214.4
GEV Parameters					
Shape	0	0	0	0	0
Scale	9.725	9.618	8.489	10.739	10.031
Location	29.668	29.727	29.919	29.423	29.672
Kolmogorov-Smirnov Test:					
D	0.123	0.122	**0.105**	0.137	0.129

Table 5.8.B.3
Comparison of Methods to Determine Yearly Total Rainfall (the Site)

Return Period	**24-Hour Maximum Rainfall [mm]**				
	Method of Moments	**Method of L-Moments**	**Method of Maximum Likelihood**	**Gumbel's Fitting Method**	**Method of Least Squares**
10	471.7	471.1	484.5	484.3	476.3
100	613.3	611.9	640.1	640.7	622.9
1000	752.3	750.1	793.0	794.2	766.8
10000	891.1	888.1	945.6	947.5	910.5
100000	1029.9	1026.1	1098.1	1100.7	1054.1
1000000	1168.7	1164.1	1250.6	1254.0	1197.8
10000000	1307.5	1302.1	1403.2	1407.2	1341.4
100000000	1446.2	1440.1	1555.7	1560.5	1485.0
GEV Parameters					
Shape	0	0	0	0	0
Scale	60.270	59.925	66.248	66.554	62.381
Location	336.024	336.210	335.388	334.509	335.932
Kolmogorov-Smirnov Test:					
D	0.101	**0.100**	0.114	0.119	0.105

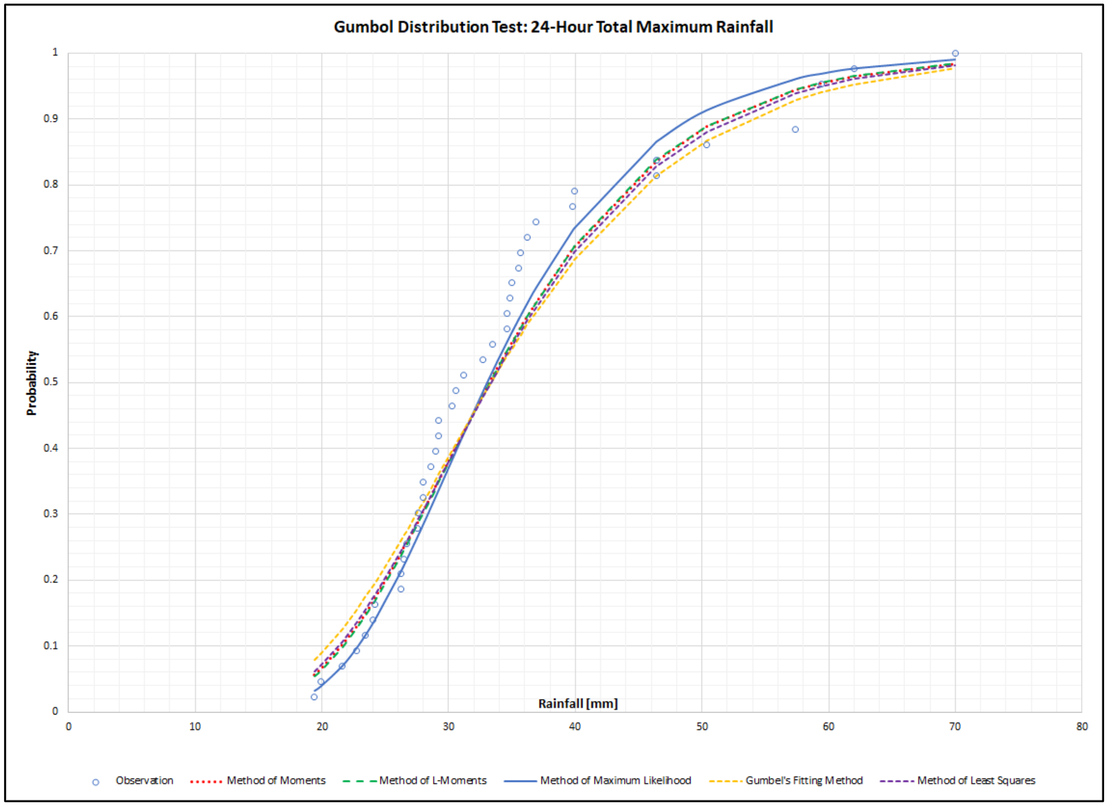

Figure 5.8.B.1
Goodness of Fit Test: Annual Total Rainfall (43-Year Dataset)

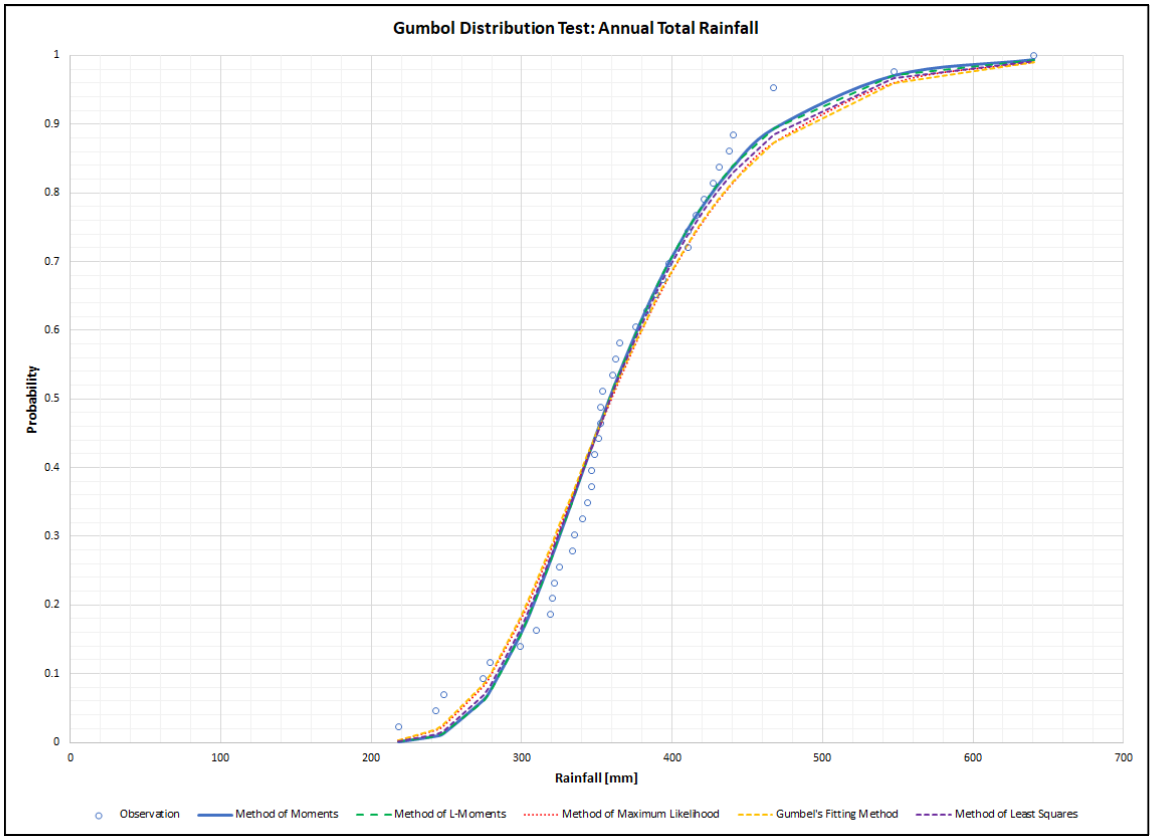

Figure 5.8.B.2

Goodness of Fit Test: Annual Total Rainfall (43-Year Dataset)

Caution should be exercised in attempting to fit an extreme value distribution to a data set representing only a few years of records. If extrapolations are carried out over very long periods of time by means of a statistical technique, due regard should be given to the physical limits of the variable of interest (International Atomic Energy Agency, 2011). Care should also be taken in extrapolating to time intervals well beyond the duration of the available records (such as for ‘return’ periods greater than four times the duration of the sample) (International Atomic Energy Agency, 2011). The extreme values with small probabilities down to the required 1x10^{-8} per year (100 000 000-year return period) should recognise that extrapolation to these events carries a significant uncertainty, since they are based on a data set of only 43 years.

Table A-5.8.B.2 is a summary of the estimated extreme rainfall totals and the calculated 95 per cent confidence interval as estimated using the Jackknife sampling method. Jackknife samples are computed by leaving out one observation from the set of observations at a time. Each Jackknife sample is then used to evaluate the mean and standard deviation of the estimate. The 95 per cent confidence calculated as 1.96 of the standard error, assuming a normal distribution. These are also illustrated in These distribution functions are also illustrated in ***Figure 5.8.B.3*** (24-hour storm) and ***Figure 5.8.B.4*** (annual total rainfall) together with the actual observed values.

Table 5.8.B.4
Maximum 24-Hour and Annual Total Rainfall Extremes (the Site)

Return Period	**Rainfall [mm]**			
	24-Hour Total Max	**95% Confidence Interval**	**Annual Total**	**95% Confidence Interval**
10	49.0	± 7.3	471.1	± 45.3
100	69.0	± 12.8	611.9	± 85.7
1000	88.6	± 18.3	750.1	± 127.0
10000	108.1	± 23.7	888.1	± 168.7
100000	127.7	± 29.2	1026.1	± 210.5
1000000	147.2	± 34.7	1164.1	± 252.4
10000000	166.7	± 40.2	1302.1	± 294.4
100000000	186.3	± 45.7	1440.1	± 336.4

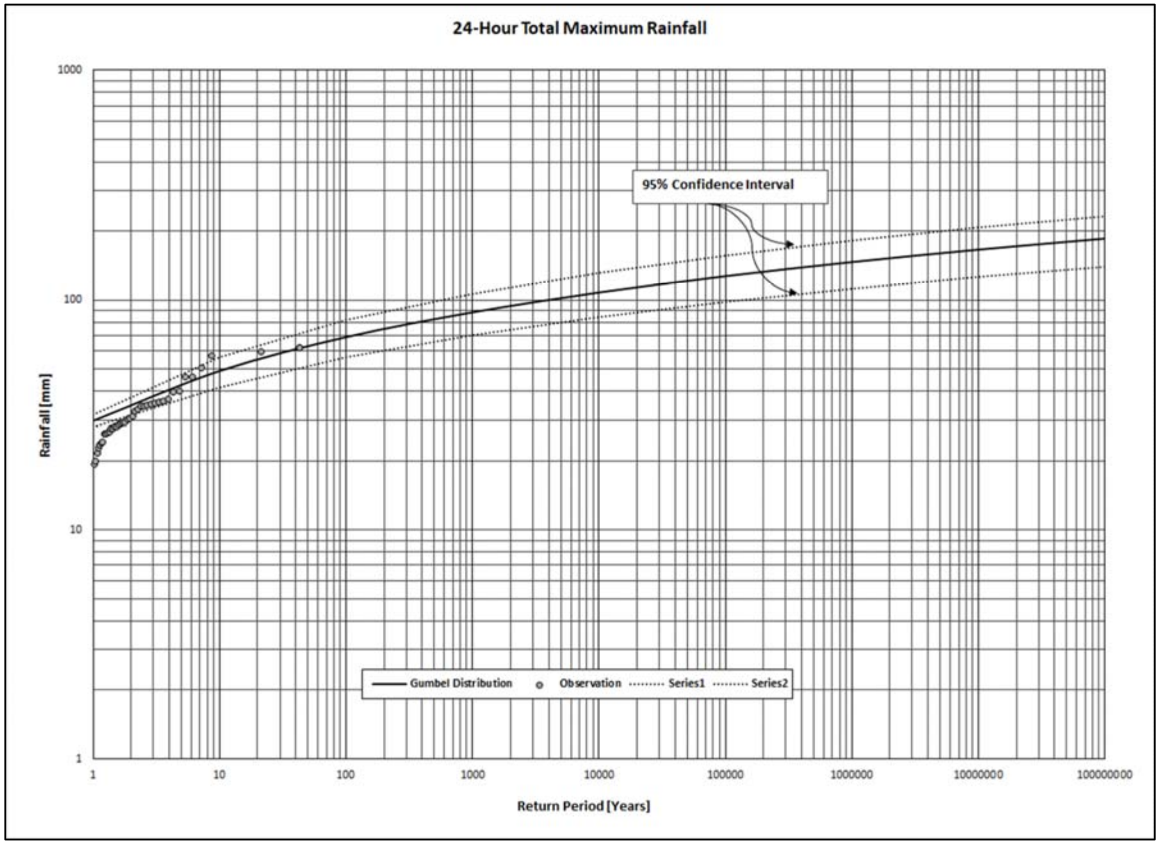

Figure 5.8.B.3

Gumbel Distribution Fit to 24-Hour Storm Events (40-Year Dataset)

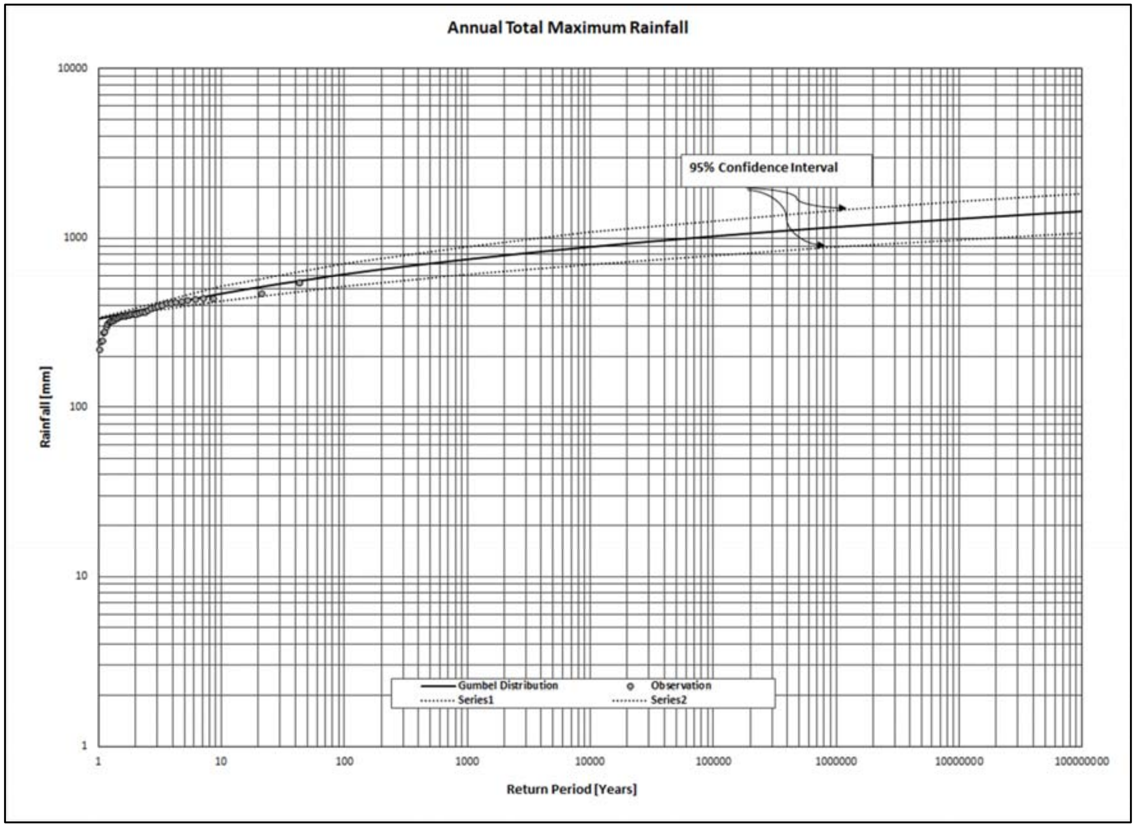

Figure 5.8.B.4

Gumbel Distribution Fit to Annual Total Rainfall (40-Year Dataset)

Extreme Temperature

The 25-years (1998-2022) of dry-bulb temperature which were observed at the 10-m level of the 120-m tower at the Site are summarised in ***Table 5.8.B.5***. These data were used to fit an appropriate GEV using the five methods discussed in the previous section.

The results from the distribution fit (shape *k*, scale *α*, location *ξ* and Kolmogorov–Smirnov test statistic, *D*) are summarised in ***Table 5.8.B.6*** (minimum hourly average temperature) and ***Table 5.8.B.7*** (maximum hourly average temperature). The tables include the extremes for return periods 10- to 100 000 000-years using the four methods. The method of least Squares performed the best for both the minimum and maximum temperatures.

These distribution functions are also illustrated in ***Figure 5.8.B.5*** (minimum hourly average temperature) and ***Figure 5.8.B.6*** (maximum hourly average temperature).

Table 5.8.B.5
Maximum and Minimum Hourly Average Temperature (the Site)

Year	Hourly Average Temperature [°C]		Year	Hourly Average Temperature [°C]	
	Minimum	Maximum		Minimum	Annual
1998	5.8	34.8	2011	5.8	35
1999	5.0	35.5	2012	3.9	35.7
2000	4.2	36.7	2013	4.5	33.1
2001	5.0	35.2	2014	3.9	35.6
2002	4.1	36.6	2015	5.0	38.8
2003	4.4	36.4	2016	4.5	33.5
2004	4.8	37.3	2017	5.4	35.7
2005	4.5	35.6	2018	5.6	37.1
2006	5.3	35.3	2019	5.0	35.9
2007	5.0	35.6	2020	3.4	31.2
2008	6.2	34.2	2021	3.0	36.1
2009	5.5	35.3	2022	4.9	32.1
2010	3.2	36.0			

Table 5.8.B.6
Comparison of Methods to Determine Minimum Hourly Average Dry Bulb Temperature (the Site)

Return Period	24-Hour Maximum Rainfall [mm]				
	Method of Moments	Method of L-Moments	Method of Maximum Likelihood	Gumbel's Fitting Method	Method of Least Squares
10	3.6	3.5	3.2	3.4	3.5
100	1.8	1.6	-0.9	1.3	1.6
1000	0.0	-0.3	1.3	-0.7	-0.2
10000	-1.7	-2.1	3.5	-2.8	-2.1
100000	-3.5	-4.0	5.7	-4.8	-3.9
1000000	-5.2	-5.9	7.9	-6.8	-5.8
10000000	-7.0	-7.7	10.1	-8.8	-7.6
100000000	-8.8	-9.6	12.3	-10.9	-9.5
GEV Parameters					
Shape	0	0	0	0	0
Scale	0.764	0.811	0.959	0.879	0.803
Location	5.305	5.332	5.346	5.331	5.305
Kolmogorov-Smirnov Test:					
D	0.151	0.155	**0.138**	0.143	0.145

Table 5.8.B.7
Comparison of Methods to Determine Maximum Hourly Average Dry Bulb Temperature (the Site)

Return Period	24-Hour Maximum Rainfall [mm]				
	Method of Moments	**Method of L-Moments**	**Method of Maximum Likelihood**	**Gumbel's Fitting Method**	**Method of Least Squares**
10	37.5	37.5	38.6	37.9	37.5
100	40.5	40.4	42.9	41.3	40.4
1000	43.4	43.4	47.0	44.6	43.3
10000	46.3	46.3	51.2	48.0	46.2
100000	49.2	49.2	55.4	51.3	49.1
1000000	52.1	52.1	59.6	54.7	52.0
10000000	55.0	55.0	63.7	58.0	54.9
100000000	57.9	57.9	67.9	61.4	57.8
GEV Parameters					
Shape	0	0	0	0	0
Scale	0.939	0.950	1.163	1.090	0.984
Location	35.137	35.130	35.095	35.679	35.140
Kolmogorov-Smirnov Test:					
D	0.245	0.245	**0.223**	0.236	0.236

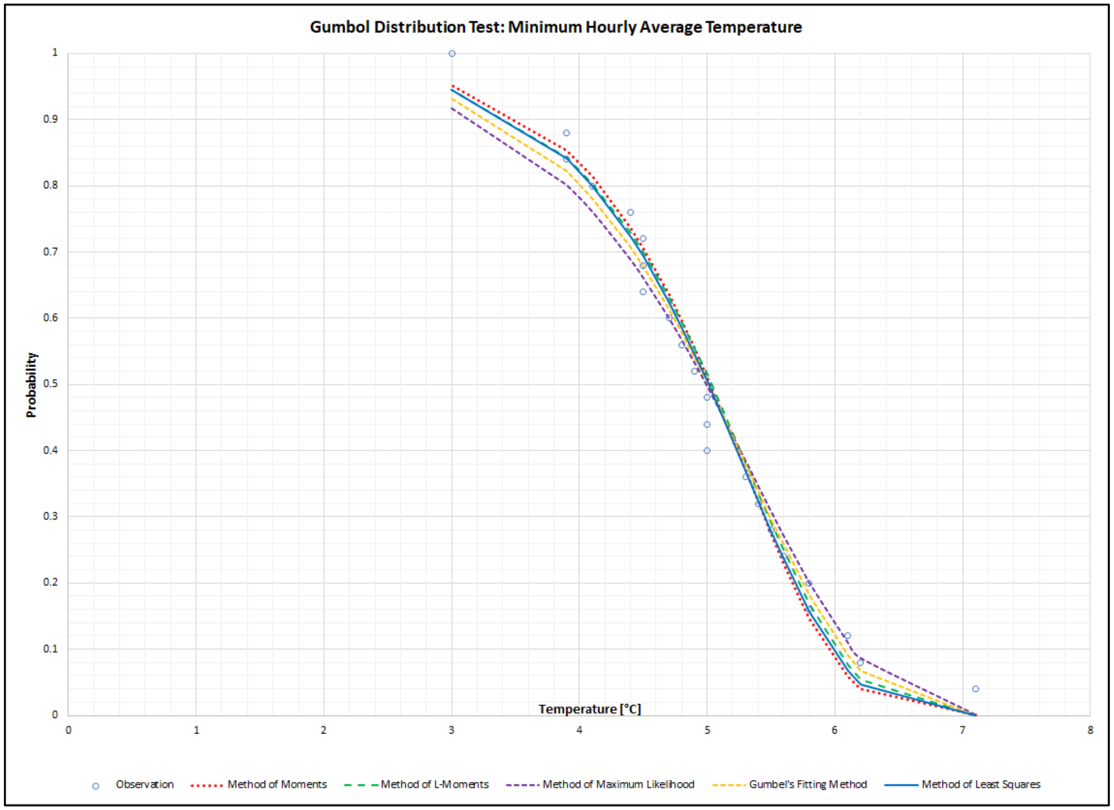

Figure 5.8.B.5
Goodness of Fit Test: Minimum Hourly Average Temperature (25-Year Dataset)

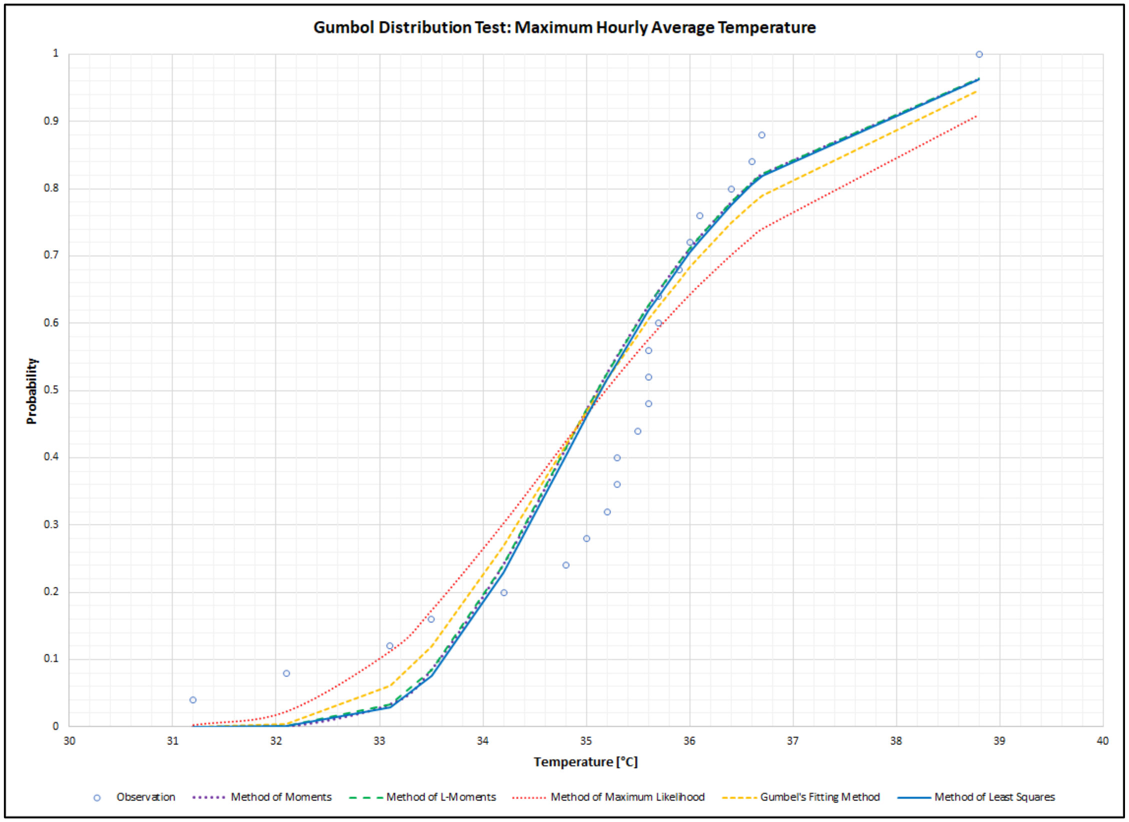

Figure 5.8.B.6

Goodness of Fit Test: Maximum Hourly Average Temperature (25-Year Dataset)

Table 5.8.B.8 is a summary of the estimated minimum and maximum temperatures and the calculated 95 per cent confidence interval as estimated using the method of least squares. These are also illustrated in These distribution functions are also illustrated in ***Figure 5.8.B.7*** (minimum hourly average temperature) and ***Figure 5.8.B.8*** (maximum hourly average temperature) together with the actual observed values.

Since the extreme analyses were based on 23 years of data, caution should be exercised in the use of the projections for very low probabilities.

Table 5.8.B.8
Minimum and Maximum Hourly Average Temperature Extremes (the Site)

Return Period	Hourly Average Temperature [°C]			
	Minimum	95% Confidence Interval	Maximum	95% Confidence Interval
10	3.5	± 0.5	37.5	± 0.9
100	1.6	± 1.0	40.4	± 2.0
1000	-0.2	± 1.5	43.3	± 3.2
10000	-2.1	± 2.0	46.2	± 4.3
100000	-3.9	± 2.5	49.1	± 5.5
1000000	-5.8	± 3.0	52.0	± 6.7
10000000	-7.6	± 3.5	54.9	± 7.9
100000000	-9.5	± 4.0	57.8	± 9.0

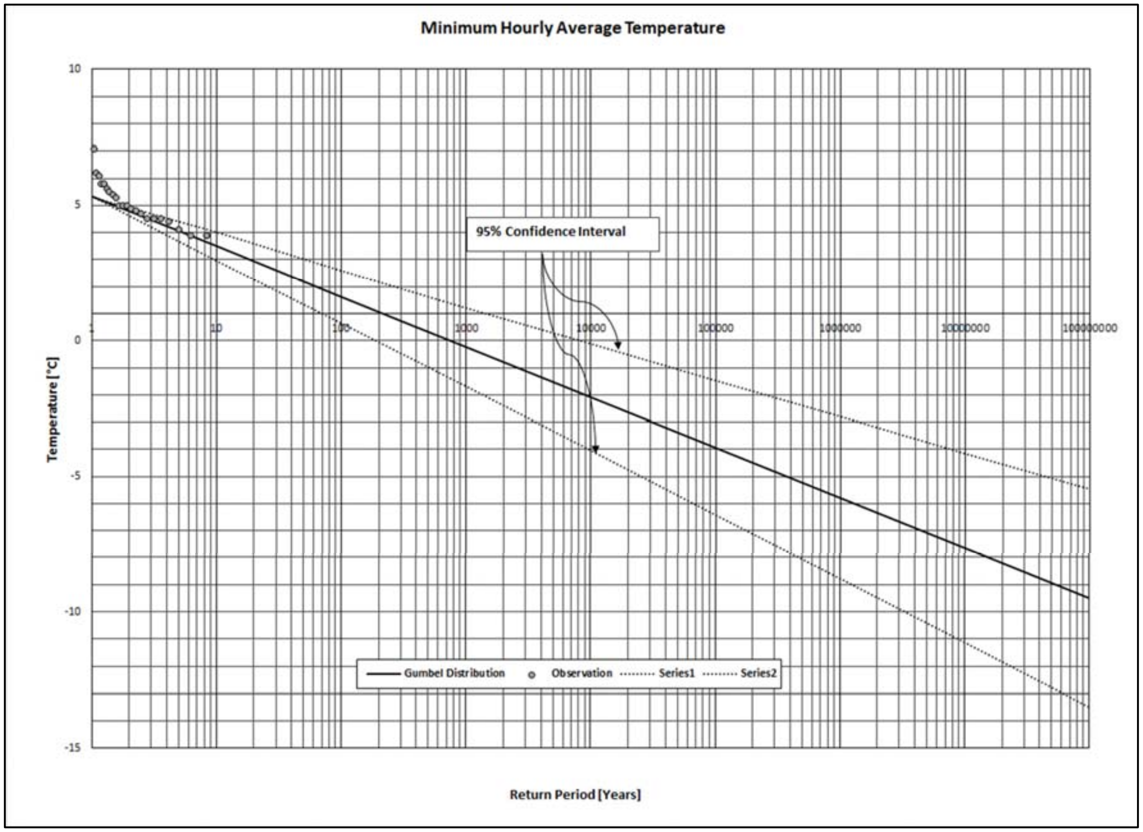

Figure 5.8.B.7

Gumbel Distribution Fit to Minimum Hourly Average Temperature (25-Year Dataset)

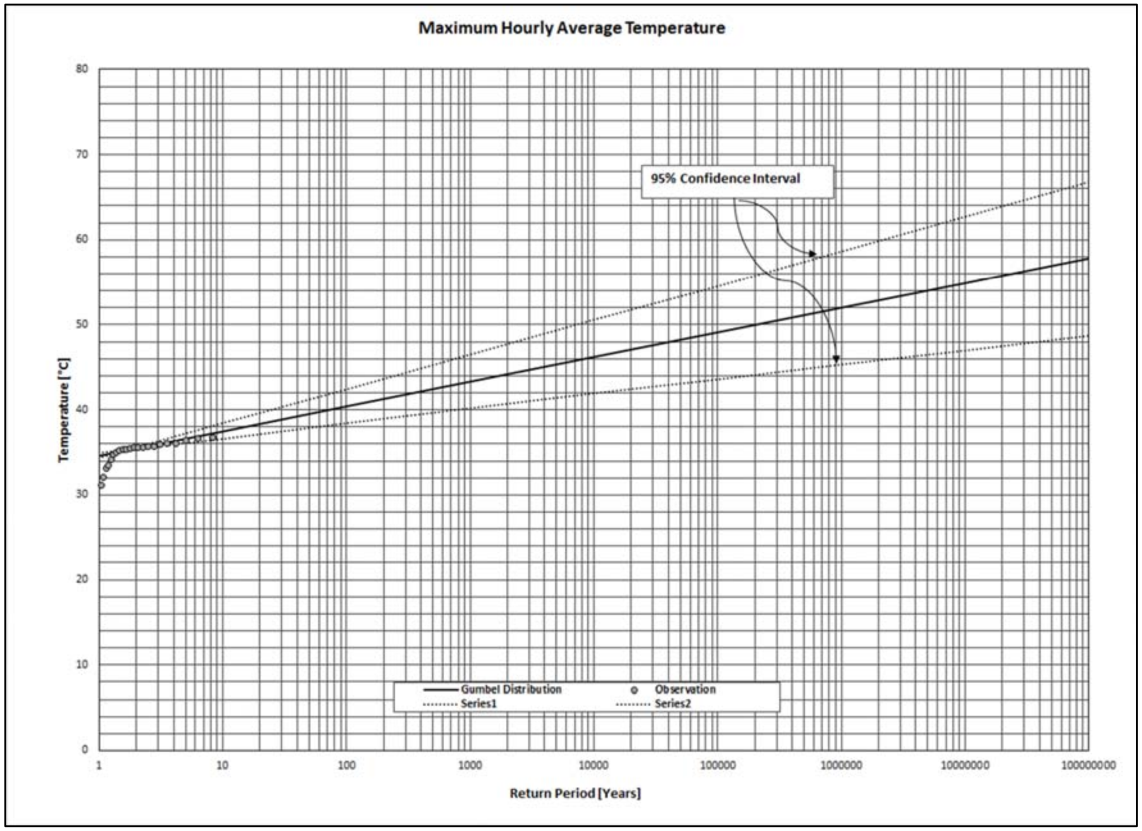

Figure 5.8.B.8

Gumbel Distribution Fit to Maximum Hourly Average Temperature (25-Year Dataset)

Extreme Wind Speed

The 40-years (1980-2019) of hourly average wind speed maxima and sort duration gusts which were observed at the 10-m level of the 120-m tower at the Site are summarised in ***Table 5.8.A.8***. These data wereas used to fit an appropriate GEV with the results from each of the methods for the distribution fit (shape *k*, scale *α*, location *ξ* and Kolmogorov–Smirnov test statistic, *D*) summarised in ***Table 5.8.B.9*** (maximum hourly averages) and ***Table 5.8.B.10*** (wind gusts). The tables also include the extremes for return periods 10- to 100 000 000 years. The method of maximum likelihood performed the best for the maximum hourly average wind speed data and the Gumbel's fitting method performing best for the wind gust data. These distribution functions are also illustrated in ***Figure 5.8.B.9*** (maximum hourly averages) and ***Figure 5.8.B.10*** (wind gusts).

Table 5.8.B.8
Maximum Hourly Average Wind Speeds and Wind Gusts (the Site)

Year	Wind Speed [m/s]		Year	Wind Speed [m/s]	
	Hourly Average	Gust		Hourly Average	Gust
1980	14.9	22.6	2002	15.7	36.9
1981	14.7	23.9	2003	12.6	21.9
1982	16.3	22.4	2004	12.8	20.6
1983	15.8	20.8	2005	15.7	24.3
1984	17.2	28.2	2006	13.9	22.1
1985	10.8	31.5	2007	14.4	28.1
1986	10.2	35.9	2008	16.2	31.2
1987	9.8	38.8	2009	16.0	31.2
1988	9.4	24.2	2010	14.3	28.0
1989	10.5	27.2	2011	14.1	23.6
1990	10.5	24.7	2012	14.1	24.5
1991	15.0	30.6	2013	13.3	22.4
1992	12.3	27	2014	13.8	24.9
1993	11.2	37.1	2015	12.5	23.5
1994	11.2	34.4	2016	13.4	22.6
1995	11.1	24.6	2017	14.4	28.1
1996	11.3	25.2	2018	12.9	23.5
1997	9.3	24.5	2019	15.8	27.3
1998	13.1	25.6	2020	16.5	31.0
1999	14.4	24.5	2021	13.7	21.4
2000	14.9	30.6	2022	12.7	23.0
2001	15.4	28.9			

Table 5.8.B.9
Comparison of Methods to Determine Extreme Hourly Average Wind Speeds (the Site)

Return Period	**Maximum Hourly Average Wind Speed [m/s]**				
	Method of Moments	**Method of L-Moments**	**Method of Maximum Likelihood**	**Gumbel's Fitting Method**	**Method of Least Squares**
10	16.2	16.4	16.9	16.5	16.2
100	20.0	20.5	21.6	20.8	20.0
1000	23.8	24.5	26.3	24.9	23.8
10000	27.5	28.5	30.9	29.1	27.5
100000	31.3	32.6	35.5	33.2	31.3
1000000	35.1	36.6	40.2	37.4	35.0
10000000	38.8	40.6	44.8	41.5	38.8
100000000	42.6	44.6	49.4	45.7	42.5
GEV Parameters					
Shape	0	0	0	0	0
Scale	1.632	1.746	2.009	1.802	1.628
Location	12.521	12.455	12.406	12.480	12.553
Kolmogorov-Smirnov Test:					
D	0.150	0.147	**0.126**	0.136	0.145

Table 5.8.B.10
Comparison of Methods to Determine Extreme Wind Gusts (the Site)

Return Period	Wind Gusts [m/s]				
	Method of Moments	Method of L-Moments	Method of Maximum Likelihood	Gumbel's Fitting Method	Method of Least Squares
10	33.0	33.1	32.4	33.8	33.3
100	41.6	41.9	40.4	43.3	42.3
1000	50.1	50.6	48.3	52.7	51.1
10000	58.6	59.3	56.1	62.0	60.0
100000	67.1	67.9	64.0	71.4	68.8
1000000	75.5	76.6	71.8	80.8	77.6
10000000	84.0	85.3	79.6	90.1	86.4
100000000	92.5	93.9	87.5	99.5	95.3
GEV Parameters					
Shape	0	0	0	0	0
Scale	3.681	3.760	3.407	4.064	3.832
Location	24.697	24.650	24.724	24.605	24.679
Kolmogorov-Smirnov Test:					
D	0.123	0.119	0.125	**0.117**	0.123

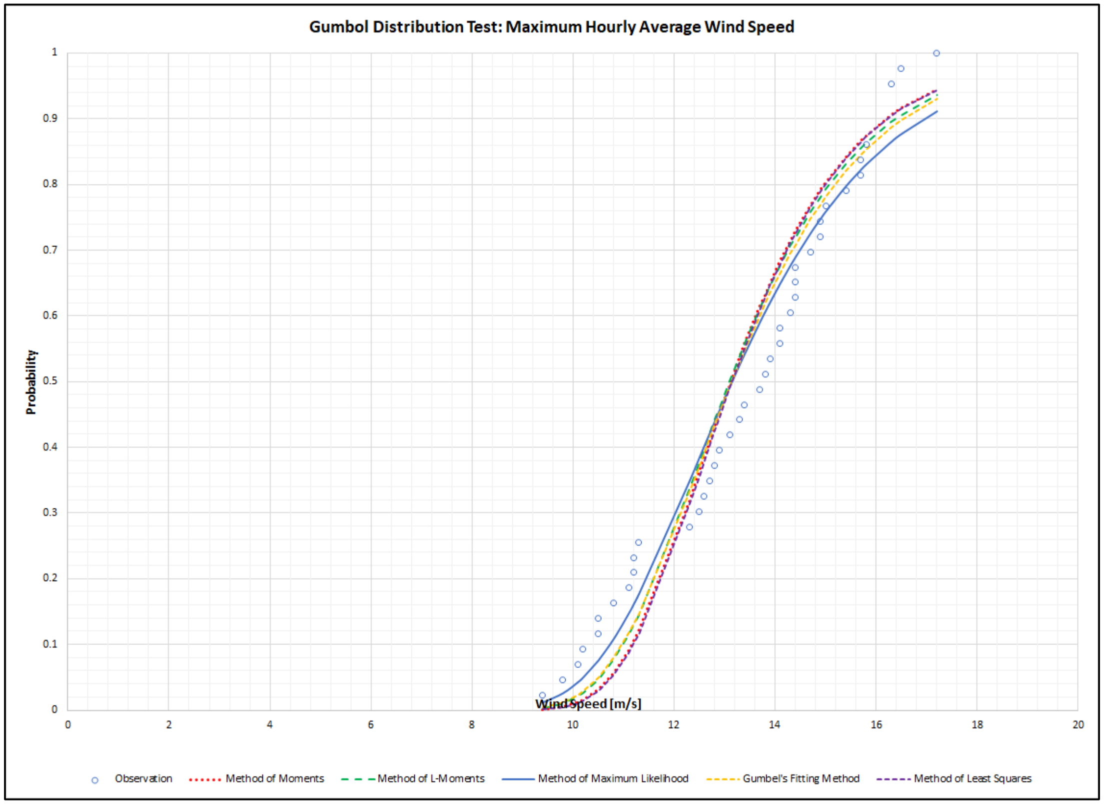

Figure 5.8.B.9
Goodness of Fit Test: Maximum Hourly Average Wind Speed (43-Year Dataset)

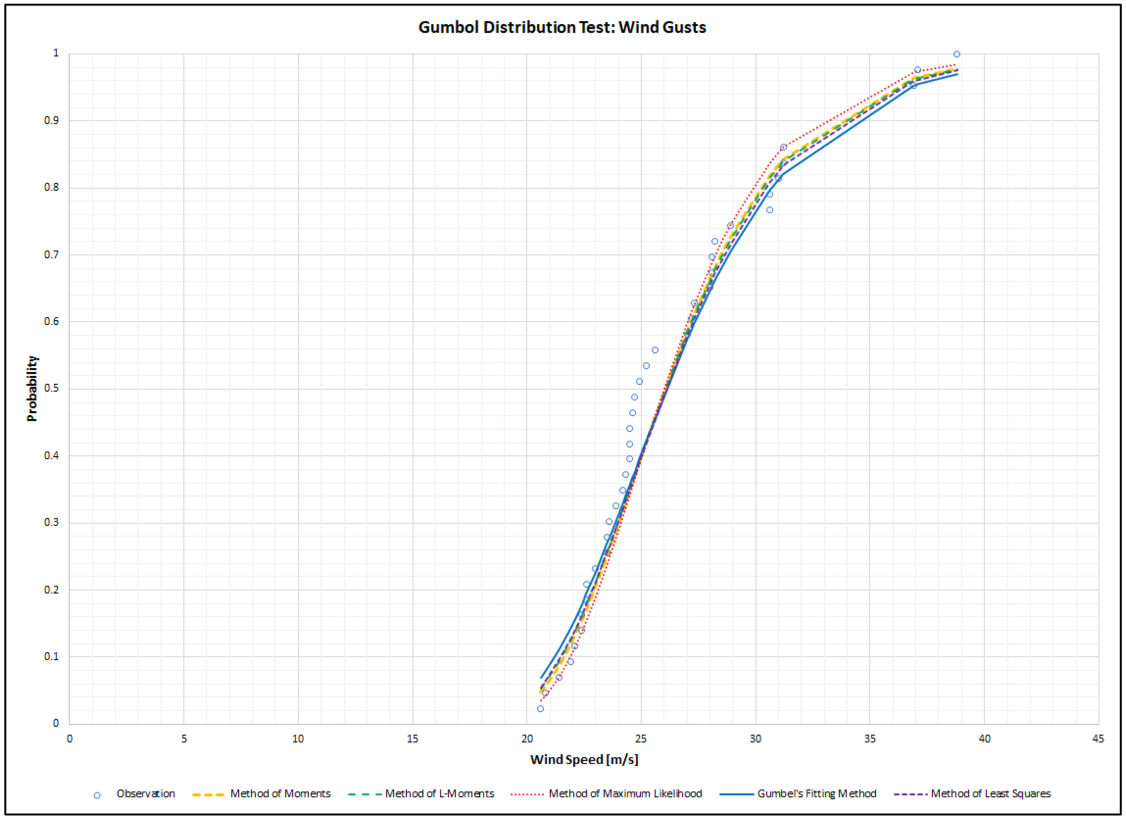

Figure 5.8.B.10

Goodness of Fit Test: Wind Gusts (43-Year Dataset)

Table 5.8.B.11 is a summary of the estimated extreme wind speeds using the method of maximum likelihood performed for the maximum hourly average wind speed data and the Gumbel's fitting method performing for the wind gust data. The table also includes the calculated 95 per cent confidence interval as estimated using the Jackknife sampling method. These results are illustrated in ***Figure 5.8.B.11*** (maximum hourly average) and ***Figure 5.8.B.12*** (wind gusts) together with the actual observed values.

Table 5.8.B.11
Maximum Hourly Average Wind Speeds and Wind Gust Extremes (the Site)

Return Period	**Wind Speed [m/s]**			
	Hourly Average Wind Speed	**95% Confidence Interval**	**Wind Gust**	**95% Confidence Interval**
10	16.9	± 1.0	33.8	± 2.7
100	21.6	± 1.5	43.3	± 4.8
1000	26.3	± 2.2	52.7	± 6.8
10000	30.9	± 2.8	62.0	± 8.9
100000	35.5	± 3.5	71.4	± 11.0
1000000	40.2	± 4.2	80.8	± 13.1
10000000	44.8	± 4.8	90.1	± 15.2
100000000	49.4	± 5.5	99.5	± 17.3

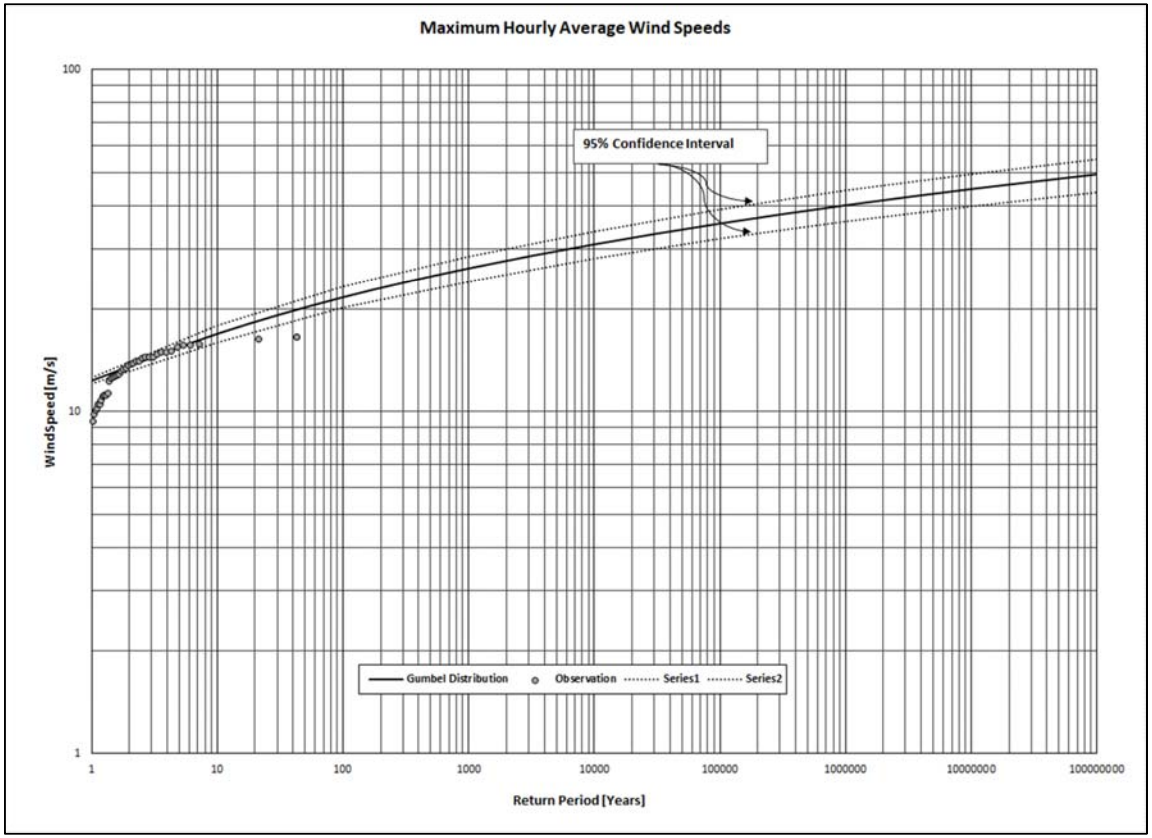

Figure 5.8.B.11

Gumbel Distribution Fit to Maximum Hourly Average Wind Speeds (43-Year Dataset)

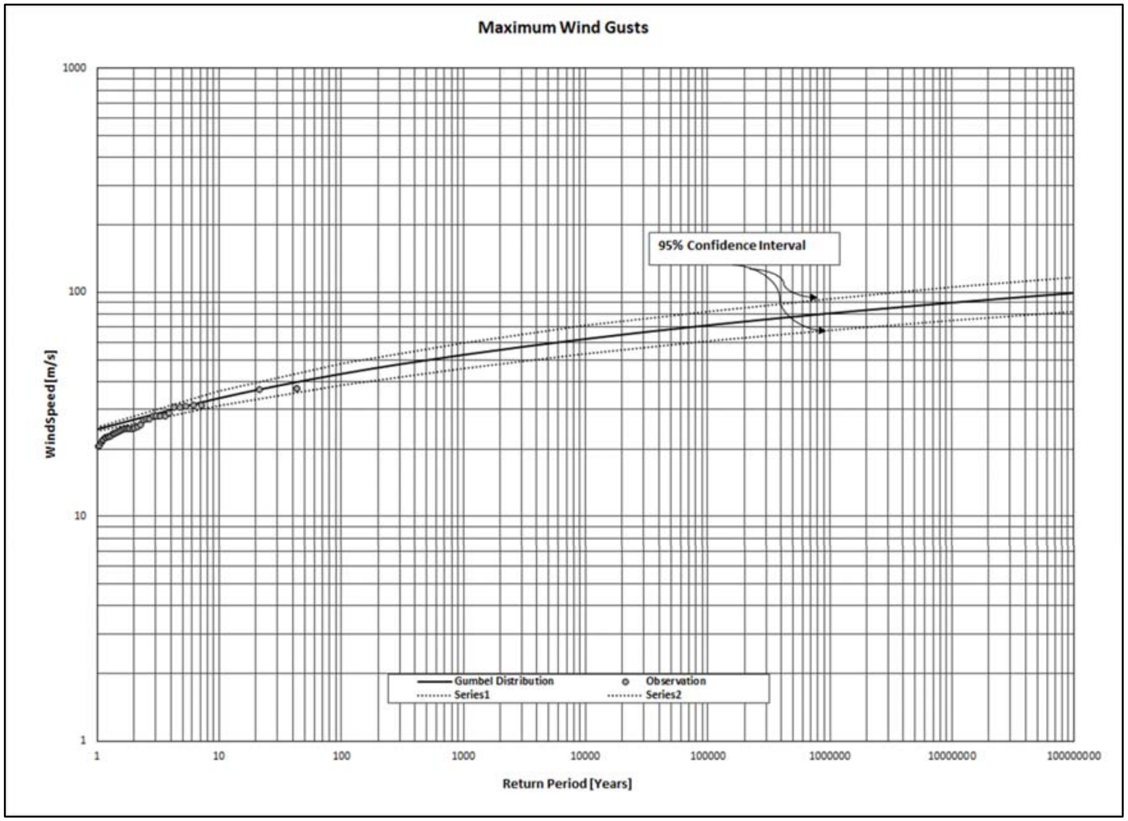

Figure 5.8.B.12

Gumbel Distribution Fit to Wind Gust Events (40-Year Dataset)

Appendix 5.8.C: Evapotranspiration Rate Estimation

The classical form for the Penman (Penman, 1948; Penman, 1963) equation to estimate potential evaporation or evapotranspiration is:

$$E_{PEN} = \frac{\Delta}{\Delta + \gamma}\left(\frac{R_n}{\lambda}\right) + \frac{\gamma}{\Delta + \gamma}\left(\frac{6.43 f_u D}{\lambda}\right)$$

where

E_{PEN} = potential, open water evaporation or evapotranspiration (mm/d)

R_n = net radiation at the surface (MJ/m²/d)

Δ = slope of the saturation vapour pressure curve (kPa/°C) obtained from

$$\Delta = \frac{4098 e_s}{(237.3 + T)^2}$$

with e_s being the saturation vapour pressure at temperature T (°C)

γ = psychrometric coefficient (kPa/°C), given by

$$\gamma = 0.00064734P$$

P = atmospheric pressure (kPa)

λ = 2.45 is latent heat of vaporization (MJ/kg)

D = (e_s - e_a) is the vapour pressure deficit (kPa), where

e_s is the saturation vapour pressure (kPa)

e_a is the actual vapour pressure (kPa)

f_n = wind function: $f_n = a_u + b_u u_2$ where a_u and b_u are wind function coefficients and u_2 is the wind speed at 2 m height (m/s)

For the original Penman (Penman, 1948; Penman, 1963) equation a_u = 1, b_u = 0.537.

A slight variation of the Penman equation is the Penman-Monteith equation (Shuttleworth, 1993):

$$E_{PM} = \frac{0.408\Delta(R_n - G) + \gamma \frac{900}{T + 273} u_2 D}{\Delta + \gamma(1 + 0.34 u_2)}$$

where

E_{PM} is the vegetation evaporation (mm/d)

G is the soil heat flux density (MJ/m²/d)

The soil heat flux density is approximately 10% of the net radiation, R_n.

The saturation vapour pressure $e_s(T)$ can be calculated with (Shuttleworth, 1993).

$$e_s(T) = 0.6108exp\left(\frac{17.27T}{273.3 + T}\right)$$

where T is the air temperature in °C.

The actual vapour pressure is obtained from

$$e_a(T) = \frac{RH}{100} e_s(T)$$

where RH is the relative humidity in %.

The *net radiation* (R_n) is computed as the difference between the incoming *net short wave radiation* (R_{ns}) and the *net long wave radiation* (R_L). The incoming net short wave radiation (R_{ns}) is calculated as:

$$R_{ns} = (1 - \alpha)R_s$$

where R_s is the *measured incoming solar radiation* (MJ/m².day) at the site and α is reflection coefficient or *albedo*. Albedo indicates the relative amount of solar radiation retained by the earth's surface. Variations in albedo of the earth's land surface are broad. Bare, moist dark soils reflect as little as 0.08, grasslands 0.26 and sandy deserts 0.37 (Johnston, 1983). For open water surfaces a = 0.08 (Shuttleworth, 1993). The albedo for the site vary between 0.097 in January and 0.118 in June (Johnston, 1983).

The net long-wave radiation R_L (MJ/m².day) is calculated from:

$$R_l = R_{Li} - R_{Lo}$$

where R_{Li} is the *incoming long wave radiation* (MJ/m².day) and R_{Lo} is the *outgoing long wave radiation* (MJ/m².day). The outgoing long wave radiation R_{Lo} is calculated from:

$$R_{Li} = f\xi_s\sigma(T_s + 273.15)^4$$

where

f = an adjustment for cloud cover
ξ_{as} = soil surface emissivity (= 0.95 for dry sand)
σ = 4.903x10^{-9} (MJ/m²/K^4/d) is Stephan-Boltzman constant
T_s = soil surface temperature in °C

The incoming long-wave radiation R_{Li} is calculated from:

$$R_{Li} = f\xi_a\sigma(T + 273.15)^4$$

where

f = an adjustment for cloud cover

ξ_a = net emissivity between the atmosphere and the ground

σ = 4.903x10^{-9} (MJ/m²/K^4/d) is Stephan-Boltzman constant

T = air temperature in °C

The adjustment for cloud cover *f* calculated from the measured incoming solar radiation, R_s and the clear sky radiation R_{s0}, as follows (Shuttleworth, 1993):

$$f = 1.35\frac{R_s}{R_{s0}} - 0.35$$

And the *clear sky radiation* from

$$R_{s0} = (0.57 + 0.00002Z)R_A$$

where R_A is the *extraterrestrial solar radiation* (MJ/m²/d) and *Z* is the station elevation above sea level (m).

The extraterrestrial solar radiation is computed from the relative position of the earth to the sun. This is approximated as follows (Shuttleworth, 1993)

$$R_A = \frac{12(60)}{\pi}d_rG_{SC}[(\omega_2 - \omega_1)\sin\varphi\sin\delta + \cos\varphi\cos\delta\,(\sin\omega_2 - \sin\omega_1)]$$

where the inverse relative Earth-Sun distance, d_r is given by

$$d_r = 1 + 0.033\cos\left(\frac{2\pi}{365}J\right)$$

and the solar declination, δ is given by

$$\delta = 0.409sin\,\left(\frac{2\pi}{365}J - 1.39\right)$$

with

G_{SC} = 0.0820 MJ/m²-min is the solar constant

J = the Julian day (1 = 1 January consecutively counting to 31 December)

ω_1 and ω_2 are the solar time angle (radians) at the beginning and end of the monitoring period, computed from

$$\omega_1 = \omega - \frac{\pi t_1}{24}$$

$$\omega_2 = \omega + \frac{\pi t_1}{24}$$

and ω the solar time angle (radians) at midpoint of the hourly, or shorter period, t_1 length of the calculation period (hour), e.g., 1 for an hourly period or 0.17 for a 10-minute period, computed from

$$\omega_s = \frac{\pi}{12}[t + 0.06667(15GMT - L_m) + S_c - 12]$$

with

t the standard clock time (hour)

GMT hours different from Greenwich Meantime (i.e., 2 hours in South Africa)

L_m is the longitude (degrees, positive towards the east starting at Greenwich)

S_C is the seasonal correction for solar time (hour) obtained from

$$S_c = 0{,}1645 sin(2b) - 0{,}1255 cos(b) - 0{,}025 sin(b)$$

$$b = \frac{2\pi(J - 81)}{364}$$

The following applies:

if $\omega_1 < -\omega_s$ then $\omega_1 = -\omega_s$

if $\omega_2 > \omega_s$ then $\omega_2 = \omega_s$

The most important parameters in the calculation of the evapotranspiration rates, as discussed above, are given in ***Table 5.8.C.1*** to ***Table 5.8.C.3*** for a 24-hour example.

Table 5.8.C.1
Evapotranspiration Calculation Parameters(1)

JD	Hour	Temperature (°C)	Pressure (Pa)	Relative Humidity (%)	Wind Speed at 10 m (m/s)	Wind Speed at 10 m (m/s)	Solar Radiation (W/m^2)	Inverse relative Earth-Sun distance (d_r)	Solar Declination	Hour Angle	w1	w2	Extraterrestrial Ra (MJ/m^2-h)
11	1	17.7	1004	96.3	2.4	1.413	0.1	1.032	-0.381	-2.821	-2.952	-2.690	-2.6294
11	2	17.2	1003	94.3	2.1	1.236	0.1	1.032	-0.381	-2.560	-2.690	-2.429	-2.1867
11	3	17.2	1003	88.7	1.8	1.059	0.2	1.032	-0.381	-2.298	-2.429	-2.167	-1.5227
11	4	17.7	1002	86.8	1.8	1.059	0.1	1.032	-0.381	-2.036	-2.167	-1.905	-0.6826
11	5	17.2	1002	93.9	3.2	1.883	0.2	1.032	-0.381	-1.774	-1.905	-1.643	0.2765
11	6	16.8	1002	96.6	1.7	1.001	0.1	1.032	-0.381	-1.512	-1.643	-1.381	1.2891
11	7	17	1001	87.3	1.8	1.059	20.6	1.032	-0.381	-1.251	-1.381	-1.120	2.2862
11	8	18.9	1001	77.1	1.2	0.706	167	1.032	-0.381	-0.989	-1.120	-0.858	3.1998
11	9	21.8	1001	70.5	1.1	0.647	381.1	1.032	-0.381	-0.727	-0.858	-0.596	3.9678
11	10	25.4	1000	53.3	1.9	1.118	609.5	1.032	-0.381	-0.465	-0.596	-0.334	4.5378
11	11	28.2	1000	60.3	2.5	1.471	813	1.032	-0.381	-0.203	-0.334	-0.072	4.8709
11	12	24.4	999	70.6	3.4	2.001	969	1.032	-0.381	0.058	-0.072	0.189	4.9444
11	13	22.4	1000	82.8	4	2.354	1065	1.032	-0.381	0.320	0.189	0.451	4.7534
11	14	21.4	1000	85.5	5.8	3.414	1087	1.032	-0.381	0.582	0.451	0.713	4.3107
11	15	20.9	999	81.4	7.8	4.591	1051	1.032	-0.381	0.844	0.713	0.975	3.6467
11	16	20.3	999	84.7	8.9	5.238	802	1.032	-0.381	1.106	0.975	1.237	2.8066
11	17	19.6	999	89	8	4.709	500.5	1.032	-0.381	1.367	1.237	1.498	1.8475
11	18	19.7	999	87.1	7.2	4.238	529.6	1.032	-0.381	1.629	1.498	1.760	0.8349
11	19	19.8	1000	85.4	6.3	3.708	339.8	1.032	-0.381	1.891	1.760	2.022	-0.1622
11	20	19.6	1000	96.9	5.8	3.414	91.4	1.032	-0.381	2.153	2.022	2.284	-1.0759
11	21	19.1	1002	96.4	6.1	3.590	5.2	1.032	-0.381	2.415	2.284	2.546	-1.8438
11	22	20.3	1003	96.5	5.1	3.002	0.4	1.032	-0.381	2.676	2.546	2.807	-2.4138
11	23	20.4	1004	99.5	5.3	3.120	0.2	1.032	-0.381	2.938	2.807	3.069	-2.7469
11	24	20.5	1004	99.2	4.4	2.590	0.3	1.032	-0.381	3.200	3.069	3.331	-2.8204

Table 5.8.C.2
Evapotranspiration Calculation Parameters(2)

JD	Hour	Seasonal correction (Sc) (hour)	Gamma (Pa/°C)	Saturation Vapour Pressure (Pa)	Actual Vapour Pressure (Pa)	delta (Pa/°C)	Clear sky radiation (R_{s0}) (MJ/m²/d)	f-adjustment	Net Emissivity	Net Longwave Radiation (R_L) (W/m²)	Net Radiation (Rn) (W/m²)	Soil Heat Flux (W/m²)
11	1	-0.1302	65.8836	2026.0394	1951.0759	127.6849	-47.4168	-0.350	0.144	0.0000	0.0770	0.0077
11	2	-0.1302	65.8180	1963.0682	1851.1733	124.2029	-39.4348	-0.350	0.150	0.0000	0.0770	0.0077
11	3	-0.1302	65.8180	1963.0682	1741.2415	124.2029	-27.4603	-0.351	0.155	0.0000	0.1540	0.0154
11	4	-0.1302	65.7523	2026.0394	1758.6022	127.6849	-12.3092	-0.351	0.154	0.0000	0.0770	0.0077
11	5	-0.1302	65.7523	1963.0682	1843.3211	124.2029	4.9859	-0.345	0.150	0.0000	0.1540	0.0154
11	6	-0.1302	65.7523	1913.9322	1848.8585	121.4756	23.2463	-0.349	0.150	0.0000	0.0770	0.0077
11	7	-0.1302	65.6867	1938.3638	1692.1916	122.8329	41.2277	-0.292	0.158	0.0000	15.8620	1.5862
11	8	-0.1302	65.6867	2184.4369	1684.2008	136.3808	57.7047	-0.012	0.158	0.0000	128.5900	12.8590
11	9	-0.1302	65.6867	2612.7271	1841.9726	159.4892	71.5543	0.271	0.150	17.4705	275.9765	27.5976
11	10	-0.1302	65.6211	3245.1045	1729.6407	192.6995	81.8328	0.519	0.156	36.4514	432.8636	43.2864
11	11	-0.1302	65.6211	3825.4242	2306.7308	222.3937	87.8396	0.730	0.127	43.4823	582.5277	58.2528
11	12	-0.1302	65.5555	3057.3134	2158.4633	182.9382	89.1655	0.918	0.134	54.8171	691.3129	69.1313
11	13	-0.1302	65.6211	2709.9695	2243.8547	164.6616	85.7200	1.000	0.130	56.4069	763.6431	76.3643
11	14	-0.1302	65.6211	2549.6052	2179.9124	156.1177	77.7381	1.000	0.133	56.9330	780.0570	78.0057
11	15	-0.1302	65.5555	2472.5794	2012.6796	151.9881	65.7635	1.000	0.141	59.9781	749.2919	74.9292
11	16	-0.1302	65.5555	2382.8393	2018.2649	147.1550	50.6124	1.000	0.141	59.3742	558.1658	55.8166
11	17	-0.1302	65.5555	2281.7527	2030.7599	141.6812	33.3173	1.000	0.140	58.5536	326.8314	32.6831
11	18	-0.1302	65.5555	2295.9599	1999.7811	142.4525	15.0569	1.000	0.142	59.2712	348.5208	34.8521
11	19	-0.1302	65.6211	2310.2445	1972.9488	143.2273	-2.9245	-13.902	0.143	0.0000	261.6460	26.1646
11	20	-0.1302	65.6211	2281.7527	2211.0183	141.6812	-19.4014	-0.899	0.132	0.0000	70.3780	7.0378
11	21	-0.1302	65.7523	2211.8636	2132.2366	137.8778	-33.2511	-0.368	0.136	0.0000	4.0040	0.4004
11	22	-0.1302	65.8180	2382.8393	2299.4399	147.1550	-43.5295	-0.351	0.128	0.0000	0.3080	0.0308
11	23	-0.1302	65.8836	2397.5952	2385.6072	147.9514	-49.5364	-0.350	0.124	0.0000	0.1540	0.0154
11	24	-0.1302	65.8836	2412.4309	2393.1315	148.7514	-50.8623	-0.351	0.123	0.0000	0.2310	0.0231

Table 5.8.C.3
Evapotranspiration Calculation Parameters(3)

JD	Hour	Penman (mm/day)	Penman-Monteith (mm/day)
11	1	0.0050	0.0041
11	2	0.0071	0.0055
11	3	0.0133	0.0095
11	4	0.0157	0.0111
11	5	0.0093	0.0084
11	6	0.0039	0.0027
11	7	0.0299	0.0226
11	8	0.1520	0.1201
11	9	0.3203	0.2602
11	10	0.5418	0.4386
11	11	0.7286	0.5907
11	12	0.8016	0.6211
11	13	0.8352	0.6201
11	14	0.8409	0.5758
11	15	0.8217	0.5259
11	16	0.6142	0.3781
11	17	0.3589	0.2279
11	18	0.3841	0.2518
11	19	0.2983	0.2059
11	20	0.0776	0.0537
11	21	0.0122	0.0111
11	22	0.0077	0.0077
11	23	0.0012	0.0012
11	24	0.0018	0.0017

Appendix 5.8.D: Instrument Specifications

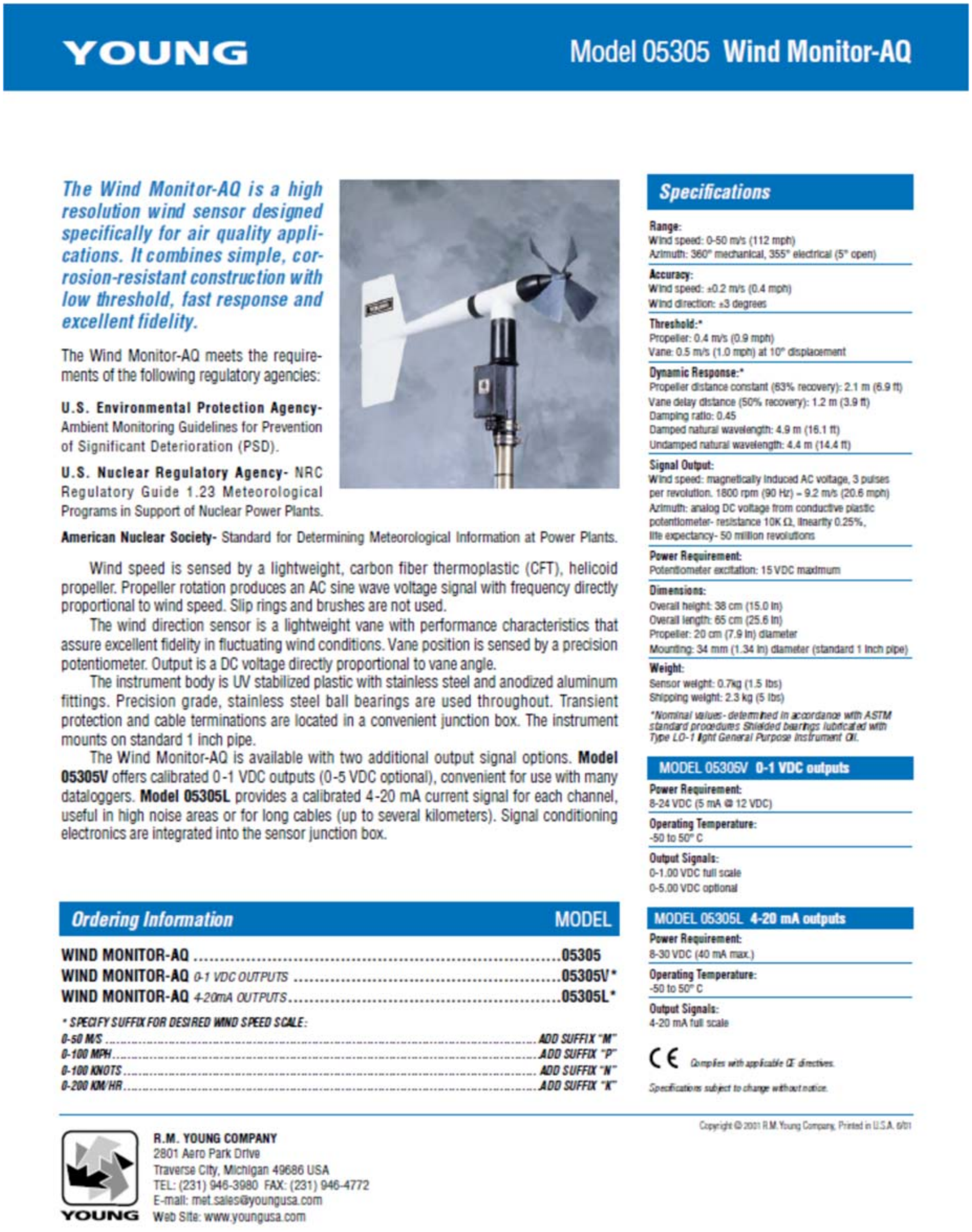

YOUNG Model 05305 **Wind Monitor-AQ**

The Wind Monitor-AQ is a high resolution wind sensor designed specifically for air quality applications. It combines simple, corrosion-resistant construction with low threshold, fast response and excellent fidelity.

The Wind Monitor-AQ meets the requirements of the following regulatory agencies:

U.S. Environmental Protection Agency- Ambient Monitoring Guidelines for Prevention of Significant Deterioration (PSD).

U.S. Nuclear Regulatory Agency- NRC Regulatory Guide 1.23 Meteorological Programs in Support of Nuclear Power Plants.

American Nuclear Society- Standard for Determining Meteorological Information at Power Plants.

Wind speed is sensed by a lightweight, carbon fiber thermoplastic (CFT), helicoid propeller. Propeller rotation produces an AC sine wave voltage signal with frequency directly proportional to wind speed. Slip rings and brushes are not used.

The wind direction sensor is a lightweight vane with performance characteristics that assure excellent fidelity in fluctuating wind conditions. Vane position is sensed by a precision potentiometer. Output is a DC voltage directly proportional to vane angle.

The instrument body is UV stabilized plastic with stainless steel and anodized aluminum fittings. Precision grade, stainless steel ball bearings are used throughout. Transient protection and cable terminations are located in a convenient junction box. The instrument mounts on standard 1 inch pipe.

The Wind Monitor-AQ is available with two additional output signal options. **Model 05305V** offers calibrated 0-1 VDC outputs (0-5 VDC optional), convenient for use with many dataloggers. **Model 05305L** provides a calibrated 4-20 mA current signal for each channel, useful in high noise areas or for long cables (up to several kilometers). Signal conditioning electronics are integrated into the sensor junction box.

Ordering Information	MODEL
WIND MONITOR-AQ	**05305**
WIND MONITOR-AQ *0-1 VDC OUTPUTS*	**05305V***
WIND MONITOR-AQ *4-20mA OUTPUTS*	**05305L***

** SPECIFY SUFFIX FOR DESIRED WIND SPEED SCALE:*

0-50 M/S	*ADD SUFFIX "M"*
0-100 MPH	*ADD SUFFIX "P"*
0-100 KNOTS	*ADD SUFFIX "N"*
0-200 KM/HR	*ADD SUFFIX "K"*

Specifications

Range:
Wind speed: 0-50 m/s (112 mph)
Azimuth: 360° mechanical, 355° electrical (5° open)

Accuracy:
Wind speed: ±0.2 m/s (0.4 mph)
Wind direction: ±3 degrees

Threshold:*
Propeller: 0.4 m/s (0.9 mph)
Vane: 0.5 m/s (1.0 mph) at 10° displacement

Dynamic Response:*
Propeller distance constant (63% recovery): 2.1 m (6.9 ft)
Vane delay distance (50% recovery): 1.2 m (3.9 ft)
Damping ratio: 0.45
Damped natural wavelength: 4.9 m (16.1 ft)
Undamped natural wavelength: 4.4 m (14.4 ft)

Signal Output:
Wind speed: magnetically induced AC voltage, 3 pulses per revolution. 1800 rpm (90 Hz) = 9.2 m/s (20.6 mph)
Azimuth: analog DC voltage from conductive plastic potentiometer- resistance 10K Ω, linearity 0.25%, life expectancy- 50 million revolutions

Power Requirement:
Potentiometer excitation: 15 VDC maximum

Dimensions:
Overall height: 38 cm (15.0 in)
Overall length: 65 cm (25.6 in)
Propeller: 20 cm (7.9 in) diameter
Mounting: 34 mm (1.34 in) diameter (standard 1 inch pipe)

Weight:
Sensor weight: 0.7kg (1.5 lbs)
Shipping weight: 2.3 kg (5 lbs)

**Nominal values- determined in accordance with ASTM standard procedures Shielded bearings lubricated with Type LO-1 light General Purpose Instrument Oil.*

MODEL 05305V **0-1 VDC outputs**

Power Requirement:
8-24 VDC (5 mA @ 12 VDC)

Operating Temperature:
-50 to 50° C

Output Signals:
0-1.00 VDC full scale
0-5.00 VDC optional

MODEL 05305L **4-20 mA outputs**

Power Requirement:
8-30 VDC (40 mA max.)

Operating Temperature:
-50 to 50° C

Output Signals:
4-20 mA full scale

CE *Complies with applicable CE directives.*

Specifications subject to change without notice.

YOUNG
R.M. YOUNG COMPANY
2801 Aero Park Drive
Traverse City, Michigan 49686 USA
TEL: (231) 946-3980 FAX: (231) 946-4772
E-mail: met.sales@youngusa.com
Web Site: www.youngusa.com

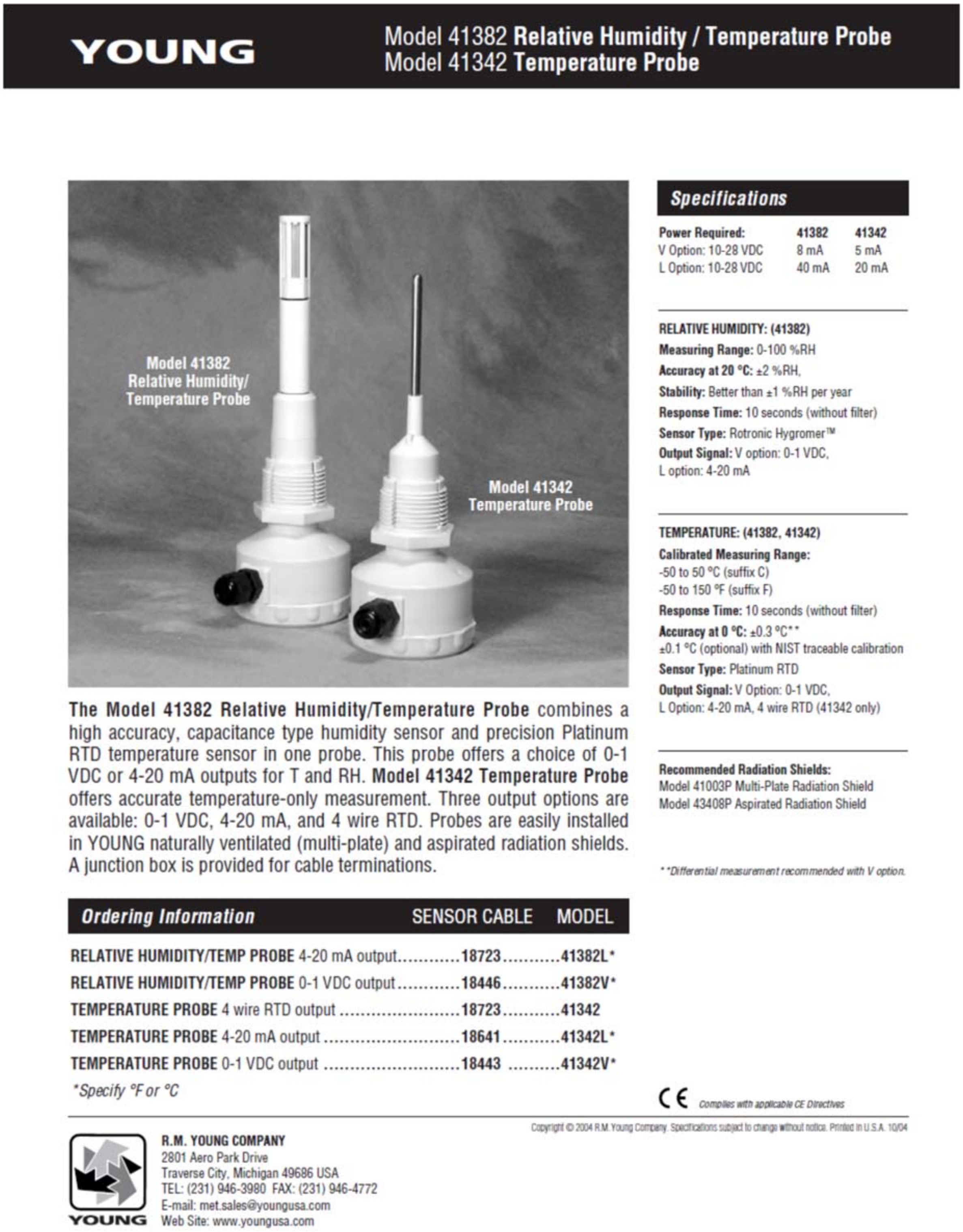

YOUNG

Model 41382 **Relative Humidity / Temperature Probe**
Model 41342 **Temperature Probe**

Model 41382 Relative Humidity/ Temperature Probe

Model 41342 Temperature Probe

The Model 41382 Relative Humidity/Temperature Probe combines a high accuracy, capacitance type humidity sensor and precision Platinum RTD temperature sensor in one probe. This probe offers a choice of 0-1 VDC or 4-20 mA outputs for T and RH. **Model 41342 Temperature Probe** offers accurate temperature-only measurement. Three output options are available: 0-1 VDC, 4-20 mA, and 4 wire RTD. Probes are easily installed in YOUNG naturally ventilated (multi-plate) and aspirated radiation shields. A junction box is provided for cable terminations.

Ordering Information	SENSOR CABLE	MODEL
RELATIVE HUMIDITY/TEMP PROBE 4-20 mA output	**18723**	**41382L***
RELATIVE HUMIDITY/TEMP PROBE 0-1 VDC output	**18446**	**41382V***
TEMPERATURE PROBE 4 wire RTD output	**18723**	**41342**
TEMPERATURE PROBE 4-20 mA output	**18641**	**41342L***
TEMPERATURE PROBE 0-1 VDC output	**18443**	**41342V***

**Specify °F or °C*

Specifications

Power Required:	**41382**	**41342**
V Option: 10-28 VDC	8 mA	5 mA
L Option: 10-28 VDC	40 mA	20 mA

RELATIVE HUMIDITY: (41382)

Measuring Range: 0-100 %RH

Accuracy at 20 °C: ±2 %RH,

Stability: Better than ±1 %RH per year

Response Time: 10 seconds (without filter)

Sensor Type: Rotronic Hygromer™

Output Signal: V option: 0-1 VDC,
L option: 4-20 mA

TEMPERATURE: (41382, 41342)

Calibrated Measuring Range:
-50 to 50 °C (suffix C)
-50 to 150 °F (suffix F)

Response Time: 10 seconds (without filter)

Accuracy at 0 °C: ±0.3 °C**
±0.1 °C (optional) with NIST traceable calibration

Sensor Type: Platinum RTD

Output Signal: V Option: 0-1 VDC,
L Option: 4-20 mA, 4 wire RTD (41342 only)

Recommended Radiation Shields:
Model 41003P Multi-Plate Radiation Shield
Model 43408P Aspirated Radiation Shield

***Differential measurement recommended with V option.*

CE *Compiles with applicable CE Directives*

YOUNG
R.M. YOUNG COMPANY
2801 Aero Park Drive
Traverse City, Michigan 49686 USA
TEL: (231) 946-3980 FAX: (231) 946-4772
E-mail: met.sales@youngusa.com
Web Site: www.youngusa.com

YOUNG

Model 41003 Multi-Plate Radiation Shield

The Multi-Plate Radiation Shield protects temperature and relative humidity sensors from error-producing solar radiation and precipitation. Compact size and light weight make this shield useful for many applications.

The multiple plates have a unique profile that blocks direct and reflected solar radiation, yet permits easy passage of air. Enlarged top plate and steep edge profile minimize moisture accumulation from precipitation and dew. The plate material is specially formulated for high reflectivity, low thermal conductivity, and maximum weather resistance. The rugged U-bolt mounting clamp attaches easily to any vertical pipe up to 2 inches diameter.

Model 41003 employs a universal clamp-type adapter to securely hold sensors up to 12.5 mm diameter. **Model 41003P** features a special mounting adapter that is custom sized to fit a sensor from 12.5 mm to 26 mm diameter; please specify the sensor diameter when ordering.

The Temperature Probe is a precision Platinum RTD encased in a stainless steel protective sheath. The sensor assembly is securely mounted in a convenient junction box that fits YOUNG radiation shields. For special applications, the temperature probe is available with various output options. The 4-20 mA current output is useful in high noise, industrial settings or for long cable lengths. The 0-1 VDC option provides a calibrated voltage output signal. Low power circuitry makes it ideal for field studies and remote data-logging applications.

The Relative Humidity/Temperature Probe combines a high-accuracy humidity sensor and temperature sensor into one compact unit. The probe is available with 0-1 VDC or 4-20 mA outputs to satisfy a wide variety of applications.

Ordering Information

	MODEL
MULTI-PLATE RADIATION SHIELD *Includes universal adapter for sensors to 15 mm diameter.*	41003
MULTI-PLATE RADIATION SHIELD *With custom sensor adapter. Specify diameter from 12.5 mm to 26 mm.*	41003P
TEMPERATURE PROBE - RTD OUTPUT	41342
4-20 mA OUTPUT*	41342L*
0-1 VDC OUTPUT*	41342V*
RELATIVE HUMIDITY/TEMPERATURE PROBE:	
4-20 mA OUTPUT*	41382L*
0-1 VDC OUTPUT*	41382V*
ACCESSORY JUNCTION BOX *Specify sensor diameter (10 mm max.)*	41390

Specifications

Sensor Types:
Accommodates temperature and humidity sensors up to 26 mm (1 in) diameter

Radiation Error:
@ 1080 W/m² intensity- Dependent on wind speed
0.4° C (0.7°F) RMS @ 3 m/s (6.7 mph)
0.7° C (1.3°F) RMS @ 2 m/s (4.5 mph)
1.5° C (2.7°F) RMS @ 1 m/s (2.2 mph)

Construction:
UV stabilized white thermoplastic plates
Aluminum mounting bracket, white powder coated
Stainless steel U-bolt clamp

Dimensions:
13 cm (5.1 in) diameter x 26 cm (10.2 in) high
Mounting fits vertical pipe 25-50 mm (1-2 in) diameter

Weight:
Net weight: 0.7 kg (1.5 lb)
Shipping weight: 1.4 kg (3 lb)

MODEL 41342 Platinum Temp. Probe

Sensor Type:
1000 Ω Platinum RTD

Range:
Temperature: -50° C to +50° C (-50° to +150° F)

Accuracy:
±0.3° C at 0° C (standard)
±0.1° C at 0° C (optional)

Available Outputs: (Power Requirement)
4 wire RTD 41342
4-20 mA (12-30 VDC, 20 mA) 41342L
0-1 VDC (8-24 VDC, 5 mA) 41342V

MODEL 41382 Rel. Humidity/Temp. Probe

Sensor Type:
Temperature: 100 Ω Platinum RTD
Humidity: Capacitive Polymer

Range:
Temperature: -50° C to +50° C (-50° to +150° F)
Humidity: 0 to 100% RH

Accuracy:
Temperature: ±0.3° C
Humidity: ±2% RH

Available Outputs: (Power Requirement)
4-20 mA (10-28 VDC, 20 mA) 41382L
0-1 VDC (10-28 VDC, 8 mA) 41382V

SPECIFY TEMPERATURE SCALING:
-50 to +50° C add suffix C
-50 to +150° F add suffix F

YOUNG
R.M. YOUNG COMPANY
2801 Aero Park Drive
Traverse City, Michigan 49686 USA
TEL: (231) 946-3980 FAX: (231) 946-4772
E-mail: met.sales@youngusa.com
Web Site: www.youngusa.com

YOUNG Model 52202 Tipping Bucket Rain Gauge

The YOUNG Tipping Bucket Rain Gauge meets the specifications of the World Meteorological Organization (WMO).

The design uses a proven tipping bucket mechanism for simple and effective rainfall measurement. The bucket geometry and material are specially selected for maximum water release, thereby reducing contamination and errors.

Catchment area of 200 cm^2 and measurement resolution of 0.1 mm meet the recommendations of the WMO. Leveling screws and bullseye level are built-in for easy and precise adjustment in the field. Measured precipitation is discharged through a collection tube for verification of total rainfall.

Model 52202 is heated for operation in cold temperatures. An unheated version, 52203, is available for use in moderate climates.

To discourage birds from perching on the funnel rim, accessory bird wire assembly may be attached to the gauge.

Specifications

Size:
18 cm dia. x 30 cm high, (39 cm high with mounting base)

Catchment Area:
200 cm^2

Resolution:
0.1 mm per tip
0.2 mm per tip (optional)

Accuracy:
2% up to 25 mm/hr
3% up to 50 mm/hr

Output:
Magnetic reed switch (N.O.), rating 24VAC/DC 500mA

Operating Temperature:
-20°C to +50°C (heated)

Power:
18 Watts for heater only

Mounting:
Clamp for 1" (1.34" dia.) iron pipe
or 3 bolts on 160mm dia. circle

Other:
Leveling adjustment, thermostatic control for heater, intake screen

Ordering Information	MODEL
TIPPING BUCKET RAIN GAUGE (HEATED)	52202
TIPPING BUCKET RAIN GAUGE (UNHEATED)	52203
BIRD WIRE ASSEMBLY	52250

CE *Complies with applicable CE directives.*
Specifications subject to change without notice.

R.M. YOUNG COMPANY
2801 Aero Park Drive
Traverse City, Michigan 49686 USA
TEL: (231) 946-3980 FAX: (231) 946-4772
E-mail: met.sales@youngusa.com
Web Site: www.youngusa.com

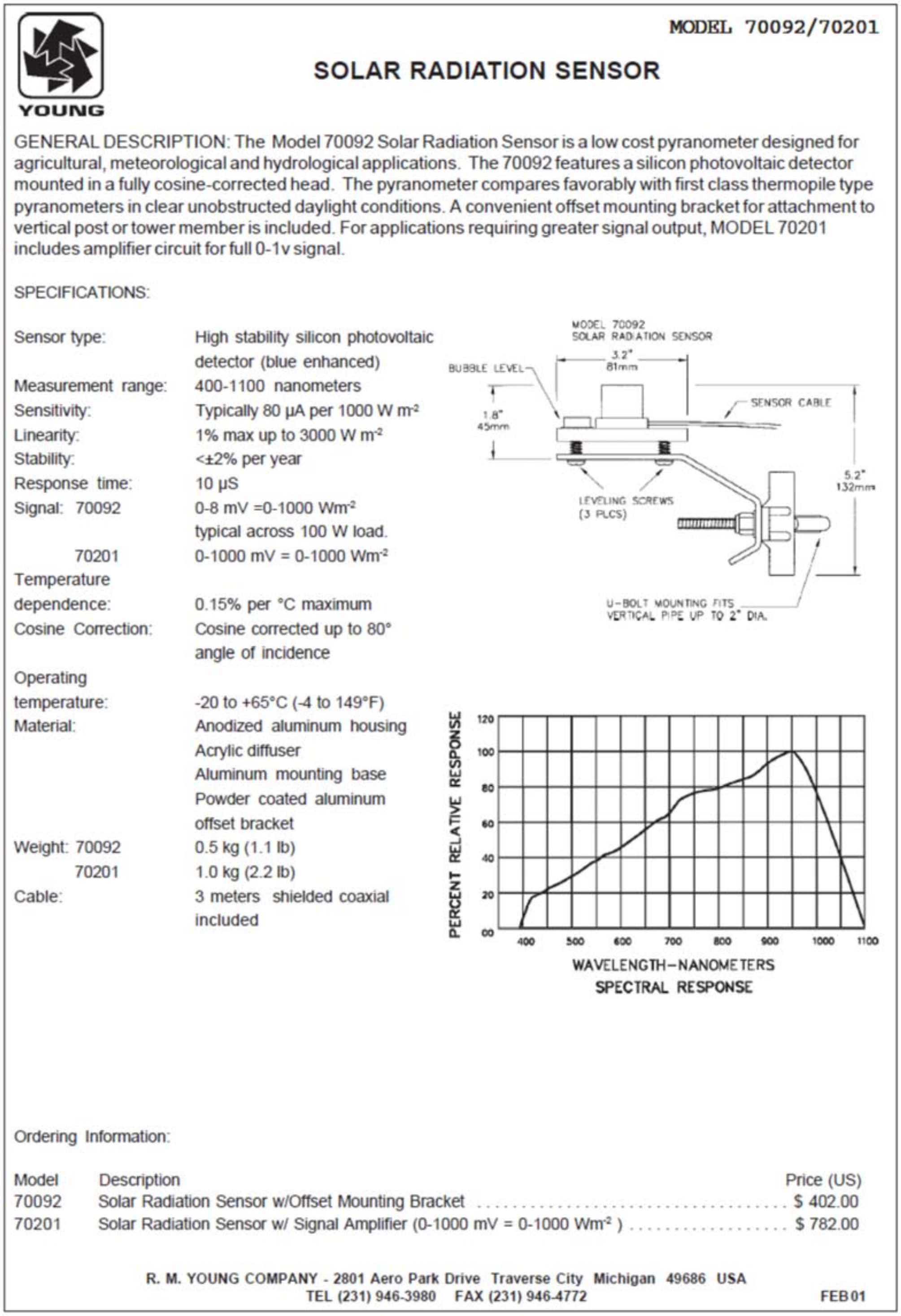

MODEL 70092/70201

SOLAR RADIATION SENSOR

GENERAL DESCRIPTION: The Model 70092 Solar Radiation Sensor is a low cost pyranometer designed for agricultural, meteorological and hydrological applications. The 70092 features a silicon photovoltaic detector mounted in a fully cosine-corrected head. The pyranometer compares favorably with first class thermopile type pyranometers in clear unobstructed daylight conditions. A convenient offset mounting bracket for attachment to vertical post or tower member is included. For applications requiring greater signal output, MODEL 70201 includes amplifier circuit for full 0-1v signal.

SPECIFICATIONS:

Sensor type:	High stability silicon photovoltaic detector (blue enhanced)
Measurement range:	400-1100 nanometers
Sensitivity:	Typically 80 µA per 1000 W m^{-2}
Linearity:	1% max up to 3000 W m^{-2}
Stability:	<±2% per year
Response time:	10 µS
Signal: 70092	0-8 mV =0-1000 Wm^{-2} typical across 100 W load.
70201	0-1000 mV = 0-1000 Wm^{-2}
Temperature dependence:	0.15% per °C maximum
Cosine Correction:	Cosine corrected up to 80° angle of incidence
Operating temperature:	-20 to +65°C (-4 to 149°F)
Material:	Anodized aluminum housing Acrylic diffuser Aluminum mounting base Powder coated aluminum offset bracket
Weight: 70092	0.5 kg (1.1 lb)
70201	1.0 kg (2.2 lb)
Cable:	3 meters shielded coaxial included

Ordering Information:

Model	Description	Price (US)
70092	Solar Radiation Sensor w/Offset Mounting Bracket	$ 402.00
70201	Solar Radiation Sensor w/ Signal Amplifier (0-1000 mV = 0-1000 Wm^{-2})	$ 782.00

R. M. YOUNG COMPANY - 2801 Aero Park Drive Traverse City Michigan 49686 USA
TEL (231) 946-3980 FAX (231) 946-4772

FEB01

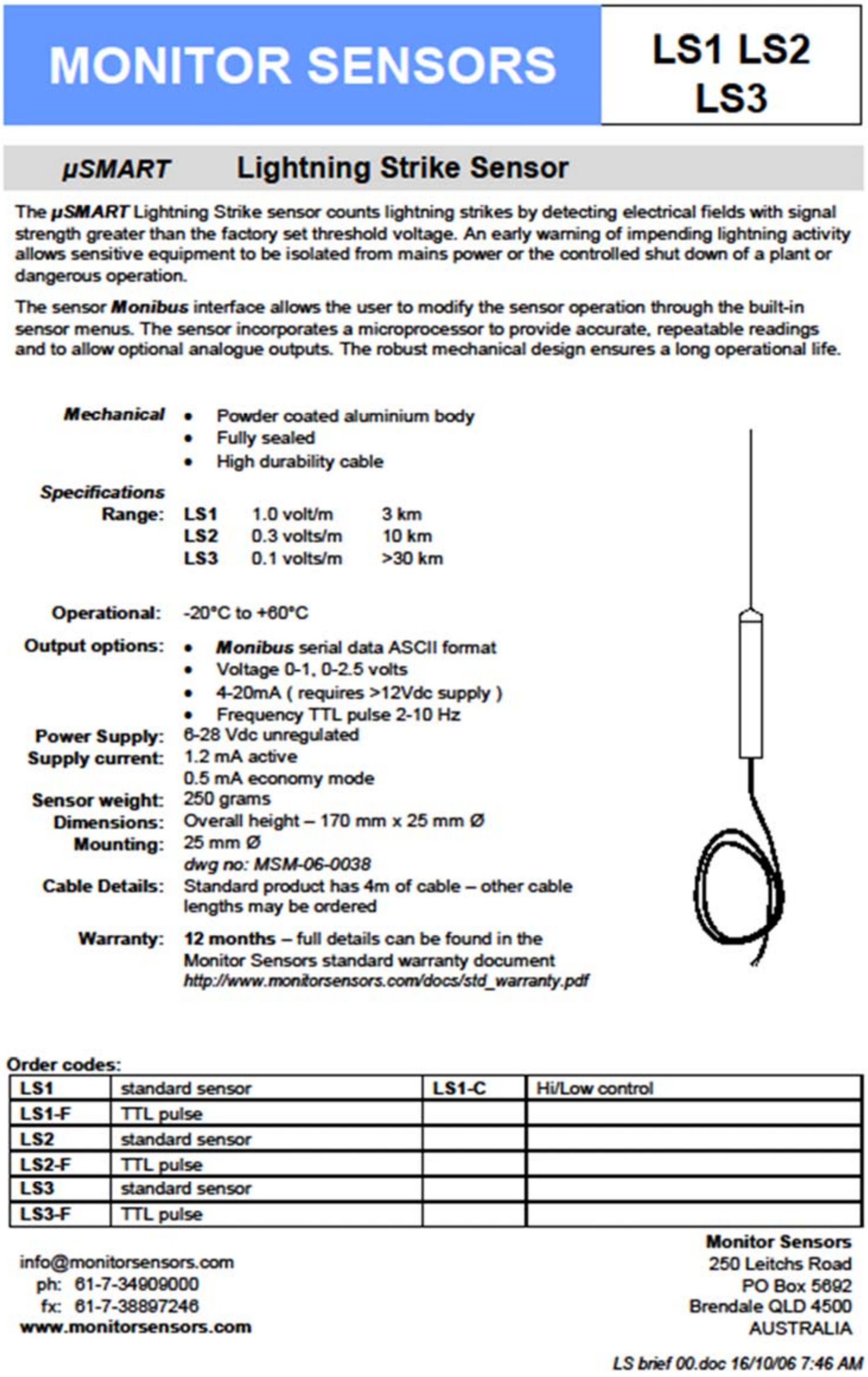

MONITOR SENSORS

LS1 LS2 LS3

µSMART Lightning Strike Sensor

The ***µSMART*** Lightning Strike sensor counts lightning strikes by detecting electrical fields with signal strength greater than the factory set threshold voltage. An early warning of impending lightning activity allows sensitive equipment to be isolated from mains power or the controlled shut down of a plant or dangerous operation.

The sensor ***Monibus*** interface allows the user to modify the sensor operation through the built-in sensor menus. The sensor incorporates a microprocessor to provide accurate, repeatable readings and to allow optional analogue outputs. The robust mechanical design ensures a long operational life.

Mechanical
- Powder coated aluminium body
- Fully sealed
- High durability cable

Specifications

Range:

LS1	1.0 volt/m	3 km
LS2	0.3 volts/m	10 km
LS3	0.1 volts/m	>30 km

Operational: -20°C to +60°C

Output options:
- ***Monibus*** serial data ASCII format
- Voltage 0-1, 0-2.5 volts
- 4-20mA (requires >12Vdc supply)
- Frequency TTL pulse 2-10 Hz

Power Supply: 6-28 Vdc unregulated

Supply current: 1.2 mA active
0.5 mA economy mode

Sensor weight: 250 grams

Dimensions: Overall height – 170 mm x 25 mm Ø

Mounting: 25 mm Ø
dwg no: MSM-06-0038

Cable Details: Standard product has 4m of cable – other cable lengths may be ordered

Warranty: **12 months** – full details can be found in the Monitor Sensors standard warranty document
http://www.monitorsensors.com/docs/std_warranty.pdf

Order codes:

LS1	standard sensor	**LS1-C**	Hi/Low control
LS1-F	TTL pulse		
LS2	standard sensor		
LS2-F	TTL pulse		
LS3	standard sensor		
LS3-F	TTL pulse		

info@monitorsensors.com
ph: 61-7-34909000
fx: 61-7-38897246
www.monitorsensors.com

Monitor Sensors
250 Leitchs Road
PO Box 5692
Brendale QLD 4500
AUSTRALIA

LS brief 00.doc 16/10/06 7:46 AM

YOUNG

Model 73000 Sentry™ Visibility Sensor

The YOUNG Sentry™ Visibility Sensor measures atmospheric visibility (meteorological optical range) by determining the amount of light scattered by particles in the air (smoke, dust, haze, fog, rain, & snow).

Performance in all weather conditions is achieved with an integrated design that keeps all cabling internal to the sensor for complete protection from hazards. The sensor is made from anodized aluminum and rugged, UV-resistant fiberglass enclosures. Based on the proven field experience of the NWS and FAA, the sensor uses a "look down" geometry to reduce window contamination and clogging from blowing snow. The optical windows have continuous duty anti-dew heaters. Optional thermostatically controlled external hood heaters are available for additional protection in extreme environments. All power and signal lines to the Sentry™ are protected with surge and EMI filtering to ensure uninterrupted service for the life of the sensor.

Installation and maintenance are simple with the Sentry™. A sturdy mounting flange located on the bottom of the main enclosure mates with a user-supplied 1-1/2 inch IPS mounting pipe. Power and signal cables are installed through waterproof cable glands on the bottom of the main enclosure to terminal boards for simple but reliable connections.

Calibration of the Sentry™ in the field is as simple as attaching a factory supplied calibration fixture and following a procedure that takes less than 30 minutes.

Ordering Information

73000 Sentry™ Visibility Sensor
73004 Sentry™ Visibility Sensor with Hood Heating

Power – select one:
- **A** AC Power, 200-240 VAC, 50/60 Hz
- **D** DC Power, 10-36 VDC

Signal Output – select one:
- **V** 0-5 VDC (no control relays)
- **W** 0-10 VDC
- **L** 4-20 mA
- **M** 4-20 mA isolated
- **S** RS-232
- **T** RS-422
- **U** RS-485

Control Output – optional
- **C** Single Control Relay (NA w/ output option V)
- **D** Diagnostic Relay
- **E** 2 Control Relays (NA w/ output option V)
- **F** Control Relay and Diagnostic Relay (NA w/ output option V)
- **G** 2 Control Relays, Diagnostic Relay (NA w/ output option V)**

** NOTE: Option G not available with Options S, T or U

☐ – ☐ ☐ ☐

EXAMPLE: 73004-DWF – Sentry™ Visibility Sensor with hood heating, DC power, 0-10 VDC output, single control relay and single diagnostic relay

Accessories

73062 Calibration Fixture – recommended
74050 Mounting Bracket – for vertical surfaces including walls, traffic poles and Rohn-type towers
73038 Hood Extensions

Specifications

Visibility Range:	30 m – 16 km
Accuracy:	+/- 10% RMSE
Time Constant:	60 sec
Scatter Angle:	42 deg nominal
Output Options:	0-10 VDC 0-5 VDC 4-20 mA 4-20 mA isolated RS-232, RS-422 or RS-485
Relay Options:	2 Control 1 Diagnostic
Power: AC Version:	100-240 VAC, 24 VA Nominal 75 VA w/ hood heating
DC Version:	10-36 VDC, 6 VA Nominal 18 VA w/ hood heating
Operating Temperature:	-40 to +60 C
Humidity:	0 to 100% RH
Protection:	IP66 (NEMA-4X)
Weight:	8 kg (18 lb)
Dimensions: (W x H x D)	889 mm x 292 mm x 305 mm 35" x 11.5" x 12"
Mounting:	48 mm (1.9 inch) diameter (standard 1.5 inch IPS pipe)
Optional:	34 mm (1.3 inch) diameter (standard 1 inch IPS pipe)
Construction:	Frame: Anodized Aluminum Enclosures: Fiberglass, UV Resistant
Certifications:	This equipment is in compliance with the essential requirements and other provisions of Low Voltage Directives 73/23/EEC and 89/336/ EEC as amended by Directive 93/68/EEC.

CE Complies with applicable CE directives.

R.M. YOUNG COMPANY
2801 Aero Park Drive
Traverse City, Michigan 49686 USA
TEL: (231) 946-3980 FAX: (231) 946-4772
E-mail: met.sales@youngusa.com
Web Site: www.youngusa.com

Appendix 5.8.E: Second Edition of the ISO Corrosion Standard

Provided in electronic format.

Appendix 5.8.F: Calibration Certificates

Calibration Date - 29 September 2017

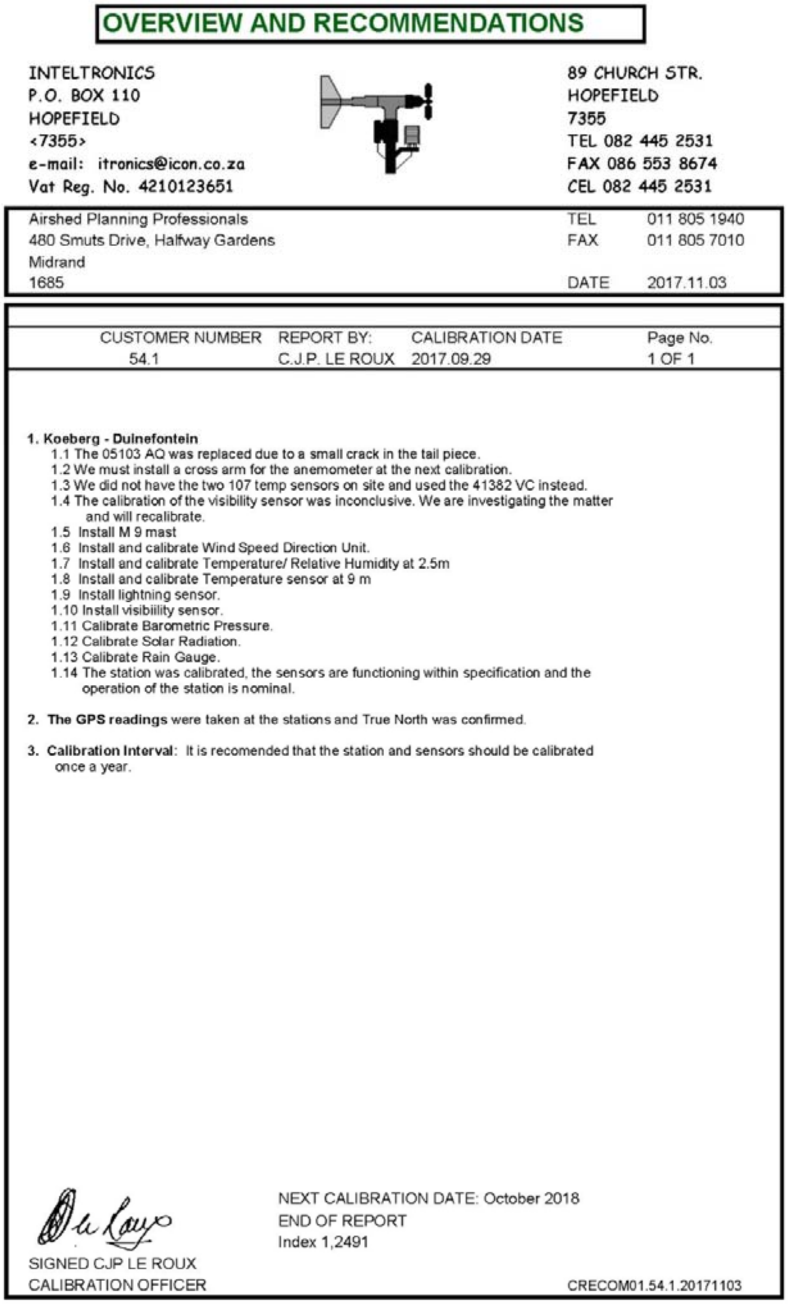

OVERVIEW AND RECOMMENDATIONS

INTELTRONICS
P.O. BOX 110
HOPEFIELD
<7355>
e-mail: itronics@icon.co.za
Vat Reg. No. 4210123651

89 CHURCH STR.
HOPEFIELD
7355
TEL 082 445 2531
FAX 086 553 8674
CEL 082 445 2531

Airshed Planning Professionals
480 Smuts Drive, Halfway Gardens
Midrand
1685

TEL 011 805 1940
FAX 011 805 7010
DATE 2017.11.03

CUSTOMER NUMBER	REPORT BY:	CALIBRATION DATE	Page No.
54.1	C.J.P. LE ROUX	2017.09.29	1 OF 1

1. **Koeberg - Duinefontein**
   - 1.1 The 05103 AQ was replaced due to a small crack in the tail piece.
   - 1.2 We must install a cross arm for the anemometer at the next calibration.
   - 1.3 We did not have the two 107 temp sensors on site and used the 41382 VC instead.
   - 1.4 The calibration of the visibility sensor was inconclusive. We are investigating the matter and will recalibrate.
   - 1.5 Install M 9 mast
   - 1.6 Install and calibrate Wind Speed Direction Unit.
   - 1.7 Install and calibrate Temperature/ Relative Humidity at 2.5m
   - 1.8 Install and calibrate Temperature sensor at 9 m
   - 1.9 Install lightning sensor.
   - 1.10 Install visibiility sensor.
   - 1.11 Calibrate Barometric Pressure.
   - 1.12 Calibrate Solar Radiation.
   - 1.13 Calibrate Rain Gauge.
   - 1.14 The station was calibrated, the sensors are functioning within specification and the operation of the station is nominal.

2. **The GPS readings** were taken at the stations and True North was confirmed.

3. **Calibration Interval**: It is recomended that the station and sensors should be calibrated once a year.

Du Lou

SIGNED CJP LE ROUX
CALIBRATION OFFICER

NEXT CALIBRATION DATE: October 2018
END OF REPORT
Index 1,2491

CRECOM01.54.1.20171103

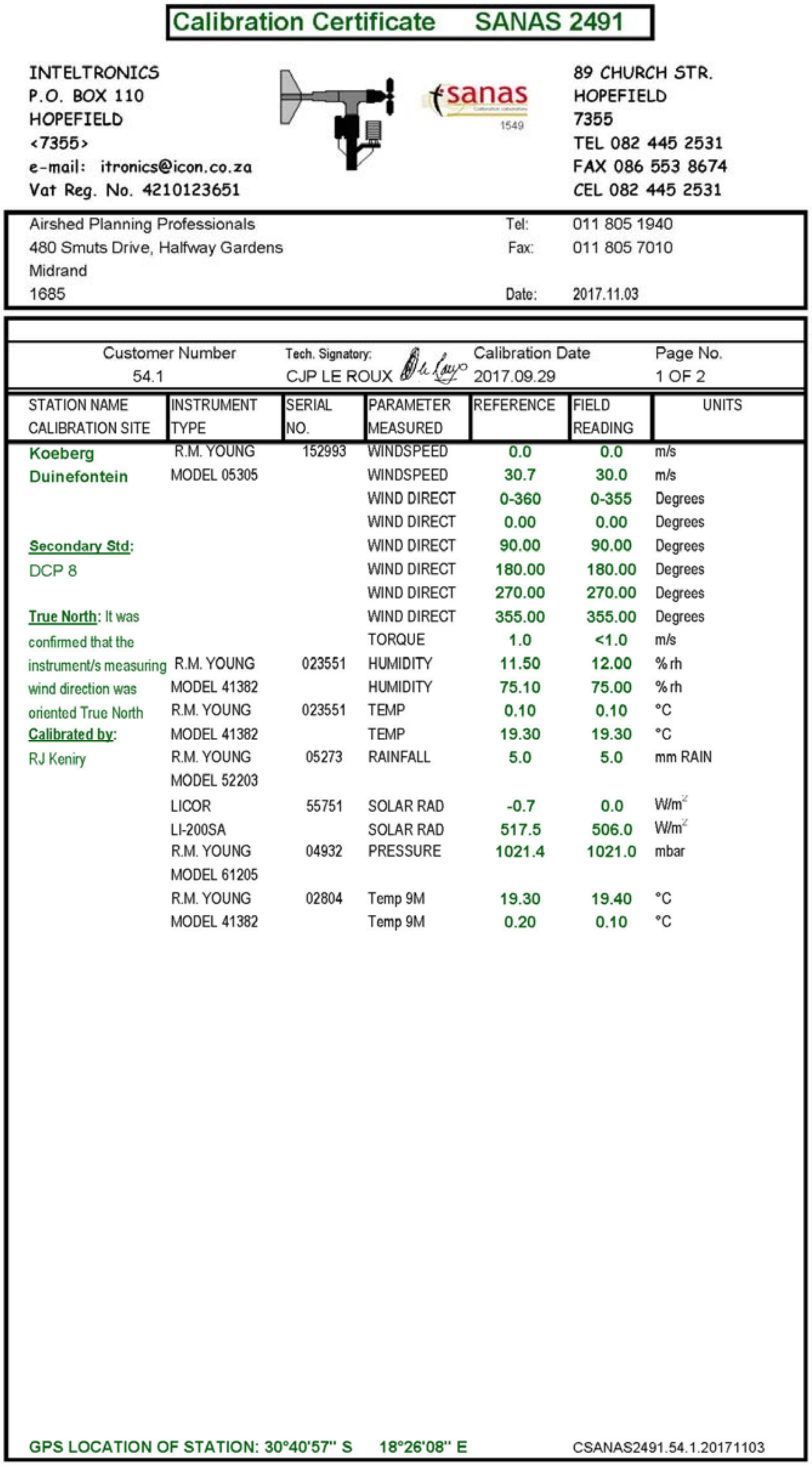

Calibration Certificate SANAS 2491

INTELTRONICS
P.O. BOX 110
HOPEFIELD
<7355>
e-mail: itronics@icon.co.za
Vat Reg. No. 4210123651

sanas
1549

89 CHURCH STR.
HOPEFIELD
7355
TEL 082 445 2531
FAX 086 553 8674
CEL 082 445 2531

Airshed Planning Professionals
480 Smuts Drive, Halfway Gardens
Midrand
1685

Tel: 011 805 1940
Fax: 011 805 7010
Date: 2017.11.03

Customer Number	Tech. Signatory:	Calibration Date	Page No.
54.1	CJP LE ROUX	2017.09.29	1 OF 2

STATION NAME CALIBRATION SITE	INSTRUMENT TYPE	SERIAL NO.	PARAMETER MEASURED	REFERENCE	FIELD READING	UNITS
Koeberg	R.M. YOUNG	152993	WINDSPEED	0.0	0.0	m/s
Duinefontein	MODEL 05305		WINDSPEED	30.7	30.0	m/s
			WIND DIRECT	0-360	0-355	Degrees
			WIND DIRECT	0.00	0.00	Degrees
Secondary Std:			WIND DIRECT	90.00	90.00	Degrees
DCP 8			WIND DIRECT	180.00	180.00	Degrees
			WIND DIRECT	270.00	270.00	Degrees
True North: It was			WIND DIRECT	355.00	355.00	Degrees
confirmed that the			TORQUE	1.0	<1.0	m/s
instrument/s measuring	R.M. YOUNG	023551	HUMIDITY	11.50	12.00	% rh
wind direction was	MODEL 41382		HUMIDITY	75.10	75.00	% rh
oriented True North	R.M. YOUNG	023551	TEMP	0.10	0.10	°C
Calibrated by:	MODEL 41382		TEMP	19.30	19.30	°C
RJ Keniry	R.M. YOUNG	05273	RAINFALL	5.0	5.0	mm RAIN
	MODEL 52203					
	LICOR	55751	SOLAR RAD	-0.7	0.0	W/m^2
	LI-200SA		SOLAR RAD	517.5	506.0	W/m^2
	R.M. YOUNG	04932	PRESSURE	1021.4	1021.0	mbar
	MODEL 61205					
	R.M. YOUNG	02804	Temp 9M	19.30	19.40	°C
	MODEL 41382		Temp 9M	0.20	0.10	°C

GPS LOCATION OF STATION: 30°40'57'' S 18°26'08'' E

CSANAS2491.54.1.20171103

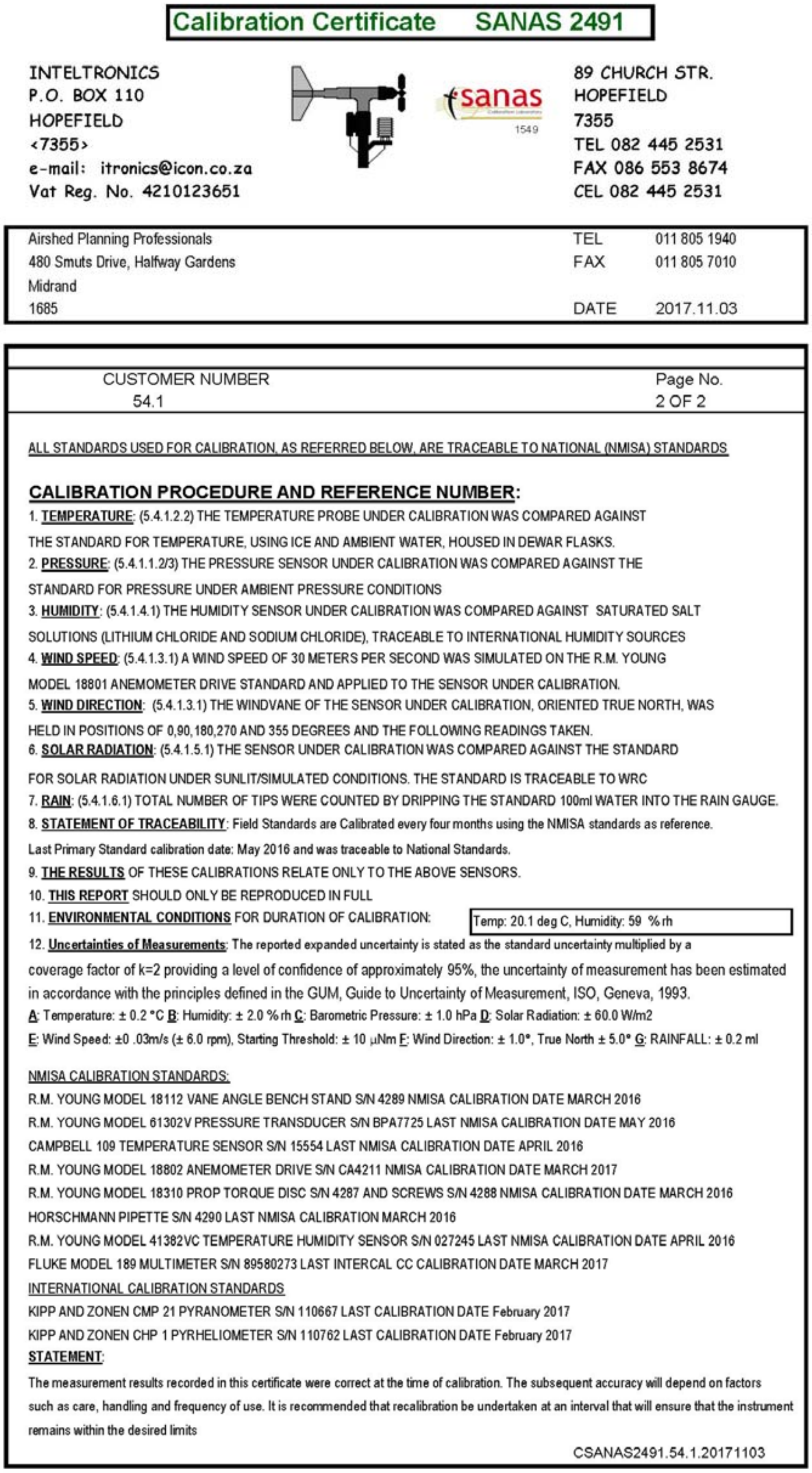

Calibration Certificate SANAS 2491

INTELTRONICS
P.O. BOX 110
HOPEFIELD
<7355>
e-mail: itronics@icon.co.za
Vat Reg. No. 4210123651

sanas
1549

89 CHURCH STR.
HOPEFIELD
7355
TEL 082 445 2531
FAX 086 553 8674
CEL 082 445 2531

Airshed Planning Professionals
480 Smuts Drive, Halfway Gardens
Midrand
1685

TEL 011 805 1940
FAX 011 805 7010
DATE 2017.11.03

CUSTOMER NUMBER	Page No.
54.1	2 OF 2

ALL STANDARDS USED FOR CALIBRATION, AS REFERRED BELOW, ARE TRACEABLE TO NATIONAL (NMISA) STANDARDS

CALIBRATION PROCEDURE AND REFERENCE NUMBER:

1. **TEMPERATURE**: (5.4.1.2.2) THE TEMPERATURE PROBE UNDER CALIBRATION WAS COMPARED AGAINST THE STANDARD FOR TEMPERATURE, USING ICE AND AMBIENT WATER, HOUSED IN DEWAR FLASKS.
2. **PRESSURE**: (5.4.1.1.2/3) THE PRESSURE SENSOR UNDER CALIBRATION WAS COMPARED AGAINST THE STANDARD FOR PRESSURE UNDER AMBIENT PRESSURE CONDITIONS
3. **HUMIDITY**: (5.4.1.4.1) THE HUMIDITY SENSOR UNDER CALIBRATION WAS COMPARED AGAINST SATURATED SALT SOLUTIONS (LITHIUM CHLORIDE AND SODIUM CHLORIDE), TRACEABLE TO INTERNATIONAL HUMIDITY SOURCES
4. **WIND SPEED**: (5.4.1.3.1) A WIND SPEED OF 30 METERS PER SECOND WAS SIMULATED ON THE R.M. YOUNG MODEL 18801 ANEMOMETER DRIVE STANDARD AND APPLIED TO THE SENSOR UNDER CALIBRATION.
5. **WIND DIRECTION**: (5.4.1.3.1) THE WINDVANE OF THE SENSOR UNDER CALIBRATION, ORIENTED TRUE NORTH, WAS HELD IN POSITIONS OF 0,90,180,270 AND 355 DEGREES AND THE FOLLOWING READINGS TAKEN.
6. **SOLAR RADIATION**: (5.4.1.5.1) THE SENSOR UNDER CALIBRATION WAS COMPARED AGAINST THE STANDARD FOR SOLAR RADIATION UNDER SUNLIT/SIMULATED CONDITIONS. THE STANDARD IS TRACEABLE TO WRC
7. **RAIN**: (5.4.1.6.1) TOTAL NUMBER OF TIPS WERE COUNTED BY DRIPPING THE STANDARD 100ml WATER INTO THE RAIN GAUGE.
8. **STATEMENT OF TRACEABILITY**: Field Standards are Calibrated every four months using the NMISA standards as reference. Last Primary Standard calibration date: May 2016 and was traceable to National Standards.
9. **THE RESULTS** OF THESE CALIBRATIONS RELATE ONLY TO THE ABOVE SENSORS.
10. **THIS REPORT** SHOULD ONLY BE REPRODUCED IN FULL
11. **ENVIRONMENTAL CONDITIONS** FOR DURATION OF CALIBRATION: Temp: 20.1 deg C, Humidity: 59 %rh
12. **Uncertainties of Measurements**: The reported expanded uncertainty is stated as the standard uncertainty multiplied by a coverage factor of k=2 providing a level of confidence of approximately 95%, the uncertainty of measurement has been estimated in accordance with the principles defined in the GUM, Guide to Uncertainty of Measurement, ISO, Geneva, 1993.

A: Temperature: ± 0.2 °C B: Humidity: ± 2.0 %rh C: Barometric Pressure: ± 1.0 hPa D: Solar Radiation: ± 60.0 W/m2
E: Wind Speed: ±0 .03m/s (± 6.0 rpm), Starting Threshold: ± 10 µNm F: Wind Direction: ± 1.0°, True North ± 5.0° G: RAINFALL: ± 0.2 ml

NMISA CALIBRATION STANDARDS:
R.M. YOUNG MODEL 18112 VANE ANGLE BENCH STAND S/N 4289 NMISA CALIBRATION DATE MARCH 2016
R.M. YOUNG MODEL 61302V PRESSURE TRANSDUCER S/N BPA7725 LAST NMISA CALIBRATION DATE MAY 2016
CAMPBELL 109 TEMPERATURE SENSOR S/N 15554 LAST NMISA CALIBRATION DATE APRIL 2016
R.M. YOUNG MODEL 18802 ANEMOMETER DRIVE S/N CA4211 NMISA CALIBRATION DATE MARCH 2017
R.M. YOUNG MODEL 18310 PROP TORQUE DISC S/N 4287 AND SCREWS S/N 4288 NMISA CALIBRATION DATE MARCH 2016
HORSCHMANN PIPETTE S/N 4290 LAST NMISA CALIBRATION MARCH 2016
R.M. YOUNG MODEL 41382VC TEMPERATURE HUMIDITY SENSOR S/N 027245 LAST NMISA CALIBRATION DATE APRIL 2016
FLUKE MODEL 189 MULTIMETER S/N 89580273 LAST INTERCAL CC CALIBRATION DATE MARCH 2017

INTERNATIONAL CALIBRATION STANDARDS
KIPP AND ZONEN CMP 21 PYRANOMETER S/N 110667 LAST CALIBRATION DATE February 2017
KIPP AND ZONEN CHP 1 PYRHELIOMETER S/N 110762 LAST CALIBRATION DATE February 2017

STATEMENT:

The measurement results recorded in this certificate were correct at the time of calibration. The subsequent accuracy will depend on factors such as care, handling and frequency of use. It is recommended that recalibration be undertaken at an interval that will ensure that the instrument remains within the desired limits

CSANAS2491.54.1.20171103

Calibration Date - 12 April 2018

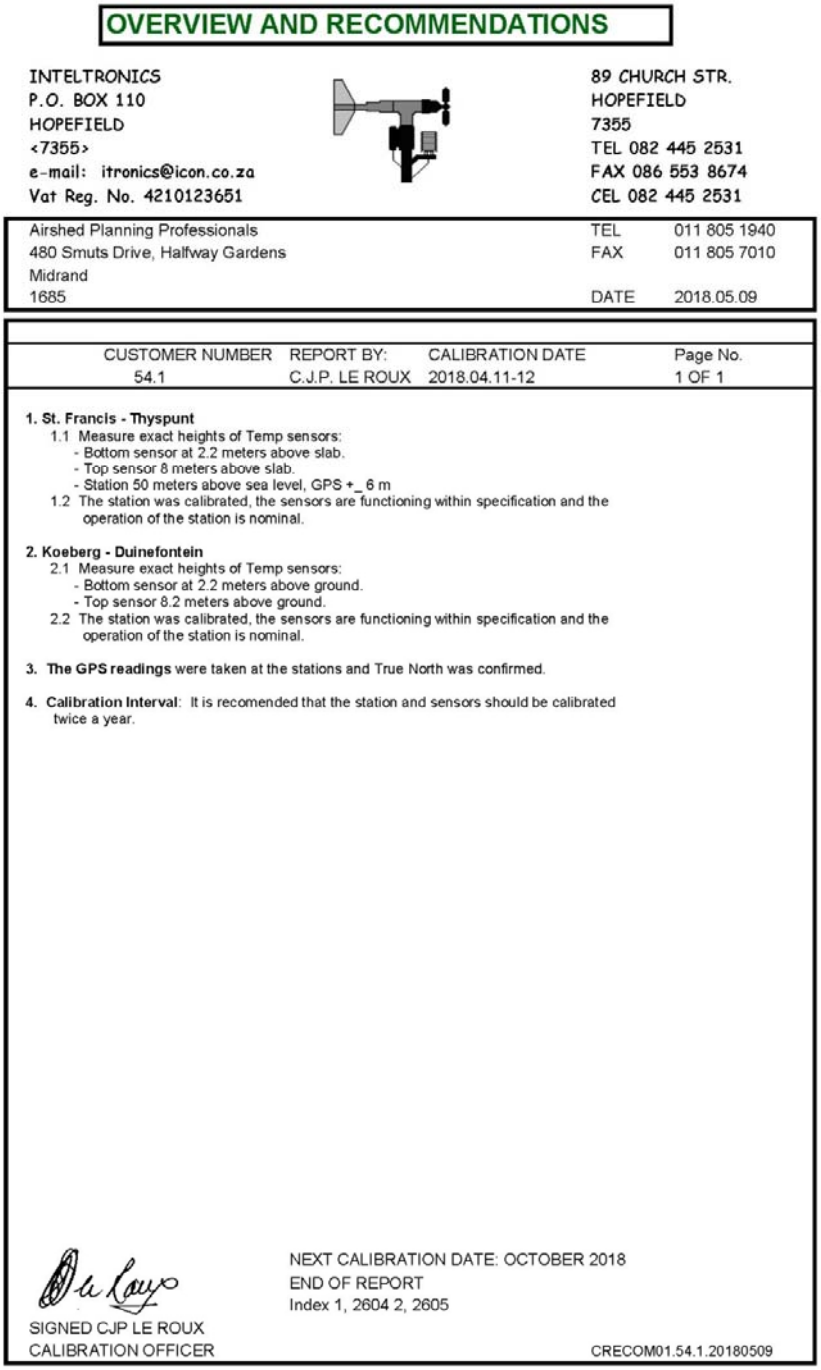

OVERVIEW AND RECOMMENDATIONS

INTELTRONICS
P.O. BOX 110
HOPEFIELD
<7355>
e-mail: itronics@icon.co.za
Vat Reg. No. 4210123651

89 CHURCH STR.
HOPEFIELD
7355
TEL 082 445 2531
FAX 086 553 8674
CEL 082 445 2531

Airshed Planning Professionals
480 Smuts Drive, Halfway Gardens
Midrand
1685

TEL 011 805 1940
FAX 011 805 7010
DATE 2018.05.09

CUSTOMER NUMBER	REPORT BY:	CALIBRATION DATE	Page No.
54.1	C.J.P. LE ROUX	2018.04.11-12	1 OF 1

1. St. Francis - Thyspunt

1.1 Measure exact heights of Temp sensors:
- Bottom sensor at 2.2 meters above slab.
- Top sensor 8 meters above slab.
- Station 50 meters above sea level, GPS +_ 6 m

1.2 The station was calibrated, the sensors are functioning within specification and the operation of the station is nominal.

2. Koeberg - Duinefontein

2.1 Measure exact heights of Temp sensors:
- Bottom sensor at 2.2 meters above ground.
- Top sensor 8.2 meters above ground.

2.2 The station was calibrated, the sensors are functioning within specification and the operation of the station is nominal.

3. **The GPS readings** were taken at the stations and True North was confirmed.

4. **Calibration Interval**: It is recomended that the station and sensors should be calibrated twice a year.

NEXT CALIBRATION DATE: OCTOBER 2018
END OF REPORT
Index 1, 2604 2, 2605

SIGNED CJP LE ROUX
CALIBRATION OFFICER

CRECOM01.54.1.20180509

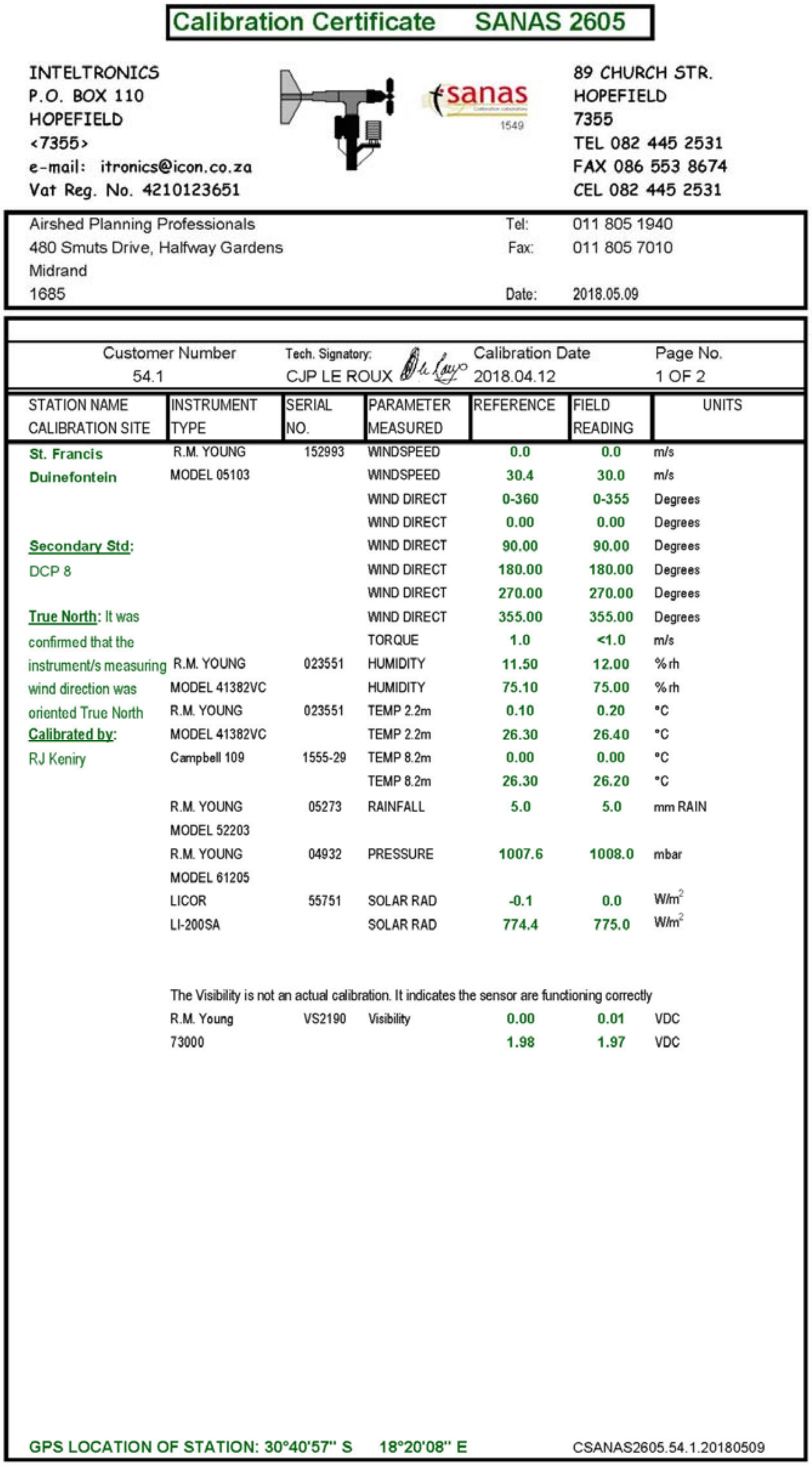

Calibration Certificate SANAS 2605

INTELTRONICS
P.O. BOX 110
HOPEFIELD
<7355>
e-mail: itronics@icon.co.za
Vat Reg. No. 4210123651

sanas
1549

89 CHURCH STR.
HOPEFIELD
7355
TEL 082 445 2531
FAX 086 553 8674
CEL 082 445 2531

Airshed Planning Professionals
480 Smuts Drive, Halfway Gardens
Midrand
1685

Tel: 011 805 1940
Fax: 011 805 7010
Date: 2018.05.09

Customer Number	Tech. Signatory:	Calibration Date	Page No.
54.1	CJP LE ROUX	2018.04.12	1 OF 2

STATION NAME CALIBRATION SITE	INSTRUMENT TYPE	SERIAL NO.	PARAMETER MEASURED	REFERENCE	FIELD READING	UNITS
St. Francis	R.M. YOUNG	152993	WINDSPEED	0.0	0.0	m/s
Duinefontein	MODEL 05103		WINDSPEED	30.4	30.0	m/s
			WIND DIRECT	0-360	0-355	Degrees
			WIND DIRECT	0.00	0.00	Degrees
Secondary Std:			WIND DIRECT	90.00	90.00	Degrees
DCP 8			WIND DIRECT	180.00	180.00	Degrees
			WIND DIRECT	270.00	270.00	Degrees
True North: It was			WIND DIRECT	355.00	355.00	Degrees
confirmed that the			TORQUE	1.0	<1.0	m/s
instrument/s measuring	R.M. YOUNG	023551	HUMIDITY	11.50	12.00	%rh
wind direction was	MODEL 41382VC		HUMIDITY	75.10	75.00	%rh
oriented True North	R.M. YOUNG	023551	TEMP 2.2m	0.10	0.20	°C
Calibrated by:	MODEL 41382VC		TEMP 2.2m	26.30	26.40	°C
RJ Keniry	Campbell 109	1555-29	TEMP 8.2m	0.00	0.00	°C
			TEMP 8.2m	26.30	26.20	°C
	R.M. YOUNG	05273	RAINFALL	5.0	5.0	mm RAIN
	MODEL 52203					
	R.M. YOUNG	04932	PRESSURE	1007.6	1008.0	mbar
	MODEL 61205					
	LICOR	55751	SOLAR RAD	-0.1	0.0	W/m^2
	LI-200SA		SOLAR RAD	774.4	775.0	W/m^2

The Visibility is not an actual calibration. It indicates the sensor are functioning correctly

R.M. Young	VS2190	Visibility	0.00	0.01	VDC
73000			1.98	1.97	VDC

GPS LOCATION OF STATION: 30°40'57" S 18°20'08" E

CSANAS2605.54.1.20180509

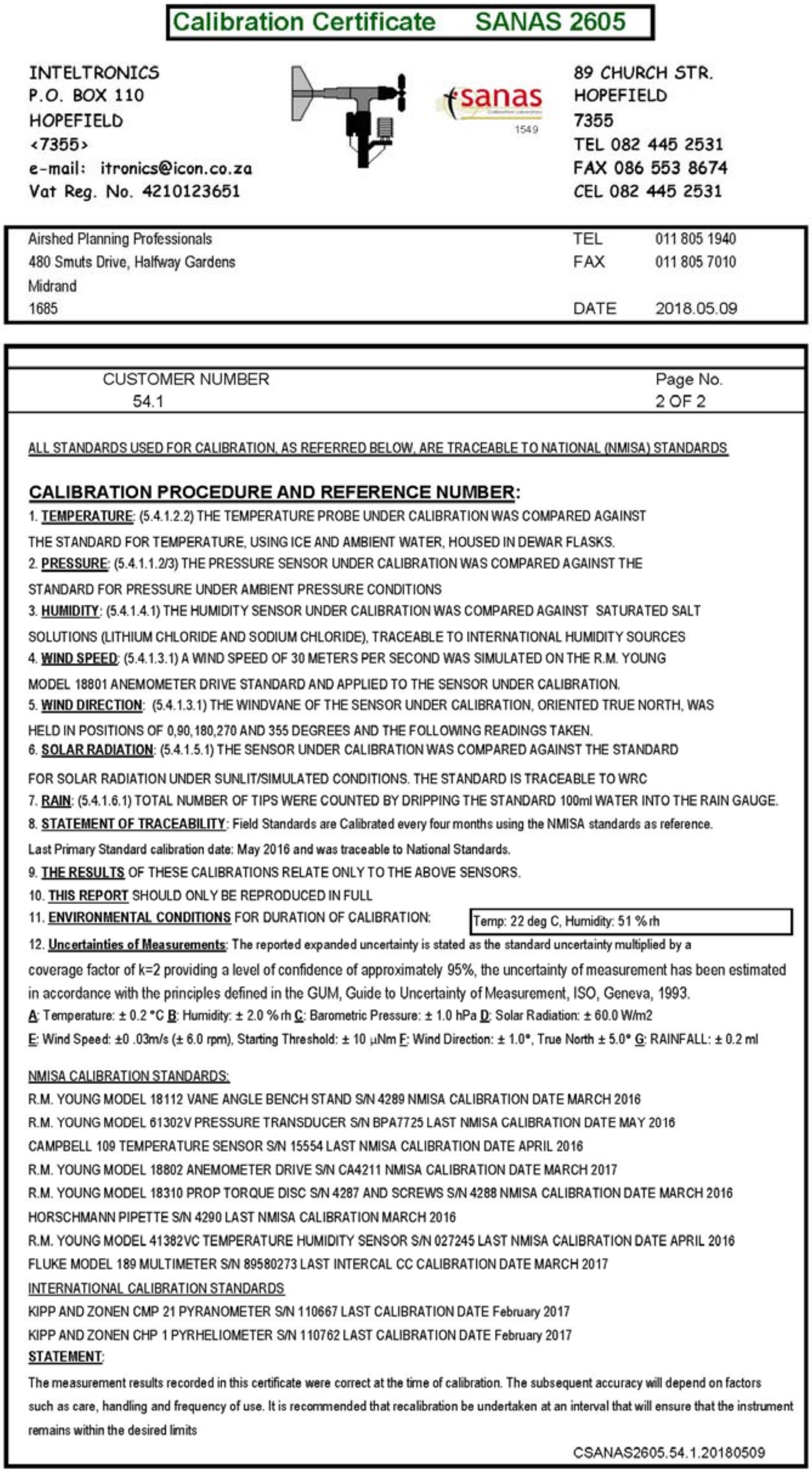

Calibration Certificate SANAS 2605

INTELTRONICS
P.O. BOX 110
HOPEFIELD
<7355>
e-mail: itronics@icon.co.za
Vat Reg. No. 4210123651

sanas
1549

89 CHURCH STR.
HOPEFIELD
7355
TEL 082 445 2531
FAX 086 553 8674
CEL 082 445 2531

Airshed Planning Professionals
480 Smuts Drive, Halfway Gardens
Midrand
1685

TEL 011 805 1940
FAX 011 805 7010
DATE 2018.05.09

CUSTOMER NUMBER	Page No.
54.1	2 OF 2

ALL STANDARDS USED FOR CALIBRATION, AS REFERRED BELOW, ARE TRACEABLE TO NATIONAL (NMISA) STANDARDS

CALIBRATION PROCEDURE AND REFERENCE NUMBER:

1. **TEMPERATURE**: (5.4.1.2.2) THE TEMPERATURE PROBE UNDER CALIBRATION WAS COMPARED AGAINST THE STANDARD FOR TEMPERATURE, USING ICE AND AMBIENT WATER, HOUSED IN DEWAR FLASKS.
2. **PRESSURE**: (5.4.1.1.2/3) THE PRESSURE SENSOR UNDER CALIBRATION WAS COMPARED AGAINST THE STANDARD FOR PRESSURE UNDER AMBIENT PRESSURE CONDITIONS
3. **HUMIDITY**: (5.4.1.4.1) THE HUMIDITY SENSOR UNDER CALIBRATION WAS COMPARED AGAINST SATURATED SALT SOLUTIONS (LITHIUM CHLORIDE AND SODIUM CHLORIDE), TRACEABLE TO INTERNATIONAL HUMIDITY SOURCES
4. **WIND SPEED**: (5.4.1.3.1) A WIND SPEED OF 30 METERS PER SECOND WAS SIMULATED ON THE R.M. YOUNG MODEL 18801 ANEMOMETER DRIVE STANDARD AND APPLIED TO THE SENSOR UNDER CALIBRATION.
5. **WIND DIRECTION**: (5.4.1.3.1) THE WINDVANE OF THE SENSOR UNDER CALIBRATION, ORIENTED TRUE NORTH, WAS HELD IN POSITIONS OF 0,90,180,270 AND 355 DEGREES AND THE FOLLOWING READINGS TAKEN.
6. **SOLAR RADIATION**: (5.4.1.5.1) THE SENSOR UNDER CALIBRATION WAS COMPARED AGAINST THE STANDARD FOR SOLAR RADIATION UNDER SUNLIT/SIMULATED CONDITIONS. THE STANDARD IS TRACEABLE TO WRC
7. **RAIN**: (5.4.1.6.1) TOTAL NUMBER OF TIPS WERE COUNTED BY DRIPPING THE STANDARD 100ml WATER INTO THE RAIN GAUGE.
8. **STATEMENT OF TRACEABILITY**: Field Standards are Calibrated every four months using the NMISA standards as reference. Last Primary Standard calibration date: May 2016 and was traceable to National Standards.
9. **THE RESULTS** OF THESE CALIBRATIONS RELATE ONLY TO THE ABOVE SENSORS.
10. **THIS REPORT** SHOULD ONLY BE REPRODUCED IN FULL
11. **ENVIRONMENTAL CONDITIONS** FOR DURATION OF CALIBRATION: Temp: 22 deg C, Humidity: 51 % rh
12. **Uncertainties of Measurements**: The reported expanded uncertainty is stated as the standard uncertainty multiplied by a coverage factor of k=2 providing a level of confidence of approximately 95%, the uncertainty of measurement has been estimated in accordance with the principles defined in the GUM, Guide to Uncertainty of Measurement, ISO, Geneva, 1993.

A: Temperature: ± 0.2 °C B: Humidity: ± 2.0 % rh C: Barometric Pressure: ± 1.0 hPa D: Solar Radiation: ± 60.0 W/m2
E: Wind Speed: ±0 .03m/s (± 6.0 rpm), Starting Threshold: ± 10 µNm F: Wind Direction: ± 1.0°, True North ± 5.0° G: RAINFALL: ± 0.2 ml

NMISA CALIBRATION STANDARDS:
R.M. YOUNG MODEL 18112 VANE ANGLE BENCH STAND S/N 4289 NMISA CALIBRATION DATE MARCH 2016
R.M. YOUNG MODEL 61302V PRESSURE TRANSDUCER S/N BPA7725 LAST NMISA CALIBRATION DATE MAY 2016
CAMPBELL 109 TEMPERATURE SENSOR S/N 15554 LAST NMISA CALIBRATION DATE APRIL 2016
R.M. YOUNG MODEL 18802 ANEMOMETER DRIVE S/N CA4211 NMISA CALIBRATION DATE MARCH 2017
R.M. YOUNG MODEL 18310 PROP TORQUE DISC S/N 4287 AND SCREWS S/N 4288 NMISA CALIBRATION DATE MARCH 2016
HORSCHMANN PIPETTE S/N 4290 LAST NMISA CALIBRATION MARCH 2016
R.M. YOUNG MODEL 41382VC TEMPERATURE HUMIDITY SENSOR S/N 027245 LAST NMISA CALIBRATION DATE APRIL 2016
FLUKE MODEL 189 MULTIMETER S/N 89580273 LAST INTERCAL CC CALIBRATION DATE MARCH 2017

INTERNATIONAL CALIBRATION STANDARDS
KIPP AND ZONEN CMP 21 PYRANOMETER S/N 110667 LAST CALIBRATION DATE February 2017
KIPP AND ZONEN CHP 1 PYRHELIOMETER S/N 110762 LAST CALIBRATION DATE February 2017

STATEMENT:

The measurement results recorded in this certificate were correct at the time of calibration. The subsequent accuracy will depend on factors such as care, handling and frequency of use. It is recommended that recalibration be undertaken at an interval that will ensure that the instrument remains within the desired limits

CSANAS2605.54.1.20180509

Calibration Date - 17 October 2018

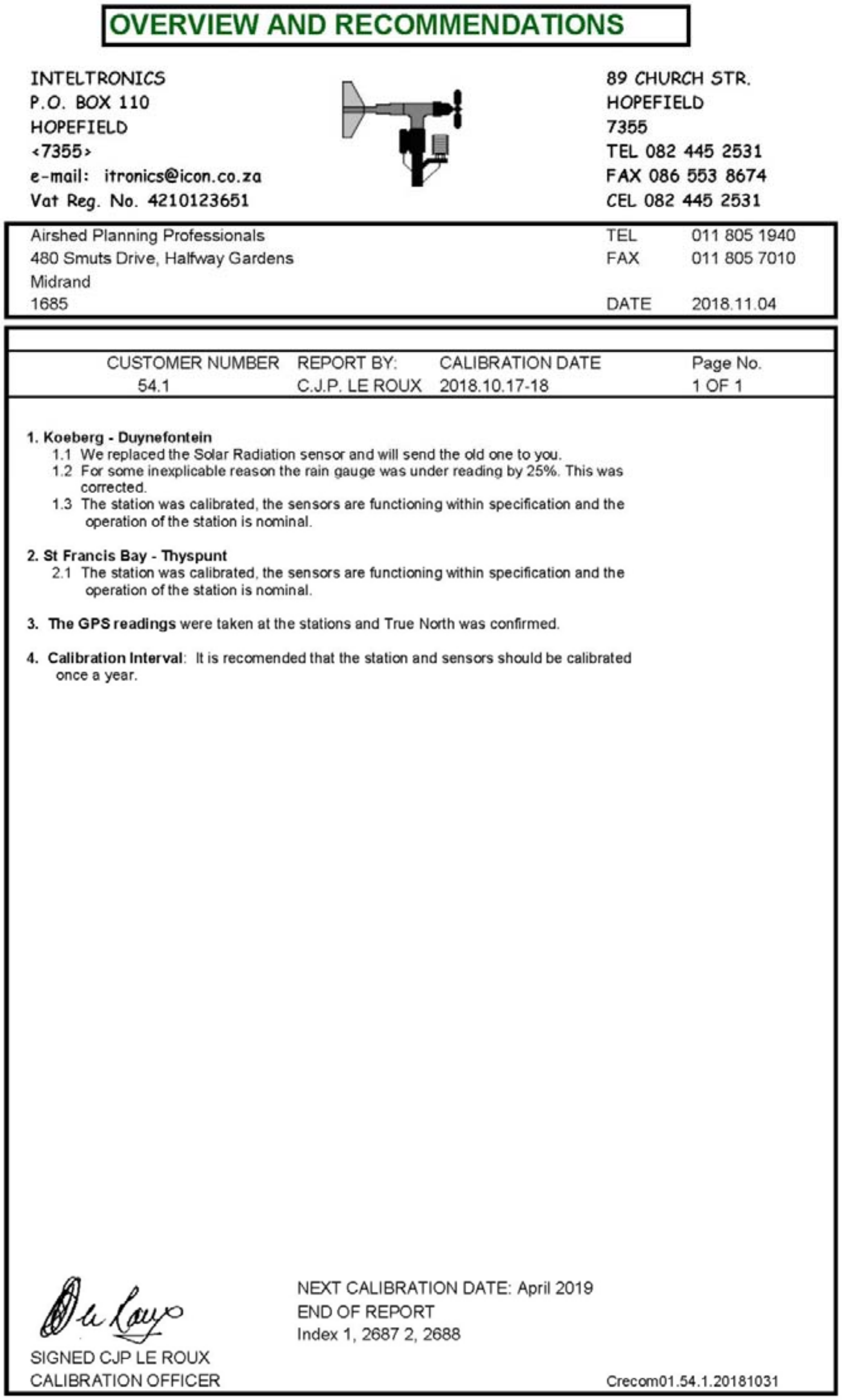

OVERVIEW AND RECOMMENDATIONS

INTELTRONICS
P.O. BOX 110
HOPEFIELD
<7355>
e-mail: itronics@icon.co.za
Vat Reg. No. 4210123651

89 CHURCH STR.
HOPEFIELD
7355
TEL 082 445 2531
FAX 086 553 8674
CEL 082 445 2531

Airshed Planning Professionals
480 Smuts Drive, Halfway Gardens
Midrand
1685

TEL 011 805 1940
FAX 011 805 7010
DATE 2018.11.04

CUSTOMER NUMBER	REPORT BY:	CALIBRATION DATE	Page No.
54.1	C.J.P. LE ROUX	2018.10.17-18	1 OF 1

1. Koeberg - Duynefontein

- 1.1 We replaced the Solar Radiation sensor and will send the old one to you.
- 1.2 For some inexplicable reason the rain gauge was under reading by 25%. This was corrected.
- 1.3 The station was calibrated, the sensors are functioning within specification and the operation of the station is nominal.

2. St Francis Bay - Thyspunt

- 2.1 The station was calibrated, the sensors are functioning within specification and the operation of the station is nominal.

3. **The GPS readings** were taken at the stations and True North was confirmed.

4. **Calibration Interval**: It is recomended that the station and sensors should be calibrated once a year.

SIGNED CJP LE ROUX
CALIBRATION OFFICER

NEXT CALIBRATION DATE: April 2019
END OF REPORT
Index 1, 2687 2, 2688

Crecom01.54.1.20181031

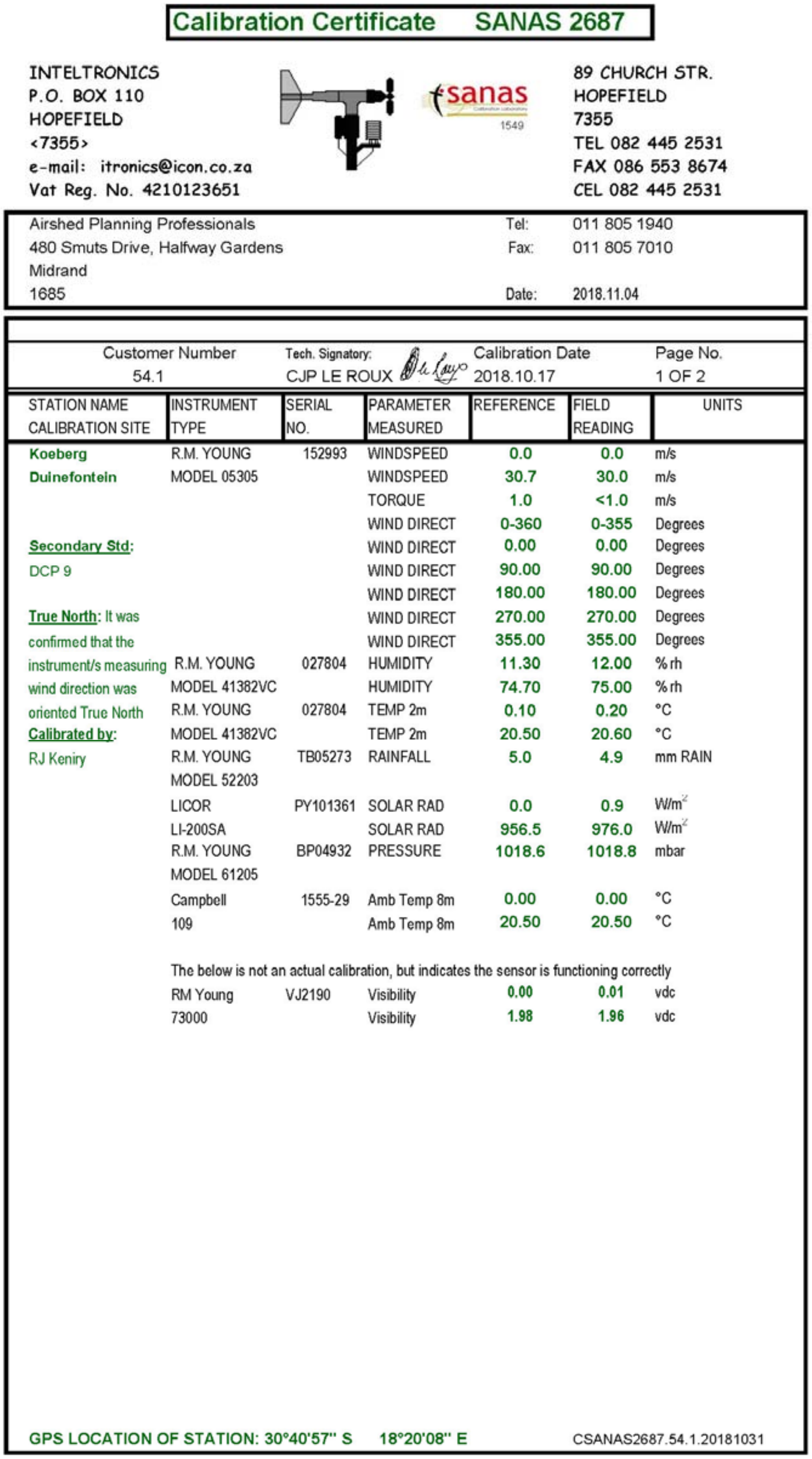

Calibration Certificate SANAS 2687

INTELTRONICS
P.O. BOX 110
HOPEFIELD
<7355>
e-mail: itronics@icon.co.za
Vat Reg. No. 4210123651

sanas 1549

89 CHURCH STR.
HOPEFIELD
7355
TEL 082 445 2531
FAX 086 553 8674
CEL 082 445 2531

Airshed Planning Professionals
480 Smuts Drive, Halfway Gardens
Midrand
1685

Tel: 011 805 1940
Fax: 011 805 7010
Date: 2018.11.04

Customer Number	Tech. Signatory:	Calibration Date	Page No.
54.1	CJP LE ROUX	2018.10.17	1 OF 2

STATION NAME CALIBRATION SITE	INSTRUMENT TYPE	SERIAL NO.	PARAMETER MEASURED	REFERENCE	FIELD READING	UNITS
Koeberg	R.M. YOUNG	152993	WINDSPEED	0.0	0.0	m/s
Duinefontein	MODEL 05305		WINDSPEED	30.7	30.0	m/s
			TORQUE	1.0	<1.0	m/s
			WIND DIRECT	0-360	0-355	Degrees
Secondary Std:			WIND DIRECT	0.00	0.00	Degrees
DCP 9			WIND DIRECT	90.00	90.00	Degrees
			WIND DIRECT	180.00	180.00	Degrees
True North: It was			WIND DIRECT	270.00	270.00	Degrees
confirmed that the			WIND DIRECT	355.00	355.00	Degrees
instrument/s measuring	R.M. YOUNG	027804	HUMIDITY	11.30	12.00	% rh
wind direction was	MODEL 41382VC		HUMIDITY	74.70	75.00	% rh
oriented True North	R.M. YOUNG	027804	TEMP 2m	0.10	0.20	°C
Calibrated by:	MODEL 41382VC		TEMP 2m	20.50	20.60	°C
RJ Keniry	R.M. YOUNG	TB05273	RAINFALL	5.0	4.9	mm RAIN
	MODEL 52203					
	LICOR	PY101361	SOLAR RAD	0.0	0.9	W/m^2
	LI-200SA		SOLAR RAD	956.5	976.0	W/m^2
	R.M. YOUNG	BP04932	PRESSURE	1018.6	1018.8	mbar
	MODEL 61205					
	Campbell	1555-29	Amb Temp 8m	0.00	0.00	°C
	109		Amb Temp 8m	20.50	20.50	°C

The below is not an actual calibration, but indicates the sensor is functioning correctly

RM Young	VJ2190	Visibility	0.00	0.01	vdc
73000		Visibility	1.98	1.96	vdc

GPS LOCATION OF STATION: 30°40'57" S 18°20'08" E

CSANAS2687.54.1.20181031

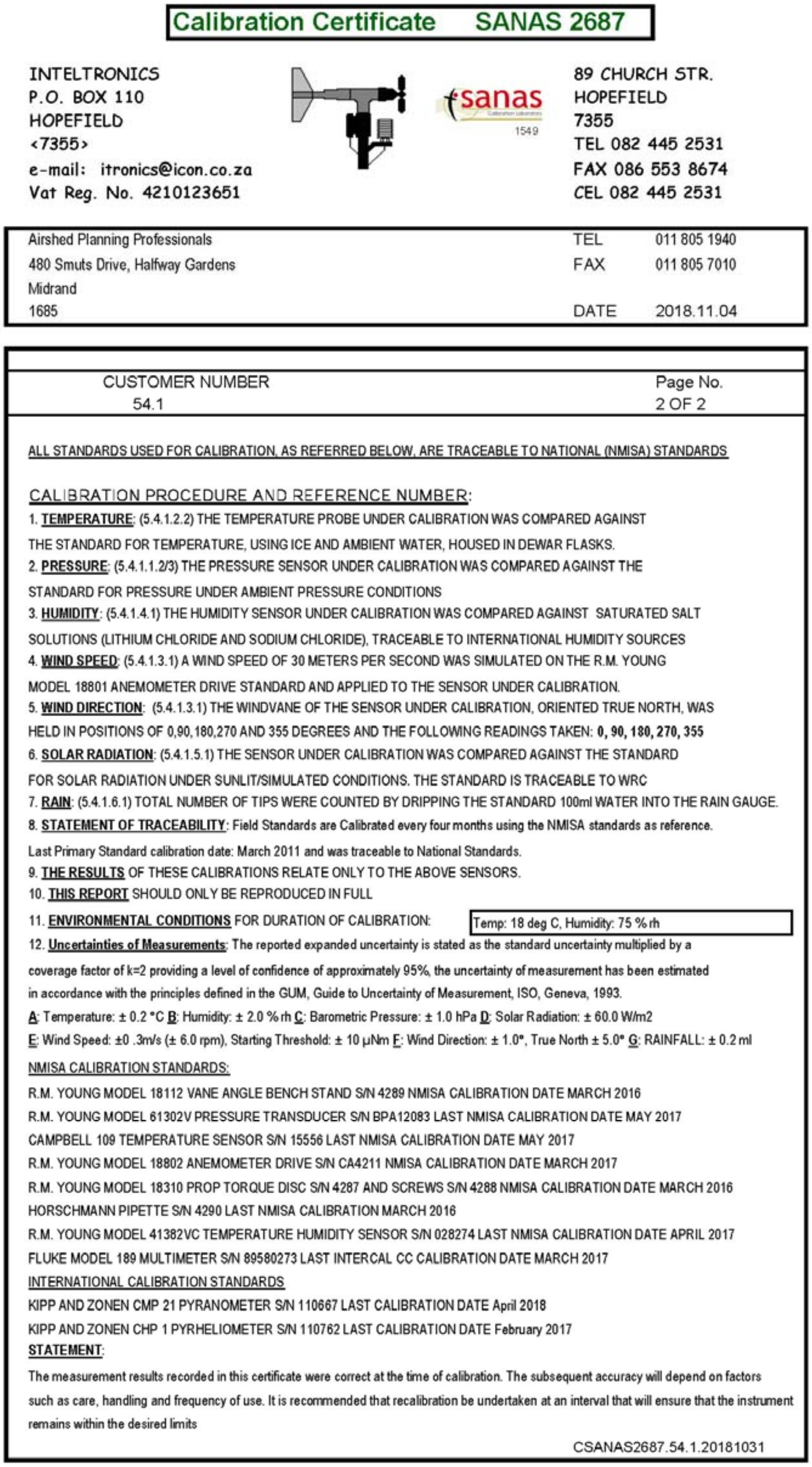

Calibration Certificate SANAS 2687

INTELTRONICS
P.O. BOX 110
HOPEFIELD
<7355>
e-mail: itronics@icon.co.za
Vat Reg. No. 4210123651

sanas
1549

89 CHURCH STR.
HOPEFIELD
7355
TEL 082 445 2531
FAX 086 553 8674
CEL 082 445 2531

Airshed Planning Professionals
480 Smuts Drive, Halfway Gardens
Midrand
1685

TEL 011 805 1940
FAX 011 805 7010
DATE 2018.11.04

CUSTOMER NUMBER
54.1

Page No.
2 OF 2

ALL STANDARDS USED FOR CALIBRATION, AS REFERRED BELOW, ARE TRACEABLE TO NATIONAL (NMISA) STANDARDS

CALIBRATION PROCEDURE AND REFERENCE NUMBER:

1. **TEMPERATURE**: (5.4.1.2.2) THE TEMPERATURE PROBE UNDER CALIBRATION WAS COMPARED AGAINST THE STANDARD FOR TEMPERATURE, USING ICE AND AMBIENT WATER, HOUSED IN DEWAR FLASKS.
2. **PRESSURE**: (5.4.1.1.2/3) THE PRESSURE SENSOR UNDER CALIBRATION WAS COMPARED AGAINST THE STANDARD FOR PRESSURE UNDER AMBIENT PRESSURE CONDITIONS
3. **HUMIDITY**: (5.4.1.4.1) THE HUMIDITY SENSOR UNDER CALIBRATION WAS COMPARED AGAINST SATURATED SALT SOLUTIONS (LITHIUM CHLORIDE AND SODIUM CHLORIDE), TRACEABLE TO INTERNATIONAL HUMIDITY SOURCES
4. **WIND SPEED**: (5.4.1.3.1) A WIND SPEED OF 30 METERS PER SECOND WAS SIMULATED ON THE R.M. YOUNG MODEL 18801 ANEMOMETER DRIVE STANDARD AND APPLIED TO THE SENSOR UNDER CALIBRATION.
5. **WIND DIRECTION**: (5.4.1.3.1) THE WINDVANE OF THE SENSOR UNDER CALIBRATION, ORIENTED TRUE NORTH, WAS HELD IN POSITIONS OF 0,90,180,270 AND 355 DEGREES AND THE FOLLOWING READINGS TAKEN: **0, 90, 180, 270, 355**
6. **SOLAR RADIATION**: (5.4.1.5.1) THE SENSOR UNDER CALIBRATION WAS COMPARED AGAINST THE STANDARD FOR SOLAR RADIATION UNDER SUNLIT/SIMULATED CONDITIONS. THE STANDARD IS TRACEABLE TO WRC
7. **RAIN**: (5.4.1.6.1) TOTAL NUMBER OF TIPS WERE COUNTED BY DRIPPING THE STANDARD 100ml WATER INTO THE RAIN GAUGE.
8. **STATEMENT OF TRACEABILITY**: Field Standards are Calibrated every four months using the NMISA standards as reference. Last Primary Standard calibration date: March 2011 and was traceable to National Standards.
9. **THE RESULTS** OF THESE CALIBRATIONS RELATE ONLY TO THE ABOVE SENSORS.
10. **THIS REPORT** SHOULD ONLY BE REPRODUCED IN FULL
11. **ENVIRONMENTAL CONDITIONS** FOR DURATION OF CALIBRATION: Temp: 18 deg C, Humidity: 75 % rh
12. **Uncertainties of Measurements**: The reported expanded uncertainty is stated as the standard uncertainty multiplied by a coverage factor of k=2 providing a level of confidence of approximately 95%, the uncertainty of measurement has been estimated in accordance with the principles defined in the GUM, Guide to Uncertainty of Measurement, ISO, Geneva, 1993.

A: Temperature: ± 0.2 °C **B**: Humidity: ± 2.0 % rh **C**: Barometric Pressure: ± 1.0 hPa **D**: Solar Radiation: ± 60.0 W/m2
E: Wind Speed: ±0 .3m/s (± 6.0 rpm), Starting Threshold: ± 10 µNm **F**: Wind Direction: ± 1.0°, True North ± 5.0° **G**: RAINFALL: ± 0.2 ml

NMISA CALIBRATION STANDARDS:

R.M. YOUNG MODEL 18112 VANE ANGLE BENCH STAND S/N 4289 NMISA CALIBRATION DATE MARCH 2016
R.M. YOUNG MODEL 61302V PRESSURE TRANSDUCER S/N BPA12083 LAST NMISA CALIBRATION DATE MAY 2017
CAMPBELL 109 TEMPERATURE SENSOR S/N 15556 LAST NMISA CALIBRATION DATE MAY 2017
R.M. YOUNG MODEL 18802 ANEMOMETER DRIVE S/N CA4211 NMISA CALIBRATION DATE MARCH 2017
R.M. YOUNG MODEL 18310 PROP TORQUE DISC S/N 4287 AND SCREWS S/N 4288 NMISA CALIBRATION DATE MARCH 2016
HORSCHMANN PIPETTE S/N 4290 LAST NMISA CALIBRATION MARCH 2016
R.M. YOUNG MODEL 41382VC TEMPERATURE HUMIDITY SENSOR S/N 028274 LAST NMISA CALIBRATION DATE APRIL 2017
FLUKE MODEL 189 MULTIMETER S/N 89580273 LAST INTERCAL CC CALIBRATION DATE MARCH 2017

INTERNATIONAL CALIBRATION STANDARDS

KIPP AND ZONEN CMP 21 PYRANOMETER S/N 110667 LAST CALIBRATION DATE April 2018
KIPP AND ZONEN CHP 1 PYRHELIOMETER S/N 110762 LAST CALIBRATION DATE February 2017

STATEMENT:

The measurement results recorded in this certificate were correct at the time of calibration. The subsequent accuracy will depend on factors such as care, handling and frequency of use. It is recommended that recalibration be undertaken at an interval that will ensure that the instrument remains within the desired limits

CSANAS2687.54.1.20181031

Calibration Date - 8 October 2019

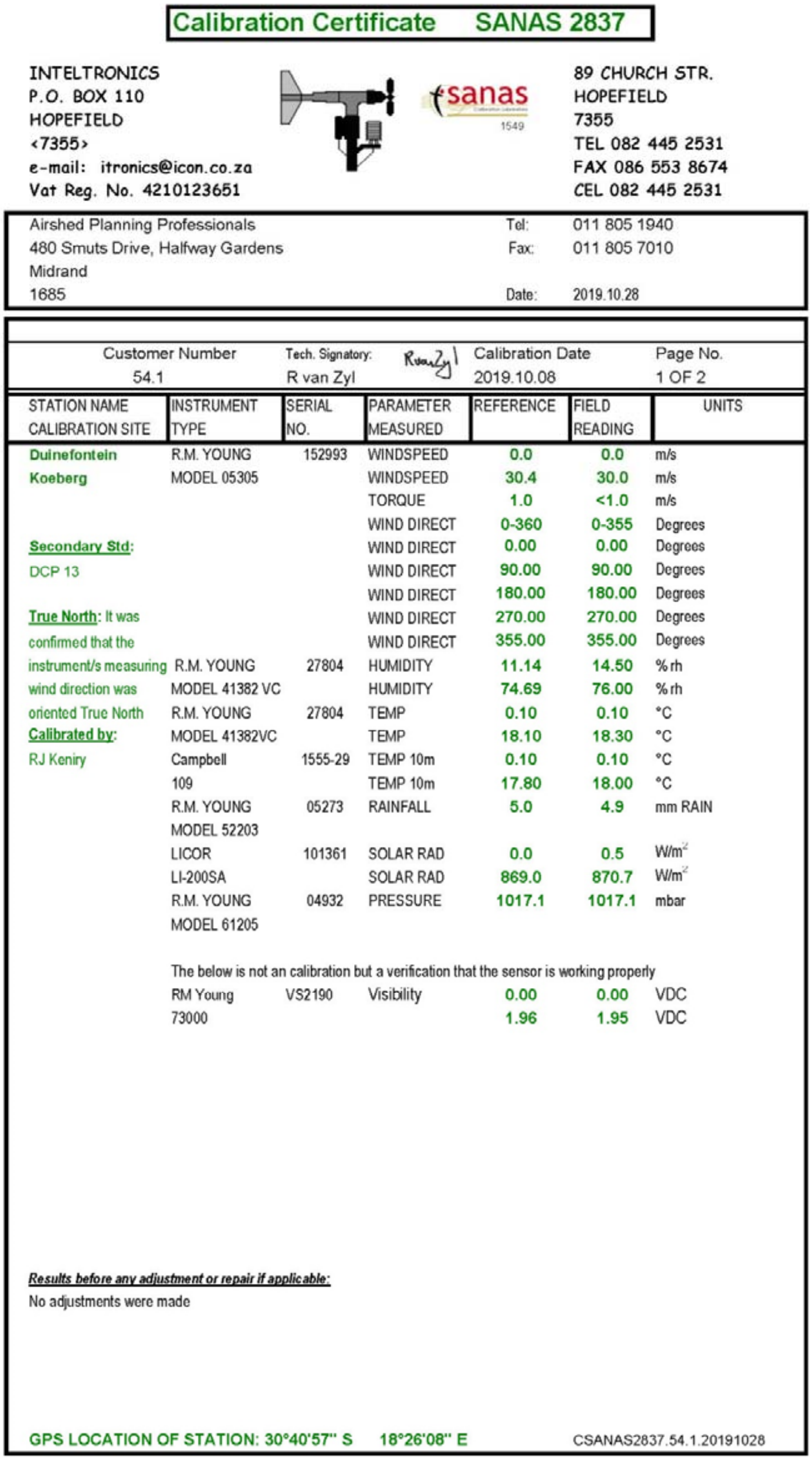

Calibration Certificate SANAS 2837

INTELTRONICS
P.O. BOX 110
HOPEFIELD
<7355>
e-mail: itronics@icon.co.za
Vat Reg. No. 4210123651

sanas
1549

89 CHURCH STR.
HOPEFIELD
7355
TEL 082 445 2531
FAX 086 553 8674
CEL 082 445 2531

Airshed Planning Professionals
480 Smuts Drive, Halfway Gardens
Midrand
1685

Tel: 011 805 1940
Fax: 011 805 7010
Date: 2019.10.28

Customer Number	Tech. Signatory:	Calibration Date	Page No.
54.1	R van Zyl	2019.10.08	1 OF 2

STATION NAME CALIBRATION SITE	INSTRUMENT TYPE	SERIAL NO.	PARAMETER MEASURED	REFERENCE	FIELD READING	UNITS
Duinefontein	R.M. YOUNG	152993	WINDSPEED	0.0	0.0	m/s
Koeberg	MODEL 05305		WINDSPEED	30.4	30.0	m/s
			TORQUE	1.0	<1.0	m/s
			WIND DIRECT	0-360	0-355	Degrees
Secondary Std:			WIND DIRECT	0.00	0.00	Degrees
DCP 13			WIND DIRECT	90.00	90.00	Degrees
			WIND DIRECT	180.00	180.00	Degrees
True North: It was			WIND DIRECT	270.00	270.00	Degrees
confirmed that the			WIND DIRECT	355.00	355.00	Degrees
instrument/s measuring	R.M. YOUNG	27804	HUMIDITY	11.14	14.50	%rh
wind direction was	MODEL 41382 VC		HUMIDITY	74.69	76.00	%rh
oriented True North	R.M. YOUNG	27804	TEMP	0.10	0.10	°C
Calibrated by:	MODEL 41382VC		TEMP	18.10	18.30	°C
RJ Keniry	Campbell	1555-29	TEMP 10m	0.10	0.10	°C
	109		TEMP 10m	17.80	18.00	°C
	R.M. YOUNG	05273	RAINFALL	5.0	4.9	mm RAIN
	MODEL 52203					
	LICOR	101361	SOLAR RAD	0.0	0.5	W/m^2
	LI-200SA		SOLAR RAD	869.0	870.7	W/m^2
	R.M. YOUNG	04932	PRESSURE	1017.1	1017.1	mbar
	MODEL 61205					

The below is not an calibration but a verification that the sensor is working properly

RM Young	VS2190	Visibility	0.00	0.00	VDC
73000			1.96	1.95	VDC

Results before any adjustment or repair if applicable:

No adjustments were made

GPS LOCATION OF STATION: 30°40'57" S 18°26'08" E

CSANAS2837.54.1.20191028

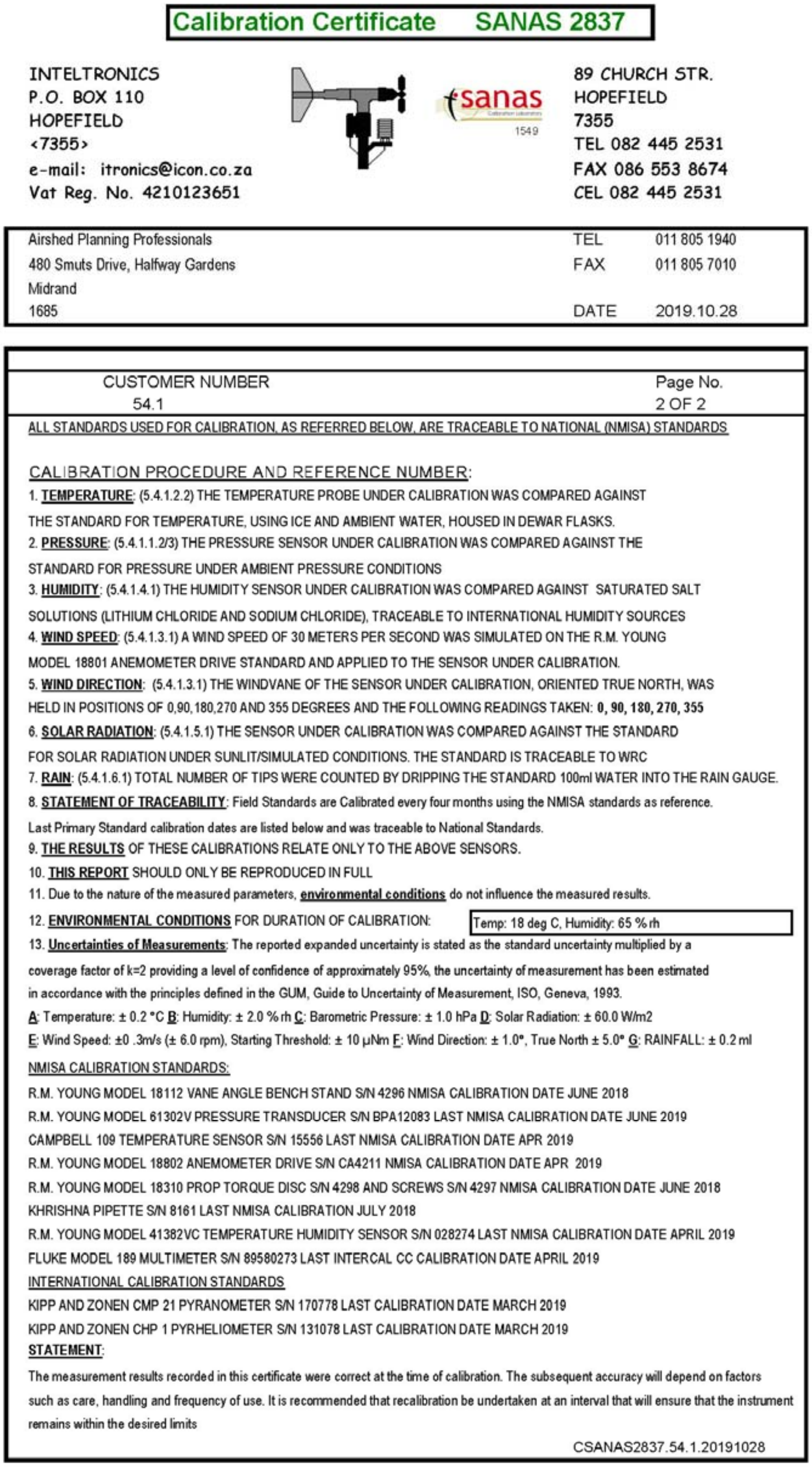

Calibration Certificate SANAS 2837

INTELTRONICS
P.O. BOX 110
HOPEFIELD
<7355>
e-mail: itronics@icon.co.za
Vat Reg. No. 4210123651

sanas
1549

89 CHURCH STR.
HOPEFIELD
7355
TEL 082 445 2531
FAX 086 553 8674
CEL 082 445 2531

Airshed Planning Professionals
480 Smuts Drive, Halfway Gardens
Midrand
1685

TEL 011 805 1940
FAX 011 805 7010
DATE 2019.10.28

CUSTOMER NUMBER
54.1

Page No.
2 OF 2

ALL STANDARDS USED FOR CALIBRATION, AS REFERRED BELOW, ARE TRACEABLE TO NATIONAL (NMISA) STANDARDS

CALIBRATION PROCEDURE AND REFERENCE NUMBER:

1. **TEMPERATURE**: (5.4.1.2.2) THE TEMPERATURE PROBE UNDER CALIBRATION WAS COMPARED AGAINST THE STANDARD FOR TEMPERATURE, USING ICE AND AMBIENT WATER, HOUSED IN DEWAR FLASKS.
2. **PRESSURE**: (5.4.1.1.2/3) THE PRESSURE SENSOR UNDER CALIBRATION WAS COMPARED AGAINST THE STANDARD FOR PRESSURE UNDER AMBIENT PRESSURE CONDITIONS
3. **HUMIDITY**: (5.4.1.4.1) THE HUMIDITY SENSOR UNDER CALIBRATION WAS COMPARED AGAINST SATURATED SALT SOLUTIONS (LITHIUM CHLORIDE AND SODIUM CHLORIDE), TRACEABLE TO INTERNATIONAL HUMIDITY SOURCES
4. **WIND SPEED**: (5.4.1.3.1) A WIND SPEED OF 30 METERS PER SECOND WAS SIMULATED ON THE R.M. YOUNG MODEL 18801 ANEMOMETER DRIVE STANDARD AND APPLIED TO THE SENSOR UNDER CALIBRATION.
5. **WIND DIRECTION**: (5.4.1.3.1) THE WINDVANE OF THE SENSOR UNDER CALIBRATION, ORIENTED TRUE NORTH, WAS HELD IN POSITIONS OF 0,90,180,270 AND 355 DEGREES AND THE FOLLOWING READINGS TAKEN: **0, 90, 180, 270, 355**
6. **SOLAR RADIATION**: (5.4.1.5.1) THE SENSOR UNDER CALIBRATION WAS COMPARED AGAINST THE STANDARD FOR SOLAR RADIATION UNDER SUNLIT/SIMULATED CONDITIONS. THE STANDARD IS TRACEABLE TO WRC
7. **RAIN**: (5.4.1.6.1) TOTAL NUMBER OF TIPS WERE COUNTED BY DRIPPING THE STANDARD 100ml WATER INTO THE RAIN GAUGE.
8. **STATEMENT OF TRACEABILITY**: Field Standards are Calibrated every four months using the NMISA standards as reference. Last Primary Standard calibration dates are listed below and was traceable to National Standards.
9. **THE RESULTS** OF THESE CALIBRATIONS RELATE ONLY TO THE ABOVE SENSORS.
10. **THIS REPORT** SHOULD ONLY BE REPRODUCED IN FULL
11. Due to the nature of the measured parameters, **environmental conditions** do not influence the measured results.
12. **ENVIRONMENTAL CONDITIONS** FOR DURATION OF CALIBRATION: Temp: 18 deg C, Humidity: 65 % rh
13. **Uncertainties of Measurements**: The reported expanded uncertainty is stated as the standard uncertainty multiplied by a coverage factor of k=2 providing a level of confidence of approximately 95%, the uncertainty of measurement has been estimated in accordance with the principles defined in the GUM, Guide to Uncertainty of Measurement, ISO, Geneva, 1993.

A: Temperature: ± 0.2 °C B: Humidity: ± 2.0 % rh C: Barometric Pressure: ± 1.0 hPa D: Solar Radiation: ± 60.0 W/m2
E: Wind Speed: ±0 .3m/s (± 6.0 rpm), Starting Threshold: ± 10 µNm F: Wind Direction: ± 1.0°, True North ± 5.0° G: RAINFALL: ± 0.2 ml

NMISA CALIBRATION STANDARDS:

R.M. YOUNG MODEL 18112 VANE ANGLE BENCH STAND S/N 4296 NMISA CALIBRATION DATE JUNE 2018
R.M. YOUNG MODEL 61302V PRESSURE TRANSDUCER S/N BPA12083 LAST NMISA CALIBRATION DATE JUNE 2019
CAMPBELL 109 TEMPERATURE SENSOR S/N 15556 LAST NMISA CALIBRATION DATE APR 2019
R.M. YOUNG MODEL 18802 ANEMOMETER DRIVE S/N CA4211 NMISA CALIBRATION DATE APR 2019
R.M. YOUNG MODEL 18310 PROP TORQUE DISC S/N 4298 AND SCREWS S/N 4297 NMISA CALIBRATION DATE JUNE 2018
KHRISHNA PIPETTE S/N 8161 LAST NMISA CALIBRATION JULY 2018
R.M. YOUNG MODEL 41382VC TEMPERATURE HUMIDITY SENSOR S/N 028274 LAST NMISA CALIBRATION DATE APRIL 2019
FLUKE MODEL 189 MULTIMETER S/N 89580273 LAST INTERCAL CC CALIBRATION DATE APRIL 2019

INTERNATIONAL CALIBRATION STANDARDS

KIPP AND ZONEN CMP 21 PYRANOMETER S/N 170778 LAST CALIBRATION DATE MARCH 2019
KIPP AND ZONEN CHP 1 PYRHELIOMETER S/N 131078 LAST CALIBRATION DATE MARCH 2019

STATEMENT:

The measurement results recorded in this certificate were correct at the time of calibration. The subsequent accuracy will depend on factors such as care, handling and frequency of use. It is recommended that recalibration be undertaken at an interval that will ensure that the instrument remains within the desired limits

CSANAS2837.54.1.20191028

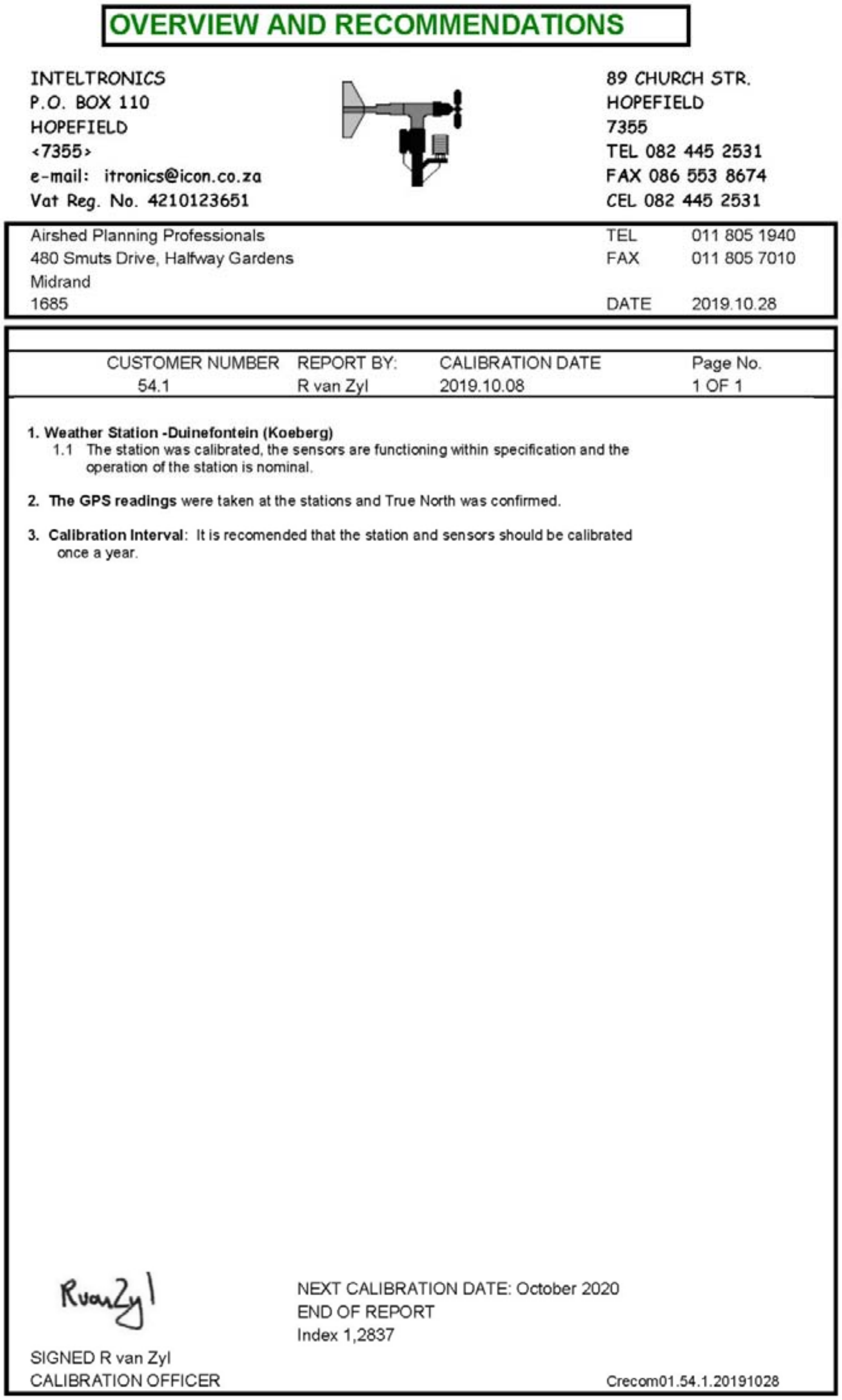

OVERVIEW AND RECOMMENDATIONS

INTELTRONICS
P.O. BOX 110
HOPEFIELD
<7355>
e-mail: itronics@icon.co.za
Vat Reg. No. 4210123651

89 CHURCH STR.
HOPEFIELD
7355
TEL 082 445 2531
FAX 086 553 8674
CEL 082 445 2531

Airshed Planning Professionals
480 Smuts Drive, Halfway Gardens
Midrand
1685

TEL 011 805 1940
FAX 011 805 7010

DATE 2019.10.28

CUSTOMER NUMBER	REPORT BY:	CALIBRATION DATE	Page No.
54.1	R van Zyl	2019.10.08	1 OF 1

1. **Weather Station -Duinefontein (Koeberg)**
   1.1 The station was calibrated, the sensors are functioning within specification and the operation of the station is nominal.

2. **The GPS readings** were taken at the stations and True North was confirmed.

3. **Calibration Interval**: It is recomended that the station and sensors should be calibrated once a year.

RvanZyl

SIGNED R van Zyl
CALIBRATION OFFICER

NEXT CALIBRATION DATE: October 2020
END OF REPORT
Index 1,2837

Crecom01.54.1.20191028

Calibration Date – 20 May 2020

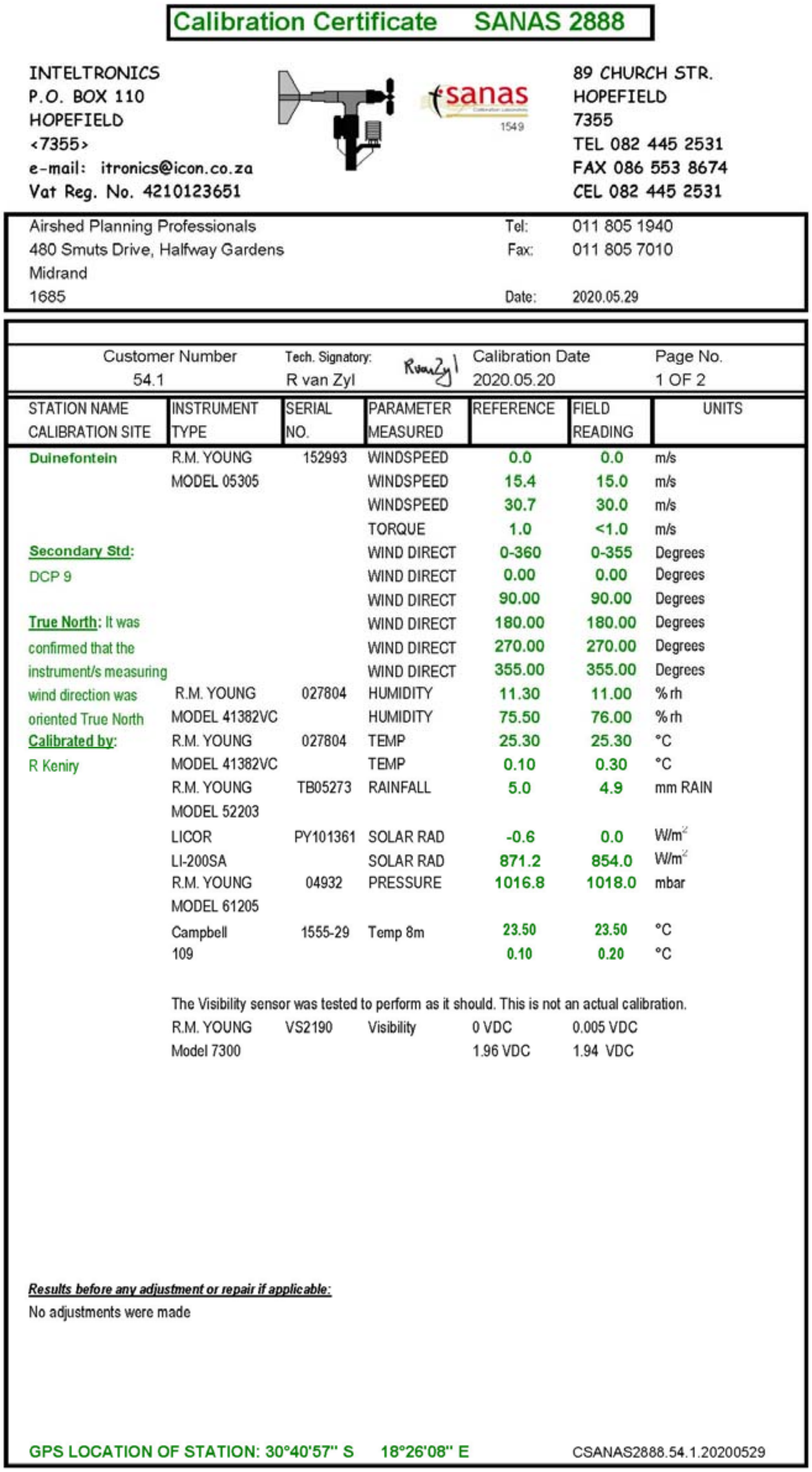

Calibration Certificate SANAS 2888

INTELTRONICS
P.O. BOX 110
HOPEFIELD
<7355>
e-mail: itronics@icon.co.za
Vat Reg. No. 4210123651

sanas
1549

89 CHURCH STR.
HOPEFIELD
7355
TEL 082 445 2531
FAX 086 553 8674
CEL 082 445 2531

Airshed Planning Professionals
480 Smuts Drive, Halfway Gardens
Midrand
1685

Tel: 011 805 1940
Fax: 011 805 7010
Date: 2020.05.29

Customer Number	Tech. Signatory:	Calibration Date	Page No.
54.1	R van Zyl	2020.05.20	1 OF 2

RvanZyl

STATION NAME CALIBRATION SITE	INSTRUMENT TYPE	SERIAL NO.	PARAMETER MEASURED	REFERENCE	FIELD READING	UNITS
Duinefontein	R.M. YOUNG	152993	WINDSPEED	0.0	0.0	m/s
	MODEL 05305		WINDSPEED	15.4	15.0	m/s
			WINDSPEED	30.7	30.0	m/s
			TORQUE	1.0	<1.0	m/s
Secondary Std:			WIND DIRECT	0-360	0-355	Degrees
DCP 9			WIND DIRECT	0.00	0.00	Degrees
			WIND DIRECT	90.00	90.00	Degrees
True North: It was			WIND DIRECT	180.00	180.00	Degrees
confirmed that the			WIND DIRECT	270.00	270.00	Degrees
instrument/s measuring			WIND DIRECT	355.00	355.00	Degrees
wind direction was	R.M. YOUNG	027804	HUMIDITY	11.30	11.00	%rh
oriented True North	MODEL 41382VC		HUMIDITY	75.50	76.00	%rh
Calibrated by:	R.M. YOUNG	027804	TEMP	25.30	25.30	°C
R Keniry	MODEL 41382VC		TEMP	0.10	0.30	°C
	R.M. YOUNG	TB05273	RAINFALL	5.0	4.9	mm RAIN
	MODEL 52203					
	LICOR	PY101361	SOLAR RAD	-0.6	0.0	W/m^2
	LI-200SA		SOLAR RAD	871.2	854.0	W/m^2
	R.M. YOUNG	04932	PRESSURE	1016.8	1018.0	mbar
	MODEL 61205					
	Campbell	1555-29	Temp 8m	23.50	23.50	°C
	109			0.10	0.20	°C

The Visibility sensor was tested to perform as it should. This is not an actual calibration.

R.M. YOUNG	VS2190	Visibility	0 VDC	0.005 VDC
Model 7300			1.96 VDC	1.94 VDC

Results before any adjustment or repair if applicable:

No adjustments were made

GPS LOCATION OF STATION: 30°40'57" S 18°26'08" E

CSANAS2888.54.1.20200529

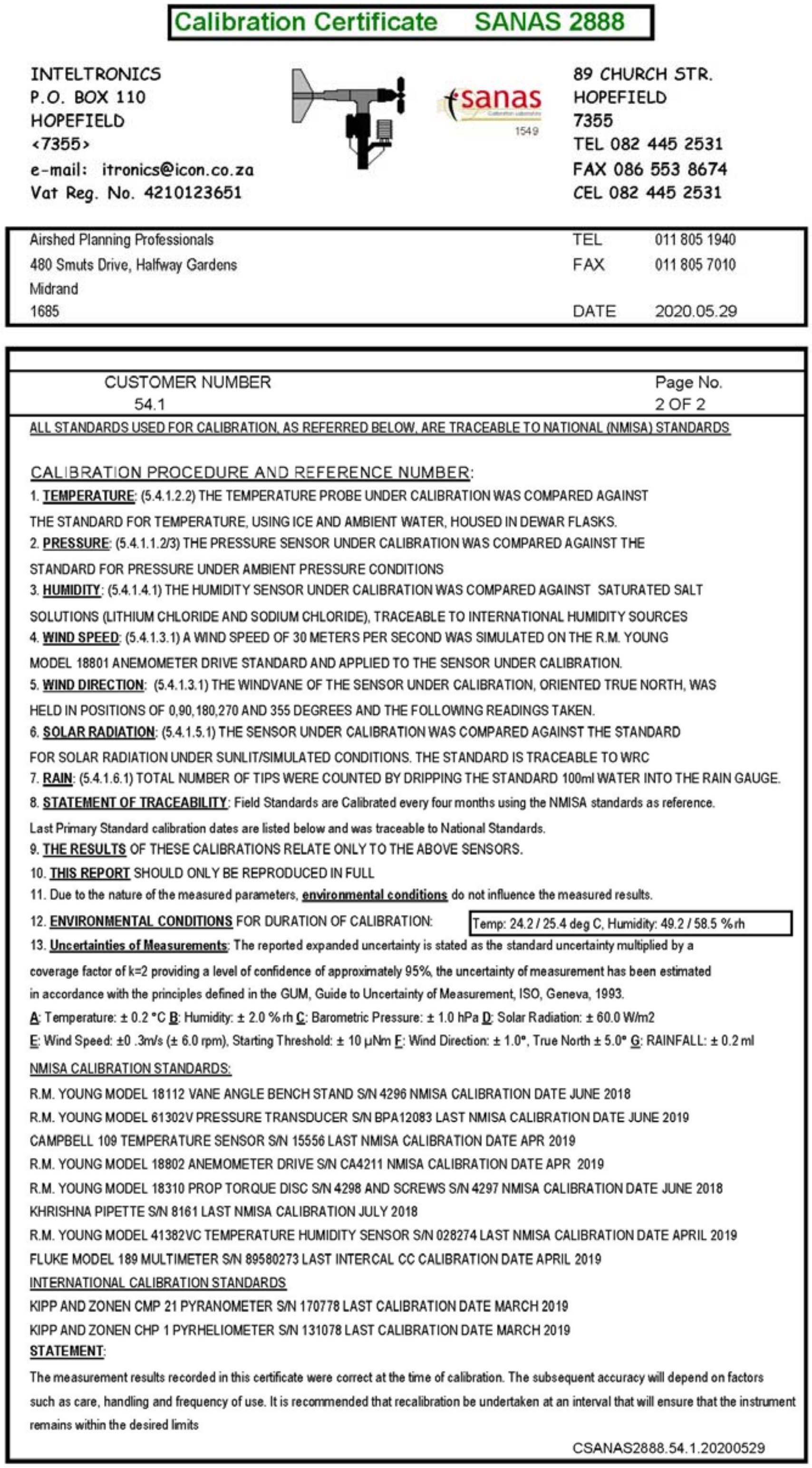

Calibration Certificate SANAS 2888

INTELTRONICS
P.O. BOX 110
HOPEFIELD
<7355>
e-mail: itronics@icon.co.za
Vat Reg. No. 4210123651

89 CHURCH STR.
HOPEFIELD
7355
TEL 082 445 2531
FAX 086 553 8674
CEL 082 445 2531

Airshed Planning Professionals
480 Smuts Drive, Halfway Gardens
Midrand
1685

TEL 011 805 1940
FAX 011 805 7010
DATE 2020.05.29

CUSTOMER NUMBER 54.1

Page No. 2 OF 2

ALL STANDARDS USED FOR CALIBRATION, AS REFERRED BELOW, ARE TRACEABLE TO NATIONAL (NMISA) STANDARDS

CALIBRATION PROCEDURE AND REFERENCE NUMBER:

1. **TEMPERATURE**: (5.4.1.2.2) THE TEMPERATURE PROBE UNDER CALIBRATION WAS COMPARED AGAINST THE STANDARD FOR TEMPERATURE, USING ICE AND AMBIENT WATER, HOUSED IN DEWAR FLASKS.
2. **PRESSURE**: (5.4.1.1.2/3) THE PRESSURE SENSOR UNDER CALIBRATION WAS COMPARED AGAINST THE STANDARD FOR PRESSURE UNDER AMBIENT PRESSURE CONDITIONS
3. **HUMIDITY**: (5.4.1.4.1) THE HUMIDITY SENSOR UNDER CALIBRATION WAS COMPARED AGAINST SATURATED SALT SOLUTIONS (LITHIUM CHLORIDE AND SODIUM CHLORIDE), TRACEABLE TO INTERNATIONAL HUMIDITY SOURCES
4. **WIND SPEED**: (5.4.1.3.1) A WIND SPEED OF 30 METERS PER SECOND WAS SIMULATED ON THE R.M. YOUNG MODEL 18801 ANEMOMETER DRIVE STANDARD AND APPLIED TO THE SENSOR UNDER CALIBRATION.
5. **WIND DIRECTION**: (5.4.1.3.1) THE WINDVANE OF THE SENSOR UNDER CALIBRATION, ORIENTED TRUE NORTH, WAS HELD IN POSITIONS OF 0,90,180,270 AND 355 DEGREES AND THE FOLLOWING READINGS TAKEN.
6. **SOLAR RADIATION**: (5.4.1.5.1) THE SENSOR UNDER CALIBRATION WAS COMPARED AGAINST THE STANDARD FOR SOLAR RADIATION UNDER SUNLIT/SIMULATED CONDITIONS. THE STANDARD IS TRACEABLE TO WRC
7. **RAIN**: (5.4.1.6.1) TOTAL NUMBER OF TIPS WERE COUNTED BY DRIPPING THE STANDARD 100ml WATER INTO THE RAIN GAUGE.
8. **STATEMENT OF TRACEABILITY**: Field Standards are Calibrated every four months using the NMISA standards as reference. Last Primary Standard calibration dates are listed below and was traceable to National Standards.
9. **THE RESULTS** OF THESE CALIBRATIONS RELATE ONLY TO THE ABOVE SENSORS.
10. **THIS REPORT** SHOULD ONLY BE REPRODUCED IN FULL
11. Due to the nature of the measured parameters, **environmental conditions** do not influence the measured results.
12. **ENVIRONMENTAL CONDITIONS** FOR DURATION OF CALIBRATION: Temp: 24.2 / 25.4 deg C, Humidity: 49.2 / 58.5 %rh
13. **Uncertainties of Measurements**: The reported expanded uncertainty is stated as the standard uncertainty multiplied by a coverage factor of k=2 providing a level of confidence of approximately 95%, the uncertainty of measurement has been estimated in accordance with the principles defined in the GUM, Guide to Uncertainty of Measurement, ISO, Geneva, 1993.

A: Temperature: ± 0.2 °C B: Humidity: ± 2.0 %rh C: Barometric Pressure: ± 1.0 hPa D: Solar Radiation: ± 60.0 W/m2
E: Wind Speed: ±0 .3m/s (± 6.0 rpm), Starting Threshold: ± 10 µNm F: Wind Direction: ± 1.0°, True North ± 5.0° G: RAINFALL: ± 0.2 ml

NMISA CALIBRATION STANDARDS:

R.M. YOUNG MODEL 18112 VANE ANGLE BENCH STAND S/N 4296 NMISA CALIBRATION DATE JUNE 2018
R.M. YOUNG MODEL 61302V PRESSURE TRANSDUCER S/N BPA12083 LAST NMISA CALIBRATION DATE JUNE 2019
CAMPBELL 109 TEMPERATURE SENSOR S/N 15556 LAST NMISA CALIBRATION DATE APR 2019
R.M. YOUNG MODEL 18802 ANEMOMETER DRIVE S/N CA4211 NMISA CALIBRATION DATE APR 2019
R.M. YOUNG MODEL 18310 PROP TORQUE DISC S/N 4298 AND SCREWS S/N 4297 NMISA CALIBRATION DATE JUNE 2018
KHRISHNA PIPETTE S/N 8161 LAST NMISA CALIBRATION JULY 2018
R.M. YOUNG MODEL 41382VC TEMPERATURE HUMIDITY SENSOR S/N 028274 LAST NMISA CALIBRATION DATE APRIL 2019
FLUKE MODEL 189 MULTIMETER S/N 89580273 LAST INTERCAL CC CALIBRATION DATE APRIL 2019

INTERNATIONAL CALIBRATION STANDARDS

KIPP AND ZONEN CMP 21 PYRANOMETER S/N 170778 LAST CALIBRATION DATE MARCH 2019
KIPP AND ZONEN CHP 1 PYRHELIOMETER S/N 131078 LAST CALIBRATION DATE MARCH 2019

STATEMENT:

The measurement results recorded in this certificate were correct at the time of calibration. The subsequent accuracy will depend on factors such as care, handling and frequency of use. It is recommended that recalibration be undertaken at an interval that will ensure that the instrument remains within the desired limits

CSANAS2888.54.1.20200529

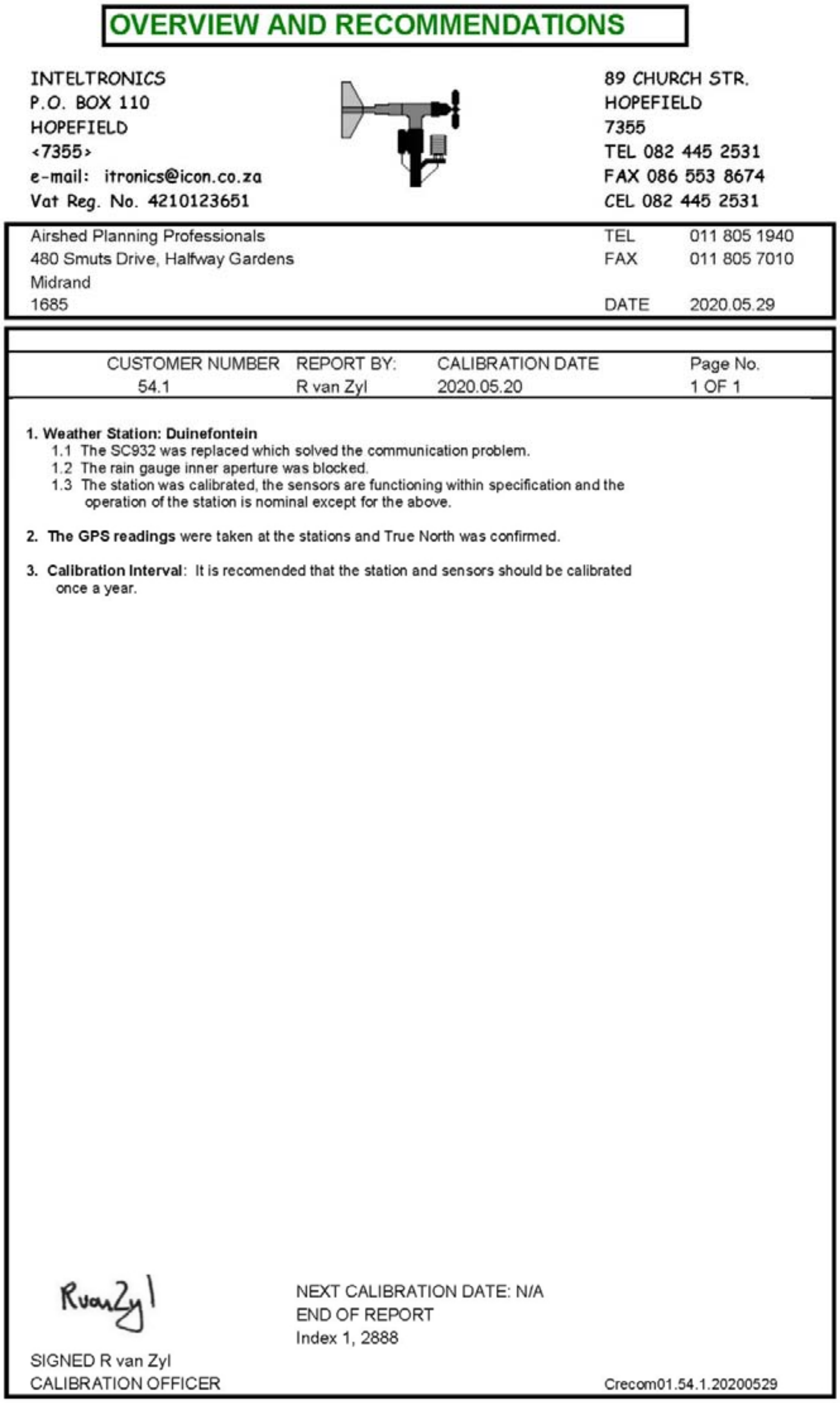

OVERVIEW AND RECOMMENDATIONS

INTELTRONICS
P.O. BOX 110
HOPEFIELD
<7355>
e-mail: itronics@icon.co.za
Vat Reg. No. 4210123651

89 CHURCH STR.
HOPEFIELD
7355
TEL 082 445 2531
FAX 086 553 8674
CEL 082 445 2531

Airshed Planning Professionals
480 Smuts Drive, Halfway Gardens
Midrand
1685

TEL 011 805 1940
FAX 011 805 7010

DATE 2020.05.29

CUSTOMER NUMBER	REPORT BY:	CALIBRATION DATE	Page No.
54.1	R van Zyl	2020.05.20	1 OF 1

1. **Weather Station: Duinefontein**
   - 1.1 The SC932 was replaced which solved the communication problem.
   - 1.2 The rain gauge inner aperture was blocked.
   - 1.3 The station was calibrated, the sensors are functioning within specification and the operation of the station is nominal except for the above.

2. **The GPS readings** were taken at the stations and True North was confirmed.

3. **Calibration Interval**: It is recomended that the station and sensors should be calibrated once a year.

RvanZyl

SIGNED R van Zyl
CALIBRATION OFFICER

NEXT CALIBRATION DATE: N/A
END OF REPORT
Index 1, 2888

Crecom01.54.1.20200529

Calibration Date – 27 November 2020

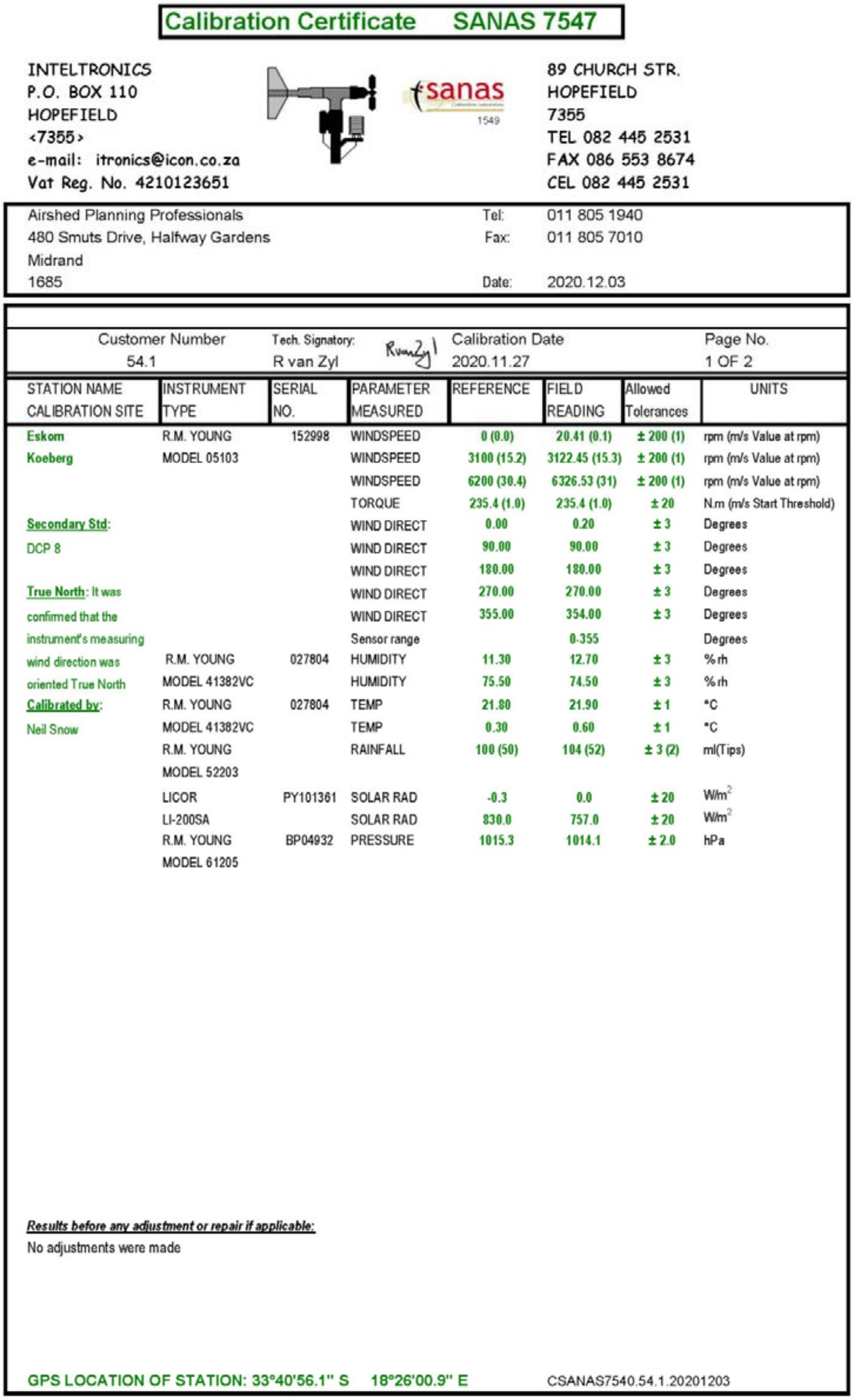

Calibration Certificate SANAS 7547

INTELTRONICS
P.O. BOX 110
HOPEFIELD
<7355>
e-mail: itronics@icon.co.za
Vat Reg. No. 4210123651

sanas 1549

89 CHURCH STR.
HOPEFIELD
7355
TEL 082 445 2531
FAX 086 553 8674
CEL 082 445 2531

Airshed Planning Professionals
480 Smuts Drive, Halfway Gardens
Midrand
1685

Tel: 011 805 1940
Fax: 011 805 7010

Date: 2020.12.03

Customer Number
54.1

Tech. Signatory:
R van Zyl
RvanZyl

Calibration Date
2020.11.27

Page No.
1 OF 2

STATION NAME CALIBRATION SITE	INSTRUMENT TYPE	SERIAL NO.	PARAMETER MEASURED	REFERENCE	FIELD READING	Allowed Tolerances	UNITS
Eskom	R.M. YOUNG	152998	WINDSPEED	0 (0.0)	20.41 (0.1)	± 200 (1)	rpm (m/s Value at rpm)
Koeberg	MODEL 05103		WINDSPEED	3100 (15.2)	3122.45 (15.3)	± 200 (1)	rpm (m/s Value at rpm)
			WINDSPEED	6200 (30.4)	6326.53 (31)	± 200 (1)	rpm (m/s Value at rpm)
			TORQUE	235.4 (1.0)	235.4 (1.0)	± 20	N.m (m/s Start Threshold)
Secondary Std:			WIND DIRECT	0.00	0.20	± 3	Degrees
DCP 8			WIND DIRECT	90.00	90.00	± 3	Degrees
			WIND DIRECT	180.00	180.00	± 3	Degrees
True North: It was			WIND DIRECT	270.00	270.00	± 3	Degrees
confirmed that the			WIND DIRECT	355.00	354.00	± 3	Degrees
instrument's measuring			Sensor range		0-355		Degrees
wind direction was	R.M. YOUNG	027804	HUMIDITY	11.30	12.70	± 3	% rh
oriented True North	MODEL 41382VC		HUMIDITY	75.50	74.50	± 3	% rh
Calibrated by:	R.M. YOUNG	027804	TEMP	21.80	21.90	± 1	°C
Neil Snow	MODEL 41382VC		TEMP	0.30	0.60	± 1	°C
	R.M. YOUNG		RAINFALL	100 (50)	104 (52)	± 3 (2)	ml(Tips)
	MODEL 52203						
	LICOR	PY101361	SOLAR RAD	-0.3	0.0	± 20	W/m^2
	LI-200SA		SOLAR RAD	830.0	757.0	± 20	W/m^2
	R.M. YOUNG	BP04932	PRESSURE	1015.3	1014.1	± 2.0	hPa
	MODEL 61205						

Results before any adjustment or repair if applicable:

No adjustments were made

GPS LOCATION OF STATION: 33°40'56.1" S 18°26'00.9" E

CSANAS7540.54.1.20201203

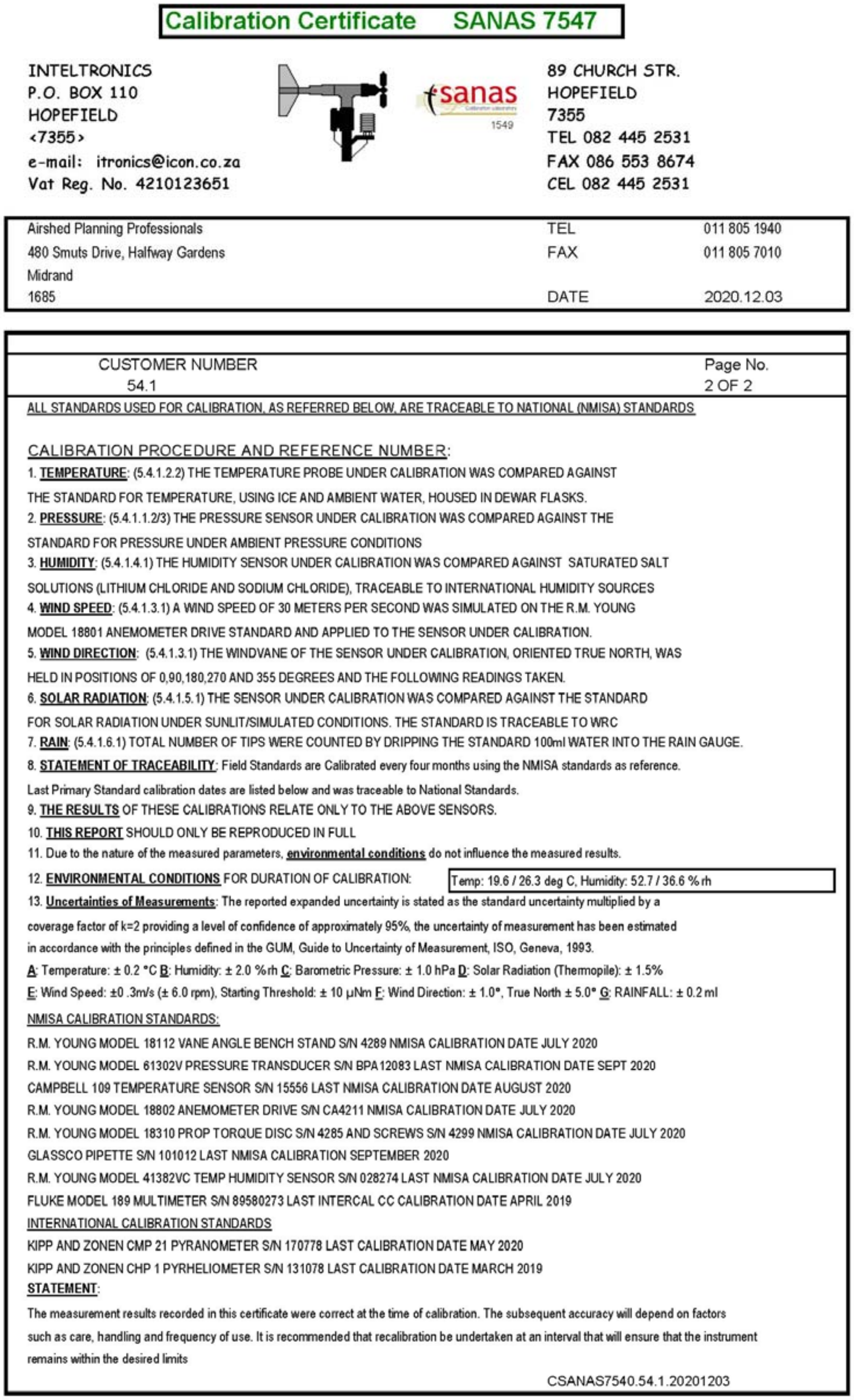

Calibration Certificate SANAS 7547

INTELTRONICS
P.O. BOX 110
HOPEFIELD
<7355>
e-mail: itronics@icon.co.za
Vat Reg. No. 4210123651

sanas
1549

89 CHURCH STR.
HOPEFIELD
7355
TEL 082 445 2531
FAX 086 553 8674
CEL 082 445 2531

Airshed Planning Professionals
480 Smuts Drive, Halfway Gardens
Midrand
1685

TEL 011 805 1940
FAX 011 805 7010
DATE 2020.12.03

CUSTOMER NUMBER
54.1

Page No.
2 OF 2

ALL STANDARDS USED FOR CALIBRATION, AS REFERRED BELOW, ARE TRACEABLE TO NATIONAL (NMISA) STANDARDS

CALIBRATION PROCEDURE AND REFERENCE NUMBER:

1. **TEMPERATURE**: (5.4.1.2.2) THE TEMPERATURE PROBE UNDER CALIBRATION WAS COMPARED AGAINST THE STANDARD FOR TEMPERATURE, USING ICE AND AMBIENT WATER, HOUSED IN DEWAR FLASKS.
2. **PRESSURE**: (5.4.1.1.2/3) THE PRESSURE SENSOR UNDER CALIBRATION WAS COMPARED AGAINST THE STANDARD FOR PRESSURE UNDER AMBIENT PRESSURE CONDITIONS
3. **HUMIDITY**: (5.4.1.4.1) THE HUMIDITY SENSOR UNDER CALIBRATION WAS COMPARED AGAINST SATURATED SALT SOLUTIONS (LITHIUM CHLORIDE AND SODIUM CHLORIDE), TRACEABLE TO INTERNATIONAL HUMIDITY SOURCES
4. **WIND SPEED**: (5.4.1.3.1) A WIND SPEED OF 30 METERS PER SECOND WAS SIMULATED ON THE R.M. YOUNG MODEL 18801 ANEMOMETER DRIVE STANDARD AND APPLIED TO THE SENSOR UNDER CALIBRATION.
5. **WIND DIRECTION**: (5.4.1.3.1) THE WINDVANE OF THE SENSOR UNDER CALIBRATION, ORIENTED TRUE NORTH, WAS HELD IN POSITIONS OF 0,90,180,270 AND 355 DEGREES AND THE FOLLOWING READINGS TAKEN.
6. **SOLAR RADIATION**: (5.4.1.5.1) THE SENSOR UNDER CALIBRATION WAS COMPARED AGAINST THE STANDARD FOR SOLAR RADIATION UNDER SUNLIT/SIMULATED CONDITIONS. THE STANDARD IS TRACEABLE TO WRC
7. **RAIN**: (5.4.1.6.1) TOTAL NUMBER OF TIPS WERE COUNTED BY DRIPPING THE STANDARD 100ml WATER INTO THE RAIN GAUGE.
8. **STATEMENT OF TRACEABILITY**: Field Standards are Calibrated every four months using the NMISA standards as reference. Last Primary Standard calibration dates are listed below and was traceable to National Standards.
9. **THE RESULTS** OF THESE CALIBRATIONS RELATE ONLY TO THE ABOVE SENSORS.
10. **THIS REPORT** SHOULD ONLY BE REPRODUCED IN FULL
11. Due to the nature of the measured parameters, **environmental conditions** do not influence the measured results.
12. **ENVIRONMENTAL CONDITIONS** FOR DURATION OF CALIBRATION: Temp: 19.6 / 26.3 deg C, Humidity: 52.7 / 36.6 %rh
13. **Uncertainties of Measurements**: The reported expanded uncertainty is stated as the standard uncertainty multiplied by a coverage factor of k=2 providing a level of confidence of approximately 95%, the uncertainty of measurement has been estimated in accordance with the principles defined in the GUM, Guide to Uncertainty of Measurement, ISO, Geneva, 1993.

A: Temperature: ± 0.2 °C B: Humidity: ± 2.0 %rh C: Barometric Pressure: ± 1.0 hPa D: Solar Radiation (Thermopile): ± 1.5%
E: Wind Speed: ±0 .3m/s (± 6.0 rpm), Starting Threshold: ± 10 μNm F: Wind Direction: ± 1.0°, True North ± 5.0° G: RAINFALL: ± 0.2 ml

NMISA CALIBRATION STANDARDS:

R.M. YOUNG MODEL 18112 VANE ANGLE BENCH STAND S/N 4289 NMISA CALIBRATION DATE JULY 2020
R.M. YOUNG MODEL 61302V PRESSURE TRANSDUCER S/N BPA12083 LAST NMISA CALIBRATION DATE SEPT 2020
CAMPBELL 109 TEMPERATURE SENSOR S/N 15556 LAST NMISA CALIBRATION DATE AUGUST 2020
R.M. YOUNG MODEL 18802 ANEMOMETER DRIVE S/N CA4211 NMISA CALIBRATION DATE JULY 2020
R.M. YOUNG MODEL 18310 PROP TORQUE DISC S/N 4285 AND SCREWS S/N 4299 NMISA CALIBRATION DATE JULY 2020
GLASSCO PIPETTE S/N 101012 LAST NMISA CALIBRATION SEPTEMBER 2020
R.M. YOUNG MODEL 41382VC TEMP HUMIDITY SENSOR S/N 028274 LAST NMISA CALIBRATION DATE JULY 2020
FLUKE MODEL 189 MULTIMETER S/N 89580273 LAST INTERCAL CC CALIBRATION DATE APRIL 2019

INTERNATIONAL CALIBRATION STANDARDS

KIPP AND ZONEN CMP 21 PYRANOMETER S/N 170778 LAST CALIBRATION DATE MAY 2020
KIPP AND ZONEN CHP 1 PYRHELIOMETER S/N 131078 LAST CALIBRATION DATE MARCH 2019

STATEMENT:

The measurement results recorded in this certificate were correct at the time of calibration. The subsequent accuracy will depend on factors such as care, handling and frequency of use. It is recommended that recalibration be undertaken at an interval that will ensure that the instrument remains within the desired limits

CSANAS7540.54.1.20201203

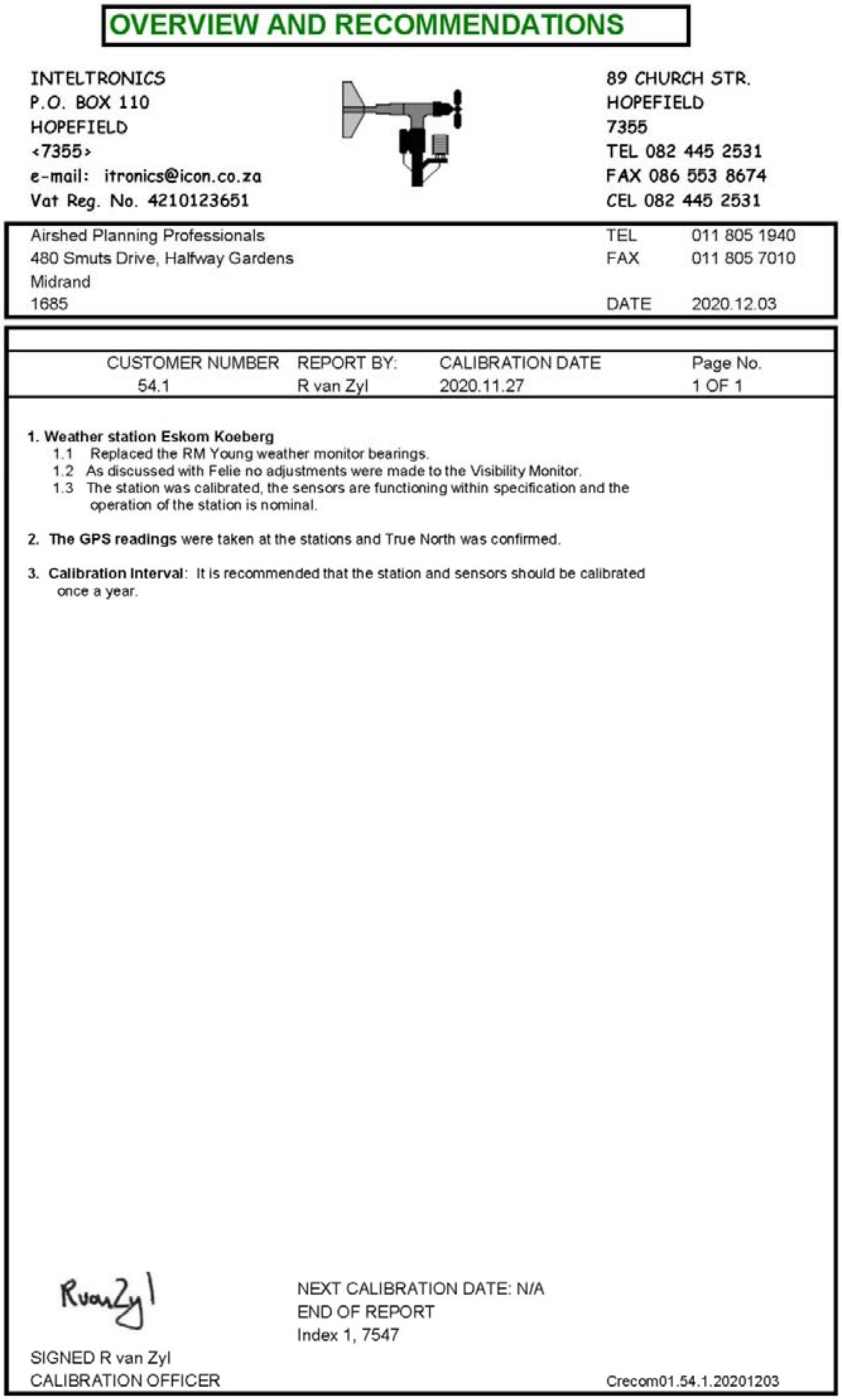

OVERVIEW AND RECOMMENDATIONS

INTELTRONICS
P.O. BOX 110
HOPEFIELD
<7355>
e-mail: itronics@icon.co.za
Vat Reg. No. 4210123651

89 CHURCH STR.
HOPEFIELD
7355
TEL 082 445 2531
FAX 086 553 8674
CEL 082 445 2531

Airshed Planning Professionals
480 Smuts Drive, Halfway Gardens
Midrand
1685

TEL 011 805 1940
FAX 011 805 7010

DATE 2020.12.03

CUSTOMER NUMBER	REPORT BY:	CALIBRATION DATE	Page No.
54.1	R van Zyl	2020.11.27	1 OF 1

1. Weather station Eskom Koeberg
  - 1.1 Replaced the RM Young weather monitor bearings.
  - 1.2 As discussed with Felie no adjustments were made to the Visibility Monitor.
  - 1.3 The station was calibrated, the sensors are functioning within specification and the operation of the station is nominal.

2. **The GPS readings** were taken at the stations and True North was confirmed.

3. **Calibration Interval**: It is recommended that the station and sensors should be calibrated once a year.

RvanZyl

SIGNED R van Zyl
CALIBRATION OFFICER

NEXT CALIBRATION DATE: N/A
END OF REPORT
Index 1, 7547

Crecom01.54.1.20201203

Calibration Date – 19 November 2021

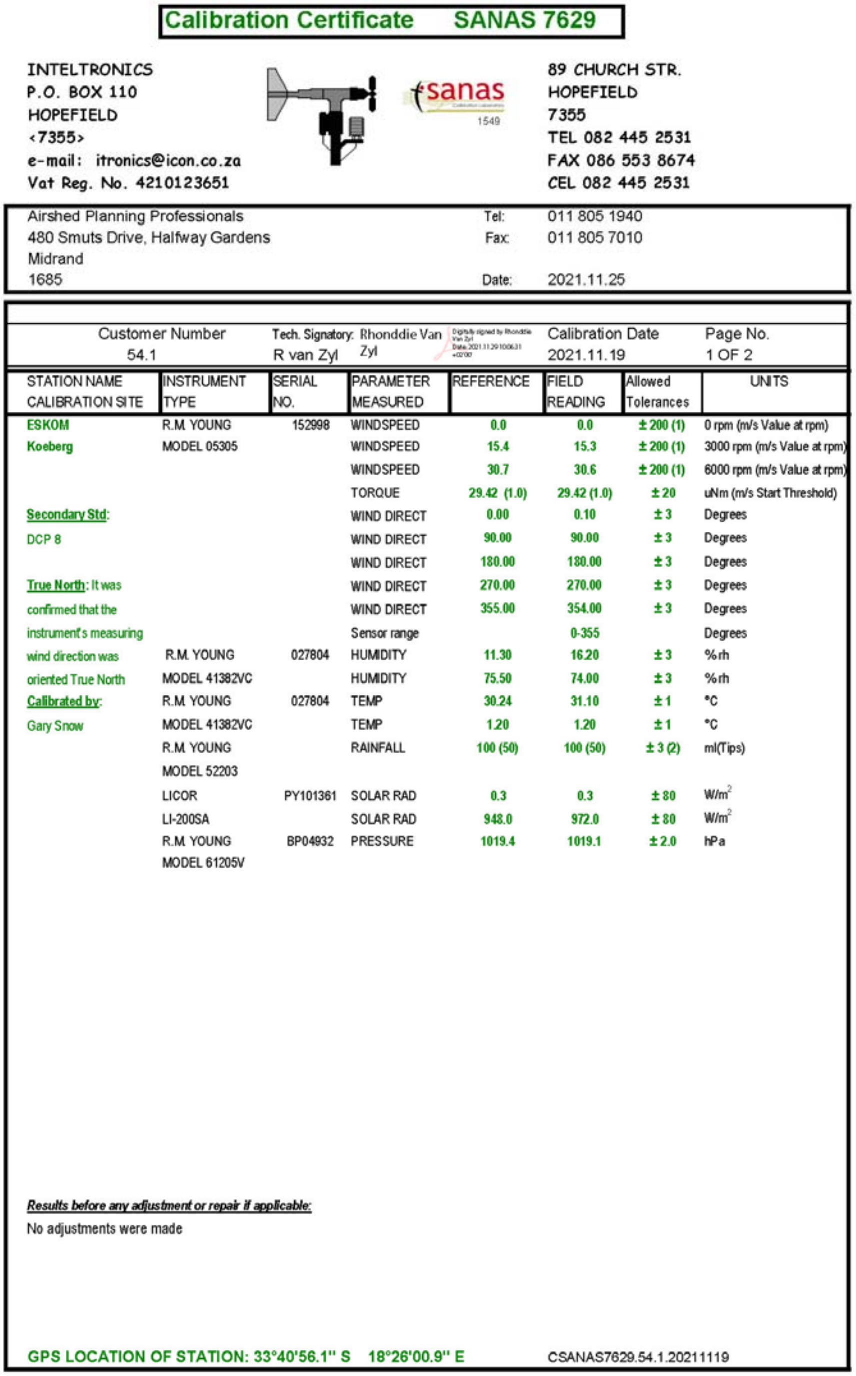

Calibration Certificate SANAS 7629

INTELTRONICS
P.O. BOX 110
HOPEFIELD
<7355>
e-mail: itronics@icon.co.za
Vat Reg. No. 4210123651

sanas
1549

89 CHURCH STR.
HOPEFIELD
7355
TEL 082 445 2531
FAX 086 553 8674
CEL 082 445 2531

Airshed Planning Professionals
480 Smuts Drive, Halfway Gardens
Midrand
1685

Tel: 011 805 1940
Fax: 011 805 7010
Date: 2021.11.25

Customer Number	Tech. Signatory:	Calibration Date	Page No.
54.1	R van Zyl Rhonddie Van Zyl Digitally signed by Rhonddie Van Zyl Date: 2021.11.29 10:06:31 +02'00'	2021.11.19	1 OF 2

STATION NAME CALIBRATION SITE	INSTRUMENT TYPE	SERIAL NO.	PARAMETER MEASURED	REFERENCE	FIELD READING	Allowed Tolerances	UNITS
ESKOM	R.M. YOUNG	152998	WINDSPEED	0.0	0.0	± 200 (1)	0 rpm (m/s Value at rpm)
Koeberg	MODEL 05305		WINDSPEED	15.4	15.3	± 200 (1)	3000 rpm (m/s Value at rpm)
			WINDSPEED	30.7	30.6	± 200 (1)	6000 rpm (m/s Value at rpm)
			TORQUE	29.42 (1.0)	29.42 (1.0)	± 20	uNm (m/s Start Threshold)
Secondary Std:			WIND DIRECT	0.00	0.10	± 3	Degrees
DCP 8			WIND DIRECT	90.00	90.00	± 3	Degrees
			WIND DIRECT	180.00	180.00	± 3	Degrees
True North: It was			WIND DIRECT	270.00	270.00	± 3	Degrees
confirmed that the			WIND DIRECT	355.00	354.00	± 3	Degrees
instrument's measuring			Sensor range		0-355		Degrees
wind direction was	R.M. YOUNG	027804	HUMIDITY	11.30	16.20	± 3	%rh
oriented True North	MODEL 41382VC		HUMIDITY	75.50	74.00	± 3	%rh
Calibrated by:	R.M. YOUNG	027804	TEMP	30.24	31.10	± 1	°C
Gary Snow	MODEL 41382VC		TEMP	1.20	1.20	± 1	°C
	R.M. YOUNG		RAINFALL	100 (50)	100 (50)	± 3 (2)	ml(Tips)
	MODEL 52203						
	LICOR	PY101361	SOLAR RAD	0.3	0.3	± 80	W/m^2
	LI-200SA		SOLAR RAD	948.0	972.0	± 80	W/m^2
	R.M. YOUNG	BP04932	PRESSURE	1019.4	1019.1	± 2.0	hPa
	MODEL 61205V						

Results before any adjustment or repair if applicable:

No adjustments were made

GPS LOCATION OF STATION: 33°40'56.1" S 18°26'00.9" E

CSANAS7629.54.1.20211119

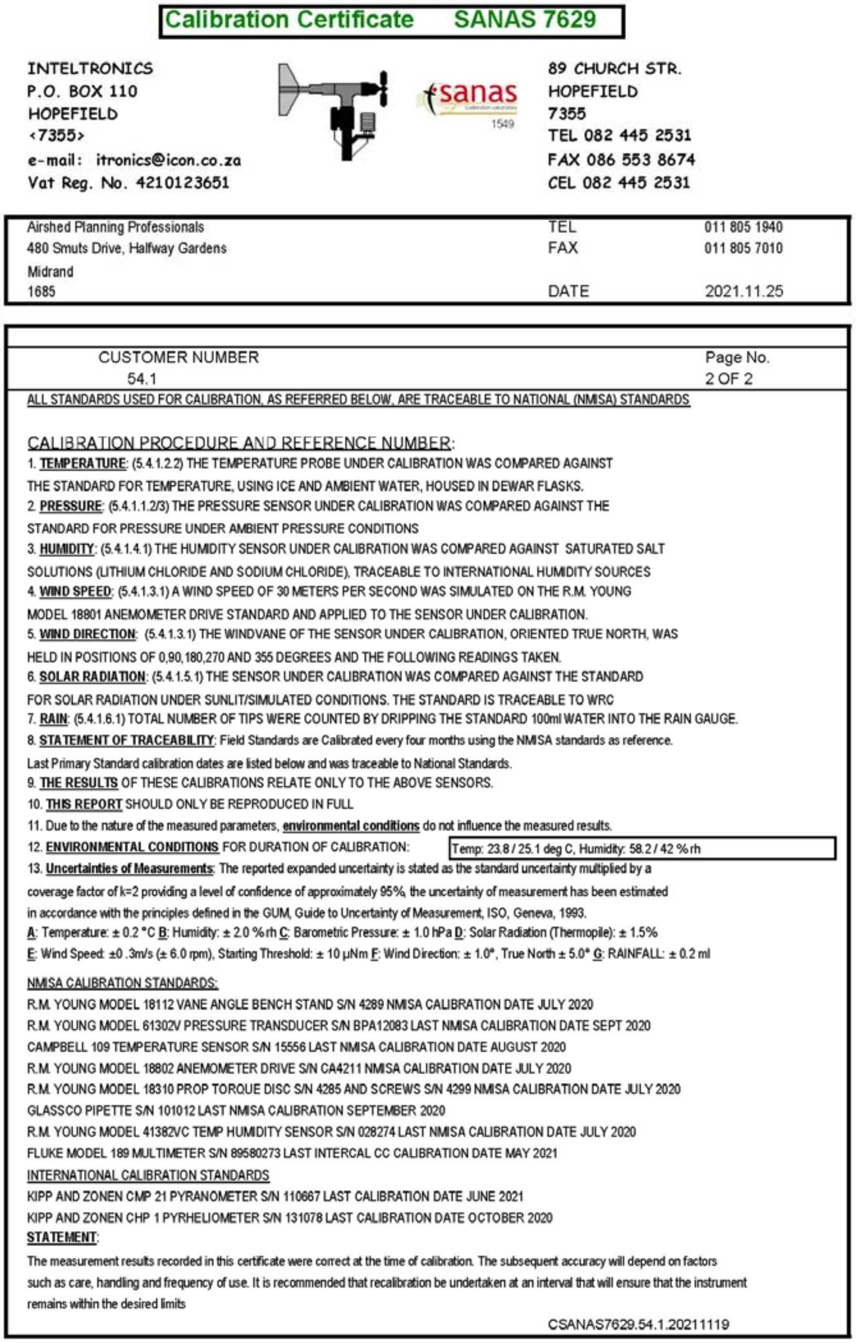

Calibration Certificate SANAS 7629

INTELTRONICS
P.O. BOX 110
HOPEFIELD
<7355>
e-mail: itronics@icon.co.za
Vat Reg. No. 4210123651

sanas
1549

89 CHURCH STR.
HOPEFIELD
7355
TEL 082 445 2531
FAX 086 553 8674
CEL 082 445 2531

Airshed Planning Professionals	TEL	011 805 1940
480 Smuts Drive, Halfway Gardens	FAX	011 805 7010
Midrand		
1685	DATE	2021.11.25

CUSTOMER NUMBER
54.1

Page No.
2 OF 2

ALL STANDARDS USED FOR CALIBRATION, AS REFERRED BELOW, ARE TRACEABLE TO NATIONAL (NMISA) STANDARDS

CALIBRATION PROCEDURE AND REFERENCE NUMBER:

1. **TEMPERATURE**: (5.4.1.2.2) THE TEMPERATURE PROBE UNDER CALIBRATION WAS COMPARED AGAINST THE STANDARD FOR TEMPERATURE, USING ICE AND AMBIENT WATER, HOUSED IN DEWAR FLASKS.
2. **PRESSURE**: (5.4.1.1.2/3) THE PRESSURE SENSOR UNDER CALIBRATION WAS COMPARED AGAINST THE STANDARD FOR PRESSURE UNDER AMBIENT PRESSURE CONDITIONS
3. **HUMIDITY**: (5.4.1.4.1) THE HUMIDITY SENSOR UNDER CALIBRATION WAS COMPARED AGAINST SATURATED SALT SOLUTIONS (LITHIUM CHLORIDE AND SODIUM CHLORIDE), TRACEABLE TO INTERNATIONAL HUMIDITY SOURCES
4. **WIND SPEED**: (5.4.1.3.1) A WIND SPEED OF 30 METERS PER SECOND WAS SIMULATED ON THE R.M. YOUNG MODEL 18801 ANEMOMETER DRIVE STANDARD AND APPLIED TO THE SENSOR UNDER CALIBRATION.
5. **WIND DIRECTION**: (5.4.1.3.1) THE WINDVANE OF THE SENSOR UNDER CALIBRATION, ORIENTED TRUE NORTH, WAS HELD IN POSITIONS OF 0,90,180,270 AND 355 DEGREES AND THE FOLLOWING READINGS TAKEN.
6. **SOLAR RADIATION**: (5.4.1.5.1) THE SENSOR UNDER CALIBRATION WAS COMPARED AGAINST THE STANDARD FOR SOLAR RADIATION UNDER SUNLIT/SIMULATED CONDITIONS. THE STANDARD IS TRACEABLE TO WRC
7. **RAIN**: (5.4.1.6.1) TOTAL NUMBER OF TIPS WERE COUNTED BY DRIPPING THE STANDARD 100ml WATER INTO THE RAIN GAUGE.
8. **STATEMENT OF TRACEABILITY**: Field Standards are Calibrated every four months using the NMISA standards as reference. Last Primary Standard calibration dates are listed below and was traceable to National Standards.
9. **THE RESULTS** OF THESE CALIBRATIONS RELATE ONLY TO THE ABOVE SENSORS.
10. **THIS REPORT** SHOULD ONLY BE REPRODUCED IN FULL
11. Due to the nature of the measured parameters, **environmental conditions** do not influence the measured results.
12. **ENVIRONMENTAL CONDITIONS** FOR DURATION OF CALIBRATION: Temp: 23.8 / 25.1 deg C, Humidity: 58.2 / 42 %rh
13. **Uncertainties of Measurements**: The reported expanded uncertainty is stated as the standard uncertainty multiplied by a coverage factor of k=2 providing a level of confidence of approximately 95%, the uncertainty of measurement has been estimated in accordance with the principles defined in the GUM, Guide to Uncertainty of Measurement, ISO, Geneva, 1993.

A: Temperature: ± 0.2 °C B: Humidity: ± 2.0 %rh C: Barometric Pressure: ± 1.0 hPa D: Solar Radiation (Thermopile): ± 1.5%
E: Wind Speed: ±0 .3m/s (± 6.0 rpm), Starting Threshold: ± 10 μNm F: Wind Direction: ± 1.0°, True North ± 5.0° G: RAINFALL: ± 0.2 ml

NMISA CALIBRATION STANDARDS:

R.M. YOUNG MODEL 18112 VANE ANGLE BENCH STAND S/N 4289 NMISA CALIBRATION DATE JULY 2020
R.M. YOUNG MODEL 61302V PRESSURE TRANSDUCER S/N BPA12083 LAST NMISA CALIBRATION DATE SEPT 2020
CAMPBELL 109 TEMPERATURE SENSOR S/N 15556 LAST NMISA CALIBRATION DATE AUGUST 2020
R.M. YOUNG MODEL 18802 ANEMOMETER DRIVE S/N CA4211 NMISA CALIBRATION DATE JULY 2020
R.M. YOUNG MODEL 18310 PROP TORQUE DISC S/N 4285 AND SCREWS S/N 4299 NMISA CALIBRATION DATE JULY 2020
GLASSCO PIPETTE S/N 101012 LAST NMISA CALIBRATION SEPTEMBER 2020
R.M. YOUNG MODEL 41382VC TEMP HUMIDITY SENSOR S/N 028274 LAST NMISA CALIBRATION DATE JULY 2020
FLUKE MODEL 189 MULTIMETER S/N 89580273 LAST INTERCAL CC CALIBRATION DATE MAY 2021

INTERNATIONAL CALIBRATION STANDARDS

KIPP AND ZONEN CMP 21 PYRANOMETER S/N 110667 LAST CALIBRATION DATE JUNE 2021
KIPP AND ZONEN CHP 1 PYRHELIOMETER S/N 131078 LAST CALIBRATION DATE OCTOBER 2020

STATEMENT:

The measurement results recorded in this certificate were correct at the time of calibration. The subsequent accuracy will depend on factors such as care, handling and frequency of use. It is recommended that recalibration be undertaken at an interval that will ensure that the instrument remains within the desired limits

CSANAS7629.54.1.20211119

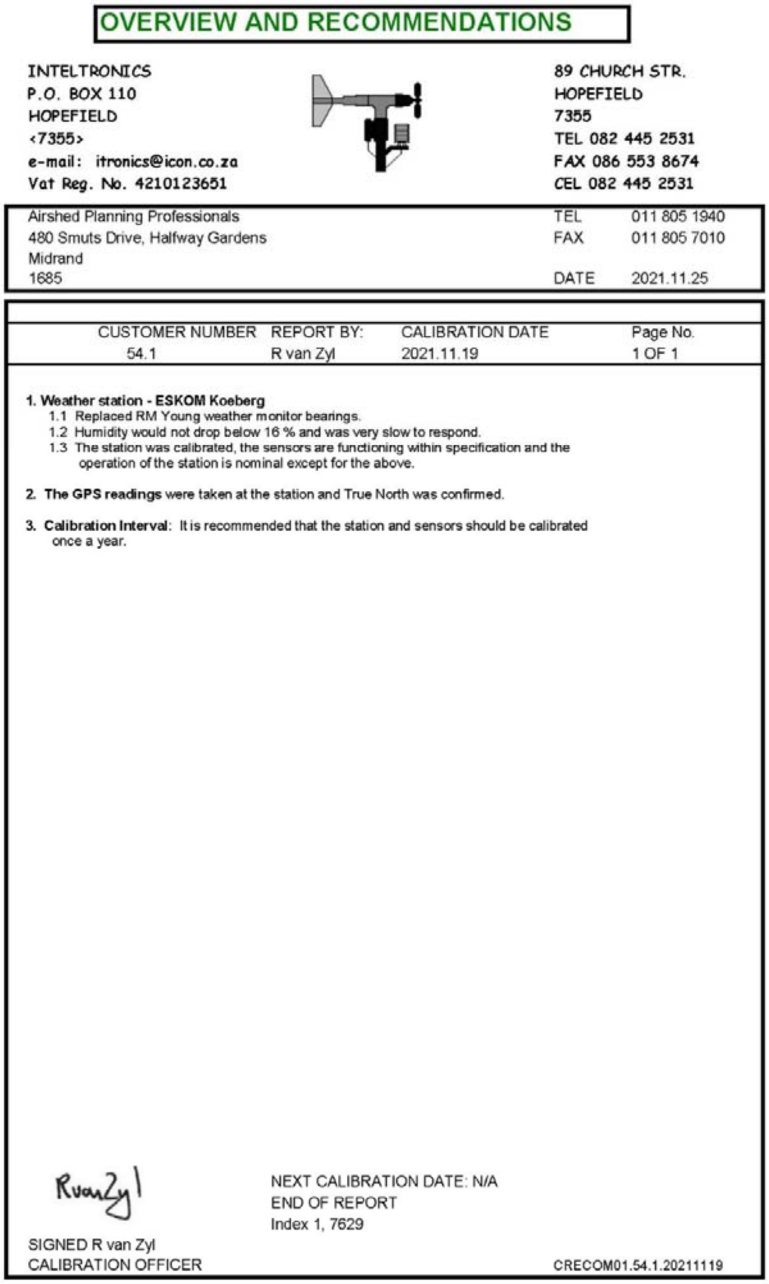

OVERVIEW AND RECOMMENDATIONS

INTELTRONICS
P.O. BOX 110
HOPEFIELD
<7355>
e-mail: itronics@icon.co.za
Vat Reg. No. 4210123651

89 CHURCH STR.
HOPEFIELD
7355
TEL 082 445 2531
FAX 086 553 8674
CEL 082 445 2531

Airshed Planning Professionals
480 Smuts Drive, Halfway Gardens
Midrand
1685

TEL 011 805 1940
FAX 011 805 7010
DATE 2021.11.25

CUSTOMER NUMBER	REPORT BY:	CALIBRATION DATE	Page No.
54.1	R van Zyl	2021.11.19	1 OF 1

1. **Weather station - ESKOM Koeberg**
   1.1 Replaced RM Young weather monitor bearings.
   1.2 Humidity would not drop below 16 % and was very slow to respond.
   1.3 The station was calibrated, the sensors are functioning within specification and the operation of the station is nominal except for the above.

2. **The GPS readings** were taken at the station and True North was confirmed.

3. **Calibration Interval**: It is recommended that the station and sensors should be calibrated once a year.

RvanZyl

SIGNED R van Zyl
CALIBRATION OFFICER

NEXT CALIBRATION DATE: N/A
END OF REPORT
Index 1, 7629

CRECOM01.54.1.20211119

Calibration Date – 19 May 2021

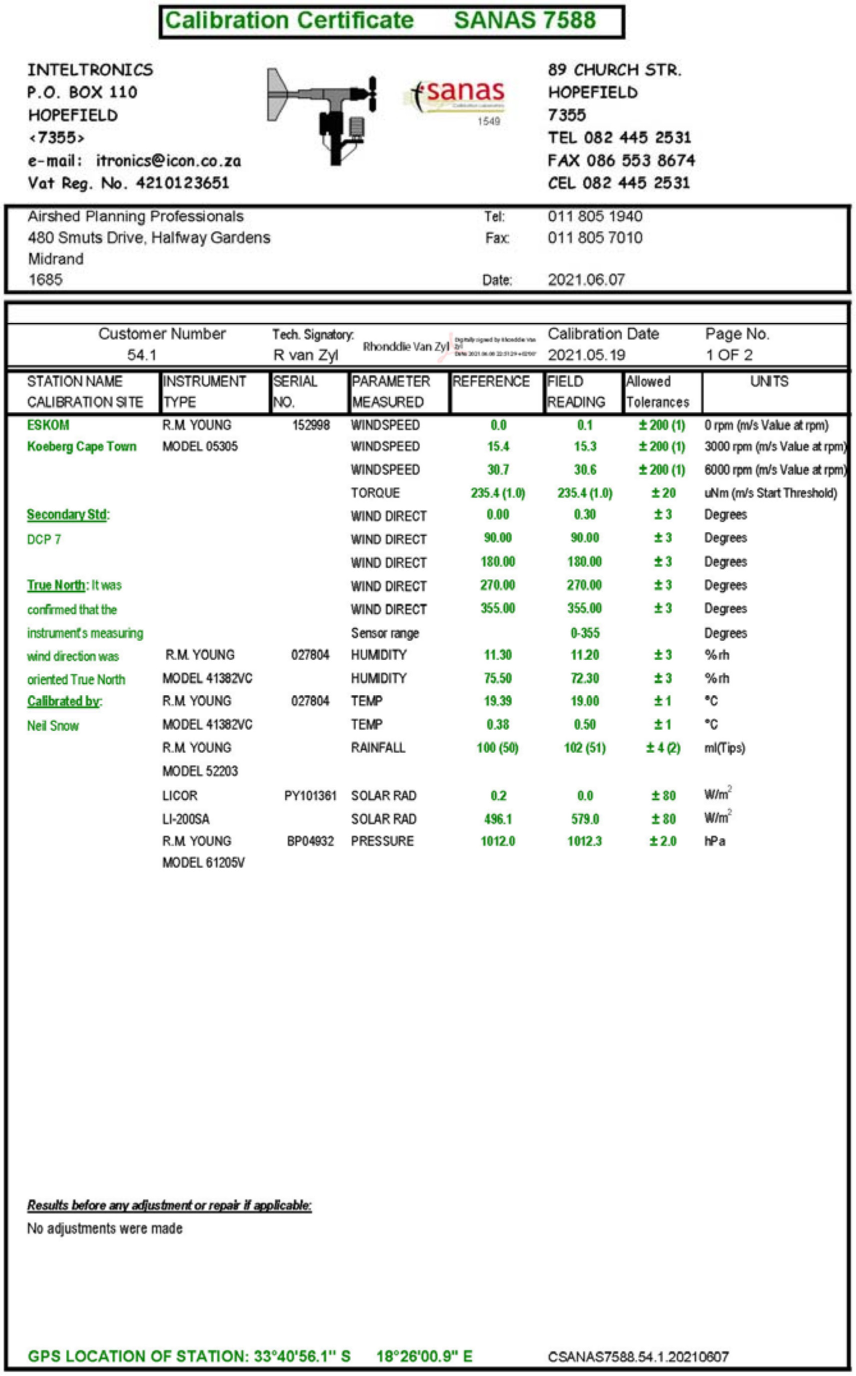

Calibration Certificate SANAS 7588

INTELTRONICS
P.O. BOX 110
HOPEFIELD
<7355>
e-mail: itronics@icon.co.za
Vat Reg. No. 4210123651

sanas
1549

89 CHURCH STR.
HOPEFIELD
7355
TEL 082 445 2531
FAX 086 553 8674
CEL 082 445 2531

Airshed Planning Professionals
480 Smuts Drive, Halfway Gardens
Midrand
1685

Tel: 011 805 1940
Fax: 011 805 7010
Date: 2021.06.07

Customer Number	Tech. Signatory:	Calibration Date	Page No.
54.1	R van Zyl Rhonddie Van Zyl	2021.05.19	1 OF 2

STATION NAME CALIBRATION SITE	INSTRUMENT TYPE	SERIAL NO.	PARAMETER MEASURED	REFERENCE	FIELD READING	Allowed Tolerances	UNITS
ESKOM	R.M. YOUNG	152998	WINDSPEED	0.0	0.1	± 200 (1)	0 rpm (m/s Value at rpm)
Koeberg Cape Town	MODEL 05305		WINDSPEED	15.4	15.3	± 200 (1)	3000 rpm (m/s Value at rpm)
			WINDSPEED	30.7	30.6	± 200 (1)	6000 rpm (m/s Value at rpm)
			TORQUE	235.4 (1.0)	235.4 (1.0)	± 20	uNm (m/s Start Threshold)
Secondary Std:			WIND DIRECT	0.00	0.30	± 3	Degrees
DCP 7			WIND DIRECT	90.00	90.00	± 3	Degrees
			WIND DIRECT	180.00	180.00	± 3	Degrees
True North: It was			WIND DIRECT	270.00	270.00	± 3	Degrees
confirmed that the			WIND DIRECT	355.00	355.00	± 3	Degrees
instrument's measuring			Sensor range		0-355		Degrees
wind direction was	R.M. YOUNG	027804	HUMIDITY	11.30	11.20	± 3	%rh
oriented True North	MODEL 41382VC		HUMIDITY	75.50	72.30	± 3	%rh
Calibrated by:	R.M. YOUNG	027804	TEMP	19.39	19.00	± 1	°C
Neil Snow	MODEL 41382VC		TEMP	0.38	0.50	± 1	°C
	R.M. YOUNG		RAINFALL	100 (50)	102 (51)	± 4 (2)	ml(Tips)
	MODEL 52203						
	LICOR	PY101361	SOLAR RAD	0.2	0.0	± 80	W/m^2
	LI-200SA		SOLAR RAD	496.1	579.0	± 80	W/m^2
	R.M. YOUNG	BP04932	PRESSURE	1012.0	1012.3	± 2.0	hPa
	MODEL 61205V						

Results before any adjustment or repair if applicable:

No adjustments were made

GPS LOCATION OF STATION: 33°40'56.1" S 18°26'00.9" E

CSANAS7588.54.1.20210607

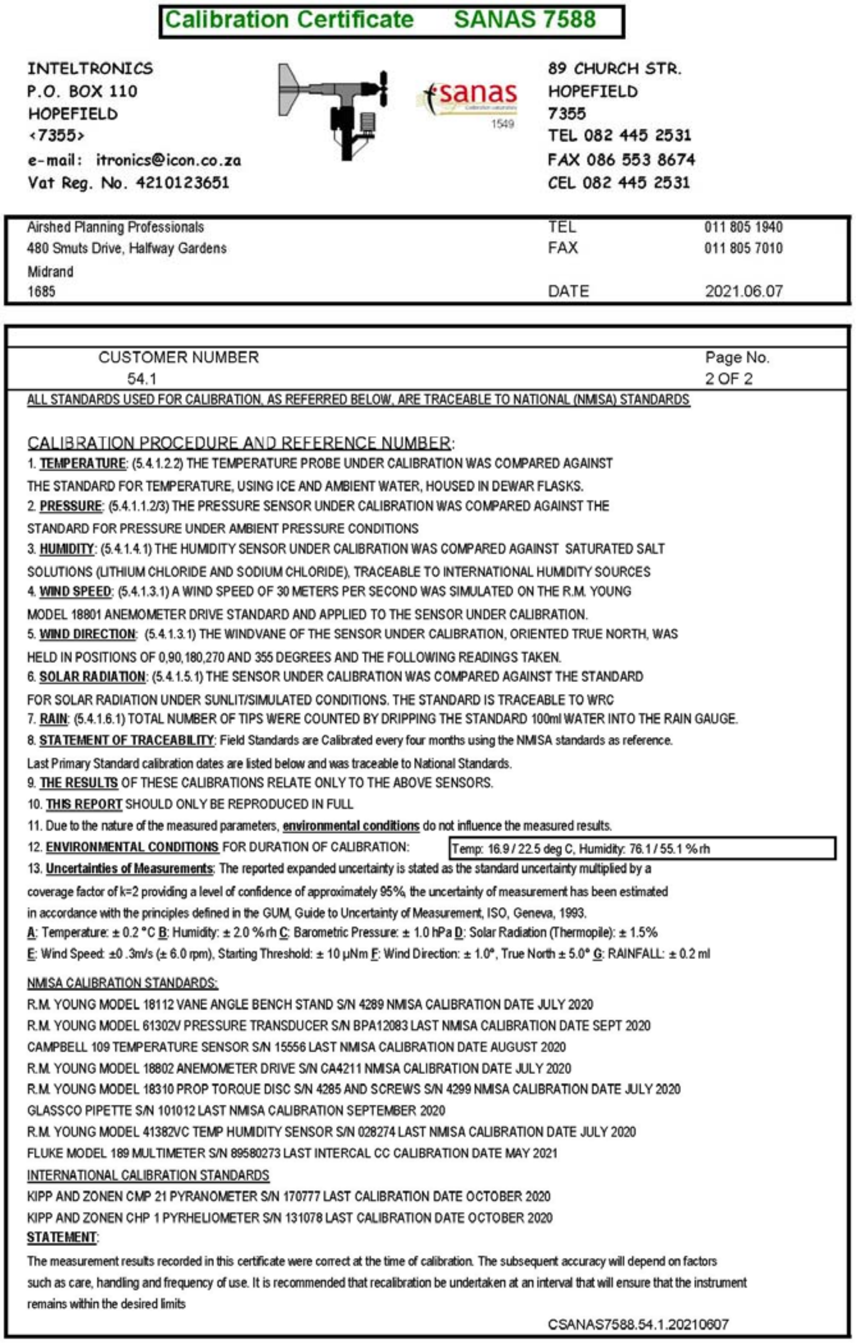

Calibration Certificate SANAS 7588

INTELTRONICS
P.O. BOX 110
HOPEFIELD
<7355>
e-mail: itronics@icon.co.za
Vat Reg. No. 4210123651

sanas
1549

89 CHURCH STR.
HOPEFIELD
7355
TEL 082 445 2531
FAX 086 553 8674
CEL 082 445 2531

Airshed Planning Professionals	TEL	011 805 1940
480 Smuts Drive, Halfway Gardens	FAX	011 805 7010
Midrand		
1685	DATE	2021.06.07

CUSTOMER NUMBER 54.1	Page No. 2 OF 2

ALL STANDARDS USED FOR CALIBRATION, AS REFERRED BELOW, ARE TRACEABLE TO NATIONAL (NMISA) STANDARDS

CALIBRATION PROCEDURE AND REFERENCE NUMBER:

1. **TEMPERATURE**: (5.4.1.2.2) THE TEMPERATURE PROBE UNDER CALIBRATION WAS COMPARED AGAINST THE STANDARD FOR TEMPERATURE, USING ICE AND AMBIENT WATER, HOUSED IN DEWAR FLASKS.
2. **PRESSURE**: (5.4.1.1.2/3) THE PRESSURE SENSOR UNDER CALIBRATION WAS COMPARED AGAINST THE STANDARD FOR PRESSURE UNDER AMBIENT PRESSURE CONDITIONS
3. **HUMIDITY**: (5.4.1.4.1) THE HUMIDITY SENSOR UNDER CALIBRATION WAS COMPARED AGAINST SATURATED SALT SOLUTIONS (LITHIUM CHLORIDE AND SODIUM CHLORIDE), TRACEABLE TO INTERNATIONAL HUMIDITY SOURCES
4. **WIND SPEED**: (5.4.1.3.1) A WIND SPEED OF 30 METERS PER SECOND WAS SIMULATED ON THE R.M. YOUNG MODEL 18801 ANEMOMETER DRIVE STANDARD AND APPLIED TO THE SENSOR UNDER CALIBRATION.
5. **WIND DIRECTION**: (5.4.1.3.1) THE WINDVANE OF THE SENSOR UNDER CALIBRATION, ORIENTED TRUE NORTH, WAS HELD IN POSITIONS OF 0,90,180,270 AND 355 DEGREES AND THE FOLLOWING READINGS TAKEN.
6. **SOLAR RADIATION**: (5.4.1.5.1) THE SENSOR UNDER CALIBRATION WAS COMPARED AGAINST THE STANDARD FOR SOLAR RADIATION UNDER SUNLIT/SIMULATED CONDITIONS. THE STANDARD IS TRACEABLE TO WRC
7. **RAIN**: (5.4.1.6.1) TOTAL NUMBER OF TIPS WERE COUNTED BY DRIPPING THE STANDARD 100ml WATER INTO THE RAIN GAUGE.
8. **STATEMENT OF TRACEABILITY**: Field Standards are Calibrated every four months using the NMISA standards as reference. Last Primary Standard calibration dates are listed below and was traceable to National Standards.
9. **THE RESULTS** OF THESE CALIBRATIONS RELATE ONLY TO THE ABOVE SENSORS.
10. **THIS REPORT** SHOULD ONLY BE REPRODUCED IN FULL
11. Due to the nature of the measured parameters, **environmental conditions** do not influence the measured results.
12. **ENVIRONMENTAL CONDITIONS** FOR DURATION OF CALIBRATION: Temp: 16.9 / 22.5 deg C, Humidity: 76.1 / 55.1 %rh
13. **Uncertainties of Measurements**: The reported expanded uncertainty is stated as the standard uncertainty multiplied by a coverage factor of k=2 providing a level of confidence of approximately 95%, the uncertainty of measurement has been estimated in accordance with the principles defined in the GUM, Guide to Uncertainty of Measurement, ISO, Geneva, 1993.

A: Temperature: ± 0.2 °C B: Humidity: ± 2.0 %rh C: Barometric Pressure: ± 1.0 hPa D: Solar Radiation (Thermopile): ± 1.5%
E: Wind Speed: ±0 .3m/s (± 6.0 rpm), Starting Threshold: ± 10 µNm F: Wind Direction: ± 1.0°, True North ± 5.0° G: RAINFALL: ± 0.2 ml

NMISA CALIBRATION STANDARDS:
R.M. YOUNG MODEL 18112 VANE ANGLE BENCH STAND S/N 4289 NMISA CALIBRATION DATE JULY 2020
R.M. YOUNG MODEL 61302V PRESSURE TRANSDUCER S/N BPA12083 LAST NMISA CALIBRATION DATE SEPT 2020
CAMPBELL 109 TEMPERATURE SENSOR S/N 15556 LAST NMISA CALIBRATION DATE AUGUST 2020
R.M. YOUNG MODEL 18802 ANEMOMETER DRIVE S/N CA4211 NMISA CALIBRATION DATE JULY 2020
R.M. YOUNG MODEL 18310 PROP TORQUE DISC S/N 4285 AND SCREWS S/N 4299 NMISA CALIBRATION DATE JULY 2020
GLASSCO PIPETTE S/N 101012 LAST NMISA CALIBRATION SEPTEMBER 2020
R.M. YOUNG MODEL 41382VC TEMP HUMIDITY SENSOR S/N 028274 LAST NMISA CALIBRATION DATE JULY 2020
FLUKE MODEL 189 MULTIMETER S/N 89580273 LAST INTERCAL CC CALIBRATION DATE MAY 2021

INTERNATIONAL CALIBRATION STANDARDS
KIPP AND ZONEN CMP 21 PYRANOMETER S/N 170777 LAST CALIBRATION DATE OCTOBER 2020
KIPP AND ZONEN CHP 1 PYRHELIOMETER S/N 131078 LAST CALIBRATION DATE OCTOBER 2020

STATEMENT:

The measurement results recorded in this certificate were correct at the time of calibration. The subsequent accuracy will depend on factors such as care, handling and frequency of use. It is recommended that recalibration be undertaken at an interval that will ensure that the instrument remains within the desired limits

CSANAS7588.54.1.20210607

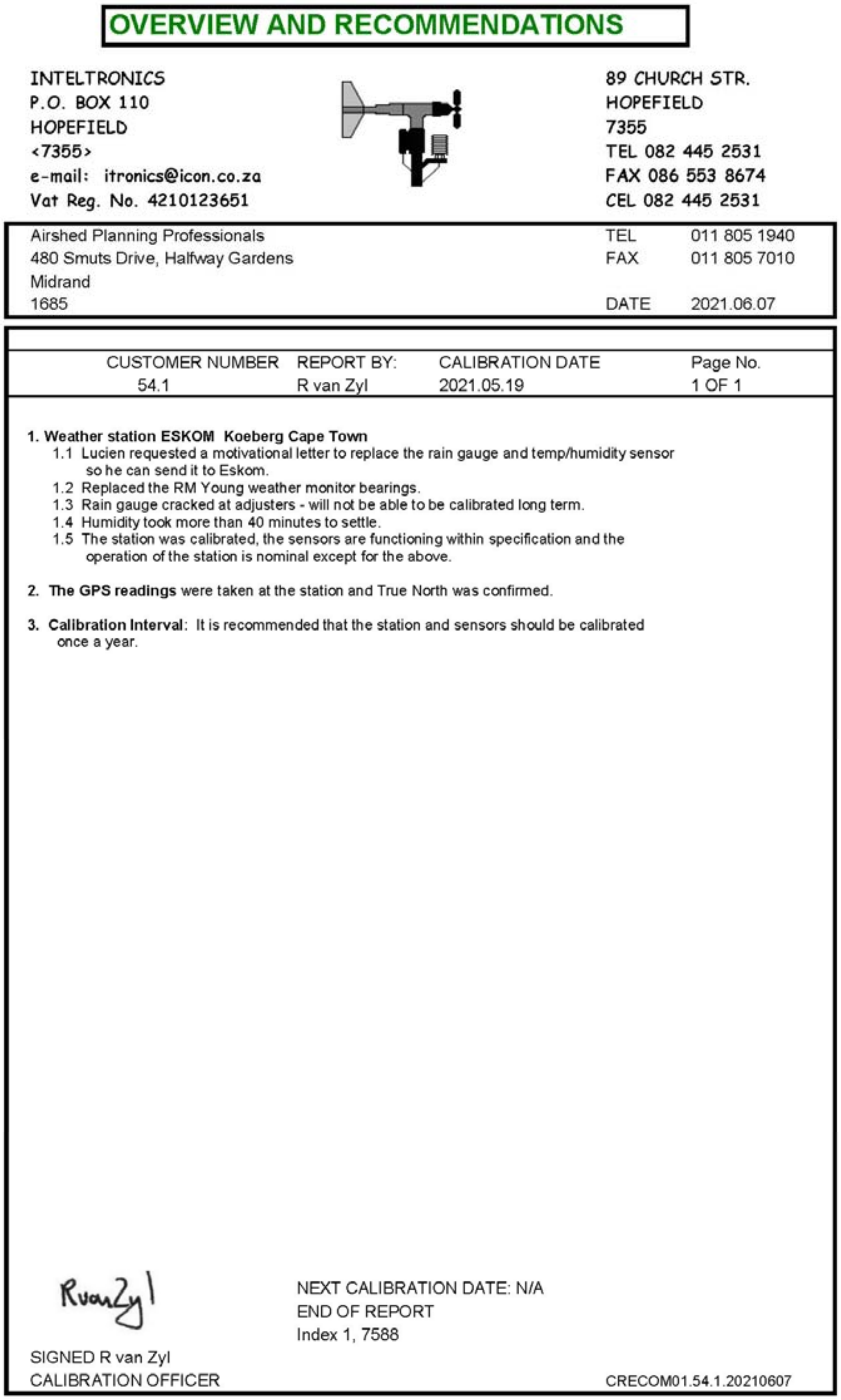

OVERVIEW AND RECOMMENDATIONS

INTELTRONICS
P.O. BOX 110
HOPEFIELD
<7355>
e-mail: itronics@icon.co.za
Vat Reg. No. 4210123651

89 CHURCH STR.
HOPEFIELD
7355
TEL 082 445 2531
FAX 086 553 8674
CEL 082 445 2531

Airshed Planning Professionals
480 Smuts Drive, Halfway Gardens
Midrand
1685

TEL 011 805 1940
FAX 011 805 7010
DATE 2021.06.07

CUSTOMER NUMBER	REPORT BY:	CALIBRATION DATE	Page No.
54.1	R van Zyl	2021.05.19	1 OF 1

1. **Weather station ESKOM Koeberg Cape Town**
    - 1.1 Lucien requested a motivational letter to replace the rain gauge and temp/humidity sensor so he can send it to Eskom.
    - 1.2 Replaced the RM Young weather monitor bearings.
    - 1.3 Rain gauge cracked at adjusters - will not be able to be calibrated long term.
    - 1.4 Humidity took more than 40 minutes to settle.
    - 1.5 The station was calibrated, the sensors are functioning within specification and the operation of the station is nominal except for the above.

2. **The GPS readings** were taken at the station and True North was confirmed.

3. **Calibration Interval**: It is recommended that the station and sensors should be calibrated once a year.

RvanZyl

SIGNED R van Zyl
CALIBRATION OFFICER

NEXT CALIBRATION DATE: N/A
END OF REPORT
Index 1, 7588

CRECOM01.54.1.20210607

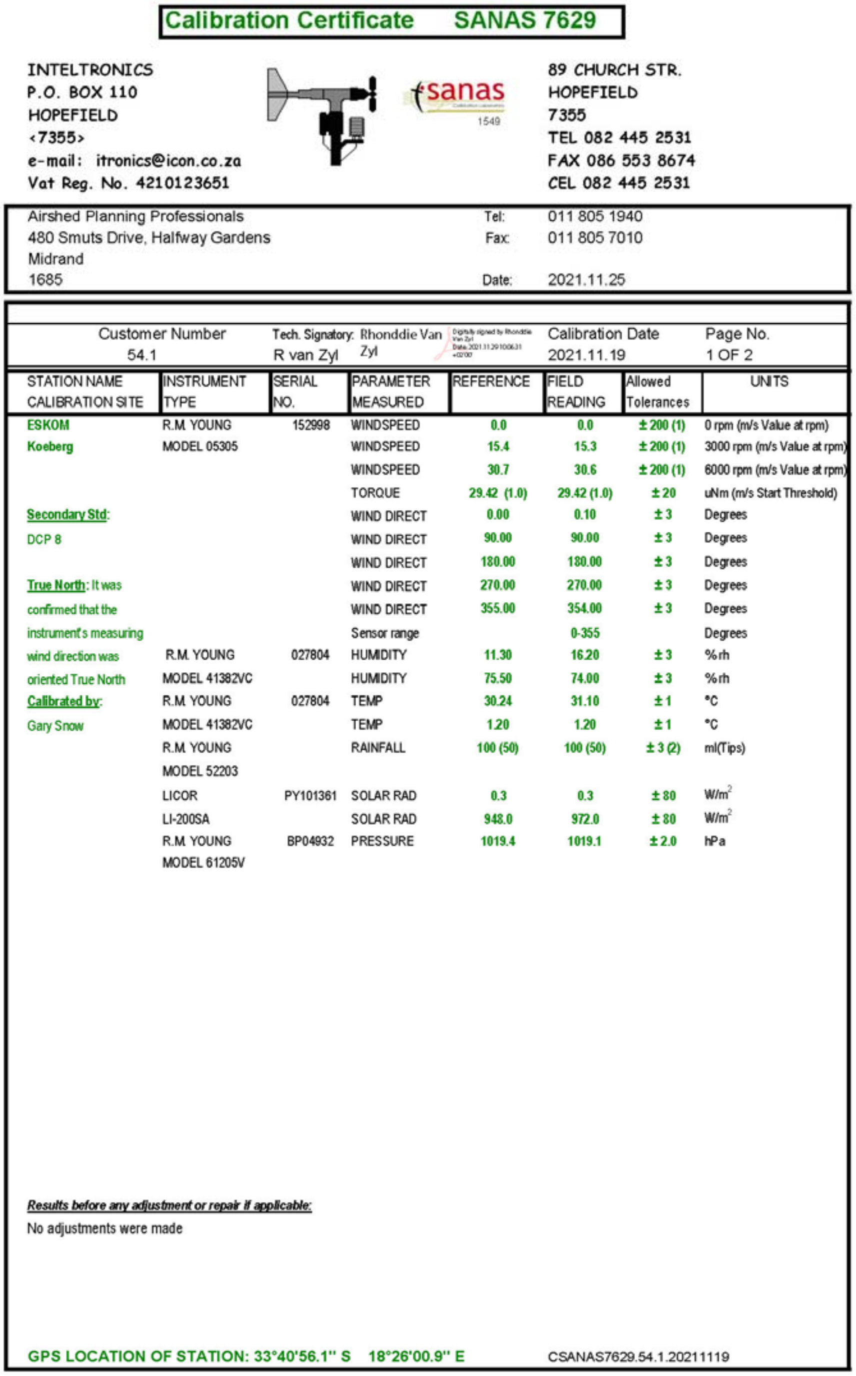

Calibration Certificate SANAS 7629

INTELTRONICS
P.O. BOX 110
HOPEFIELD
<7355>
e-mail: itronics@icon.co.za
Vat Reg. No. 4210123651

sanas
1549

89 CHURCH STR.
HOPEFIELD
7355
TEL 082 445 2531
FAX 086 553 8674
CEL 082 445 2531

Airshed Planning Professionals
480 Smuts Drive, Halfway Gardens
Midrand
1685

Tel: 011 805 1940
Fax: 011 805 7010
Date: 2021.11.25

Customer Number	Tech. Signatory:	Calibration Date	Page No.
54.1	R van Zyl Rhonddie Van Zyl Digitally signed by Rhonddie Van Zyl Date: 2021.11.29 10:06:31 +02'00'	2021.11.19	1 OF 2

STATION NAME CALIBRATION SITE	INSTRUMENT TYPE	SERIAL NO.	PARAMETER MEASURED	REFERENCE	FIELD READING	Allowed Tolerances	UNITS
ESKOM	R.M. YOUNG	152998	WINDSPEED	0.0	0.0	± 200 (1)	0 rpm (m/s Value at rpm)
Koeberg	MODEL 05305		WINDSPEED	15.4	15.3	± 200 (1)	3000 rpm (m/s Value at rpm)
			WINDSPEED	30.7	30.6	± 200 (1)	6000 rpm (m/s Value at rpm)
			TORQUE	29.42 (1.0)	29.42 (1.0)	± 20	uNm (m/s Start Threshold)
Secondary Std:			WIND DIRECT	0.00	0.10	± 3	Degrees
DCP 8			WIND DIRECT	90.00	90.00	± 3	Degrees
			WIND DIRECT	180.00	180.00	± 3	Degrees
True North: It was			WIND DIRECT	270.00	270.00	± 3	Degrees
confirmed that the			WIND DIRECT	355.00	354.00	± 3	Degrees
instrument's measuring			Sensor range		0-355		Degrees
wind direction was	R.M. YOUNG	027804	HUMIDITY	11.30	16.20	± 3	%rh
oriented True North	MODEL 41382VC		HUMIDITY	75.50	74.00	± 3	%rh
Calibrated by:	R.M. YOUNG	027804	TEMP	30.24	31.10	± 1	°C
Gary Snow	MODEL 41382VC		TEMP	1.20	1.20	± 1	°C
	R.M. YOUNG		RAINFALL	100 (50)	100 (50)	± 3 (2)	ml(Tips)
	MODEL 52203						
	LICOR	PY101361	SOLAR RAD	0.3	0.3	± 80	W/m^2
	LI-200SA		SOLAR RAD	948.0	972.0	± 80	W/m^2
	R.M. YOUNG	BP04932	PRESSURE	1019.4	1019.1	± 2.0	hPa
	MODEL 61205V						

Results before any adjustment or repair if applicable:

No adjustments were made

GPS LOCATION OF STATION: 33°40'56.1'' S 18°26'00.9'' E

CSANAS7629.54.1.20211119

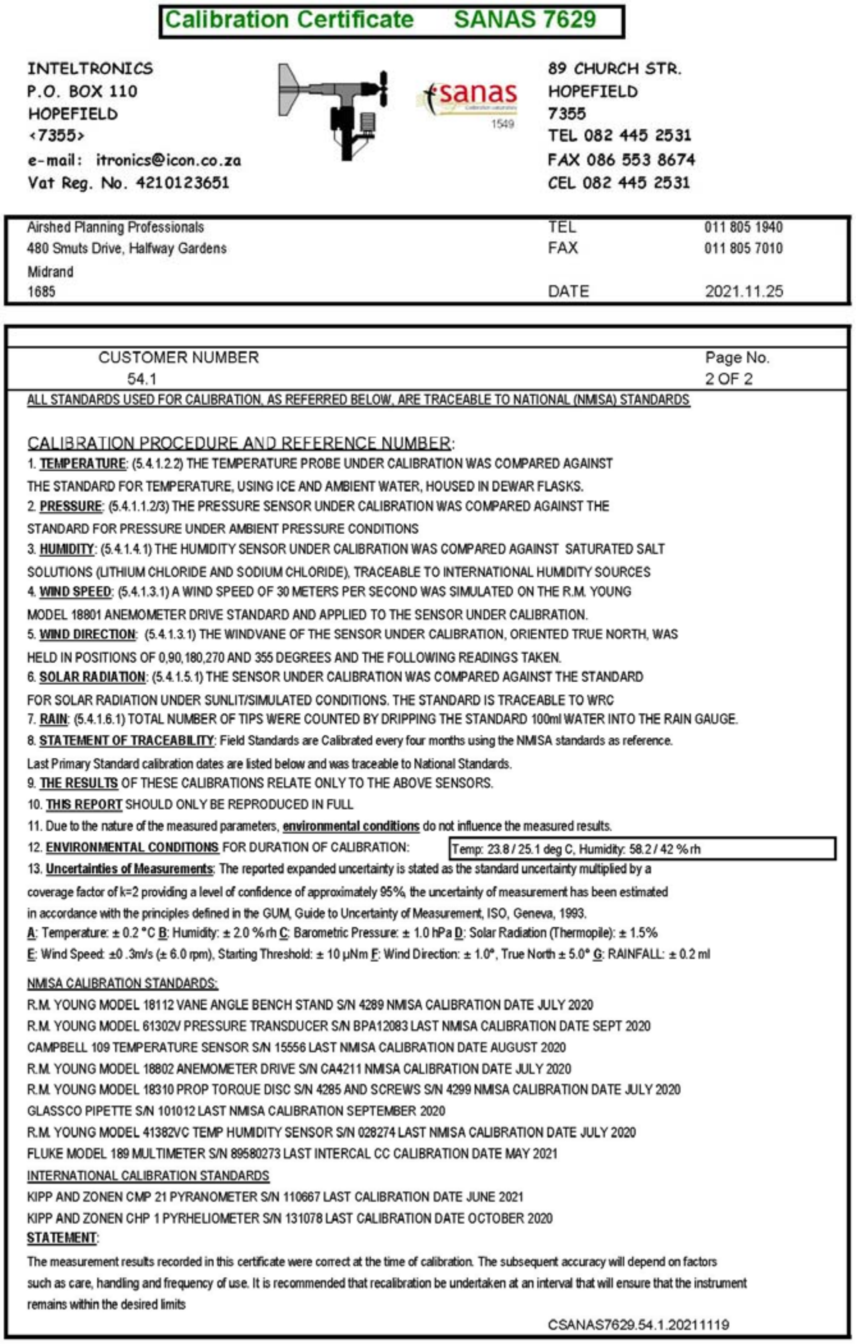

Calibration Certificate SANAS 7629

INTELTRONICS
P.O. BOX 110
HOPEFIELD
<7355>
e-mail: itronics@icon.co.za
Vat Reg. No. 4210123651

sanas
1549

89 CHURCH STR.
HOPEFIELD
7355
TEL 082 445 2531
FAX 086 553 8674
CEL 082 445 2531

Airshed Planning Professionals
480 Smuts Drive, Halfway Gardens
Midrand
1685

TEL 011 805 1940
FAX 011 805 7010
DATE 2021.11.25

CUSTOMER NUMBER	Page No.
54.1	2 OF 2

ALL STANDARDS USED FOR CALIBRATION, AS REFERRED BELOW, ARE TRACEABLE TO NATIONAL (NMISA) STANDARDS

CALIBRATION PROCEDURE AND REFERENCE NUMBER:

1. **TEMPERATURE**: (5.4.1.2.2) THE TEMPERATURE PROBE UNDER CALIBRATION WAS COMPARED AGAINST THE STANDARD FOR TEMPERATURE, USING ICE AND AMBIENT WATER, HOUSED IN DEWAR FLASKS.
2. **PRESSURE**: (5.4.1.1.2/3) THE PRESSURE SENSOR UNDER CALIBRATION WAS COMPARED AGAINST THE STANDARD FOR PRESSURE UNDER AMBIENT PRESSURE CONDITIONS
3. **HUMIDITY**: (5.4.1.4.1) THE HUMIDITY SENSOR UNDER CALIBRATION WAS COMPARED AGAINST SATURATED SALT SOLUTIONS (LITHIUM CHLORIDE AND SODIUM CHLORIDE), TRACEABLE TO INTERNATIONAL HUMIDITY SOURCES
4. **WIND SPEED**: (5.4.1.3.1) A WIND SPEED OF 30 METERS PER SECOND WAS SIMULATED ON THE R.M. YOUNG MODEL 18801 ANEMOMETER DRIVE STANDARD AND APPLIED TO THE SENSOR UNDER CALIBRATION.
5. **WIND DIRECTION**: (5.4.1.3.1) THE WINDVANE OF THE SENSOR UNDER CALIBRATION, ORIENTED TRUE NORTH, WAS HELD IN POSITIONS OF 0,90,180,270 AND 355 DEGREES AND THE FOLLOWING READINGS TAKEN.
6. **SOLAR RADIATION**: (5.4.1.5.1) THE SENSOR UNDER CALIBRATION WAS COMPARED AGAINST THE STANDARD FOR SOLAR RADIATION UNDER SUNLIT/SIMULATED CONDITIONS. THE STANDARD IS TRACEABLE TO WRC
7. **RAIN**: (5.4.1.6.1) TOTAL NUMBER OF TIPS WERE COUNTED BY DRIPPING THE STANDARD 100ml WATER INTO THE RAIN GAUGE.
8. **STATEMENT OF TRACEABILITY**: Field Standards are Calibrated every four months using the NMISA standards as reference. Last Primary Standard calibration dates are listed below and was traceable to National Standards.
9. **THE RESULTS** OF THESE CALIBRATIONS RELATE ONLY TO THE ABOVE SENSORS.
10. **THIS REPORT** SHOULD ONLY BE REPRODUCED IN FULL
11. Due to the nature of the measured parameters, **environmental conditions** do not influence the measured results.
12. **ENVIRONMENTAL CONDITIONS** FOR DURATION OF CALIBRATION: Temp: 23.8 / 25.1 deg C, Humidity: 58.2 / 42 % rh
13. **Uncertainties of Measurements**: The reported expanded uncertainty is stated as the standard uncertainty multiplied by a coverage factor of k=2 providing a level of confidence of approximately 95%, the uncertainty of measurement has been estimated in accordance with the principles defined in the GUM, Guide to Uncertainty of Measurement, ISO, Geneva, 1993.

A: Temperature: ± 0.2 °C B: Humidity: ± 2.0 % rh C: Barometric Pressure: ± 1.0 hPa D: Solar Radiation (Thermopile): ± 1.5%
E: Wind Speed: ±0 .3m/s (± 6.0 rpm), Starting Threshold: ± 10 μNm F: Wind Direction: ± 1.0°, True North ± 5.0° G: RAINFALL: ± 0.2 ml

NMISA CALIBRATION STANDARDS:

R.M. YOUNG MODEL 18112 VANE ANGLE BENCH STAND S/N 4289 NMISA CALIBRATION DATE JULY 2020
R.M. YOUNG MODEL 61302V PRESSURE TRANSDUCER S/N BPA12083 LAST NMISA CALIBRATION DATE SEPT 2020
CAMPBELL 109 TEMPERATURE SENSOR S/N 15556 LAST NMISA CALIBRATION DATE AUGUST 2020
R.M. YOUNG MODEL 18802 ANEMOMETER DRIVE S/N CA4211 NMISA CALIBRATION DATE JULY 2020
R.M. YOUNG MODEL 18310 PROP TORQUE DISC S/N 4285 AND SCREWS S/N 4299 NMISA CALIBRATION DATE JULY 2020
GLASSCO PIPETTE S/N 101012 LAST NMISA CALIBRATION SEPTEMBER 2020
R.M. YOUNG MODEL 41382VC TEMP HUMIDITY SENSOR S/N 028274 LAST NMISA CALIBRATION DATE JULY 2020
FLUKE MODEL 189 MULTIMETER S/N 89580273 LAST INTERCAL CC CALIBRATION DATE MAY 2021

INTERNATIONAL CALIBRATION STANDARDS

KIPP AND ZONEN CMP 21 PYRANOMETER S/N 110667 LAST CALIBRATION DATE JUNE 2021
KIPP AND ZONEN CHP 1 PYRHELIOMETER S/N 131078 LAST CALIBRATION DATE OCTOBER 2020

STATEMENT:

The measurement results recorded in this certificate were correct at the time of calibration. The subsequent accuracy will depend on factors such as care, handling and frequency of use. It is recommended that recalibration be undertaken at an interval that will ensure that the instrument remains within the desired limits

CSANAS7629.54.1.20211119

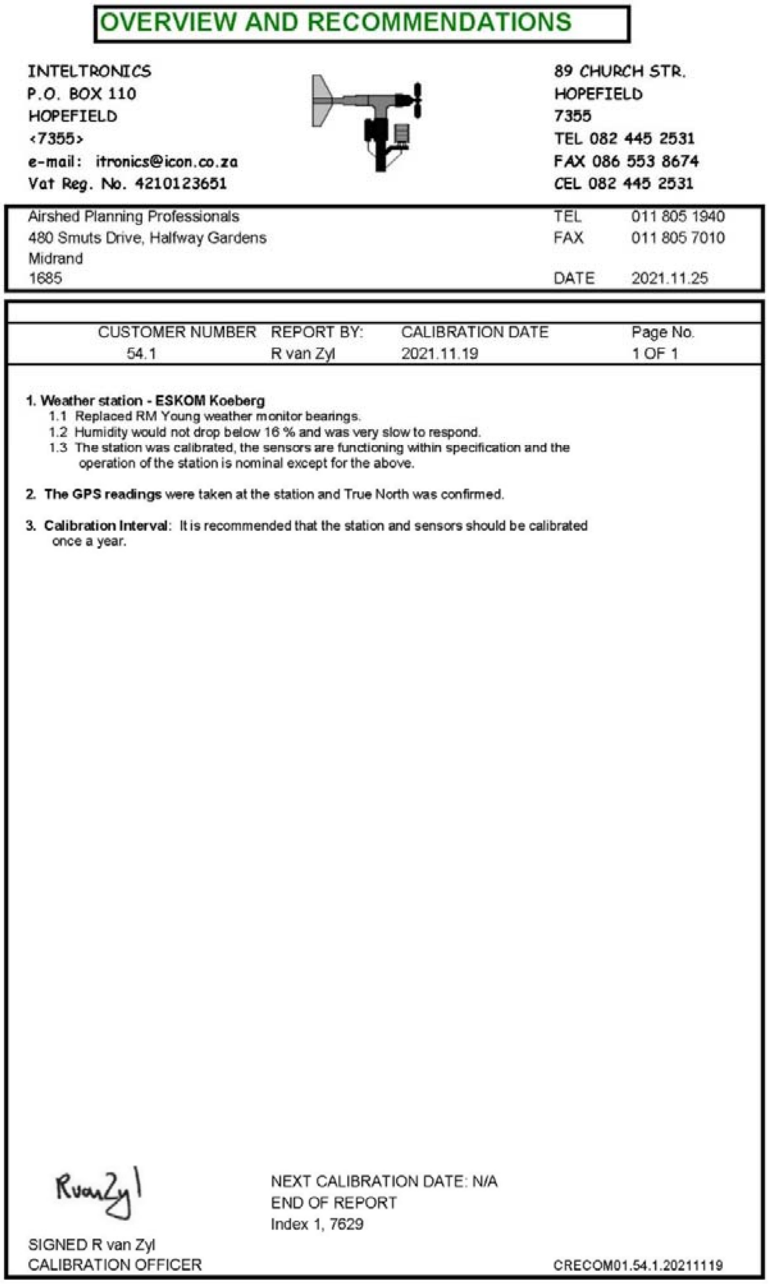

OVERVIEW AND RECOMMENDATIONS

INTELTRONICS
P.O. BOX 110
HOPEFIELD
<7355>
e-mail: itronics@icon.co.za
Vat Reg. No. 4210123651

89 CHURCH STR.
HOPEFIELD
7355
TEL 082 445 2531
FAX 086 553 8674
CEL 082 445 2531

Airshed Planning Professionals
480 Smuts Drive, Halfway Gardens
Midrand
1685

TEL 011 805 1940
FAX 011 805 7010
DATE 2021.11.25

CUSTOMER NUMBER	REPORT BY:	CALIBRATION DATE	Page No.
54.1	R van Zyl	2021.11.19	1 OF 1

1. **Weather station - ESKOM Koeberg**
   1.1 Replaced RM Young weather monitor bearings.
   1.2 Humidity would not drop below 16 % and was very slow to respond.
   1.3 The station was calibrated, the sensors are functioning within specification and the operation of the station is nominal except for the above.
2. **The GPS readings** were taken at the station and True North was confirmed.
3. **Calibration Interval**: It is recommended that the station and sensors should be calibrated once a year.

RvanZyl

SIGNED R van Zyl
CALIBRATION OFFICER

NEXT CALIBRATION DATE: N/A
END OF REPORT
Index 1, 7629

CRECOM01.54.1.20211119

Appendix 5.8.G: Data Collection and Validation Procedure

Meteorological monitoring data from the automatic weather station at the site are downloaded on a two-weekly basis (or more frequently). This is done remotely with communication via Campbell Scientific Inc Loggernet Software. A cell phone connection allows data retrieval with password protection. Once the site is selected in the software, the telecommunication connection is made and the data are downloaded from the CR1000 Logger. The user may decide to download all or only since the previous download placeholder.

The raw data are copied into a living Excel Spreadsheet (‘Met Table (Duynefontein).xls’. The original data text files are kept separately. The data are also duplicated in a similarly living ‘validated’ Excel Spreadsheet (‘Met Table (Duynefontein) Validated.xls’ in which a number of data screening tests are done and recorded.

All the meteorological parameters in the ‘validated’ worksheet are screened, averaged and stored as hourly average parameters according to the criteria given in ***Table 5.8.G.1***. Data values that fail the Range Test, are replaced by a missing parameter (‘-9999’) placeholder. Each occurrence of a Data Change Test 1 and Data Change Test 2, is manually inspected to see whether an instrument failure occurred; if found to be the case, the value is replaced by the missing parameter ‘-9999’.

Specific care is taken in rainfall measurements. Originally these measurements were found to observe spurious readings at high wind speeds, i.e. above 9.4 m/s. This was particularly prevalent when the rain gauges were fixed to the 10-metre mast. The rain gauges were subsequently isolated from the mast. Although the interference no longer appears to occur, a check is nevertheless made to see that when rainfall occurs with a relative humidity below 70%, that the wind speed is not above 9 m/s. If this is the situation, the rainfall data are replaced by the missing parameter. The original recordings, the test results and the final, manually changed data are all kept in the ‘validated’ spreadsheets for reference.

Data values recorded during the bi-annual calibration tests are also removed and replaced with the missing parameter ‘-9999’. This is noted in the ‘validated’ spreadsheets.

Only the hourly averaged data are provided to the SSR project team. This is generally done every third month. The data are accompanied by the Meteorological Data Checking and Approval Certificate (***Table 5.8.G.2***).

Table 5.8.G.1
Recorded Meteorological Data Screening Parameters

Parameter	Range Test				Data Change Test 1				Data Change Test 2			
	Instrument Minimum	**Instrument Maximum**	**Local Minimum**	**Local Maximum**	**Minimum or Maximum Change**	**Delta Value**	**Duration**	**Time Unit**	**Minimum or Maximum Change**	**Delta Value**	**Duration**	**Time Unit**
Wind Speed (m/s)	0	60	0	45	Minimum	0.1	6	hours	Minimum	0.5	24	hours
Wind Direction (°)	0	360	0	360	Minimum	0.1	3	hours	Minimum	2	24	hours
Dry Bulb Temperature (°C)	-50	50	-1	41	Maximum	5	2	hours	Minimum	0.2	12	hours
Relative Humidity *%)	0	100	10	100	Minimum	0.1	18	hours	Minimum	1	36	hours
Solar Radiation (W/m^2)	0	1400	0	1300	Minimum	10	12	hours	Minimum	100	12	hours
Barometric Pressure (hPa)	900	1100	960	1060	Maximum	6	3	hours	Minimum	1	48	hours
Rainfall (mm)	0	50	0	50	Maximum	50	2	hours	Minimum	0.1	1	month

Table 5.8.G.2

Meteorological Data Checking and Approval Certificate

METEOROLOGICAL DATA CHECKING AND APPROVAL CERTIFICATE					
Project: *Nuclear-1 Site Safety Reports – Onsite Meteorological Data*				**Reference:** *10/005*	
Item #	**Reference and Description**		**Prepared by (Name)**	**Checked/Verified (Signature and Date)**	**Approved for Use (Signature and Date)**
	Data Reference	**Title**			
1	*Met data (Duynefontein & Bantamsklip) 3 October 2010.xls*	*Duynefontein Onsite Hourly Average Validated Meteorological Data*	*L Burger*		
2	*Met data (Duynefontein & Bantamsklip) 3 October 2010.xls*	*Bantamsklip Onsite Hourly Average Validated Meteorological Data*	*L Burger*		

Appendix 5.8.H: Particle Size Distribution

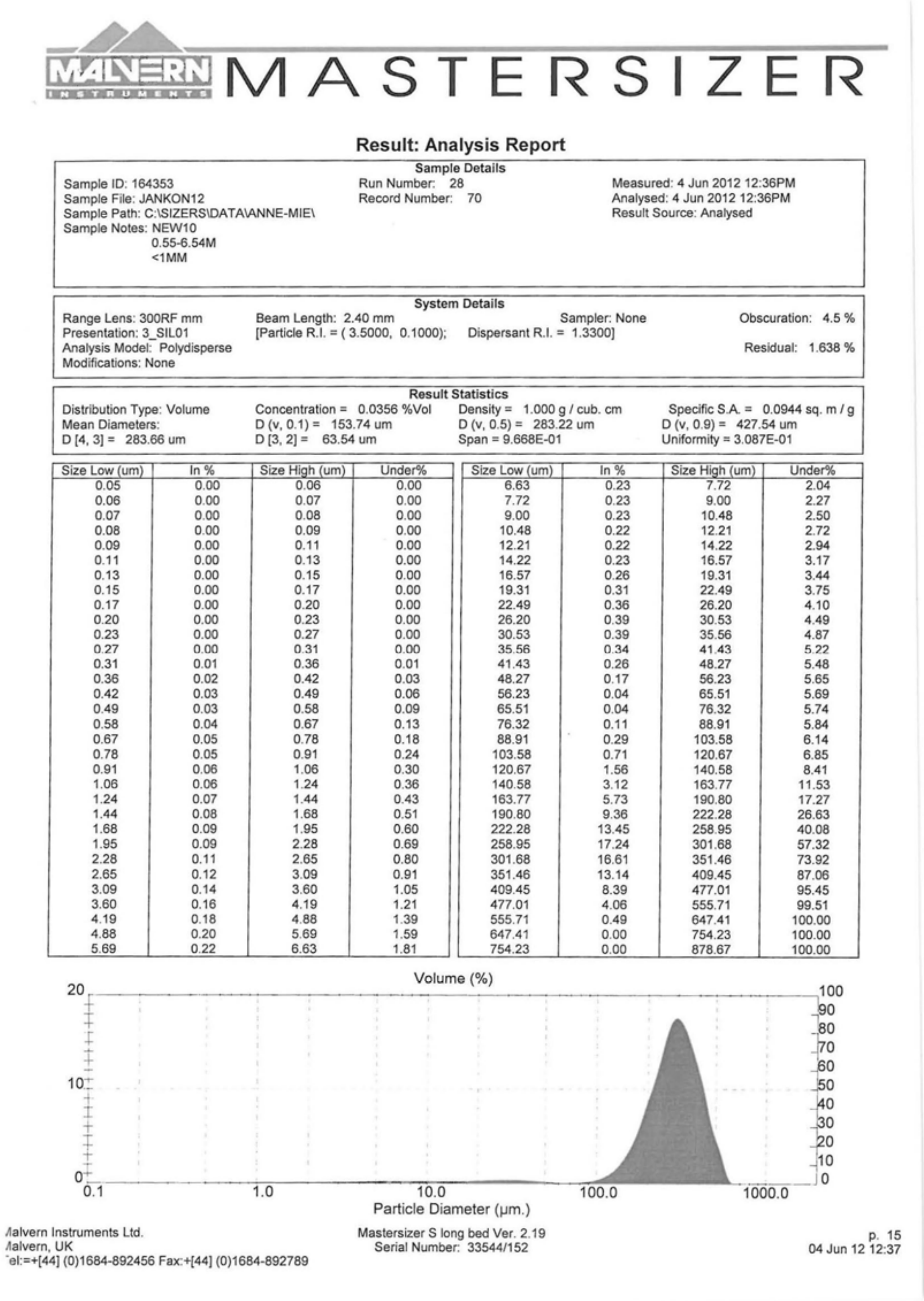

MALVERN INSTRUMENTS MASTERSIZER

Result: Analysis Report

Sample Details

Sample ID: 164353
Sample File: JANKON12
Sample Path: C:\SIZERS\DATA\ANNE-MIE\
Sample Notes: NEW10
0.55-6.54M
<1MM

Run Number: 28
Record Number: 70

Measured: 4 Jun 2012 12:36PM
Analysed: 4 Jun 2012 12:36PM
Result Source: Analysed

System Details

Range Lens: 300RF mm
Presentation: 3_SIL01
Analysis Model: Polydisperse
Modifications: None

Beam Length: 2.40 mm
[Particle R.I. = (3.5000, 0.1000); Dispersant R.I. = 1.3300]

Sampler: None

Obscuration: 4.5 %
Residual: 1.638 %

Result Statistics

Distribution Type: Volume
Mean Diameters:
D [4, 3] = 283.66 um

Concentration = 0.0356 %Vol
D (v, 0.1) = 153.74 um
D [3, 2] = 63.54 um

Density = 1.000 g / cub. cm
D (v, 0.5) = 283.22 um
Span = 9.668E-01

Specific S.A. = 0.0944 sq. m / g
D (v, 0.9) = 427.54 um
Uniformity = 3.087E-01

Size Low (um)	In %	Size High (um)	Under%	Size Low (um)	In %	Size High (um)	Under%
0.05	0.00	0.06	0.00	6.63	0.23	7.72	2.04
0.06	0.00	0.07	0.00	7.72	0.23	9.00	2.27
0.07	0.00	0.08	0.00	9.00	0.23	10.48	2.50
0.08	0.00	0.09	0.00	10.48	0.22	12.21	2.72
0.09	0.00	0.11	0.00	12.21	0.22	14.22	2.94
0.11	0.00	0.13	0.00	14.22	0.23	16.57	3.17
0.13	0.00	0.15	0.00	16.57	0.26	19.31	3.44
0.15	0.00	0.17	0.00	19.31	0.31	22.49	3.75
0.17	0.00	0.20	0.00	22.49	0.36	26.20	4.10
0.20	0.00	0.23	0.00	26.20	0.39	30.53	4.49
0.23	0.00	0.27	0.00	30.53	0.39	35.56	4.87
0.27	0.00	0.31	0.00	35.56	0.34	41.43	5.22
0.31	0.01	0.36	0.01	41.43	0.26	48.27	5.48
0.36	0.02	0.42	0.03	48.27	0.17	56.23	5.65
0.42	0.03	0.49	0.06	56.23	0.04	65.51	5.69
0.49	0.03	0.58	0.09	65.51	0.04	76.32	5.74
0.58	0.04	0.67	0.13	76.32	0.11	88.91	5.84
0.67	0.05	0.78	0.18	88.91	0.29	103.58	6.14
0.78	0.05	0.91	0.24	103.58	0.71	120.67	6.85
0.91	0.06	1.06	0.30	120.67	1.56	140.58	8.41
1.06	0.06	1.24	0.36	140.58	3.12	163.77	11.53
1.24	0.07	1.44	0.43	163.77	5.73	190.80	17.27
1.44	0.08	1.68	0.51	190.80	9.36	222.28	26.63
1.68	0.09	1.95	0.60	222.28	13.45	258.95	40.08
1.95	0.09	2.28	0.69	258.95	17.24	301.68	57.32
2.28	0.11	2.65	0.80	301.68	16.61	351.46	73.92
2.65	0.12	3.09	0.91	351.46	13.14	409.45	87.06
3.09	0.14	3.60	1.05	409.45	8.39	477.01	95.45
3.60	0.16	4.19	1.21	477.01	4.06	555.71	99.51
4.19	0.18	4.88	1.39	555.71	0.49	647.41	100.00
4.88	0.20	5.69	1.59	647.41	0.00	754.23	100.00
5.69	0.22	6.63	1.81	754.23	0.00	878.67	100.00

alvern Instruments Ltd.
alvern, UK
el:=+[44] (0)1684-892456 Fax:+[44] (0)1684-892789

Mastersizer S long bed Ver. 2.19
Serial Number: 33544/152

p. 15
04 Jun 12 12:37

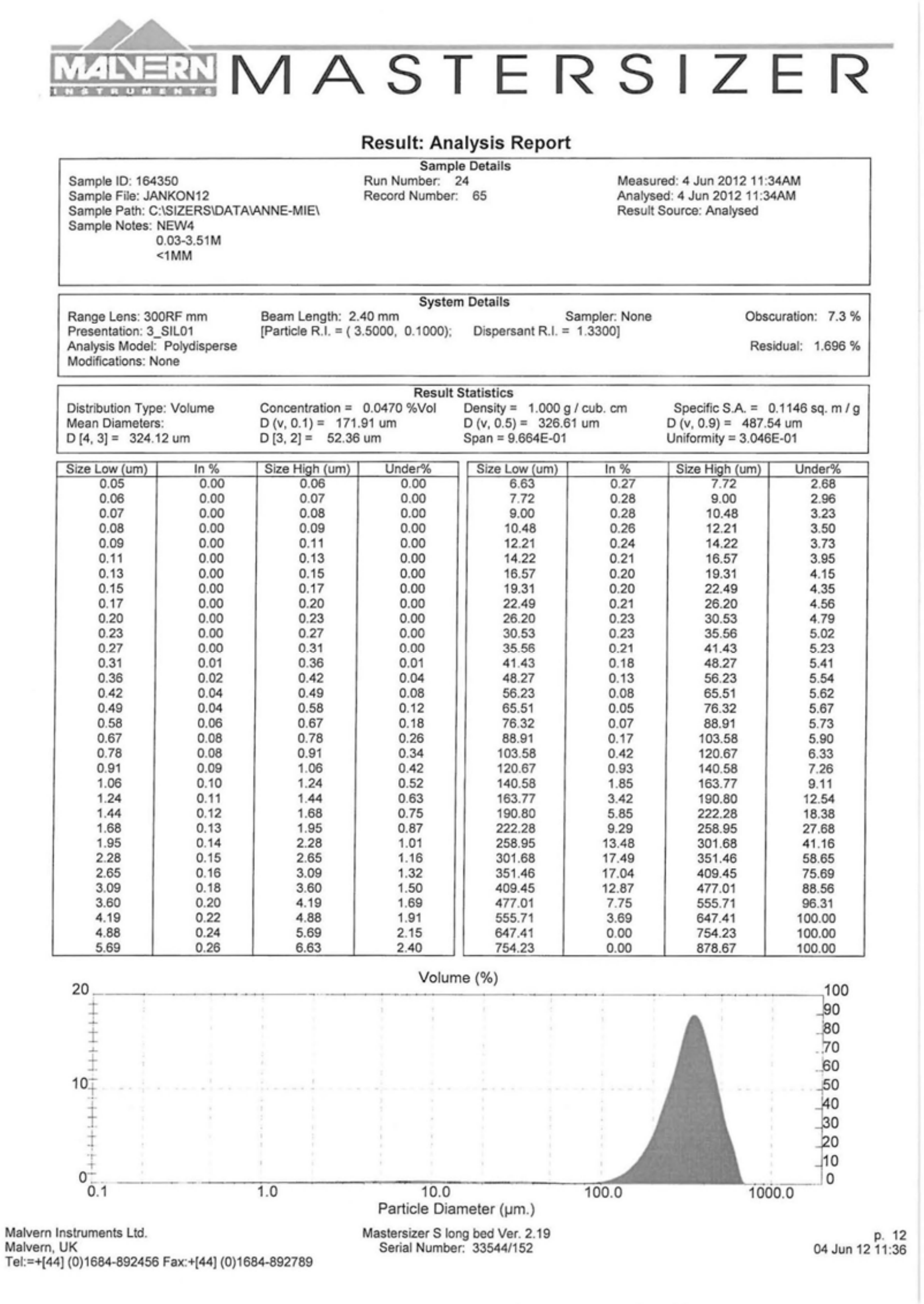

MALVERN INSTRUMENTS MASTERSIZER

Result: Analysis Report

Sample Details

Sample ID: 164350
Sample File: JANKON12
Sample Path: C:\SIZERS\DATA\ANNE-MIE\
Sample Notes: NEW4
0.03-3.51M
<1MM

Run Number: 24
Record Number: 65

Measured: 4 Jun 2012 11:34AM
Analysed: 4 Jun 2012 11:34AM
Result Source: Analysed

System Details

Range Lens: 300RF mm
Presentation: 3_SIL01
Analysis Model: Polydisperse
Modifications: None

Beam Length: 2.40 mm
[Particle R.I. = (3.5000, 0.1000); Dispersant R.I. = 1.3300]

Sampler: None

Obscuration: 7.3 %
Residual: 1.696 %

Result Statistics

Distribution Type: Volume
Mean Diameters:
D [4, 3] = 324.12 um

Concentration = 0.0470 %Vol
D (v, 0.1) = 171.91 um
D [3, 2] = 52.36 um

Density = 1.000 g / cub. cm
D (v, 0.5) = 326.61 um
Span = 9.664E-01

Specific S.A. = 0.1146 sq. m / g
D (v, 0.9) = 487.54 um
Uniformity = 3.046E-01

Size Low (um)	In %	Size High (um)	Under%
0.05	0.00	0.06	0.00
0.06	0.00	0.07	0.00
0.07	0.00	0.08	0.00
0.08	0.00	0.09	0.00
0.09	0.00	0.11	0.00
0.11	0.00	0.13	0.00
0.13	0.00	0.15	0.00
0.15	0.00	0.17	0.00
0.17	0.00	0.20	0.00
0.20	0.00	0.23	0.00
0.23	0.00	0.27	0.00
0.27	0.00	0.31	0.00
0.31	0.01	0.36	0.01
0.36	0.02	0.42	0.04
0.42	0.04	0.49	0.08
0.49	0.04	0.58	0.12
0.58	0.06	0.67	0.18
0.67	0.08	0.78	0.26
0.78	0.08	0.91	0.34
0.91	0.09	1.06	0.42
1.06	0.10	1.24	0.52
1.24	0.11	1.44	0.63
1.44	0.12	1.68	0.75
1.68	0.13	1.95	0.87
1.95	0.14	2.28	1.01
2.28	0.15	2.65	1.16
2.65	0.16	3.09	1.32
3.09	0.18	3.60	1.50
3.60	0.20	4.19	1.69
4.19	0.22	4.88	1.91
4.88	0.24	5.69	2.15
5.69	0.26	6.63	2.40
6.63	0.27	7.72	2.68
7.72	0.28	9.00	2.96
9.00	0.28	10.48	3.23
10.48	0.26	12.21	3.50
12.21	0.24	14.22	3.73
14.22	0.21	16.57	3.95
16.57	0.20	19.31	4.15
19.31	0.20	22.49	4.35
22.49	0.21	26.20	4.56
26.20	0.23	30.53	4.79
30.53	0.23	35.56	5.02
35.56	0.21	41.43	5.23
41.43	0.18	48.27	5.41
48.27	0.13	56.23	5.54
56.23	0.08	65.51	5.62
65.51	0.05	76.32	5.67
76.32	0.07	88.91	5.73
88.91	0.17	103.58	5.90
103.58	0.42	120.67	6.33
120.67	0.93	140.58	7.26
140.58	1.85	163.77	9.11
163.77	3.42	190.80	12.54
190.80	5.85	222.28	18.38
222.28	9.29	258.95	27.68
258.95	13.48	301.68	41.16
301.68	17.49	351.46	58.65
351.46	17.04	409.45	75.69
409.45	12.87	477.01	88.56
477.01	7.75	555.71	96.31
555.71	3.69	647.41	100.00
647.41	0.00	754.23	100.00
754.23	0.00	878.67	100.00

Malvern Instruments Ltd.
Malvern, UK
Tel:=+[44] (0)1684-892456 Fax:+[44] (0)1684-892789

Mastersizer S long bed Ver. 2.19
Serial Number: 33544/152

p. 12
04 Jun 12 11:36

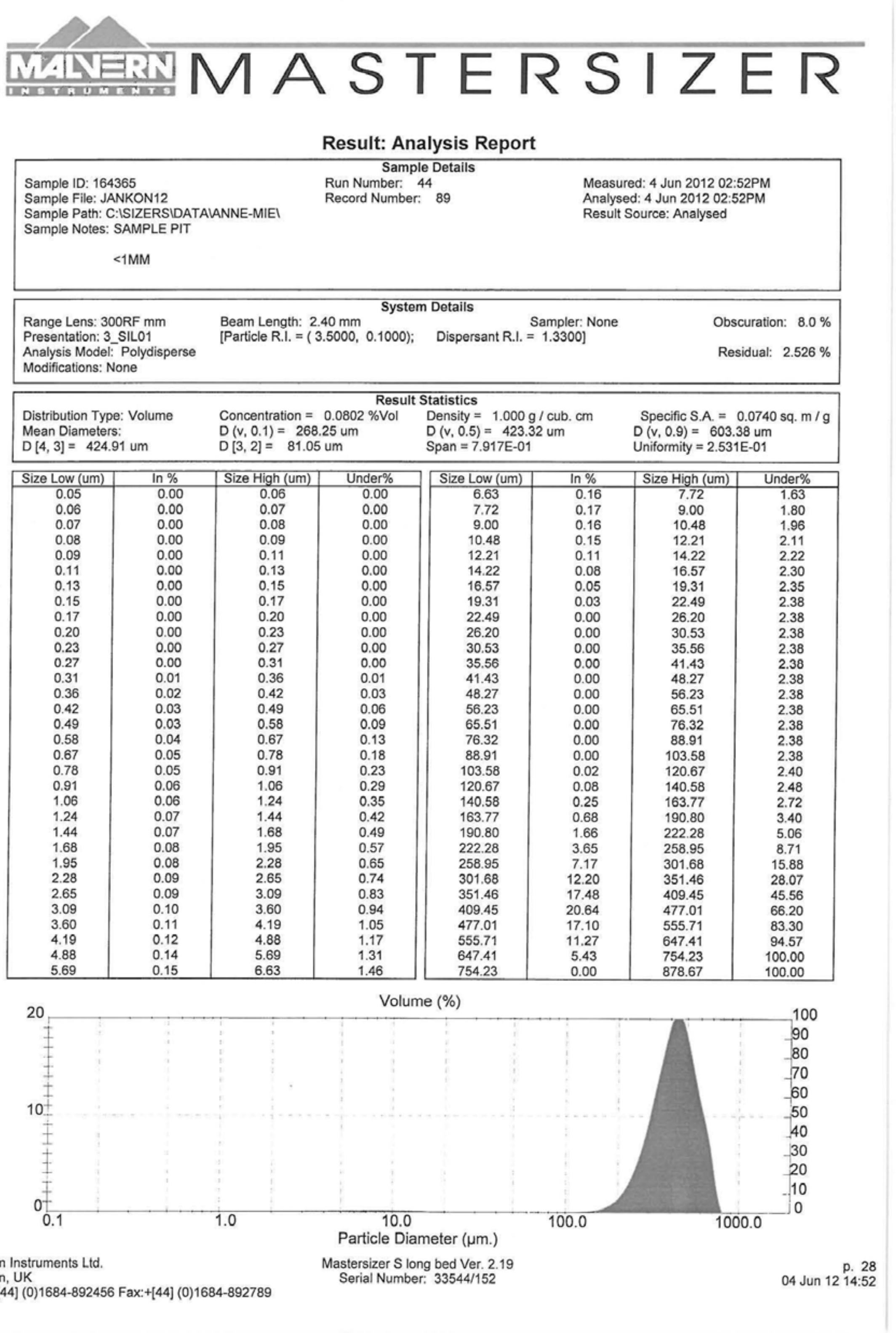

MALVERN INSTRUMENTS MASTERSIZER

Result: Analysis Report

Sample Details

Sample ID: 164365
Sample File: JANKON12
Sample Path: C:\SIZERS\DATA\ANNE-MIE\
Sample Notes: SAMPLE PIT

<1MM

Run Number: 44
Record Number: 89

Measured: 4 Jun 2012 02:52PM
Analysed: 4 Jun 2012 02:52PM
Result Source: Analysed

System Details

Range Lens: 300RF mm
Presentation: 3_SIL01
Analysis Model: Polydisperse
Modifications: None

Beam Length: 2.40 mm
[Particle R.I. = (3.5000, 0.1000); Dispersant R.I. = 1.3300]

Sampler: None

Obscuration: 8.0 %
Residual: 2.526 %

Result Statistics

Distribution Type: Volume
Mean Diameters:
D [4, 3] = 424.91 um

Concentration = 0.0802 %Vol
D (v, 0.1) = 268.25 um
D [3, 2] = 81.05 um

Density = 1.000 g / cub. cm
D (v, 0.5) = 423.32 um
Span = 7.917E-01

Specific S.A. = 0.0740 sq. m / g
D (v, 0.9) = 603.38 um
Uniformity = 2.531E-01

Size Low (um)	In %	Size High (um)	Under%
0.05	0.00	0.06	0.00
0.06	0.00	0.07	0.00
0.07	0.00	0.08	0.00
0.08	0.00	0.09	0.00
0.09	0.00	0.11	0.00
0.11	0.00	0.13	0.00
0.13	0.00	0.15	0.00
0.15	0.00	0.17	0.00
0.17	0.00	0.20	0.00
0.20	0.00	0.23	0.00
0.23	0.00	0.27	0.00
0.27	0.00	0.31	0.00
0.31	0.01	0.36	0.01
0.36	0.02	0.42	0.03
0.42	0.03	0.49	0.06
0.49	0.03	0.58	0.09
0.58	0.04	0.67	0.13
0.67	0.05	0.78	0.18
0.78	0.05	0.91	0.23
0.91	0.06	1.06	0.29
1.06	0.06	1.24	0.35
1.24	0.07	1.44	0.42
1.44	0.07	1.68	0.49
1.68	0.08	1.95	0.57
1.95	0.08	2.28	0.65
2.28	0.09	2.65	0.74
2.65	0.09	3.09	0.83
3.09	0.10	3.60	0.94
3.60	0.11	4.19	1.05
4.19	0.12	4.88	1.17
4.88	0.14	5.69	1.31
5.69	0.15	6.63	1.46

Size Low (um)	In %	Size High (um)	Under%
6.63	0.16	7.72	1.63
7.72	0.17	9.00	1.80
9.00	0.16	10.48	1.96
10.48	0.15	12.21	2.11
12.21	0.11	14.22	2.22
14.22	0.08	16.57	2.30
16.57	0.05	19.31	2.35
19.31	0.03	22.49	2.38
22.49	0.00	26.20	2.38
26.20	0.00	30.53	2.38
30.53	0.00	35.56	2.38
35.56	0.00	41.43	2.38
41.43	0.00	48.27	2.38
48.27	0.00	56.23	2.38
56.23	0.00	65.51	2.38
65.51	0.00	76.32	2.38
76.32	0.00	88.91	2.38
88.91	0.00	103.58	2.38
103.58	0.02	120.67	2.40
120.67	0.08	140.58	2.48
140.58	0.25	163.77	2.72
163.77	0.68	190.80	3.40
190.80	1.66	222.28	5.06
222.28	3.65	258.95	8.71
258.95	7.17	301.68	15.88
301.68	12.20	351.46	28.07
351.46	17.48	409.45	45.56
409.45	20.64	477.01	66.20
477.01	17.10	555.71	83.30
555.71	11.27	647.41	94.57
647.41	5.43	754.23	100.00
754.23	0.00	878.67	100.00

Malvern Instruments Ltd.
Malvern, UK
Tel:=+[44] (0)1684-892456 Fax:+[44] (0)1684-892789

Mastersizer S long bed Ver. 2.19
Serial Number: 33544/152

p. 28
04 Jun 12 14:52

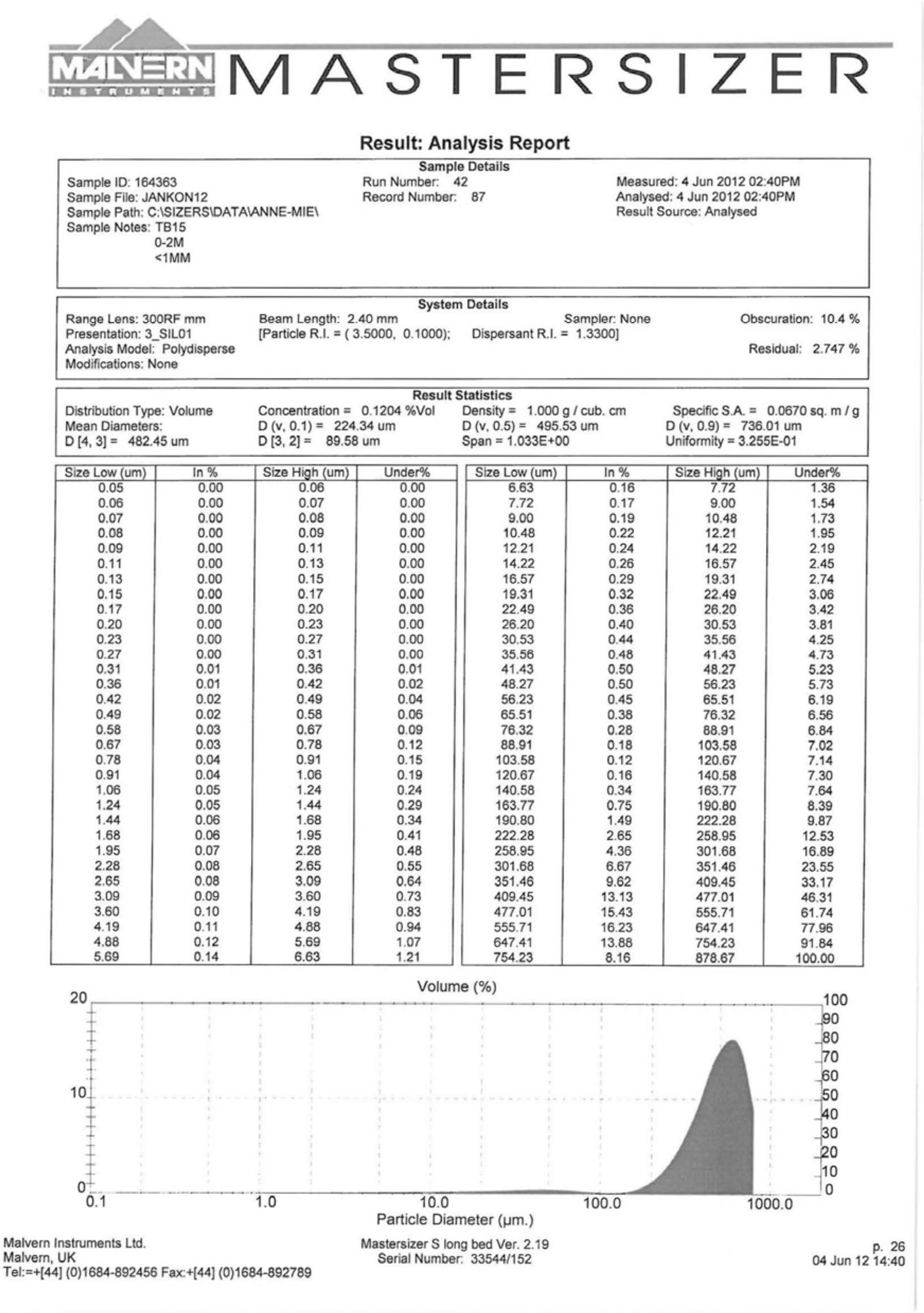

Result: Analysis Report

Sample Details

Sample ID: 164363
Sample File: JANKON12
Sample Path: C:\SIZERS\DATA\ANNE-MIE\
Sample Notes: TB15
0-2M
<1MM

Run Number: 42
Record Number: 87

Measured: 4 Jun 2012 02:40PM
Analysed: 4 Jun 2012 02:40PM
Result Source: Analysed

System Details

Range Lens: 300RF mm
Presentation: 3_SIL01
Analysis Model: Polydisperse
Modifications: None

Beam Length: 2.40 mm
[Particle R.I. = (3.5000, 0.1000); Dispersant R.I. = 1.3300]

Sampler: None

Obscuration: 10.4 %
Residual: 2.747 %

Result Statistics

Distribution Type: Volume
Mean Diameters:
D [4, 3] = 482.45 um

Concentration = 0.1204 %Vol
D (v, 0.1) = 224.34 um
D [3, 2] = 89.58 um

Density = 1.000 g / cub. cm
D (v, 0.5) = 495.53 um
Span = 1.033E+00

Specific S.A. = 0.0670 sq. m / g
D (v, 0.9) = 736.01 um
Uniformity = 3.255E-01

Size Low (um)	In %	Size High (um)	Under%
0.05	0.00	0.06	0.00
0.06	0.00	0.07	0.00
0.07	0.00	0.08	0.00
0.08	0.00	0.09	0.00
0.09	0.00	0.11	0.00
0.11	0.00	0.13	0.00
0.13	0.00	0.15	0.00
0.15	0.00	0.17	0.00
0.17	0.00	0.20	0.00
0.20	0.00	0.23	0.00
0.23	0.00	0.27	0.00
0.27	0.00	0.31	0.00
0.31	0.01	0.36	0.01
0.36	0.01	0.42	0.02
0.42	0.02	0.49	0.04
0.49	0.02	0.58	0.06
0.58	0.03	0.67	0.09
0.67	0.03	0.78	0.12
0.78	0.04	0.91	0.15
0.91	0.04	1.06	0.19
1.06	0.05	1.24	0.24
1.24	0.05	1.44	0.29
1.44	0.06	1.68	0.34
1.68	0.06	1.95	0.41
1.95	0.07	2.28	0.48
2.28	0.08	2.65	0.55
2.65	0.08	3.09	0.64
3.09	0.09	3.60	0.73
3.60	0.10	4.19	0.83
4.19	0.11	4.88	0.94
4.88	0.12	5.69	1.07
5.69	0.14	6.63	1.21

Size Low (um)	In %	Size High (um)	Under%
6.63	0.16	7.72	1.36
7.72	0.17	9.00	1.54
9.00	0.19	10.48	1.73
10.48	0.22	12.21	1.95
12.21	0.24	14.22	2.19
14.22	0.26	16.57	2.45
16.57	0.29	19.31	2.74
19.31	0.32	22.49	3.06
22.49	0.36	26.20	3.42
26.20	0.40	30.53	3.81
30.53	0.44	35.56	4.25
35.56	0.48	41.43	4.73
41.43	0.50	48.27	5.23
48.27	0.50	56.23	5.73
56.23	0.45	65.51	6.19
65.51	0.38	76.32	6.56
76.32	0.28	88.91	6.84
88.91	0.18	103.58	7.02
103.58	0.12	120.67	7.14
120.67	0.16	140.58	7.30
140.58	0.34	163.77	7.64
163.77	0.75	190.80	8.39
190.80	1.49	222.28	9.87
222.28	2.65	258.95	12.53
258.95	4.36	301.68	16.89
301.68	6.67	351.46	23.55
351.46	9.62	409.45	33.17
409.45	13.13	477.01	46.31
477.01	15.43	555.71	61.74
555.71	16.23	647.41	77.96
647.41	13.88	754.23	91.84
754.23	8.16	878.67	100.00

Malvern Instruments Ltd.
Malvern, UK
Tel:=+[44] (0)1684-892456 Fax:+[44] (0)1684-892789

Mastersizer S long bed Ver. 2.19
Serial Number: 33544/152

p. 26
04 Jun 12 14:40

Appendix 5.8.I: Reportable Meteorological Incidents

Table 5.8.I.1
Summary of Severe Phenomena Recorded in the Region

Event	Location	Year	Consequences
Floods	Stellenbosch	1705	One third of the wheat crop was destroyed, 5 people killed
Strong wind	Cape town	1722	Eleven ships destroyed and 660 people drowned
Strong wind	Cape town	1728	75 people drowned
Strong wind	Cape town	1728	1 shipwrecked and 90 people drowned
Strong wind	Cape town	1737	Eight ships wrecked and 207 people drowned
Strong wind	Cape town	1773	One ship destroyed and many people died
Strong wind	Cape town	1822	Seven ships destroyed
Floods	Somerset west	1822	25 homes destroyed
Strong wind	Cape town	1842	Three ships destroyed
Strong wind	Cape town	1857	Two ships destroyed
Strong wind	Cape town	1857	26 ships were destroyed in three days
Strong wind	Cape town	1865	18 ships destroyed and 89 people died
Tornado	Malmesbury	1905	Some loss of life
Strong wind	Cape town	1940	Several ships wrecked
Strong wind	Cape town	1956	Several people injured - 40 families left homeless in Mowbray
Floods	Tulbach	1956	Massive vineyard and orchard damage
Floods	Cape town	1957	Many people injured
Hail	Ceres	1958	R140000 in damages
Strong wind	Cape town	1959	12 m swell in the harbour
Floods	Paarl	1976	Worst flood in 25 years
Floods	Wellington	1976	Worst flood in 25 years
Floods	Cape town	1983	Millions of Rands worth of damage
Floods	Malmesbury	1983	Millions of Rands worth of damage
Floods	Cape town	1983	Millions of Rands worth of damage
Hail	Hopefield	1988	Hen's egg size hail
Hail	Ceres	1990	R1.5 million in damages
Extreme cold	Cape town	1990	6 babies died on the cape flats
Fire	Piketberg	1991	Fire raged for 12 days - 12 000 ha of grassland was destroyed
Fire	Porterville	1992	Millions of Rands in damages
Fire	Cape town	1992	Lightning sparked the fire
Fire	Paarl	1992	200 ha of pine forest destroyed

Event	Location	Year	Consequences
Strong wind	Grabouw	1992	20% loss of the apple crop
Floods	Hermanus	1993	Highest flood in Breede River in 50 years
Floods	Cape town	1993	Described as the worst storms in 30 years
Severe heat	Worcester	1994	Fruit crops severely damaged and farmers had to use sprays in chicken batteries to prevent poultry deaths
Floods	Cape town	1994	400 people left homeless
Fire	Cape town	1994	400 families were left homeless in Khayelitsha
Strong wind	Cape town	1994	400 families were left homeless in Khayelitsha
Fire	Paarl	1994	200 ha pine plantation destroyed on 4 farms
Fire	Porterville	1994	10 000 ha of vegetation destroyed - millions of Rands in damages
Strong wind	Langebaan	1994	1 yachtsman killed
Fog	Cape town	1997	Resulted in motor vehicle accidents in which 12 people were killed and 51 injured
Fire	Cape town	1998	The fire in a luxury house was sparked by lightning
Frost	Worcester	1998	10 000 ton of wine grapes destroyed
Fog	Saldanha	1998	1 person died in an aeroplane accident in the fog
Hail	Tulbach	1999	R20 million in damages
Strong wind	Cape town	1999	Millions of Rands in damages to ships and an oil rig in the harbour
Floods	Cape town	1999	Flooding was accompanied by mud slides
Fire	Franschhoek	1999	500 ha of plantations were destroyed
Fire	Paarl	1999	500 ha of plantations were destroyed
Fire	Grabouw	1999	5 000 people left homeless - fires were fanned by strong winds
Tornado	Cape town	1999	5 000 people left homeless - 5 people died and 180 were injured
Fire	Cape town	2000	R20 million in damages
Floods	Cape town	2001	3500 people left homeless
Floods	Cape town	2001	3500 people left homeless
Floods	Bakoven	2002	Millions Rands damage
Floods	Betty's bay	2002	Millions Rands damage
Floods	Bloubergstrand	2002	Millions Rands damage
Floods	Hermanus	2002	Millions Rands damage
Strong wind	Langebaan	2002	Millions Rands damage
Floods	Langebaan	2002	Millions Rands damage
Fire	Betty's bay	2002	22 ha fynbos and alien vegetation destroyed
Fire	Pringle bay	2002	21 ha fynbos and alien vegetation destroyed
Floods	Cape town	2002	1000 people displaced
Floods	Cape town	2003	Thousands homeless
Fire	Piketberg	2003	30 homes damaged
Floods	Worcester	2004	Extensive damage to property
Floods	Cape town	2004	200 homes damaged
Strong wind	Cape town	2004	200 homes damaged
Floods	Overstrand	2005	People left homeless
Floods	Theewaterskloof	2005	People left homeless
Fire	Khayelitsha	2005	One person died and 1104 left homeless

Event	Location	Year	Consequences
Floods	Khayelitsha	2005	20 shacks affected
Strong wind	Cape town	2005	100-year-old Breede River yellowwood 'magic tree' in Kirstenbosch garden was blown over
Floods	Cape town	2005	100 shacks affected
Strong wind	Cape town	2006	1 killed
Strong wind	Cape town	2006	1 death
Veld fires and strong winds	Hermanus	2008	Destroyed three houses and damaged several others
Heavy rains and floods	Donkerhoek	2008	A man drowned
Strong winds and fires	Cape Town	2008	left more than 100 people homeless
Veld fires and gale-force winds	Overberg	2008	Damaging nine houses.
Veld fires and gale-force winds	Betty's Bay	2008	Four homesteads burnt to the ground.
Veld fires and gale-force winds	Fish Hoek	2008	Destroyed eight shacks leaving 32 people homeless
Heavy rains and floods	Cape Flats	2008	About 5500 people accommodated in community halls
Heavy rains and floods	Cape Flats	2008	About 16 000 people and 3 600 dwellings in 23 informal settlements negatively affected. Three thousand people had to be housed in community halls.Roads were flooded leading to a number of road accidents. Food and blankets were distributed to affected people.
Tornado	Western Cape	2008	Twelve light aircrafts at the Western Cape Micro-light Club were damaged by a tornado. The tornado totally destroyed some hangers while leaving others almost completely intact. Doors were blown off hangers and deposit some 3 to 4 km away.
Veld fires and strong winds	Western Cape	2008	Four people killed
Gales force winds	Ysterplaat	2008	The strong wind lifted a Dakota aircraft and smashed it into Shackleton Maritime aircraft, both parked on a concrete slab 30m apart.
Veld fires	Paarl	2009	Damage of at least R400 million
Veld fires, very hot conditions and strong winds	Western Cape	2009	Damage suffered by the agricultural industry to be between R150 million and R200 million.
Winter storms	Cape Town	2009	Nearly 500 houses, affecting more than 1 700 people in 28 informal settlements in Cape Town, were flooded
Heavy rains, gale-force winds and floods	Western Cape	2009	Heavy rain accompanied by gale-force winds caused flood damage in informal settlements as well as power outages in several suburbs in the Western Cape.
Strong wind-gust	Milnerton	2009	A kite surfer killed
Heavy rain and floods	Western Cape	2009	Thousands of shack dwellers were left homeless

Event	Location	Year	Consequences
Storm, heavy swells and gale-force winds	Western Cape	2009	A five-year-old girl was killed
Strong wind	Cape Peninsula	2009	The gale-force winds that reached speeds as high as 165km/h flattened trees and damaged roofs and power lines across the Cape Peninsula.
Very hot conditions	Western Cape	2010	Temperatures as high as 42 degrees Celsius were recorded. Some stations in the Western Cape recorded temperatures as high as 44 and even 46 degrees Celsius.
Rough seas and big waves	Cape Town	2010	Waves hit houses and the NSRI station in Bakoven, Cape Town as rough seas went through the coastline
Raw weather	Kleinmond	2010	Characterized by hail and wind speeds of 70 km/h.
Heavy rains	Cape Flats	2010	Five hundred residents of informal settlements were affected after heavy rain waterlogged about 200 shacks in Kanana, Gugulethu and the Cape Flats.
Gale-force winds	Cape Peninsula	2011	Several people on motorcycles and bicycles were blown over. Four members of a family in Melkbosstrand narrowly escape death when the wall of a double-storey house under construction, collapsed.
Heavy rains, strong winds and high waves	Western Cape	2011	People in low-lying areas were affected when their homes were flooded following heavy rain. More than 22 informal settlements including some in Strand, Khayelitsha, Gugulethu, Crossroads and Phillipi were affected. According to reports a total of 1895 households and 7300 people were affected. Heavy rain disrupted schools and causing mudslides. Windows were blown out by strong winds.
Volcanic ash clouds	Cape Town	2011	The volcanic ash cloud that originated from the Puyehue-Cordon Caulle volcanic complex in south-central Chile, South America on 4 June 2011, affected flights to and from Cape Town on 18 and 19 June 2011. A total of 13 flights to and 12 flights from the Cape Town International Airport were delayed.
Dense Fog	Mitchell’s Plain	2011	At least 11 people were injured in two pileups that took place in dense fog on the R300 in Mitchells Plain near Cape Town. Nine vehicles were involved in the one pileup on the one side of the road while five vehicles were involved in the second pileup on the same road, but in the opposite direction.
Dense Fog	Cape Town	2011	At least 8 car accidents occurred between 07:00 and 10:00 in the Cape Metro pole. According to reports dense fog could have contributed to the occurrence of the accidents. Luckily no serious injuries occurred.
Veld fires and strong winds	Franschhoek	2012	
Hot conditions	Cape Town	2012	Extremely hot conditions prevailed in Cape Town during the Cape Argus cycling race.
Strong winds	Stellenbosch	2012	Three passengers in a hot-air balloon were injured when the balloon crashed during strong-wind conditions on a farm outside Stellenbosch.

Event	Location	Year	Consequences
Heavy rain	Cape Town	2012	Extensive flooding occurred across the city of Cape Town and thousands of people were displaced when their shacks were flooded after heavy rain. In the Europe informal settlement 250 shacks were flooded resulting in the displacement of at least 750 people, in the Kanana informal settlement 266 shacks were flooded with 800 people being displaced, and in the Egoli informal settlement 250 shacks were flooded and 1000 people displaced. Areas that were affected by the flooding included amongst others Philippi, Strandfontein, Khayelitsha, Delft, Gugulethu and Hout Bay
Heavy Rain	Observatory	2012	Heavy rain also led to several roads being flooded while, due to the rising water level of the Liesbeek River, about 60 people were evacuated from the River Club premises in Observatory for safety reasons. During the whole weekend the disaster management team assisted more than 2500 people in the flood-affected areas.
Snow and heavy rain			Sir Lowry's Pass was closed on the 15th after large boulders crashed down the Hottentots-Holland Mountain onto the road. At least 12 people were injured in several incidents. The Montagu Pass was also closed after power lines fell across the road.
Heavy rain and strong winds	Cape Peninsula	2012	About 5000 people were affected as hundreds of homes across the Cape Peninsula were flooded during heavy rain conditions over the weekend. Gale-force winds and low temperatures worsened the conditions.
Strong winds	Goodwood	2012	Trains to and from Cape Town were delayed for about 2 hours after strong winds blew a tree over on overhead power cables near the Goodwood station.
Strong winds	Table Bay	2012	Strong winds and big swells broke an abandoned bulk carrier, which ran aground near Table Bay in Cape Town during September 2009, apart during the night of 31 Aug/1 Sep spilling oil into the ocean. Bad weather conditions hampered the clean-up operations along the Table Bay coastline, but much of the oil had been cleared. At least 15 oiled penguins were captured and cleaned.
Heavy rains and flooding	Bredardorp	2012	Thirty-two hikers were airlifted by helicopter from the Whale Trail near Bredasdorp after they were trapped following heavy rain in the area. Six secondary roads in the Overberg region were closed due to flooding and several people were forced to evacuate their homes. Four persons were rescued in two incidents in the Overberg after their vehicles were washed away.
Gale-force winds	Cape Town	2012	At least 20 people were injured and one person died outside Cape Town Stadium when strong winds gusting at gale-force strength caused the collapse of a sponsor's stand. Three people were in a critical

Event	Location	Year	Consequences
			condition while a further 11 were also taken to hospital for treatment.
Wind gusts	Cape Town	2012	A large blue-gum tree in Bergvliet, Cape Town was uprooted by a wind gust obstructing the main road for about an hour.
Fires and strong winds	Hermanus	2012	A fire ignited by lightning near Hermanus was fanned by gale-force winds and wreaked havoc over a distance of approximate 12km. The fire was brought under control the following day, but with a change in the wind direction three days later it flared up again and caused further damage. About 20,000 ha veld and fynbos was destroyed between Hermanus and Stanford. Extensive damage was suffered at the Hermanus yacht-club where at least 12 caravans, 15 boats, several trailers and a two-bedroom house were destroyed.
Lightning	Ceres	2013	Lightning ignited a fire in Cederberg between Clanwilliam and Wupperthal leaving one person dead. Tourists were also evacuated from a Cape guest lodge.
Strong winds	Cape Town	2013	Windy conditions in early February prevented ships from entering or leaving Cape Town harbour for up to eight days causing delays in shipment of fresh produce and other products to international markets.
Very hot conditions	Table Mountain	2013	Two hiking tourists were airlifted off Table Mountain in separate incidents during very hot conditions. Both were treated for dehydration.
Heavy rain	Cape Peninsula	2013	Heavy rain that occurred over the Cape Peninsula resulted in several vehicles lining up along waterlogged roads. The heavy rain also affected more than 200 people whose houses were flooded in Masiphumelele and Mitchells Plain in Cape Town
Dense fog	Cape Town	2013	Dense fog disrupted air traffic at the Cape Town International Airport and airplanes could not land or depart including several flights to Johannesburg.
Heavy rain and gale-force winds	Cape Town	2013	Heavy rain and gale-force winds hit Cape Town causing severe flooding and damage in at least 23 residential areas. The affected areas included Phillipi, Gugulethu, Khayelitsha, Hout Bay, Bishop Lavis, Strand, Atlantis, Blackheath, Elsie River, Kalkfontein, Langa, Lavender Hill, Lotus River, Milnerton and Parkwood. About 547 shacks were damaged with 2266 people displaced At least 8 houses lost their roofs while trees were uprooted and lamp posts as well as power lines brought down.
Cold and wet conditions	Western Cape	2013	More than 26 000 people were affected by heavy rains and cold weather in the Western Cape. One woman died from hypothermia in Robertson, while another one died in Wynberg due to exposure to cold weather. A man died in a rock fall that occurred on the Franschhoek Pass near Paarl. Five people died and several sustained injuries in accidents related to

Event	Location	Year	Consequences
			wet conditions in Grabouw, Brackenfell, De Doorns, Parow and Prince Alfred Hamlet. According to reports at least 17 car accidents occurred in wet weather conditions across the Western Cape.
Hail	Cape Town and Surrounding Area	2013	Small pellets of hail fell in Cape Town and surrounding areas. Reports of hail were also received from Boston in Bellville, Bothasig, Stellenbosch, Paarl, Moorreesburg and Malmesbury
Heavy rain	Cape Town	2013	Heavy rain hit the city of Cape Town causing damage to shacks as well as flooding roads. A low bridge on Main Road in Lakeside collapsed. Flooding also occurred in the Isiqalo informal settlement next to Vanguard Drive near Mitchells Plain
Heavy Rain	Cape Town	2013	The Berg River in Paarl burst its banks forcing the residents of Mbekweni, an informal settlement to leave their homes. Some 160 people were evacuated from their homes and given shelter in a community hall. At least two bridges and a number of roads in the Drakenstein Municipality area were closed due to the flooding, while Chapman's Peak Drive was closed after a mudslide. Franschhoek Pass was also closed following a rock fall and mudslide.
Strong winds	Cape Town	2013	A fire, fanned by strong winds, destroyed at least 350 shacks in the Agstelaan informal settlement of Valhalla Park near Cape Town. About 1400 people were left homeless, while 8 firefighters were treated for smoke inhalation. In another incident fire also destroyed 2 shacks in Phase Six, Wallacedene affecting at least 9 people.
Gale-force winds and rough seas	Cape Town	2014	Participants in the Cape 2 Rio race, which started on the 4th, were seriously affected by gale-force winds and rough seas. About 25% of the fleet that started the race withdrew when the boats sailed into rough seas about 75 nautical miles from the start, where they encountered swells of up to 8 m and gale-force winds of between 74 and 111 km/h. One crewman died while several others were injured.
Flooding	Cape Town	2014	Continuous rainfall that occurred during the first half of the month resulted in localized flooding affecting more than 20 000 people in informal settlements around Cape Town. The most affected areas included Khayelitsha, Strand, Vrygrond, Lotus River, Gugulethu, Makhaza, Taiwan, Delft and Philippi. Khayelitsha was the worst hit area with about 7000 people affected.
Heavy rains and flooding	Cape Town	2014	Heavy rain that occurred in Cape Town and surrounding areas affected more than 30 000 people. Relief aid was provided to nearly 25 700 people on the 5th and a further 6 400 on the 6th. The most affected areas included Khayelitsha, Nyanga, Philippi, Gugulethu, Strand and Somerset West. During the first weekend of the month traffic

Event	Location	Year	Consequences
			gridlocked with at least 24 motor vehicle accidents and more than 100 roads that were flooded. One person died in one of the accidents. The Civic Centre in Cape Town was also flooded. Chapman's Peak Drive as well as the Table Mountain Cableway was closed for safety reasons.
Gale-force winds	Kleinmond	2014	Winds gusting up to 60 km/h resulted in the suspension of the 2nd round of a golf tournament that took place in Kleinmond, Western Cape
Heavy rains and flooding	Cape Town	2014	Damage caused by flooding occurred in several low-lying areas as well as informal settlements in and around Cape Town, Western Cape following heavy rain. According to reports at least 3 000 home structures were effected with about 10 000 people in need of some sort of assistance.
Heavy seas and tidal waves		2014	Heavy seas as well as tidal surges causing waves with heights up to 8,5 m hit areas from Melkbosstrand along the West Coast to the False Bay coast. Coincidently with this, a spring tide reaching its peak aggravating the situation. An 18-year-old man drowned after being swept away by strong currents at Strand beach while trying to rescue his 13-year-old cousin.
Strong winds	Sea Point and Paarl	2015	Gale-force winds caused damage in parts of the Western Cape, including palm-trees that were blown over in Sea Point. The N1 was closed at the Huguenot Tunnel during the evening after the gale-force winds blew a truck over; due to the strong winds it could only be removed the next morning when the road was opened again.
Heavy rain	Cape Town	2015	Heavy rain occurred in areas of the Western Cape. In the Cape Flats several homes were flooded, especially those in Khayelitsha, Philippi and Guguletu leaving more than 1 000 people homeless
Gale force winds	Paarl	2015	Near-gale to gale-force southeasterly winds caused havoc in parts of the Western Cape. The Huguenot Tunnel on the N1 was closed after four trucks were blown over near the tunnel. The Bain's Kloof Pass was also closed following trees that were blown over onto the road. Motorists had to use alternative roads.
Lightning	Sunningdale	2015	A pylon collapsed onto the roof of a house in Sunningdale near Cape Town, Western Cape after it was struck by lightning. According to reports it seems as if the cables wrapped around each other until the structure fell.
Strong winds and veld fires	Cape Peninsula	2015	At least 240 firefighters from 30 stations were battling to deal with 60 vegetation fires that started in Simon's Town, Western Cape. Some properties were completely destroyed, while a number of residents were forced to evacuate their homes. The fires were fanned by strong south-easterly winds, but the wind changed direction during the night, which aggravated

Event	Location	Year	Consequences
			the situation.
Strong winds and veld fires	Khayelitsha	2016	Thick smoke coming from a vegetation fire fanned by strong winds caused poor visibility. As a result a section of the N2 freeway near Khayelitsha, between Spine Road and Baden Powell Drive, was closed for 4 hours with traffic being diverted.
Strong winds and veld fires	Stellenbosch & Franschhoek	2016	A runaway fire that raged in gale-force winds in the area between Stellenbosch and Franschhoek from the 19th caused extensive damage. More than 800 ha was destroyed across farms and wineries. Apart from thousands of Rand damage to the vineyards, a Telkom tower on Simonsberg was also damaged.
Black frost	Worcester and Ceres	2016	Black frost that occurred in areas of the Western Cape caused widespread and extensive damage to vineyards of Breedekloof, De Doorns, Brandvlei, Nuy, and De Wet, all near Worcester, as well as the Witzenberg Valley near Ceres. The damage on some of the wine farms is estimated between 30 to 40%.
Strong winds and veld fires	Somerset West	2016	Veld fires fanned by strong southeasterly winds caused extensive damage in the Western Cape during the first week. Hundreds of firefighters from across the country were deployed to the Western Cape to fight the fires. About 3000 hectares of veld was destroyed on the Lourensford and Vergelegen Estates in Somerset West. For Vergelegen Estate it was about 40% of the wine farm. Several helicopters were used to water bombed the fires. Seven residential properties in Somerset West were damaged or destroyed in the blaze. The estimated structural damage was more than R53 million.
Strong winds and veld fires	Western Cape	2017	A fire, fanned by strong winds, spread from the Du Toitskloof Mountain to Wellington. About 650 hectares of vegetation was destroyed overnight. Fires also occurred in Paarl and on the lower slopes of Table Mountain. Other areas that were also affected by fires included Simon's Town, Tulbagh, Rawsonville, Grabouw, Stilbaai, Blanco area in George as well as Oudtshoorn. The fires also affected the electricity supply to numerous areas. A fire that broke out near Bainskloof in Wellington, Western Cape was fanned by strong south-easterly winds and burnt out of control. Another fire broke out in the mountains surrounding Du Toitskloof Pass causing a two-day road closure over the weekend of the 5th. More than 1 500 hectares of fynbos and other vegetation burnt down. No serious injuries or structural damages were reported. A veld fire that was fanned by strong winds spread to Tafelberg Road on Table Mountain in the Western

Event	Location	Year	Consequences
			Cape where flames engulfed a car. There were no reports of any injuries and no properties were damaged by the car blaze. A fire raged out of control in Pringle Bay. At least 50 families were evacuated from their homes, while 3 homes that were severely damaged. About 90 firefighters were on the scene struggling to contain the blaze, fanned by strong winds. Another fire, fanned by strong south-easterly winds, started on Signal Hill, Cape Town. Other areas that were also affect by wild fires included Kylemore, La Motte and Banghoek as well as the Bredasdorp and Hout Bay areas.
Drought	Western Cape	2017	The drought conditions in the Western Cape continued and level 3b water restrictions were implemented by the City of Cape Town. The collective dam levels for the city stood at about 39%. Many dam levels are at an all time low.
Gale-force winds	Parl and Stellenbosch	2017	The fourth shift of the international Tour of Good Hope road cycle tour was cancelled due to gale-force winds causing extremely dangerous conditions for the cyclists in the Dutoitskloof and Bainskloof passes outside Paarl. In Stellenbosch a tree was blown over. A sailing-yacht also got in trouble southwest of Hermanus due to the gale-force winds and the National Sea Rescue Institute was called for help.
Gale-force winds	Cape Peninsula	2017	Gale-force winds gusting nearly 100 km/h in the Cape Peninsula causing a serious safety risk and a devastating fire blazing at Imizamo, Hout Bay contributed to the cancelling of the Cape Town Cycle Tour shortly after it started. According to reports more than 1000 homes were destroyed by the fire
High temperatures	Hermanus	2017	The Cape Epic Mountain cycle tour took place in extremely hot conditions and high humidity. The second shift of this tour, between Hermanus and Caledon, was shortened due to the extremely dangerous weather conditions.
Drought	Western Cape	2017	Drought continues to affect the agricultural sectors in the Western Cape, which might cause job losses, with farmers being requested to cut water usage by 30% in order to increase quantities available for residential use. Several plans to supplement the water supply are investigated and stronger water restrictions were implemented.
Thunderstorms, lightning and hail	Cape Town and Durbanville	2017	hit a large part of the Western Cape. In Durbanville a tall palm tree was set alight when hit by lightning. Hail as big as marbles also occurred in some parts of Cape Town.
Drought	Western Cape	2017	The persistent lack of rain in the Western Cape continues to affect dam levels and water restrictions in the province due to drought. The major dam levels

Event	Location	Year	Consequences
			in the province have reached a critical low of less than 20%. The effects of drought have left various farmers, from smallholder to commercial counting losses in both livestock and crop production. The food prices and other commodities also went up affecting the poor. The persistent lack of rain in the Western Cape continues to affect dam levels and water restrictions in the province due to drought. The Premier of the Western Cape declared the province a disaster area on the 22nd. The disaster period would be for 3 months, with an option to extend the period if needed.
Gale-force winds, storm and lightning	Cape Peninsula	2017	A severe storm accompanied by gale-force winds, lightning and heavy rainfall caused havoc in the Western Cape starting from the evening of the 6th and on the 7th. Six people died and more than 2 000 had to be displaced. Two adults and 3 children died tragically on a farm in Kraaifontein when lightning hit a tree, which fell on their house, setting a fire and they burnt to death on the 7th. A 69-year-old man died when a wall collapsed on top of his Wendy house in Lavender Hill in the southern Cape Peninsula. According to the Western Cape Education Department at least 170 schools in the Western Cape were damaged by the storms, with the total damage estimated at R124 million. Reported damages include roofs that were blown off, water damage to classrooms, fallen trees and damage to fences. Roofs were also blown off over a large area including Strand, Kalkfontein, Delft, Mfuleni, Mandalay and Lavender Hill, where 2 people were injured. Trees were also uprooted over a large area including Plumstead, Durbanville, Delft, Plattekloof, Paarl, Kenilworth, and Somerset West. Reports of electricity cables that were blown down came from Athlone, Weltevreden Valley, Pelican Park, Schaapkraal, Goodwood, Boston and Parow Valley, resulting in about 46 000 homes without electricity. Power failures occurred over an extensive area including Albertinia, Stilbaai, Tulbagh, Caledon, Greyton, De Doorns, Touwsrivier, Ladismith, Franschhoek, Worcester, Citrusdal, Darling, Yzerfontein, Palmiet, Voëlklip, and Villiersdorp. Evacuations took place with emergency alternative accommodation provided to more than 2 000 residents in Imizamo Yethu and Macassar Village in Hout Bay. Evacuations also took place in Makhaza in Khayelitsha, Villiersdorp, Bot River, Franschhoek, George and the Kannaland Municipality. Chapman's Peak Drive between Noordhoek and Hout Bay was closed due to mudslides, while rock falls occurred on

Event	Location	Year	Consequences
			Clarence Drive between Gordon's Bay and Rooi Els. Furthermore, the railway line between Wellington and Bellville was closed. As a safety precaution all schools and four universities in the Western Cape were closed on the 7th of June 2017
Black Frost	Worcester	2017	Severe damage was caused to vineyards in Worcester, Aan de Doorns and Rawsonville when black frost occurred. All indications are that the grape harvest could be between 2 000 and 3 000 tons less.
Gale-force winds	Cape Metropole, Cape Columbine and Cape Hanglip	2017	Gale-force south-easterly winds that swept the Cape Metropole, Cape Columbine and Cape Hanglip led to road closures and traffic delays. The city was forced to close roads for the safety of residents and prevention of damage to vehicles. The construction site of a new building in Roeland Street was damaged, while equipment used on the high-story building blew off and landed in Roeland Street and surrounding areas. Streets that were closed included Roeland Street and Phillip Kgosana Drive.
Strong winds and veld fires	Western Cape	2017	Gale-force winds fanned several fires in areas of the Western Cape. Hundreds of people were left destitute. Firefighters responded to a shack fire in Jim se Bos informal settlement in Philippi. The fire was extinguished early on the 10th with 15 structures destroyed and about 50 people displaced. No injuries were reported. About 270 people, of whom 83 were children under the age of 10, were left destitute in Chicago, Paarl East after a fire broke out on the 10th. Fourteen housing units located at Grysbok Flats as well as 42 informal settlements in the Chicago neighbourhood were destroyed. Another three housing units in Grysbok Flats were damaged.
Cloudburst and strong winds	Tulbagh	2018	A cloudburst accompanied by strong winds caused extensive damage to several fruit farms in the Tulbagh region, Western Cape. According to reports 30 mm of rain occurred within about 10 minutes, while strong winds ripped fruit as well as branches from trees. Some farmers estimated the damage to plum and pear harvests on more than 50%. Farm roads were also washed away preventing farmers from reaching the town. Flooding also occurred in Hermanus where houses and businesses were flooded. Some of the streets were closed preventing cars to drive through the water and pushing more water from the flooded roads into adjacent buildings.
Heavy rain	Cape Town	2018	Heavy rain occurred in the Greater Cape Town area causing extensive damage to homes in informal settlements in Strand, Khayelitsha, Mfuleni, and Macassar affecting about 2 000 people. Streets in Epping, Bishop Lavis and Guguletu were flooded, and several streets were closed due to the flooding

Event	Location	Year	Consequences
			including amongst other Koeberg Road between Table View and Milnerton, Blaauberg Road near the Bayside Center, Belrail Road in Bellville and the crossing at Jan van Riebeeck Drive and Jan Smuts Drive, as well as Epping Lane in Parow.
Sandstorm	Grabouw	2018	The continuous drought in the Western Cape had another consequence when a strong north-westerly wind blew sand from the dry Theewaterskloof Dam and caused a sandstorm that disrupted traffic on the R321 between Villiersdorp and Grabouw in the Western Cape. Visibility was very low while vehicles were also stuck in the sand that was blown on the road. The road was closed, and motorists were advised to use other roads. The Theewaterskloof Dam was about 11% full on the 7th of May 2018
Heavy rain and gale-force winds	Cape Town	2018	Heavy rain and gale-force winds occurred in areas of the Western Cape. In the Sir Lowry's Pass area, the roofs of a house and a shop were ripped off by the gale-force winds. Mud spills along Chapmans Piek Drive as well as in Hout Bay and the area of the Twelve Apostles resulted in the temporary closure of roads. Several trees were uprooted, and power failures occurred amongst others in Parow Valley, Langa, Durbanville, Mfuleni, Bridgetown, Constantia, Cape Farms and Clovelly. Day clinics in Belhar, Parow and Ravensmead were flooded and patients had to be transferred to other health facilities. About 150 homes were affected by the flooding. A person suffered slight head and neck injuries when a tree fell over on his car in Constantia.
Floods	Cape Town	2018	Heavy rain occurred in the Cape Metropole, Western Cape causing floods in informal settlements in areas of Khayelitsha, Langa, Strand, Strandfontein, Philippi, Kengsington and Atlantis. More than 500 structures were affected, and several roads were flooded. Power failures occurred in Bridgetown, Athlone, while trees were uprooted in Kenilworth, Parow Industria and Goodwood.
Heavy rain	Western Cape	2019	A cold front that moved over the Western Cape caused heavy rain and localized flooding in Langa, Gugulethu, Imizamo Yethu, Mitchells Plain, Philippi, Khayelitsha and Manenberg. There was a request from residents in the Burundi informal settlement near Mfuleni to be evacuated from the area. A tree in Imizamo Yethu was uprooted and fell on two informal dwellings. According to Disaster Management reports at least 700 house in informal settlements in Khayelitsha, Strand, Gugulethu and Cross Roads were flooded. Other areas where flooding occurred included Gatesville, Diep River, Athlone and Wallace Dene. In Manenberg, the

Event	Location	Year	Consequences
			canal in Silverstream Road overflowed, leaving a number of houses flooded.
Storm with strong wind	Cape Town	2019	A storm with heavy rain and strong winds, estimated between 40 and 60 km/h, caused extensive damage to properties in Cape Town and surrounding areas, Western Cape. Several trees were uprooted in Strand, Somerset-West, Theewaterskloof and Genadendal, while roofs were blown off in Macassar and Strand during the same period. There were reports of windows that were blown out in Strand while multiple incidents of power outages occurred across portions of Gordon’s Bay and Somerset West, as well as in Stellenbosch. Luckily, no injuries were reported.
Heavy rain, flooding and strong winds	Cape Town	2019	The city of Cape Town recorded a number of incidents, including flooding in Cape Town and surrounding areas. There was flooding in informal settlements in Masiphumelele in Fish Hoek, Imizamo Yethu in Hout Bay, Burundi, Wallacedene and Makhaza in Khayelitsha where approaximately 3640 structures were affected following heavy rain. Seven dwellings were destroyed by an uprooted tree in Imizamo Yethu. Strong winds damaged roofs and led to power outages in Mamre, Strand, Gugulethu, as well as in Belhar. Roadways were flooded across the city in Southfield, Grassy Park, Killarney, Kraaifontein, Atlantis, Mamre, Hout Bay, Kuils River, Mitchells Plain, Macassar, Parow and Durbanville. Power outages were recorded in Strand, Bonteheuwel, Observatory, Noordhoek, Joe Slovo Park, Athlone, Wynberg, Gugulethu, Nyanga, Sunnydale, Rondebosch, Philippi, Mitchells Plain, Hout Bay,Plumstead, Plattekloof and Rylands. Fallen trees were reported in Parow, Edgemead, Crawford, Panorama, Durbanville and Brackenfell
Gale-force winds	Cape Town	2020	The black south-Easter wreaked havoc across the city of Cape Town and surrounding areas when roofs were blown off, trees uprooted, delivery scooters stopped and people scurrying away from the flying debris. Several roofs were damaged by the strong winds in areas including Fresnaye, the Bo-Kaap, Bonteheuwel, Bokmakierie, Macassar, Philippi and Sea Point. Shack dwellers in the Vygieskraal informal settlement tried to stay indoors after witnessing objects being flung around dangerously by the winds. The wind caused excessive damage in the area. There were also electricity disruptions experienced in Pinelands, Bridgetown, Wynberg, Parow, Richmond Estate, Bellville, Sea Point, Strand, Claremont, Heideveld and Three Anchor Bay because of the wind. Large trees were uprooted in Gordon’s Bay, Newlands,

Event	Location	Year	Consequences
			Mowbray, Rylands and Bonteheuwel. No death or injuries were reported. Several events that were scheduled to take place were cancelled due to the safety of people. The wind also affected the repair of underwater cables that failed and left parts of the continent with slow internet.
Heavy rain and flooding	Khayelitsha	2020	Heavy rain flooded houses in Zwezwe informal settlement in Khayelitsha as well as other areas in the Western Cape. The other affected areas include Overcome Heights, Phola Park, Goliath Estate, Langa, Masiphumele, Khayelitsha and Philippi. Many trees were uprooted across the City in Durbanville, Ravensmead, Atlantis, Eversdal and Somerset West. Power outages were also experienced in Philippi, Pelican Heights, Samora Machel, Strand and Nyanga.
Gale-force winds	Cape Peninsula	2019	Gale-force winds blew over the Peninsula in the Western Cape leaving few dangerous incidents. Trees were uprooted in various areas including the Cape Town, Goodwood, N1 city and other suburbs. A truck overturned after the driver lost control in the winds on the N1 near the Huguenot toll tunnel. Public artworks in Sea Point were also blown over during the night. A blue sculpture had its head blown off.

APPENDICES 5.8.J to 5.8.T

Data in the following appendices are provided in electronic format:

Appendix 5.8.J: AERMOD Dispersion Model Concentration Input File 5 Km by 5 Km Model Domain

Appendix 5.8.K: AERMOD Dispersion Model Concentration Input File 40 Km by 40 Km Model Domain

Appendix 5.8.L: AERMOD Dispersion Model Deposition Input File 5 Km by 5 Km Model Domain

Appendix 5.8.M: AERMOD Dispersion Model Deposition Input File 40 Km by 40 Km Model Domain

Appendix 5.8.N: AERMET Meteorology Surface Data File

Appendix 5.8.O: AERMET Meteorology Profile File

Appendix 5.8.P: AERMAP Terrain and Land Use File

Appendix 5.8.Q: AERMOD Dispersion Model Concentration Output File 5 Km by 5 Km Model Domain

Appendix 5.8.R: AERMOD Dispersion Model Concentration Output File 40 Km by 40 Km Model Domain

Appendix 5.8.S: AERMOD Dispersion Model Deposition Output File 5 Km by 5 Km Model Domain

Appendix 5.8.T: AERMOD Dispersion Model Deposition Output File 40 Km by 40 Km Model Domain